IAHS Publication no. 246
ISSN 0144-7815

FRIEND'97—Regional Hydrology: Concepts and Models for Sustainable Water Resource Management

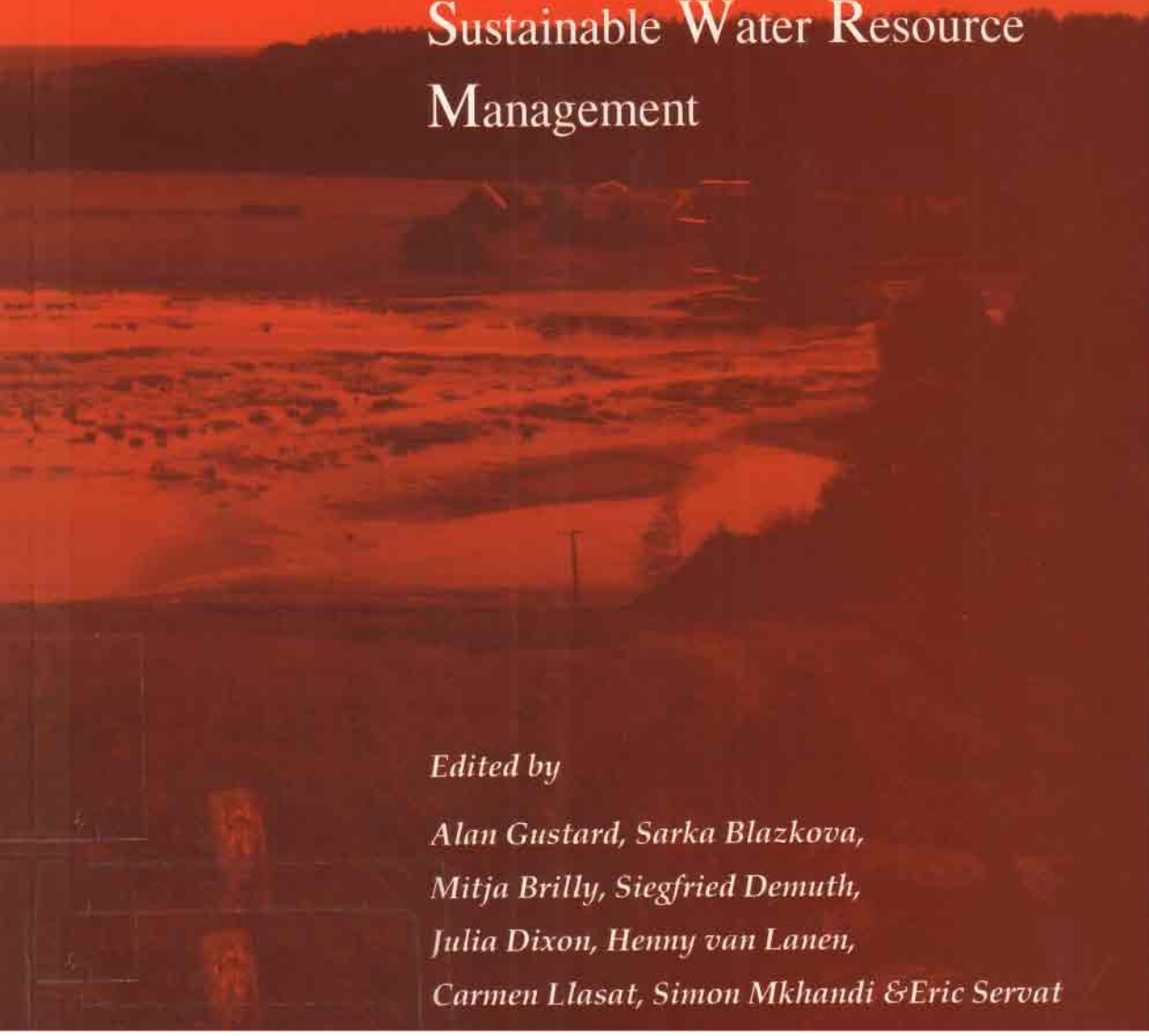

Edited by

Alan Gustard, Sarka Blazkova, Mitja Brilly, Siegfried Demuth, Julia Dixon, Henny van Lanen, Carmen Llasat, Simon Mkhandi &Eric Servat

FRIEND'97—Regional Hydrology:

Concepts and Models for Sustainable Water Resource Management

Edited by

ALAN GUSTARD
Institute of Hydrology, Wallingford, Oxfordshire OX10 8BB, UK

SARKA BLAZKOVA
T G Masaryk Water Research Institute, Podbabská 30, 160-62 Prague 6, Czech Republic

MITJA BRILLY
FAGG Hydraulics Division, University of Ljubljana, Hajdrihova 28, 61000 Ljubljana, Slovenia

SIEGFRIED DEMUTH
Department of Hydrology, University of Freiburg, Werderring 4, D-79085 Freiburg, Germany

JULIA DIXON
Institute of Hydrology, Wallingford, Oxfordshire OX10 8BB, UK

HENNY VAN LANEN
Department of Water Resources, Agricultural University, Nieuwe Kanaal 11, 6709 PA Wageningen, The Netherlands

CARMEN LLASAT
Department of Astronomy and Meteorology, University of Barcelona, Avda Diagonal 647, 08028 Barcelona, Spain

SIMON MKHANDI
Department of Civil Engineering, University of Dar es Salaam, PO Box 35131, Dar es Salaam, Tanzania

ERIC SERVAT
Antenne Hydrologique, 06 BP 1203, Cidex 1, Abidjan 06, Côte d' Ivoire

Proceedings of the Third International Conference on FRIEND held at Postojna, Slovenia, from 30 September to 4 October 1997. The conference was convened jointly by the steering committee of the Alpine Mediterranean Hydrology (AMHY) FRIEND project with the support of other FRIEND groups: Northern European FRIEND, Southern African FRIEND, West and Central African FRIEND and the National Committee of Slovenia for the International Hydrological Programme of the United Nations Educational, Scientific and Cultural Organization (UNESCO) and the Operational Hydrological Programme of World Meteorological Organization (WMO). The conference was sponsored by UNESCO, WMO, the European Commission, the International Association of Hydrological Sciences (IAHS) and the Ministry of Science and Technology, Republic of Slovenia.

IAHS Publication no. 246
in the IAHS Series of Proceedings and Reports

Published by the International Association of Hydrological Sciences 1997
IAHS Press, Institute of Hydrology, Wallingford, Oxfordshire OX10 8BB, UK
IAHS Publication no. 246
ISBN 1-901502-35-X

British Library Cataloguing-in-Publication Data.
A catalogue record for this book is available from the British Library.

IAHS is indebted to the Institute of Hydrology, Wallingford, UK, for the support and services provided that enabled the editor-in-chief to work effectively and efficiently. IAHS is similarly indebted to the employers of the co-editors for the support they provided.

The Editors wish to acknowledge Penny Kisby of IAHS Press for the preparation of the camera-ready copy; the editorial assistance of the conference convenors; and the authors of the papers for their patience and cooperation during the editing process.

The camera-ready pages were assembled by Penny Kisby (IAHS Press, Wallingford, UK) using files of the edited papers provided by the Editor.

Printed in The Netherlands by Krips Repro Meppel.

Preface

The FRIEND—Flow Regimes from International Experimental and Network Data—research programme is an international collaborative study into regional hydrology. It is Project 1.1 of UNESCO's Fifth International Hydrological Programme. The primary objective of the FRIEND project has been to improve understanding of hydrological variability and similarity across time and space in order to develop hydrological science and practical design methods. To achieve this it has been essential to permit hydrological research to cross national boundaries. This has been done in three ways. Firstly, by developing international hydrological databases of time series and spatial data. Secondly, by establishing project groups that could exchange models and analysis techniques and interpret the results using a common approach. Thirdly, by encouraging the exchange of scientists: promoting collaborative links between operational and research organizations and by running workshops and training courses in database management and regional hydrology. Since its inception in northern Europe in 1985, the project has developed to embrace six major international groups with around 75 participating countries. Two previous proceedings have been published by IAHS presenting the scientific results of the FRIEND project at conferences held in Bolkesjø, Norway (IAHS Publ. no. 187, April 1989) and in Braunschweig, Germany (IAHS Publ. no. 221, August 1994). To complement the papers published in these proceedings CEMAGREF has published the third major FRIEND international report.

As we approach the end of the twentieth century, we face increasing uncertainty, not only in the extremes of floods and droughts but in the entire hydrological regime which controls our domestic, agricultural, industrial, energy and environmental use of water. The objectives of these proceedings are to address these issues by developing scientific, technical and applied links between regional hydrology and the development of integrated catchment management systems.

Alan Gustard
Editor-in-chief
Institute of Hydrology, Wallingford, UK

Contents

8 Hydrological Processes

1 International Hydrological Databases

WHYCOS, a programme supporting regional and global hydrology

SERGE A. PIEYNS & DIETER KRAEMER
Hydrology and Water Resources Department, WMO, 41 Avenue Giuseppe Motta, CH-1211 Geneva 2, Switzerland

Abstract Regional and global hydrology are relatively new concepts. They both depend on reliable national hydrological information systems and on the willingness of the countries to cooperate at regional and global levels, notably through the exchange and dissemination of good quality data and information. Unfortunately, recent studies and international conferences have stressed that hydrological information systems are inadequate or do not exist in many countries, and that regional and international cooperation is rather limited. For these reasons, the World Meteorological Organization (WMO), with the support of the World Bank (WB) and other partners, started to promote, in 1993, the World Hydrological Cycle Observing System (WHYCOS), a programme aimed at supporting the establishment and improvement of hydrological information systems. This global approach is being implemented through components (HYCOSs) established at the level of hydrological, economic and political regions.

INTRODUCTION

Regional and global hydrology are relatively new concepts. These "new" ways of approaching hydrological processes correspond to real demands both from the scientific (knowledge base) point of view as well as from the sustainable development one.

It should be recalled that the International Conference on Water and the Environment (ICWE, 1992), held in Dublin (Ireland), stated that "the most appropriate geographical entity for the planning and the management of water resources was the basin", which very often extend beyond the national border of a single country. Obviously, regional and global hydrology will be extremely helpful in this regard.

Similarly, the UN Commission on Sustainable Development (UNCSD, 1994) declared that "many countries face a water crisis with rapid deterioration of water quality, serious water shortages and reduced availability of freshwater, which effects severely human health, the ecosystem and economic development". CSD urged UN agencies, including WMO, "to strengthen their efforts towards a comprehensive assessment of the world freshwater resources, with the aim of identifying the availability of such resources, making projections of future needs and identifying problems to be considered by the 1997 Special Session of the General Assembly" (UNCSD, 1994). Once again, the new concepts will be very appropriate tools for undertaking reliable periodical assessments. Above all, they will be instrumental for a better knowledge of the hydrological cycle (quantity and quality) which, according to Chapter 18 of Agenda 21 (UNCED, 1992), is essential for the efficient and

sustainable management of the water resources, since life on this planet takes place at the mercy of the water cycle (Falkenmark, 1994), which imposes its constraints to both the social sphere (socio-economic development) and the landscape sphere (environment), within which the development takes place.

Finally, several global initiatives which need a thorough knowledge of the hydrological cycle at the appropriate scales will benefit from regional and global hydrology such as: the World Climate Research Programme (WCRP) and the Global Climate Observing System (GCOS), aimed at improving regional and global climate models to predict seasonal and interannual climate variability, to detect climate change and to reduce uncertainties in climate prediction; the Global Ocean Observing System (GOOS); and the Global Environment Monitoring System (GEMS), etc.

Regional and global hydrology require international cooperation and collaboration, notably through data exchange and dissemination and the establishment of easily accessible regional and international hydrological databases. The FRIEND project of UNESCO has already succeeded in establishing some of these databases with selected sets of historical data for northwest Europe, the Alpine and Mediterranean countries, southern and west and Central Africa, etc. However, hydrological databases are only one piece of a much broader set of activities, harmoniously integrated in what could be called a **hydrological information system**. This system should include collection and dissemination of data and "plays an important role in estimating the quantity and quality of water available, as well as the current and prospective water use and demand patterns" (World Bank, 1994). An example is shown in Fig. 1. Databases are totally dependant from the quality, timeliness, consistency and sustainability of the data flow which feed them. At the basin, regional and international levels this can only be achieved, in a sustainable way, if the national information systems are operational and have more or less reached the same status of development and if the countries have institutionalized their willingness to cooperate, notably by disseminating and exchanging data and information.

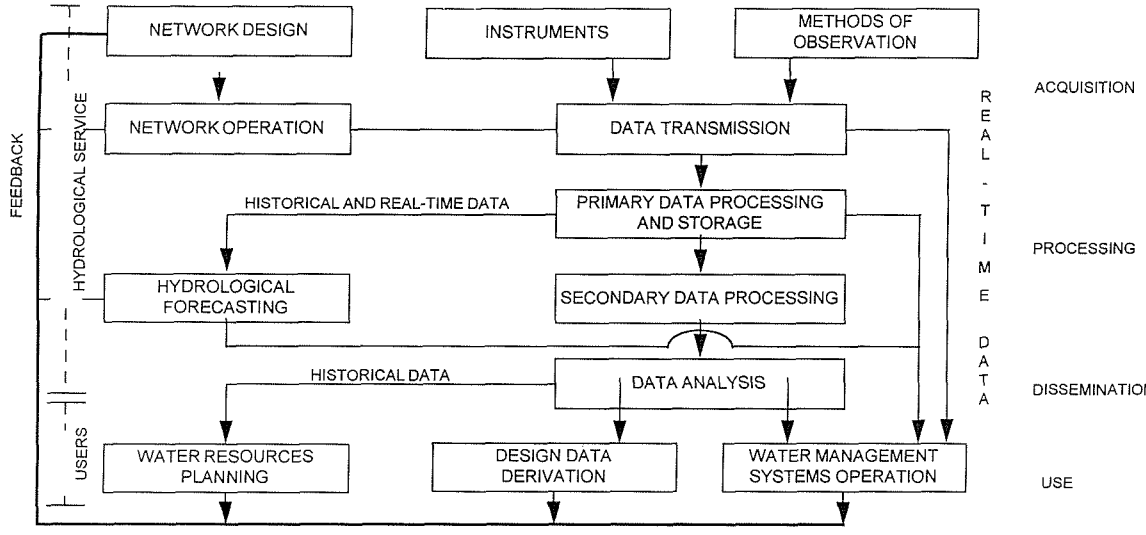

Fig. 1 Hydrological information system.

THE STATUS OF HYDROLOGICAL INFORMATION SYSTEMS

Both Chapter 18, the ICWE report and the WMO/UNESCO report (1991) on water resources assessment (WRA), clearly indicate that in many regions of the world these systems are not working correctly or do not exist at all. Fig. 2, which was prepared by using information collected by WMO for the preparation of the 1995 edition of the INFOHYDRO Manual (WMO, 1995), illustrates the situation which is prevailing in the different Regional Associations (RAs) of WMO. There is a great disparity between the measurement activities within the various regions. For example, in 1994 there were 5703 stations for river discharge measurement in Africa (the second largest continent) and 20 008 such stations in Europe. For water quality stations, the figures were 5297 and 55 379 respectively. Although the number of national data banks grew substantially between the Mar del Plata Conference held in 1977 and 1994, the WRA report (WMO/UNESCO, 1991) notes that in the later part of the 1980s and into 1990s some ground gained in the early 1980s has been lost in both water data collection and management.

Moreover, the Comprehensive Freshwater Assessment, prepared for the CSD by UN agencies, including WMO, and the Stockholm Environment Institute, clearly indicates that the access to reliable data is presently inadequate and that there is a need for national and internationally harmonized information systems, including

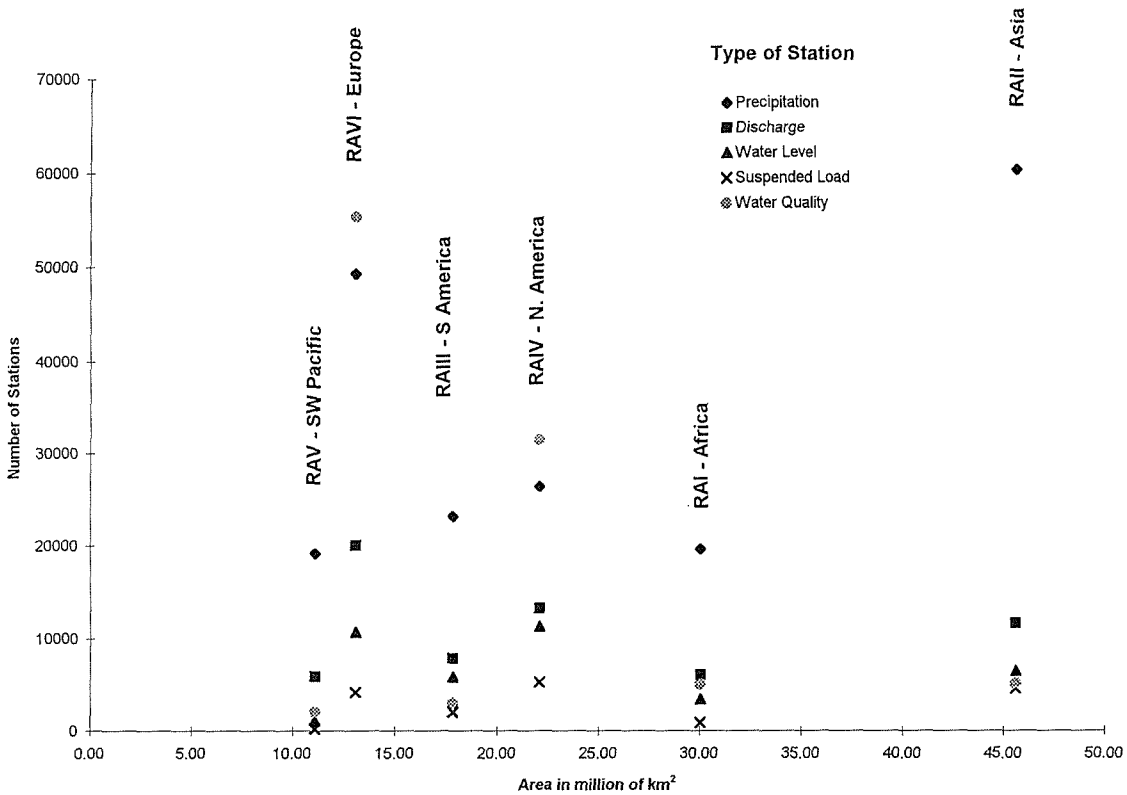

Fig. 2 Number of hydrological stations by area of WMO region.

hydrological ones, that provide data needed for planning and decision making, as well as common ways of analysing the information.

As an example of this situation, the conclusions of the sub-Saharan Africa Hydrological Assessment (SSAHA), executed by the World Bank from 1988 to 1995 with the financial support of UNDP, the African Development Bank (ADB), the European Community and the French Government, demonstrate that the situation of most of the hydrological information systems, and of the services which are responsible for these in the Region, is declining rapidly.

The causes of this situation were discussed during the Addis Ababa Conference organized in Ethiopia by WMO and the United Nations Economic Commission for Africa (ECA), in March 1995 (WMO/ECA, 1995). There is no doubt that the fundamental cause for the decline of water resources assessment and management systems (at national, subregional and international river basin levels), is the slow-down or even reversal of socio-economic progress in a large number of the countries of the Region. In addition, the adverse economic situation has emphasized other historical and structural pre-existing causes.

As a general rule, politicians and decision makers, facing a number of problems, are not aware of the degree of priority of the water sector and for the need for integrated and sustainable development. Above all, in many cases they have generally no idea of the economic value, direct and indirect, of hydrological information systems. It is therefore not surprising that they are not willing to disburse the meagre available funds for the assessment and monitoring of the water resources. Moreover, the general public largely ignore the status of water resources in terms of supply and demand, quantity, scarcity and ecological value. In addition, the National Hydrological Services (NHSs) have increasingly been confined to data collection, network maintenance and operation, with too little involvement in the socio-economic development and promotion of their activities.

This experience, gained from SSAHA, cannot be transferred directly to the other regions of the world. However, the fact that the knowledge-base related to the global hydrological cycle is not adequate has become more and more evident, notably during the recent assessment of global water resources undertaken by WMO/UNESCO, as part of the Comprehensive Freshwater Assessment Project requested by the UNCSD (1994).

ONE POSSIBLE WAY FORWARD

WMO, with the support of the World Bank and other partners, started in 1993 (Rodda *et al.*, 1993) to promote the World Hydrological Cycle Observing System (WHYCOS).

Basic concept and objectives

The underlying principle of this worldwide programme is cooperation between the participating countries in the domain of water resources assessment and management.

The objective of the WHYCOS initiative is to provide a scientific basis for water resources monitoring, assessment and integrated development and management, at different time and space scales, through the improvement of exchange of consistent, reliable and timely available data and information. It will contribute to the knowledge of hydrological processes in their interaction with climate and the environment, and will encourage intersectoral sharing of water resource data and information for development and natural capital management.

Improved cooperation between the participating countries would notably help to address ensuing problems by:

(a) improving consistency in data acquisition, transmission, processing and use; and
(b) strengthening technology transfer and capacity building; and
(c) promoting the free exchange and dissemination of data and information.
(d) supporting the NHSs throughout the world, by carrying out more accurate, sustainable and cost-effective monitoring and management of the world water resources.

Implementation

Originally this programme was essentially conceived to be based on the implementation of a global network of reference stations (hydrological observatories), with real-time data transmission, through satellite whenever possible, to enable the development of consistent, high-quality and constantly updated distributed national, regional and international databases on river flow, water quality and key climatic variables.

The programme however progressively moved from this technological approach to an integrated one, aimed at improving not only the collection of consistent and reliable data, but also the preparation and the dissemination of relevant information on the hydrological cycle at national, basin, regional and international levels, through the implementation/improvement of hydrological information systems meeting the demand.

The vision of the programme is to create a sustainable basis and a logical framework for the "revival" of operational hydrology, demand driven and action oriented, in order to put at the disposal of the end-users information in different domains of application (WMO, 1996).

This revival has to be undertaken with the participation of decision makers, and users at national, regional and international levels and, when necessary, funding agencies. It has to be adapted to the actual short and medium term possibilities of the countries, using first of all the existing resources in terms of personnel, equipment and knowledge. This revival has also to be harmonized with other related ongoing or planned projects in domains such as health, famine and poverty alleviation.

To reach this objective, WHYCOS is being implemented through a two-pronged fully integrated approach with, on the one side, a **global conceptual basis** providing a framework and general guidance based on the improvement of cooperation between the participating countries in the field of water resources assessment and management; and, on the other, **a number of operational activities**, which are being developed interactively and concurrently through the implementation of regional

components: the HYCOSs. This approach allows an independent implementation of each component, notably to be able to establish the institutional and financial agreements which best fit the specific needs and conditions prevailing in the region.

The intention is that the regional projects would be implemented by a Pilot Regional Centre (PRC), hosted by an operational organization existing in the region, either a NHS or a regional organization, under the control of a Regional Technical Committee (RTC) with representatives of all participating countries. According to the situation, a Steering Committee with representatives from the funding agencies, countries and executing agency, might be set up. At the global level, the need for a coordinating body is being considered. The different HYCOSs projects, programmes such as the Global Runoff Data Centre (GRDC) and FRIEND, global observing systems, and users from both public and private sectors, should be represented.

Expected products

Installation of networks of key stations These stations will be multi sensor-equipped Data Collection Platforms (DCPs) to establish a basic network of benchmark stations sited on major rivers for the collection and transmission of several variables related to water resources monitoring. A small number of significant lakes and reservoirs will also be monitored. The stations will be proposed by the participating countries from existing stations which might be easily upgraded to meet a common WHYCOS technical standard.

The stations will be selected according to the WHYCOS criteria: (a) availability of long historic series record; (b) stable calibration curves; (c) regional significance of data collected; and (d) needs expressed. They will transmit data to regional and national centres, mainly through meteorological satellites (METEOSAT, GOES, etc.) and the Global Telecommunication System (GTS) of the World Weather Watch (WWW) of WMO. The variables the programme intends to collect are listed in Table 1.

Development and implementation of regional databases These databases are aimed at providing consistent, good quality, updated and timely available data They will be designed on the basis of the needs expressed by the users. In order to facilitate easy access, the database will have an integrated Web server. Modalities for accessing data and information will be decided by the participating countries, notably on the basis of international recommendations and regulations, such as Resolution 40 of WMO's Twelfth Congress for the exchange of meteorological data and its equivalent for hydrological data (in preparation). It is proposed that during the implementation phase the regional database be developed and installed at the PRC. Later on, the countries might decide to establish a distributed database by interconnecting the national bases using the regional computer network.

Implementation of regional computer networks These networks are aimed at monitoring the regional water resources and promoting data exchange, and encouraging regional and international collaboration between governments, NHSs and other research or operational institutions and organizations. The network will also enable the exchange of information with other databases.

Table 1 WHYCOS: Data to be collected and transmitted.

		Frequency of measurement per day
Environmental variables		
1.	Water level (upstream)	1 to 6 (depending on size of river)
2.	Water level (downstream)	1 to 6 (depending on size of river)
3.	Water conductivity	1
4.	Water temperature	1
5.	Turbidity	1
6.	Air temperature	8 (synoptic hours)
7.	Rainfall	24, plus daily total
8.	Relative humidity	8 (synoptic hours)
9.	Wind speed	8 (synoptic hours)
10.	Wind direction	8 (synoptic hours)
11.	Net radiation	8 (synoptic hours)
Housekeeping variables		
12.	Battery voltage	1
13.	Solar panel voltage	1
14.	Memory status	1
15.	Temperature inside instrument housing	1

Hydrological products These products will be prepared using the data available in the regional database and those made available from other sources at national, regional and international levels. During the first step of the implementation, these products will be developed on a regional basis by the PRC, in cooperation and collaboration with the NHSs of the participating countries and other partners, as necessary. The products will be distributed using several ways such as: the Web of the Internet which will allow a dynamic presentation of the information, E-mail, CD-ROM and other traditional ways. The dissemination will be targeted to the greatest possible number of users. A survey of the impact of these products will be conducted and new products developed, in line with the results of the survey. Later on, NHSs of participating countries will be trained to develop products at national level and therefore create/improve the market for hydrological information.

Training The NHSs will be in charge for installing, operating and maintaining the WHYCOS hydrological stations, carrying out regular stage/discharge calibration, maintaining databases and network connections, and validating raw data. Additional observational and telecommunication instrumentation might be provided for the upgrading of the selected stations forming the WHYCOS network. When necessary, the NHSs will also be provided with hardware and software for the national databases, and for the preparation of hydrological products and their dissemination. Relevant training programmes will be developed to cover all aspects of the programme, including marketing, promotion and public relation.

STATUS OF THE PROGRAMME

Several regional projects are at different stages of development or implementation:

(a) **MED-HYCOS** (Mediterranean rim), is being implemented with WMO as the executing agency, with support from the World Bank and other partners. The PRC is hosted by the French Scientific Research Institute for Development through Cooperation (Orstom), in Montpellier (France). The installation of the first 20 DCPs is being done and a regional telecommunication system, based on the use of existing segments of the GTS and of Internet, is being developed concurrently with relevant training sessions. The implementation of the project would be extended to the Black Sea, as new funds become available.

(b) **SADC-HYCOS** (Southern Africa Development Community). The project document was prepared by SADC and WMO at the request of the European Union (EU) which is now funding the implementation of the project under the Lomé Fund, with WMO as the supervising agency. The PRC will be hosted by the Directorate of Hydrology, in Pretoria (South Africa) and 50 DCPs would be installed during the year 1997.

(c) **AOC-HYCOS** (West and Central Africa). The project document has been prepared by WMO and local experts, through a contract signed with the French Ministry of Cooperation, and presented to the Ministry in the early 1997. Web sites for MED-HYCOS and for a pilot AOC-HYCOS project can be reached through WMO's home page (http:// wmo.www.ch) under Hydrology and Water Resources Programme.

(d) **Congo-HYCOS** (Congo River basin). Would be part of a Regional Environment Information Management Project for the Central Africa Region (REIMP-CAR). The preparation of the project document by WMO is funded directly by the European Commission, under a contract signed with WMO in February 1997.

(e) **Aral Sea-HYCOS** (central Asia). The relevant project document has been prepared by WMO in cooperation with Swiss experts. It would be one of the components in a World Bank's Aral Sea Programme. Other HYCOSs are under consideration for the preparation of the corresponding project documents such as **IGAD-HYCOS** (Eastern Africa), **CARIB-HYCOS** (Caribbean region) and **NILE-HYCOS** (Nile basin).

CONCLUSION

A number of surveys, reports, and international Conferences have recently highlighted the **absence or the inadequacy of the hydrological information systems** mainly, but not exclusively, in developing countries. Moreover, **regional cooperation for the assessment and management of shared water resources is difficult to establish and to sustain.**

These are obviously **limiting factors** for the development of regional and global hydrology, which at the same time are responding to needs expressed by users ranging from national to international agencies.

In addition to the economic problems, which a number of countries are facing, there is an absence of a real understanding by the decision makers of the role of the hydrological cycle in the socio-economic development and in environment and biodiversity protection.

Therefore, WHYCOS is being implemented in order to participate in the sustainable revival of these systems and of the regional and international cooperation in the field of water resources assessment and management. The approach chosen is regional and integrated, through the utilization of appropriate and well-tried tools, development of human resources, tailored and targeted financial support, promotion and dialogue with the users at national, regional and international levels in a new information context.

Thus, the WHYCOS programme of WMO and the FRIEND programme of UNESCO are working hand-in-hand for the development/improvement of regional and global hydrology for the benefit of knowledge and sustainable socio-economic development.

REFERENCES

Falkenmark, M. (1994) Landscape as a life support provider: water-related limitations. In: *Population—The Complex Reality. A Report of the Population Summit of the World's Scientific Academies* (ed. by Sir Francis Graham-Smith). The Royal Society, London.

ICWE (1992) International Conference on Water and the Environment (Dublin, Ireland, 26–31 January 1992). The Dublin Statement and Report of the Conference.

Rodda, J. C., Pieyns, S. A., Sehmi, N. S. & Matthews, G. (1993) Towards a world hydrological cycle observing system. *Hydrol. Sci. J.* **38**(5).

UNCED (1992) *Agenda 21: The United Nations Programme of Action from Rio.* Chapter 18: Protecting and managing fresh water.

UNCSD (1994) UN Commission for Sustainable Development: Report of the Second Session on Water, New York.

WMO (1995) Hydrological information reference service. *Operational Hydrology Report no. 28.* OMM no. 683.

WMO (1996) *Guide to Hydrological Practices.* Chapter 3, OMM no. 168.

WMO/ECA (1995) African Conference on Water Resources. Policy and Assessment. (Addis-Ababa, Ethiopia, 20–25 March 1995). Report of the Conference.

WMO/UNESCO (1991) *Water Resources Assessment. Progress in the Implementation of the Mar del Plata Action Plan and a Strategy for the 1990s.*

World Bank (1994) A guide to the formulation of Water Resources Strategy. *Technical Document no. 263.*

FRIEND'97 — Regional Hydrology: Concepts and Models for Sustainable Water Resource Management
(Proceedings of the Postojna, Slovenia, Conference, September–October 1997). IAHS Publ. no. 246, 1997.

Information transfer in hydrology: experiences of the Global Runoff Data Centre

WOLFGANG E. GRABS
Global Runoff Data Centre (GRDC) c/o Federal Institute of Hydrology, PO Box 309, D-56068 Koblenz, Germany

Abstract Politicians and decision-makers are faced with water-related problems of geopolitical importance which have a large influence on life on our planet and which have to be resolved now. The global exchange of hydrological information is a necessary precondition in this situation. A global hydrological database is essential for research and application-oriented hydrological and climatological programmes at global, regional and basin scales. The Global Runoff Data Centre (GRDC) advocates the controlled access to global hydrological data which allows free access to the data under the provision that the interests of the data providers and the data users are balanced. In this respect, the participation of hydrological services in international science programmes is essential to create a transmission belt between scientific projects and the interests and the capacity of hydrological services. National and international aspects of hydrological information transfer requires the development of more effective transfer mechanisms both: Technically and through simplified procedural processes. To improve information transfer in hydrology, the transfer of hydrological information should be embedded in an information feedback cycle which provides benefits for both: The data provider and the data user. An additional benefit of this feedback cycle is the possibility to network research and application-oriented programmes and thus contribute to economizing the rising cost for regional and global hydrological research and its applications to operational hydrology issues. In this respect, several policy options for information transfer are discussed in this paper and an outlook is provided into emerging issues of data exchange in hydrology.

INTRODUCTION

The principal objective of the GRDC is to facilitate and optimize the information exchange in surface water hydrology. Another important objective is to provide decision-makers with hydrological information needed to resolve hydrological problems, e.g. in the management of international river basins. These tasks are fulfilled through intense interaction with water-related programmes of UN agencies, foremost those of WMO, UNEP and UNESCO, other governmental and nongovernmental organizations and data users. At present, the demand for data and information from the different user groups in hydrology is not matched by the supply of hydrological information from data providers.

FROM DATA TO PRODUCTS

The transfer of hydrological information is the end of a process chain which involves the collection of data, its quality control, processing the data into user-specific

information and the transfer process of data and information itself. The technologies used for the transfer of information along this process chain determine the technical efficiency of the system and its integrity. The decisions and resulting regulations for data collection and processing on one hand and the adopted policies which regulate the information flow and access to information determine the overall effectiveness of the hydrological information transfer process. The importance of data management and information to execute global change programmes can be highlighted with a figure from the 1995 budget of the US Global Change Research Programme: Out of a total budget of US$1814.8 million, 382.0 or 23% are dedicated for data management and information alone (US General Accounting Office, 1995).

RATIONAL FOR GLOBAL HYDROLOGICAL INFORMATION TRANSFER

Perhaps the singlemost important rational for the transfer of hydrological information on a global scale is that no single country today is able to bear alone the enormous costs of a global observing system from which national economies could benefit. Regional monitoring and warning of flood and drought events, coupling of atmospheric with land and ocean models, the pollution of the world's oceans through transport of pollutants from rivers discharging into the oceans are top agenda issues. These tasks, problems and the possible solutions to the problems indicated above have a truly global dimension and cannot be viewed from the catchment scale perspective alone. National decision-makers should be convinced that the development interests of individual countries are directly served through the participation in global exchange and the institutionalized sharing of hydrological and related information. WMO has set the frame in which the exchange of information may happen. At its Twelfth Congress in 1995, WMO adopted Resolution 21 (Cg-XII) "Global Runoff Data Centre" which encourages Members "to support the GRDC through the provision of the hydrological data and related information that it needs" (WMO, 1996). In an analogy to resolution 40 (Cg-XII), the Commission of Hydrology (CHy) in December 1996 adopted a draft resolution regarding the exchange of hydrological data and related information which will be discussed by the Executive Council of WMO in June 1997.

TRANSFER OF HYDROLOGICAL INFORMATION: THE NATIONAL PERSPECTIVE

Hydrological services until recently have been viewed in most cases by their governments as basic statistical services which were expected to collect and archive hydrological information of the national territory. As these services in many cases operate under civil service rules and regulations, active marketing of the benefit of hydrological information for the national development and the response to user requirements with meaningful data products has not been a priority of national hydrological services. Thus, despite the growing sectoral demand for water related data and initial investments in hydrological services, the advantages and benefits of

hydrological data transfer are not known or simply are not a priority for governmental and nongovernmental organizations. Diminishing support for "traditional" hydrological services and the taking over of data collection programmes by other, more project and market-oriented (semi)-privatized organizations has led to a further fragmentation of data holdings. This continuing process further complicates the exchange of data. The situation is sometimes worse in federally organized countries, where riparian states on top of sectoral competition for water uses also have difficulties to agree on a mutually satisfying allocation scheme.

TRANSFER OF HYDROLOGICAL INFORMATION: THE INTERNATIONAL PERSPECTIVE

Hydrological services have usually a clearly national scope for their operations. Only very few services have the mandate and the capacity to deal with international partners in hydrology and water resources management. Therefore, at the very basic levels, the understanding of the importance of internationally shared data is little understood and promoted. In addition to institutional weaknesses of services, especially in developing countries, comes the issue of political decisions which impede the cross-border transfer of hydrological information. The idea of possessing an information monopoly of this vital resource is often combined with disagreements between riparian countries regarding water distribution. The opinion that water resources are tied to the national security, integrity and development potential of a nation is a strong factor which severely limits the transfer of information. The situation is worse in the compilation of hydrological information over entire regions. The point is made here that a good part of the problem of international transfer of hydrological information could be solved if national governments defined the value of hydrological information for the national development and—based on this assessment—highlighted the role of hydrological information in the national development plan for each country. In countries with transboundary river basins, the political will and technical ability of governments must be demonstrated to cooperate with other riparian countries.

It may be important to recognize that conflicts between riparian states are maintained in a climate of mutual distrust which in its technical component can be traced to the lack or absence of shared data and information. The sharing of data and information would be a first step in a series of confidence-building measures to overcome a conflict situation on the basis of equal information which can be shared by all partners. The International Law Association (International Law Association, 1987) has formulated the Helsinki rules (International Law Association 1966 with several amendments in 1986). Article 29 recommends that each basin state "furnish relevant and reasonably available information to the other basin states concerning the waters of a drainage basin within its territory and its use of, and activities with respect to, such waters". Though the value of these rules is generally not disputed, its practical implementation e.g. the transfer of hydrological information is slow in many and pending in some cases. Bearing in mind however that over 60% of the world`s freshwater resources are shared in only 200 international river basins, the global importance of information transfer becomes apparent.

LESSONS LEARNED FROM THE EXCHANGE OF HYDROLOGICAL INFORMATION

The transfer of hydrological information requires first of all the vision and political will for regional and even global cooperation in hydrology and water resources management between governments and their hydrological services.

(a) While the collection of data is the prime objective of hydrological services, with an often much lesser priority or capacity to process the data adequately for water resources management purposes, the transmission of information halts at the question "Why should I?".

(b) Looking at the national and international aspects of hydrological information transfer and related GRDC experience, the development of more effective transfer mechanisms of hydrological information should be prioritized. Information transfer from providers to users is in many cases organized on an *ad hoc* basis without clearly defined policies.

(c) Fragmented data holding and the just evolving concept of the management of distributed databases lead to the development of sector-oriented, project-focused data collection programmes with limited access to cross-sectoral or international users.

(d) The limited programmatic scope of many hydrological services is a hindrance to promote the exchange of data which usually is circulated only between government agencies, selected users and contractors.

(e) The recognition of the potential economic value of hydrological information which, in many cases cannot be realized by hydrological services, creates an effective block to transfer information: The information is withheld in the expectation that in an indistinct future the service may have the capacity to fully analyse the data and transfer only customized information and not the data.

(f) The low level of public recognition of the tasks and capacities of hydrological services has lead to a mental setting where the idea of an information monopoly is created which could be exploited for the benefit of an individual service or a position holder.

(g) There is hardly a "transmission belt" between ambitious international scientific programmes and their needs for regional or global data sets on one side and the objectives of national services on the other side. Likewise, scientific programmes hardly find a proper communication channel to include hydrological services as partners and participants of their far-reaching efforts but rather as "data-servants"; an unsatisfactory role for most hydrological services. The possibility of capacity building within these scientific programmes is under-utilized.

WMO has a attained a lead role in the development of effective transfer mechanisms where the World Weather Watch Programme can serve as an example. In hydrology, the GRDC is presently the only operational hydrological databank working on a global scale with continued dataflow. Further efforts including an increasing share of funds for Technical Development projects are necessary to maintain and improve this lead role.

CONCEPTS FOR THE EXCHANGE OF HYDROLOGICAL INFORMATION

The international dissemination of hydrological information does not have a long

history and many nations are simply hesitating to allow access to data because potential gains and perceived losses cannot be judged with confidence. The latter can be largely attributed to an insufficient exchange of national experiences in data exchange and the insufficient recognition of positive national feedback when hydrological data is shared on a regional and global basis. In the view of the GRDC, two major concepts to the exchange of hydrological data can be identified:

(a) The concept that data acquired from public funds in a civil service structure should be freely accessible and unrestricted for the benefit not only to the national population (who paid indirectly for the data acquisition with their tax contribution), but also to the scientific community whose research results are regional or even global in nature so that a trans-national benefit can be achieved. Access to and exchange of information is also perceived as a confidence building measure between and across nations.

(b) The concept that hydrological data are crucial for the socio-economic development of a nation. Therefore it is perceived as politically important that data should be protected from improper use. This could be e.g. in the case of conflicting interests between riparian countries or in a situation where decision-makers suspect that the access to hydrological information would indirectly reveal internally sensitive issues such as power production, industrial development, agricultural production etc.

MODELS FOR INFORMATION TRANSFER

Four basic models for the transfer of hydrological data are identified in this paper:

(a) Dissemination of data and products to identified users. This would mean a controlled access. From the experience of the GRDC this approach has helped a lot to network researchers who work in related fields and is able to make use of synergistic potentials in research which are less evident with an anonymous access to data and products. This approach also supports the information need of data providers who need feedback as to who is using the data for which purposes and thus underlines the participatory approach of data providers in information processing. This approach requires "User rules" which regulate the dissemination of data.

(b) Dissemination of the data through the Internet: This provides free, unrestricted, uncontrolled access except perhaps for commercial purposes. This model requires least administration efforts and follows the "Freedom of Information"—philosophy of the United States. It also allows the widest possible dissemination of the data and products. There is no need felt to monitor who is using the data in what context and for what purpose. The data providers do not have feedback on the use of the data. The data may be used without reference of the source and update verification.

(c) Dissemination of data for project participants only, until the project has proceeded to a stage where the project participants decide to make data and results public. This approach is close to the data transfer policy of UNESCO's regionally implemented programme Flow Regimes from International and

Experimental Network Data (FRIEND). The assembly of global data sets and the principle of free and undiscriminatory access to data are difficult to achieve.

(d) Case-to-case decision which datasets are open and which datasets should have a controlled access. This model takes into account that many datasets may already be in the public domain (e.g. data from historic archives etc.) and others are restricted for use only for defined purposes. The practical implementation of this model in a daily routine is problematic from an administrative point of view.

Though there is a common understanding that data should be provided free for research, it becomes increasingly difficult to distinguish between research and applications as much of today's research is application-oriented. It is a good assumption that many of the expensive global research programmes are funded because of the awareness of funding agencies of the potential or even immediate socio-economic value of the research.

Whereas the "free access" model follows the example of the United States, European countries tend to operate various schemes of differential charging of data, which has been an effective regulation instrument in terms of use and access to data. Where the cost of data and its inherent value is becoming apparent in this way, cash-scarce programmes and participants especially in developing countries cannot afford research. In a drive for the commercialization of services, costs emerge as an effective barrier to access hydrological data.

MILESTONES FOR INFORMATION EXCHANGE

Information exchange in hydrology is only taking place when this is politically desired. From the experience of the GRDC, several milestones need to be reached to accomplish the transfer of global hydrological information: Governments and hydrological services must be informed about the benefits of shared information and about the value-added benefit which can be derived from this. The interests of data providers and data users must be recognized and adequately embedded in a data exchange policy. The protocols for the transfer of information must be known to the public and be transparent for all participants. Feedback mechanisms about the use of transferred information and results must be established to close the information transfer cycle. Feedback is also an important motivator to provide information. Programmes of WMO and other organizations which rely wholly or in part on the supply of hydrological data should develop an outreach for a truly participatory approach of hydrological services to participate in these programmes and projects.

Though the limited success of international agencies to mediate international water treaties is recognized, little has been done to spell out, categorize and analyse the political reasons for restrictions in information flow in hydrology.

The concept of information transfer must clearly spell out where the mutual benefits become evident and intelligible for all partners. This requires grass-root efforts to communicate (and learn how to communicate!) regional and global hydrological issues and their data requirements to the level of hydrological services.

Specifically the hydrological advisors and members of working groups in hydrology have a responsibility to "educate" and inform their own services about the international use of data which these services collect and provide guidance and

information for national decision-makers who decide about the transfer of hydrological information.

Transfer of hydrological information should be embedded in an information feedback cycle which provides benefits for both: The data provider and the data user. An additional benefit of this feedback cycle is the possibility to network research and application-oriented programmes and thus contribute to economize the rising cost for regional and global hydrological research and its applications to operational hydrology issues.

REFERENCES

International Law Association (1987) *Helsinki Rules on the Uses of the Waters of International Rivers*. Adopted at the 52nd Conference of ILA (Helsinki 20 August 1966). ILA, London.

WMO (1996) Twelfth World Meteorological Congress. *Abridged Final Report with Resolutions*. Geneva 1995.

2 The Spatial and Temporal Variability of Hydrological Regimes: *Mean Runoff*

FRIEND'97 — Regional Hydrology: Concepts and Models for Sustainable Water Resource Management
(Proceedings of the Postojna, Slovenia, Conference, September–October 1997). IAHS Publ. no. 246, 1997.

The derivation of a runoff grid for southern Africa for climate change impact analyses

NICHOLAS REYNARD, ANTHONY ANDREWS
Institute of Hydrology, Wallingford, Oxfordshire OX10 8BB, UK

NIGEL ARNELL
University of Southampton, Southampton SO17 1BJ, UK

Abstract One of the most significant impacts of global climate change will be on the hydrological system and hence river flows and water resources. This will be particularly true in semiarid areas such as southern Africa. The recent droughts of 1992 and 1995 have highlighted the sensitivity of the regions' water resources to variation in climate, especially rainfall. This implies that the sensitivity of water resources to climate changes on national and regional scales must be addressed. This paper describes the derivation of a map of gridded runoff for southern Africa as the first step in a regional climate change impact analysis. The southern Africa FRIEND database provided both raingauge and catchment runoff data for validation purposes. The results show that the model tends to overestimate the annual runoff, but in a consistent manner suggesting that the model is conceptually sound but lacking the high quality, accurate input data necessary for better simulations.

INTRODUCTION

Regional-scale hydrological modelling can provide much needed guidance for national and international water resource issues. One of these is the potential impact of climate change due to global warming over the next century. Before any assessment of climate change impacts is possible the baseline that these changes are measured against must be defined. In this study a baseline period of 1961–1990 is used. No hydrological model can possibly simulate the runoff of an entire region in detail, so an approach has been developed that divides the region into regular grids, usually 0.5° longitude by 0.5° latitude, and then simulates the runoff in each of these cells to obtain the regional picture (Arnell & Reynard, 1993; 1996).

This gridded map of monthly and annual average runoff for southern Africa was developed as part of a wider study assessing the potential impacts and implications of climate change in the Southern African Development Community (SADC) region (Hulme, 1996). The study assessed the potential impacts of climate change in various sectors, covering water availability, vegetation, agriculture, disease and ungulate diversity. In addition, the study discusses some of the possible policy responses to these changes. This paper describes the methods used and the hydrological model applied to generate the runoff grid, and in addition, outlines the validation of the runoff that was undertaken using the southern Africa FRIEND database, as a contribution to the southern Africa FRIEND project (UNESCO, Project 1.1 of IHP-V).

HYDROLOGICAL MODEL AND RUNOFF GENERATION

The runoff map is derived using a rainfall–runoff modelling technique, based on a regular 0.5° grid. Each cell is treated as an independent catchment and the resultant map shows the runoff generated over each cell, with no routing of the runoff through the cells or via the river network. The model used is a conceptual rainfall–runoff model, with the parameters derived from physical and climatic characteristics, rather than by calibration. It is based on Moore's probability distributed model (PDM) which has a soil moisture store with a capacity that varies across each cell, and a groundwater store (Moore, 1985). The parameters define the size of the stores and the rate of removal of water from them. The inputs are daily rainfall and potential evaporation, and the model works through the simple accounting procedure for each cell on each day:

$$S_t = S_{t-1} + P_t - AE_t - Q_t - D_t \quad (1)$$

The soil moisture content at the end of the current day (S_t) is calculated as a function of the soil moisture content at the end of the previous day (S_{t-1}), the rainfall (P_t) and the actual evaporation (AE_t). The soil moisture is reduced by the drainage of water from the soil into the groundwater store (D_t), and the direct runoff (Q_t) when the soil is saturated:

$$Q_t = (P_t - AE_t - D_t) - (S_{max} - S_t) \quad (2)$$

where S_{max} is the maximum amount of water that may be held in the soil.

The rainfall input is derived from a database of monthly rainfall for the 1961–1990 period, provided by the Climatic Research Unit, Norwich, UK. The daily rainfall data (P_t) are generated by dividing the monthly totals by the long-term average number of raindays for that month. The actual evaporation (AE_t) is estimated as a function of the potential evaporation (PE_t), whereby the actual rate is considered to be equal to the potential rate until field capacity is reached, whereafter it declines linearly to zero.

Besides the climatological inputs, physiological data are required that describe the moisture potential of the soils and the evaporation and root properties of the vegetation. To this end, the FAO dominant soil textures were extracted for each cell using Geographical Information System (GIS) techniques. The soil texture is used to describe the ability of each soil type to hold water (Arnell & Reynard, 1996; Vorosmarty *et al.*, 1989; Saxton *et al.*, 1986). The type of vegetation is important as it determines the root depth, the rate of interception of the rainfall and the evapotranspiration rates. The extent of the forest cover is estimated from the global classification of ecosystems by Olson, available at the required 0.5° resolution (Olson, 1992). For each of the ecosystem types a proportion of forest cover is assumed, distinguishing between no forest, 25%, 50%, 75% and 100% coverage. It is known that this estimation is crude and current work is examining ways of improving the quality of land-cover input data as well as the representation of the forest processes in the model. The current forest coverage will necessarily underestimate the real forest cover as it only takes account of the large forested zones, not the smaller areas of trees that undoubtedly also have an influence on the local water balance. The runoff will, as a result, tend to be overestimated. The

percentage coverage of permanent wetland is estimated from digitized maps of the region.

With this set of climatological driving variables and physiological operating data, the model is run independently for each cell in the region for the 30-year period between 1961 and 1990 to derive the baseline average annual runoff map shown in Fig. 1.

A time series of monthly runoff for this 30 year period is simulated for each cell, and from these data the coefficient of variation (CV) of monthly and annual runoff may be calculated. The grid of the CV of annual runoff for the 1961–1990 period is shown in Fig. 2. The values range from 25 to 50% over the majority of southern Africa, although they are higher along the south coast, which is subject to the somewhat erratic frontal activity during the southern hemisphere winter. This creates a time series with a few years of exceptionally high annual rainfall compared to the long-term mean.

VALIDATION OF THE RUNOFF GRID

The parameters of the hydrological model are not calibrated against measured flows, but rather derived from climatological data and physiological data, such as soil textures. Because this method is used for parameter estimation, two steps have been included in the validation process. A sensitivity test of the modelled runoff to changes in individual parameter values is included as well as the comparison of the modelled runoff values against observed catchment runoff data.

For the sensitivity test, two cells were selected and the model run several times, altering one of four parameters each time to assess the impact of the changes on the average annual runoff. The selected cells are in western Angola and eastern South Africa. The sensitivity analysis involved four parameters: the rainfall interception rate for forest as opposed to grass, the percentage cover of forest, the percentage cover of wetland and the "*b*" parameter. This *b* parameter controls the spatial variability of the maximum soil capacity across each cell, with 0.0 representing a constant capacity and 1.0 being a uniform variation. In the probability-distributed model, the spatial variability of the soil moisture capacity (c) is represented by the reflected power distribution:

$$F(c) = 1 - \left[1 - \frac{c}{c_{\max}}\right]^{b} \qquad 0 \le c \le c_{\max}$$

The parameter *b* is not derived from either climatic or physiological data and was set to 0.25 across the region for this simulation, based on the experience of running the model in other regions of the world.

Figures 3 and 4 show the results of the sensitivity test for the two cells. The grid cell in Angola has an average annual runoff of 234 mm when the parameters are set as normal, which represents a *b* value of 0.25, a forest cover of 25%, a permanent wetland cover of 0% and an interception rate of 10% of the rainfall, where the vegetation is forest. The South African cell has the same initial values for the four parameters but a simulated annual average runoff of 105 mm. The parameters were

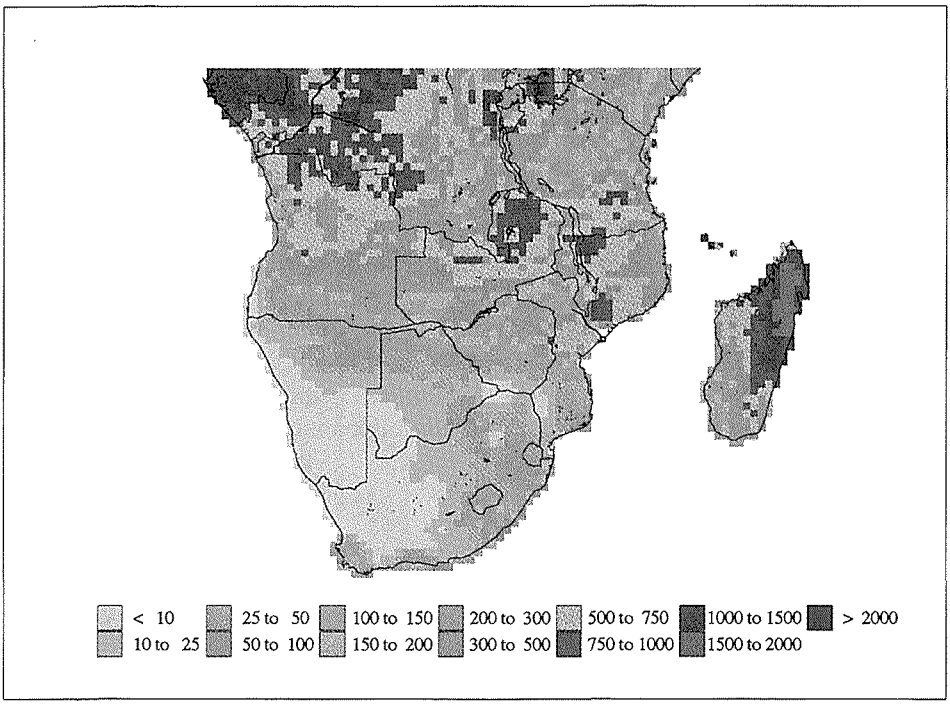

Fig. 1 Average annual runoff (mm) from 1961 to 1990.

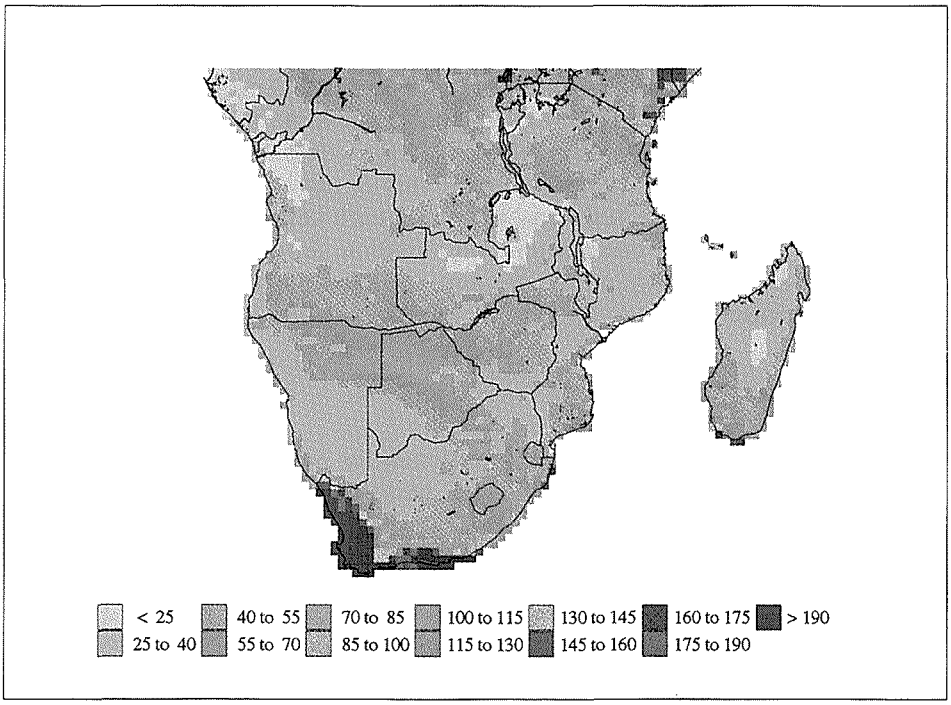

Fig. 2 Coefficient of variation (*CV*) of average annual runoff (%) from 1961 to 1990.

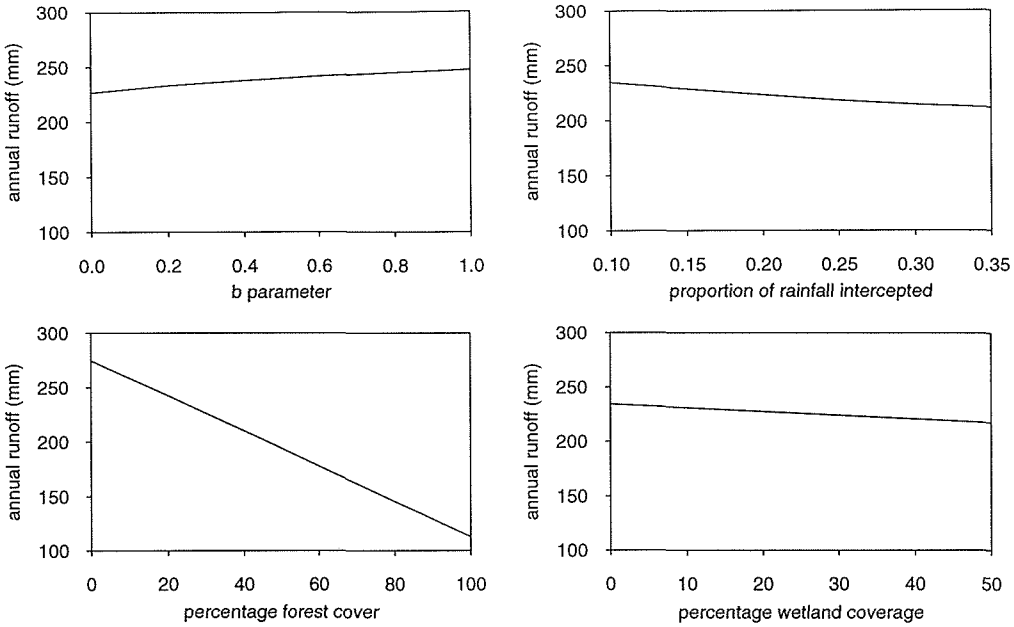

Fig. 3 Results of the sensitivity analysis for a cell in western Angola.

systematically altered, independent of each other, across a sensible range. These ranges being 0.0 to 1.0 for b, 0.10 to 0.35 for the proportion of rainfall intercepted and transpired by forests, 0 to 100% of the cell forested and 0 to 50% of the cell as a permanent wetland.

The results for Angola (Fig. 3) clearly show that runoff is most sensitive to changes in the forest cover, decreasing from 270 mm with no forest to only 110 mm

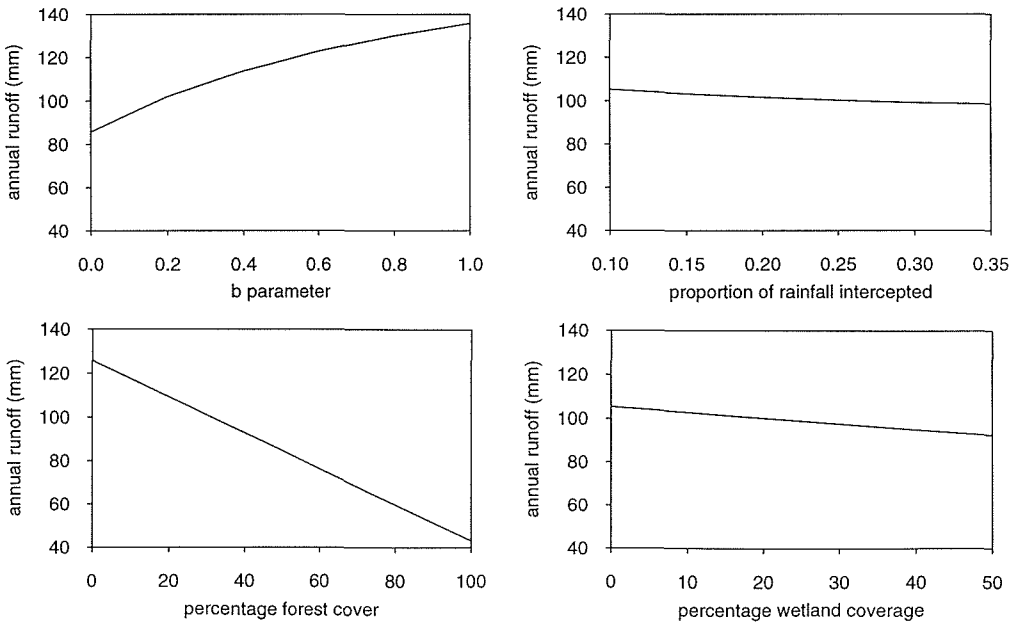

Fig. 4 Results of the sensitivity analysis for a cell in southeastern South Africa.

with 100% forest. The runoff is relatively insensitive to changes in b and the interception rate, and the additional evaporative losses from increasing the area covered by the permanent wetlands is also small.

The response in the South African cell (Fig. 4) is similar to that of the Angolan cell. The runoff is most sensitive to the assumed forest cover, ranging from 125 mm with no forest to only 45 mm with 100% forest. The sensitivity to the changes in the interception rate and the wetland coverage is again small. There is greater sensitivity to changes in b, however. As b increases from 0.0 to 0.4, the runoff increases from 85 mm to 120 mm, although thereafter the rate of increase slows so that a runoff of nearly 140 mm is reached when b reaches a value of 1.0. This change in runoff is, however, still only about half that experienced when the percentage forest cover is changed.

The second stage of the validation of the model is to compare the modelled results with observed data from the southern Africa FRIEND database. Flow records were extracted from the archive for sites with 25 or more years of complete data within the 1961–1990 baseline period. The selection was made from five of the SADC countries: Zambia, Zimbabwe, Namibia, Malawi and Swaziland. These criteria allowed the records from 42 catchments to be used, ranging in size from nearly 50 000 km^2 on the Orange River to only 7 km^2 on a small subcatchment of the Zambezi.

The set of 42 gauged flow records from the archive are representative of their upstream catchments, not the location at which the flows are measured. To compare the gridded data with these catchment data, the weighted average runoff for each catchment was calculated, using GIS techniques, according to the simulated runoff of the underlying 0.5° cells. The results for the 42 catchments are shown in Fig. 5, with the observed runoff from the FRIEND database plotted against the simulated catchment runoff. The one-to-one line is also plotted for reference with the different symbols indicating the six major river basins for which data were used in the analysis. It is apparent that there is an overestimation of runoff by the model, particularly in the high runoff areas, where this may be by as much as a factor of 2. The correlation between the observed and the simulated runoff is above 90%, suggesting that the model may be conceptually quite sound, but there is a bias in the estimates.

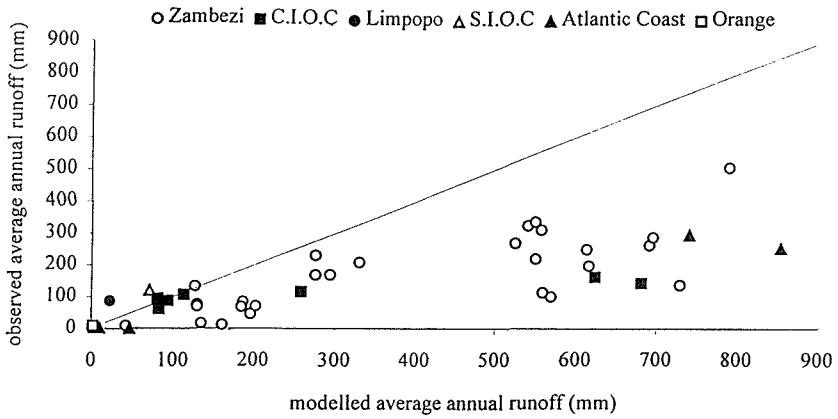

Fig. 5 Observed average annual runoff compared to simulated runoff for 42 catchments in the SADC region.

DISCUSSION

The validation exercise showed that the hydrological model tends to overestimate the observed catchment runoff quite considerably. There could be several reasons for this overestimation. The first explanation arises from the catchment data used in the validation. The modelled runoff estimates the *natural* runoff of that cell, whereas there may be some doubt about whether the flows on the FRIEND database are also truly natural. Artificial influences on river flows will tend to reduce gauged flows and so make it appear that the modelled flows are too high.

Other reasons for a bias stem from the modelling process. The model was originally developed and used in the more temperate, humid zones of northern Europe and its application in a region such as southern Africa presents new problems. The simulated runoff takes no account of the transmission losses, for example, as the water flows downstream, hence the observed flows will be higher than the modelled runoff generated in each cell.

The main driving variable of the model is the rainfall, so this gridded input was checked against a selection of raingauges from Zimbabwe, Namibia and Malawi. The results are shown in Fig. 6, plotting the observed rainfall against the gridded database. The agreement between the two sets of data is good for low rainfall, but the spread is high in those areas with annual rainfall in excess of about 900 mm. There is some evidence of a slight overestimation of the gridded rainfall, although this is not sufficiently large to account for the large bias in the simulated runoff. The second climatological driving variable is the PE. Previous studies have shown that regional estimates of Penman PE appear too low (although precise validation of these data is difficult as there are no other regional datasets for comparison, only maps of open water evaporation). However, with PE too low, particularly during the wet season when actual evaporation can approach the potential rate, runoff will, again, be overestimated. A further problem, allied to this evaporation issue, is the representation of wetlands. A new wetland coverage has recently been developed at the Institute of Hydrology, but this only includes the permanently saturated zones. Seasonal wetlands are a major influence on the water balance of the SADC region, with open water or saturated soils only during the wet season. As this season

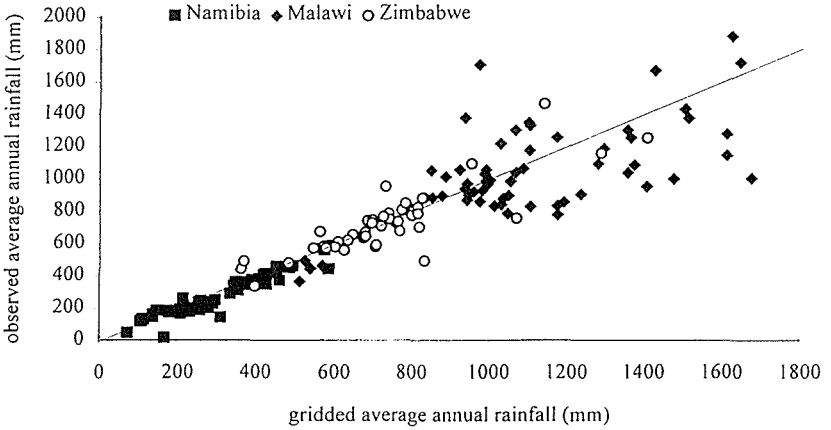

Fig. 6 Annual rainfall compared to recorded average annual rainfall in three of the SADC countries.

accounts for the vast majority of the runoff, some significant losses are being omitted, and runoff will be overestimated. The assumed forest coverage is an important parameter within the model. There is evidence, discussed earlier, that suggests the current underestimation of the true extent of the tree and forest areas can cause a significant overestimation of the modelled runoff.

Despite the apparent overestimation of runoff it is believed that the model is conceptually sound as has been shown in catchment specific studies, when the model has been calibrated and validated before the simulation run (Arnell & Reynard, 1993; 1996). In addition, the geographical distribution of annual runoff (Fig. 1) stands up to visual scrutiny, with the known areas of high and low runoff being reproduced well.

Acknowledgements The authors wish to acknowledge the contribution of the WWF International in funding much of this work. The data provision by the Climatic Research Unit and southern Africa FRIEND is also acknowledged.

REFERENCES

Arnell, N. W. & Reynard, N. S. (1993) *Impact of Climate Change on River Flow Regimes in the United Kingdom.* Institute of Hydrology Report for the UK Department of the Environment.

Arnell, N. W. & Reynard, N. S. (1996) The effects of climate change due to global warming on river flows in Great Britain. *J. Hydrol.* **183**, 397–424.

Hulme, M. (1996) *Climate Change and Southern Africa: an Exploration of some Potential Impacts and Implications in the SADC Region.* Report for WWF International, Climatic Research Unit, Norwich, UK.

Moore, R. J. (1985) The probability distributed principle and runoff production at point and basin scales. *Hydrol. Sci. J.* **30**(2), 263–297.

Olson, J. (1992) Global changes and resource management. *ASPRS/ACSM/RY92 Technical Papers 1*, 32–42.

Saxton, K. E., Rawls, W. J., Romberger, J. S. & Papendick, R. I. (1986) Estimating generalized soil-water characteristics from texture. *Soil Sci. Soc. Am. J.* **50,** 1031–1036.

Vorosmarty, C. J., Moore, B., Grace, A. L., Gildea, M. P., Melillo, J. M., Peterson, B. J., Rastetter, E. B. & Steudler, P. A. (1989) Continental scale models of water balance and fluvial transport: an application to South America. *Global Biogeochem. Cycles* **3**, 241–265.

FRIEND'97 — Regional Hydrology: Concepts and Models for Sustainable Water Resource Management
(Proceedings of the Postojna, Slovenia, Conference, September–October 1997). IAHS Publ. no. 246, 1997.

Estimation of renewable water resources in the European Union

H. G. REES, K. M. CROKER, N. S. REYNARD & A. GUSTARD
Institute of Hydrology, Wallingford, Oxfordshire OX10 8BB, UK

Abstract The over-exploitation of freshwater resources and the associated impact on commerce and the environment is a major pan-European problem. Freshwater is a finite and fragile resource, yet increases in demand by industrial, agricultural, domestic and municipal consumers have induced great stresses in the hydrological system. To prevent the degradation of freshwater resources, it is essential that techniques are developed to accurately estimate their availability across Europe. No consistent method is used to estimate the availability of water or to compare resources between different countries and regions. This paper presents a standard method to estimate the availability of water resources in Europe. The method is applied in a grid based model where the availability of water within each cell is derived from combining observed river flow data with methods for estimating flows at ungauged sites. The benefits of a grid approach is illustrated by comparing water availability with water demand to derive indicators of water stress.

INTRODUCTION

An accurate assessment of the renewable freshwater resource is essential for effective and sustainable management. Estimating the renewable freshwater resource available is, however, difficult due to the temporal and spatial variability of the hydrological regime and the complex effect of human interventions. This paper presents results of a study, commissioned by the Statistical Office of the European Communities (Eurostat), which investigated appropriate methods for estimating the renewable water resource across Europe. The study was also required to illustrate the regional variability in the renewable water resource over the European Union. To meet these objectives, gridded maps of average annual runoff were developed at a 10 km by 10 km resolution for the whole territory. For many of the grid cells, it was possible to derive estimates of the renewable water resource by using the observed gauged daily flow data and digitized catchment boundaries held on the FRIEND European Water Archive. To estimate the average annual runoff for the ungauged portion of the grid (i.e. those areas not covered by the FRIEND dataset) a critical assessment of four different estimation methods was undertaken. Each method used the same base-line climatological dataset provided by the Climate Research Unit (CRU) of the University of East Anglia. The methods considered were: regional characterization; the Budyko freshwater balance method; the Turc-Pike freshwater balance method; and the Probability Distributed Model, a conceptual model developed at the Institute of Hydrology. Grids of average annual runoff were derived from each method. By

comparing the modelled runoff with observed data, it was possible to assess the performance of the methods and ascertain which was most appropriate to apply at the European scale. A composite grid was then developed combining the observed runoff grid with the best of the modelled grids. As well as illustrating the spatial variability of the renewable water resource, the paper will then show how grids can be used to derive indicators of water stress with respect to both agricultural and urban demand.

INPUT DATA

The pan-European datasets used in the derivation of the grids of renewable water resource included:

(a) FRIEND European Water Archive, containing river flow data for over 3500 gauging stations and 2500 digital catchment boundaries;
(b) the CEC Soils Map (CEC, 1985), which provides a consistent classification of the soils in 12 countries of the European Union;
(c) baseline climatological data, developed by the Climate Research Unit (Hulme *et al.*, 1995), which provides a mean monthly climatology for the 1961–1990 period, covering the European Union and beyond, at a resolution of 0.5° latitude by 0.5° longitude. Nine variables are available: minimum, maximum and mean temperature, precipitation, sunshine hours, vapour pressure, wind speed, frost days and rain days. For this study, only the mean temperature and precipitation were used directly, but the sunshine hours, vapour pressure and wind speed were used to calculate the potential evaporation (PE) according to the Penman equation (Penman, 1948). To represent these variables on the 10 km grid, a simple linear interpolation function was used.

GRID DEVELOPMENT FOR GAUGED CATCHMENTS

The grid development described in this paper was based on data from the FRIEND European Water Archive. All catchments on the archive with both a gauged river flow record and a digitized catchment boundary were included in the analysis. The renewable water resource of each gauged catchment is calculated using all available flow data. Once the renewable resource of each gauged catchment has been determined, the 10 km grid is overlain on to a map of digitized catchment boundaries enabling those cells for which gauged data is available to be identified. The renewable resource for each gauged grid cell is then estimated using the same weighted area technique described by Arnell in the 1993 FRIEND report (Gustard, 1993).

GRID DEVELOPMENT FOR UNGAUGED CATCHMENTS

The hydrological regime across Europe shows a high degree of spatial and temporal variability. This makes it difficult to ascribe a single method for estimating runoff at an ungauged site. A key requirement of the project was, however, to develop one

consistent method applicable to the whole of Europe. Four different approaches to estimating runoff for the ungauged grid cells were tested:

(a) The Probability Distributed Model (PDM), a conceptual water balance approach to rainfall-runoff modelling based on a soil moisture accounting procedure (Moore, 1985). The model provides estimates of the monthly runoff (in mm) generated within each 10 km grid cell independently. There is no routing of runoff through the river network, or from one cell to another.

(b) A freshwater balance approach using an empirical formula proposed by Budyko (1961):

$$\text{Runoff} = \text{AAR}.\exp(-\text{PE}/\text{AAR}) \tag{1}$$

where AAR is the average annual rainfall and PE is the potential evaporation.

(c) A second freshwater balance approach first developed by Turc (1954) and modified by Pike (1964) where the actual evaporation (AE) is written as:

$$\text{AE} = \text{AAR}/(1 + (\text{AAR}/\text{PE})^2)^{1/2} \tag{2}$$

and

$$\text{Runoff} = \text{AAR} - \text{AE} \tag{3}$$

(d) A regional characterization approach based on multivariate regression techniques (Gustard *et al.*, 1992) in which the actual evaporation is given by the equation:

$$\text{AE} = r \cdot \text{PE} \tag{4}$$

The value of the conversion factor r increases with rainfall to reflect the proportion of water available as any soil moisture deficit is replenished. When the total annual rainfall reaches a certain threshold, the soil is assumed to be saturated and that the value of r is 1. For the UK, r can be expressed as (Gustard *et al.*, 1992):

$$r = 0.000\,61 \cdot \text{SAAR} + 0.475 \quad \text{for AAR} < 850 \text{ mm} \tag{5a}$$

$$r = 1.0 \quad \text{for AAR} \geq 850 \text{ mm} \tag{5b}$$

By comparison, the equation for the whole of Europe was calculated as:

$$r = 0.000\,13 \cdot \text{SAAR} + 0.489 \quad \text{for AAR} < 3900 \text{ mm} \tag{6a}$$

$$r = 1.0 \quad \text{for AAR} \geq 3900 \text{ mm} \tag{6b}$$

VALIDATION OF RESULTS FOR UNGAUGED CATCHMENTS

In order to compare the performance of the four models a statistical comparison of observed and modelled runoff was undertaken for each gauged grid cell. The relationship between the modelled and observed data was expressed in terms of a bias, given by:

$$\text{bias} = (\text{modelled runoff} / \text{gauged runoff}) \cdot 100\% \tag{7}$$

The observed runoff and modelled runoff were calculated for 1257 gauging stations across Europe and the bias calculated. Overall, the mean bias of the PDM model was

Table 1 Comparison of bias for countries in Europe.

Country	No stations	Mean percentage bias:			
		PDM	Budyko	Turc-Pike	Regression
All	1257	77.94	101.32	85.82	119.44
Belgium	49	105.47	144.22	121.28	168.87
Switzerland	14	99.04	109.56	99.67	122.67
Germany	145	63.52	94.80	78.38	114.98
Denmark	8	58.98	76.60	62.67	91.41
Spain	49	48.82	63.60	52.40	71.15
France	314	76.79	104.18	85.94	122.00
Italy	43	77.86	86.04	74.68	98.96
Ireland	24	96.71	108.89	99.26	122.91
Norway	63	71.74	75.75	67.80	86.50
Netherlands	6	79.08	112.71	93.36	132.98
Sweden	18	61.60	72.14	60.57	84.33
Finland	26	63.31	77.91	63.94	95.01
UK	498	83.94	107.40	92.26	127.53

approximately 78%, which suggested that the model was consistently underestimating the runoff. This compared with a mean bias of 101% using the Budyko equation, 86% using the Turc-Pike equation and 119% using the regression based approach. The mean bias for each country is given in Table 1.

The performance of each model was also considered using regression analysis to obtain statistics for the factorial standard error of each model. The relationship between the modelled runoff (RO_m) and the observed runoff (RO_o) is considered to be in the form:

$$RO_m = a \cdot RO_o^{\,b} \tag{8}$$

Therefore, linear regression analysis is undertaken on the equation in the form:

$$\log RO_m = \log a + b.\ \log RO_o \tag{9}$$

where $\log a$ is the intercept and b is the parameter estimate.

If the model (PDM, Budyko, etc.) had predicted the flows exactly, the parameters a and b, from the above regression equation, would have equalled 1. In the absence of ideal (predicted) data, these parameter estimates should be as close to one as possible, while maximizing the fit of the model, represented by the R^2 (percentage of variance explained) value, and reducing the factorial standard error. From Table 2, it can be seen that, for all models, the variance and factorial standard errors are very similar. Using this information with that for the mean bias, the Budyko method would seem the most effective method for estimating the runoff in ungauged catchments.

As Table 1 shows, the four models considered all demonstrate variations in the accuracy with which the annual runoff can be predicted across Europe and each model performs well in some regions, but not so well in others. Numerous other studies have been undertaken to identify the most appropriate method for deriving runoff from rainfall and evaporation across Europe. Arnell *et al.* (1990), compared model sensitivity to changes in rainfall and evaporation and concluded that the Turc-Pike model approximates runoff reasonably well (Budyko was not considered in Arnell's study). In Spain, Estrela *et al.* (1995), looked at the relative performance of

Table 2 Regression analysis.

Regression statistics	PDM	Budyko	Turc-Pike	Regression
Parameter estimate (*b*)	0.67	0.51	0.58	0.49
Intercept (log *a*)	0.73	1.26	1.03	1.38
a	5.38	18.16	10.82	23.75
R^2	51.63	51.97	51.72	53.80
Factorial standard error	1.48	1.35	1.40	1.32

the Budyko and Turc-Pike models and found Budyko to be more consistent with observed data, although Turc-Pike was better for low evaporation conditions. These findings would suggest that the use of a simple empirical model over Europe can indeed be justified.

COMPOSITE MAP OF RENEWABLE WATER RESOURCE

Figure 1 shows a composite map of renewable water resource, expressed in terms of the average annual runoff. The gridded map was generated from flow records, in gauged areas, and by applying the Budyko equation in the ungauged areas and includes estimates of runoff for all major drainage basins affecting the European Union.

WATER STRESS INDICATORS

In developing a grid based model of the renewable water resource, water demand information can be readily superimposed to derive grids (or maps) of water stress. Such grids were developed for the two most significant types of water demand: agriculture and urban.

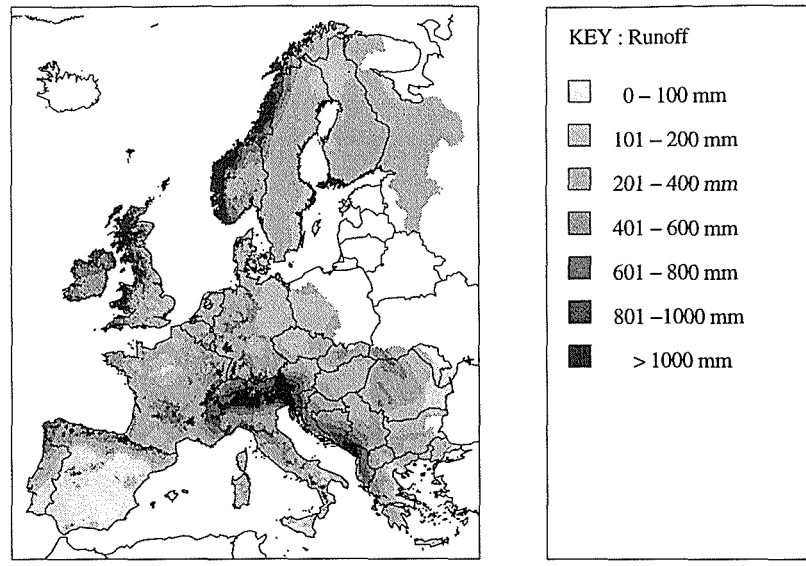

Fig. 1 Composite map of average annual runoff.

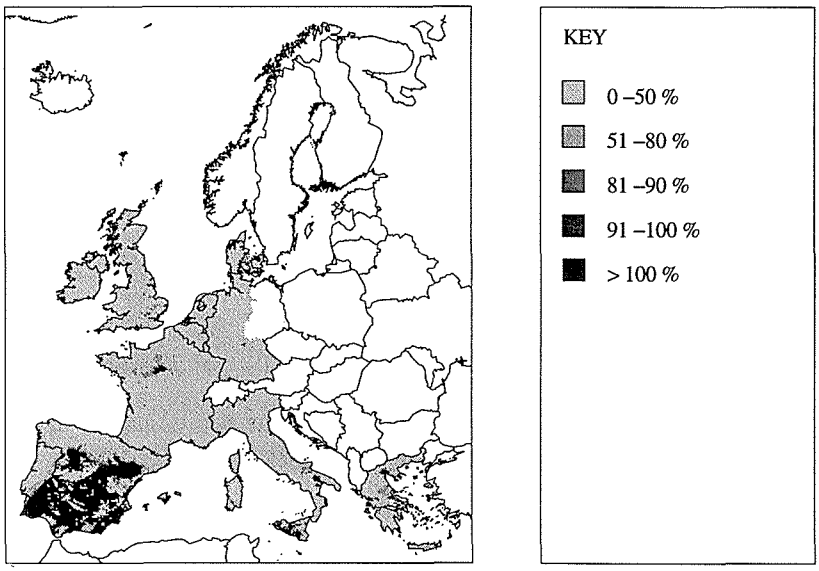

Fig. 2 Irrigation demand as a proportion of average annual runoff.

Agricultural water demand

According to the World Resources Institute (WRI, 1990), agricultural (irrigation) demand across Europe amounts to approximately 110 km^3 $year^{-1}$. In several areas, particularly in southern Europe, the demand for water is fast approaching the limits of the resource. Grids of agricultural demand were developed using the soil use information available within the CEC Soils Map. For each relevant soil use type, typical figures for the crop water requirement were assumed according to FAO guidelines (FAO, 1977). With irrigation assumed to be confined to the summer months from April to September, the net irrigation requirement was calculated by subtracting crop water requirement, from estimates of summer runoff derived from the PDM. It was further assumed that only 20% of each irrigable grid cell is irrigated using the sprinkler irrigation method at 75% efficiency. The resulting grid, representing irrigation demand as a proportion of the average annual runoff, is shown in Fig. 2. Despite the assumptions made, the grid reaffirms the existence of problems of water stress brought about by agriculture in certain areas of southern Europe.

Urban water demand

For Europe as a whole, urban water demand, which includes industrial and domestic use, accounts for over two thirds (67%) of freshwater abstractions (WRI, 1990). To derive grids of urban water stress, the Eurostat *Degree of Urbanization* data coverage was used. This presents three classes of urban density: thinly (< 100 heads of population per km^2); intermediate (100–500 heads of population per km^2); and (> 500 heads of population per km^2). A daily per capita consumption rate was assumed for each urban class on the basis of data presented in the Dobris Assessment (EEA, 1995). The resulting urban water demand grid can be directly compared with

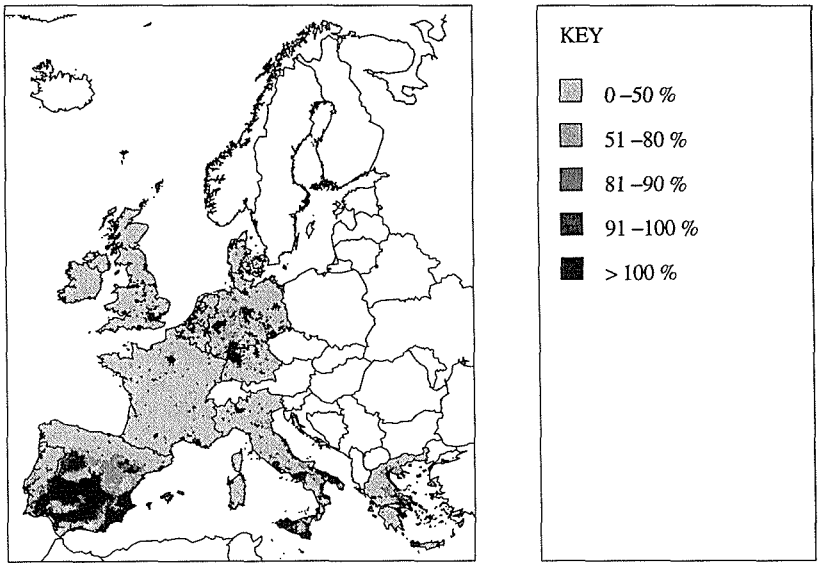

Fig. 3 Summer urban water demand as a proportion of summer runoff.

the grids of renewable water resource. Figure 3 compares an increased summer demand (120% of average demand) with summer runoff. It clearly shows there is an important need for the effective management of freshwater resources and for the provision of artificial storage or transfer facilities, especially in southern Europe and the densely populated regions of the north.

CONCLUSIONS

With the ever growing demands for freshwater, it is vitally important that reliable methods are used to assess the availability of the resource. However, few improvements can be made without better and more reliable data. The four methods considered all used the baseline climatology for Europe supplied by the Climate Research Unit (CRU). There is a recognized tendency for the CRU data to underestimate precipitation, especially in regions affected by snowmelt, while the potential evaporation, calculated according to the Penman equation, is generally over-estimated. Despite offering the best data currently available at a pan-European scale, there is general agreement that, with better station coverage and harmonized definitions of the variables, significant improvements could be made to the CRU dataset and hence estimation of the renewable water resource.

All methods demonstrated variations in the accuracy of prediction, with each performing well in some countries and not so well in others. This problem occurs as a result of using a single method for the whole of Europe, ignoring any regional discrepancies in climate and flow regime. It should be noted that the Budyko method, which was developed to represent just the annual freshwater balance only, is considered unsuitable for estimating the renewable water resource at any finer temporal resolution. With its ability to run at a daily or monthly time step, the PDM model demonstrates a versatility which is ideal for deriving estimates of the resource

at varying time intervals. Previous studies (Arnell & Reynard, 1996) have shown the PDM to be conceptually sound and, therefore, further work in developing the model on a pan-European basis should be considered.

A major advantage of a grid based approach is the ability to combine and compare, on a cell by cell basis, the renewable water resource with other spatially referenced data. The lack of detailed data on the extent of human activity posed considerable difficulties to this particular exercise with the demand estimates derived on the basis of some very broad assumptions. Despite these problems, the project succeeded to illustrate those area prone to water stress.

While good progress has been made in the course of the study, there still remains considerable scope for further work. In considering the long-term renewable water resource, no attempt has been made within the project to account for the inter-annual availability of the resource or the complex, and ever changing, influences of man. To protect freshwater resources from unsustainable exploitation, it is important that such issues are considered. With freshwater becoming an increasingly precious resource, methods of estimating the renewable water resource must continue to develop and improve.

Acknowledgements The research presented in this paper was undertaken as part of the Eurostat SUP.COM 95 project, "Estimation of Renewable Water Resources in the European Union", funded by the European Commission through the Fourth Framework Programme. The authors would like to thank both Eurostat, for allowing the results of the project to be published in this paper, and also the Climate Research Unit of the University of East Anglia, who supplied the baseline climatological data. Various other spatial data sets were kindly provided by the Eurostat GISCO service.

REFERENCES

Arnell, N. W, Brown, R. P. C. & Reynard, N. S. (1990) Impact of climatic variability and change on river flow regimes in the UK. *Inst. Hydrol., Wallingford, Report no. 107.*

Arnell, N. W. & Reynard, N. S. (1996) The effects of climate change due to global warming on river flows in Great Britain. *J. Hydrol.* **183**, 397–424.

Budyko, M. I. & Zubenok, L. I. (1961) The determination of evaporation from the land surface. *Izv. Akad, Nauk SSSR, Ser. Geogr. no. 6*, 3–17.

CEC (1985) *Soil Map of the European Communities. 1:1 000 000.* CEC-DGVI., Luxembourg.

Estrela, T., Ferrer, M. & Ardiles, L. (1995) Estimation of precipitation–runoff regional laws and runoff maps in Spain using a geographical information system. *Proc. FRIEND–AMHY Conference* (Thessalonika).

European Environment Agency (1995) *Europe's Environment—The Dobris Assessment* (ed. by D. Stanners & P. Bourdeau)

FAO (1977) Guide for Predicting Crop Water Requirements. *FAO Irrigation and Drainage Pap. no. 24C*, Revised 1977.

Gustard, A., Bullock. A. & Dixon. J. M. (1992) Low flow estimation in the United Kingdom. *Inst. Hydrol., Wallingford, Report no. 108.*

Gustard, A. (ed.) (1993) *Flow Regimes from International Experimental and Network Data (FRIEND).* Vol. I: *Hydrological Studies.* Institute of Hydrology, Wallingford, UK.

Hulme, M., Conway, D., Jones, P. D., Jiang, T., Barrow, E. & Turney, C. (1995) Construction of a 1961–90 European climatology for climate change modelling and impact implications. *Int. J. Climatol.* **15**, 1333–1363.

Moore, R. J. (1985) The probability-distributed principle and runoff production at point and basin scales. *Hydrol. Sci. J.* **30**(2), 263–297.

Penman, H. L. (1948) Evaporation in nature. *Rep. Progr. Phys.* **XI**, 366–388.

Pike, J. G. (1964) Estimation of annual run-off from meteorological data in tropical climate. *J. Hydrol.* **2**(2), 116–123.

Turc, L. (1954) Le bilan d'eau des sols, relation entre les précipitations, l'évaporation, et l'écoulement. *Ann. Agron.* **5**, 491–596.

World Resources Institute (WRI) (1990) *World Resources 1990–91.*

FRIEND'97 — Regional Hydrology: Concepts and Models for Sustainable Water Resource Management
(Proceedings of the Postojna, Slovenia, Conference, September–October 1997). IAHS Publ. no. 246, 1997.

Derivation of flow discharges from runoff maps and digital terrain models in Spain

TEODORO ESTRELA, LUIS QUINTAS & JAVIER ALVAREZ
Centro de Estudios Hidrográficos del CEDEX, Paseo Bajo de la Virgen del Puerto 3, Madrid 28005, Spain

Abstract A methodology is presented that has been developed by the Centro de Estudios Hidrográficos of CEDEX, which automatically derives the river network yield maps from runoff maps and a digital terrain model in an operational way, without it being necessary to plot the watersheds of the basins. The proposed methodology has been applied throughout the Spanish mainland.

INTRODUCTION

Knowledge of the river network yields is essentially based upon the data taken at the gauging stations, which takes into account the effect of anthropogenic actions upon the discharges. However, there is often a wish to know what the natural regime of a river is. This is the case, for example, when models are used to simulate the operation of water resource systems.

The generation of yields in a natural regime can be carried out by naturalizing the discharges, if data are available concerning water consumption, reservoir management, irrigation and urban returns, etc. This procedure is not always immediate, because most of the data are unknown. The solution involves using hydrological models that generate runoff maps (yields per unit area) on the basis of meteorological information and the characteristics of the basins.

If maps are available which reflect the spatial variability of the runoff in a specific territory, it is easy to obtain the yields for any point on the river network, by plotting the watershed of the catchment area at this point and integrating the basin runoff. This procedure can only be used if the basin watersheds are known.

When the aim is to find the yields for most of the points on a river network, a large number of digitized basins have to be available. If one wished to automate this procedure, not only would information concerning the river network topology have to be included, but the watersheds would also have to be digitized. However, the existence of digital terrain models (DTMs) is becoming increasingly common. A DTM is understood as being a raster model, in which each of the cells into which the terrain is discretized is associated with the average value for the natural terrain elevation. EUROSTAT (1996) has used a DTM to derive yield maps for the entire European Union supported on the watersheds of the large river basins.

This paper presents a procedure that has been developed to automatically derive river network yield maps in an operational way, from runoff maps and the DTM, without it being necessary to use the watersheds of the basins.

THE DIGITAL TERRAIN MODEL

The source of the digital terrain model used are the topographical maps at a scale of

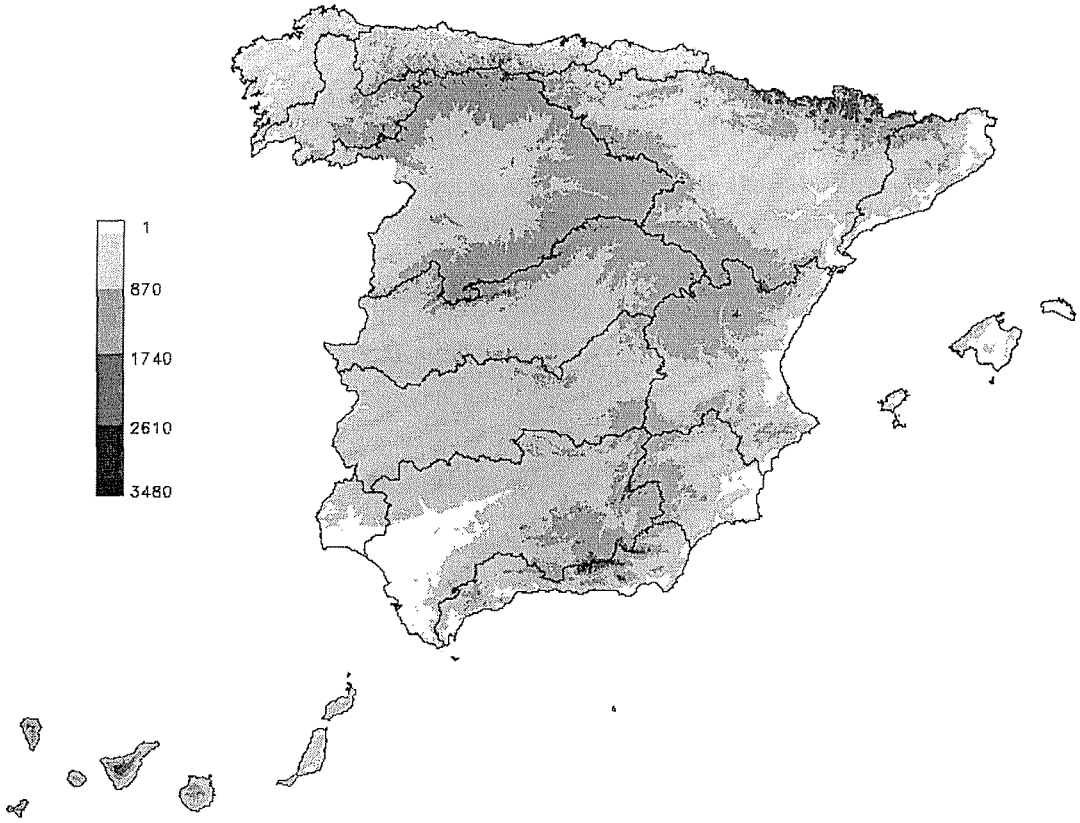

Fig. 1 Digital terrain model of the Spanish mainland.

1:50 000, from the Spanish Army Geographical Service. It is a result of digitizing the map contours, these being 20 m apart, and generating the raster model by using the interpolation commands of the Geographic Information System GRASS, developed by the US Army Corps of Engineers (1991). Cells 80 m × 80 m (Fig. 1) are the spatial resolution for the raster model on these maps, and these dimensions are considered to be sufficient for the purposes of this work.

METHODOLOGY FOR DERIVING DRAINING NETWORK MAPS AND ACCUMULATED DRAINING SURFACES

Using the DTM and runoff maps to calculate river network yields, is based upon an approach similar to the one generally used to determine draining network.

The draining networks of a territory, also called cell accumulation map, can be obtained automatically if a DTM is available. The procedure is based upon (Meijerink *et al.*, 1994; Burrough, 1986): (a) a flow direction map is determined by evaluating the maximum slope in each cell, (b) the number of cells which discharge into a specific one are determined, by analysing the draining courses from the flow direction maps, and (c) all the cells with a value greater than a specific threshold will

form part of that draining network. This threshold determines the extent to which the network is ramified.

The automatic derivation of draining networks is usually faced with the problem of having to debug the geographical data. These problems generally crop up in:

(a) *Flat zones*. Decision problems arise with regard to the algorithm to be used to determine the flow directions (Quinn *et al.*, 1993).
(b) *Sinks and endhoreic zones*. Procedures exist for defining these and considering them as such.
(c) *Zones with steep topographical gradients*. The interpolation needed to obtain the DTM raster and the cell size, require a smoothing of the real topography which, at specific points such as a river gorge, can give rise to errors in the flow directions calculated.
(d) *Zones with badly compiled topographical data*. By way of example, those which correspond to the presence of a water sheet (estuaries, reservoirs etc.), where the topographical plans usually give the height of the water sheet as the natural land height, and this causes the algorithm to get lost in search of the flow directions.

These problems have been detected in several zones in Spain, when draining networks have been automatically generated from the original 80 m × 80 m DTM. Other problems of an operational nature have also cropped up, concerning the extremely time-consuming process involved in obtaining the draining network for the whole of Spain, even with extremely powerful data-processing equipment. This would not be a serious problem if the calculation had only to be made once, but it should be borne in mind that the purpose of this work is the continuous simulation in time of river network yield maps.

In the light of the above problems, the original DTM has been used to obtain DTMs with different spatial resolutions, with a view to studying which of these produces the best draining network. The resolutions selected are 400 m × 400 m, 1000 m × 1000 m, 2000 m × 2000 m and 10 000 m × 10 000 m. The value of the terrain elevation in the cells of each one of these new DTMs is a result of averaging the original DTM for the new cell dimensions, a task which is carried out easily by using the SIG GRASS commands.

If the cell accumulation map is multiplied by a constant equal to the surface area of the cells, a new map is obtained in which each cell will have the surface of its catchment area associated.

The GRASS *watershed* command has been used to generate the accumulated draining surface map in a zone on the Spanish mainland, the inland basins of Catalonia, for each one of the above-mentioned DTMs. This zone lies in the northeast of the Iberian Peninsula, and was selected as an experimental zone, because it contains high mountains and coastal areas in a small strip of land.

With a view to analysing the reliability of the maps obtained and for comparison purposes, the digitized hydrographic network maps at a scale of 1:50 000 developed by the Spanish Army Geographical Service were used, because this mapping is the same as was used to derive the DTM. Figure 2, shows some of the comparisons made. It can be deduced from the analysis carried out, that the best results are obtained from the DTM with a 1000 m × 1000 m resolution. Although this analysis is not exhaustive, and no conclusions of a general nature have been reached, one thing which is revealed is that the optimum solution for the intended purpose, is not

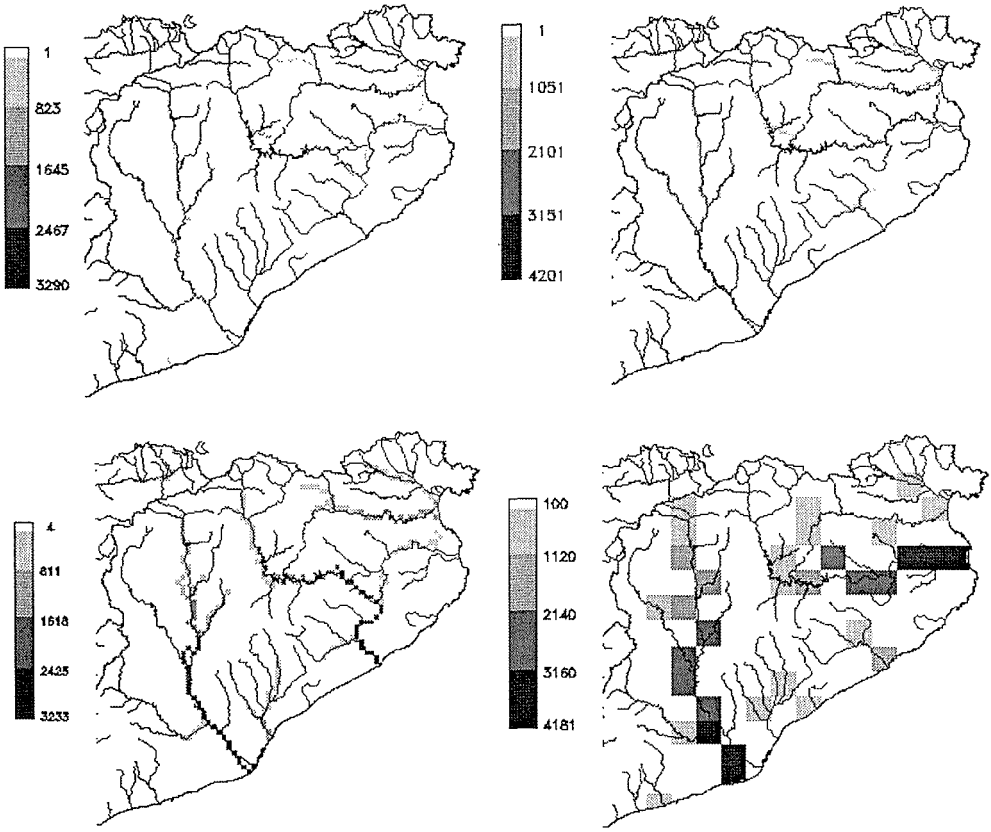

Fig. 2 Comparisons between automatically derived drainage network and the digitized hydrographic network for different DTM spatial resolutions (400 × 400, 1000 × 1000, 2000 × 2000 and 10 000 × 10 000).

the most detailed one. A cell size of 1000 m × 1000 m, also has the following advantages:

(a) It enables the user to deal with the whole Spanish mainland without this being excessively time-consuming.
(b) It is a reasonably standard resolution for many distributed hydrological models.
(c) It gives the data a certain continuity, which would be lost if the cell-sizes were greater.

The DMT with a cell-size of 1000 m × 1000 m, was then used to calculate the accumulated draining surfaces for the entire Spanish mainland. The map thus obtained was then compared with the digitized rivers map and with the surface areas of its basins. In general, the results were acceptable, in spite of the fact that certain problems had not been detected in the example used to test the validity of the method. One such problem concerned how the draining networks obtained automatically for the large reservoirs, differed from the real situation. This can be explained by the deficiencies inherent to the DTMs themselves, because they consider the reservoir water sheet to be the actual land elevation (Fig. 3).

A theoretical solution to these problems is difficult, because in most cases they are associated with the validity of the DTM. The practical solution taken, was to

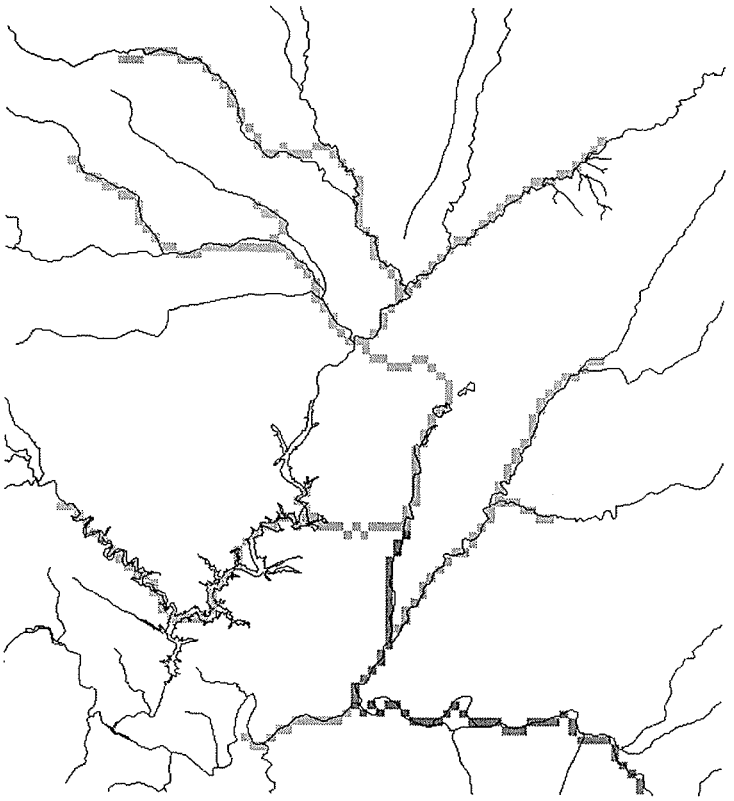

Fig. 3 Example of the problem concerning the reservoirs. Because of incorrect topographical data, the algorithm searches a wrong drainage path in spite of the real one.

review all the problems that arose and make a manual modification to the 1000 m × 1000 m DTM until they disappeared. Modifications had to be made to approximately 60 small zones, each covering a surface area of about 10 km^2. The real values of the natural land elevation, many of which were not known, were not included, fictitious ones being used that allowed for the generation of the real draining networks. The only aim of the DTM which resulted from this purification, is to solve that particular problem. It has now been shown that there are no significant errors in determining the draining networks of the water courses whose catchment area is greater than 50 km^2.

DERIVATION OF RIVER NETWORK YIELD MAPS

Raster runoff maps are required for generating river network yield maps. As part of UNESCO's FRIEND–AMHY project, Estrela *et al.* (1995) derived average annual runoff maps for Spain, assuming that a territory's runoff of internal origin is equal to the difference between the rainfall and the evapotranspiration. The precipitation in each cell was obtained by interpolating the average annual values recorded at the meteorological stations, while the real evapotranspiration was estimated by applying

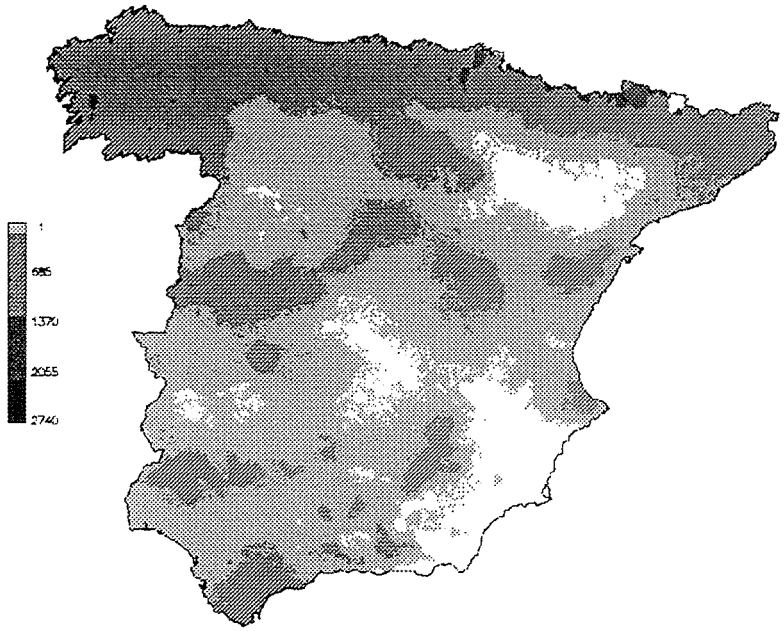

Fig. 4 Average annual runoff map for the Spanish mainland.

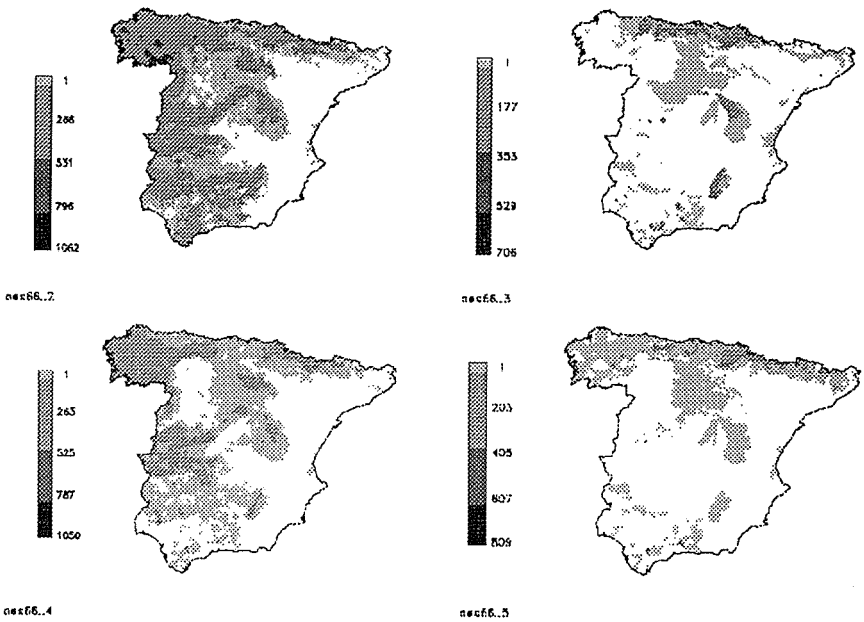

Fig. 5 Runoff maps for different months on the Spanish mainland.

Budyko's experimental law to each cell, this having been compared beforehand in the experimental Spanish basins of the FRIEND–AMHY database (Quintas *et al.*, 1995). According to that law, the real evapotranspiration is a function of the rainfall and the potential evapotranspiration. Finally, a runoff map (Figs 4 and 5) was obtained as the

difference between the rainfall maps and the evapotranspiration maps.

Ruiz *et al.* (1994) and Estrela & Quintas (1996a) developed a continuous distributed simulation runoff model which they included in the Rainfall Modelling Integrated System—Runoff, SIMPA (Estrela & Quintas, 1996b) of the Centro de Estudios Hidrográficos of CEDEX, the aim of which is to simulate on a monthly scale the different processes that constitute the hydrological cycle in a natural regime. The hydrological processes under consideration are: rainfall, evapotranspiration, infiltration, soil water storage, surface runoff, aquifer recharge, aquifer water storage, groundwater runoff and total runoff. Therefore, it generates raster runoff maps for each one of the time intervals considered.

The main purpose of this article is to develop a tool which enables the user to visualize the yields in a river network, from runoff maps like those mentioned above. In order to achieve this, a module has been developed and integrated into SIMPA for this purpose.

If the accumulated runoff map, where the value associated to each cell is the sum of the runoffs generated in cells which are inside of its catchment area, is multiplied by a constant equal to the surface of a cell, the river network yield map is obtained.

With a view to conveniently displaying the yield maps in the river network, a series of different files were defined that reclassified the yields into ranges of values, and these were associated with different colour codes. It was thus possible, for example, to display those cells which received a yield greater than a given threshold

Fig. 6 River network yield map for the Spanish mainland with threshold of 50 Hm^3 $year^{-1}$.

(Fig. 6). This would be an objective procedure for defining draining networks, on the basis of the discharges that flow through them. In Fig. 7 is shown an example of the yields in April 1970, for a Mediterranean basin to the east of the Iberian Peninsula, the Júcar basin.

DERIVATION FROM OTHER MAPS

By applying methodologies similar to those described, other types of maps can be obtained in a similar way to those for the draining network, accumulated surface draining and river network yield maps. One such map, is the map of areal values for any hydrometeorological variable. A map can be obtained, which provides for each cell, the areal value of the rainfall for the basin which drains into that particular cell. The rainfall map and a digital terrain model are needed to achieve this. The procedure consists of obtaining two maps: (a) the accumulated draining surface map and (b) the accumulated rainfall in the cells flowing into a particular cell. The quotient between the two maps, (b)/(a), directly gives the areal rainfall for the basin which flows into each cell.

Figure 8, shows the map of areal values for the average annual rainfall on the Spanish mainland. Amongst other things, this map has the following uses: (a) it directly provides the areal value of the rainfall in the basin which flows into any cell,

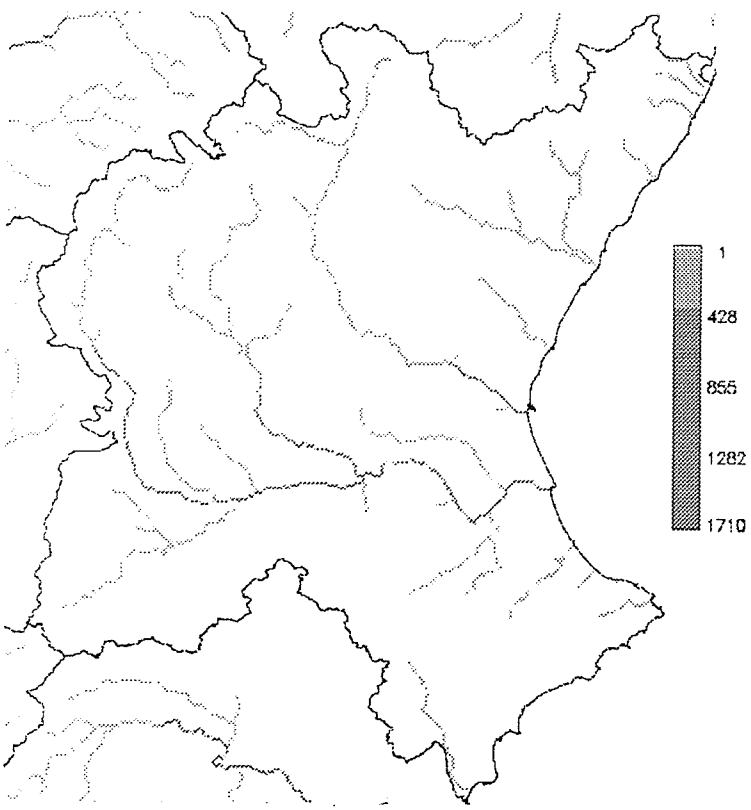

Fig. 7 Yields for the rivers in the Júcar basin in April 1970.

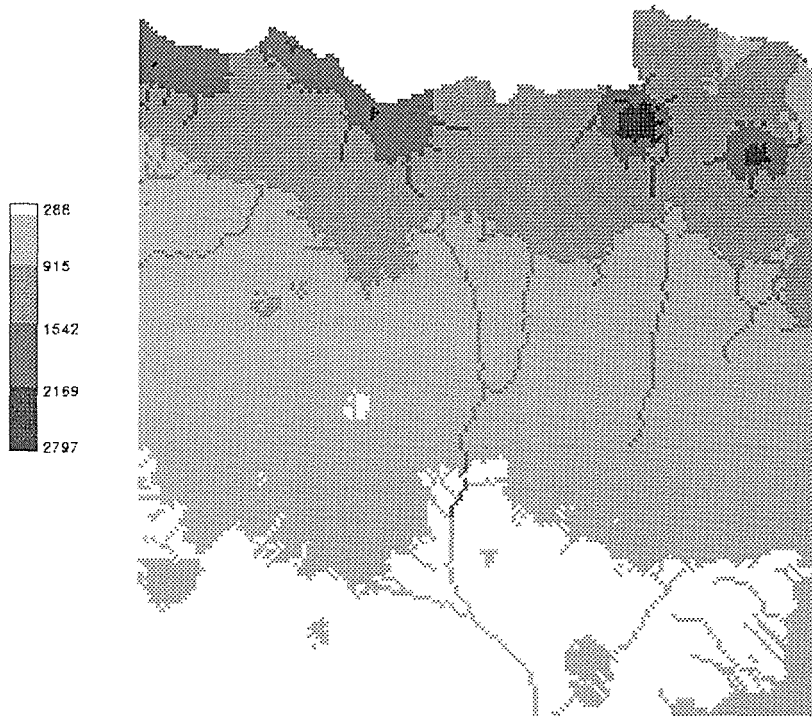

Fig. 8 Example of average annual areal rainfall in the basin draining into a particular point.

and (b) it shows the influence the rain which has fallen at far flung points, has upon the discharge point. This information will be useful for the design of network, because it shows, for example, the incidence of the data recorded at stations in the mountainous zones, upon the areal value.

CONCLUSIONS

A methodology has been presented, which enables the user to automatically and operationally derive river network yield maps from runoff maps and digital terrain models (DTMs), based upon an approach similar to the one which is generally used to determine draining networks. The main target was to obtain these yield maps directly at any point of the Spanish territory avoiding the digitalization of the watersheds. This aim was reached optimizing the size of the DTM cells. A spatial resolution of 1000 m $\times$ 1000 m was found to be the best to obtain draining maps, though it was necessary to debug the terrain data of a few sets of cells. This procedure assures no significant errors in the determination of water courses whose catchment area is greater than 50 km^2. This methodology can also be applied to derive the areal value of any hydrometeorological variable for the basin which drains into a certain cell.

REFERENCES

Burrough, P. A. (1986) *Principles of Geographical Information Systems for Land Resource Assessment*. Clarendon Press, Oxford, UK.

Estrela, T. & Quintas, L. (1996a) A distributed hydrological model for water resources assessment in large basins. In: *Proceedings of 1st IWRA International Conference on Rivertech 96* (Chicago, USA, September 1996), vol. 2, 861–868.

Estrela, T. & Quintas, L. (1996b) El Sistema Integrado de Modelización Precipitación—Aportación SIMPA. *Revista de Ingeniería Civil. no. 104, CEDEX, Madrid*, 43–53. December 1996.

Estrela, T., Ferrer, M. & Ardiles, L. (1995) Estimation of precipitation–runoff regional laws and runoff maps using a GIS. Presented at AMHY FRIEND meeting (Thessaloniki, September 1995), Theme III.

EUROSTAT (1996) Estimation of renewable water resources in the European Union. Draft final report. Unpublished. Edited by Institute of Hydrology in association with CEDEX, INAG and WRc.

Meijerink, A. M. L., de Brouwer, H. A. M., Mannaerts, C. M. & Valenzuela, C. R. (1994) *Introduction to the Use of Geographic Information Systems for Practical Hydrology*. UNESCO, IHP-IV M2.3. ITC, Publ. no. 23, The Netherlands.

Quinn, P., Beven, K., Chevallier, P. & Planchon, O. (1993) The prediction of hillslope flow paths for distributed hydrological modelling using digital terrain models. In: *Terrain Analysis and Distributed Modelling in Hydrology* (ed. by K. J. Beven & I. D. Moore). Wiley.

Quintas, L., Ardiles, L. & Ferrer, M. (1995) Analysis of the Spanish data in the FRIEND AMHY database. Presented at AMHY FRIEND meeting (Thessaloniki, September 1995).

Ruiz, J. M., Estrela, T. & Quintas, L. (1994) Modelización hidrológica distribuida en el proyecto Guadiana. El modelo SIMPA. Curso sobre Utilización de los Sistemas de Información Geográfica en Hidrología. CEDEX, Madrid, España, Noviembre 1994.

US Army Corps of Engineers (1991) *Manual for the Geographical Resources Analysis Support System GRASS*. Version 4.0. CRREL ADP Report no. 87/22, July 1991.

3 The Spatial and Temporal Variability of Hydrological Regimes: *Regime Variability*

FRIEND'97 — Regional Hydrology: Concepts and Models for Sustainable Water Resource Management
(Proceedings of the Postojna, Slovenia, Conference, September–October 1997). IAHS Publ. no. 246, 1997.

Quantification of catchment discharge sensitivity to climate variability

B. VAN DER WATEREN-DE HOOG & M. R. HENDRIKS
The Netherlands Centre for Geo-ecological Research (ICG), Department of Physical Geography, Utrecht University, PO Box 80115, 3508 TC Utrecht, The Netherlands

Abstract A simple annual storage model has been developed for regional assessment of catchment discharge sensitivity to climate variability. In the model presently occurring maximum reservoir storage in catchments (s_{pm}) is linked to catchment storage capacities (s_c) and climatic input. The fraction s_{pm}/s_c as determined by the model defines present catchment sensitivity to climate variability. Using climate scenarios as determined by global circulation models (GCMs) the model can be extended to include future catchment sensitivity. Also, storage capacities can be determined for catchments where no long hydrological records are available (regionalization of the storage capacity).

INTRODUCTION

Regional assessment of catchment discharge sensitivity to expected climate variability (IPCC, 1996) is of great interest for present and future water resources management. There is a need to identify where large impacts on discharge within a region are to be expected and also to identify the variables that strongly influence the magnitude of the impact. Two important variables that influence the discharge from catchments can readily be identified from literature research: (a) the varying, climatically induced input to a catchment system, and (b) the water-holding capacity of a catchment.

A lot of research has been done on the catchment system input. For this time series analyses have been used, e.g. studies by Arnell (1987) and Karl & Riebsame (1989). The importance of the second variable, the water-holding capacity has been deduced from research into the effects of geology and land use change on catchment discharge (e.g. Farvolden, 1963; Robinson, 1986). Because of the difference in approaches and the variety of catchments involved in both types of analyses, it is extremely difficult to obtain a clear view of the interactional effect of the above stated variables on catchment discharge. Recently, research incorporating both important variables is carried out to quantify the impact of climate change, e.g. Lettenmaier & Gan (1990) and Bultot *et al.* (1988) In these analyses daily to monthly conceptual or distributed discharge models are run with inputs obtained from climate scenarios. However, a number of problems are still apparent:

(a) since the analyses have been carried out on one or only a few catchments, they yield only local estimates of the impact of climate change;
(b) the results of the studies are, again, difficult to compare as different discharge models and climate change scenarios are used;
(c) the climate scenarios are taken from the results of global circulation models, which are not yet capable to simulate accurately present/future climate (IPCC, 1996), and

(d) the climate scenarios are projections of the climate into the twenty-first century. Vegetation and thus the hydrological system will have already (partly) adapted to any predicted climate change. It is however impossible to predict accurately the size of this change on a local scale, as this mainly depends on future natural and economic factors.

A model was developed to regionally assess catchment discharge sensitivity to climate variability: (a) with variables that are relatively easy to determine, (b) that can be applied at a regional scale, and (c) that enables comparisons between catchments within the region. To enable verification, such a model should be developed and tested by using knowledge deduced from previous climate variability, keeping in mind that the range of monitored climate variability is thought to be smaller than the expected climate change in the (near-)future.

From the literature review described previously it is clear that the main factors influencing catchment discharge sensitivity are the input to the catchment and the catchment water-holding capacity. The catchment water-holding capacity is mainly determined by its geology. To quantify catchment discharge sensitivity to climate variability a regional model that involves both catchment storage capacity and its input is presented in this study.

THE REGIONAL MODEL

Flow duration curve analyses of dry and wet periods of several years in the Upper Loire basin, France (Van der Wateren-de Hoog, 1995) show that catchment discharge sensitivity does not only depend on the size of the storage reservoir, but also on the highest storage which is reached under present climate conditions, i.e. the present maximum reservoir storage. This is in accordance with the earlier mentioned literature, as the present maximum reservoir storage obviously depends on the climatic input to the system. A simple annual storage model was developed to link the present maximum reservoir storage (s_{pm}) to the storage capacity (s_c) and the climatic input (Van der Wateren-de Hoog, 1997). In this model the present maximum storage is expressed as a fraction of the storage capacity. This fraction (s_{pm}/s_c) can be used to present catchment discharge sensitivity to climate variability. This can be visualized as follows: a nearly empty reservoir at present (low s_{pm}/s_c) can easily store water under wetter conditions, but does not have much water to overcome near-future dry conditions. In such catchments drought can have a large impact on water resources management. On the other hand, a catchment with a nearly full reservoir at present (high s_{pm}/s_c) cannot store large amounts of precipitation in the near-future. Excess precipitation will be discarded in the form of floods and this, obviously, also provides a risk for water management.

Catchment discharge sensitivity (s_{pm}/s_c) is a function of the storage capacity (s_c) and the net precipitation (precipitation - evapotranspiration) to the reservoir. An unknown part will not reach the storage reservoir at all, but will leave the catchment as direct discharge. Therefore, the precipitation reaching the storage reservoir is only a fraction (d) of the average annual net precipitation (P_{AAN}). The following nonlinear relationship for the fraction describing catchment discharge sensitivity is proposed:

$$\frac{s_{pm}}{s_c} = s_c \exp - \left[\frac{s_c}{d * P_{AAN}} \right] \quad (1)$$

The variables are expressed in length units (mm), if divided by catchment area. To apply the above relationship, the variables s_{pm}, s_c and P_{AAN} need to be quantified. P_{AAN} can simply be approximated by multiplying average annual precipitation with the runoff ratio (runoff/precipitation). s_{pm} can be quantified by means of recession analysis from time series of daily discharge using the approach as described by Tallaksen (1989). For each recession period the discharge derived solely from storage at the beginning of a recession period ($t = 0$) and its recession constant are determined. From this, following linear groundwater theory, the amount of storage in the catchment at time $t = 0$ can be calculated (+ in Fig. 1). The s_{pm} is then defined from all studied catchment recession periods as the average storage plus two standard deviations (Fig. 1). s_c is defined by catchment volume and geological properties (equation (2)). Assuming linear groundwater theory under the Dupuit(-Forchheimer) assumption allows s_c to be described by catchment slope (*Sl*, dimensionless), catchment shape (*Re*, dimensionless: Schumm, 1956), the average catchment recession constant (α_c, day^{-1}), and *K*. *K* combines catchment hydraulic conductivity and the quadratic proportion of drainable aquifers (Van der Wateren-de Hoog, 1997). Theoretically estimated values for the exponents in equation (2) are $a = 2$, $b = 1$ and $c = 4$.

$$s_c = \frac{K Sl^a}{\alpha_c^b Re^c} \quad (2)$$

The use of groundwater theory to develop the model limits its application to catchments for which the Dupuit assumption is valid. This essentially means that the catchments should have homogeneous and isotropic geology and not too steep slopes. In practice catchments with slopes less than 5% and stable recession constants along the whole range of monitored discharges can be used (Van der Wateren-de Hoog, 1997). To apply the model (i.e. equations (1) and (2)) for regional assessment of catchment discharge sensitivity (s_{pm}/s_c) to climate variability, using average annual net precipitation (P_{AAN}) as input, five parameters: the exponents *a*, *b* and *c*, the

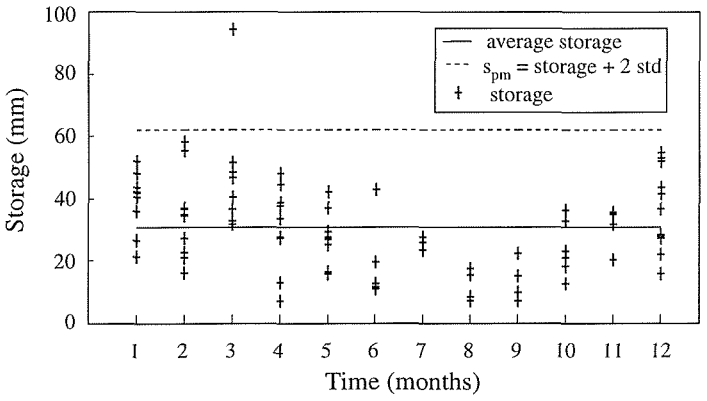

Fig. 1 Storage (+) determined for the Sioule catchment from recession analysis for the period 1970–1983 (1: January...12: December).

fraction d and the variable K first need to be calibrated for the specific region under study.

CALIBRATION AND VERIFICATION OF THE REGIONAL MODEL

The Upper Loire basin in France (Fig. 2) was selected as the study region. The European Water Archive (Gustard, 1993) provided the necessary catchment variables and discharge data for 15 catchments in this region. The Dupuit assumption as well as the statistical assumptions necessary for regional application, i.e. insignificant correlation between predictor variables and normal distribution of s_{pm} were valid for these catchments.

Statistical calibration was carried out with the nonlinear estimation procedure of the statistical software package CSS-Statistica using the quasi-Newton method and with least squares loss function. Calibration of the model using observed s_{pm} (Fig. 1) of 15 catchments resulted in a coefficient of determination (r^2) of 0.86 and values of the exponential parameters a, b and c of 0.32, 1.57 and 0.73 respectively, a value for the fraction d of 0.76, and a value for K of 5.06. The values of a, b and c do not approximate the theoretically estimated values stated above. However, since the theoretical values are approximations based on a number of assumptions, this is acceptable. The value 0.76 for the fraction d reaching the storage reservoir is

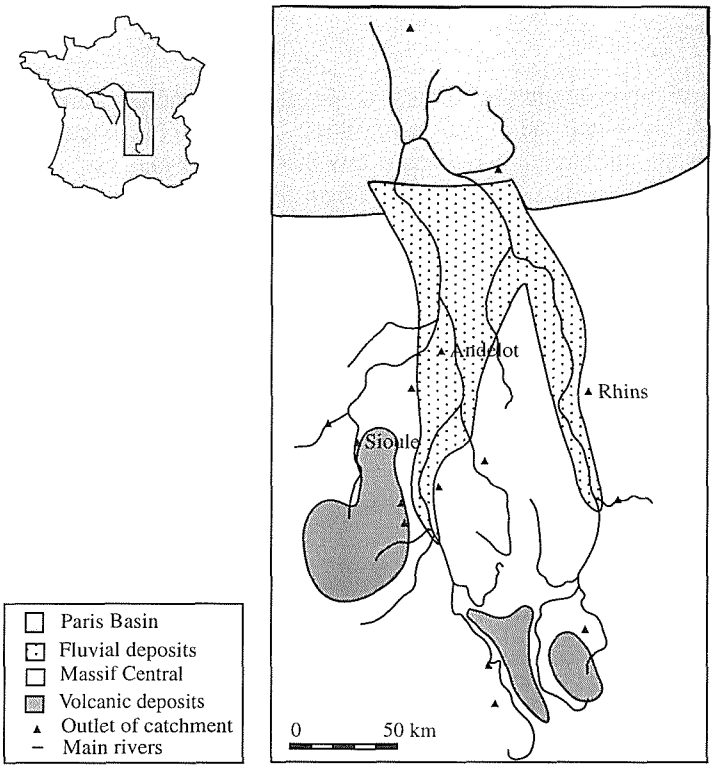

Fig. 2 The locations of the outlets of the catchments used in the regional model are shown by small black triangles.

probable. The same is true for the fitted value for variable K.

As the model is calibrated for only 15 catchments it needs verification to gain confidence in its practical use. The model was statistically and physically verified. The statistical verification consisted of a 15 times repetition of the calibration routine, excluding a different catchment each time to test for stability in the outcome of the above described parameters. This jack-knifing exercise showed only small variations in outcome, thus confirming the stability of the proposed regional model. The physical background of the regional model was verified using a daily discharge model (PDM, Moore, 1996). The storage capacity simulated with the discharge model closely resembled the regionally determined s_c. Storage capacity was a sensitive parameter in the PDM model. Simulation of discharge during dry and wet periods by the PDM model indicated that groundwater storage causes the main differences in the catchment reaction to climate variability. Both investigations, described in Van der Wateren-de Hoog (submitted), indicate that the physical background of the regional model is sound. The statistical and physical verification of the developed regional model confirm its value for practical use.

PRACTICAL USE OF THE REGIONAL MODEL

With the calibrated model spatial and temporal analyses within the Upper Loire basin can be carried out. By inserting the appropriate values for the catchment specific variables Sl, Re and α_c and the region specific parameters a, b, c, d and K in equations (1) and (2), spatial analyses can be carried out to determine catchment storage capacities within the region. Figure 3 presents storage capacities (s_c) for catchments used in the analysis together with their present maximum storage (s_{pm}) as predicted by the model as well as the observed values of s_{pm}, determined from recession analysis.

Temporal analyses can be carried out to assess catchment discharge sensitivity to climate variability by applying the model equations with either actual or hypothetical data for the annual net precipitation (P_{AN}). As an example this was done for three catchments (Fig. 2) with actual data (Fig. 4). A high ratio of modelled s_{pm}/s_c for current P_{AN} conditions in Fig. 4 indicates that a catchment is dominated by direct flow. These catchments are flood prone (Rhins, Sioule). Baseflow dominated

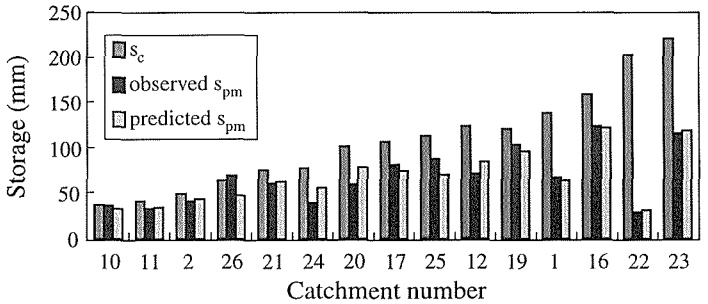

Fig. 3 Predicted storage capacity (s_c) and observed and predicted present maximum reservoir storage (s_{pm}) for 15 catchments as determined by the regional model (10: Rhins, 21: Sioule, 22: Andelot catchment).

catchments can be identified by a flat slope of the initial, left-hand part of the modelled s_{pm}/s_c curve (Andelot). This identifies drought prone catchments. On the other hand, catchments with a high variability of discharge show a steep slope in the initial, left-hand part of the modelled curve. These catchments can both be drought and flood prone.

Concluding, Fig. 4 summarizes present conditions and may be used for future annual net precipitation conditions. Both are important for catchment water management with respect to floods, droughts and the impact of climate variability/change. For all catchments the modelled curves of s_{pm}/s_c indicate their sensitivity. With the regional model it is possible to produce maps of current sensitivity as well as future sensitivity.

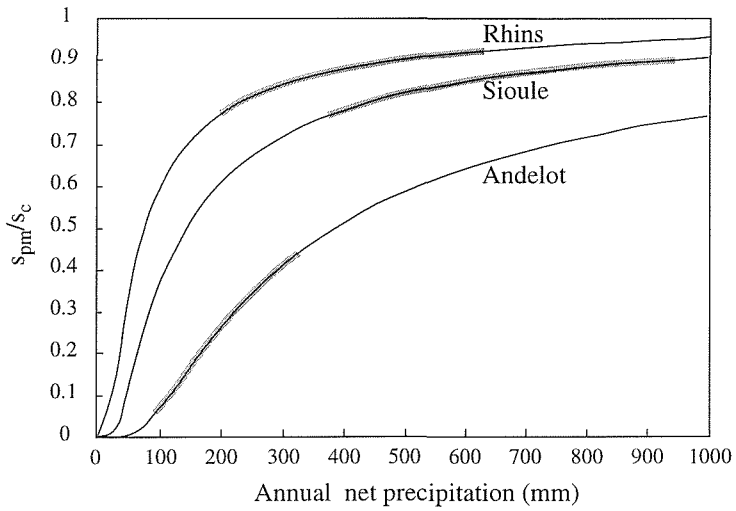

Fig. 4 Catchment discharge sensitivity (s_{pm}/s_c) for the Andelot, Sioule and Rhins catchment. The thick grey lines show the range of annual net precipitation for the period 1970–1983.

CONCLUSIONS

This paper summarizes the development, calibration and verification of a regional model that quantifies catchment discharge sensitivity to climate variability. Catchment discharge sensitivity depends on present maximum reservoir storage and storage capacity. The developed regional model has high potential for large-scale application, assuming that the model concept is also valid for catchments in other regions. Regional catchment sensitivities and catchment storage capacities can be determined using readily available data.

Potential applications of the regional model for present and future water resources management are:

(a) the identification of flood and drought prone catchments, i.e. the present catchment discharge sensitivity;
(b) the incorporation of storage capacity in GCMs and in large-scale discharge models such as Rhineflow (Kwadijk, 1993);

(c) the identification of catchments where large impacts are to be expected, i.e. future catchment discharge sensitivity as influenced by climate change;
(d) the determination of storage capacities for catchments where no long hydrological records are available (regionalization of the storage capacity).

There are some limitations to the applicability of the model; the most severe being that the Dupuit assumption should be valid for catchments included in the analysis, and that discharge data are needed to set up the regional model. Further research is needed to investigate these drawbacks. The necessary geological homogeneity of catchments to be included in the regional model needs to be investigated and further development of the regional model is necessary to apply the model to catchments which are inhomogeneous or that have steep slopes. Furthermore, research into the derivation of the catchment recession constant, independently from discharge data could further enhance the models applicability.

Acknowledgement The authors wish to thank METEO-FRANCE and AMHY for the provision of climate data. This research is financed by NWO (Dutch Scientific Organization) and is a contribution to FRIEND theme 3.

REFERENCES

Arnell, N. W. (1987) Changing frequency of extreme hydrological events in northern and western Europe. In: *FRIENDS in Hydrology* (ed. by L. Roald, K. Nordseth & K. Anker Hassel) (Proc. Bolkesjø Symp., Norway, April 1989), 237–249. IAHS Publ. no. 187.

Bultot, F., Coppens, A., Dupries, G. L., Gellens, D. & Meulenberghs, F. (1988) Repercussions of a CO_2 doubling on the water cycle and on the water balance—a case study for Belgium. *J. Hydrol.* **99**, 319–347.

Farvolden, R. N. (1963) Geologic controls on ground-water storage and base flow. *J. Hydrol.* **1**, 219–249.

Gustard, A. (ed.)(1993) *Flow Regimes from International Experimental and Network Data, (FRIEND)*, vols I, II. Institute of Hydrology, Wallingford.

IPCC (1996) *Climate Change 1995: Impacts, Adaptations and Mitigation of Climate Change*. Scientific-Technical Analyses, Cambridge Press.

Karl, T. R. & Riebsame, W. E. (1989) The impact of decadal fluctuations in mean precipitation and temperature on runoff: a sensitivity study over the United States. *Climatic Change* **15**, 423–447.

Kwadijk, J. C. J. (1993) The impact of climate change on the discharge of the river Rhine. PhD Thesis, Utrecht University, The Netherlands.

Lettenmaier, D. P. & Gan, T. Y. (1990) Hydrologic sensitivities of the Sacramento–San Joaquin river basin, California, to global warming. *Wat. Resour. Res.* **26**, 69–86.

Moore, R. J. (1996) *A Guide to the PDM*. Institute of Hydrology, Wallingford.

Robinson, M. (1986) Changes in catchment runoff following drainage and afforestation. *J. Hydrol.* **86**, 71–84.

Schumm, S. A. (1956) Evolution of drainage systems and slopes in badlands at Perth Amboy, New Jersey. *Bull. Am. Geol. Soc.* **67**, 579–646.

Tallaksen, L. (1989) Analysis in time variability in recessions. In: *FRIENDS in Hydrology* (ed. by L. Roald, K. Nordseth & K. Anker Hassel) (Proc. Bolkesjø Symp., Norway, April 1989), 85–96. IAHS Publ. no. 187.

Van der Wateren-de Hoog, B. (1995) The effect of climate variability on discharge, as dependent on catchment characteristics in the Upper Loire basin, France. *Hydrol. Sci. J.* **40**, 633–646.

Van der Wateren-de Hoog, B. (1997) A regional model to assess the hydrological sensitivity of medium sized catchments to climate variability. *Hydrol. Processes* (in press).

Van der Wateren-de Hoog, B. Catchment sensitivity to climate variability as dependent on: 1. Catchment storage capacity. (submitted to *Hydrol. Processes*)

Van der Wateren-de Hoog, B. Catchment sensitivity to climate variability as dependent on: 2. Catchment storage. (submitted to *Hydrol. Processes*)

The variability of hydrological series due to extreme climate conditions and the possible change of the hydrological characteristics with respect to potential climate change

OLGA MAJERČÁKOVÁ
Slovak Hydrometeorological Institute, Jeséniova 17, 833 15 Bratislava, Slovak Republic

MIRIAM FENDEKOVÁ
Department of Hydrogeology, PRIF UK, Mlynská Dolina, 842 15 Bratislava, Slovak Republic

DANICA LEŠKOVÁ
Slovak Hydrometeorological Institute, Jeséniova 17, 833 15 Bratislava, Slovak Republic

Abstract In recent years Slovak hydrology has been more oriented towards evaluation of water resources, their variability and possible changes and also towards evaluation of the territory from the point of view of water resources. The results documented significant decrease in the runoff from Slovak streams after 1980. The decrease is most significant in November, negligible decrease was identified in May and in the spring months. The absolute minimum annual discharge for the whole observed period occurred in 1993 in 19% of all water gauging stations considered. The main starting time of decreasing spring yields in Slovakia was in 1987–1988. The decrease in yield will reach up to 60% by 2010.

NATURAL CONDITIONS

The Slovak Republic (SR) is an inland country in central Europe, with an area of 49 036 km^2. Slovakia lies on the roof of Europe and occupies territory between the River Danube and the Tatra Mountains. One of the main European watershed divides passes through northern Slovakia. From an orographic point of view, the territory of SR is very heterogeneous, the altitude varying between 94 m a.s.l. (southeastern Slovakia) and 2655 m a.s.l. (Gerlach mountain in the High Tatras). Slovakia is a mostly mountainous country, 60% of the territory being higher than 300 m a.s.l. The country lies in the mild climate zone, where the effects of the ocean and continent meet. The territory is characterized by a regular rotation of four seasons and variable weather throughout the whole year. The mean annual temperature ranges from 10.4°C (south of the Danube Lowland) to –3.7°C (Lomnický štít in the High Tatras). The mean annual precipitation is about 750 mm.

The runoff of surface and subsurface water is relatively quick; the surface and groundwater resources are filled largely by the precipitation. The next source of water is the River Danube, which flows through southwestern Slovakia and saturates the groundwater in near surroundings.

The density of the river network varies from 0 to 2000 m km^{-2} while on average it is 920 m km^{-2}. Approximately 2% of the territory is covered by water. For water balance and optimal management of rivers, the territory of Slovakia is divided into 10 main basins (Fig. 1).

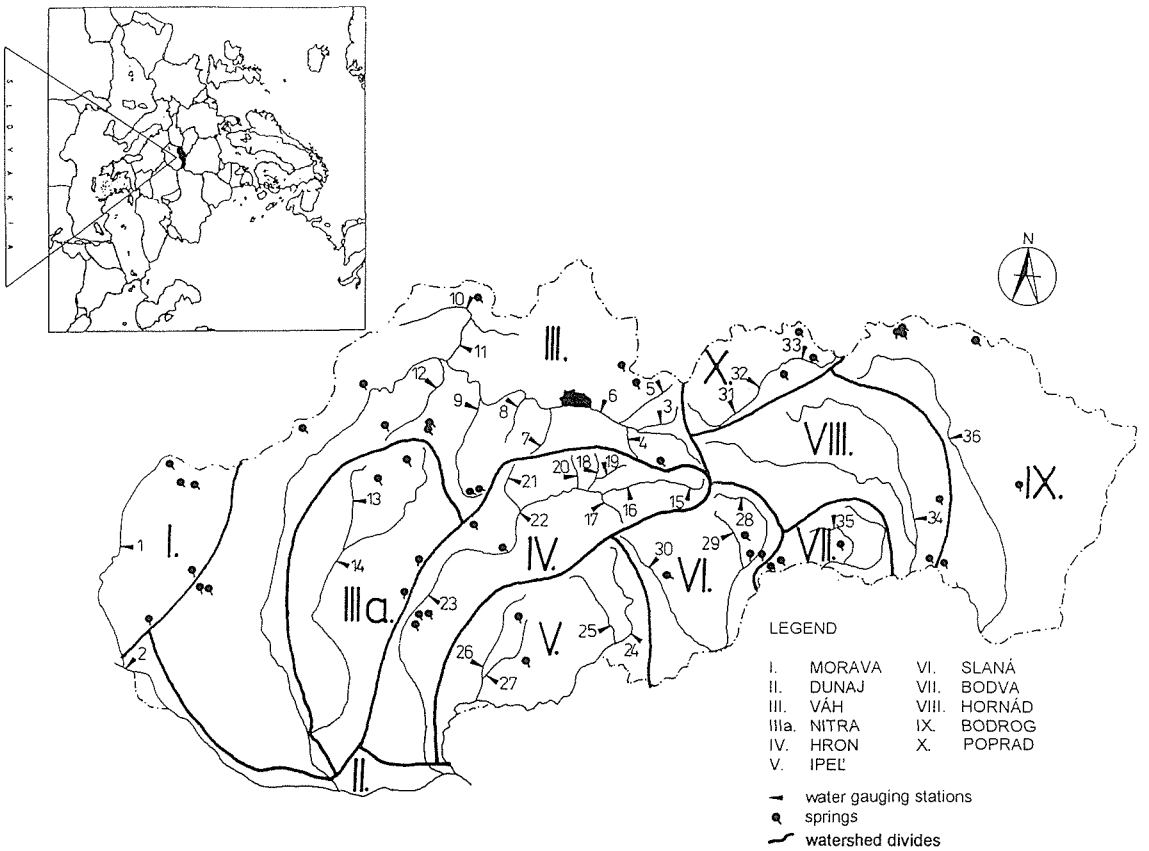

Fig. 1 Slovakia: main river basins. Water gauging stations and springs selected for NCP and FRIEND.

The natural conditions determine the relatively dense network of hydrological and climatological observations. The mean daily discharges are measured at about 450 gauging stations. The spring yields and the groundwater levels are measured once a week at some 700 and 1200 points, respectively.

DESCRIPTION OF THE PROBLEM

The long-term water balance of Slovak territory has been derived for the period 1931–1980:

753 mm (Precipitation) = 261 mm (Runoff) + 492 mm (Evaporation)

At the Slovak hydrological service, 1931–1980 is considered as a reference period and is the basis for the main long-term hydrological characterization.

After 1980 came the series of climatically unfavourable years from the point of view of water resources filling. This unfavourable situation peaked in 1993 and ended in 1994 (year 1994 was the warmest one in the history of measurements). The period 1981–1993 can be characterized by a deficit of precipitation and runoff. The

Table 1 Runoff in 1993 for the main river basins in Slovakia (in % of long-term mean annual runoff).

No.	Basin	R_{1993} in % of $R_{avg.}$
I	Morava	50–60%
II	Dunaj	90% main stream, 50% tributaries
III	Váh	55–70%
IIIa	Nitra	40–80%
IV	Hron	20–40%
V	Ipel	10–45%
VI	Slaná	20–50%
VII	Bodva	<30%
VIII	Hornád	40–80%
IX	Bodrog	60–90%
X	Poprad	55–70%

Note: Basins 1–X (96% of territory) belong to the Black Sea; basin X (4% of territory) belongs to the Baltic Sea.

differences compared with the long-term averages were –6% for precipitation and –20% for runoff. These values varied during the period 1981–1993 as well as over the territory. For instance, in 1993 in 34% of the territory (southern and southeastern Slovakia) runoff was less than 50% of the long-term average (Table 1).

Most Slovak river basins regularly have the low flow season at the end of the summer and during the autumn. During the last 15 relatively dry years this fact was particularly remarkable.

It is out of the hydrologists' domain to judge the causes of the climate variability. However, the advent of potential climate change shifts hydrology from evaluation of the past and short term future to prognoses of possible development of the hydrological cycle and water balance. These prognoses are based on the recommended climate scenarios.

The hydrological situations of the last 15 years or so create the need for re-evaluation of long-term hydrological characteristics. Among possible tasks for this forthcoming need are:

- the analysis of variability of hydrological series and the judgement of the series stationarity;
- the analysis of the change of low flow characteristics;
- the possible impact of potential climate change on the hydrological characteristics which quantify the water resources.

The solution of these presented problems was possible due to the support of national and international projects, mainly: the FRIEND project, the National Climate Programme and the Country Study Programme.

DATA

The basic data which were used in the solution of the above-mentioned tasks were:

- Sixty-four of the discharge series—daily, mean monthly and mean annual discharge series observed at least from 1931. Thirty-six of these series were included in the National Climate Programme (NCP), 20 in the FRIEND project and 45 were used to evaluate the low flow characteristics.

- Sixty-four series of spring yields (mean monthly yield series), the most important of them included in Fig. 1.
- In parallel the series of precipitation, air temperatures and meteorological data were evaluated (by the climatological service of SHMI).
- Climate scenarios:
  - the results according to GCMs (scenarios CCCM, GISS and GFD3),
  - the results of NCP experts (scenarios SD and WP) (Lapin *et al.*, 1995).

The selection of hydrological series was determined by the following criteria:

- the measurement of discharges at least from 1931; the observation of spring yields over as long a period as possible (starting in the 1970s);
- the series representing the watersheds of various sizes, various physio-geographical and hydrogeological regions (from all 10 main basins);
- the perspective series (with high probability of further observation);
- the series are relatively reliable (the reliability of series means that the series are of good quality and are representative). The verification of reliability was based on the history of measurements, on known activities in watersheds as well as on homogeneity testing (Majerčáková & Šedík, 1994a).

MAIN RESULTS

Analysis of discharge series variability and their stationarity

The results of homogeneity testing, of low frequencies filters (moving averages) and trend analysis of series until 1990 identify the remarkable decrease of the runoff in Slovak streams after 1980. The decrease is most significant in November and following autumn–winter months. Negligible decrease was identified in May and some following spring months, respectively. An example is shown in Fig. 2, where the course of mean annual, May and November discharges is supplemented by linear trends on the Litava watershed at the Pláštovce gauging station.

The runoff decrease in SR territory is different. The most influenced basins are: Ipel, Slaná and Bodva (south and southeastern Slovakia), where the runoff after 1980 was decreased by 30–40%. Behind them follow the basins of Hron, Nitra, Poprad and upper Váh, where the decrease did not exceed 15–20%. The lowest decrease (to 5–10%) was recorded in northwestern, western and northeastern Slovakia.

From the statistical analysis of series it is evident that many of them are non-stationary (in the observed interval). For instance, the proof of the non-stationarity can be significant non-homogeneity, which is not evident throughout the entire year but only in some months. In the future this fact will have to change the methods (or the philosophy) of the series evaluation as well as the derivation of long-term characteristics (Majerčáková & Šedík, 1994b).

Analysis of the spring yield series variability

The results of homogeneity testing and trend analysis of spring yields time series up to 1994 identify the same remarkable decrease of mean, minimum and maximum

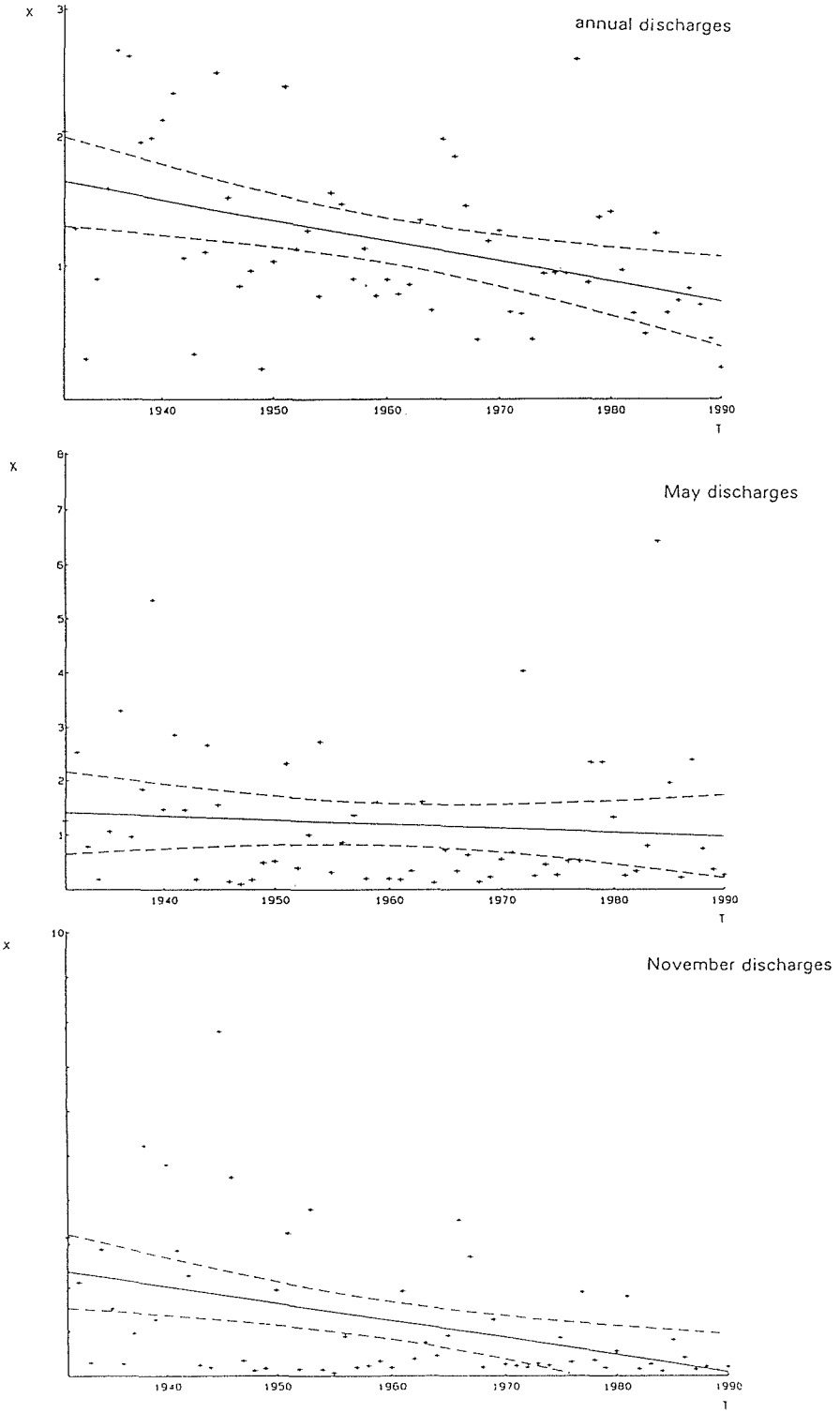

Fig. 2 Linear trend course of mean annual, May and November discharges for the Litava basin in Pláštovce.

monthly spring yields in almost all cases. The main difference is in the commencement of decreasing trends. In some cases it started in 1982 (two years later than in the case of identified runoff decrease), but the most frequent starting point of spring yield decrease were years 1987–1988 (Fendeková *et al.*, 1995; Kullman, 1995; Fendeková, 1996). The influence of the documented last warm climate period 1988–1994 on Slovak territory was very distinct for the springs located in structures of sedimentary flysch rocks (alternation of sandstones and clays) and in karst limestone areas, but not so strong in the areas of neo-volcanic rocks.

The spatial distribution of decreasing yield is very variable. The most remarkable decreasing trends were documented in the southern part of Slovak territory by springs from karst environment and also in northeastern and northern Slovakia by springs from flysch rocks. It is interesting that decreasing trends were documented as being more distinct in the case of mean and maximum yields. Minimum yields are quite stable.

Analysis of low flow characteristics

The climatological situation after 1980 has evoked an interest in re-evaluating the low flow characteristics, (e.g. Majerčáková *et al.*, 1995). We can say that the low flow characteristics have responded to this situation with some delay. For example, the absolute minima occurred only since 1984. Two examples illustrate the change of these characteristics:

1. *The minimum annual discharges*: up to 1986 the minimum annual discharges were only slightly under the long-term average in approximately 40% of territory. From 1987 a rising number of cases occurred when $Q_{\text{minann.}} < Q_{\text{minavg}}$. In 1993 the minimum annual discharges were half of their long-term averages at almost 30% of water gauging stations and 70% of stations had the minimum annual discharge less than the average. The mean minimum discharge for the period 1931–1993 was less than the mean for the period 1931–1980 by about 5–10% at 40% of stations.
2. *Occurrence of the absolute minimum discharges*: during the period 1981–1993 the absolute minima occurred rarely, examples occurring in 1984 (at 11% of stations), in 1992 (at 17% of stations) and this phenomenon peaked in 1993 (at 19% of all considered gauging stations). According to the presented and other low flow characteristics, the year 1993 can be considered as the second driest year in our country (Lešková, 1996).

Possible impact of potential climate change on the characteristics which quantify the water resources

Runoff The statistical methods for the analysis of runoff series variability were used only exceptionally for the prediction. The hydrological scenarios were based mostly on the application of already developed models (WatBal, DAIR etc.) and on application of the author's methods. For the prediction of the mean monthly and annual runoff change due to potential climate change a statistical linear regression

model was used of the type $R = f(P_{-i}, P, T, r, R_{-1})$, where R is the runoff, P = precipitation, T = air temperature, r = relative air humidity; indexes with the negative sign indicate the mean monthly values of elements in previous months (Majerčáková & Šedík, 1995). This model was applied on 12 watersheds in central SR, (Majerčáková *et al.*, 1996). The results can be summarized in the following way:

- A significant runoff increase over the whole territory during the winter (from December to March). In the northern regions a smaller increase is expected (about 20%) of longer duration (from November to April—due to the altitude). In central and southern regions there is a more intensive increase in winter runoff (to 40%) but of shorter duration (only January and February).
- During the spring and summer until September a very significant decrease can occur; with only one exception which results from the GFD3 scenario. In northern regions the decrease in runoff can reach from 20 to 25%, while in southern regions it can be from 30 to 40% and exceptionally 60%.
- According to GCM scenarios we can expect a slight increase in the runoff from October into the winter, the opposite situation to that indicated by the NCP scenarios—a slight or moderate decrease.
- The intensity of the runoff change will grow as the year 2075 approaches and will be higher in the southern and southeastern parts of Slovakia.
- Although the annual sums of the runoff change can be relatively small, the significant seasonal and monthly changes can influence to a very large extent water management and the other sectors dependent on water.

Spring yield The prediction of spring yields was made by statistical methods of trend analysis. The decrease of spring yields varies from 10 to 65% of mean yield for the whole period of observation. The prediction to the year 2000 was made for springs flowing from karstic structures. The values obtained varied from 0 to 63% decrease. According to Kullman (1996) the decrease of spring yield in accordance with parameters of climatic scenarios GISS, GFD3, CCCM and others, and the decrease of mean yearly yield in crystalline range mountains will reach, in the year 2010, values in the range 10–60%. Only in a few cases was an increase of spring yields documented.

CONCLUSIONS

In recent years Slovak hydrology has been increasingly oriented towards evaluation of water resources, their variability and possible changes, and also on evaluation of the territory from the point of view of water resources. The interest in hydrological processes was less than in the 1960s and 1970s. This orientation was also supported by some of the international projects mentioned previously.

The relatively dry and warm years were not favourable for the water resources saturation or for water management (furthermore at a time of economic and social transformation). In the history of hydrological measurements such a long dry period has not before been identified. This is the main reason for describing the present situation, presenting some results from recent years and making some predictions about the future.

REFERENCES

Fendeková, M. (1996) Spring regimes of selected hydrogeological units of Slovakia (in Slovak with English summary). *Podzemná Voda* 2/1996, SAH, 23–31.

Fendeková, M., Gavurník, J., Kullman, E., Jr & Sadloňová, K. (1995) Influence of global climate change on spring yields on Slovak territory (in Slovak). In: *AQUA 95* (Trenčín), 8–18.

Kullman, E. (1995) Decrease in the yield of groundwater resources in Slovakia and an appraisal of its causes (in Slovak with English summary). *Podzemná Voda* 1/1995, SAH, 58–74.

Kullman, E. (1996) Interpretation of possible impacts of climatic and hydrologic condition changes on estimation on the disposable groundwater supply changes. *Slovak Republic's Country Study*, element 2iii. SHMÚ, Bratislava.

Lapin, M., Nieplová, E. & Faško, P. (1995) Climate change scenarios for air temperature and precipitation change in Slovakia (in Slovak with extended English summary). In: *NKP* 3/95 (National Climate Programme SR), 19–57.

Lešková, D. (1996) Selected statistical and probable characteristics of low flow. *Report for FRIEND Project 1996*. SHMU, Bratislava.

Majerčáková, O. & Šedík, P. (1994a) The selection of hydrological monthly series and the analysis of their variability and reliability (in Slovak). *Final Report for NCP SR*. SHMÚ, Bratislava.

Majerčáková, O. & Šedík, P. (1994b) The runoff change of the Slovak rivers (in Slovak with extended English summary). In: *NKP* 2/94 (National Climate Programme SR), 107–137.

Majerčáková, O. & Šedík, P. (1995) The estimation of the possible runoff change during the year on the basis of the statistical model (in Slovak). *Report for NCP SR*. SHMÚ, Bratislava.

Majerčáková, O., Lešková, D. & Šedík, P. (1995) Selected characteristics of low flows of Slovak rivers. *J. Hydrol. Hydromech.* **43**(4–5), 331–353.

Majerčáková, O., Minárik, B. & Šedík, P. (1996) The possible runoff change during the year on the Slovak streams due to potential climate change. *Slovak Republic's Country* Study, element 2iii. SHMÚ, Bratislava.

FRIEND'97 — Regional Hydrology: Concepts and Models for Sustainable Water Resource Management
(Proceedings of the Postojna, Slovenia, Conference, September–October 1997). IAHS Publ. no. 246, 1997.

Hydrological regimes in the FRIEND–AMHY area: space variability and stability

VIOREL ALEXANDRU STANESCU & VALENTINA UNGUREANU
National Institute of Meteorology and Hydrology, Sos. Bucuresti-Ploiesti 97, 71552 Bucharest, Romania

Abstract The characteristics of the climate determine the "macro-types" of hydrological regimes each of them encompassing "subtypes" of river flow regimes, the occurrence of which is generated by the orographic characteristics of specific sub-areas. Thus, the low temperature during the winter time in the high mountainous zones result in a "shifting" of the low flows toward late January or February, as well as the high flows toward the summer months due to an appreciable delay in the snow melting. This shifting leads to a differentiation of the subtypes of hydrological regimes which are defined on the basis of an analysis of the mean monthly flow variation at the considered hydrological stations in the FRIEND–AMHY area. The degree of their stability is quantitatively assessed.

INTRODUCTION

A river flow regime type is defined by the variation of the flow throughout the year as the timing of the maximum and minimum flow seasons and range in the discharges during each flow phase dependent on its origin and the basin characteristics.

In the report on "European River Flow Regimes" (Arnell *et al.*, 1993) nine types of regimes, adapted from Gottschalk *et al.* (1979) and Krasovskaia & Gottschalk (1992), have been established in Europe. The regime types refer to the widely-distributed areas where they are found, the periods of the year when the high and low flows occur, and the type of water supply (rainfall and/or snowmelt). The river flow regimes presented in this work refer to a European scale and are dependent on the main climate features. At a finer scale, the effects of a particular climate on river flow regimes are considerably controlled by the physiographical properties of the basin. Among these, the altitude plays the most important role as it expresses the gradual variation on the vertical of a particular macro-type of the climate and implicitly reflects the configuration of the hydrographical network, channel and slope gradients, soil and land cover. Thus the diversity and the features of the regimes are connected with the time and space scale at which the hydrological analysis is made.

The present work describes the regime types at a finer scale, concentrating on (a) means of representation of the flow regimes, (b) types of regimes defined by the timing of the high and low flow phases, (c) regionalization of some "micro-types" in some countries from the FRIEND–AMHY area, and (d) stability of the river flow regimes.

MEANS OF REPRESENTATION OF THE RIVER FLOW REGIMES

The following types of hydrographs may offer an image of a river flow regime:

- *Typical hydrograph* which is drawn on the basis of the most frequent phases of the flow expressed in terms of the timing (earliest, mean, latest) as well as by the characteristic values of their daily discharges (Stanescu, 1967). In Fig. 1 a typical hydrograph of a river in Romania is presented (Diaconu & Serban, 1994). The typical hydrograph may be relevant for the schematic representation of the river flow regime provided that the occurrence of the phases does not vary too much in time. This assumes a relatively high stability of the occurrence of the characteristic phases of the flow as well as a high degree of the natural regulation of the flow. Hence, the use of such a representation is generally applicable for the basins of medium and large areas.
- *Daily flow hydrograph* in the characteristic (wet, dry and average) years. An example of such a hydrograph in the average year (50% probability) for a river in Romania is presented in Fig. 2.

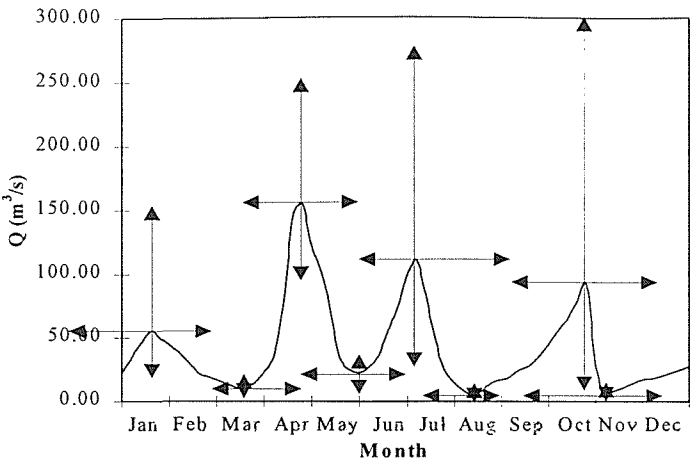

Fig. 1 Typical hydrograph.

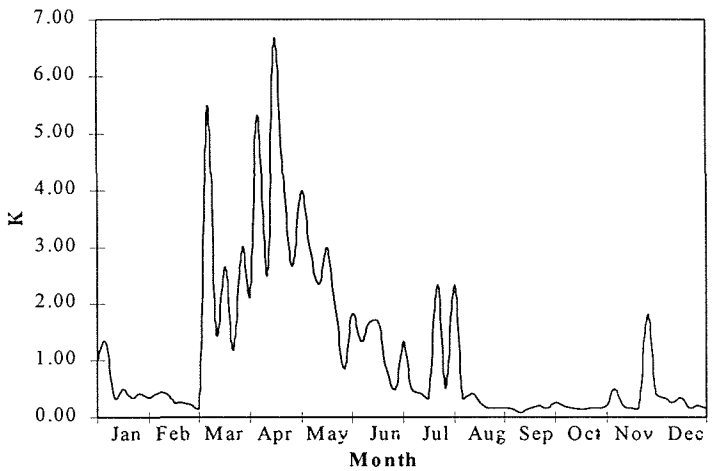

Fig. 2 Hydrograph in the average year (50% probability). K = ratio of the daily flow against the mean annual discharge.

- *Mean monthly flow hydrograph* which significantly represents the seasonal flow regime but, due to the averaging of the monthly flows in individual years, cannot reflect the occurrence of the characteristic phases of the daily flows. Nevertheless, taking into account that only mean monthly flow data have been available, such monthly-based representation has been used in establishing at the finer scale the river flow regimes of the considered countries from the FRIEND–AMHY area: Romania, Yugoslavia, Greece, Switzerland and Spain.

PERIODS OF HIGH AND LOW FLOWS

For the analysis, data from the FRIEND–AMHY database were used in addition to data published in the yearbooks of Romania and Yugoslavia and data kindly provided by the national coordinators for topic III–AMHY from Spain, Switzerland and Greece (Table 1).

Table 1 Data used in the considered countries from FRIEND–AMHY area.

Country	Number of stations	Period (years)
Romania	350	45–65
Spain	18	35–80
Yugoslavia	61	15–45
Greece	2	18–24
Switzerland	12	61–80

The classification of the hydrological regimes was made by the assessment of the *discriminating periods* defined by the first, the second and the third highest and lowest monthly flows, noted with MAX1, MAX2, MAX3, MIN1, MIN2, MIN3 respectively.

The river flow regimes at a finer scale in the FRIEND–AMHY area are influenced by: (a) the Mediterranean circulation, (b) the oceanic circulation and (c) the pronounced variation in altitude of the basins. As an indicator of the elevation of the basin, the mean altitude ($\overline{H}$) has been considered. Mention should be made about the relationship between the space (ranges in altitude) and time (monthly flow) scale considered in the analysis. In Fig. 3 the mean monthly flows for three sub-basins of different mean altitudes, embedded in a same basin controlled by a particular climate, are presented. For the sub-basin of Arges Superior at a high altitude, at the Tunel station ($\overline{H} = 1442$ m) the MAX1 value occurs in May followed by MAX2 in June. This timing is due to the late snowmelt combined with the abundant rainfalls caused in the period April–June by a Mediterranean circulation, more intense over this span of time. For the Argesel basin at a medium altitude at the Mioveni station ($\overline{H} = 668$ m), the flows MAX1 and MAX2, practically equal, occur in April and May. This "shifting back" from June–May to May–April is explained by the earlier snowmelt due to the lower altitude. For the Cervenia station in the Vedea basin which is at a low altitude ($\overline{H} = 176$ m) the snowmelt ends in early spring resulting in the occurrence of MAX1 in March and of MAX2 in February. Thus, an elevation range of about 500–700 m (space scale) is sensitive to one month (time scale) shifting.

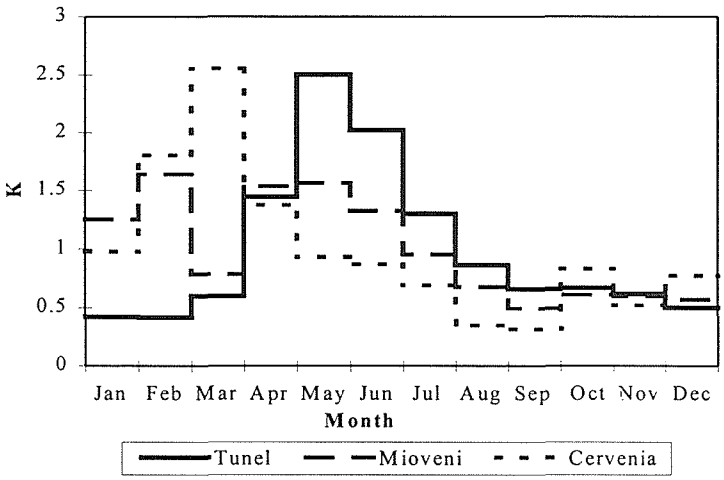

Fig. 3 Mean monthly flows for three sub-basins of different mean altitudes. K = ratio of the mean monthly flow against the mean annual discharge.

The shifting of the low flows MIN1 and MIN2 of the sub-basins situated at low altitude from August–September towards December–February for those of a high altitude, is explained by the occurrence of the long-lasting very low temperatures in the mountainous zones.

Thus, under a given climate influence, the situation of the basins of different altitudes results in a diversification of the flow regime types with particular features.

TYPES OF RIVER FLOW REGIME AND THEIR REGIONALIZATION

Relying upon the available data at the stations considered in Romania, Spain, Yugoslavia, Greece and Switzerland, the discriminating periods which define a particular river flow regime have been determined (Table 2). The existence of different zones which are quasi-homogeneous from the physiographical properties stand point, expressed by their mean altitudes, allows hydrological regionalization to be carried out. In Fig. 4 the mapping of the river flow regime zones for Romania (a) and Yugoslavia (b) is presented. The mean monthly flows defining several regime types in Spain, Greece and Switzerland are shown in Fig. 5.

STABILITY OF THE RIVER FLOW REGIMES

The stability of a certain flow regime may be quantitatively expressed by the sum of the entropies of the occurrence of the regime characteristics (maximum MAX1, MAX2, MAX3 and minimum MIN1, MIN2, MIN3 values) in the discriminating periods (Shannon & Weaver, 1941; Krasovskaia, 1995).

The occurrence of a certain pattern of flow out of n types during individual years in a series is considered as an event E_i, the probability of which is $p_i = p(E_i)$ and $\sum_{i=1}^{n} p_i = 1$. The entropy H of the occurrence of each characteristic is given by:

Table 2 River flow regimes and discriminating periods for the considered countries from FRIEND–AMHY area.

Zone	Regime type	MAX1	MAX2	MAX3	MIN1	MIN2	MIN3
Romania							
1	South-plain: rainfall (snowmelt) origin	II–III	II–IV	II–IV	VIII–X	VIII–X	VIII–X
2	Western and south-western: rainfall–snowmelt origin	II–IV	II–IV	II–IV	IX–XI	VIII–X	VIII–X
3	Central plateau: rainfall–snowmelt origin	III–IV	III–IV	III–VI	IX–XI	VIII–XI	VIII–XI
4	Eastern plateau: rainfall (snowmelt) origin	III–IV	III–V	III–V	VIII–X	VIII–X	VIII–X
5	Southern and eastern Carpathian: rainfall–snowmelt origin	IV–VI	IV–VII	IV–VII	XII–II	XI–II	XI–II
6	Southeastern Black Sea side: rainfall origin	II–VI	II–VII	II–VII	IX–XI	IX–XII	IX–XII
Spain							
1	Western and southwestern zone: oceanic circulation influence	XII–III	XII–III	XII–IV	VIII–IX	VIII–IX	VII–IX
2	Central zone: transition from oceanic to Mediterranean circulation	I–V (IV)	I–V	I–VI	VIII–IX	VII–IX	VII–X
3	Eastern and southeastern zone: *Mediterranean circulation influence*	II–V	II–VI	II–VI	VI–VIII	VII–IX	VII–IX
Yugoslavia							
1	North plain—low altitude: rainfall (snowmelt) origin	II–III	II–IV	II–V	VIII–X	VIII–X	VIII–X
2	Southeastern zone—Juzna Morava: rainfall–snowmelt origin	III–IV	II–IV	II–V	VIII–IX	VIII–X	VIII–X
3	Eastern zone: rainfall–snowmelt origin	III–IV	II–IV	II–V	VIII–IX	VIII–IX	VIII–X
4	Southwestern zone: rainfall–snowmelt origin	IV–V	IV–V	III–V	VIII–IX	VIII–IX	VIII–X
5	Central zone—Zapadna Morava: rainfall–snowmelt origin	III–IV	III–V	III–V	VIII–IX	VIII–X	IX–X
6	Southern zone—high altitude: rainfall–snowmelt origin	IV–V	IV–V	III–V	VIII–IX	IX–X	VIII–X
Greece							
1	Northern high altitude-temperate influence): rainfall–snowmelt origin	II–V	III–VI	III–VI	VIII–IX	VII–IX	VII–X
2	Central zone—Mediterranean influence: rainfall origin	XII–II	II–IV	III–IV	VIII–IX	VII–IX	VII–X
Switzerland (after *The Hydrological Atlas of Switzerland*)							
1	Glaciare A (66% glaciers)	VII–VIII	VII–VIII	VI–IX	I–II	I–II	I–II
2	Glaciare B (33% glaciers)	VI–VIII	VI–VIII	V–VIII	I–II	I–II	XII–III
3	Glacio-snowmelt A (17% glaciers)	VI–VII	VI–VIII	V–VIII	I–II	XII–II	XII–II
4	Glacio-snowmelt B (7% glaciers)	VI–VII	VI–VIII	V–IX	XII–III	XII–III	I–III
5	Snowmelt Glaciare	VI–VII	V–VII	V–VIII	I–III	I–III	I–III
6	*Snowmelt alpine*	V–VI	V–VII	IV–VIII	I–II	I–II	XII–II
7	Snowmelt of transition	IV–VII	IV–VIII	IV–VIII	I–II	XII–II	XII–III
8	Snowmelt–rainfall subalpine	IV–VII	IV–VII	III–VII	I–II	XI–II	XII–II
9	Rainfall origin (inferior and superior)	XII–III	XII–IV	XII–IV	VII–IX	VII–X	VII–X
10	Jura rainfall origin	XII–III	XII–IV	XII–IV	VII–X	VII–X	VII–XI
11	Jura snowmelt–rainfall origin	I–IV	XII–IV	XII–IV	VIII–X	VII–X	VII–X
12	Southern snowmelt origin	VI–VII	V–VII	V–VIII	I–III	I–III	XII–III

$$H = -\sum_{i=1}^{n} p_i \times \ln(p_i) \tag{1}$$

The entropy has the maximum value when $p_1 = p_2 \ldots = p_n$ (complete incertitude or instability of the regime) and minimum value when $\forall p_i = 1$ (complete certitude or

(a) ROMANIA

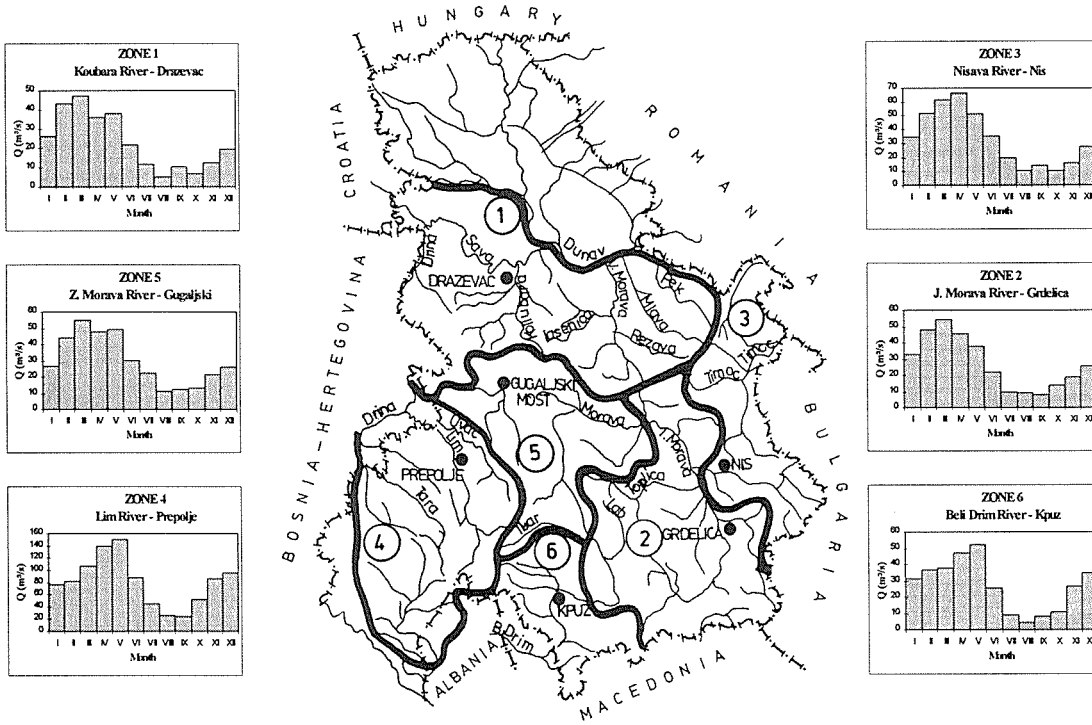

(b) YUGOSLAVIA

Fig. 4 Mapping of the river flow regime zones for Romania (a) and Yugoslavia (b).

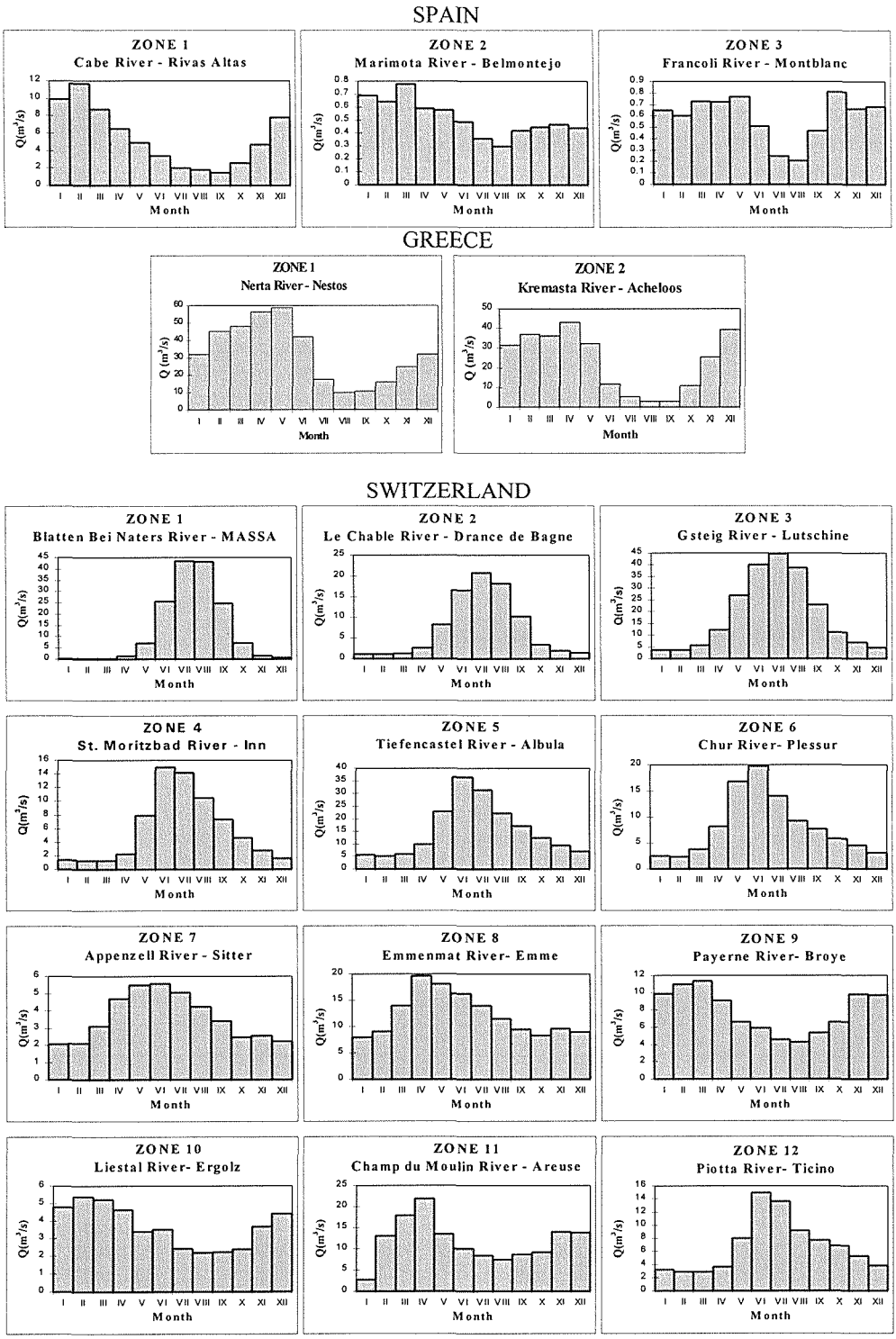

Fig. 5 Mean monthly flow defining several regimes types in Spain, Greece and Switzerland.

stability). Using property of addition of the entropy the sum of the entropies of each characteristic (total entropy) expresses the entropy of the flow pattern and therefore the degree of its stability. In equation (1) consider the values p_i of the percentage of years in the series having a certain regime type, and compute for each p_i the total entropy. In terms of this total the degree of stability of the flow pattern (river flow regime) is established (Table 3).

The total entropy computed for a certain pattern is then compared with the entropy corresponding to a particular value of p_i which results in establishing the degree of stability. In Table 4 the entropy and the stability of the river flow regimes established for each characteristic zone are presented.

Mention is made that very stable and stable types of regimes have been found in the high mountainous zones of Switzerland and Romania, where the feed in high flows from the melting of the glaciers and snow (which is significant as compared with the rainfall) occurs with some regularity in time and the low flows are strongly influenced by the river frost.

Relatively stable regimes have been found in the medium altitudes (ranging between 800 and 1200 m) from Romania, Spain and Switzerland where the rainfall feed caused by a particular atmospheric circulation has a more stable periodicity of occurrence.

Table 3 Regime stability character function of the entropy.

p_i	Character of the regime	Entropy
95%	Very stable	1.188
90%	Very stable	1.950
85%	Stable	2.536
80%	Stable	3.000
75%	Relatively stable	3.374
70%	Relatively stable	3.665
65%	Relatively stable	3.885
60%	Relatively unstable	4.038
55%	Relatively unstable	4.128
50%	Unstable	4.158

Table 4 Stability of the regime types for the considered countries from the FRIEND–AMHY area.

Zone	Entropy	p_i (%)	Stability	Zone	Entropy	p_i (%)	Stability
Romania				**Switzerland**			
1	3.852	66.0	Rel. unstable	1	1.340	94.0	Very stable
2	3.805	67.0	Rel. unstable	2	1.933	90.0	Very stable
3	3.659	71.0	Rel. stable	3	1.527	93.0	Very stable
4	3.847	66.0	Rel. unstable	4	1.129	95.5	Very stable
5	2.769	83.0	Stable	5	1.249	94.5	Very stable
6	4.158	50.0	Unstable	6	2.028	89.0	Stable
Spain				7	3.379	74.5	Rel. stable
1	3.194	77.0	Rel. stable	8	3.580	71.2	Rel. stable
2	3.365	74.5	Rel. stable	9	3.758	66.5	Rel. unstable
3	3.403	73.5	Rel. stable	10	3.487	73.0	Rel. stable
Greece				11	3.797	66.0	Rel. unstable
1	2.910	81.0	Stable	12	2.578	84.5	Stable
2	2.182	88.5	Stable				

Unstable and relatively unstable regimes are found in the low altitude zones where the flows originate from rainfall-snowmelt and when, during some winters with much snow, the earlier snowmelt in the spring time is not synchronous with the rainfall period (which is usually April–June).

CONCLUSIONS

- The significant variation in altitude of a zone or basin subject to the influence of a particular climate leads to a differentiation of several micro-types of flow regimes. If a zone is found under the control of the intersection of many atmospheric circulations the micro-regime is a result of their combination with the altitude influence.
- An appropriate index of the stability of a particular flow regime is the total entropy of the occurrence of the characteristics discriminating a flow pattern.

REFERENCES

Arnell, N., Oancea, V. & Oberlin, G. (1993) *European River Flow Regimes. A Contribution to "Europe's Environment 1993"*. Report to the European Environment Agency Task Force. CEMAGREF, Lyon, and Institute of Hydrology, Wallingford.

Diaconu, C. & Serban, P. (1994) *Synthesis and Regionalization in Hydrology* (in Romanian). Editura Tehnica, Bucharest.

Gottschalk, L., Jensen, J. L., Lundquist, D., Solantie, R. & Tollan, A. (1979) Hydrological regions in the Nordic countries. *Nordic Hydrol.* **10**, 273–286.

Krasovskaia, I. (1995) Quantification of the stability of the river flow regimes. *Hydrol. Sci. J.* **40**(5), 587–598.

Krasovskaia, I. & Gottschalk, L. (1992) Stability of river flow regimes. *Nordic Hydrol.* **23**, 137–154.

Shannon, C. E. & Weaver, W. (1941) *The Mathematical Theory of Communication*. University of Illinois Press, Urbana, USA.

Stanescu, V. A. (1967) *Danube between Bazias and Ceatal Izmail* (in Romanian). ISCH Press, Bucharest.

FRIEND'97—Regional Hydrology: Concepts and Models for Sustainable Water Resource Management
(Proceedings of the Postojna, Slovenia, Conference, September–October 1997). IAHS Publ. no. 246, 1997.

Spatial and temporal variability in European river flows and the North Atlantic oscillation

C. A. SHORTHOUSE & N. W. ARNELL
Department of Geography, University of Southampton, Highfield, Southampton SO17 1BJ, UK

Abstract Europe has recently experienced a number of extensive droughts and floods, raising concerns about the potential impacts of climate change. This paper explores the relationships between inter-annual climatic variability—as measured by the North Atlantic Oscillation Index (NAOI)—and spatial patterns of anomalous hydrological behaviour across Europe, using the FRIEND European Water Archive. Results show that in winters with a high NAOI, characterized by stronger than average westerly circulation patterns, river flows are above average in northern Europe, but below average in the south. Correlations are strong and statistically significant, and the spatial patterns are consistent with those in temperature and precipitation.

INTRODUCTION

Over the last few years, anomalous hydrological behaviour in Europe has caught the attention of water managers and scientists. Large parts of Europe have suffered drought, sometimes lasting several years, whilst other parts have experienced unprecedented large flows. Arnell (1994) demonstrated that seasonal runoff in Europe showed both non-random temporal patterns, and strong spatial patterns. He found that most of western Europe experienced the same types of hydrological anomaly, with the western part of Scandinavia showing a different pattern of variation. Also, years with above, or below, average seasonal runoff tended to cluster together, producing multi-year runs of anomalous behaviour.

This paper presents preliminary results from a spatial analysis of hydrological variability across Europe, focusing here on the links between the North Atlantic Oscillation—a characteristic of inter-annual climate variability in Europe—and hydrological response. The research uses data from the FRIEND European Water Archive, and is a contribution to the FRIEND project.

SPATIAL AND TEMPORAL VARIABILITY IN EUROPEAN HYDROLOGICAL BEHAVIOUR

Spatial and temporal patterns in European hydrological behaviour must be related to patterns in anomalous climatic behaviour. The weather of western Europe is dominated by westerly airflows, particularly the passage of depressions, whilst the continental part is more affected by stable anticyclonic conditions. The details of these controls, however, vary seasonally and from year to year. The most important features controlling European climate are the Icelandic Low and the Azores High. Their precise position and relative magnitudes affect the location and strength of westerlies, which are stronger in winter. Their ingress into the continent, however,

is prevented by high pressure over Siberia. In summer, pressure is less high over continental Eurasia, but the westerlies do not penetrate far to the east because they are weaker than during winter. Storm track positions are also affected by sea surface temperatures, and tend to be further north when sea surface temperatures in the North Atlantic are below average (Moene, 1986). Under some climatic conditions, a blocking anticyclone is created, most commonly over Scandinavia in spring, which diverts the normal eastward movement of depressions either to the northeast—considerably further north than usual—or to the southeast. The detailed anomalies, however, depend on the strength and position of the block.

Inter-annual variation in the strength and, to a lesser extent, position of westerlies is termed the North Atlantic Oscillation (NAO), which describes variations in the meridional pressure gradient across the North Atlantic. The NAO is characterized by the North Atlantic Oscillation Index (NAOI), a measure of the difference in standardized pressures between the Icelandic Low and Azores High (Hurrell, 1995). When the NAOI is high (the pressure gradient is greatest), westerlies are more powerful, penetrate further into Europe, and bring high temperatures and increased rainfall to northern Europe: this is particularly apparent during winter (Hurrell, 1995; 1996). When the NAOI is low, westerlies are weaker, winter temperatures are influenced more by the cold high pressure located over Eurasia, and precipitation is lower. Figure 1 shows the time series of the NAOI for winter (December, January, February), between 1865 and 1995. There are clear patterns in the index. The NAOI was persistently low during the early and mid 1960s—generally cold winters in western Europe—and since the late 1980s has been persistently high.

The El Niño Southern Oscillation (ENSO) is a well-studied feature of climate variability in the southern Pacific, which has documented teleconnections with climate anomalies across large parts of the southern hemisphere and around the Pacific (Glantz, 1996). ENSO signals have been found in various aspects of

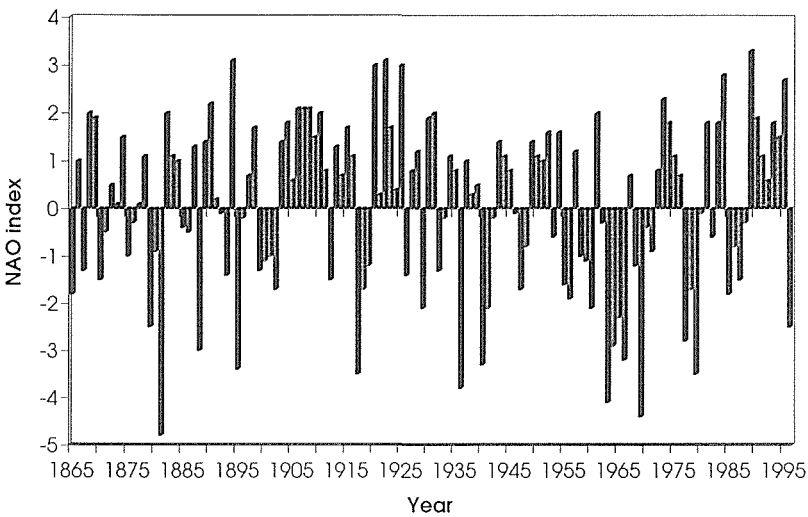

Fig. 1 Time series of the North Atlantic Oscillation Index, based of normalized sea level pressures (SLP) between Ponta Delagda, Azores and Stykkisholmur, Iceland from 1965 to 1995.

European climate (Fraedrich & Muller, 1992; Wilby, 1993; Fraedrich, 1994), although the direct effect of ENSO is small. In the winter following a warm ENSO event, for example, precipitation and temperature are higher than normal across western and central Europe, due largely to changes in depression tracks—although it is clearly very difficult to separate the ENSO signal from the NAO effect.

In recent years, several studies have explored the links between atmospheric anomalies and hydrological variability. Most studies have looked at relationships between ENSO variability and hydrological response in a few drainage basins (Dracup & Kahya, 1994; Kahya & Dracup, 1994; Ely *et al.*, 1994; Marengo, 1995; Mechoso & Iribarren, 1992; Waylen & Caviedes, 1990), and relatively few have explored the spatial hydrological response to atmospheric anomaly (Peterson *et al.*, 1987; Redmond & Koch, 1991). None of these studies have been in Europe. This paper focuses on the relationships between variability in the North Atlantic Oscillation and resulting spatial and temporal hydrological anomalies.

METHODS

Analysis was based on regional average monthly runoff series, derived from drainage basins on the European Water Archive, with regions defined as the FRIEND hydrometric areas. Initially, all basins with an area of less than 500 km^2, and with flow data between 1961 and 1990 were selected, resulting in a total of 477 selected basins. Many areas are relatively data poor, and parts of Europe were not represented by basins selected by this first procedure. A supplementary set of data was, therefore, selected with at least 20 years of data within the 1961-1990 period. This brought the total to 744 selected basins in a total of 233 hydrometric areas.

Regional flow indices were derived in order to investigate spatial patterns in flow anomalies across Europe. Firstly, monthly flow indices for the selected drainage basins were calculated by:

$$F_{ij} = \frac{X_{ij} - \overline{X}_j}{S_j}$$

where:

F_{ij} = index for year i and month j;

X_{ij} = monthly flow for year i and month j;

$\overline{X}_j$ = mean monthly flow for month j;

S_j = standard deviation of monthly flows, for month j;

in order to evenly weight the contribution of each basin to the mean regional index. These indices were then averaged to give a mean regional index, for each year and month, and for each hydrometric area. Seasonal indices for each area have also been derived based on seasonal flow data. These flow indices have been mapped, using the ARC/INFO GIS, to show spatial patterns in flow anomalies across Europe, and for different months and years.

The monthly and seasonal regional indices for all 233 areas were correlated against the NAOI, using the Pearson product moment correlation coefficient. Maps

of correlation and significance of correlation have been produced, for seasonal against seasonal and monthly against monthly data.

RESULTS

Figure 2 shows spatial patterns in flow anomalies across Europe, at two different times, with positive anomalies indicating above average flows, and negative anomalies defining below average flows. These two maps, and others not shown, set the stage for further analyses as they clearly show spatial patterns in flow anomalies at different times. These kind of maps produced describe the problem, that patterns in flow variability exist, and the reasons for which will be investigated in further analyses.

During January 1970 (Fig. 2(a)), it can be seen that different parts of Europe exhibit different flow anomalies at the same point in time. There is, in fact, a gradient in flow anomaly magnitudes across Europe during the month, with southern areas, especially Spain, experiencing high flows, in opposition with the low flows exhibited in the Nordic region. June 1976 (Fig. 2(b)), during a very significant European-scale drought, shows flows across most of Europe as being either low or very low, although a few areas in Norway and Sweden actually experienced relatively high flows at the time.

Figure 3 shows the correlation between winter (December, January, February) NAOI and winter regional runoff, and clearly shows strong spatial patterns across Europe. The values of the correlation coefficient are high in many areas, up to between -0.6 and -0.7 in parts of Spain, and between 0.6 and 0.7 in small areas of Norway. Northern parts of Europe reveal positive correlations with the NAO index, where flows are greater with higher NAOI. The Nordic region and the western UK and Ireland in particular, and also parts of Germany and The Netherlands, exhibit positive correlations. More southern areas, Spain and France in particular, show negative correlations with the NAOI resulting in lower flows when the NAOI is higher.

Even January against January correlations show distinct spatial patterns, and show a strong gradient of correlation, but with a slightly more northeast/southwest orientation. The region of positive correlation extends further into continental Europe than the winter/winter maps of correlation.

The significance of these winter correlations are presented in Fig. 4, which shows that Spain has the most significant negative associations, and Norway, Sweden and parts of Finland have the most significant positive associations with NAOI. There is a slight clustering of low, or insignificant relationships in France, in the middle of these two regions of strongly opposing association.

DISCUSSION

The results from these preliminary analyses show strong spatial patterns in the relationships between river flows, from right across Europe, and the NAOI. These findings are entirely consistent with the findings of Hurrell (1995; 1996), Hurrell &

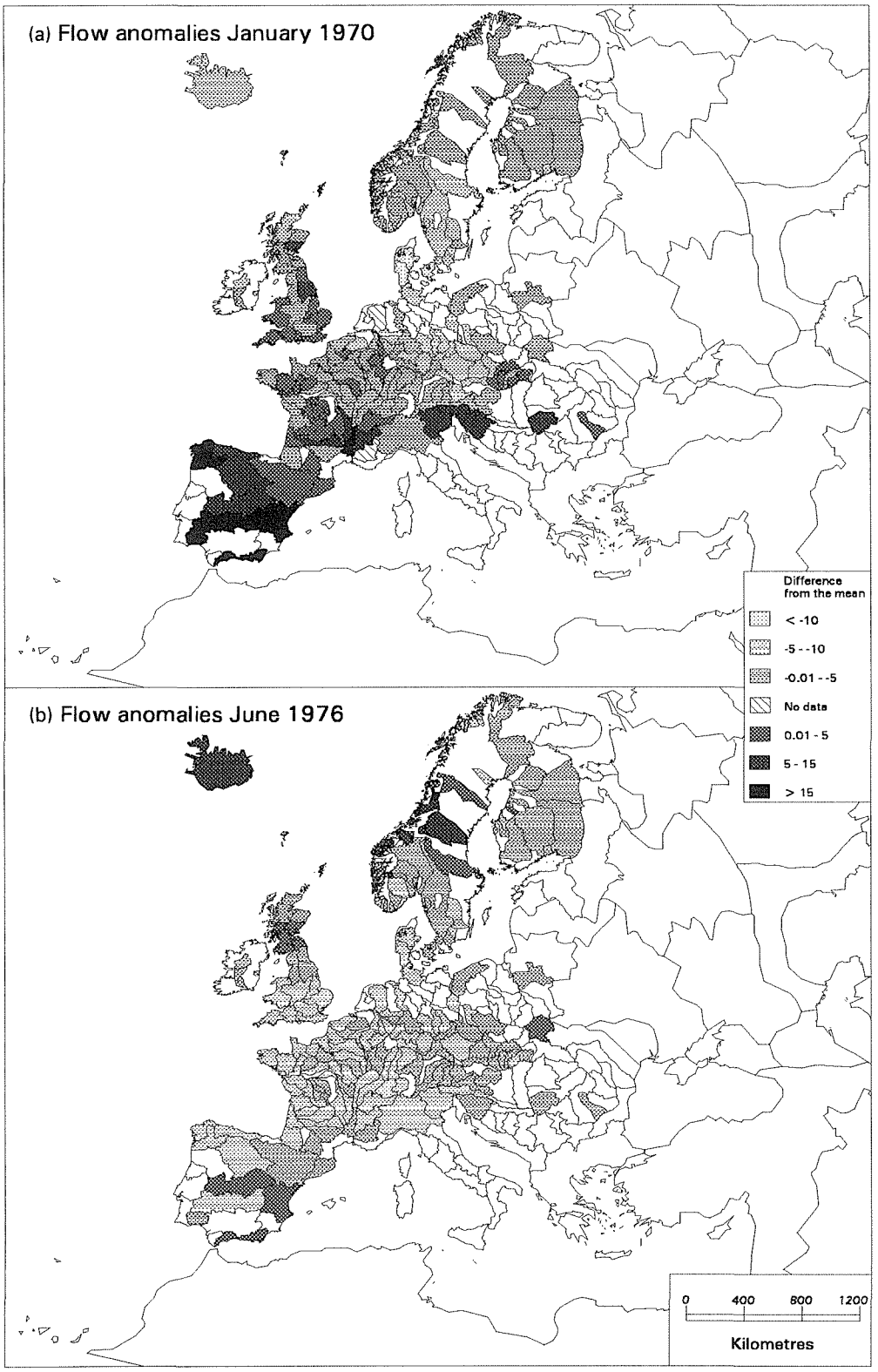

Fig. 2 Map to show flow anomalies for (a) January 1970 and (b) June 1976. Shadings show the values of the standardized flow indices, with zero representing the mean.

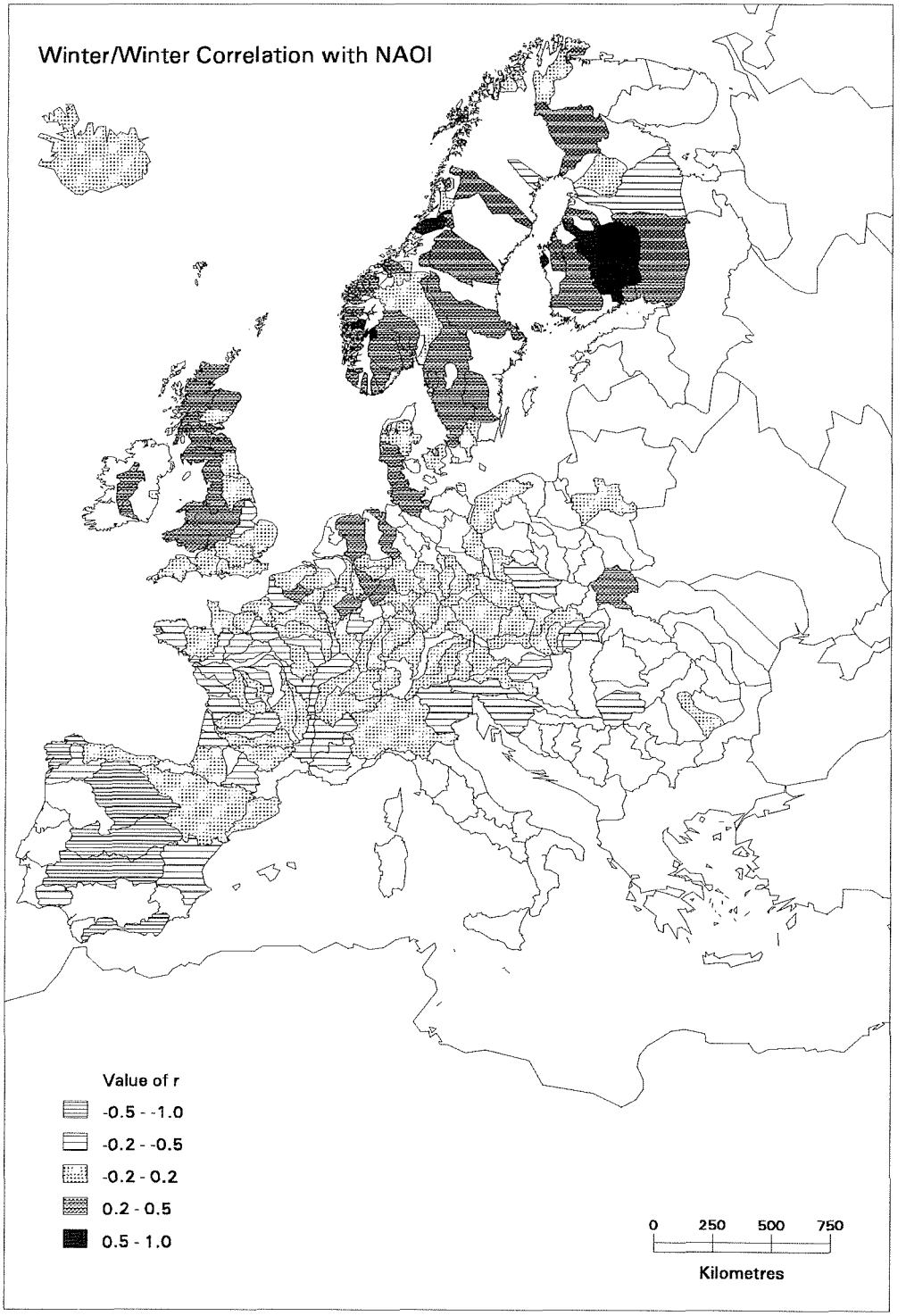

Fig. 3 Map to show winter against winter correlation between regional flow indices and NAOI. The value of *r* is shown.

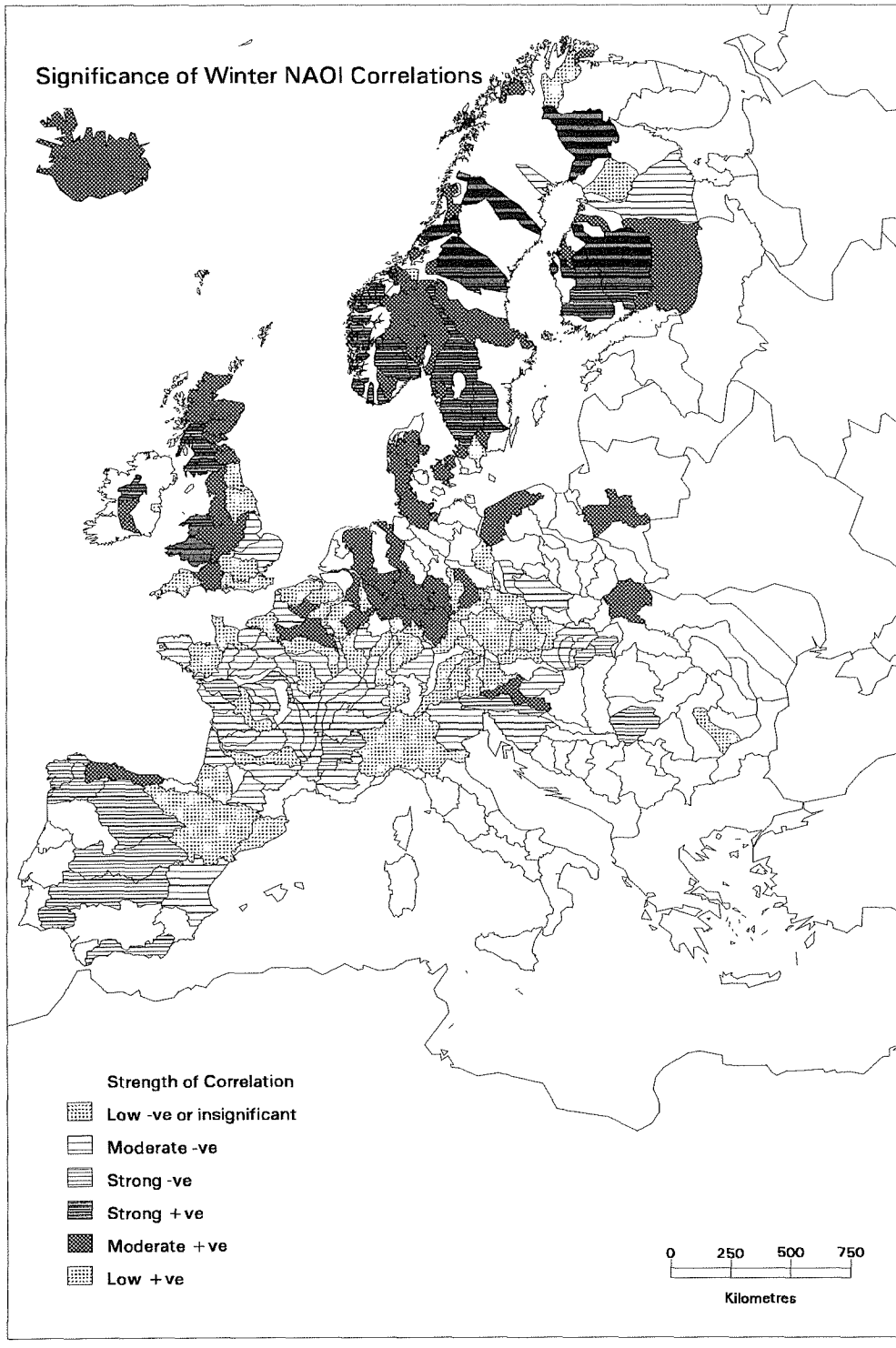

Fig. 4 Map to show the significance of the computed winter against winter correlations. Low significance equates to the 0.8, or below, level of significance, moderate is up to 0.02 significance and highly significant relates to a 0.02 or 0.01 level of significance.

van Loon (in press) and Wilby *et al.* (in press), who were concerned with temperature and precipitation.

Changes in circulation patterns over the North Atlantic lead to changes in temperature and precipitation across Europe. These changes are also reflected in runoff patterns across Europe, and these patterns have a strong spatial component. When the NAOI is high, westerlies are stronger, which is particularly apparent during winter, due to the associated low pressure anomalies in the region of the Icelandic low and anomously high pressures across the subtropical Atlantic. During periods of high NAOI, the axis of maximum moisture transport shifts to a more southwest-to-northeast orientation across the Atlantic, and extends much further to the north and east on to northern Europe and Scandinavia. This brings about enhanced rainfall over northern Europe and Scandinavia whilst a significant reduction of the total atmospheric moisture transport occurs over parts of central and southern Europe, and the Mediterranean. During periods of low NAOI, westerlies are weaker and therefore the climate is more influenced by Eurasian high pressure, bringing about colder and drier winter conditions in northern Europe.

CONCLUSIONS

European river flows vary over both space and time. It has been shown here that European river flows are strongly correlated, most particularly in winter, with the North Atlantic Oscillation and that this relationship exhibits a strong spatial pattern. northern European river flows, particularly in the Nordic region, tend to be positively correlated with the NAOI, and rivers in southern Europe reveal negative correlations with the index. This is consistent with the previously explored correlations between the NAO and precipitation.

This paper presents preliminary results, indicating the nature of the associations between atmospheric circulation and river flows in Europe, for part of the year. Further work is required in explaining the nature of the relationship during spring, summer and autumn, and in examining correlations between sea surface temperature anomalies, Gulf Stream position, upper atmosphere characteristics (such as Jetstream position), mean storm track position and ENSO, on the one hand and hydrological anomalies on the other. The effect of catchment characteristics, principally geology, on the links between atmospheric and hydrological anomalies will also be explored.

Acknowledgements This work is a contribution to the Northwest European FRIEND project and uses data from the European Water Archive. The NAOI data was provided by Dr J. Hurrell, at NCAR. Caroline Shorthouse is a NERC funded research student, co-supervised by Dr Nigel Arnell and Dr Alan Gustard (Institute of Hydrology, Wallingford, Oxfordshire, UK).

REFERENCES

Arnell, N. W. (1994) Variations over time in European hydrological behaviour: a spatial perspective. In: *FRIEND: Flow Regimes from International Experimental and Network Data* (ed. by P. Seuna, A. Gustard, N. W. Arnell & G. A. Cole), 179-184. IAHS Publ. no. 221.

Dracup, J. A. & Kahya, E. (1994) The relationships between U.S. streamflow and La Niña events. *Wat. Resour. Res.* **30**, 2133-2141.

Ely, L. L., Enzel, Y. & Cayan, R. (1994) Anomalous North Pacific atmospheric circulation and large winter floods in the southwestern United States. *J. Climate* **7**, 977-987.

Freadrich, K. (1994) An ENSO impact on Europe: a review. *Tellus* Series A*: Dynamic Meteorology and Oceanography* **46**, 541-552.

Fraedrich, K. & Muller, K. (1992) Climate anomalies in Europe associated with ENSO extremes. *Int. J. Climatol.* **12**, 25-31.

Glantz, M. H. (1996) *Currents of Change: El Niño's Impact on Climate and Society*. Cambridge University.

Hurrell, J. W. (1995) Decadal trends in the North Atlantic Oscillation: regional temperature and precipitation. *Science* **269**, 676-679.

Hurrell, J. W. (1996) Influence of variations in extratropical wintertime teleconnections on Northern Hemisphere temperature. *Geophys. Res. Lett.* **23**, 665-668.

Hurrell, J. W. & van Loon, H. (in press) Decadal variations in climate associated with the North Atlantic Oscillation. *Weather*.

Kahya, E. & Dracup, J. A. (1994) The influence of Type 1 El Niño and La Niña events on streamflows in the Pacific Southwest of the United States. *J. Climate* **7**, 965-976.

Marengo, J. A. (1995) Variations and change in South American streamflow. *Climatic Change* **31**, 99-117.

Mechoso, C. R. & Iribarren, G. P. (1992) Streamflow in southeastern South America and the Southern Oscillation. *J. Climate* **5**, 1535-15359.

Moene, A. (1986) Associations between North Atlantic sea surface temperature anomalies, latitude of the polar front zone, and precipitation over northwest Europe. *Mon. Weath. Rev.* **114**, 636-643.

Peterson, D. H., Cayan, D. R., Dileo-Stevens, J. & Ross, T. G. (1987) Some effects of climatic variability on hydrology in western North America. In: *The Influence of Climatic Change and Climatic Variability on Hydrologic Regime and Water Resources* (ed. by S. I. Solomon, M. Beran & W. Hogg), 45-62. IAHS Publ. no. 168.

Redmond, K. T. & Koch, R. W. (1991) Surface climate and streamflow variability in the western United States and their relationship to large-scale circulation indices. *Wat. Resour. Res.* **27**, 2381-2399.

Waylen, P. R. & Caviedes, C. N. (1990) Annual and seasonal fluctuations of precipitation and streamflow in the Aconcagua River basin, Chile. *J. Hydrol.* **120**, 79-102.

Wilby, R. L. (1993) Evidence of ENSO in the synoptic climate of the British Isles since 1880. *Weather* **48**, 234-239.

Wilby, R. L., O'Hare, G. O. & Barnsley, N. (in press) The North Atlantic Oscillation and British Isles climate variability. *Weather*.

FRIEND'97 — Regional Hydrology: Concepts and Models for Sustainable Water Resource Management
(Proceedings of the Postojna, Slovenia, Conference, September–October 1997). IAHS Publ. no. 246, 1997.

Historical runoff variation in the Nordic countries

LARS A. ROALD, HEGE HISDAL
Norwegian Water Resources and Energy Administration, PO Box 5091 Majorstua, N-0301 Oslo, Norway

TAPANI HILTUNEN, VELI HYVÄRINEN
Finnish Environment Agency, Helsinki, Finland

TORBJØRN JUTMAN
Swedish Meteorological and Hydrological Institute (SMHI), Norrköping, Sweden

KRISTINN GUDMUNDSSON, PÁLL JONSSON
Orkustofnun, Reykjavik, Iceland

NIELS BERING OVESEN
National Environmental Research Institute (DMU), Silkeborg, Denmark

Abstract The regional variability of the runoff in the Nordic countries has been examined by analysing 160 long-term series of daily discharge. The study area was grouped into 13 regions with similar temporal behaviour of the annual runoff. Index series were developed for each region. The series were tested for trend and jumps. An increase has been found in southwest Norway and in Denmark, especially since 1980. Series from southern Sweden show a decrease at the same time. The increase in the maritime exposed areas are most significant in the autumn and early winter. The behaviour of the runoff series has been compared to the behaviour of selected precipitation series. The increase in runoff in southwest Norway is reflected in a similar increase in the precipitation in the same period.

INTRODUCTION

Based on scenarios of future temperatures and precipitation and a modified rainfall–runoff model, simulation experiments indicate changes in the runoff regime of the Nordic countries as shown by Sælthun *et al.* (1994). A rise in the temperature will reduce the accumulation of snow, which has a dominating effect on the present seasonal regime. The effects should be possible to identify in the long-term time series of runoff data.

The long-term variation of the runoff has been examined in a number of national studies by Roald & Sælthun (1990), Jutman (1991), and Hiltunen & Hyvärinen (1992). Lindstrøm (1993) has studied trends in floods in Sweden. Long-term variability in meteorological time series has been studied by Aune (1989), Førland & Bauer (1992), Alexandersson & Eriksson (1989), Frich (1990) and Heino (1994). Hiltunen (1994) has shown that long periodic fluctuations in runoff in Finland are linked to changes in precipitation and evaporation. Tveito & Hisdal (1994) have compared long homogeneous time series of precipitation and runoff to identify variation in time and space. Clark *et al* (1992) have studied trends in precipitation, evaporation and runoff from nine catchments in Denmark. This paper summarizes results of an ongoing study by the Hydrological Institutions in the Nordic countries (Hisdal *et al.*, 1995, 1996). WMO (1988) has also done a regional study on long-term variability of the runoff.

DATA

The Norwegian Water Resources and Energy Administration, NVE, serves as a regional data centre for the Nordic countries in FRIEND-NE. A subset of the FRIEND database has been implemented as an extension of the national Norwegian hydrological database. The selection of data from the Nordic countries was supplemented with daily flow data from a number of long-term stations, mostly from larger basins than in the original FREND database, resulting in a Nordic data set of 160 stations long-term data series. Data was also obtained from Estonia, Greenland and the Faeroe Islands. The data series from Greenland and the Faeroe Islands were, however, too short and too incomplete to be applicable to this study.

Some of the data series are unaffected by reservoirs or diversions for hydropower production or other human activities. These data series were considered as suitable for study of the seasonal variability as well as the extremes. For other series affected by regulations, naturalized flow series have been calculated. These series were considered suitable for study of the seasonal variability, but not for study of the extremes. Some series are affected by reservoirs, but not by diversions in or out of the upstream basin. Because very few reservoirs operate as buffers over several years, these series were considered suitable for analysis of annual values. The data set was thus divided into three quality categories according to their suitability for analysis of extremes, seasonality and annual values.

A map showing the location of the gauging stations included in the study is shown in Fig. 1. The part of the database used in this study is summarized in Table 1.

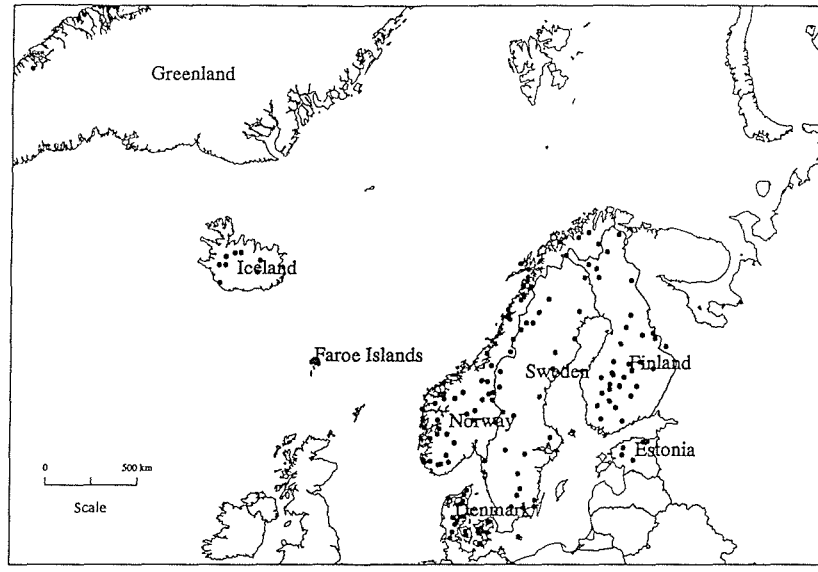

Fig. 1 Map of the study area. The centre points of the basins for the stations included in the study are shown on the map.

Table 1 Summary of the discharge series on the Nordic FRIEND database.

Country	No. of series	Record length (years)	Quality category: 1	2	3
Denmark	25	41–75	23	2	
Estonia	5	47–67	5	-	
Faroes	6	4–11	6	-	1
Finland	34	41–144	25	-	9
Greenland	2	10–13	2	-	
Iceland	7	40–61	6	1	
Norway	55	41–111	47	6	2
Sweden	25	68–152	18	2	5

Quality categories are:
1. Annual values, seasonal values and extremes,
2. Annual and seasonal values and
3. Annual values only.

Some series were later discarded because of unsatisfactory record lengths or because of suspicion of inhomogeneities in the series.

REGIONALIZATION

The study area was divided into 13 regions with similar behaviour of the annual runoff based on the following procedure (Arnell *et al.*, 1989):

(a) Calculation of annual values.
(b) Standardization of each series in order to remove scale effects due to differences in the size of the drainage basin. Each annual series was standardized by subtracting the long-term mean value and by division by the long-term standard deviation.
(c) Identify spatially coherent groups of series with similar temporal behaviour based on the cross-correlations between the series.
(d) For each region an index series was derived based on the annual values expressed as percentages of the long-term average of each series. The regional mean value was calculated by averaging the percentages for all series within the region for each year. Since the individual series comprising a region was of different length, a correction was applied. This correction was based on two averages: The average for the common period of all series in the region and the average for the common period of the series for the specific year.

The resulting regionalization is summarized in Table 2.

The timing and degree of the snowmelt contribution to the seasonal cycle differ from basin to basin and from region to region. One or two "typical" series were therefore chosen for each region as basis for an analysis based on seasonal and extreme values. Each of the selected typical series was analysed for four seasons, based on a division of the year into seasons, depending on the seasonal regime in each region.

STATISTICAL ANALYSES

The following analyses were applied to the regional index series and the seasonal runoff series: Visualization of the general behaviour by Gauss filtering, as shown in

Table 2 Summary of the regionalization.

Region	Name	No. of series	First year*	Last year
I	Iceland	6	1947	1991
II	Northwest Norway	25	1901	1991
III	Southwest Norway	9	1892	1991
IV	Central Scandinavia	15	1872	1991
V	Northern Finland, Sweden and northeast Norway	8	1911	1991
VI	Central and southern Finland	29	1871	1991
VII	Estonia	5	1922	1989
VIII	Southeast Norway and Central Sweden	20	1871	1991
IX	Southern Sweden	7	1871	1991
X	Eastern Denmark	13	1918	1991
XI	Western Denmark	12	1918	1991
XII	Glaciers Iceland	2	1939	1991
XIII	Glaciers Norway	2	1900	1991

* This is normally the first year of the longest series. Some series start earlier (1847 in Region VI, 1807 in Region VIII and 1858 in Region IX), but have not been included in the analysis.

Fig. 2. The following trend tests were applied: Spearmann and Mann test. Schumann (1994) has developed a jump test based on split sample techniques to identify sudden shifts in a time series. The jump test includes: (a) Mann-Whitney-Wilcoxon (rank) test, (b) chi-square test (on the assumption of normal or log-normal distribution), (c) *F*-test (on differences of the variances), and (d) *t*-test (on differences of the mean). The non-randomness of the index series was examined by the run test and by calculating the autocorrelations. A significance level of 5% was chosen for all tests.

RESULTS

The regional annual index series are shown in Fig. 3 for all the regions. Figure 4 summarizes the regional distribution of changes in the annual runoff for the period

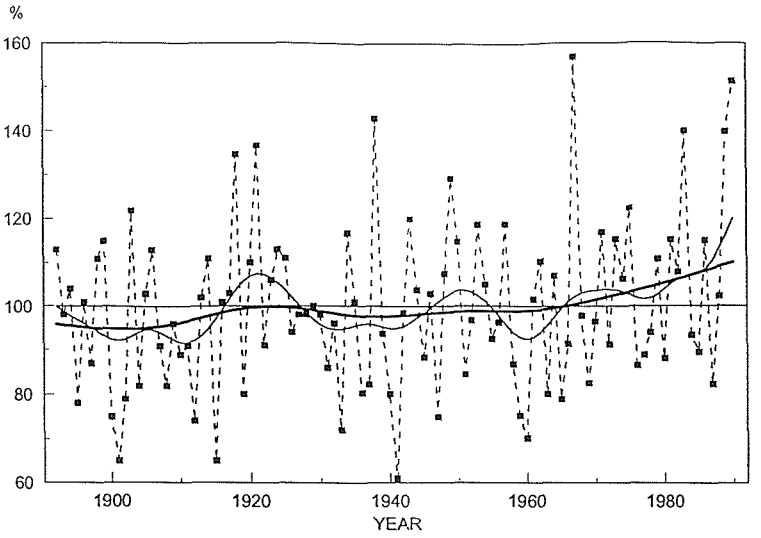

Fig. 2 The regional series from region III, southwestern Norway. The runoff is given as percentage of the long-term mean value. Broken lines: Yearly mean values, thin solid lines: Filtered values, filter width approximately 9 years, thick solid lines: filter width approximately 27 years.

1930–1980. The seasonal index series for the autumn are shown in Fig. 5. Figure 6 summarizes the regional distribution of changes for all four seasons.

The only region with a significant trend for the annual index series is region IX—southern Sweden. This decreasing trend is also significant for all the seasons. The positive trend in region III—southwest Norway and in region XI and X—Denmark is not significant for annual values, but is strongly significant from 1960 onwards. The positive trend in the autumn series is significant for region III and significant for all seasons in region XI. The jump test indicates a clustering of positive jumps from 1960 to 1980, with negative jumps in earlier periods. Combining the results of the trend test, the jump test and the Gauss filtered values, we conclude that the runoff has increased in regions III, XI and X, and has decreased for region IX and XI. The runoff in Iceland seems to decrease when it is increasing in other parts of the study area. The higher flow values at the start and at the end of

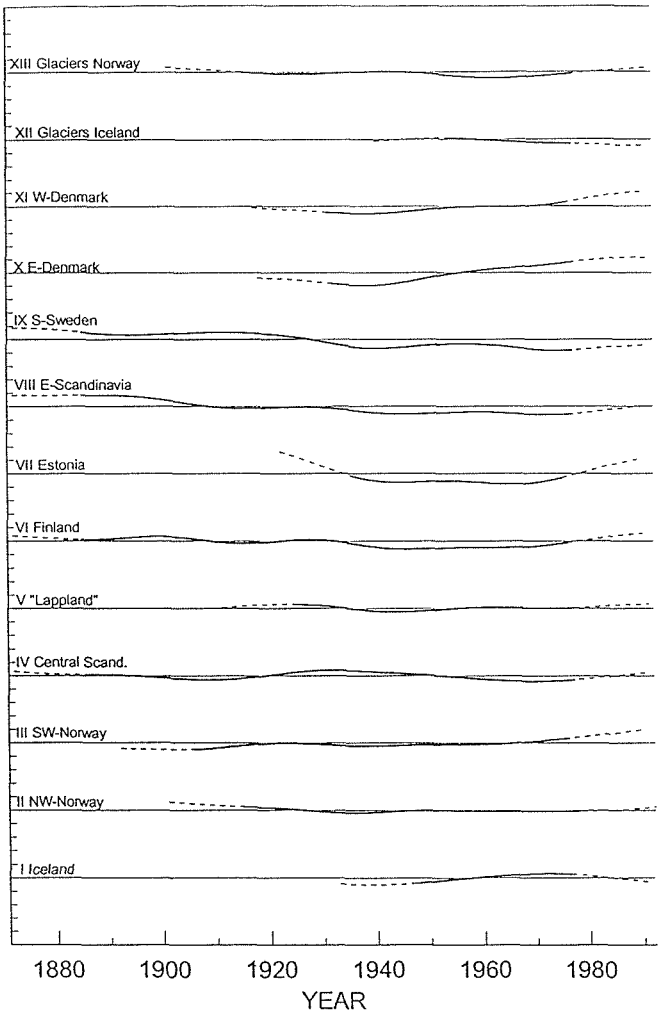

Fig. 3 Gauss filtered regional series (filter width approximately 27 years) for all regions.

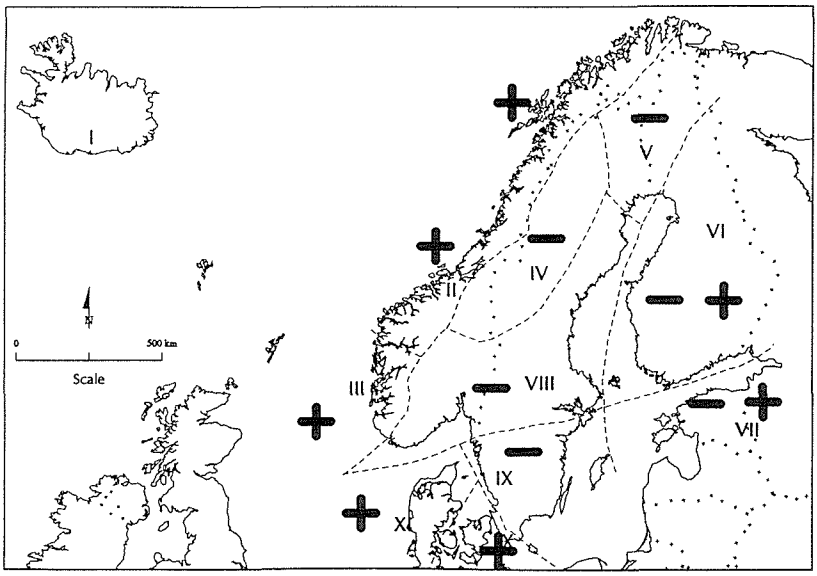

Fig. 4 Map showing regional trends in the annual series for the period 1930–1980. The delimitation between the various regions is also shown in the map. The trends indicated in the various regions is based both on results of the trend analysis and the jump test.

the period for Estonia seems also to be present in some degree in series from Finland. This pattern is also found in Russia by Semyonov & Alexeyeva (1994).

COMPARISON WITH METEOROLOGICAL TIME SERIES

A number of long-term monthly precipitation and temperature series has been

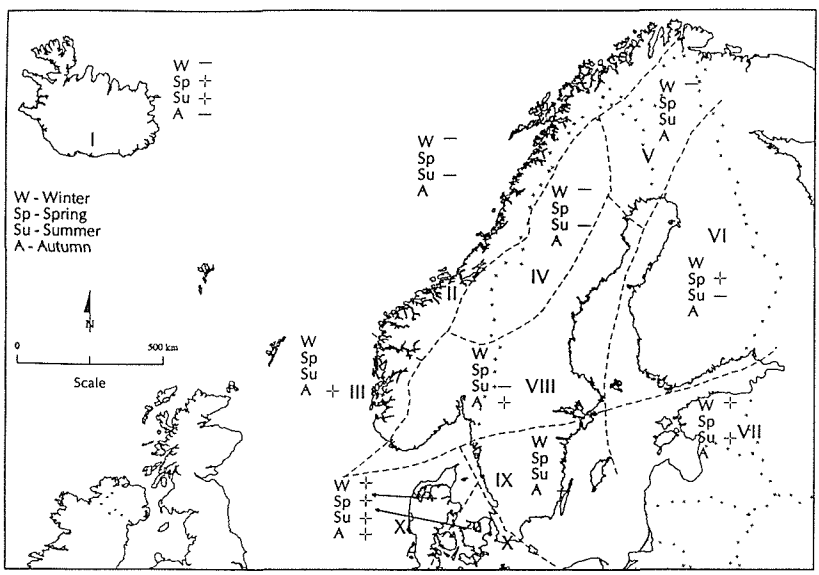

Fig. 5 Map showing seasonal trends for the period 1930–1980. W: winter, Sp: spring, Su: summer, A: autumn. Increasing seasonal runoff +, decreasing seasonal runoff –.

selected and added to the database. The series were selected to be representative for the basins of the "typical" series. For the Finnish basins area precipitation series were obtained, otherwise the series were observed at locations within or near each basin. Some of these series have been homogenized. Linear trends were fitted to the precipitation and runoff series in order to quantify the magnitude of the trends for two standard periods: (1921–1990) and (1960–1990). The series were also tested for jumps for the same periods. The results have been compared, and the results are summarized in Table 3. The difference between observed precipitation and runoff was also examined. For Iceland and Norway the specific runoff expressed in mm per year exceeds the observed precipitation considerably, in particular in the mountainous areas, where the precipitation stations are located at low altitudes.

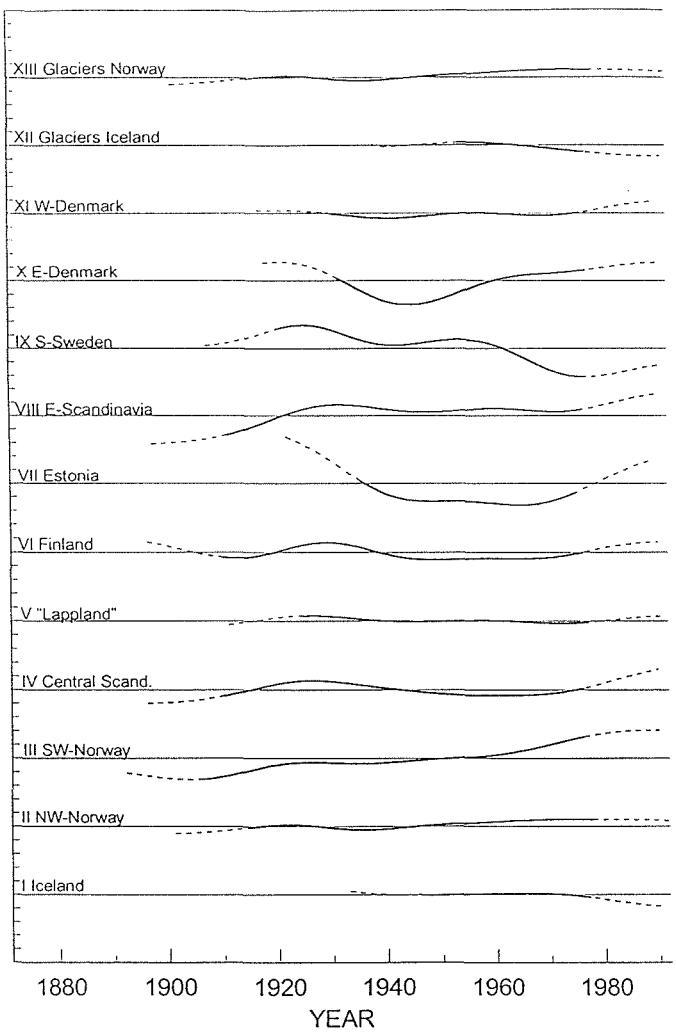

Fig. 6 Gauss filtered regional series (filter width approximately 27 years) for the autumn season.

Table 3 Summary of the comparison of trends and jumps in the precipitation and runoff series.

Period	No. of series	No. of series with matching trends*	Significant trends either parameter	Matching jumps
1921–1990	15	8	7	
1961–1990	28	17	7	13

* Not necessarily significant.

DISCUSSION

A regional index series will be smoother than the individual index series within the region. Since few series are contributing to the early part of the series, compared to the latter, this smoothing will be most pronounced towards the end of the series. By applying trend tests, it is expected that there will be a less significant trend than by analysis of single series. The results do not indicate that a linear trend is a realistic model for describing the variability of the time series. Trend analysis is dependent on the start and end value of the series under consideration. By simply moving the period one year, the sign of a linear trend can be reversed as shown by Jutman (1991). The seasonal analysis is based on "typical" series, where man-induced redistribution of the seasonal flow is not expected to occur. Trends occur more significant in these series, and this reflects to some degree real seasonal redistribution, but some noise will be generated by the procedure of splitting the year into fixed seasons.

By looking at the longest series within the data set we see that each series comprises humid periods with spells of dryer years in between. The humid periods are often characterized by more floods and droughts than in other parts of the series. In southern Norway and Sweden, such a spell can be found in the 1860s and into the 1870s, from the mid 1920s to 1940 and from the 1980s. Comparison of dry and wet spells in different regions, demonstrates that a wet spell in one region is frequently accompanied by a dry spell in a region on the other side of a mountain range. The run test indicates significant non-randomness in regions I, II, VII, VIII, IX and XI. The autocorrelations of the regional series differ from region to region, but few significant autocorrelations have been found. The jump test indicates that the shift from a humid period to a dry period, occurs as one or more jumps rather than as a gradual trend. A possible explanation of this may be found in a change of the general circulation over the study area, a topic which is studied by Førland (ed., 1996). The Scandinavian Peninsula is characterized by mountain ranges to the west, with lowland to the east. A small change in the circulation can therefore easily lead to significant changes in the precipitation and runoff as found in this study.

The analysis of annual precipitation series for standard periods of 1921–1990 and 1961–1990 indicates that the recent trend occurring in the flow in west Norway is reflected in the trends of the seasonal series of the annual precipitation. Most regions did not have significant trends in the runoff. The lack of similarity in the trends is also caused by lack of representativity of the precipitation station selected for the study. Some basins are quite large (up to 68 000 km^2). One or two precipitation stations are obviously insufficient to define an index of the area precipitation for such basins. The precipitation series may also be affected by changes in exposure and measuring procedures over time. The Norwegian meteorological institute has applied

corrections to homogenize a number of long series, but there may still be inhomogenities in the series. The flow series does also most likely contain some inhomogenities because of gradual land use changes and errors in the rating curves. Hanssen-Bauer *et al.* (1996) have shown that the measuring error of precipitation is likely be reduced by increasing temperatures. The loss caused by catch deficiency is considerably higher for snow than for rainfall. This could result in false trends in precipitation series.

The annual runoff is not only dependent on precipitation but also on the evapotranspiration, which is likely to have more effect in the eastern drier lowland. Examples of this have been found in eastern Sweden. This is expected to be more related to the air temperature in the warm season. The study includes also some basins with a considerable fraction of glaciers. The annual discharge is also more dependent on the temperature of the melting season for these series. The dependencies on the temperature will be examined in the next phase of the project.

CONCLUSION

The long-term variability of number of long-term runoff series from the Nordic countries has been analysed. Based on annual flow indices, 13 regions with similar temporal flow patterns have been identified for the study area. Although a significant long-term trend has been found for only one regional series of annual values, clear regional patterns can be identified for parts of the study area, in particular the western part where a rise has occurred in recent years. Similar increases have also been noted for series in parts of UK, Arnell *et al.* (1990), in the Netherlands and in the Rhine basin.

By analysis of seasonal averages of "typical" series more significant trends can be found. There are some indications of a seasonal redistribution of the flow with a significant increase in autumn flow, in particular in southwest Norway and in western Denmark which can be explained by a similar increase in the precipitation.

Acknowledgement The project has been funded by the research project: EM 1991:8—Climate Change and Energy Production and by the participating institutions as a part of the Nordic Hydrological Programme. The authors would like to thank to their respective institutions for providing data and the meteorological institutes in Finland, Iceland and Norway for providing long-term temperature and precipitation series. Acknowledgement is also given to Astrid Voksø for producing the maps.

REFERENCES

Alexandersson, H. & Eriksson, B. (1989) Climate fluctuations in Sweden 1860–1989. *SMHI RMK. no. 58, Norrköping, Sweden.*

Arnell, N. W., Gustard, A., Roald, L. A, Demuth, S., Lumadjeng, H. S. & Ross, R. (1989) *Flow Regimes from Experimental and Network Data.* Vol. I: *Hydrological Studies*, 50–57 and 114–117. Institute of Hydrology, Wallingford, UK.

Arnell, N. W., Brown, R. P. C. & Reynard, N. S. (1990) Impact of climate variability and change on river flow regimes in the UK. *Report no. 107, Institute of Hydrology, Wallingford, UK.*

Aune, B. (1989) Air temperature and precipitation in Norway. Variations during the period of instrumental observations (in Norwegian). *DNMI-Report no. 26/89, Oslo, Norway.*

Clark, D. R., Olesen, J. E., Mikkelsen, H. E., Clausen, S. U. & Waagepetersen, J. (1992) Historical trends in precipitation, evapotranspiration, and runoff from nine Danish catchments. *Landbrugsministeriet—Statens Planteavlsforsøg, Tidsskrift for Planteavls Specialserie, Beretning ne. S 2177-1992, Denmark.*

Frich, P. (1990) Changes in the Danish climate from 1931–60 to 1961–90 (in Danish). *Vejret* **44**, 12–19.

Førland, E. J. & Hanssen-Bauer, I. (1992) Analysis of long precipitation series (in Norwegian). *DNMI-Report no. 01/92, Oslo, Norway.*

Førland, E. J. (ed.) Alexandersson, H., Frich, P., Hanssen-Bauer, I., Heino, R., Helminen, J., Jónsson, T., Nordli, P. Ø., Pálsdottir, T., Schmidt, T., Tuomenvirta, H. & Tveito, O. E. (1996) REWARD: "Relating Extreme Weather to Atmospheric circulation using a Regionalized Dataset". *Progress Report 01.01.1996–30.09.1996. DNMI-Report no. 30/96 KLIMA, Oslo, Norway.*

Hanssen-Bauer, I.., Førland, E. J. & Nordli, P. Ø. (1996) Measured and true precipitation at Svalbard. *DNMI-Report no. 31/96 KLIMA, Oslo, Norway.*

Heino, R. (1994) Climate in Finland during the period of meteorological observations. *Finnish Meteorological Institute, Contributions no. 12, Helsinki, Finland.*

Hiltunen, T. & Hyvärinen, V. (1992) Evaluation of changes in hydrological time series. *Publications of the Academy of Finland 3/92, Helsinki, Finland.*

Hiltunen, T. (1994) What do hydrological time series tell about climate changes? *Publications of the Water and Environment Research Institute, National Board of Waters and the Environment, no 17, Helsinki, Finland*, 37–50.

Hisdal, H., Erup, J., Gudmundsson, K., Hiltunen, T., Jutman, T., Ovesen, N. B. & Roald, L. A. (1995) Historical runoff variations in the Nordic countries. *Nordic Hydrological Programme, NHP Report no. 37, Oslo, Norway.*

Hisdal, H., Erup, J., Hyvärinen, V., Jónsson, P., Jutman, T., Ovesen, N. B. & Roald, L. A. (1996) The dependence of runoff on precipitation. In: *Nordic Hydrological Conference 1996. Nordic Hydrological Programme, NHP Report no. 40, Reykjavik, Iceland,* 369–378.

Jutman, T. (1991) Analysis of runoff trends in Sweden (in Swedish). *SMHI Hydrologi no. 30, Norrköping, Sweden.*

Lindström, G. (1993) Floods in Sweden—trends and occurrence. *SMHI TH no. 6, Norrköping, Sweden.*

Roald, L. A. & Sælthun, N. R. (1990) Long-term variations in Norwegian runoff (in Norwegian). *NVE-notat, Oslo, Norway.*

Schumann, A. (1994) Description of the "Jump3" programme. Internal Pap. Ruhr-Universität, Bochum, Germany.

Semyonov, V. A. & Alexeyeva, A. K. (1994) Regional particulars of the rivers in Russia and adjacent Eurasian areas. In: *FRIEND: Flow Regimes from International Experimental and Network Data* (ed. by P. Seuna, A. Gustard, N. W. Arnell & G. A. Cole) (Proc. Braunschweig Conference, October 1993), 193–149. IAHS Publ. no. 221.

Sælthun, N. R., Bergstrøm, S., Thomsen, T. & Vehviläinen, B. (1994) Simulation of climate change impact on runoff in the Nordic countries. Part B—climate and runoff scenarios. In: *Nordic Hydrological Conference 1994, NHP-Report no. 34, Copenhagen, Denmark*, 13–26.

Tveito, O. E. & Hisdal, H. (1994) A study of regional trends in annual and seasonal precipitation and runoff series. *NVE, Report no. 09-94, Oslo, Norway.*

WMO (1988) Analysing long time series of hydrological data with respect to climate variability. Project description. *WMO/TD-no. 224.*

FRIEND'97 — Regional Hydrology: Concepts and Models for Sustainable Water Resource Management
(Proceedings of the Postojna, Slovenia, Conference, September–October 1997). IAHS Publ. no. 246, 1997.

Temporal variability in the hydrologic regimes of the United States

E. F. HUBBARD
US Geological Survey, 415 National Center, Reston, Virginia 20192, USA

J. M. LANDWEHR
US Geological Survey, 431 National Center, Reston, Virginia 20192, USA

A. R. BARKER
US Geological Survey, 415 National Center, Reston, Virginia 20192, USA

Abstract Discharge records where flows have not been subject to overt anthropogenic controls have been identified for over 1500 streamflow gauging stations throughout the United States in the US Geological Survey Hydro-Climatic Data Network. These stations fall within all 21 water resources regions of the United States. Analysis of runoff in 20 regions, where long-term daily records are available, shows an increasing trend in 16 regions. Further analysis using a stratified subset of 65 sites shows an increase in baseflow at approximately 90% of the sites during the past 50 years, regardless of the size of the drainage area. Because anthropogenic alterations of watershed characteristics cannot explain these hydrologic changes, then meteorological or climatic forces are implicated.

INTRODUCTION

The purpose of this paper is to show the temporal variation in the surface-water resources of the United States over the last century, the period in which the US Geological Survey has maintained records of streamflow. Both average runoff and baseflow are examined for trends.

Water resources regions

The United States is divided into 21 major geographic areas, or regions (Fig. 1). The regions, which are hydrologic divisions based on topography, encompass the drainage areas of major rivers or the combined drainage areas of a series of smaller rivers. Eighteen regions (1–18) define the conterminous United States. Alaska is region 19; the Hawaiian Islands are region 20; and Puerto Rico and outlying Caribbean Islands are region 21.

Hydro-Climatic Data Network

The Hydro-Climatic Data Network (Slack *et al.*, 1993) is a database of continuous-records of streamflow that are suitable for climatic analyses. The network is comprised of 1659 active and discontinued streamgauges throughout the United States that are relatively free of anthopogenic influences. The database contains over 73 000 station water years of daily mean discharges. Figure 2 shows the distribution of Hydro-Climatic Data Network sites across the United States.

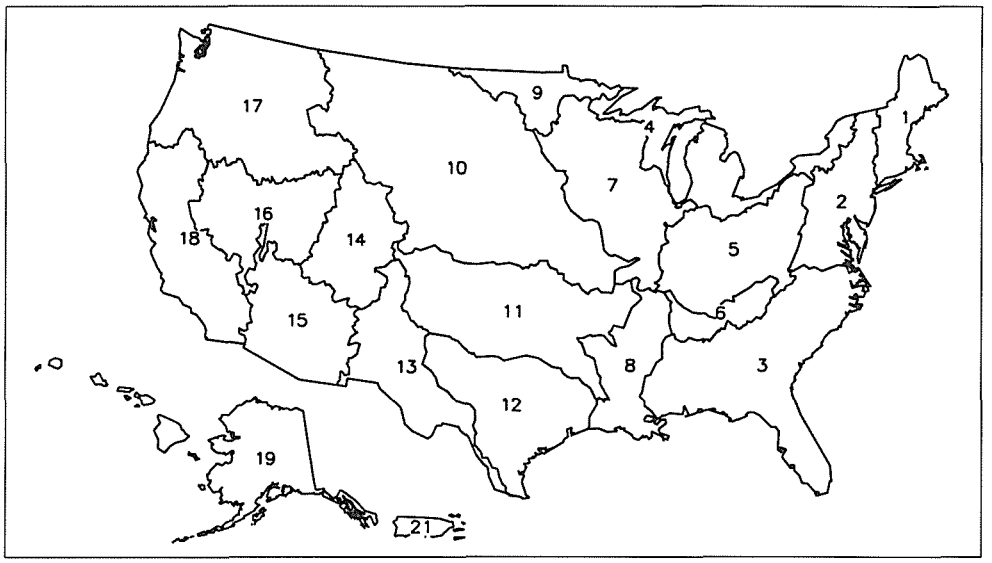

Fig. 1 Water resources regions of the United States.

The network was selected from approximately 19 000 sites where continuous records of streamflow have been collected by the US Geological Survey. Of these gauged sites, 7000 are currently active. The database, which has records as early as 1874, extends through the 1988 water year.

Criteria for selection of the network sites include:

- Data were based on direct measurements, not reconstructed flows.
- Data are in electronic form.

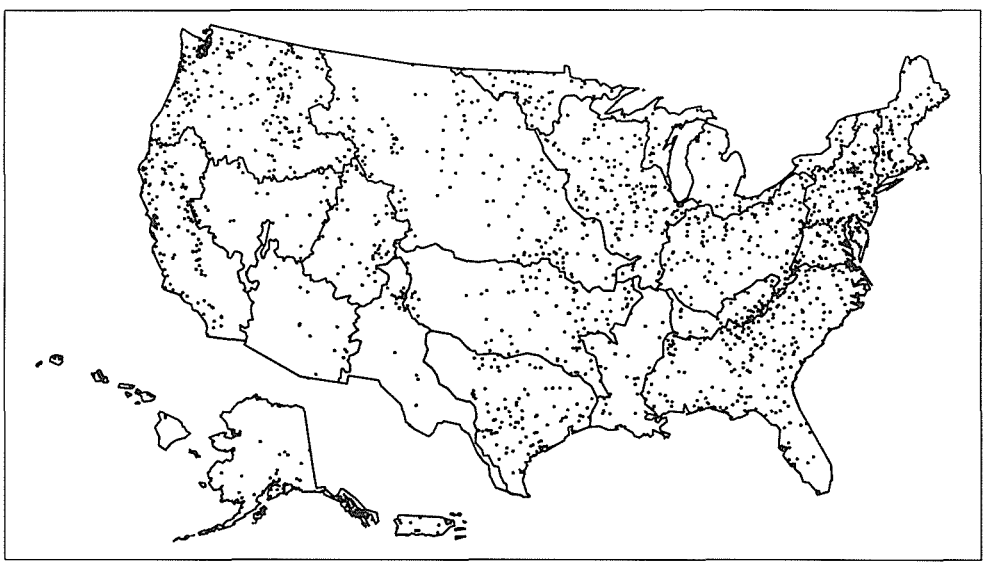

Fig. 2 Location of Hydro-Climatic Network stations.

- An existing record of at least 20 years, if consistent with good geographical coverage of the USA.
- Records rated as "good" or better and collected by established USGS and international standards.
- No appreciable diversion or regulation of flow were part of the record.
- Relatively little change in land use during the period of record.

ANALYSIS

The analysis addressed the question of long-term patterns, if any, in average-runoff and baseflow data from each of the 21 water resources regions of the United States.

Average runoff

More than 1500 gauged sites from the Hydro-Climatic Data Network, for which daily discharge data were available, were examined for long-term patterns in annual average discharge. The period from 1879 to 1988 were divided into 10 overlapping 20-year sub-periods. Table 1 shows the number of sites for which data were available in each 20-year period by water resources region. Due to the sparcity of data in early

Table 1 Number of Hydro-Climatic Data Network stations with daily average records available overlapping for 20-year periods during 1879–1988, for water resources regions of the United States.

Water resources region	Total sites	Periods of 20 years:									
		1879–1898	1889–1908	1899–1918	1909–1928	1919–1938	1929–1948	1939–1958	1949–1968	1959–1978	1969–1988
01	**62**				2	8	**11**	**26**	**42**	**46**	**37**
02	**144**				3	17	**40**	**88**	**107**	**96**	**90**
03	**173**			2	1	1	**17**	**81**	**108**	**101**	**111**
04	**46**			1	1	7	**9**	**19**	**28**	**38**	**30**
05	**94**			1	3	11	**30**	**49**	**79**	**77**	**77**
06	**37**					1	**16**	**20**	**28**	**24**	**20**
07	**123**	2	2	2	4	22	**34**	**63**	**102**	**99**	**82**
08	**21**						1	**12**	**13**	**15**	**18**
09	**38**						2	**9**	**14**	**23**	**25**
10	**141**					6	**29**	**48**	**78**	**87**	**97**
11	**85**					1	**13**	**30**	**44**	**46**	**62**
12	**90**				2	8	**17**	**22**	**32**	**43**	**73**
13	**22**						2	8	**10**	**13**	**14**
14	**44**				1	5	6	**22**	**23**	**25**	**21**
15	**17**					1	3	6	**9**	**9**	**16**
16	**32**				1	4	6	**9**	**15**	**21**	**27**
17	**190**				3	9	**53**	**92**	**106**	**101**	**114**
18	**115**			1	3	10	**23**	**33**	**48**	**81**	**94**
19	**29**							1	4	**13**	**16**
20	**42**					5	**17**	**11**	**12**	**15**	**20**
21	**15**										7
	1560										

NOTE: Bold figures in main body of Table 1 indicate number of stations used in computing weighted average runoff, for the region and time period, from which runoff trends analysis was done.

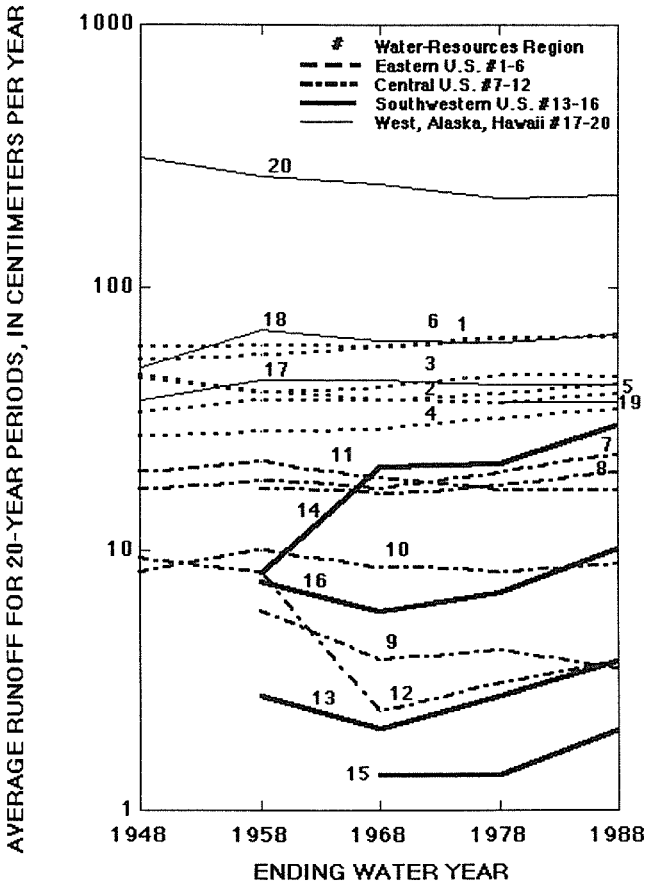

Fig. 3 Runoff, averaged for overlapping 20-year periods, for water resources regions 1–20 in the United States.

years, this work focused on the five overlapping 20-year periods ending in 1948, 1958, 1968, 1978, and 1988. Region 21, which includes Puerto Rico and outlying Caribbean Islands, was not included because there were too few stations to compute a stable average.

For each water resources region an average unit discharge weighted by drainage area was computed for each 20-year sub-period. This weighted unit discharge was then converted to average runoff in centimetres per year, using the appropriate factor (1 cubic foot per second per square mile = 34.5 cm $year^{-1}$).

From Fig. 3 it can be seen that annual runoff has tended to increase for 16 of the 20 water resources regions (see also Landwehr *et al.*, 1995). This tendency has been most dramatic in the southwestern United States (water resources regions 13–16), where increases have been in the order of 50 to 300%. Decreased flows have been most dramatic in the Pacific regions (water resources regions 17 and 20).

It is possible that the increasing trends could be an artifact of the method of analysis, or there could be subtle changes in the basins brought about by anthropogenic activities such as changes in land use, increases in irrigation, or other factors. If these kinds of anthropogenic effects can be considered minimal, then the

trends might result from a natural variation in climate or a shift induced by greenhouse gases in the atomosphere. To examine this question a hydrograph of the long-term streamflow record, Mississippi River at Clinton, Iowa, is shown in Fig. 4. Like most of the records in the database, the average annnual runoff at Clinton is increasing, especially since 1939. This longer record shows, however, that a decreasing trend occurred during the first part of the century prior to the onset of increasing runoff. Could this be evidence of a return to earlier wetter conditions in the north-central part of the United States and perhaps elsewhere?

Baseflow

A hydrograph separation program (Rutledge, 1993) was used to separate the direct runoff (overland flow) at Clinton from that contributed by the groundwater system as baseflow. As can be seen in Fig. 4, the baseflow exhibits a decreasing, then increasing, trend very similar to the total runoff–runoff hydrograph. The remaining component, the direct runoff, however, exhibits a strong upward trend for the entire period of record.

To investigate the national trends in baseflow, a stratified sample of 65 gauging sites throughout the United States, several from each of the 21 water resources regions, were selected in an attempt to represent a broad range of hydrologic conditions nationally and a diversity of drainage area sizes regionally (see also Landwehr *et al.*, 1996). Stations in separate hydrological units and having records of daily mean discharge which spanned contiguously all (or as much as available) of the period 1939–1988 were selected from those records available in the Hydro-Climatic

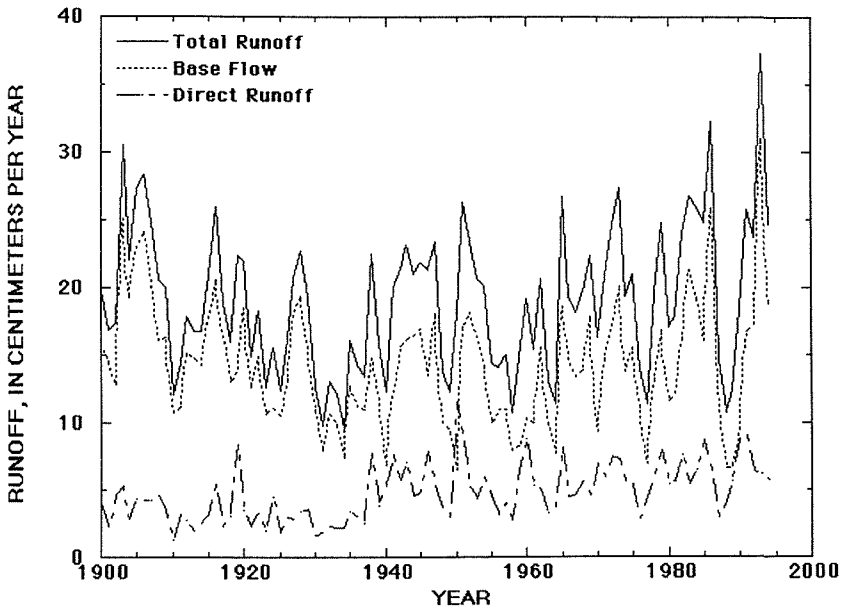

Fig. 4 Total runoff, baseflow, and direct runoff (overland flow) for Mississippi River at Clinton, Iowa, with drainage area of 221 704 km^2.

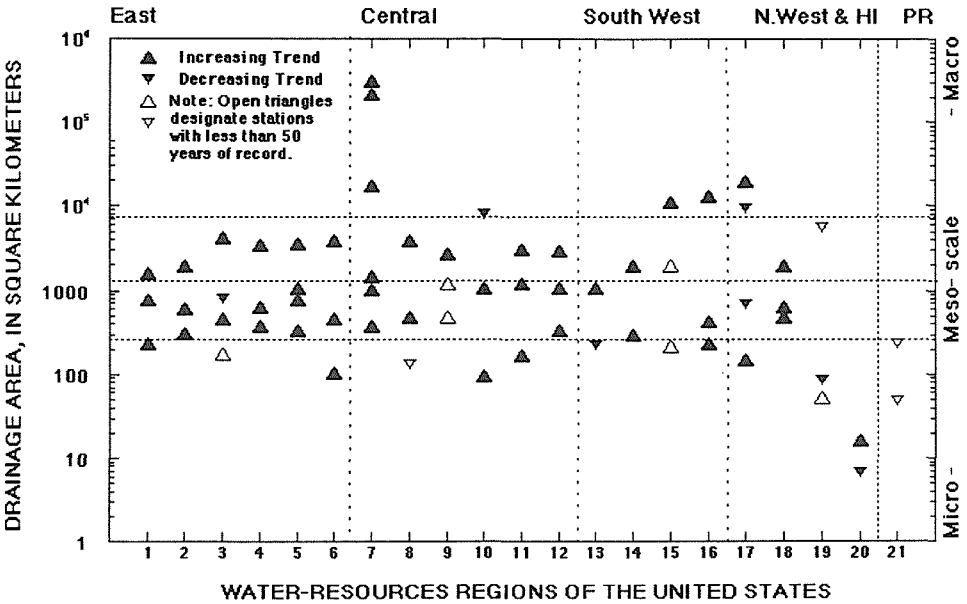

Fig. 5 Trends in baseflow for gauging stations used in this study.

categories, spanning the spatial domains of micro- to mesoscale processes. An attempt was made to identify a record in each water resources region that represented discharge from a watershed of each drainage-area category.

Rutledge's (1993) program was used to determine the baseflow runoff from the selected sites.

The 50-year records of derived baseflow exhibited positive trends (in linear and quadratic regression) at approximately 90% of the stations in the conterminous United States (Fig. 5). This is statistically significantly different from the 50% expected by chance ($p = 0.999$). The size of the drainage area was not a distinguishing factor between stations showing positive trends and those not showing positive trends. Of the five stations in Alaska and Hawaii, only two showed positive trends. The two Caribbean stations both exhibited decreasing baseflows, but records there spanned only the most recent 29 years.

DISCUSSION

There appears to be a low-intensity but consistent pattern of increasing runoff observed throughout the continental United States continuing through, or begining in, the period 1929–1988. Baseflow over the 50-year period ending in 1988 also shows an unmistakeable increasing trend. The size of the database makes it unlikely that the apparent intensified flux in the hydrologic system would be an artifact of the methods of analysis. Records for basins with overt anthropogenic changes were not included in the Hydro-Climatic Data Network, so unless some subtle anthropogenic forcing is responsbile for the trends, then meteorological or climatic forces are implicated. The findings herein are consistent with the observation (by Karl *et al.*, 1995) that over the past century there has been a rather steady increase in

precipitation, both in an increased frequency of days with precipitation and in the magnitude of extreme 1-day precipitation events, and a systematic decrease in the day-to-day variations in temperature.

Acknowledgement The authors thank Messrs C. Lamar Sanders and Michael G. Zalants of the US Geological Survey, whose help with statistical computations of the streamflow data made this paper possible.

REFERENCES

Karl, T. R., Knight, R. W., Easterling, D. R. & Quayle, R. G. (1995) Trends in US Climate during the twentieth century. *Consequences* **1**(1), 3–12.

Landwehr, J. M., Hubbard, E. F. & Slack, J. R. (1995) Centennial and continental-scale variation in the surface-water resources of the United States. In: *IUGG XXI General Assembly, Abstracts* Week B, p. B208.

Landwehr, J. M., Barker, A. R. & Hubbard, E. F. (1996) Variation in baseflow for streamflow systems of various sizes throughout the United States in this century. In: *Second International Scienticfic Conference on the Global Energy and Water Cycles*, 182–183.

Rutledge, A. T. (1993) Computer programs for describing the recession of ground-water discharge and for estimating ground-water recharge and discharge from the streamflow records. *US Geol. Survey Water Resources Investigations Report 93-4121*, 45 pages with computer diskette.

Slack, J. R., Lumb, A. M. & Landwehr, J. M. (1993) Hydro-Climatic Data Network (HCDN): streamflow data set, 1874–1988. *US Geol. Survey Wat. Resour. Invest. Report 93-4076*, CD-ROM. Also, on World Wide Webb at http://wwwrvares.er.usgs.gov/hcdn_cdrom/1st_page.html

4 Hydrological Extremes: *Low Flows*

FRIEND'97 — Regional Hydrology: Concepts and Models for Sustainable Water Resource Management
(Proceedings of the Postojna, Slovenia, Conference, September–October 1997). IAHS Publ. no. 246, 1997.

Using regional hydrology for assessing European water resources

A. GUSTARD, H. G. REES, K. M. CROKER & J. M. DIXON
Institute of Hydrology, Wallingford, Oxfordshire OX10 8BB, UK

Abstract The analysis of time series of gauged daily flows enables the temporal and spatial variability of European hydrological regimes to be described. The temporal variability includes seasonality, the distribution of annual maximum floods and annual minimum discharges for different durations. Spatial variability has focused either on mapping regime characteristics or developing relationships between flow statistics and catchment characteristics. This paper presents two examples of analysing either the spatial or temporal regimes which have been carried out at the pan European scale. They illustrate the application of generic analysis techniques to a wide range of hydrological regimes over Europe.

INTRODUCTION

There is a wide variety of low flow measures which describe properties of the flow regime. These include the flow duration curve, which describes the proportion of time a given flow is exceeded, and the flow frequency curve, which can be used to determine the return periods of drought. Table 1 summarizes the various low flow measures in use. Where reliable river flow data are available at the site of interest these measures can be derived directly from the observed data. However, in many situations no flow data is available and, hence, techniques have been developed to estimate low flows at ungauged sites. Past studies in Europe have included those of Martin & Cunnane (1976) in Ireland, Lundquist & Krokli (1985) in Norway, Gustard *et al.* (1992) in the UK, and Demuth (1994) in Germany. Until recently there have been few studies at a pan European scale because of problems in obtaining river flow data or because of the lack of consistent physiographical data in a readily accessible form. The establishment of the European Water Archive within the FRIEND project has succeeded in overcoming many of these problems by providing easy access to a variety of truly international hydrological datasets (Rees & Roald, 1995). One of the first pan European studies to benefit from the FRIEND data was a low flows study focusing on a subset of countries in western and northern Europe (Gustard *et al.*, 1989; Gustard, 1993). Other notable examples of European scale studies include Arnell's (1995) regionalized mean flow estimation over Europe and Tallaksen & Hisdal's (1997) study of seasonal droughts. Recently these approaches have been extended into Eastern Europe (Gustard & Cole, 1997).

These regional studies have provided an invaluable insight into the physical controls on European hydrological regimes and have developed useful techniques for identifying the seasonal variability of the regimes. This paper presents two further developments in estimating the spatial and temporal variability of low flows. The first focuses on a regional assessment of low flows with potential applications in the field of water resource management or for estimating small scale hydropower

Table 1 Summary of low flow measures.

Low flow measure	Property described	Application
Flow duration curve	Proportion of time a given flow is exceeded	Licensing abstractions or effluents, hydropower
Flow frequency curve(annual minimum)	Proportion of years in which the mean discharge over a given duration is below a given magnitude	Return period of drought, preliminary storage yield analysis
Low flow spells (duration of deficiency periods)	Frequency with which the flow remains continuously below a threshold for a given duration	Water quality problems Instream ecology Amenity Navigation
Deficiency volumes	Frequency of requirement of a given volume of make-up water to maintain a threshold flow	Regulating reservoir design
Storage yield	Frequency of requirement for a given volume of storage to supply a given yield	Review of or preliminary storage yield design
Time to accumulate runoff volume	Time to accumulate a given volume of runoff with a given frequency of occurrence	Probability of reservoir refill in drought conditions Reservoir control curves

potential. The second method highlights an innovative approach to analyse the development and decay of European droughts.

LOW FLOW ESTIMATION IN THE EUROPEAN UNION

The available freshwater resource is often represented in terms of the long-term average annual runoff and expressed as a uniform depth in units of millimetres over the area concerned. This statistic, though providing a measure of the average availability of the resource, gives no indication of its seasonal variability or the water available under extreme dry conditions. An alternative to the runoff is the $Q90$, a flow statistic representing the daily flow which is exceeded or equalled 90 percent of the time. Expressed in millimetres or as a percentage of the mean flow, the $Q90$ can be used by planners and engineers to determine the resource available in periods of low flow or drought.

This paper presents the results of a pan European study of $Q90$ which was undertaken as part of a project commissioned by Eurostat (Rees & Cole, 1997). Output from the study included grids of $Q90$, at a spatial resolution of 10 km by 10 km, for the majority of the European Union.

*Q*90 in gauged catchments

Using the time series of river flows and the digitized catchment boundaries held on the FRIEND European Water Archive, it was possible, using a computer program, to directly calculate the $Q90$ for a significant portion of the European Union. The $Q90$ was expressed in relative terms, as a percentage of the mean flow, in order to remove the scale effects of different sized catchments with differing rainfall and evaporation characteristics. Using the ARC/INFO Geographical Information System the values of observed $Q90$ were assigned to the appropriate catchment areas. A weighted area technique was then used to ascribe values of $Q90$ to those grid cells

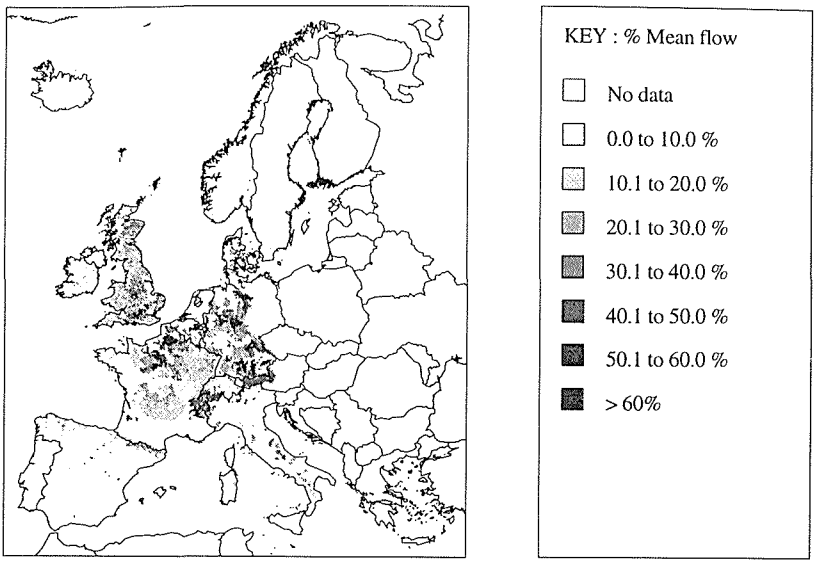

Fig. 1 Grid of $Q90$ (as % mean flow) derived from gauged flow data.

which happened to coincide with one, or more, of the digitized catchment boundaries. The resulting grid is shown in Fig. 1. As can be seen, for gauging stations in Scandinavia and Ireland, where flow data existed but no catchment boundaries were available, the observed $Q90$ value was simply assigned to the grid cell within which the gauging station was located.

$Q90$ in ungauged areas

A variety of multivariate regression models were used to derive estimates of $Q90$ for the remaining "ungauged" cells. Across mainland Europe, a regression model developed by Gustard & Irving (1993) was used. The model provided a relationship between the significant soil associations (as defined by the CEC soil classification (CEC, 1985)) and the 95 percentile flow. The complete CEC soil classification contains 312 soil associations grouped into 61 different Soil Typological Units. Of these, 28 significant soil types were identified in northern Europe. These soil types were further grouped into nine SOIL classes based on the relationship between the soils and the Base Flow Index (BFI). From this, a single weighted SOIL variable could be derived representing the percentage cover of each soil association in a catchment.

The equation for estimating the $Q95$ (in $m^3\ s^{-1}$) is given in the form:

$$Q95 = 2.55 \times 10^{-8}\ \mathrm{AREA}^{1.05}\ \mathrm{AAR}^{1.69}\ \mathrm{SOIL}^{0.90} \quad (1)$$

Flow duration curves from gauging stations were grouped together according to $Q95$ (as a percentage of mean flow), and a family of 20 flow duration type curves were identified. Having obtained an estimate of the $Q95$ (expressed as a percentage of the mean flow) a typical flow duration curve for the ungauged cell can be identified, from which an estimate of the $Q90$ can be derived.

In the UK, a more detailed classification of the soils had been undertaken which resulted in soils being assigned to one of 28 classes based on the hydrogeological properties of soils. This classification is referred to as the Hydrology of Soil Types (HOST) classification (Boorman & Hollis, 1990, Boorman *et al.*, 1995). These hydrological soil classes were further grouped into 12 Low Flow HOST Groups (LFHG) (Gustard *et al.*, 1992) to develop an equation for estimating the $Q95$, as a percentage of mean flow, in the following form:

$$Q95 = 40.8\,\text{LFHG1} + 31.9\,\text{LFHG2} + 65.7\,\text{LFHG3} + 25.0\,\text{LFHG4} + 49.0\,\text{LFHG5} + 6.5\,\text{LFHG6} + 10.7\,\text{LFHG7} + 1.1\,\text{LFHG8} + 15.0\,\text{LFHG9} + 6.8\,\text{LFHG10} + 29.4\,\text{LFHG11} + 65.1\,\text{LFHG12} \quad (2)$$

Using this equation, a gridded database of $Q95$ for the UK was produced at a resolution of 1 km × 1 km. The $Q95$ grid was resampled in ARC/INFO to create a 10 km × 10 km grid and, for each grid square, the $Q95$ was used to identify the typical flow duration curve and hence the $Q90$ (expressed as a percentage of the mean flow).

For Spain, models which had been developed as part of a project for the European Small Hydropower Association were used (Irving *et al.*, 1995). In this study the $Q95$ flow was found to be zero in a number of catchments and therefore could not be used as a hydrogeological index. A regression model was developed based on the relationship between the $Q90$ flow statistic and the CEC soil classification. However, it was found that the climate within Spain had a significant impact on the flow regimes and soil characteristics and the country was therefore subdivided into two regions with each of the models taking the form:

$$Q90 = 19.14\,\text{U} + 17.86\,\text{Bh} + 47.26\,\text{Id} + 13.73\,(\text{Bg} + \text{Bk}) \quad (3)$$

for the northern coastal region, and

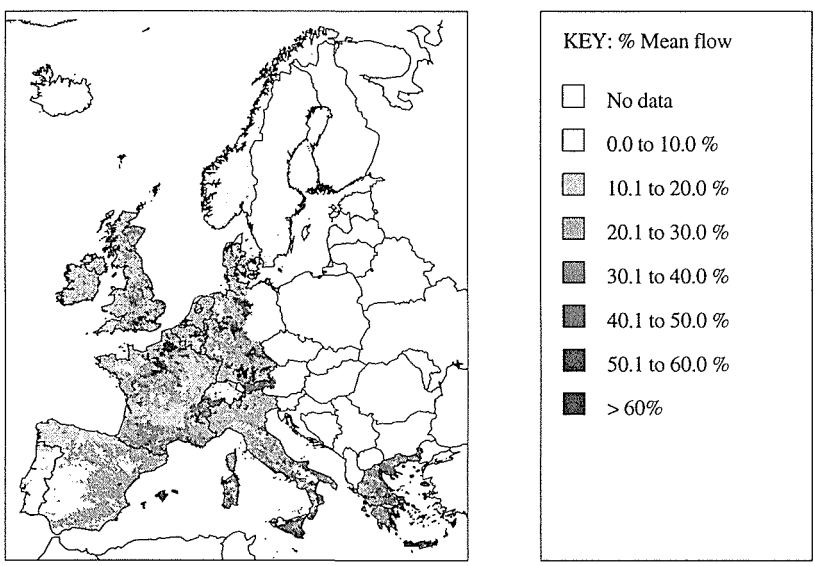

Fig. 2 Distribution of $Q90$ (% mean flow) using gauged and predicted data.

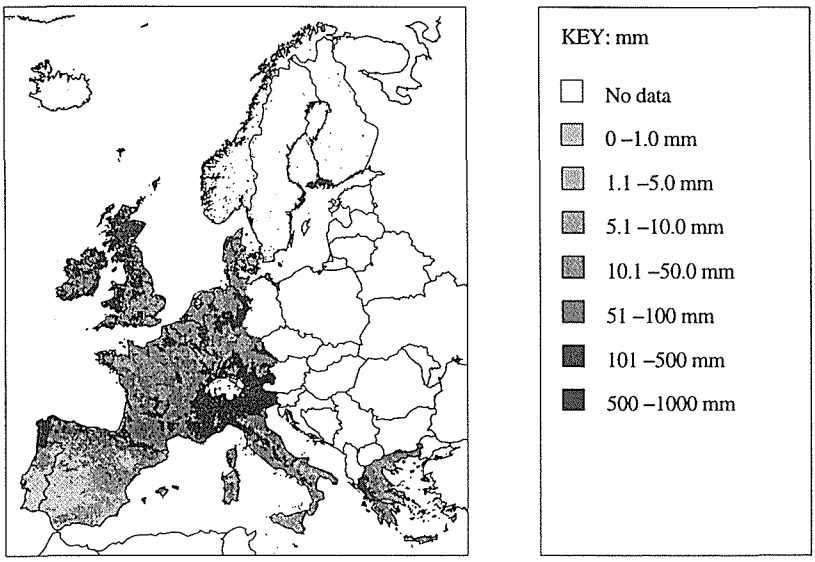

Fig. 3 Distribution of $Q90$ (mm) using gauged and predicted data.

$$Q90 = 10.59\ U + 8.84\ Bh + 2.99\ Id + 21.62\ (Bg + Bk) \quad (4)$$

for the rest of Spain.

The symbols U, Bh, Bg, Bk, Id, Je, Lcr and Lv refer to the CEC soil units of Ranker, Humic Cambisol, Gleyic Cambisol, Calcic Cambisol, Dystric Lithosol, Eutric Lithosol, Rhodo-Chromic Lithosol, and Vertic Luvisol respectively. A full description of these soil units and their characteristics can be found in the documentation of the CEC Soil Map (1985).

Composite grid of $Q90$

A composite map of gridded $Q90$, expressed relative to the mean flow, was constructed (Fig. 2) using observed values in gauged areas and predicted (regression based)— values in ungauged areas. This map, while useful for illustrating the spatial variability of relative $Q90$ across Europe, has limited value in terms of water resources assessment unless it is combined with an estimate of the mean flow to give absolute values for $Q90$. In Fig. 3 each cell's relative $Q90$ value has been multiplied by the corresponding average annual runoff value to derive a grid of $Q90$ expressed in absolute terms of millimetres. The derivation of the average annual runoff grid is described in the paper by Rees *et al.* (1997).

Comparing Figs 2 and 3 the distribution of $Q90$ changes significantly. The change is particularly visible where the mean flow (or average annual runoff) is low, such as in southern parts of Portugal, Spain, Italy or Greece. Here, absolute values of $Q90$ are unavoidably low, despite the fact that the relative $Q90$ is high. The converse is true in the wetter regions of north-west Europe (e.g. Scotland, Ireland, northern Spain) where the absolute values of $Q90$ are high even though the relative $Q90$ is very low.

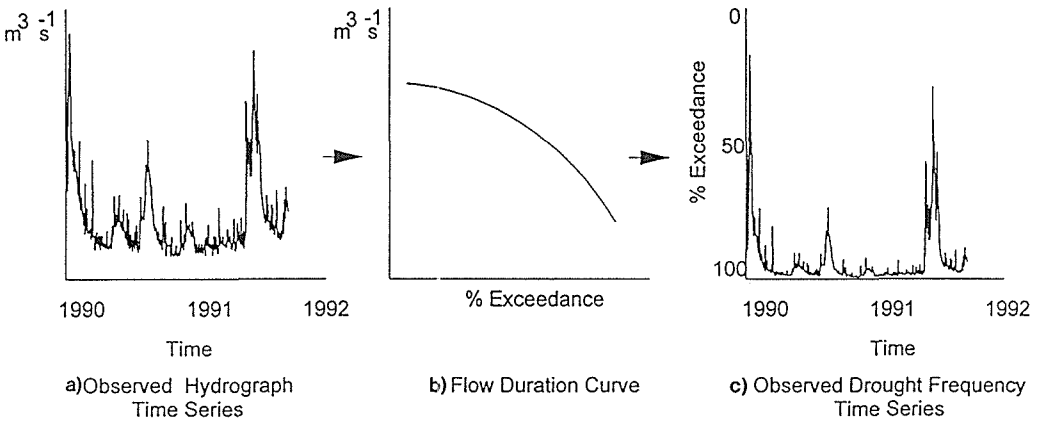

Fig. 4 Deriving time series of drought frequency.

Spatial coherence of European droughts

Figures 2 and 3 illustrate the spatial variability of a single flow statistic, $Q90$, over Europe. However, a more detailed temporal and spatial analysis can be achieved by calculating the flow duration percentile experienced on each day of the year and to map its variation across Europe. The method is illustrated in Fig. 4 and consists of:

(a) Retrieving the observed daily flow time series from the European Water Archive.
(b) Deriving the flow duration curve (cumulative frequency diagram) from the observed data.
(c) Transforming the daily flow time series to a daily exceedance series by transforming the observed daily flow duration curve.

This produces a continuous drought time series expressed as the percentage of time a given discharge is exceeded for every day of record for each flow series. The frequencies can then be mapped at the European scale to illustrate the spatial variability of drought frequency (Fig. 5).

A program, accessing the European Water Archive, has been written to convert daily flow values into exceedance percentiles. Individual catchments have been colour coded to represent the exceedance frequency ranging from dark blue (high flows, low exceedance) through green, yellow, orange and red for low flows, high exceedance.

Although the procedure is simple for individual catchments, nested catchments present problems in displaying the data adequately. The approach which has been used is to shade the polygon of an upstream catchment according to its exceedance value. The polygon of the residual catchment area between the upstream and next downstream gauging station is allocated the exceedance value of the downstream flow record.

Using this approach, an initial set of maps have been produced for the European catchments illustrating the development of the 1976 drought from February to August. From a relatively uniform frequency map in February, a wide range of frequencies are experienced in April and June with extreme conditions experienced over nearly the entire region in August. This large scale analysis is appropriate for considering the climatic impact on the spatial coherence of droughts at the European

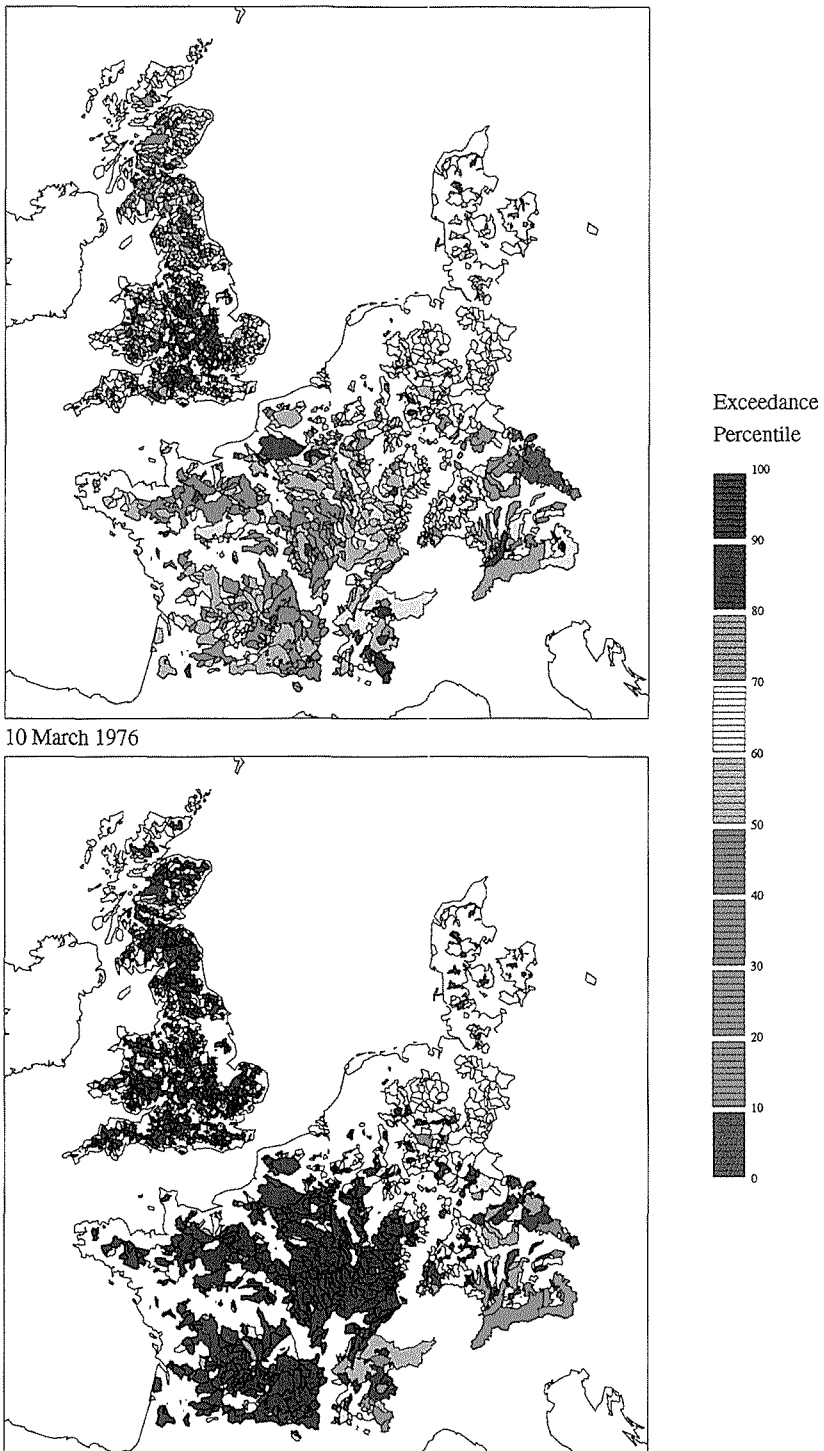

Fig. 5 Exceedance percentiles for European catchments on selected dates in 1976.

scale. However, it is not suitable for analysing the more localized control of catchment response and hydrogeological properties. This was achieved by studying how the exceedance values vary within nested catchments.

One of the weaknesses of the above approach is the allocation of the downstream exceedance percentile to the upstream residual area in the nested catchment case. Clearly the downstream exceedance should be allocated to the entire upstream catchment area or the residual flow exceedance should be calculated and allocated to the residual catchment area. This can be determined by deriving a new time series of flows from the difference between the up and downstream time series and deriving percentile exceedances from this new series. To compensate for river routing the analysis can be carried out on a seven day moving average.

In practice this approach has proved difficult as a result of gaps in time series restricting the ability to derive residual flow series. Two procedures have been adopted; the first is to use only matching flow sequences, the second is to infill missing data. For the regional European synoptic analysis the advantages of more accurate illustration of observed frequencies are small. However, for analysis and deriving relationships with thematic data there are clear advantages of a more realistic spatial analysis of nested catchments. It is an interesting feature of this study that a small data set without nested catchments is easier to analyse. The addition of more data introduces computational and display problems. Residual catchment flows estimated from the difference between upstream and downstream gauges have larger errors than the individual station data. In this case the addition of this extra data leads to an apparent increase in spatial variability as a result of increased errors of derived time series. An additional advancement of the technique is to use seasonal flow duration curves instead of annual curves in order to determine exceedance frequency on any day.

CONCLUSIONS

This paper has described the application of regional low flow estimation techniques for calculating renewable water resources at the pan European scale. The method of using both gauged and ungauged estimates maximizes the use of available data for resource estimation. The techniques used were objective and thus provide consistent estimation of resource availability. Of increasing concern in Europe is the apparent increased frequency of European droughts. These characteristics can be described by severity, frequency, duration and spatial extent. The method described in this paper introduces an innovative technique for evaluating the growth and decay of droughts at the European scale. Further work is, however, required if the method is to have any practical application or operational value. This work will include an objective analysis of a number of droughts to see if there are any detectable features indicating how droughts develop and decay. Methods will also need to be developed to map the progression of droughts in ungauged areas. This work will ultimately lead to an ability to assess the severity of a drought as it occurs, in real time. Such a tool would have considerable value to water resource engineers, farmers and environmentalists enabling them to react quicker to drought event, thus helping to avoid restrictions on water use, to protect crops from failure and to prevent ecological damage to rivers, streams and lakes.

Acknowledgements The authors gratefully acknowledge the following groups or organizations who have contributed data to the analysis presented in this paper: FRIEND—Northern Europe; FRIEND—AMHY; the European Small Hydropower Association; the Altener Programme of the European Union; the Eurostat GISCO service; and the Climate Research Unit of the University of East Anglia. Some of the research presented was undertaken as part of the Eurostat SUP.COM95 project, "Estimation of Renewable Water Resources in the European Union" funded by the European Commission through the Fourth Framework Programme.

REFERENCES

Arnell, N. W. (1995) Grid mapping of river discharge. *J. Hydrol.* 107, 39–56.

Boorman, D. B. & Hollis, J. M. (1990) Hydrology of soil types. A hydrologically-based classification of the soils of England and Wales. MAFF Conference on River and Coastal Engineering (Loughborough University).

Boorman, D. B., Hollis, J. M. & Lilley, A. (1995) Hydrology of soil types: a hydrologically-based classification of the soils of the United Kingdom. *Report no. 126, Institute of Hydrology, Wallingford, Oxfordshire, UK.*

CEC (1985) *Soil Map of the European Communities. 1:1 000 000.* CEC-DGVI, Luxembourg.

Demuth, S. (1994) Regionalization of low flows using a multiple regression approach. A review. In: *XVIIth Conference of Danube Countries* (Budapest, 5–7 September 1994), vol. 1, 115–122.

Gustard, A. (ed.) (1993) *Flow Regimes from International Experimental and Network Data (FRIEND)*; vol. I, *Hydrological Studies*; vol. II, *Hydrological Data*; vol. III, *Inventory of Streamflow Generation Studies*. Institute of Hydrology, Wallingford, Oxfordshire, UK.

Gustard, A. & Cole, G. (ed.) (1997) *Advances in Regional Hydrology through East European Cooperation*. Report to the Commission of the European Communities. Institute of Hydrology, Wallingford, Oxfordshire, UK.

Gustard, A. & Irving, K. M. (1993) Classification of the low flow response of European Soils. In: *Flow Regimes from International Experimental and Network Data*, vol. I, *Hydrological Studies* (ed. by A. Gustard), 98–108. Institute of Hydrology, Wallingford, Oxfordshire, UK.

Gustard, A., Bullock, A. & Dixon, J. M. (1992) Low flow estimation in the United Kingdom. *Report no. 108, Institute of Hydrology, Wallingford, Oxfordshire, UK.*

Gustard, A., Roald, L., Demuth, S., Lumadjeng, H. & Gross, R. (1989) *Flow regimes from experimental and network data (FREND)*, 2 vols. Institute of Hydrology, Wallingford, Oxfordshire, UK.

Gustard, A., Irving, K. M., Rees, G. & Young, A. (1995) Hydrological models for small scale hydropower assessment. In: *Proc. Hidroenergia '94—4th International Conference and Exhibition* (Milan, Italy, 18–20 September 1995).

Irving, K. M., Young, A., Rees, H. G. & Gustard, A. (1995) *European Atlas of Small-Scale Hydropower Resources*. Phase II, Part 2, *Spain and Italy*. Client Report.

Lundquist, D. & Krokli, B. (1985) *Low Flow Analysis*. Norwegian Water Resources and Energy Administration, Oslo.

Martin, J. V. & Cunnane, C. (1976) *Analysis and Prediction of Low-flow and Drought Volumes for Selected Irish Rivers*. The Institution of Engineers of Ireland.

Rees, H. G. & Cole, G. A. (eds) (1997) *Estimation of Renewable Water Resources in the European Union*. Report to the Commission of European Communities: Eurostat. Institute of Hydrology, Wallingford, Oxfordshire, UK.

Rees, H. G. & Roald, L. A. (1995) The FRIEND European Water Archive. Design and Operation of an International Hydrological Database. In: *Proc. of UNESCO IHP International Symposium on Rivers and People in South-east Asia and the Pacific—Partnership for the 21st Century* (United Nations University, Tokyo, Japan, 23–27 October 1995).

Rees, H. G., Croker, K. M., Reynard, N. S. & Gustard, A. (1997) Estimation of renewable water resources in the European Union. In: *FRIEND'97 — Regional Hydrology: Concepts and Models for Sustainable Water Resource Management* (ed. by. A. Gustard *et al.*) (Proc. Postojna, Slovenia, Conference, September–October 1997). IAHS Publ. no. 246 (this volume).

Tallaksen, L. M. & Hisdal, H. (1997) Regional analysis of extreme streamflow drought duration and deficit volume. In: *FRIEND'97 — Regional Hydrology: Concepts and Models for Sustainable Water Resource Management* (ed. by A. Gustard *et al.*) (Proc. Postojna, Slovenia, Conference, September–October 1997). IAHS Publ. no. 246 (this volume).

FRIEND'97 — Regional Hydrology: Concepts and Models for Sustainable Water Resource Management
(Proceedings of the Postojna, Slovenia, Conference, September–October 1997). IAHS Publ. no. 246, 1997.

Water information management system and low flow analysis in Slovenia

MITJA BRILLY
FAGG Hydraulics Division, University of Ljubljana, Hajdrihova 28, 61000 Ljubljana, Slovenia

MIRA KOBOLD
Hydrometeorological Institute, Vojkova 1a, 1000 Ljubljana, Slovenia

ANDREJ VIDMAR
Ministry of the Environment and Physical Planning, Vojkova 1a, 1000 Ljubljana, Slovenia

Abstract Low flow estimation is essential for water management in Slovenia. Therefore Slovenia is subdivided into 572 sub-basins. In the analysis of daily flows two low flow parameters were used: i.e. the streamflow which is exceeded in 95% of days ($Q95$), and the 20-year return period of the annual minimum flow ($20Q$). Specific flow characteristics ($q95$ and $20q$) were also computed for all available gauging stations. The $20q$ was determined for each sub-basin and a national map was made using a GIS. A nonlinear regression model obtained from 11 experimental basins in Slovenia was used to calculate the low flow parameters for gauging stations and each sub-basin by GIS. Measured and calculated low flow characteristics for gauging stations and sub-basins were analysed. The methodology and derived relationships are already useful for water management, although analysis methods still need to be improved because of observed discrepancies between measured and calculated characteristics.

INTRODUCTION

Slovenia has a great variety of hydrological regimes between the Adriatic Sea, the Alpine region, and the Pannonian plain. The jagged mountain tops rise to more than 2500 m in the northwest. In the southeast, the country slowly transforms from a mountainous landscape into a wide plateau, usually over 1000 m altitude where different types of high-level karst have been developed. The lower karst (the limestone region with underground rivers, gorges and caves) which gave its name to all karst areas around the world, extends through a wide belt in south and southwest Slovenia (Fig. 1). The eastern part of the country gradually transforms into the Pannonian plain. It is mostly an area of hills, interrupted by extensive plains with a gravel aquifer.

Slovenia is a small country (barely 20 000 km^2) with large water resources. The annual precipitation varies from 4000 mm in the Alpine region to 750 mm in the Pannonian plain. The mean value for the whole territory of Slovenia is 1500 mm per year and the mean yearly runoff is 1000 mm. The runoff from 81% of the Slovenian area flows to the Danube river; the remaining runoff of the other 19% of the area flows to the Adriatic Sea.

The hydrogeological map of Slovenia has nine geological units (VGI, 1991). For low flow analysis the geological units have been aggregated in four units: i.e. karst,

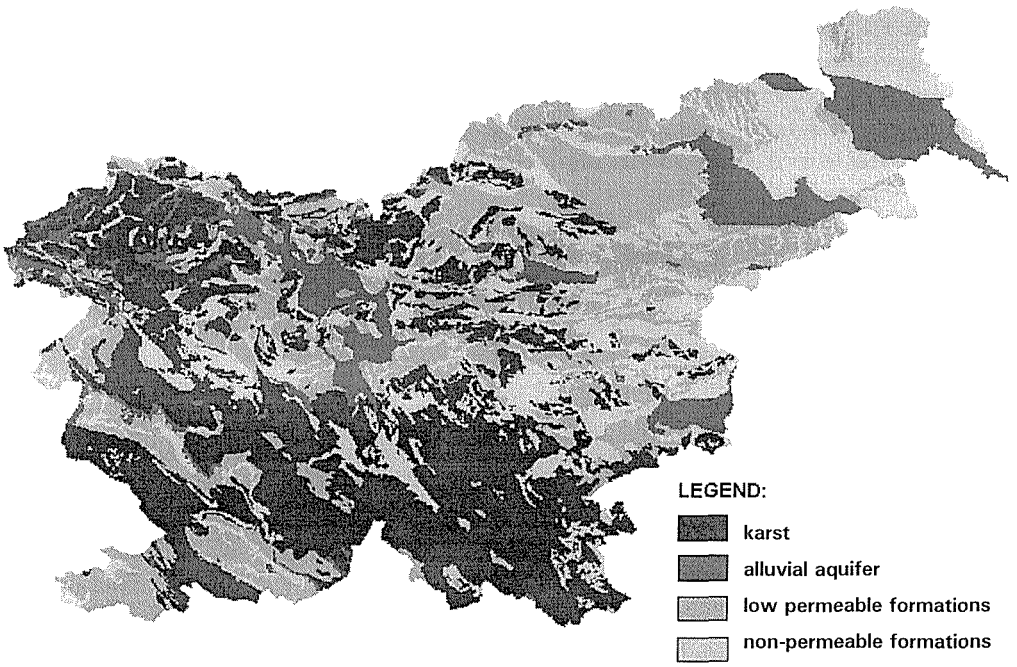

Fig. 1 The hydrogeological units of Slovenia.

alluvial aquifer, low permeable formation and non permeable formation (Fig. 1). The units cover 34%, 12%, 34% and 20% of the Slovenian area, respectively. In areas with low permeable and non permeable rocks the huge precipitation excess causes the development of a dense stream network. The karst region is without surface water streams; huge springs and many caves with water occur there. Slovenia is divided into 27 main basins and 572 sub-basins of less than 50 km^2 (Fig. 2). The only exceptions are in the karst region where large basins could not be divided in smaller sub-basins. The basin divides and codes are given according to the LAWA methodology (LAWA, 1993, Brilly & Vidmar, 1994).

Low flow estimation is essential for water management in Slovenia. Although large water resources are available, in dry periods there is not enough water in the streams for all requirements including nature and wildlife. Therefore water management which includes water planning, water rights of the consumer, water quality standards for wastewater, should also aim at low flows. The objective of this study is to analyse low flows and to map its characteristics for the whole of Slovenia.

LOW FLOW ANALYSIS AND MAPPING WITH RUNOFF DATA

The Hydrometeorological Institute of Slovenia (HMZ) is responsible for meteorological, hydrological and environmental monitoring. The institute takes care of 250 meteorological and 126 runoff stations. Some stations have a record of more than 100 years. Many stations have been monitored temporarily and abandoned with time series of 20 years or less.

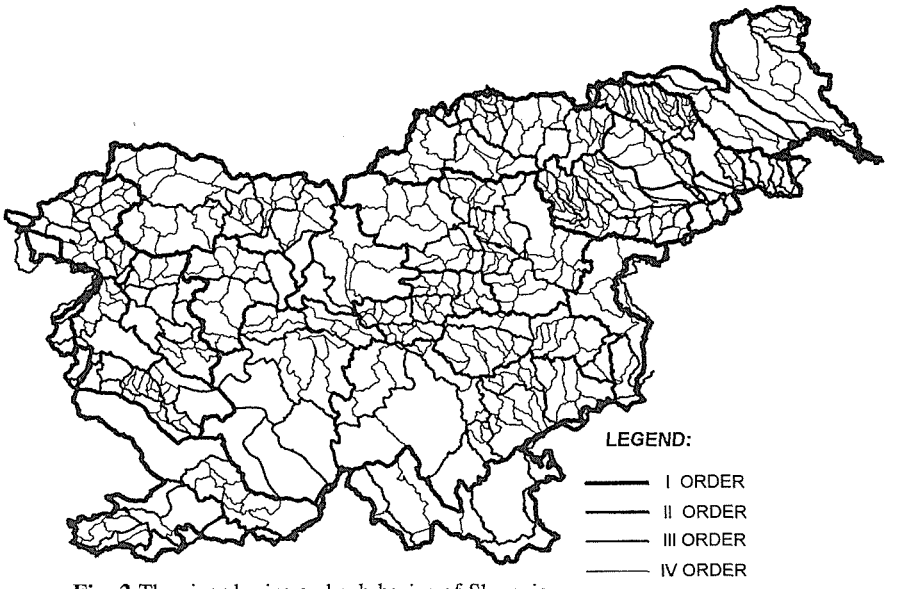

Fig. 2 The river basins and sub-basins of Slovenia.

In the framework of this study the period from 1961 to 1990 was selected for the low flow analysis. In this period HMZ has monitored 55 stations in basins smaller than 300 km^2 with daily flow data available. Other stations have not been used because either the time series was incomplete or the basin area was larger than 300 km^2.

In the low flow analysis, two parameters were used: a) the streamflow, which is exceeded in 95% of days ($Q95$), to be derived from the flow duration curve, and b) the 20-year return period of the annual minimum flow ($20Q$). The $Q95$ and $20Q$ were estimated for all 55 stations. Specific runoff or low flow yield per unit area was also calculated and indicated as $q95$ and $20q$.

A shorter 15-year period sample was extracted from the 1961–1990 data set. Statistics of both samples are presented in Table 1. The difference between the $Q95$ from the two samples is small, but significant. A linear correlation should be used for calculation of the $Q95$ for the period 1961–1990 from incomplete samples. The difference in the $20Q$ from the two samples is almost negligible, and data from gauged stations with incomplete time series could be used for mapping of low flows. The relationship between $Q95$ and $20Q$ is given in Fig. 3, which shows a high correlation (R^2 = 0.935). Specific low flows $q95$ and $20q$ also have a good

Table 1 Low flow statistics ($Q95$ and $20Q$) for 15 and 30 year samples.

Statistics	$Q95$ (m^3 s^{-1}):		$20Q$ (m^3 s^{-1}):	
	15 year	30 year	15 year	30 year
Mean	1.123	1.081	0.637	0.625
Standard deviation	1.205	1.230	0.831	0.834
Sample variance	1.452	1.514	0.690	0.696
Minimum	0.059	0.075	0.006	0.005
Maximum	5.752	5.778	3.703	3.502

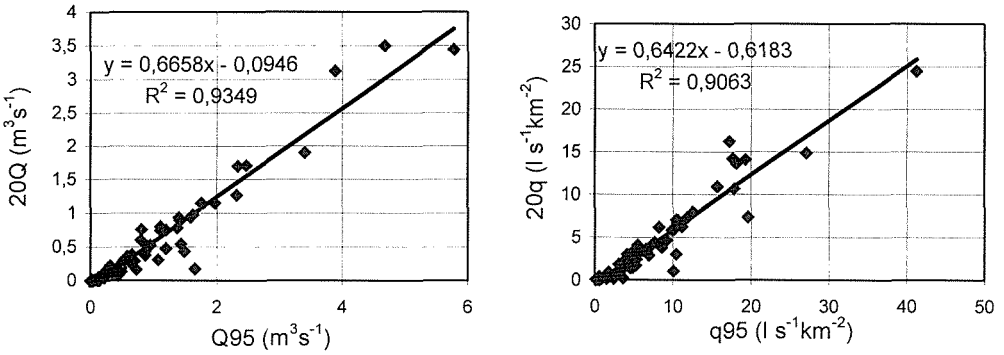

Fig. 3 Relationships between the flow exceeded in 95% of the days and the 20-year return period annual minimum flow.

correlation (R^2 = 0.906, Fig. 3). The low flow analysis shows that water reservoirs, water supply and highly permeable aquifers along the stream have a strong impact on low flows. Surface water flow is almost zero in the alluvial plains under dry conditions. Drainage of large ground water reservoirs causes constant low flows with a low decrease of the flow related to the return period. Data from 21 stations was eliminated from the sample of 55 stations, related to these conditions and the correlation recalculated (Fig. 3). The correlation is significantly better, with R^2 = 0.97 for $Q95$ and $20Q$, and R^2 = 0.95 for specific low flow $q95$ and $20q$.

We used all the available data of the specific $20q$ low flow to map low flows. Specific low flow data ($20q$) for all gauged stations (55 stations with a 30 year period and 25 stations with incomplete time series) were incorporated in the Geographic Information System (GIS) of the national water management information system (WMIS) and linked to the sub-basins (Fig. 2). The highest value (24 l s^{-1} km^{-2}) is

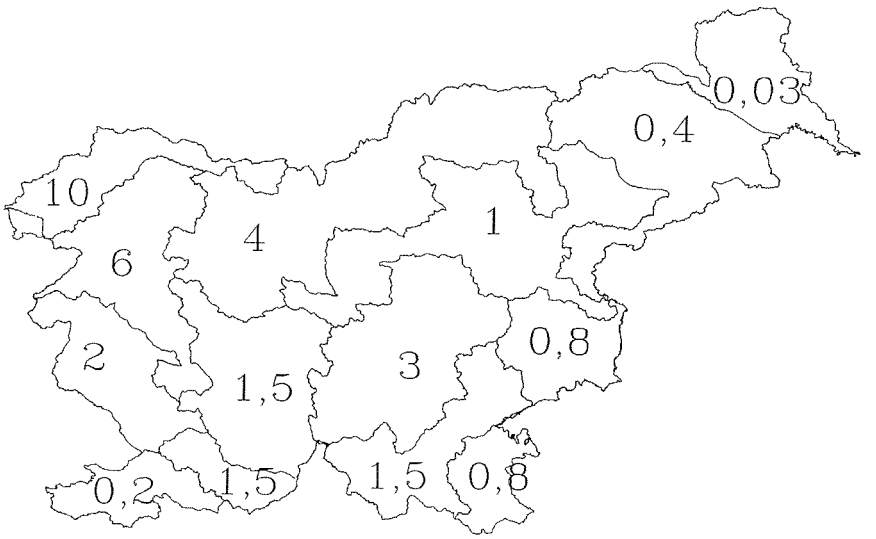

Fig. 4 The specific annual minimum low flow for the 20-year return period ($20q$ in l s^{-1} km^{-2}).

found in the northern Alpine part of country and the lowest value is only 0.024 l s^{-1} km^{-2} and prevails in the eastern and drier region. The result (regionalized 20*q*) is presented on a map with low flows regions (Fig. 4).

REGIONALIZATION OF LOW FLOW WITH NONLINEAR REGRESSION MODELS

The nonlinear regression model obtained from the experimental basins in Slovenia (Kobold & Brilly, 1994) was simplified and adapted to accept only readily available data: i.e. basin area (AREA), mean annual rainfall (AAR) and index of geology (GEO). Low flow characteristics were determined as follows:

$$Q\text{lw} = a * \text{AREA}^b \text{AAR}^c \text{GEO}^d \quad (1)$$

and specific low flow ($b = 0$):

$$q\text{lw} = a * \text{AAR}^c \text{GEO}^d \quad (2)$$

*Q*lw is either *Q*95 or 20*Q* and *q*lw is *q*95 or 20*q*. Data for both models (AREA, AAR, GEO, *Q*95, 20*Q*, *q*95 and 20*q*) estimated from the 11 basins are given in Table 2. The coefficients of the models are given in Table 3. The previous model for the *Q*95 (Kobold & Brilly, 1994) fits better to the data from the experimental basins ($R^2 = 0.741$) than the current model ($R^2 = 0.6387$). The reason is the better estimation of GEO in the previous model. Models for 20*Q* and 20*q* fit better than models for *Q*95 and *q*95.

Table 2 Data from the experimental basins and low flow characteristics.

Gauging station	Parameter:			Low flow characteristics:			
	AREA (km^2)	AAR (mm)	GEO	*Q*95 (m^3 s^{-1})	20*Q* (m^3 s^{-1})	*q*95 (l s^{-1} km^{-2})	20*q* (l s^{-1} km^{-2})
Zamusani	477	963	0.038	0.663	0.288	1.388	0.603
Sostanj	131	1287	0.021	0.578	0.108	4.405	0.823
Podhom	165	2279	0.036	1.921	1.160	11.600	7.005
Krsovec	157	3140	0.027	2.718	1.786	17.289	11.361
Suha	566	1922	0.022	4.410	2.594	7.787	4.580
Hotescek	442	2406	0.021	5.237	3.595	11.826	8.118
Vipava	105	2186	0.024	1.204	0.788	11.407	7.466
Precna	294	1270	0.026	1.671	0.905	5.680	3.076
Cerk.mlin	332	2011	0.019	0.604	0.230	1.817	0.692
Petrina	460	1832	0.018	3.376	1.550	7.339	3.370
Gradac	221	1328	0.026	0.507	0.170	2.291	0.768

Table 3 The model coefficients and statistics.

Low flow characteristic	Coefficient:			Statistics:		
	a	*b*	*c*	*d*	R^2	SE
*Q*95	$4.08.10^{-8}$	0.810	1.828	0.207	0.6387	1.86
*q*95	$1.12.10^{-5}$		1.918	0.323	0.6067	1.81
20*Q*	$7.66.10^{-11}$	1.106	2.737	0.993	0.6905	2.18
20*q*	$1.59.10^{-7}$		2.686	0.928	0.6609	2.08

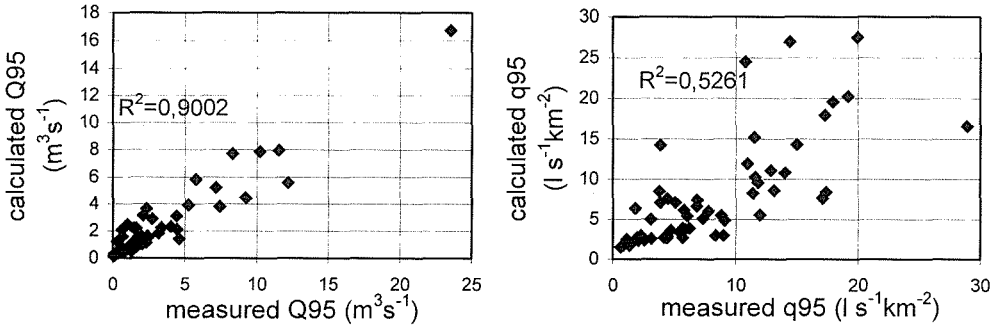

Fig. 5 Relationships between calculated and measured flows exceeded in 95% of the days. Discharge ($Q95$, left graph) and specific flow ($q95$, right graph).

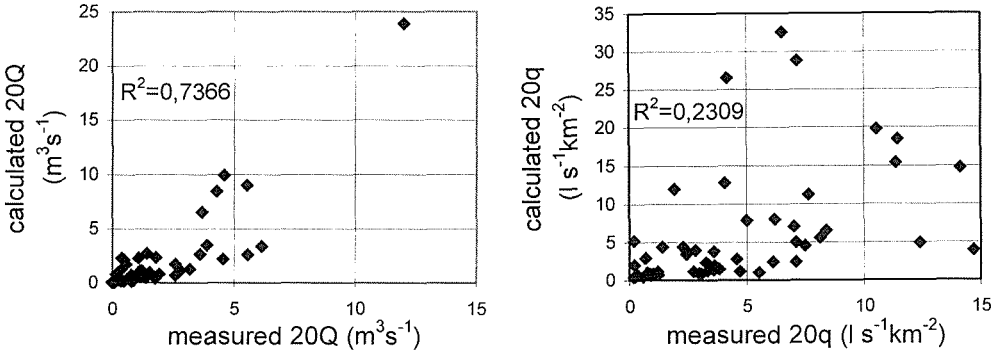

Fig. 6 Relationships between calculated and measured 20-year return period of the annual minimum flow. Discharge ($20Q$, left graph) and specific flow ($20q$, right graph).

The model parameters AREA, AAR and GEO were estimated for each of the 572 sub-basins in the WMIS and the gauging stations with a 1961–1990 data set. The low flow characteristics $Q95$, $q95$, $20Q$, and $20q$ were calculated for the gauging stations and sub-basins by using a GIS.

Measured (i.e. characteristics derived from measured time series) and calculated low flow characteristics for the gauging stations are presented in Figs 5 and 6. The characteristics of low flows fit better than those of the specific flows. The best fit is for the $Q95$ (R^2 = 0.9002, Fig. 5). The $20Q$ and $95q$ have a R^2 of 0.7366 and 0.5261 (Figs 6 and 5). The measured and calculated $20q$ show a poor correlation (R^2 = 0.2309, Fig. 6).

Data for specific flow with a 20-year return period ($20q$) were calculated for each sub-basin (Fig. 2) by the nonlinear regression model (equation 2) with the coefficients presented in Table 3. These values were plotted (Fig. 7) against the regionalized $20q$ values presented in Fig. 4. The statistics of the comparison are given in Table 4. The values of the units presented in Fig. 4 fit in the range between the minimum and maximum $20q$ values of the sub-basins belonging to a particular unit (except the regionalized $20q$ of 3 l s^{-1} km^{-2}). Low streamflow and groundwater flow should be linked in a region with large alluvial formations.

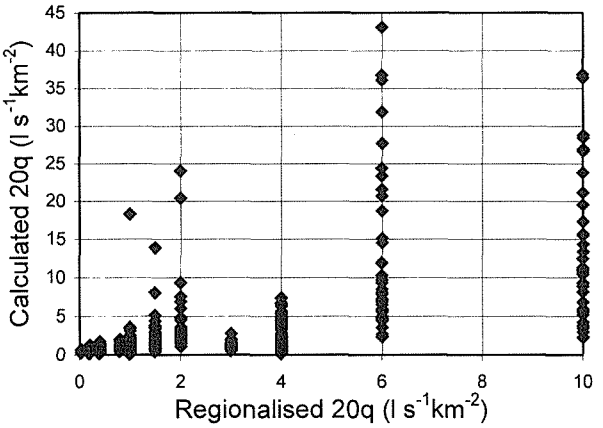

Fig. 7 Relationships between the calculated 20*q* for the 571 sub-basins in Slovenia and the regionalized 20*q* (Fig. 4).

RECOMMENDATIONS AND CONCLUSIONS

Hydrology of low flows is too complex to analyse it by very simplified models only. The discrepancies between measured and calculated low flow characteristics are caused by:

(a) infiltration of surface water, and groundwater flow in the alluvial plains and large karst regions,
(b) water management,
(c) estimation of geological (GEO) and rainfall (AAR) parameters,
(d) simplifications of the model.

The differences between measured and calculated low flow characteristics should be analysed carefully. Low streamflow and groundwater flow in a region with large alluvial deposits should be linked. Furthermore low flow in sub-basins in the karst region should be carefully analysed. Models with different parameters could be used

Table 4 Comparison between regionalized 20*q* values (Fig. 4) and the calculated 20*q* of the 572 sub-basins in Slovenia (Fig. 7).

Regionalized 20*q* ($l\ s^{-1}\ km^{-2}$)	20*q* of sub-basins ($l\ s^{-1}\ km^{-2}$): Mean	Standard deviation	Minimum	Maximum	Number of sub-basins
0.03	0.447	0.148	0.280	0.717	22
0.20	0.516	0.359	0.154	1.299	12
0.40	0.644	0.342	0.155	1.773	87
0.80	1.012	0.462	0.461	2.049	27
1.00	1.208	1.822	0.078	18.280	107
1.50	2.164	2.160	0.420	13.917	54
2.00	4.520	5.039	1.131	24.038	32
3.00	1.123	0.473	0.480	2.772	51
4.00	2.407	2.001	0.172	7.438	98
6.00	11.821	10.075	2.389	43.11	45
10.00	14.384	9.926	2.275	36.839	37

in this context. The geological parameters should be recalculated and for the AAR parameter in the $20Q$ model a rainfall map for the dry period should be used.

The methodology and derived interdependencies are already useful for water management. The observed discrepancies between measured and calculated low flow characteristics, however, need to result in a more sophisticated analysis of low flow phenomena.

Acknowledgements The authors gratefully acknowledge the support of the Hydrometeorological Institute and the Ministry of the Environment and Physical Planning for supplying the river flow and WMIS data.

REFERENCES

Brilly, M. & Vidmar, A. (1994) River basin coding. In: *Hydroinformatics'94* (ed. by A. Verwey, A. W. Minns, V. Babovic & C. Maksimovic) (Proc. Delft Symp.), 531–533. A. A. Balkema, Rotterdam.

Kobold, M. & Brilly, M. (1994) Low flow discharge analysis in Slovenia. In: *FRIEND: Flow Regimes from International Experimental and Network Data* (ed. by P. Seuna, A. Gustard, N. W. Arnell & G. A. Cole) (Proc. Braunschweig Symp., October 1993), 119–131. IAHS Publ. no. 221.

LAWA (1993) *Richtlinie fur die Gebietsbezeichnung und die Verschlusselung von Fliesgewassern* (Guideline for the coding of waterways and their basin) (in German). Landerarbeitsgemeinschaft Wasser.

VGI (1991) *Vodnogospodarske osnove Slovenije* (The water resources of Slovenia) (in Slovin). Ministry of the Environment and Physical Planning, Ljubljana, Slovenia.

FRIEND'97 — Regional Hydrology: Concepts and Models for Sustainable Water Resource Management
(Proceedings of the Postojna, Slovenia, Conference, September–October 1997). IAHS Publ. no. 246, 1997.

Regional low-flow studies in South Africa

VLADIMIR Y. SMAKHTIN
Institute for Water Research, Rhodes University, PO Box 94, Grahamstown 6140, South Africa

Abstract The high variability of South African river low-flow regimes and varying availability of daily streamflow records necessitates the application of different low-flow estimation techniques in different regions of the country. The paper describes several possible approaches for the estimation of low-flow characteristics (use of the rainfall–runoff simulation technique, regionalization of flow duration curves, use of synthetic monthly streamflow data) and illustrates their applicability using example case studies in several catchments in South Africa. The first approach allows a variety of low-flow characteristics to be estimated and is preferable for detailed low-flow studies. The other two make use of flow duration curves and have a logical link with the database of synthetic monthly flow data for a number of ungauged subcatchments in the country.

INTRODUCTION

An increasing scarcity of water in many regions of South Africa and a recent shift towards more integrated management of limited water resources attracts a permanently growing attention to the low-flow part of a total streamflow hydrograph. Detailed daily low-flow information is required in design of run-of-river schemes, in water quality studies as well as for the determination of ecological Instream Flow Requirements of rivers. The high spatial variability of South African daily low-flow regimes (e.g. Smakhtin *et al.*, 1995), varying availability and, frequently, insufficient quality of observed streamflow data, limit in the South African context the possibilities for the development and application of regional regression models widely used for low-flow assessment elsewhere (Gustard *et al.*, 1992; Nathan & McMahon, 1992), put more emphasis on the application of daily streamflow generation methods and imply that: (a) the problem of low-flow estimation should preferably be addressed at the scale of large catchments, and (b) that different low-flow estimation techniques are likely to be required in different regions. The paper illustrates the example applications of different daily low-flow estimation techniques in several South African catchments and discusses their limitations and potential value.

LOW-FLOW ESTIMATION SOFTWARE

Low-flow estimations rely on the availability of either observed or simulated daily streamflow time series by an appropriate model, and therefore a certain software package is required to calculate various low-flow characteristics from the time series data. The software package developed at the Institute for Water Research (Smakhtin

et al., 1995; Smakhtin & Watkins, in press), includes the following analyses which are normally in demand in different water related fields: (a) the construction of flow duration curves; (b) analysis of continuous low-flow intervals below specified threshold flows (low-flow spells); (c) the construction of low-flow frequency curves; (d) procedures to calculate baseflow and recession characteristics. Several other modules for general hydrological analysis are also included.

The modules are written in "C" code, make extensive use of computer graphics, are entirely menu driven and form part of a more general computer software package —HYMAS (HYdrological Modelling Application System), which represents a flexible environment in which to set up and run hydrological models and to analyse observed and simulated hydrological variables.

LOW-FLOW ASSESSMENT FROM SIMULATED DATA

Daily low-flow information is frequently required at a finer level of spatial resolution than that provided by streamflow gauging. The other usual requirement is for low-flow characteristics in natural and present-day conditions in a study catchment. In such cases the use may be made of deterministic rainfall–runoff simulation techniques. The in-house developed VTI (Variable Time Interval) model, used in this study is a semi-distributed physically based model of a modular structure where each module describes a separate component of catchment hydrological cycle: interception, evapotranspiration, rainfall intensity controlled runoff, soil moisture redistribution and saturated surface runoff, catchment routing, channel transmission losses and flow routing (Hughes & Sami, 1994). The model also describes several surface–subsurface water interaction processes which determine low-flow regimes: (a) drainage from a soil into a percolating storage; (b) the re-emergence of percolating water as springs above the regional water table; (c) piezometric surface dynamics resulting from changes in aquifer storage; (d) groundwater seepage from the intersection of the water table with the surface. The model operates with a daily time step equal to input data time resolution, but switches to shorter time intervals during significant floods. A modelled catchment is represented by a set of interlinked subareas which are relatively homogeneous in terms of catchment physiographic parameters and/or water use development. The variability of hydrological processes within each subarea is described by means of probability distribution functions of model parameters.

The model has been applied in the Sabie catchment (area 5713 km^2) in the Mpumalanga Province, the Berg catchment (4012 km^2) in the Western Cape, several major tributaries of the Tugela River (29 000 km^2) in KwaZulu-Natal (Fig. 1). The catchments represent different physiographic conditions and low-flow generating mechanisms as well as the availability of hydrometeorological and water resource development data necessary to calibrate and run the model. The results of model calibration at gauged sites within each selected catchment have been assessed using fit statistics for untransformed and log-transformed flows (e.g. coefficients of determination (R^2) and efficiency (*CE*)). A particular emphasis in evaluating the model results has been placed on the model's ability to reproduce different aspects of low-flow regimes. The model's performance in the low-flow domain has therefore

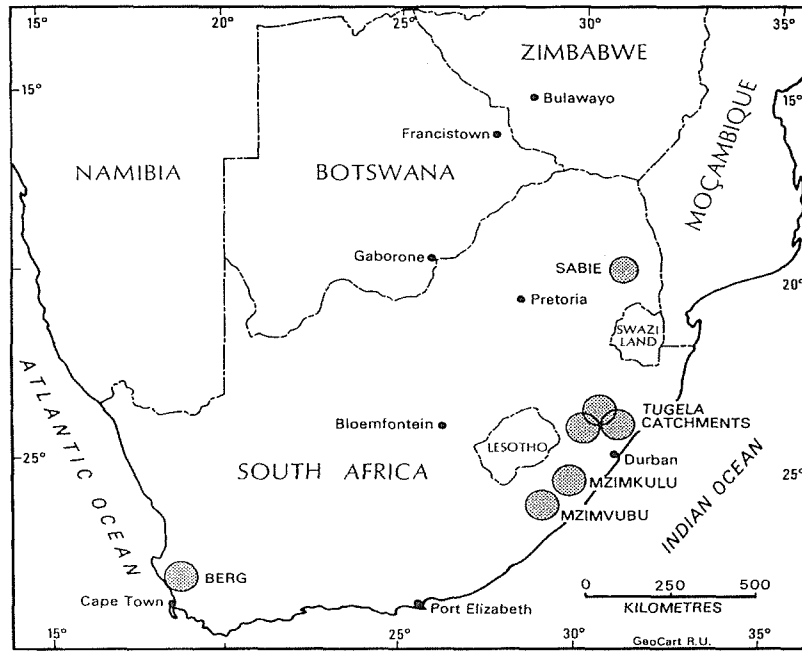

Fig. 1 Location of the study basins in South Africa.

been assessed through the comparison of observed and simulated flow duration curves, low-flow spells, baseflow volumes and recession characteristics (Smakhtin & Watkins, in press). In most of the cases the model performed satisfactorily in terms of both conventional fit statistics (R^2 and *CE* were in the range 0.6–0.9) and low-flow criteria (low-flow characteristics calculated from observed and simulated daily flow time series were in close agreement).

The calibrated model has been used to simulate a satisfactorily long daily flow time series representing natural and present-day conditions in a catchment. To simulate natural flow conditions all present artificial impacts (farm dams, direct river abstractions, forestry, etc.) have been removed from a parameter set and some of the parameter values have been modified (e.g. to account for different interception and/or evaporative demand of natural vegetation). A variety of low-flow indices can be estimated for each subarea from simulated streamflow time series. Figure 2 illustrates the spatial distribution of a 7-day average flow exceeded 95% of the time ($Q95(7)$, mm annum^{-1}) in natural conditions in the Sabie catchment. Most of the low-flows are generated in the western upstream steeply sloping parts of the catchment, whereas the more arid downstream parts are characterized by zero increments to baseflow.

The degree of change in low-flow regimes can be assessed by comparing flow duration curves constructed from simulated data in natural and present-day conditions. Figure 3 illustrates that the flow regime in the Berg River catchment has been considerably modified (due to numerous domestic and irrigation abstractions) with the largest relative effect on low flows. (The flow exceeded 75% of the time ($Q75$) at present is 5 times less than that in the natural conditions. At the same time the present-day flow exceeded 95% of the time ($Q95$) is almost two orders of magnitude lower than the corresponding natural flow value.)

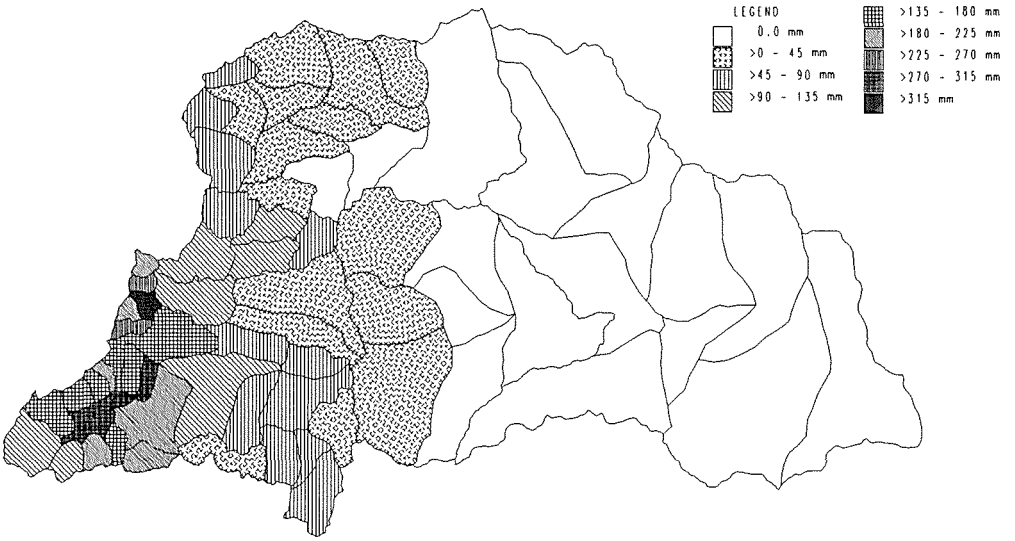

Fig. 2 The distribution of $Q95(7)$ flow values (mm annum^{-1}) in the Sabie basin.

The use of the VTI daily rainfall–runoff model is a very flexible and attractive approach for catchmentwide low-flow assessment. However, the applicability of such complex and labour intensive techniques is limited to those areas where exist: (a) sufficient knowledge about catchment physiographic characteristics, (b) adequate data on water resource development, (c) sufficient rainfall input data.

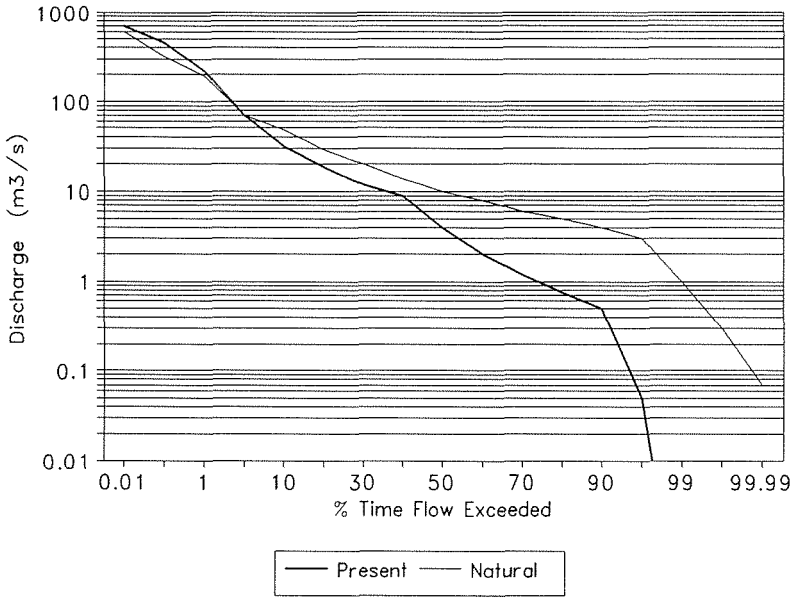

Fig. 3 One-day flow duration curves in the Berg River at Misverstand Bridge (catchment area 4012 km^2) at present and natural conditions.

REGIONAL FLOW DURATION CURVES

For small scale water projects the flow information summarized in a form of a flow duration curve (FDC) may suffice. A FDC for an ungauged site may be established through the regionalization. The ordinates of all individual curves constructed on the basis of gauged data in a hydrologically homogeneous region are normalized by the mean daily flow and an average regional non-dimensional FDC is calculated. Regional FDCs may be established for the year, season or for each calendar month. The actual FDC at an ungauged site may be calculated by multiplying back the non-dimensional ordinates of a corresponding regional FDC by the estimate of the mean flow. The latter may be calculated for 1946 small ungauged drainage subdivisions throughout the country (quaternary subcatchments) from synthetic monthly flow information presented in a nationwide study on Surface Water Resources of South Africa (WR90, 1994).

The method of regional FDCs has been applied in the northeastern part of the Eastern Cape Province to the south of Lesotho, which includes such well-watered and largely untapped at present catchments as Mzimvubu (area 19 852 km^2) and Mzimkhulu (area 6678 km^2, Fig. 1). The need for appropriate low-flow estimation techniques in the region becomes particularly relevant with the increasing development of small rural water supply schemes.

Normalized 1-day FDCs have been constructed for each of the 16 existing gauging stations which represent the only source of hydrological information in the entire region. The average observation period at these gauges is about 20 years. For each gauge the curves were constructed for the whole year, the four wettest months (December–March), the four driest months (June–September) and four intermediate months (April, May, October, November). In all four cases the individual FDCs appeared to lie close to each other throughout most of the time scale. The biggest differences occur in the area of extreme low flows, exceeded more than 95% of the time and high flows exceeded less then 5% of the time (Fig. 4). These differences

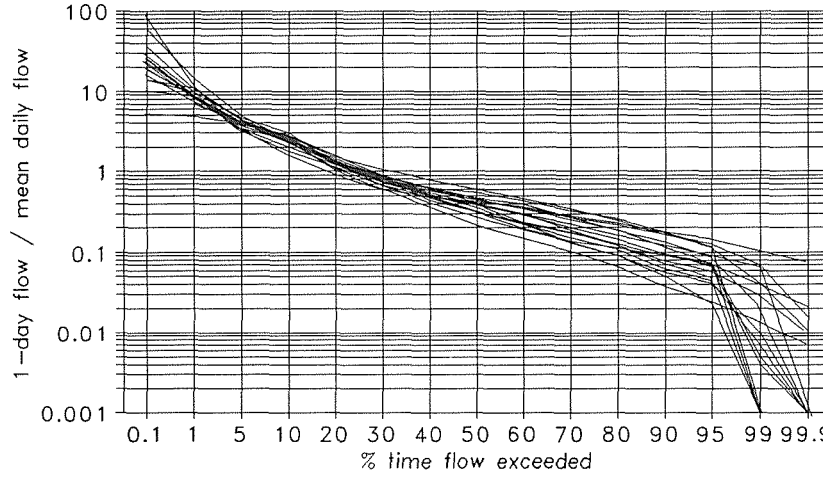

Fig. 4 Normalized 1-day annual flow duration curves for streamflow gauges in part of the Eastern Cape Province.

may be attributed to the inaccuracies of low-flow measurements, different lengths of the record period at individual gauges, and limitations of some gauging structures which are too small to measure high flows.

Using the established regional FDCs and the values of mean daily flow from WR90 (1994), the low-flow characteristics can be estimated for any large river basin in the region at least at quaternary subcatchment level of spatial resolution. Figure 5 illustrates the spatial distribution of flow exceeded 75% of the time ($Q75$, mm annum^{-1}) in the Mzimvubu catchment.

Regionalization of flow duration curves is most likely to succeed only in physiographically homogeneous areas with limited water resource development and satisfactorily long streamflow records.

ESTIMATING DAILY LOW FLOWS FROM SYNTHETIC MONTHLY DATA

Synthetic monthly streamflow time series data are available in South Africa for every quaternary subcatchment (WR90, 1994) and may be utilized for the estimation of daily low-flow characteristics. One possible option is to convert a FDC based on monthly flow volumes to FDCs based on daily discharges. The most straightforward form of a relationship between the two is a "ratio curve". Once two curves at a site are constructed using similar units, the ratios of daily to monthly flows for several

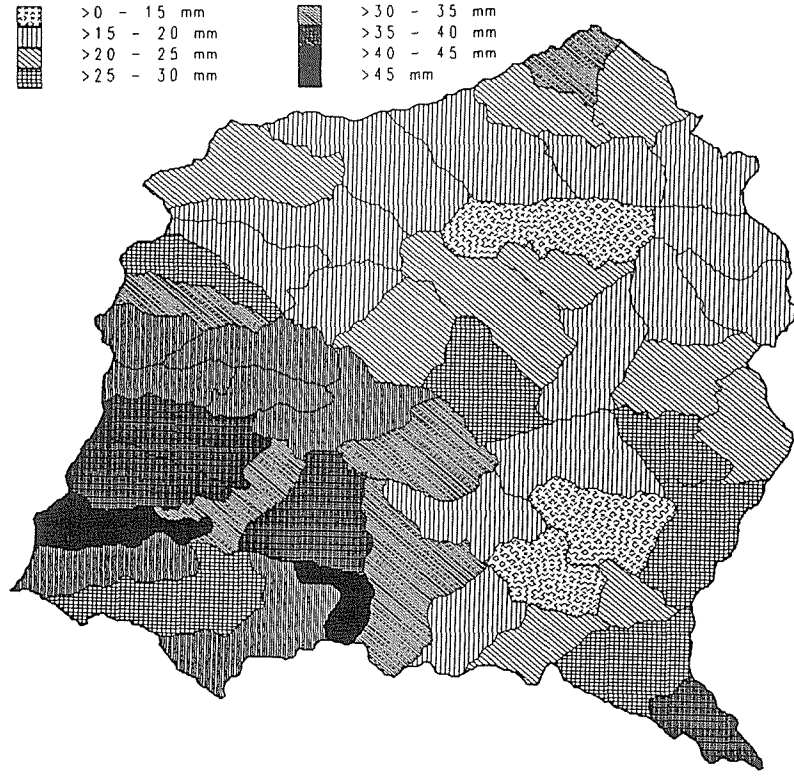

Fig. 5 The distribution of $Q75$ flow values (mm annum^{-1}) in the Mzimvubu basin.

fixed percentage points are calculated and plotted against the percentage point values producing the "ratio curve" for a site. The procedure is repeated for each gauge in a specified region. The next step is to group these ratio curves. This is largely based on the premise that the within-month variation of daily flows in similar sized catchments within a hydrologically homogeneous region might be expected to be equally similar. The desired result is therefore a regional "ratio curve" which can be used to convert the ordinates of a 1-month FDC for a quaternary catchment (e.g. established using synthetic monthly flow data) to the ordinates of a 1-day FDC.

The approach has been tested in the Sabie and Tugela catchments. These preliminary tests have demonstrated that the regional relationships between the two types of FDCs may be established, although difficulties are experienced is selecting good quality records for such analysis.

The 1-day FDC for an ungauged site derived by either regionalization of observed FDCs or from synthetic monthly data, may be used further for generation of a complete continuous daily streamflow hydrograph at a site in a combination with nonlinear spatial interpolation technique described by Hughes & Smakhtin (1997). This technique is based on 1-day FDCs for each calendar month of a year and has a purpose of transferring the gauged daily data to ungauged sites. The algorithm represents a pragmatic alternative to more complex simulation methods and has been successfully applied for daily data generation in parts of the Eastern Cape Province of South Africa (Smakhtin & Watkins, in press). The generated continuous daily hydrographs are then used for the estimation of other low-flow characteristics.

CONCLUSIONS

The applicability of three different approaches for low-flow estimation have been tested using example case studies in several catchments in South Africa. The daily rainfall–runoff simulation approach (the VTI model) is very attractive for detailed catchmentwide studies since it allows a variety of low-flow characteristics to be estimated at a required level of spatial resolution. However, it is a complex and time-consuming approach which requires detailed knowledge about catchment physiographic characteristics, water resource development and sufficient rainfall input data.

The other two methods concentrate on the estimation of 1-day flow duration curves (and related low-flow indices). They are less time consuming and have a logical link with existing national database of synthetic monthly streamflow characteristics for a number of ungauged drainage subdivisions throughout South Africa. A flow duration curve established at an ungauged location by any of the two latter methods may be converted into a continuous daily hydrograph from which other low-flow characteristics may be estimated. The limitations of these techniques mostly relate to the quality and amount of the available observed daily streamflow records.

Acknowledgements The financial support of the Water Research Commission of South Africa is gratefully acknowledged. Thanks are due to the Department of Water Affairs and Forestry for supplying the streamflow data used in this study.

REFERENCES

Gustard, A., Bullock, A. & Dixon, J. M. (1992) Low flow estimation in the United Kingdom. *Institute of Hydrology Report no. 108, Wallingford, Oxfordshire, UK.*

Hughes, D. A. & Sami, K. (1994) A semi-distributed, variable time interval model of catchment hydrology—structure and parameter estimation procedures. *J. Hydrol.* **155**, 265–291.

Hughes, D. A. & Smakhtin, V. Y. (in press) Daily flow data time series patching or extension: a spatial interpolation approach based on flow duration curves. *Hydrol. Sci. J.* **41**, 851–871.

Nathan, R. J. & McMahon, T. A. (1992) Estimating low flow characteristics in ungauged catchments. *Wat. Res. Manage.* **6**, 85–100.

Smakhtin, V. Y., Watkins, D. A. & Hughes, D. A. (1995) Preliminary analysis of low-flow characteristics of South African rivers. *Water SA* **21**, 201–210.

Smakhtin, V. Y. & Watkins, D. A. (in press) Low-flow estimation in South Africa. *WRC Report, Pretoria.*

WR90: Surface Water Resources of South Africa 1990 (1994) *WRC Report no. 298/1/94, Pretoria.*

FRIEND'97 — Regional Hydrology: Concepts and Models for Sustainable Water Resource Management
(Proceedings of the Postojna, Slovenia, Conference, September–October 1997). IAHS Publ. no. 246, 1997.

Frequency analysis of low flows by the PPCC test in Turkey

ATIL BULU & BIHRAT ONOZ
Istanbul Technical University, Civil Engineering Faculty, Maslak, 80626 Istanbul, Turkey

Abstract This study attempts to find the best fitted distribution function to the minimum D-day low flows for the Meric and Sakarya river basins in Turkey. For this purpose, the W2 and LN2 distribution functions were used. The Probability Plot Correlation Coefficient (PPCC) test was applied for the suitability of the selected distribution functions. It was found that the W2 distribution function conformed better than the LN2 distribution function on a station basis. A regional hypothesis test was applied to the 7-day low flow value which is the generally accepted low flow index. Similarly, the W2 distribution performed better than the LN2 distribution in both regions.

INTRODUCTION

Low river discharges will occur at some period of the year and sometimes become dry, especially in arid and semiarid regions. This usually occurs during the summer when irrigation is of primary importance. From the dilution point of view this has important consequences for the discharge of waste water into the river flows during the low flow period. If the flow decreases below a certain value, there is a direct effect on the aquatic life of the surface flow under consideration. Low flow statistics are also used in water supply planning to determine allowable water transfers and withdrawals. Other applications of low flow frequency analysis include determination of minimum downstream release requirements from hydropower, water supply, cooling plants and other facilities.

This study attempted to find out the best fitted distribution function to the low flows on the Meric and Sakarya basins in Turkey. In addition, regional analysis was applied to the stations under consideration. To determine the best fitted distribution function to the low flows and in regional analysis, the Probability Plot Correlation Coefficient (PPCC) test was used. This test is more robust than other known tests (Smirnov-Kolmogorov, chi-square) and has found frequent application in recent literature. Critical values were obtained for different distribution functions for practical applications.

In low flow research studies, seven-day and 10-year low flows ($Q_{7,10}$) have been investigated more thoroughly. This value coincides with the mean seven day minimum flows for a year and with a 10-year return period. For predicting $Q_{7,10}$ discharge, different distribution functions and parameter estimation techniques have been investigated for many years (Gumbel, 1954, 1958; Matalas, 1963; Condie & Nix, 1975). In Condie & Nix (1975), W3 (MLE) and W3 (MOM) was recommended, but Tasker (1987) suggested the log-Pearson type III (LP3-MOM) distribution. In a study using lognormal (LN2), Weibull (W2) and Gumbel

distributions performed by Vogel & Kroll (1989) in the United States, they came to the conclusion that the LN2 distribution is the best distribution for estimating $Q_{7,10}$ discharge at a station and on a regional basis.

PROBABILITY PLOT CORRELATION COEFFICIENT (PPCC) TEST

The Probability Plot Correlation Coefficient (PPCC) is a test statistic to measure linearity of the probability plot. Critical values have been obtained for normal and Gumbel distribution by Vogel (1986). The test has also been developed for the Weibull and the uniform distribution by Vogel & Kroll (1989), for the P3 distribution by Vogel & Martin (1991), for the extreme value distributions (GEV) by Chowdhury *et al.* (1991). The critical values obtained for the normal distribution can also be used for the LN2 distribution.

The correlation coefficient test statistic, r, is calculated between the ordered observed values and the inversed values of the cumulative distribution functions of the fitted distribution. If the observed values conform to the applied distribution, the r statistic should be greater than the critical value for the selected significance level. The equations that give unbiased estimates of the inverse values, have been obtained by different researchers, with the r test statistic defined as

$$r = \frac{\sum_{i=1}^{n} (x_i - \bar{x})\,(m_i - \bar{m})}{\sqrt{\sum_{i=1}^{n} (x_i - \bar{x})^2 \sum_{i=1}^{n} (m_i - \bar{m})^2}} \tag{1}$$

in which x_i ($x_1 \leq \ldots \leq x_i \leq \ldots \leq x_n$) is the ordered ith value and $\bar{x}$ is the mean of observed values.

$$m_i = \mathrm{F}_x^{-1}(p_i) \tag{2}$$

in which F(.) is the cumulative probability value and p_i is the value estimated by unbiased equations for different probability distributions.

PPCC test for the normal and the lognormal distribution

The inverse of the standard normal distribution can be obtained from Joiner & Rosenblatt (1971).

$$m_i = 4.91\left[p_i^{0.14} - (1 - p_i)^{0.14} \right] \tag{3}$$

Normal p_i values are estimated by Filliben (1975),

$$\begin{aligned} p_i &= 1 - (0.5)^{1/n} && i = 1 \\ p_i &= \frac{(i - 0.3175)}{(n + 0.365)} && i = 2, \ldots, n-1 \\ p_i &= (0.5)^{1/n} && i = n \end{aligned} \tag{4}$$

If the PPCC test statistic estimated from equation (1) between the inverse values and the ordered observed values, calculated by equations (3) and (4) is greater than the critical value for a selected significance level, then it can be said that the observed values fit to the normal distribution.

The PPCC test statistic for the two parameter lognormal distribution (LN2) is estimated between the inverse values calculated from equations (3) and (4) and the logarithms of the ordered observed values. Critical values were given by Vogel (1986).

PPCC test for the two parameter Weibull distribution (W2)

The extreme value type III or Weibull distribution is generally used for low flow analysis (Gumbel, 1954). The cumulative distribution function for a random variable y is

$$F(y) = 1 - \exp\left[-\left(\frac{y-\varepsilon}{\alpha-\varepsilon}\right)\right]^k \tag{5}$$

If the lower limit ε is taken as zero, the two parameter Weibull (W2) distribution is obtained. The estimate of PPCC test statistic r is calculated by equation (1) between the $x_i = \ln(y_i)$ values and the inverse values determined by

$$m_i = F_y^{-1}(p_i) = \ln\alpha + \frac{1}{k}\ln\left[-\ln\ (1-p_i)\right] \tag{6}$$

p_i values in equation (6) can be estimated by equation (7) that was proposed for Gumbel distribution (Gringorten, 1963) since there is a functional relationship between Weibull and Gumbel distributions. If the y variate is distributed as Weibull then the $z = -\ln(y)$ variate is distributed as Gumbel. Therefore, the equations used for one of these distributions can also be used for the other one (Stedinger *et al.*, 1993).

$$p_i = \frac{i-0.44}{n+0.12} \tag{7}$$

The estimates of α and k parameters by the probability weighted moments are

$$k = \frac{\ln(2)}{L_{2,(\ln y)}}, \qquad \alpha = \exp\left(L_{1,(\ln y)} + \frac{0.5772}{k}\right) \tag{8}$$

In these equations, L_1 is the mean of $\ln(y)$ series and L_2 is L_2-moments calculated from $\ln(y)$ series.

The information related to the probability weighted moments and the L-moments are given in Stedinger *et al.* (1993). Critical values for this distribution were given by Vogel & Kroll (1989).

PPCC test for the uniform distribution

If the random variable takes every value with the same probability for a given

interval then it is distributed as uniform. The probability density function f(x) and cumulative probability function F(x) for (a,b) interval are

$$f(x) = \frac{1}{b-a} \qquad a \le x \le b \tag{9}$$

$$F(x) = \frac{x-a}{b-a} \qquad a \le x \le b \tag{10}$$

The estimate of the PPCC test statistic, r, can be determined from equation (1) between the ordered observed values and the inverse values of the uniform distribution. The inverse value of this distribution can be calculated from equation (11).

$$m_i = F_x^{-1}(p_i) = a + (b-a)p_i \tag{11}$$

$$p_i = \frac{i}{n+1} \tag{12}$$

The PPCC test statistic is free of parameter estimation techniques used to estimate a and b parameters and0 equation (1) can be defined as (Vogel & Kroll, 1989),

$$r = \frac{\operatorname{cov}(x_i, p_i)}{\left[\operatorname{var}(x_i)\operatorname{var}(p_i)\right]^{0.5}} \tag{13}$$

Similarly, the PPCC test statistic is free of parameter estimation techniques for the estimation of parameters of the used distributions for one or two parameter distributions with constant skewness coefficients. Critical values of the test statistic have been given for the uniform distribution by Vogel & Kroll (1989).

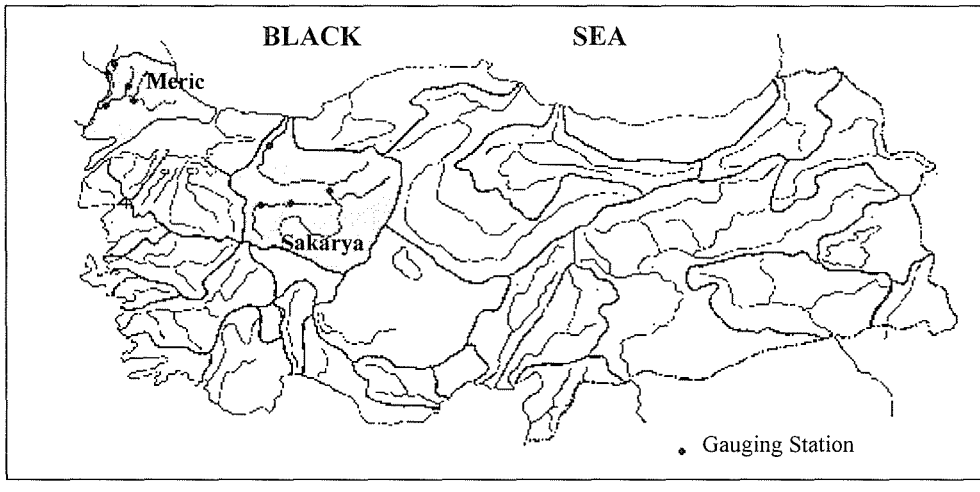

Fig. 1 Drainage basins in Turkey.

Table 1 Characteristics of the Sakarya basin.

Station	Drainage area (km^2)	Record length (years)
Besdegirmen	3 938	1935–1991 (53)
Dogancay	52 531	1952–1991 (37)
Kargi	33 847	1959–1991 (31)
Eskisehir	6 340	1969–1991 (19)

Table 2 Characteristics of the Meric basin.

Stations	Drainage area (km^2)	Record length (years)
Meric	27 251	1969–1991 (23)
Tunca	7 928	1969–1991 (23)
Ergene	10 195	1969–1990 (22)
Hayrabolu	1 318	1969–1991 (23)

CASE STUDY

Two river basins have been taken in Turkey to find out the best fitted distribution to their low flows (Fig. 1). Daily flows of four stations in each basin were used. The characteristics of the Sakarya and Meric river basins are given in Tables 1 and 2.

Mean low flows of 1, 3, 7, 10, 14, 30, 60, 90, 120, 150 and 273-days for each year were determined to check the suitability of the LN2 and W2 distributions by the PPCC test. The test statistics for the LN2 and W2 distributions for different D-day low flows are given in Tables 3 and 4. Low flows greater than zero were taken into consideration in this study. In examining Table 3, the number of D-days that the LN2 distribution is acceptable are 3 for Meric, 7 for Tunca, 3 for Ergene and 5 for Hayrabolu at $\alpha = 0.05$ significance level for different D-day low flows. Table 4 gives the results for the W2 distribution. This distribution conforms to all flows in the Meric and Hayrabolu rivers, conforms to all flows except the 30-day low flow at Tunca, and for the Ergene River it also fits to all except the 7 and 90-day low flows. It is quite apparent that the W2 distribution fits better than the LN2 distribution for the Meric River basin. The same distributions are also applied to the stations in the

Table 3 PPCC test statistics for the LN2 in the Meric region.

Day	Meric	Tunca	Ergene	Hayrabolu
1	0.944	0.965*	0.909	0.963*
3	0.945	0.971*	0.865	0.972*
7	0.944	0.974*	0.900	0.932
10	0.947	0.978*	0.856	0.938
14	0.939	0.975*	0.923	0.928
30	0.925	0.850	0.879	0.928
60	0.937	0.885	0.943	0.941
90	0.940	0.906	0.850	0.923
120	0.961*	0.952	0.992*	0.981*
150	0.964*	0.973*	0.959*	0.988*
273	0.985*	0.969*	0.978*	0.982*

* Values that are greater than the critical value at $\alpha = 0.05$ significance level.

Sakarya River basin. Tables 5 and 6 give the PPCC test results. It can be seen from Table 5 that the LN2 distribution does not conform to 3 of the D-day flows at Besdegirmen, to 8 of the D-day flows at Dogancay, 1 D-day flow at Kargi and to 2 D-day flows at Eskisehir stations. For the W2 distribution, all flows except 2 of the D-day flows for Besdegirmen, all values for Dogancay, all flows for Kargi and all values except 2 D-day flows for Eskisehir do not pass the PPCC test at $\alpha = 0.05$ significance level. It is also quite apparent for this region that the W2 is better than the LN2 distribution for the frequency analysis of low flows.

REGIONAL ANALYSIS

To check the validity of results found at the selected stations and regions, the 7-day low flows were taken for regional analysis. The PPCC test statistics and their corresponding α significance levels are given in Tables 7 and 8.

Significance levels α corresponding to the PPCC test statistic, r, are the cumulative probabilities of the distribution of r. The distribution function of α is

Table 4 PPCC test statistics for W2 in the Meric region.

Day	Meric	Tunca	Ergene	Hayrabolu
1	0.985*	0.943*	0.963*	0.991*
3	0.986*	0.951*	0.943*	0.993*
7	0.985*	0.955*	0.925	0.982*
10	0.986*	0.961*	0.936*	0.982*
14	0.980*	0.959*	0.959*	0.977*
30	0.978*	0.920	0.946*	0.970*
60	0.978*	0.948*	0.969*	0.939*
90	0.979*	0.958*	0.926	0.963*
120	0.989*	0.979*	0.971*	0.952*
150	0.984*	0.989*	0.943*	0.966*
273	0.980*	0.966*	0.981*	0.994*

* Values that are greater than the critical value at $\alpha = 0.05$ significance level.

Table 5 PPCC test statistics for LN2 in the Sakarya region.

Day	Besdegirmen	Dogancay	Kargi	Eskisehir
1	0.9734	0.9753*	0.9612	0.8609
3	0.9735	0.9652	0.9653*	0.9039
7	0.9789*	0.9686	0.9707*	0.9538*
10	0.9803*	0.9640	0.9722*	0.9817*
14	0.9805*	0.9584	0.9716*	0.9723*
30	0.9747	0.9618	0.9782*	0.9823*
60	0.9856*	0.9541	0.9858*	0.9857*
90	0.9919*	0.9568	0.9912*	0.9757*
120	0.9932*	0.9656	0.9851*	0.9872*
150	0.9964*	0.9765*	0.9948*	0.9879*
273	0.99919*	0.9855*	0.9865*	0.9895*

* Values that are greater than the critical value at $\alpha = 0.05$ significance level.

Table 6 PPCC test statistics for W2 in the Sakarya region.

Day	Besdegirmen	Dogancay	Kargi	Eskisehir
1	0.9630	0.9903*	0.9894*	0.9327
3	0.9655	0.9876*	0.9945*	0.9551*
7	0.9738*	0.9864*	0.9951*	0.9689*
10	0.9758*	0.9896*	0.9954*	0.9792*
14	0.9780*	0.9891*	0.9953*	0.9623*
30	0.9934*	0.9943*	0.9968*	0.9662*
60	0.9721*	0.9927*	0.9929*	0.9720*
90	0.9730*	0.9947*	0.9849*	0.9342
120	0.9751*	0.9940*	0.9824*	0.9613*
150	0.9768*	0.9889*	0.9752*	0.9659*
273	0.9709*	0.9772*	0.9348*	0.9485*

* Values that are greater than the critical value at $\alpha = 0.05$ significance level.

Table 7 PPCC test statistics for LN2 and W2 distributions and α-significance level for Meric.

Station	*n* (years)	*r* LN2	*r* W2	α LN2	α W2
Meric	23	0.944	0.985	0.021	0.715
Tunca	22	0.974	0.955	0.250	0.097
Ergene	14	0.900	0.925	0.010	0.180
Hayrabolu	18	0.932	0.982	0.024	0.690

Table 8 PPCC test statistics for LN2 and W2 distributions and α-significance level for Sakarya.

Station	*n* (years)	*r* LN2	*r* W2	α LN2	α W2
Besdegirmen	53	0.9754	0.9694	0.037	0.075
Dogancay	37	0.9699	0.9916	0.050	0.775
Kargi	31	0.9727	0.9950	0.130	0.972
Eskisehir	19	0.9595	0.9731	0.100	0.410

uniform at (0,1) interval (Vogel & Kroll, 1989). The theoretical mean and standard deviation of α should be 0.5 and 0.289 respectively for the sample of four. Comparison of the theoretical and observed mean and standard deviation values are shown in Tables 9 and 10. The observed mean and standard deviation values are closer to the theoretical values for the W2 distribution. The PPCC test statistic, *r*, for α significance levels are higher for the W2 distribution at both basins. These results are in agreement with the results found at the selected stations.

CONCLUSIONS

In this study, the best fitted distribution function to the low flows of Meric and Sakarya river basins in Turkey was investigated. The results were checked by a regional test. 1, 3, 7, 10, 14, 30, 60, 90, 120, 150 and 273-day mean low flow values were used for each year. The regional test was applied to the 7-day mean low

Table 9 Regional PPCC test statistics for LN2 and W2 distributions and α-significance level for Meric.

Regional Hypothesis	Significance levels Mean: Theoretical	Observed	Standard deviation: Theoretical	Observed	r
LN2	0.5	0.076	0.289	0.414	0.805
W2	0.5	0.421	0.289	0.328	0.932

Table 10 Regional PPCC test statistics for LN2 and W2 distributions and α-significance level for Sakarya.

Regional Hypothesis	Significance levels Mean: Theoretical	Observed	Standard deviation: Theoretical	Observed	r
LN2	0.5	0.08	0.289	0.043	0.979
W2	0.5	0.558	0.289	0.397	0.993

flows since this value was accepted as the low flow criteria. The results can be summarized as follows:

- The PPCC test was applied to the selected low flows described above. The W2 distribution performed better than the LN2 distribution according to the test results.
- Similarly, the W2 distribution performed better than the LN2 distribution in the regional test applied at $\alpha = 0.05$ significance level at both regions for the 7-day low flows.

Acknowledgements The authors would like to thank Istanbul Technical University Research Fund that provided support for the accomplishment of this study.

REFERENCES

Chowdhury, J. U., Stedinger, J. R. & Lu, L. H. (1991) Goodness-of-fit tests for regional generalized extreme value flood distributions. *Wat. Resour. Res.* **27**(7), 1765–1776.

Condie, R. & Nix, G. A. (1975) Modeling of low flow frequency distributions and parameter estimation. *Wat. Resour. Symp., Water for Arid Lands* (Teheran, Iran).

Filliben, J. J. (1975) The probability plot correlation coefficient test for normality. *Technometrics* **17**(1), 111–117.

Gringorten, I. I. (1963) A plotting rule for extreme probability paper. *J. Geophys. Res.* **68**(3), 813–814.

Gumbel, E. J. (1954) Statistical theory of droughts. *Proc. Hydraul. Div., ASCE* **80**, 1–10.

Gumbel, E. J. (1958) *Statistics of Extremes*. Columbia Univ. Press, New York, N.Y.

Joiner, B. L. & Rosenblatt, J. R. (1971) Some properties of the range in samples from Tukey's symmetric Lambda distributions. *J. Am. Statist. Ass.* **66**, 394–399.

Matalas, N. C. (1963) Probability distribution of low flows. *US Geol. Survey Prof. Pap. 434-A*. Government Printing Office, Washington, DC.

Stedinger, J. R., Vogel, R. M. & Foufoula-Georgiov, E. (1993) Frequency analysis of extreme events. Chapter 18 in: *Handbook of Applied Hydrology* (ed. by D. Maidment). McGraw-Hill Book Co., New York.

Tasker, G. D. (1987) A comparison of methods for estimating low flow characteristics of streams. *Wat. Resour. Bull.* **23**(6), 1077–1083.

Vogel, R. M. (1986) The probability plot correlation coefficient test for the normal, lognormal and Gumbel distributional hypotheses. *Wat. Resour. Res.* **22**(4), 587–590.

Vogel, R. M. & Kroll, C. N. (1989) Low-flow frequency analysis using probability plot correlation coefficients. *J. Wat. Resour. Planning and Manage.* **115**(3), 338–357.

FRIEND'97 — Regional Hydrology: Concepts and Models for Sustainable Water Resource Management
(Proceedings of the Postojna, Slovenia, Conference, September–October 1997). IAHS Publ. no. 246, 1997.

Regional analysis of extreme streamflow drought duration and deficit volume

LENA M. TALLAKSEN
Department of Geophysics, University of Oslo, PO Box 1022 Blindern, N-0315 Oslo, Norway

HEGE HISDAL
Norwegian Water Resources and Energy Administration, PO Box 5091 Majorstua, N-0301 Oslo, Norway

Abstract The regional characteristics of severe seasonal droughts have been studied by analysing the extreme value properties of the annual maximum series of drought duration and deficit volume. The threshold level approach is used to define drought characteristics, i.e. drought duration and deficit volume from time series of daily streamflow, and the method is evaluated for use on a Nordic data set of 52 catchments covering 60 years of flow data. The threshold level is defined by percentiles from the flow duration curve, and a low threshold level is not recommended for use due to the occurrence of a large number of years not experiencing droughts. Two different regionalization tools are compared, L-moment diagrams and empirical orthogonal functions (EOF method). L-moment diagrams showed that the generalized Pareto distribution gave the best overall fit to the annual and summer drought samples. Deficit volume exhibited a more long-tailed behaviour than the distributions obtained for duration, and a lower percentage of explained variance was found for deficit volume using the EOF method. The L-moment and EOF diagrams provided virtually the same conclusions with regard to clustering of catchments, and large scale trends were found in the data which confirms a regional pattern. A consistent regional comparison between catchments within the same summer season was hampered by the low number of stations. In future studies the number of stations should be increased at the expense of the length of the observation series.

INTRODUCTION

Droughts are regional in nature and critical drought conditions occur when there is extreme shortage of water for long durations over large areas. Drought is a relative term applicable to any climate, its occurrence depends on the ratio between water demand and water availability. Drought affects many aspects of environment and society, and future increase in the demand for water will be most critical in periods of severe and extensive droughts. The properties of severe regional droughts are not well understood, and we are presently not able to predict these droughts. Drought studies have been suffering from the lack of regional data sets and consistent methods for drought analysis. In this study focus is on hydrological droughts in terms of streamflow deficits.

Low flow studies traditionally consider only the drought magnitude by characterizing droughts in terms of the minimum annual n-day average discharge. A method that simultaneously characterizes streamflow droughts in terms of duration and deficit volume (severity) is the threshold level method presented by Yevjevich (1967), where droughts are defined as periods during which the flow is below a

certain threshold level. This definition is suitable for reservoir analysis where deficit volume is used to determine the required storage capacity, for analysing the physical factors causing severe regional droughts (which requires an objective and consistent tool for describing both the time of occurrence, duration and severity of these droughts) and regional analysis for estimating extreme events at the ungauged site. Statistical properties of drought duration have been applied with promising results using a derived distribution approach for low flow distribution functions (Gottschalk *et al.*, in press).

The threshold level approach is in this study applied for analysing streamflow droughts from a daily recorded hydrograph. Previous studies have demonstrated the potential of this method for a complete description of the stochastic process of seasonal (within-year) droughts (Tallaksen *et al.*, 1997; Zelenhasic & Salvai, 1987). Application of the method in both these studies was made on two catchments from similar climatic regions. Following the recommendations from Tallaksen *et al.* (1997), in this study the threshold level method is applied to a regional dataset comprising 52 daily streamflow series from the Nordic countries.

In a European perspective the Nordic countries show a very large variation in river flow regime (Krasovskaia *et al.*, 1994). Snow and ice affected regions generally experience their lowest flow during the winter months. Only Denmark and the southernmost parts of Sweden, Finland and Norway have a summer minimum. There are also large transition regions where the lowest flow can be found either in winter or summer. A summer drought is primarily caused by low precipitation compared with evaporation, whereas a winter drought is due to precipitation being stored as snow, and river discharge being reduced by freezing. In order to make a consistent analysis of Nordic droughts it is necessary to separate between the two events of summer and winter droughts.

The main objective of this investigation is to analyse the regional characteristics of seasonal droughts in the Nordic region. The threshold level method is applied to daily time series and the method is evaluated for use on a regional data set. The different samples of summer and winter drought catchments will be analysed by statistical methods, and thereafter series based on only summer droughts will be used to try to identify homogeneous regions with respect to the frequency distribution of the extreme values of drought duration and deficit volume. The statistical properties of the annual maximum drought series are investigated using L-moment diagrams and empirical orthogonal functions, and the regional patterns identified by the two methods are compared.

DEFINITION OF DROUGHT EVENTS

A sequence of drought events is obtained from the streamflow hydrograph by considering situations where the discharge is below a certain threshold level. Each drought event is characterized by its duration, deficit volume (severity), and time of occurrence. The time of drought occurrence is defined as the date of minimum flow in the drought. During a prolonged dry period it is often observed that the flow exceeds the threshold level in a short period of time and thereby dividing a large drought into a number of minor droughts that are mutually dependent. Following the

recommendations in Tallaksen *et al.* (1997), the moving average (MA) procedure is applied to the time series prior to selecting the droughts in order to define an independent sequence of droughts. An averaging time step of 10 days was used, and these series, labelled MA 10 days series, will be used in the following analyses.

The appearance of multi-year droughts (i.e. droughts lasting longer than 365 days) and zero-drought years (the flow never falls below the threshold level in a year) are important features when choosing a consistent threshold level. The threshold level was in Zelenhasic & Salvai (1987) and Tallaksen *et al.* (1997) defined as a percentile of the annual flow duration curve. For the MA procedure, the 50 percentile ($Q50$) was considered an upper limit with respect to the presence of multi-year droughts. On the other hand the problem of zero-drought years became more severe for lower thresholds. In this study $Q70$ and $Q90$ are used as threshold levels.

For a winter drought catchment, the use of a threshold level defined as a percentile of the annual flow duration curve, implies that very few droughts or none, will be selected from the summer period. A catchment is defined as a summer or winter drought catchment if at least 90% of the selected droughts falls within the respective seasons. An *a priori* subdivision of the streamflow data into separate subsets by season is feasible if the processes generating droughts cannot mix in each season (Rossi, 1984). This is a reasonable assumption to be made in the Nordic region, as dominating low flow in winter is only found in regions with very cold climate.

A special problem arises when a summer drought continues into a winter drought, without any clear distinction between them. Considering the Nordic climate with high precipitation in autumn and winter, this is generally due to low temperatures and precipitation falling as snow. A summer drought is therefore terminated at the start of the winter season even though the flow is still below the threshold level. Three different summer seasons have been defined for the Nordic region (Julian day numbers are given in brackets); season I, which includes inland catchments in the north (152–273), season II, which includes catchments on the coast and further to the south (121–288), and season III including only the southernmost catchments in Denmark and Sweden (121–304). By imposing a seasonal threshold level, defined relative to the seasonal flow data, a series of summer droughts can be defined for all catchments.

REGIONAL ANALYSIS

Daily flow data from 52 discharge stations in the Nordic countries were used in the study (Fig. 1). Catchment area varied between 200 and 1500 km^2, and were without glaciers. The data covered a common period of 60 years (1931–1990), with only minor exceptions. Annual maximum series (AMS) of drought duration and deficit volume were derived for all stations based on the MA 10 days series. Two different data sets were obtained: (a) annual droughts were selected using the complete flow series and a threshold level derived from the annual flow duration curve, the 70 and 90 percentiles ($Q70$ and $Q90$), and (b) a sample of summer droughts was obtained using a predefined summer period in combination with a threshold level derived from the seasonal flow duration curve ($Q70_S$ and $Q90_S$).

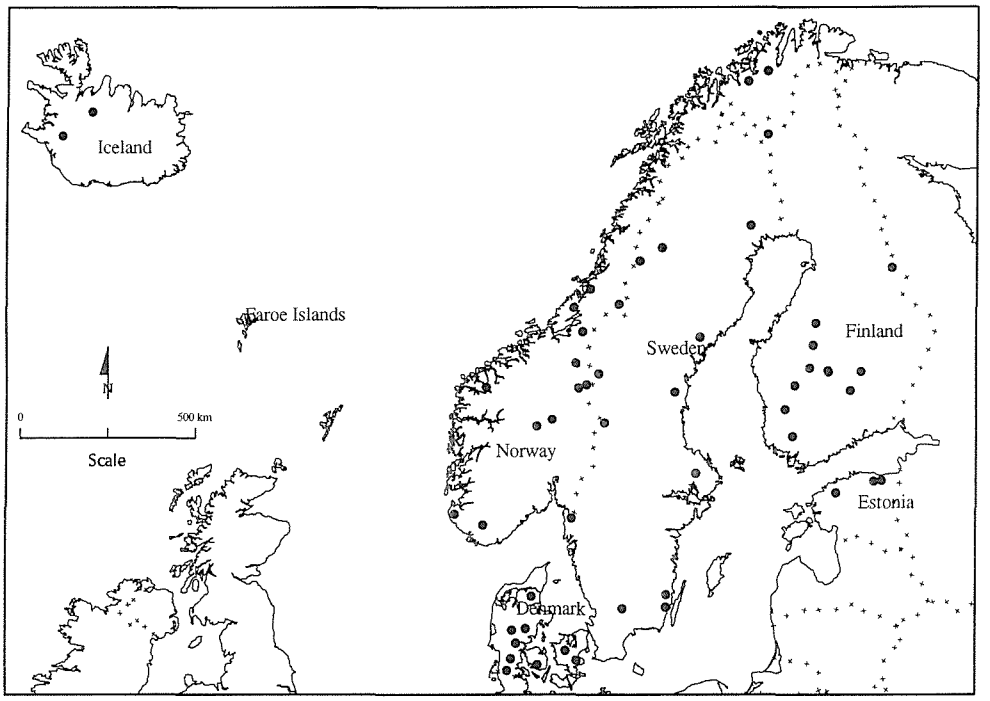

Fig. 1 Location of the 52 Nordic study catchments.

The regional characteristics of drought duration and deficit volume were investigated for both samples using L-moment diagrams and empirical orthogonal functions. L-moments are linear combinations of order statistics, and have been demonstrated to suffer less than conventional moments from the affect of sample variability (Hosking, 1990). The L-moments were estimated using unbiased estimates of the probability weighted moments (Landwehr *et al.*, 1979). L-moment ratios (coefficient of variation, skewness and kurtosis) can be defined analogous to ordinary product moments ratio, and plotted to yield an L-moment ratio diagram. The diagram summarizes basic properties of theoretical probability distributions and observed samples, and has shown to be a powerful tool to depict contrasts between different samples (Hosking & Wallis, 1993; Vogel & Fennessey, 1993). L-moment diagrams permit the identification of homogeneous regions or grouping of catchments with respect to the distribution properties of the variable of interest. At the ungauged site, the appropriate distribution is found provided some scaling factor, i.e. the mean annual quantity, is given.

A detailed description of the method of empirical orthogonal functions (EOF method) is given in Essenwanger (1976). This method is a powerful tool for analysing large data sets of spatially correlated observations. By separating temporal and spatial variations in time series the EOF method is especially suitable for extrapolation (Hisdal & Tveito, 1993) and interpolation (Hisdal & Tveito, 1992) purposes. Provided homogeneous regions have been defined, the EOF method can be used to simulate series at the ungauged location. Gottschalk (1985) used the method for a regionalization of Sweden based on time series of mean monthly runoff.

The EOF method linearly transforms the spatial correlated time series into two sets of orthogonal and thus uncorrelated functions. This linear transformation can be described as:

$$X(u,t) = \sum_{j=1}^{N} h_j(u)\beta_j(t)$$

where $X(u,t)$ are annual maximum series with u representing the location and t the time, $h_j(t)$ are spatial functions (weight coefficients) describing the transformation, and $\beta_j(t)$ are temporal or amplitude functions describing the variations common to all series. A few of the amplitude functions will contain most of the variations in the original series. They are arranged in descending order according to the proportion of variance explained by each function. Redundant information can be removed by using only a few of the amplitude functions. The weight coefficients describe the contribution of the amplitude functions to the original series. These weights can be regarded as the spatial component of the process $X(u,t)$.

If the different annual maximum series have common features from one observation point to another, the main part of the information will be in the first amplitude functions. A two-dimensional plot of $h_j(u)$ for $j = 1$ and 2 on a scatter diagram can serve to identify groups of stations with equal properties.

RESULTS

Sample estimates of L-moments for drought duration and deficit volume were compared to the theoretical relationships for a number of different distributions. A generalized Pareto distribution was found to give the best overall fit to both the annual and the summer drought samples. Annual samples of drought duration and deficit volume were labelled separately in the L-moment diagram in Fig. 2. Sample estimates of L-CV (coefficient of variation) and L-skewness using $Q90$ as a threshold level are shown in the plot together with the theoretical form of the generalized Pareto distribution. The normal distribution has zero skewness and is represented by

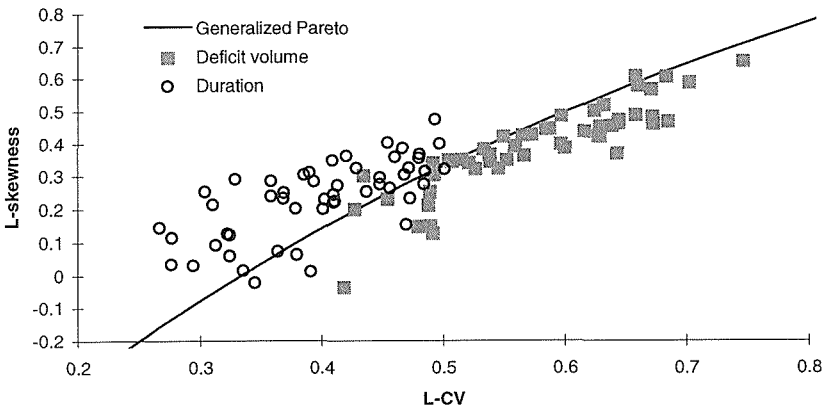

Fig. 2 L-moment diagram for annual drought duration and deficit volume using $Q90$ as a threshold level.

a horizontal line. As can be seen from the figure, drought deficit volume exhibited in general a more long-tailed behaviour than the distributions obtained for drought duration. A similar trend was observed for the highest threshold level, $Q70$, although in this case both samples were shifted towards lower L-moments.

To be able to identify groups of stations with equal properties by the EOF method, it is important that a sufficient proportion of the variance in the original data set is explained by the two first amplitude functions. Using $Q70$ as a threshold level and data for the whole year, the percentage of explained variance was 76% for duration and 63% for deficit volume. In case of $Q90$, the EOF method suffered from a large number of zero-drought years. The resultant percentage of explained variance was very low, and therefore only $Q70$ was used in the following EOF analyses.

Summer and winter droughts

It was not possible to make a clear distinction between the sample L-moments (L-moment diagram) or the weight coefficients (EOF diagram) of catchments experiencing summer droughts, winter droughts or both. All-year droughts were only found in one catchment. The winter drought catchments did, however, for both threshold levels show a general lower L-skewness and L-CV compared to the summer and mixed drought samples. This trend was most noticeable for drought duration. The EOF diagrams showed a similar clustering of winter drought catchments which was clearest for drought duration.

Summer droughts

The sample characteristics of summer droughts were also plotted in the L-moment and EOF diagrams to identify possible regional patterns in drought behaviour. Compared to the annual drought samples (Fig. 2), there was an overall shift towards lower skewness values in the L-moment diagrams. Lower L-moments and lower

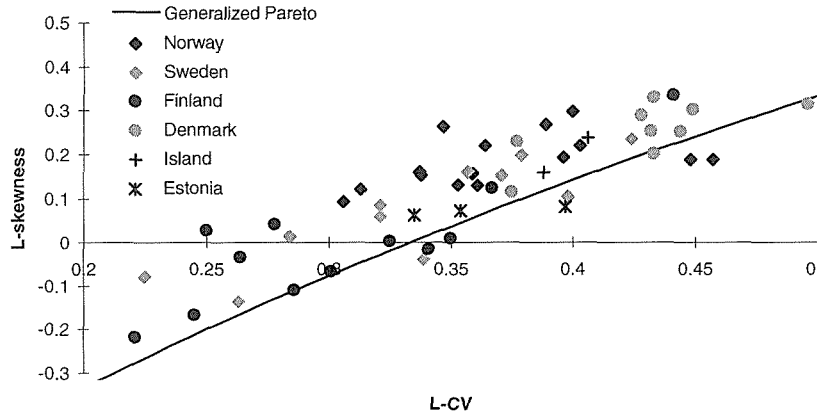

Fig. 3 L-moment diagram for summer drought duration using $Q70$ as a threshold level.

range in values were found for $Q70_S$ compared to $Q90_S$ as also observed for the annual sample. For both threshold levels the sample L-moments generally followed the Pareto distribution. For drought duration, however, the distribution is given as the lower limit of the sample (Fig. 3), whereas for deficit volume it is the upper limit. In Fig. 3 sample estimates of L-CV and L-skewness are labelled separately by countries. Although this subdivision is not based on hydrological characteristics, it is a first step to judge whether or not it is possible to identify these different geographical regions in the total sample. The figure shows the results for drought duration using $Q70$ as a threshold level, and similar pictures were obtained for $Q90$ and deficit volume.

Some main features are represented by this diagram although no unique grouping was found. Highest L-moments were found for Denmark, followed by Norway and then Finland. Swedish catchments, however, showed a large variability in values and intermingled with the other countries. The latter was not unexpected in view of Sweden's central geographical location, and the fact that it was the only country which encompassed both pure summer and winter drought catchments. The Norwegian and Finish catchments were clustered closer together in case of deficit volume.

The percentage of explained variance for the EOF method was similar for the summer samples as for the annual samples; 76% for duration and 60% for deficit volume. The weight coefficient are plotted in Fig. 4 for the same drought sample as shown in the L-moment diagram in Fig. 3. As in the L-moment diagram the Danish catchments defined the clearest group, and both Finland and Norway can be identified as clusters in the plot.

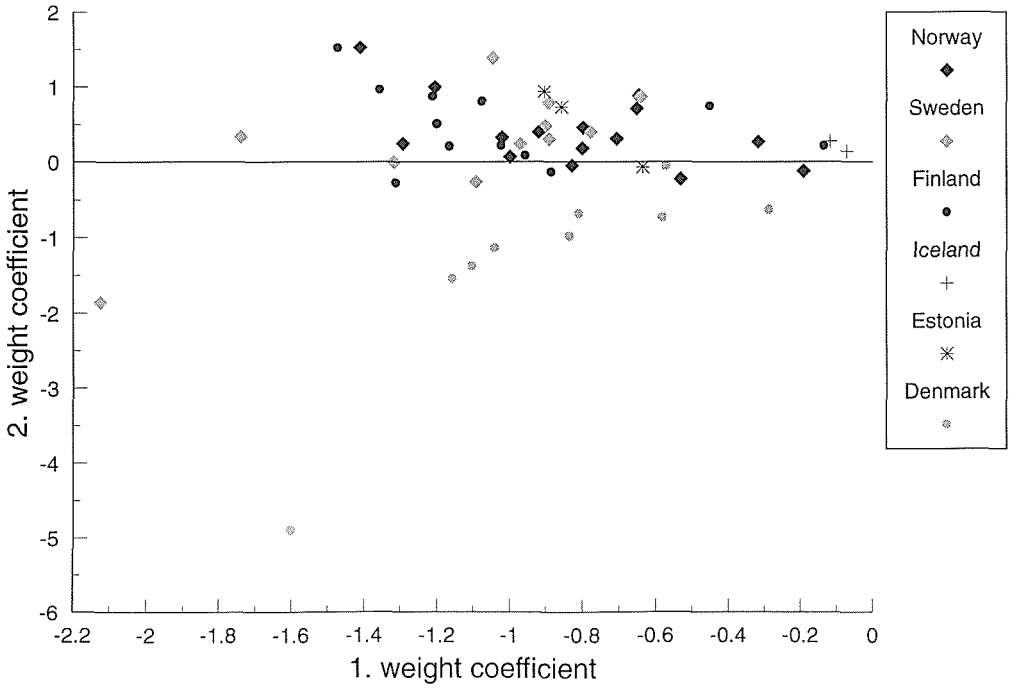

Fig. 4 EOF diagram for summer drought duration using $Q70$ as a threshold level.

However, as the summer droughts have been sampled from three different summer seasons, any regional pattern is disturbed by the fact that different season lengths will enable different drought durations and deficit volumes to be selected. To make a consistent regional comparison only catchments assigned to the same season should be compared. In the Nordic data sample, only Norway and Sweden contained catchments with more than one summer season, respectively two and three. In Fig. 5 the sample L-moments for drought durations are shown for season II. Although the sample now contain very few catchments, they tend to cluster according to geographical location. One of the Swedish catchments is plotted together with the Norwegian catchments. This is not surprising given its location close to the Norwegian border at the west coast of Sweden, whereas the other Swedish catchment is found at the east coast. The same tendency towards a better defined grouping by countries was also found for the other seasons. To compare these results with the EOF method it was necessary to run the EOF procedure again on the separate subsets of catchments. It was concluded, however, that a larger data set was required to analyse catchments assigned to the same summer season, and at this stage, further regional analysis was restricted by the low number of stations.

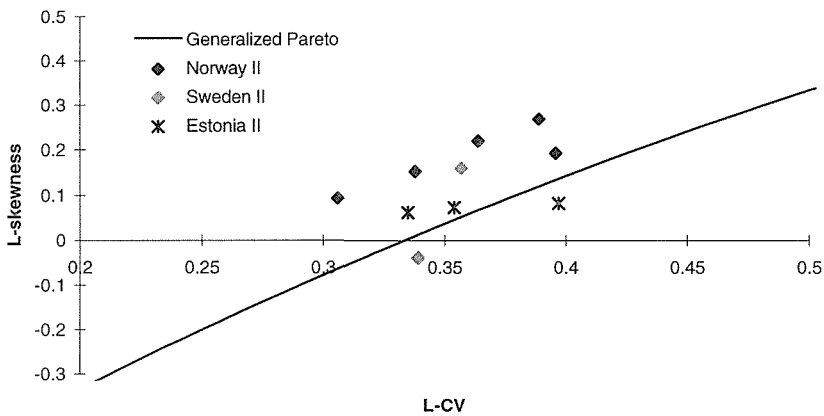

Fig. 5 L-moment diagram for summer drought duration (season II) using $Q70$ as a threshold level.

DISCUSSION AND CONCLUSIONS

The regional characteristics of drought duration and deficit volume have been analysed for a Nordic data set of 52 catchments covering 60 years (1931–1990) of streamflow data. The main objective was to try to identify homogeneous regions with respect to the extreme properties of drought characteristics. The threshold level approach was applied to daily time series, and following the recommendations given in Tallaksen *et al.* (1997), the moving average 10 days procedure was applied for pooling dependent droughts. In this study the use of the threshold level method was extended to a regional and very heterogeneous data set, and some general guidelines for modelling droughts using the threshold level approach are given.

Two threshold levels were applied, the 70 and 90 percentile of the annual and seasonal flow duration curve. Multi-year droughts were not present in any of the catchments, the problem of zero-drought years, however, was significant for the $Q90$ threshold level. The average number of droughts per year was 0.58 and 0.36 for the annual and summer drought samples, respectively. Corresponding figures for the $Q70$ threshold level were 0.93 and 0.75. There were only small differences between the distribution properties and clustering of catchments applying the $Q70$ and $Q90$ threshold levels, and $Q70$ is therefore recommended. The information content of the AMS was significantly reduced for the $Q90$ threshold level, and a similar low threshold level must be used with care in a regional study. Alternatively, a partial duration series approach can be applied. The EOF method is similarly not recommended for use if the series contains too many zero values, and in this study the method was only applied using a $Q70$ threshold level.

The L-moment diagrams showed that the generalized Pareto distribution gave the best overall fit to the annual and summer drought samples of drought duration and deficit volume. Deficit volume exhibited a longer-tailed behaviour than the distributions obtained for duration. The extreme values of drought duration and deficit volume are governed by both climate and catchment characteristics. A threshold level defined as a percentile from the flow duration curve, implies that series from different sites experience discharge below the threshold level for the same fraction of the time. The distribution of duration may vary, though, and its variation is primarily thought to be governed by climate. However, deficit volume is expected to be more related to catchment characteristics, and provided that catchment characteristics varies over a smaller scale than climate, this implies larger variability and lower spatial correlation for deficit volume. The higher L-moments found for deficit volume and the lower percentage of explained variance found in the EOF method, suggest that this is a reasonable assumption.

Catchments were grouped both by type of catchment (winter or summer droughts) and by country (only summer droughts). Two different regionalization tools were compared, the L-moment and EOF diagrams. Neither methods showed a clear pattern in the data. However, it was possible to identify a clustering of the winter drought catchments, and this was, for both methods, most noticeable for drought duration. The winter drought catchments experienced in general lower L-skewness and L-CV values as compared to the summer and mixed drought samples.

Catchments assigned to the same summer season were labelled separately by countries. This was done as a first step towards identifying possible regional patterns in drought duration and deficit volume. The results demonstrated that there were large scale trends in the data confirming a regional pattern. A more detailed regional study of summer drought, however, was hampered by the low number of stations within each summer season. The number of zero-drought years in the AMS is not a constraint for the $Q70$ threshold level, and this suggests that in future studies the number of stations can be increased at the expense of the length of the observation series. It is important that the station network is dense enough to cover the typical spatial correlation range for the drought variable of interest.

The comparison between L-moment and EOF diagrams has so far not led to any conclusions regarding choice of regionalization tool, but some factors to be considered when choosing either method must be emphasized. In the EOF method

series are grouped based on their correlations relative to the total variance of the sample, and groups can be identified although the total variance is low. The L-moments summarize distribution properties, and as opposed to the weight coefficients, a comparison is done in terms of absolute values. The interpretation of the sample L-moments, L-CV and L-skewness, is more straightforward than the weight coefficients in the EOF diagram. A physical explanation of these coefficients and corresponding amplitude functions is difficult, and although a regionalization is possible, the physical cause behind a specific grouping remains to be interpreted.

Acknowledgements As members of the FRIEND/North West Europe low flow project group, the authors would like to acknowledge the contribution of the group members through the initiation of the present drought study. Valuable discussions and critical comments on the topic have been greatly appreciated.

REFERENCES

Essenwanger, O. (1976) Applied statistics in atmospheric science. *Developments in Atmospheric Science,* **4A**, Elsevier, Amsterdam, The Netherlands.

Gottschalk, L. (1985) Hydrological regionalization of Sweden. *Hydrol. Sci. J.* **30**(1), 65–83.

Gottschalk, L., Tallaksen, L. M. & Perzyna, G. (in press) Derivation of low flow distribution functions using recession curves. *J. Hydrol.*

Hisdal, H. & Tveito, O. E. (1992) Generation of runoff series at ungauged locations using empirical orthogonal functions in combination with kriging. *Stochastic Hydrol. Hydraul.* **6**, 255–269.

Hisdal, H. & Tveito, O. E. (1993) Extension of runoff series using empirical orthogonal functions. *Hydrol. Sci. J.* **38**(1), 33–49.

Hosking, J. R. M. (1990) L-moments: analysis and estimation of distributions using linear combinations of order statistics. *J. Roy. Statist. Soc.* B, **52**(1), 105–124.

Hosking, J. R. M. & Wallis, J. R. (1993) Some statistics useful in regional frequency analysis. *Wat. Resour. Res.* **29**(2), 271–281.

Krasovskaia, I.., Arnell, N. W. & Gottschalk, L. (1994) Flow regimes in northern and western Europe: development and application of procedures for classifying flow regimes. In: *FRIEND: Flow Regimes from International Experimental and Network Data* (ed. by P. Seuna, A. Gustard, N. W. Arnell & G. A. Cole), 185–192. IAHS Publ. no. 221.

Landwehr, J. M., Matalas, N. C. & Wallis, J. R. (1979) Probability weighted moments compared with some traditional techniques in estimating Gumbel parameters and quantiles. *Wat. Resour. Res.* **15**(5), 1055–1064.

Rossi, F. (1984) Two-component extreme value distribution for flood frequency analysis. *Wat. Resour. Res.* **20**(7), 847–856.

Tallaksen, L. M., Madsen, H. & Clausen, B. (1997) On the definition and modelling of streamflow drought duration and deficit volume. *Hydrol. Sci. J.* **42**(1), 15–33.

Vogel, R. M. & Fennessey, N. M. (1993) L-moment diagrams should replace product moment diagrams. *Wat. Resour. Res.* **29**(6), 1745–1752.

Yevjevich, V. (1967) An objective approach to definition and investigations of continental hydrologic droughts. *Hydrology Papers,* **23**, Colorado State University, Fort Collins.

Zelenhasic, E. & Salvai, A. (1987) A method of streamflow drought analysis. *Wat. Resour. Res.* **23**(1), 156–168.

FRIEND'97 — Regional Hydrology: Concepts and Models for Sustainable Water Resource Management
(Proceedings of the Postojna, Slovenia, Conference, September–October 1997). IAHS Publ. no. 246, 1997.

Temporal and spatial behaviour of drought in south Germany

SIEGFRIED DEMUTH & BARBARA HEINRICH
Department of Hydrology, University of Freiburg, Werderring 4, D-79098 Freiburg, Germany

Abstract The temporal and spatial variability of drought behaviour in southern Germany has been investigated applying the theory of runs. With this approach drought duration and the deficit volume (severity) were described using $Q90$, the 90 percentile exceedance discharge as a threshold. The number of drought events within a year revealed a dryness index indicating the years 1962–1964, 1971–1973, 1976 and 1991 as dry years. Pronounced winter drought events (October–March) were found regularly in the Alpine regions resulting in small coefficient of variations (between 90 and 130%) of the annual variability of drought severity. The Pre-Alps and the River Rhine regions show in particular summer droughts with high coefficients of variations (between 170 and 220). The high value for the Rhine region indicates the irregular temporal occurrence. The study revealed the benefits of the method to detect the regional pattern of drought behaviour.

INTRODUCTION

In most European countries a growing standard of living accompanies growing pressure on limited water resources. Conflicts between competing water users arise especially during low flow periods. A better understanding of low flow characteristics is therefore important for both water resources planning and conservation management. Thus enhanced investigations are required and in the context of extreme events, the knowledge of the occurrence of low flow periods on a regional scale is important. In terms of regional resources protection it is necessary to understand not only the regional occurrences of low flow periods but also the time of the year that regions are affected. In the last few years several countries of western Europe have experienced severe droughts. Recent droughts occurred e.g. in England between 1988 and 1992 (Bryant *et al.*, 1994), in Germany the State of Brandenburg (northeast of Germany) was affected in 1992 by a severe summer drought (Gierk & Jungfer, 1992) characterized by low precipitation (between 30 and 95 mm) at the stations Cottbus and Potsdam and extreme temperatures during the summer months. The effects on agricultural productivity was significant, the crop production was reduced by nearly 22%. In this study hydrological droughts are investigated looking especially at the drought parameter duration. The research is focused on the occurrence and the space–time structure of droughts at a regional scale in south Germany.

STUDY AREA

The area under investigation is situated in the south of Germany and covers six main regions with distinct differences in climate, geology, and hydrology (Alps, Pre-Alps,

Black Forest, Bavarian Forest, Swabian and Franconian Alb, and the Upper Main region). The Alps are characterized by a nival regime with low flows occurring only during the winter season. The region exhibits a high degree of seasonality and low inter-annual variation of low flows. The maximum flow occurs in June–July due to snowmelt and a maximum of precipitation. The Pre-Alps shift from nival to pluvio-nival regime with a low degree of seasonality and low flows in winter and in summer. The low degree of seasonality indicates extended aquifers with a high storage capacity in that region. The Swabian and Franconian Alb, the Bavarian Forest and the Black Forest are characterized by nivo-pluvial and pluvial regimes with moderate inter-annual variability and low flows occurring mainly in the summer. The flow regime of the Swabian and Franconian Alb which consist mainly of limestone may be influenced by karstic phenomena. The catchments in the Upper Main region show mostly pluvial regimes with high inter-annual variation of runoff and low flows mainly in the summer (between August and September).

The hydrological data were provided by the European Water Archive (EWA), the database of the UNESCO FRIEND-Project (Flow Regimes from International Experimental and Network Data). The database includes 169 gauging stations for the investigation area. The length of the flow records varies considerably with as many as 80 years for some of the catchments and less than 10 years for others. The size of the basins selected for this study varied between 6 and 457 km^2. Due to excessive human influence on the flow regimes (e.g. abstractions and reservoir) and the need to use records of the same period, only 111 stations were selected for the drought analysis. Drought properties have been calculated for this subset of stations for the period between 1962 and 1991.

METHOD

A drought may be defined as a deficit of water in time, space, or both, but unfortunately due to the complex nature of the phenomenon there is no general view among scientists towards a comprehensive parameterization of a drought event. In general, droughts can be classified into meteorological droughts, agricultural droughts, and hydrological droughts (Beran & Rodier, 1985; Dracup *et al.*, 1980; Wilhite & Glantz, 1985). Droughts can be described through some fundamental characteristics such as duration, deficit volume (severity), and probability of recurrence (Yevjevich, 1967; Dracup *et al.*, 1980).

An objective method to identify hydrological droughts was introduced by Yevjevich (1967). The procedure is based on the theory of runs. A run is defined as an uninterrupted sequence of days with streamflow values (X) less than a chosen threshold (X_0) (see Fig. 1). The run parameters were derived from daily runoff data with threshold $Q90$ (discharge exceeded for 90% of the time) in combination with termination criterion 10%. The termination criterion was introduced to avoid the interruption of runs by small and short-lasting exceedance volumes. Therefore it allows a surplus runoff volume of 10% of the foregoing run's volume without the run being terminated. Each run is determined by the following drought parameters:
(a) drought duration with n number of days [days] with discharge values $X \leq X_0$,

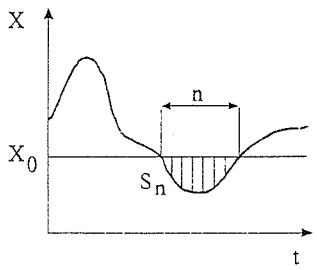

Fig. 1 The concept of runs. The duration of drought is defined by n (for $X \leq X_0$), the severity by S_n (for $X \leq X_0$) (Yevjevich 1967, modified).

(b) drought severity S_n [m^3], which is the cumulated water deficit for n days with $X \leq X_0$, and
(c) drought onset, which is the date of the first day with discharge values $X \leq X_0$.

Since during a year several drought events can occur, the annual maximum duration (AMD) and the annual maximum volume (AMV) were selected. Usually, they belong to the same run and exhibit similar behaviour. Therefore in this study the time–space variability of the AMDs is presented only.

TEMPORAL BEHAVIOUR OF DROUGHT

To study the temporal behaviour of droughts several aspects were investigated; (a) the derivation of dry and wet years and (b) the seasonal occurrence of droughts. The threshold $Q90$ is defined as the discharge exceeded for 90% of the days under investigation (1962–1991). The contribution of a single run to the derivation of $Q90$ is higher the longer it lasted and the lower discharge values were. Because flow behaviour varies between the years there exist such years for which no run can be calculated. These years are defined as zero-years. To evaluate the "dryness" of a single year, the overall drought duration of AMDs of all 111 stations was calculated for each year. The result is presented in Fig. 2. The duration ranges considerably from 339 days in 1980 up to 7736 days in 1962. The mean value accounts for 2464 days. Years showing a higher duration as the mean can be considered as dry years (1962, 1963, 1964, 1969, 1971, 1972, 1973, 1976, 1983, 1985, 1991), such with lower values as wet years. The sequences of dry years especially from 1962 to 1964

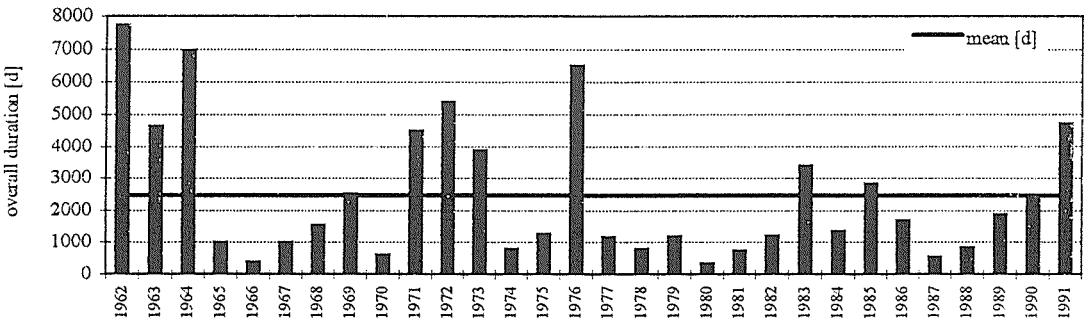

Fig. 2 Overall duration of AMDs [days] for each year of the investigation period.

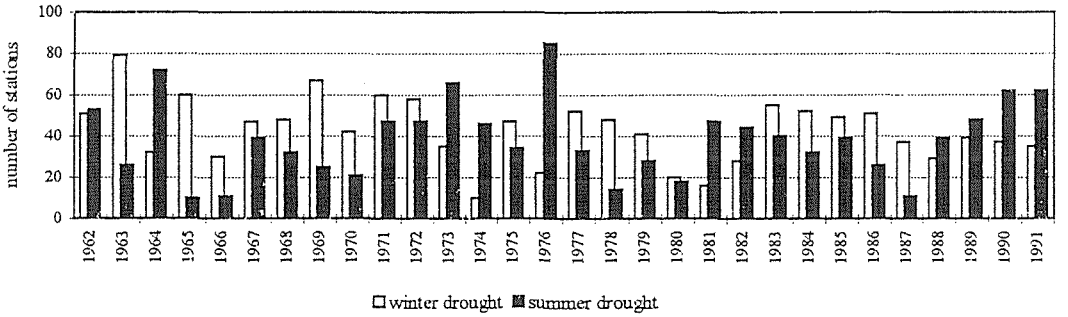

Fig. 3 Annual distribution of summer and winter droughts.

and from 1971 to 1973 indicated a memory effect (persistence) of stations towards droughts. To investigate the persistency of drought events the autocorrelation coefficients were calculated for the AMDs. A time period of $k = 10$ years was chosen. For $k = 1$, the autocorrelation coefficients were lower than 54% and indicating a none persistent behaviour.

To investigate the seasonal occurrence of droughts, the drought onsets were considered. The study revealed a distinction between winter (October–March) and summer droughts (April–September). In general, summer droughts are caused by high temperature together with evapotranspiration losses and little or no precipitation. Winter droughts are characterized by temperatures below zero degrees. As a result precipitation is stored as snow and does therefore not contribute to river discharge (Mawdsley *et al.*, 1993). Within the years under investigation, droughts occurred in both seasons (see Fig. 3). The total of drought events for the period 1962–1991 accounts for 2434 with 47% summer events and 53% winter events. In 37% (11) of the years, the greater part of events occurred during summer time, in 63% (19) during winter months. In some years the number of runs calculated for each season was almost equal (e.g. 1962, 1980). In others, a distinct difference can be seen (e.g. 1963, 1964, 1965). The 10 longest AMDs with a duration between about 4 and more than 8 months (130–259 days) occurred all except for one (131 days, 1969) during summer months. Altogether most drought events took place in winter time, but the most extreme events with regard to duration occurred during summer seasons.

SPATIAL BEHAVIOUR OF DROUGHTS

The investigation area of southern Germany is composed of six geographic regions with different physiographical, geological, and meteorological properties that influence the spatial occurrence and the characteristics of drought. To investigate the spatial behaviour of drought in southern Germany, the maximum AMD (AMD_{max}) which was calculated for each station was selected. This value reflects the spatial "drought proneness" of single years. Table 1 shows the number of stations relevant for the evaluation of each region and the percentage of the $AMDs_{max}$ per year. Grey tone indicates $AMDs_{max}$ which took place during winter months.

Table 1 presents only years in which at least one station had its AMD_{max} in either

Table 1 Regional distribution of AMD_{max}.

Geographical region	number of stations	1962	1963	1964	1966	1968	1969	1971	1972	1973	1974	1976	1979	1983	1989	1991
Alps	23	26	9		4	9	9	17	9	9				4	4	
Pre-Alps	23	34		14			5	8	39							
Swabian/Franconian Alb	7	35		13					13	13		13				13
Bavarian Forest	25	24	12	12					16		16	8		12		
Upper Main Region	17	21					7				15	43			7	7
Black Forest	16	29		29				7				7	7			21

the summer or winter season. It reveals that the regional distribution of maximum drought events varies over the years. In some years, like 1962, catchments of almost all geographic regions showed a AMD_{max}. In others, like 1969 and 1971, "drought centres" are visible (Alps and Pre-Alps). In some years (1966, 1968, 1979) only one or two stations were afflicted by $AMDs_{max}$ indicating rather "wet" years. In addition Table 1 shows regional characteristics in terms of drought onset. In the Alps, all except for one AMD_{max} (96%) took place during the winter. In the Pre-Alps, where flow regimes are still strongly influenced by the nearby Alps, the percentage accounts for 51%, and in the Bavarian Forest, 36% of all AMD_{max} took place in the months from October to March. In the remaining regions, all AMD_{max} occurred during summer. Consequently these regions are more likely to experience summer drought events with extremely long duration.

Another important factor to assess the "drought susceptibility" of a region is annual variability, expressed as the coefficient of variation of drought duration. "Zero years" were taken into account too. An increase in the differences in duration of AMDs between years results in an increase in the coefficient of variation. The coefficients of variations range between 79% in the Alps up to 223% in the Upper Main region. The mean value accounts for 152%. To get a spatial picture of the coefficients of variations the values were grouped into three classes, which are reflected by the different symbols in Fig. 4. There is a clear concentration of high values in the Upper Main region. The lowest values can be seen for the catchments located in the Alpine area and the southern part of the Black Forest. Consequently the regions that are most susceptible to extremely long drought events are those located in the northwestern part of the investigation area. The southern regions—Alps, Pre-Alps, and southern Black Forest—are clearly less afflicted by long-lasting hydrological droughts.

CONCLUSION

The study shows that with the chosen statistical method and threshold $Q90$ the characteristics of temporal and spatial drought behaviour can be found. In terms of temporal characteristics, "wet" and "dry" years could be identified for the period under investigation. With regard to the spatial behaviour characteristics of drought

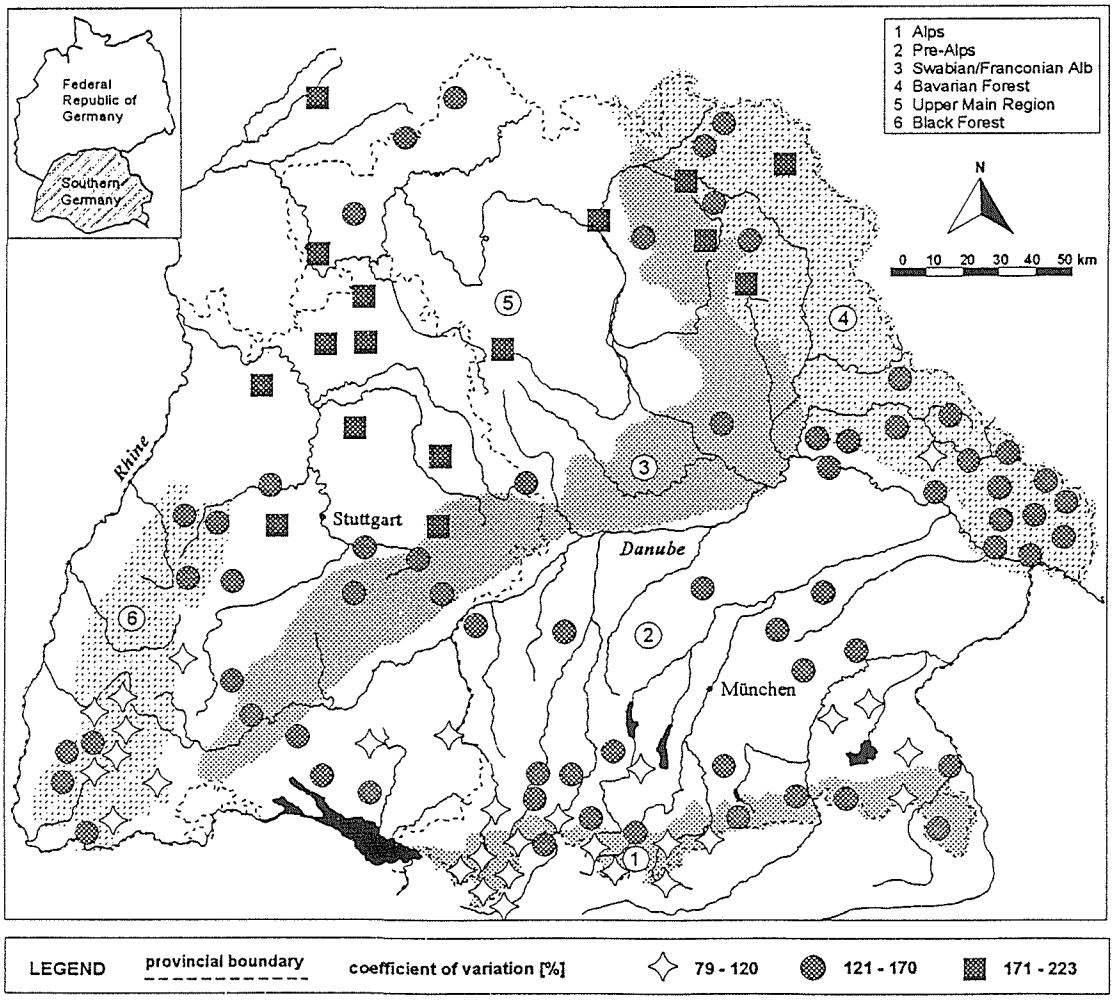

Fig. 4 Coefficients of variation of drought duration.

onset are visible. In the Alpine area and Pre-Alps most maximum events occurred during winter season. In combination with very low coefficients of variation this area is least susceptible for extreme hydrological drought. The regions north of the River Danube show a contrary pattern. Here, maximum events occurred only during summer months and the coefficients of variation are the highest ones. Consequently in this area extreme droughts are more probable. Since the threshold $Q90$ is strongly influenced by extreme low discharge values which occurred during the period under investigation the results of the study are restricted to the selected time period and cannot automatically be transferred to other time periods (Demuth & Külls, 1997).

Acknowledgements The research presented in this paper was carried out as part of the German contribution to the FRIEND (Flow Regimes from International

Experimental and Network Data) project. Support was given by the National Committee of the Federal Republic of Germany for the International Hydrological Programme (IHP). The authors would like to thank the members of the FRIEND Low-Flow Group for their many valuable discussions.

REFERENCES

Beran, M. A. & Rodier, J. A. (1985) *Hydrological Aspects of Drought*. UNESCO–WMO Studies and Reports in Hydrology no. 39.

Bryant, S. J., Arnell, N. W. & Law, F. M. (1994) The long term context for the current hydrological drought. *J. Instn Wat. Environ. Manage.* **8**, 39–51.

Demuth, S. & Külls, Ch. (1997) Probability analysis and regional aspects of droughts in southern Germany. In: *Sustainability of Water Resources under Increasing Uncertainty* (ed. by D. Rosbjerg, N.-E. Boutayeb, A. Gustard, Z. W. Kundzewicz & P. Rasmussen), 97–104. IAHS Publ. no. 240.

Dracup, J. A., Lee, K. S. & Paulson, E. G. (1980) On the definition of droughts. *Wat. Resour. Res.* **16**(2), 297–302.

Gierk, M. & Jungfer, E. (1992) Das Trockenjahr 1992 im Land Brandenburg. *Studien und Tagungsberichte Band 3, Landesumweltamt Brandenburg*, 1–23.

Mawdsley, J., Petts, J. & Walker, S. (1993) Assessment of drought severity. *BHS Occasional Pap. no. 3.*

Wilhite, D. A. &. Glantz, M. H. (1985) Understanding the drought phenomenon—the role of definitions. *Wat. International* **10**, 111–120.

Yevjevich, V. (1967) An objective approach to definition and investigation on continental hydrologic droughts. *Hydrology Pap. no. 23, Colorado State University, Fort Collins.*

FRIEND'97 — Regional Hydrology: Concepts and Models for Sustainable Water Resource Management
(Proceedings of the Postojna, Slovenia, Conference, September–October 1997). IAHS Publ. no. 246, 1997.

Probabilistic analysis of extreme low flows in selected catchments in Poland

WŁODZIMIERZ CZAMARA, WOJCIECH JAKUBOWSKI & LAURA RADCZUK
Agriculture University of Wrocław, Pl. Grunwaldzki 24, 50-363 Wrocław, Poland

Abstract The range of water deficit have been evaluated in selected catchments in Poland. For this evaluation the model of low flow analysis developed by Zelenhasič & Salvai (1987) was applied. On the basis of empirical distribution of drought occurrence and of its volume and duration, the distributions of drought maximum volume and of its maximum duration were determined. The chi-square tests of goodness of fit are taken on the level $\alpha = 0.05$.

INTRODUCTION

In Poland, a constant water deficit is observed, mainly during summer time. Thus, the sensible management of the accessible water resources becomes a necessity. Such management can be successfully carried out when the real water deficit is statistically described.

In this paper the scale of the water deficit in some catchments in different regions of Poland is evaluated. The distributions of the extreme low flow volume and time are estimated by means of the Zelenhasič & Salvai (1987) method of streamflow drought analysis. The distributions of maximum low flow volumes were determined for two catchments: the Sokołda and the Drwęca Warmińska which are regarded as typical lowland catchments and for six others: the Bystrzyca, the Czarny Potok, the Skawa, the Cicha Woda, the Krynka and the Łososina which are mountain and submontane basins (Fig. 1).

PHYSICAL AND GEOGRAPHICAL CHARACTERISTICS OF CATCHMENTS

Basic physical and geographical parameters are given in Table 1. The distribution of maximum volumes and of its durations were determined, by means of the daily flow data from 1963 to 1992. A short description of the investigated catchments follows to allow a better interpretation of the results.

The Sokołda—Sokołda gauging station The Sokołda with its tributaries drains the sandur areas of Knyszyńska Forest and zones of moraines which are at an altitude of 186 m a.s.l. There are many closed and soaked depressions and dry valleys. The sands are dominant there. The bottoms of the valleys are boggy and peaty. The catchment is covered with 90% forest.

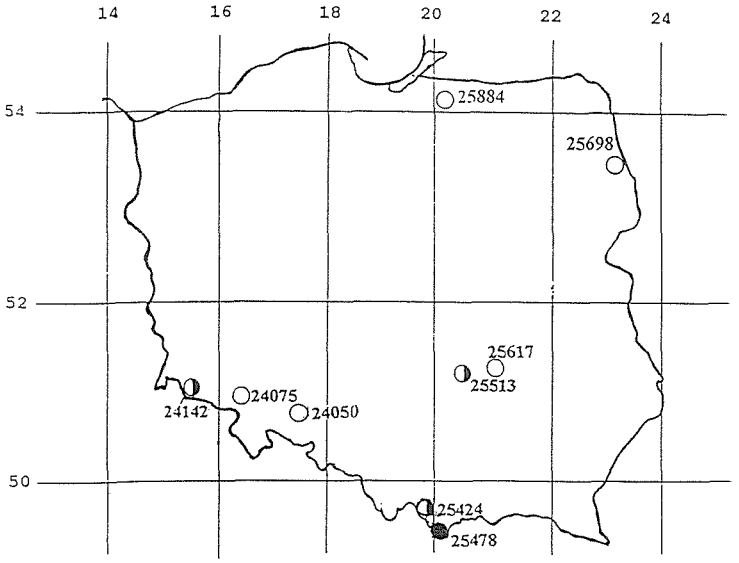

Fig. 1 Location of the investigated gauging stations in Poland.

The Drwęca Warmińska—Orneta gauging station The catchment area is covered with glacial clay and partly with sands. The river network is well developed. Forest covers 28.3% of the catchment area. There are large depressions filled with peat.

Table 1 Physical and geographical parameters of the catchments.

	River - gauging station								
	Bystrzyca-Jugowice	Czarny Potok-Mirsk	Skawa - Jordanów	Cicha Woda - Zakopane	Łososina - Bocheniec	Świślina - Nietulisko	Sokołda - Sokołda	Drwęca-Orneta	Krynka - Przeworno
station code	24075	24142	25424	25478	25513	25617	25698	25884	24050
geogr. coordinates λ	16,22	15,29	19,55	19,56	20,24	21,15	23,29	20,07	17,11
geogr. coordinates φ	50,44	50,59	49,38	49,18	50,48	50,59	53,30	54,07	50,44
catchment area km^2	122,9	55,9	96,6	58,4	300,2	405,0	464,0	306,2	163,0
altitude of station m . above sea-level	367,1	328,9	441,1	763,1	216,2	176,7	128,8	45,8	177,8
slope SL 1085 ‰	2,3	5,6	10,0	18,7	2,5	4,8	1,1	0,2	3,8
mountains %	40,0	75,0	20,0	50,0	0,0	4,0	0,0	0,0	0,0
lakes %	0,0	0,0	0,0	0,3	0,1	0,0	0,2	0,2	0,0
boggy %	0,0	0,0	0,0	0,1	0,3	1,0	9,5	8,4	0,2
forest %	36,0	12,0	32,5	32,7	32,0	22,7	24,1	28,3	19,1
urban area %	0,0	0,0	1,5	10,8	2,7	5,0	1,2	1,2	0,6

The Krynka—Przeworno gauging station The river source is a spring at 315 m a.s.l. The catchment area is covered mainly with loess, and the upper part of the catchment with glacial sands. The large and flat bed of the valley is covered with meadows incised with ditches. The catchment has a submontane character.

The Bystrzyca—Jugowice gauging station The Bystrzyca River begins 680 m a.s.l. in the eastern part of the Suche Mountains built of porphyries. The river flows through the Sowie Mountains. The valley of the river is narrow and deeply cut. Elevation ranges from 200 to 400 m. Igneous rocks dominate the geological structure of the catchment.

The Czarny Potok—Mirsk gauging station The Czarny Potok starts at the main ridge of the Izerskie Mountains. The river valley is covered with fen soils, fluvial sands and gravels as well as fluvioglacial sands and gravels. The catchment is built of different metamorphic and sedimentary rocks. Forest covers 12% of the catchment area.

The Skawa—Jordanów gauging station The valley of the Skawa River is eroded in flysch rocks. There are differences in elevation locally of over 200 m. Forest covers 32.5% of the total catchment area.

The Cicha Woda—Zakopane gauging station The source of the river is in the Tatra Mountains, then the river reaches Orawsko-Nowotarska basin filled with flish sediments from the Tertiary period. Forest covers 32.7% of the catchment area.

The Łososina—Bocheniec gauging station The source of the river is situated 300 m a.s.l., the river flows through Triassic sands covered by Quaternary sands and gravels. In depressions, the thickness of sands and gravels is up to 10 m. Below its left tributary, the Kalina River, the Łososina River flows into the part of the catchment built of Jurassic limestones. Forest covers 32% of the catchment area.

The storage capacity of the catchments depends on the catchment geological structure especially that of the river valleys. The mean daily outflow for the considered period is presented in Table 2.

DESCRIPTION OF THE MODEL

The basis of the model is the streamflow drought level. Consider the water discharge Q_t in time interval $(0, T)$. From the flow duration curve of daily discharges a truncation level Q_v is estimated. This means that streamflow droughts take place when daily discharge $Q_t < Q_v$. Necessary statistical independence between successive droughts means that v should not be lower than 80%. Then for the given truncation level v it is easy to compute the time and magnitude of successive droughts. The obtained two-dimensional sequence of raw data is elaborated in the following manner.

Table 2 Average daily and unit runoffs.

No.	River—gauge	Average runoff $\bar{Q}$ (1000 m^3 day^{-1})	Unit runoff q (l s^{-1} km^{-2})
1	Sokołda—Sokołda	204.90	5.11
2	Drwęca Warm.—Orneta	193.44	7.31
3	Bystrzyca—Jugowice	130.65	12.30
4	Krynka—Przeworno	64.39	4.57
5	Czarny Potok—Mirsk	80.72	16.71
6	Skawa—Jordanów	97.34	11.66
7	Cicha Woda—Zakopane	176.76	35.03
8	Łososina—Bocheniec	146.10	5.63
9	Świślina—Nietulisko	157.29	4.50

- From the low flow volumes D_i, $i = 1, \ldots, n$ the maximum $D_{\max}$ is chosen, and all low flow volumes lower than $\alpha \times D_{\max}$ are considered as unimportant. These have been removed from the primary raw sequence. According to Zelenhasič & Salvai (1987) we take $\alpha = 0.005$.
- Every two low flows, separated by one or two days with water discharge greater than Q_v are taken as a single one and their magnitudes and times are summed.

Now we can, according to Teodorovič & Zelenhasič (1970), start to construct the basic model. At the begining we choose the time interval $(0,t)$, because of the yearly periodicity, t cannot exceed 365 days. (Further we take $t = 356$.) Denote by:

E_t = number of droughts in time interval,
D_n = water volume at n-th streamflow drought, and
T_n = time of this drought.

These parameters are the random variables, so we also have to denote their distributions. See that the number of droughts is discrete, the two others are the continuous ones. Thus

$$F_t(x) = \Pr(D_n \le x) \tag{1}$$

and

$$H_t(\tau) = \Pr(T_n \le \tau) \tag{2}$$

The distribution (Teodorovič & Zelenhasič, 1970) of the extreme volumes is:

$$\Phi_t(x) = \Pr(\sup_n D_n \le x) = \Pr(E_t = 0) + \sum_{k=1}^{\infty} \Pr\left(\bigcap_{n=1}^{k} (D_n \le x) \bigcap (E_t = k)\right) \tag{3}$$

Similarly we can write for the time of streamflow drought, the distribution of the extreme time as:

$$\Psi_t(\tau) = \Pr(\sup_n T_n \le \tau) = \Pr(E_t = 0) + \sum_{k=1}^{\infty} \Pr\left(\bigcap_{n=1}^{k} (T_n \le \tau) \bigcap (E_t = k)\right) \tag{4}$$

The above formulae are rather impracticable. It is very difficult to determine dependency among random variables in product

$$\bigcap_{n=1}^{k} (D_n \le x) \bigcap (E_t = n)$$

and similarly in

$$\bigcap_{n=1}^{k}(T_n \le \tau)\bigcap(E_t = n)$$

Accepting the suitable independency it is easy to obtain (Teodorovič & Zelenhasič, 1970)

$$\Phi_t(x) = \Pr(E_t = 0) + \sum_{k=1}^{\infty} F_t^k(x)\Pr(E_t = k) \tag{5}$$

and

$$\Psi_t(\tau) = \Pr(E_t = 0) + \sum_{k=1}^{\infty} H_t^k(\tau)\Pr(E_t = k) \tag{6}$$

APPLICATION OF THE MODEL

The most important step is to determine the proper distribution functions, with a good fit to the empirical data. We approximate the number of droughts in time interval $(0,t)$ by a negative binomial (Pascal) distribution:

$$\Pr(E_t = n) = \binom{-v}{n} p^n q^v, \quad p+q = 1, \quad n = 0,1,2,... \tag{7}$$

or Poisson:

$$\Pr(E_t = n) = \frac{\lambda^n}{n!}e^{-2}, \qquad n = 0,1,2,... \tag{8}$$

Time and low flow volume are approximated by the following distributions with probability density functions (pdf):

$$f_1(x) = \frac{\alpha^v}{\Gamma(v)}x^{v-1}e^{-\alpha x}, \qquad x > 0 \quad \text{pdf of gamma distribution,} \tag{9}$$

Table 3 An empirical distribution of number of streamflow droughts for the Skawa River—gauge Jordanów.

Number of streamflow droughts	Number of years
0	8
1	2
2	3
3	0
4	4
5	4
6	4
7	0
8	1
9	1
10	2
11	0
12	1

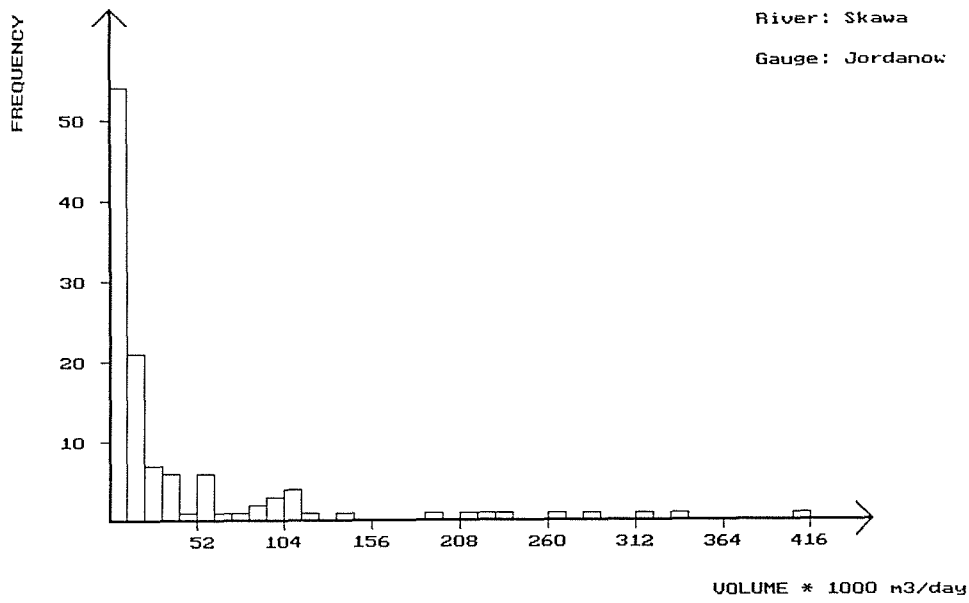

Fig. 2 An empirical distribution of low flow volumes, the Skawa River—gauge Jordanów.

$$f_2(x) = \alpha\lambda x^{\alpha-1} e^{-\lambda x^{\alpha}}, \qquad x > 0 \quad \text{pdf of Weibull distribution,} \tag{10}$$

$$f_3(x) = \frac{1}{x\sigma\sqrt{2\pi}} e^{-\frac{(\ln(x)-\mu)^2}{2\sigma^2}}, \qquad x > 0 \quad \text{pdf of lognormal distribution,} \tag{11}$$

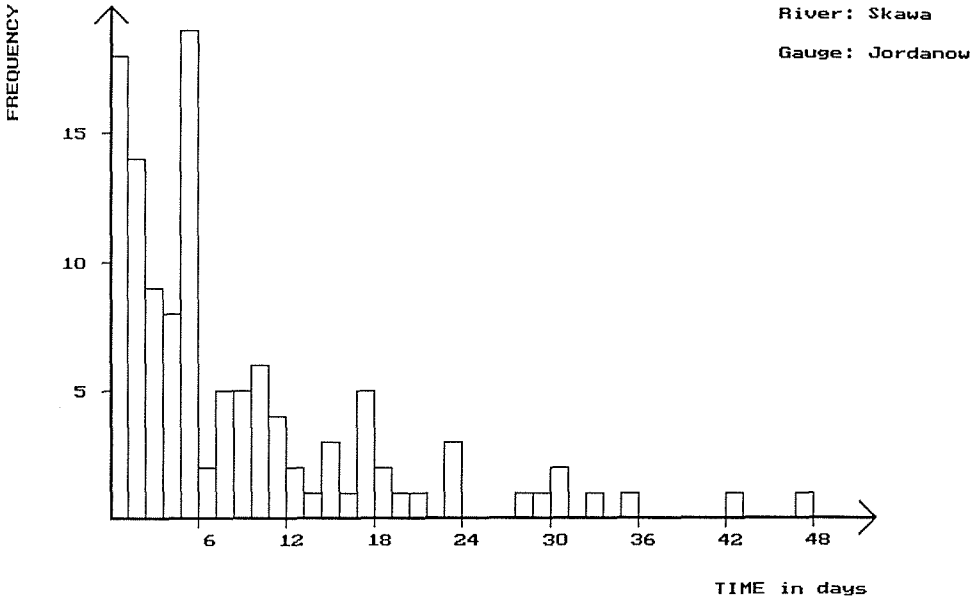

Fig. 3 An empirical distribution of the time of low flow, the Skawa River—gauge Jordanów.

For the model the distributions are taken for which chi-square tests give the best fit. Unknown parameters are obtained with the method of maximum likelihood or method of moments. The only criterion of the method is the goodness of fit of the chi-square test.

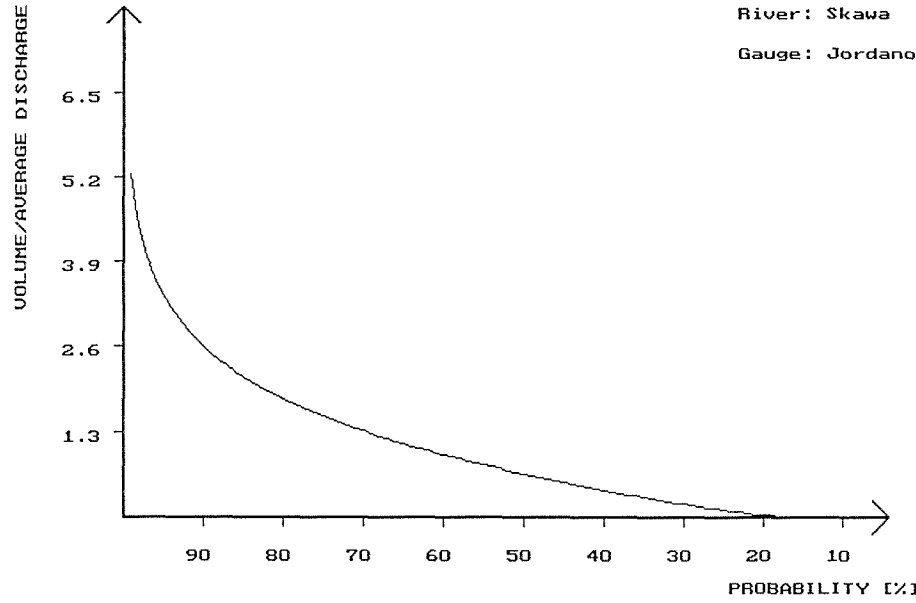

Fig. 4 The distribution of extreme low flow volumes, the mountain catchment, the Skawa River—gauge Jordanów.

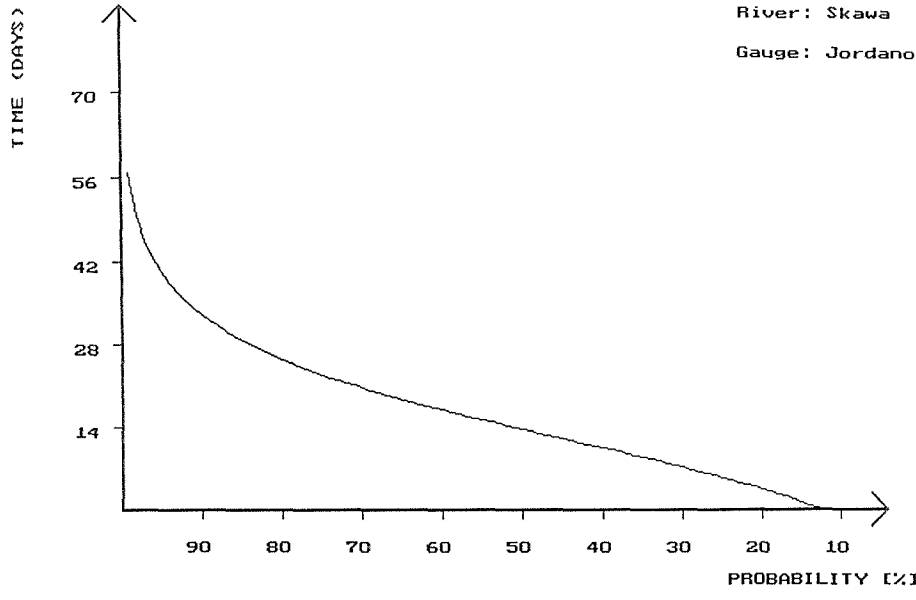

Fig. 5 The distribution of extreme time of the low flow, the mountain catchment, the Skawa River—gauge Jordanów.

To make it clear consider an example, the Jordanów gauge on the Skawa River. Take the truncation level Q_0 = 90% and a year as a basic time interval. According to the procedure given above, we obtain 117 streamflow droughts. To determine the distribution of the number of significant droughts in the year, we count how many droughts appeared every year—see Table 3.

Figures 2 and 3 show the shape of the observed pdf of water low flow volume and time of drought, and appropriate distributions of maximum low flow volume and time are presented on Figs 4 and 5.

CONCLUSIONS

Since low flow is a conventional term, it can be defined only in a conventional way because it is not possible to give a strict, well grounded definition (Ozga-Zielińska & Brzeziński, 1994). Such a definition should exactly determine the period when the flow of the river is so small that it can be considered as a drought. The most simple and the most exact definition is that the drought is a period where

$$Q_t \leq Q_0$$

To determine the boundary discharge some hydrological or economical criteria are applied. From the economical point of view low flow can be considered as a deficit of water and its duration, but if we assume hydrological criterion, we determine the volume of low flow and its duration. Since low flows as extreme phenomena do not occur every year, we assumed that boundary discharge for the considered 30 year period is

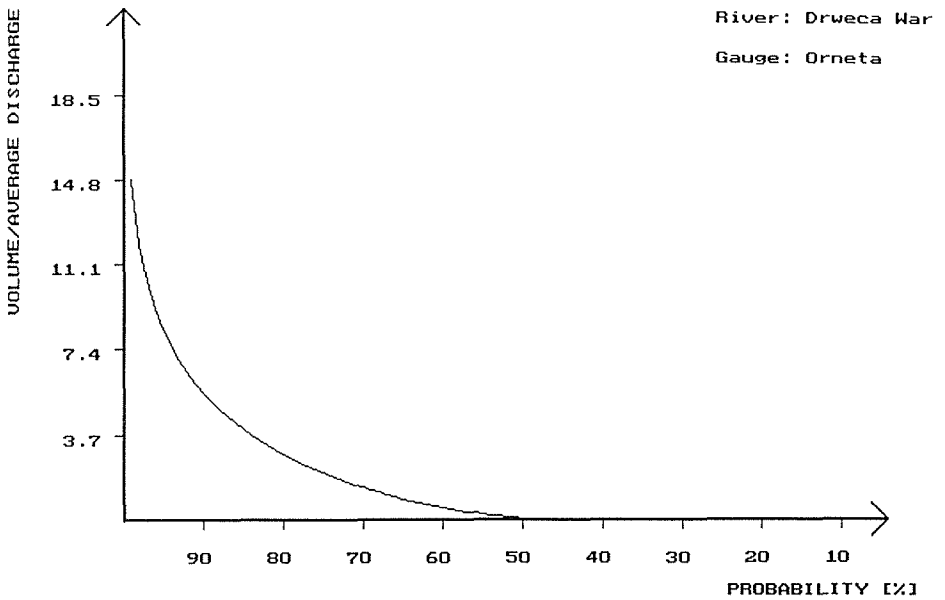

Fig. 6 The distribution of extreme low flow volumes, the lowland catchment, the Drwęca Warmińska River—gauge Orneta.

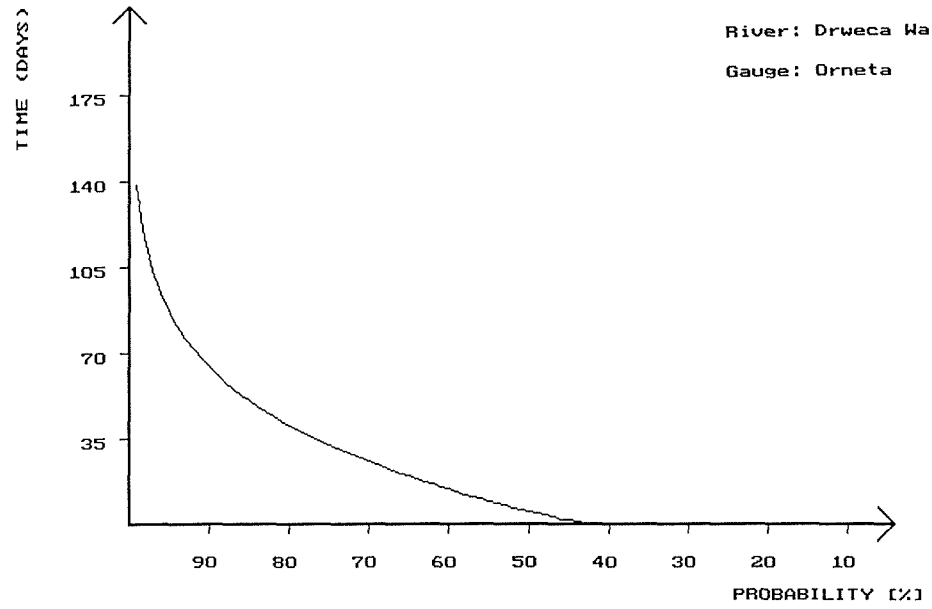

Fig. 7 The distribution of the extreme time of low flow, the lowland catchment, the Drwęca Warmińska River—gauge Orneta.

$$Q_v = Q_{90\%}$$

If we determine the low flow in this way, we have the years when we do not see low flows and years when we have more than one drought (see Table 3). The authors have presented the distribution of maximal volumes of the low flow and its duration for a typical lowland river (Figs 6, 7) and for a typical mountain one (Figs 4, 5). As a result of comparing both distributions it has been noticed that in the mountain catchments (Skawa—Jordanów) the occurrence probability p of the droughts is greater ($p = 87\%$) and their volumes do not exceed six times the mean discharge value. The duration of those droughts is much shorter (some 30–40 days). In lowland catchments (Drwęca Warmińska—Orneta) the droughts occur much more rarely ($p = 50\%$), but the low flows have more important volume(up to $15 \times \overline{Q}$) and their duration is up to 50–60 days.

Table 4 Probability of volumes and durations of droughts.

No.	River gauge	$\Pr(E_t \neq 0)$ in %	$D/\overline{Q}$		Time (days)	
			$p = 10\%$	$p = 20\%$	$p = 10\%$	$p = 20\%$
1	Sokołda—Sokołda	77	5.16	2.89	50	32
2	Drwęca Warm.—Orneta	50	5.53	2.89	64	41
3	Bystrzyca—Jugowice	76	7.57	4.43	56	37
4	Krynka—Przeworno	67	6.0	3.85	49	36
5	Czarny Potok—Mirsk	70	6.09	3.11	52	34
6	Skawa—Jordanów	87	2.60	1.80	33	25
7	Cicha Woda—Zakopane	74	3.82	2.35	47	34
8	Łososina—Bocheniec	61	4.64	2.70	39	26
9	Świślina—Nietulisko	77	2.25	1.52	29	21

The results concerning the volume and duration of low flows for the determined probability obtained for the investigated catchments are presented in Table 4. The investigations show that the stochastic low flow model allows the estimation of the quantity of low flows. We consider that Zelenhasič model can be used for the evaluation of storage capacity of a catchment. Further researches should take into consideration the relationship between drought volume and physical and geographical parameters which characterize the storage capacity of a catchment. It seems that such an approach allows determination of regional relationships.

REFERENCES

Ozga-Zielińska, M. & Brzeziński, J. (1994) *Hydrologia stosowana* (Applied hydrology) Warsaw.

Todorovič, P. & Zelenhasič, V. (1970) A stochastic model for flood analysis. *Wat. Resour. Res.* **6**(6), 1641–1648.

Zelenhasič, E. & Salvai, A. (1987) A method of streamflow drought analysis. *Wat. Resour. Res.* **23**(1), 156–168.

5 Hydrological Extremes: *Catchment Modelling*

FRIEND'97 — Regional Hydrology: Concepts and Models for Sustainable Water Resource Management
(Proceedings of the Postojna, Slovenia, Conference, September–October 1997). IAHS Publ. no. 246, 1997.

Impact of land-use, climate change and groundwater abstraction on streamflow droughts using physically-based models

E. P. QUERNER
DLO Winand Staring Centre for Integrated Land, Soil and Water Research (SC-DLO), PO Box 125, 6700 AC Wageningen, The Netherlands

L. M. TALLAKSEN
Department of Geophysics, University of Oslo, PO Box 1022, Blindern, N-0315 Oslo, Norway

L. KAŠPÁREK
T. G. Masaryk Water Research Institute, PO Box 30, 160-62 Praha 6, Czech Republic

H. A. J. VAN LANEN
Department of Water Resources, Wageningen Agricultural University, Nieuwe Kanaal 11, 6709 PA Wageningen, The Netherlands

Abstract Changes in land-use, climate and groundwater abstractions have an impact on river flows. The effect of these changes on streamflow droughts have been analysed using the models BILAN, HBVMOR, MODFLOW and MOGROW. These models are physically-based and therefore suitable to be used for potential situations with changed conditions which may affect the hydrological system. The models were applied to river basins in The Netherlands (Hupsel, Gulp and Noor), Norway (Haugland) and Scotland (Monachyle). The models were used to simulate the impact of afforestation, climate warming by 2 and 4°C in combination with an adoption of the precipitation changes in groundwater recharge and groundwater abstractions on streamflow droughts. The models are adequate tools to simulate streamflow droughts, and can be used to assess the impact of human activities.

INTRODUCTION

Floods and droughts impose serious threats to human life, environment and agriculture. A decrease in water availability resulting from natural factors, particularly in summer, causes drought to occur. These hydrological droughts are often aggravated by human activities such as change in land-use, improved land drainage or increased groundwater abstractions. A man-induced impact can be either direct, such as groundwater abstractions, or indirect such as numerous activities resulting in climate change and thus contributing to drought. Streamflow droughts are defined in this study in terms of drought duration and deficit volume using the threshold level approach, i.e. droughts are defined as periods when the streamflow is below a certain threshold level.

For the problems outlined above a regional conceptual hydrological model can be used to describe the system. Analytical models are often used to predict the changes to the hydrological system, but complex situations cannot be handled by these models. Therefore a simulation model should be physically-based, so that it can be used to synthesize historical hydrological events and to evaluate the effects of potential changes imposed on the hydrological regime.

The objective of this paper is to use several physically-based models for the assessment of human activities on streamflow drought. The analysis includes the change in land-use and climate, changes in groundwater recharge and increased groundwater abstractions for several basins across Europe.

DESCRIPTION OF RIVER BASINS

The models were applied to river basins in The Netherlands (Hupsel, Gulp and Noor), Norway (Haugland) and Scotland (Monachyle).

The Hupselse Beek basin is situated in the east of The Netherlands near the German border. The area covers 6.5 km^2 and lies between 24 and 33 m a.m.s.l. The average slope of the area is about 0.8%. The river flows through a wide valley with a gradient of 0.06–0.25%. Land-use is predominantly agricultural; about 70% is pasture, 21% is arable land (mainly maize) and 6% woodland. Within the basin the main stream is 4 km long and has seven small tributaries varying in length between 300 and 1500 m. The mean annual precipitation is about 770 mm and the average streamflow is about 70 l s^{-1}.

The Noor basin (10.6 km^2) is located in the southeast of The Netherlands and northeast of Belgium. The basin is part of the Margraten Plateau. The elevation varies between 240 m a.m.s.l. in the southeast and 91 m a.m.s.l. at the outlet in Belgium. Land-use is predominantly pasture (62%) and arable land (35%). The mean annual precipitation equals about 765 mm, and the average streamflow at the outlet is about 55 l s^{-1} for the period 1992–1994. The Noor brook has a length of 3 km and drains a dissected chalk plateau, with steep slopes to the valley. The aquifer has a large groundwater storage, which results in streamflow consisting of more than 90% from groundwater flow, i.e. baseflow.

The Gulp basin drains a dissected chalk plateau in the southeast of The Netherlands and adjacent Belgium areas. The total area of the basin is about 46 km^2, the length of the valley is 18 km, whereas the maximum width is 4 km. The Gulp brook rises at 285 m a.m.s.l. in Belgium, and joins the Geul at 88 m a.m.s.l. Permanent grassland covers more than 90% of the basin and some forest predominantly occurs on the steep, eastern slopes. The mean annual precipitation is 800 mm and the average streamflow at the outlet is about 0.5 m^3 s^{-1}.

The Haugland basin is located in the southwestern part of Norway, close to the coast. The basin area is 135 km^2, and the altitude interval is 18–424 m a.m.s.l. Bare rock (40%) and small lakes (5%) dominate in the northeast, whereas forest on a thin cover of glacial deposits (55%) is found closer to the outlet. The geology consists of Precambrian, impermeable bedrock. The mean annual precipitation is approximately 1800 mm, and the average daily streamflow for the period 1960–1991 is about 6.6 m^3 s^{-1}.

The Monachyle basin is located in the central Scottish highlands. The basin (7.7 km^2) is a steep-sided, glaciated valley (295–900 m a.m.s.l.) with shallow peat,

peaty gleys and upland brown earths overlying mica-schists and variable depths of glacial debris in the valley bottom. The mean annual precipitation ranges from 2000 mm in the valley bottom to 3500 mm near the ridge crest. The vegetation is predominantly upland pasture (50%) and heather (50%) with many rock outcrops at high altitudes. The average daily flow (1984–1988) is about 0.5 $m^3 s^{-1}$.

DESCRIPTION OF MODELS

The impacts of changes in land-use, climate change and groundwater abstraction on streamflow droughts have been analysed using the models BILAN, HBVMOR, MODFLOW and MOGROW. The water balance model BILAN consists of a number of relationships, which describe distribution of precipitation into several components, such as evaporation, percolation (recharge), various types of water storage in the basin and basic runoff components (Kašpárek & Krejčová, 1994). The HBVMOR model is composed of two separate models, a conceptual rainfall–runoff model and a physically-based evapotranspiration model (Tallaksen & Erichsen, 1994). The MODFLOW model simulates transient groundwater flow in aquifers and aquitards, using the finite difference method (McDonald & Harbaugh, 1988). The MOGROW model simulates the flow of water in the unsaturated zone, the saturated zone and the water courses in an integrated manner (Querner, 1997). The models used in this paper are evaluated for drought studies elsewhere (Van Lanen *et al.*, 1997).

DEFINITION OF DROUGHT

Natural variation in streamflow and additional effects of land-use or climate change affect the low flows and associated droughts. A drought occurs when streamflow is below a prescribed threshold discharge. A threshold can be based for instance on ecological criteria, which in turn can be derived from the flow duration curve. When the streamflow is below the threshold the period is indicated as a deficit period. A threshold discharge of $Q70$ has been used in this study. This means that 70% of the time the discharge is above the $Q70$. The measured and simulated time series of streamflow were analysed to investigate droughts using the computer code EXDEV (Řičica & Novický, 1995).

Droughts were defined in terms of duration and deficit volume. The deficit volume equals the integrated difference between the threshold discharge and the prevailing streamflow (below the threshold) over the drought period. During a prolonged dry period, short periods might be observed when the streamflow exceeds the threshold discharge thereby dividing a large drought into two or more smaller droughts. Usually these smaller droughts are pooled using an inter-event volume and/or duration criteria (Řičica & Novický, 1995; Tallaksen *et al.*, 1997). In this study a volume criterion of 0.1 was used, which implies that a drought is pooled with the next drought, if the ratio between the inter-event excess volume and the preceding deficit volume is less than 0.1.

SCENARIOS

The HBVMOR and MOGROW models were used to predict changes in flow characteristics due to afforestation. The effect on streamflow of climate change has been analysed using the BILAN model. The effect of a change in groundwater recharge and groundwater abstraction has been investigated using the groundwater model MODFLOW.

Afforestation

For the Hupsel basin the MOGROW model has been used to simulate the period 1969–1992. The average discharge measured (0.75 mm day^{-1}) and calculated (0.66 mm day^{-1}) compared reasonably well (Werkman, 1995). The increased difference between measured and calculated flows over long period might be due to a change in human activity which influences the hydrological behaviour of the basin over a long-term scale.

As an example of land-use change, a complete afforestation of the Hupsel basin showed a decrease in mean flow from 0.66 to 0.43 mm day^{-1} (Table 1). The threshold value of $Q70$ calculated for the present situation was 0.21 mm day^{-1} (period 1969–1992). A forested basin would result in a lower $Q70$ of 0.18 mm day^{-1}. Drought duration obtained using $Q70$ for the reference simulation gave 2628 days that the streamflow would be below the threshold. The forested basin gives for the same $Q70$ (reference situation) a drought duration of 2835 days, which is about 8% more days.

The HBVMOR model was applied to the Hupsel basins for the period 1980–1983 (Tallaksen & Erichsen, 1994). This period had a much higher average discharge than the period 1969–1992, but the $Q70$ was much lower. Above normal wet conditions in winter and dry conditions in summer caused this situation. Therefore the drought duration was also much larger and the simulated effect of afforestation was more pronounced. Now the increase in drought duration due to afforestation was about 30%. For the Monachyle basin with an annual precipitation of more than 2000 mm

Table 1 Simulated discharge characteristics and drought duration for non-forested and forested Hupsel and Monachyle basins.

	Streamflow (mm day^{-1}):		Drought duration* (days):	
	Reference	Forested	Reference	Forested
Hupsel (MOGROW)				
Average discharge	0.66	0.43		
$Q70$	0.21	0.18	2628	2835
Hupsel (HBVMOR)				
Average discharge	1.04	0.73		
$Q70$	0.14	0.07	393	514
Monachyle (HBVMOR)				
Average discharge	6.01	5.79		
$Q70$	1.06	1.03	133	147

* Based on the $Q70$ for the reference simulation.

the effect of afforestation resulted only in minor changes in the low flow conditions, i.e. drought duration increased by 10% (Table 1).

Impact of climate change

The impact of climate change on streamflow was studied in the Haugland and Gulp basins with the BILAN model. For the Haugland basin, data were available for the period 1960–1987, whereas for the Gulp the examined period was 1978–1985.

For both basins and for all periods with drought events (flow below the threshold level of $Q70$), the drought expressed as deficit volume per unit basin area in mm, was calculated. These deficit volumes were ranked according to their magnitude (ranked events). For the Haugland basin the curves with ranked events derived for the observed and simulated runoff were small. For the Gulp basin the simulated deficit volume was underestimated.

The first simple climate change scenario takes into account a constant (not variable in time) increase in the air temperature by 2°C and alternatively by 4°C. The temperature affects the evapotranspiration and the snow melting in BILAN. The effect of this scenario is shown in Fig. 1 for the Haugland and Gulp basins. In the Haugland basin, the deficit volume raised significantly with the increase in temperature by 2°C, while the effect of further climate warming (by an additional 2°C) was less remarkable. For the Gulp basin, the increase in deficit volume between

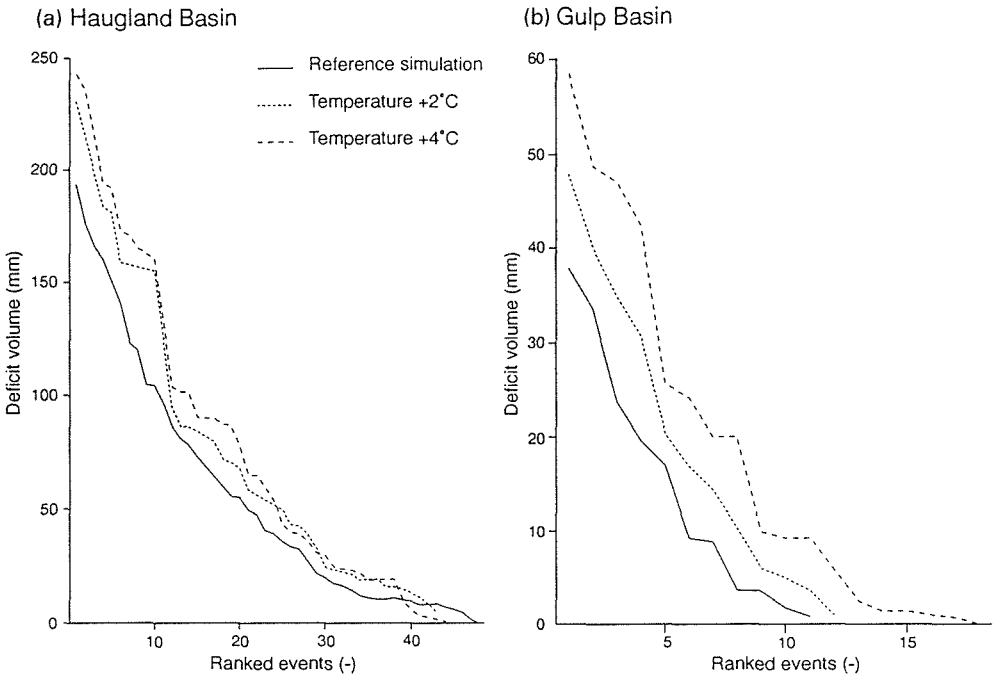

Fig. 1 Ranked deficit volumes simulated by BILAN model for the Haugland (a) and Gulp (b) basin. Sensitivity to an increase in temperature by 2 and 4°C.

the increase in temperature of 2°C and 4°C was about the same. In the Haugland basin an increase of the temperature by 2°C would result in an increase of the deficit volumes for the most severe droughts by about 15%. In the Gulp basin this increase is 25%. The difference in response between the two basins due to climate warming can probably be attributed to the fact that the drought events in Haugland, with a high annual precipitation and a low groundwater storage, are more frequent (in average 1.4 events each year) but shorter. The duration of the drought does not increase significantly with the increase in temperature. In contrast, the Gulp basin, having lower precipitation but higher water storage capacity, experiences the drought events less frequently (0.7 events each year), however, the duration was generally longer and it increased substantially with the climate warming.

In the second scenario it is assumed that air temperature is 2°C higher together with a constant increase or decrease in precipitation of 10%. Figure 2 shows for the Gulp basin the effect of these changes on the deficit volume. Frequency curves are presented for the present situation and for a change in precipitation of −10%, 0% (no change) and +10%. The increase in temperature of 2°C in combination with a decrease in precipitation caused an increase of the drought duration by about 70% (Fig. 2). An increase in precipitation by 10% would be able to compensate the effect on drought occurrence of an increase in temperature of 2°C (Fig. 2).

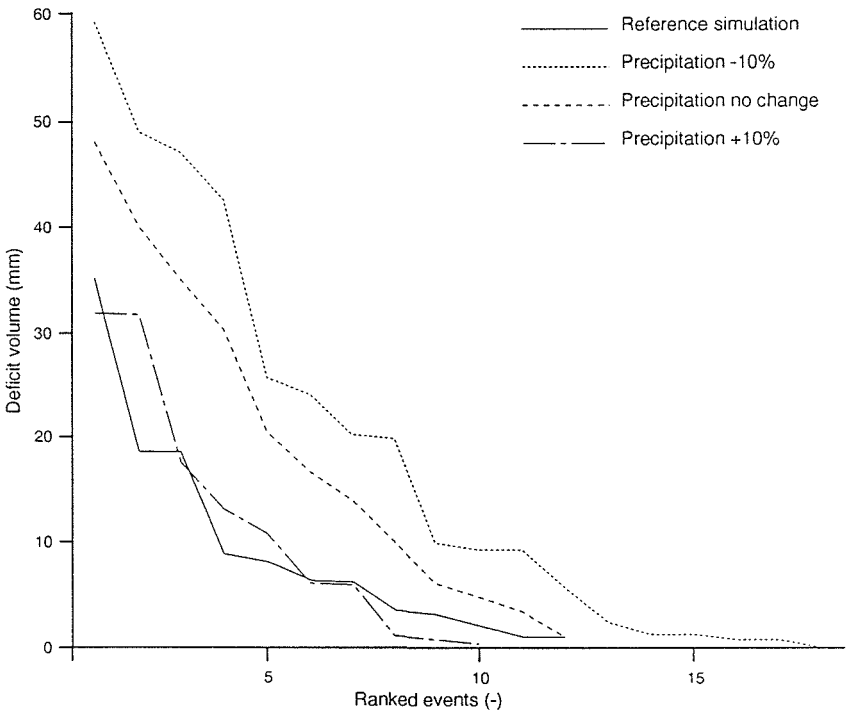

Fig. 2 Ranked deficit volumes simulated by BILAN model for the Gulp basin. Sensitivity to an increase in temperature by 2°C in combination with a change in precipitation.

Impact of groundwater recharge

The MODFLOW model was applied to the Noor basin to explore the effects of changes in recharge on the discharge of the Noor. Such variation in recharge could be the result of a change in land-use or climate. The groundwater recharge has been derived from meteorological, crop, soil and water-table depth data. In the period 1990–1994 the recharge, for grassland with deep groundwater levels, varied between 180 and 405 mm $year^{-1}$.

The effects of the natural variation in the groundwater recharge are reflected in the simulated streamflow of the Noor. Because the Noor is mainly fed by groundwater, a strong correlation between the groundwater recharge, the groundwater heads and the streamflow prevails. In years with low recharge, the discharge of the Noor varies between 25 and 60 l s^{-1}. In years with high recharge the discharge is significantly higher, i.e. 35–90 l s^{-1} (Van Lanen, 1996).

Some results of the analysis of the time series of streamflow data are presented in Fig. 3. A threshold discharge of 35 l s^{-1} was used, which equals $Q70$. In 30 out of 100 years the drought duration for the reference situation was about 140 days (Fig. 3). In 20 out 100 years the duration increased to 160 days. If the recharge decreased by 20% (80% recharge), for instance as a result of climate change, the duration will increase to 270 days in 20 out of 100 years. So, this implies an increase of the drought duration by 70%. If the recharge increased by 20% (120% recharge) in the period between 1990 and1994, the duration is less affected. In 20 out of 100 years the drought duration decreased by 30%. So, drought duration is under these conditions more sensitive to a recharge decrease of 20% than a similar increase.

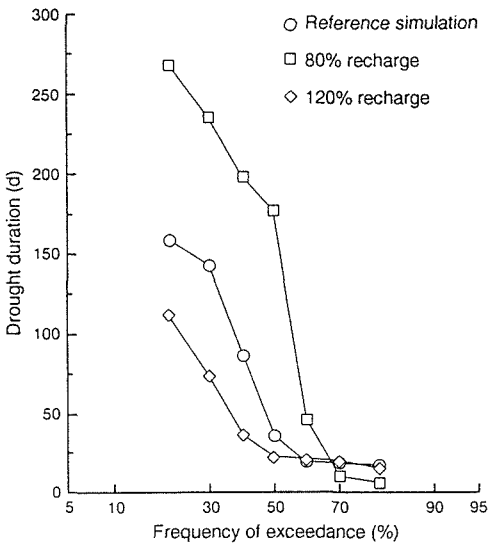

Fig. 3 Frequency of exceedance of drought duration in the Noor basin derived from simulated streamflow and scenarios with a variation in recharge.

Impact of groundwater abstraction

The MODFLOW model was applied to the Noor basin to explore the effects of changes in groundwater abstraction on streamflow and to separate the natural drought caused by a precipitation shortage from additional man-induced drought (groundwater abstraction). In Fig. 4 the effect of abstraction on the streamflow is shown. The reference situation includes the impact of all current groundwater abstractions of about 15×10^6 m^3 year^{-1}. Scenario I represents a further increase in the abstraction by 1×10^6 m^3 year^{-1} in the vicinity of the Noor catchment, as was requested by the drinking water supply company. Scenario II assumes termination of all groundwater abstractions from the Margraten Plateau.

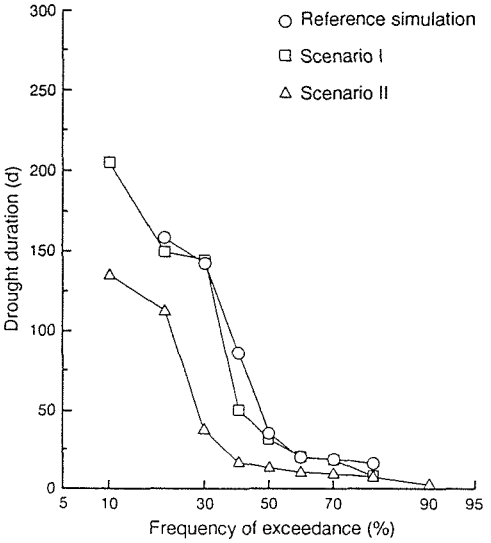

Fig. 4 Frequency of exceedance of drought duration in the Noor basin derived from simulated streamflow and scenarios with a variation in groundwater abstractions.

A small increase of the groundwater abstraction (scenario I) had hardly any effect on the drought duration (Fig. 4). Termination of all groundwater abstraction (scenario II) lead to a limited decrease of the drought duration. In 20 out of 100 years the drought duration decreased from 160 to 110 days. This decrease by 30% is small compared to the increase by the drought duration (70%) due to a 20% increase of the groundwater recharge. These streamflow simulations suggest that droughts in the Noor basin will be more affected by relatively small changes in groundwater recharge due to climatic or land-use change than current groundwater abstraction practices.

CONCLUSIONS

Physically-based models are able to simulate streamflow in selected basins in northwest and central Europe with different geology and climate conditions. The

tion results show that the models give satisfactory estimates of mean and low flow characteristics. There is an important consistency in the model results. The models are therefore adequate tools to simulate streamflow droughts, and have a potential to assess the impact of human activities, including changing climate conditions.

As an example of land-use change, a complete afforestation of the Hupsel basin (The Netherlands) shows a decrease in mean flow. This would also result in about 10–30% more days that the streamflow would be below the given threshold level of $Q70$ (70% of the flow duration curve). In the wetter Monachyle basin (Scotland) the effect of afforestation is about 10% more days with streamflow below $Q70$.

The results of the simulations, based on the simplified climate change scenarios, show that the deficit volume is very sensitive to both an increase in temperature and a change in precipitation (Norwegian and Dutch basins). Even in basins with abundant precipitation, the warming by 2°C would result in a rise in deficit volume by up to 20%. The deficit would be more severe in a basin experiencing medium–high precipitation although its water storage capacity is relatively large.

Changes in recharge (indicating a change in climate or land-use) and groundwater abstractions were simulated with the MODFLOW model for the Noor basin (The Netherlands). Variation of 20% in recharge has a larger effect on drought duration and deficit volume than changes in abstractions. Even, if all groundwater abstractions were terminated, the total impact is lower than the still limited variation in the recharge of 20%.

Acknowledgements The authors thank the members of the Low Flow Group of the FRIEND (Northwest Europe) for the valuable discussions and contributions. The MSc student W. J. Werkman performed the MOGROW simulations for the Hupselse Beek basin.

REFERENCES

Kašpárek, L. & Krejčová, K. (1994) *BILAN Water Balance Model. User's Guide and Background Information.* T. G. Masaryk Water Research Institute, Prague.

Lanen, H. A. J. van (1996) Groundwater monitoring and modelling studies: Netherlands' contribution to IHP. In: *Symposium on Hydrological Research Proceedings*, Report 96.1 Netherlands National Committee for IHP-OHP, 19–28.

Lanen, H. A. J. van, Tallaksen, L. M., Kašpárek, L. & Querner, E. P. (1997) Hydrological drought analysis in the Hupsel basin using different physically-based models. In: *FRIEND'97: Regional Hydrology—Concepts and Models for Sustainable Water Resource Management* (ed. by A. Gustard *et al.*) (Proc. Postojna Conference, September–October 1997), this volume. IAHS Publ. no. 246.

McDonald, M. G. & Harbaugh, A. W. (1988) *A Modular Three-dimensional Finite-Difference Groundwater Flow Model.* US Geological Survey.

Querner, E. P. (1997) Description and application of the combined surface and groundwater flow model MOGROW. *J. Hydrol.* (in press).

Řičica, J. & Novický, O. (1995) Experiments with deficit volumes (EXDEV). Description of the program. Edition April 1995. Czech Hydrometeorological Institute, Prague.

Tallaksen, L. M. & Erichsen, B. (1994) Modelling low flow response to evapotranspiration. In: *FRIEND: Flow Regimes from International Experimental and Network Data* (ed. by P. Seuna, A. Gustard, N. W. Arnell & G. A. Cole) (Proc. Braunschweig Conf., October 1993), 95–102. IAHS Publ. no. 221.

Tallaksen, L. M., Madsen, H. & Clausen, B. (1997) On the definition and modelling of streamflow drought duration and deficit volume. *Hydrol. Sci. J.* **42**(1), 15–33.

Werkman, W. J. (1995) Low flows in the Hupselse Beek basin. An analysis with the integrated groundwater and surface water model MOGROW (in Dutch). MSc Thesis, Wageningen Agricultural University. DLO Winand Staring Centre, Internal Report 378.

FRIEND'97 — Regional Hydrology: Concepts and Models for Sustainable Water Resource Management
(Proceedings of the Postojna, Slovenia, Conference, September–October 1997). IAHS Publ. no. 246, 1997.

Groundwater management in the Jegrznia River valley

WALDEMAR MIODUSZEWSKI, ZBIGNIEW KOWALEWSKI, ALICJA ŚLESICKA
Institute for Land Reclamation and Grassland Farming, Falenty, 05-090 Raszyn, Poland

ERIK P. QUERNER
DLO Winand Staring Centre for Integrated Land, Soil and Water Research, (SC-DLO), PO Box 125, 6700 AC Wageningen, The Netherlands

Abstract The results of field investigation and simulation of groundwater levels in the Jegrznia River Valley (Biebrza National Park, Poland) are presented. Calculations were carried out for climatic conditions prevailing in 1992 to analyse various scenarios for surface water distribution. The combined groundwater and surface water model SIMGRO has been used to predict the effect of human intervention. The research demonstrated that surface water has a minor influence on groundwater levels. In the central part of the valley, further away from the surface water, the changes in groundwater level mainly depend on weather conditions, i.e. precipitation and evapotranspiration. Spring flooding is needed to raise groundwater levels and to restore the nature potential.

INTRODUCTION

The Jegrznia River valley is part of the Biebrza National Park (BNP) in northeast Poland, which is an area of great natural value. The peatlands which can be found there are characterized by the rich natural flora and fauna typical of marshland habitats. Over the last 100 years, various hydrotechnical projects have been undertaken in the Biebrza and Jegrznia River valleys to drain the marshlands and transform them to agricultural land. The construction of the Rudzki, Woźnawiejski and Kuwasy canals have caused changes in the natural hydrographical network (Fig. 1). Natural rivers (such as the Elk and the Jegrznia) currently have a small water capacity, and the principle drainage system are the manmade canals, which very quickly drain the water from this area. The construction of the drainage system has caused lowering of groundwater levels and a significant reduction in the annual flooding which previously used to occur in spring.

The excessive drainage of the marshes has resulted in the mineralization and degradation of organic soils and unfavourable changes in the natural flora and fauna. The degradation processes show that a new water management policy is required based upon new principles to protect the natural environment of the Jegrznia valley. It is of particular importance that the groundwater level will be raised. The estimated optimum moisture conditions will prevail when the groundwater level in the summer will be maintained within 50 cm below the soil surface (Okruszko, 1990; Mioduszewski, 1994).

Renaturalization plans for the Jegrznia valley foresee a reduction in the outflow from the Woźnawiejski canal and redirection of the water to the old river bed (Fig. 1). Construction of weirs in the canal will increase the flow of water in the river and will result in higher groundwater levels. An evaluation of the impact of such intervention and the eventual changes in land use (reduction of overgrown woodlands) on the groundwater level are the main aims of this study.

DESCRIPTION OF THE STUDY AREA AND FIELD INVESTIGATIONS

Field investigations were mainly concentrated in the so called "Triangle" area which borders the old river beds of the Elk and Jegrznia and the Woźnawiejski canal (Fig. 1). In the regional groundwater flow model the research area was enlarged in an easterly direction to include the Czerwone Bagno Reserve.

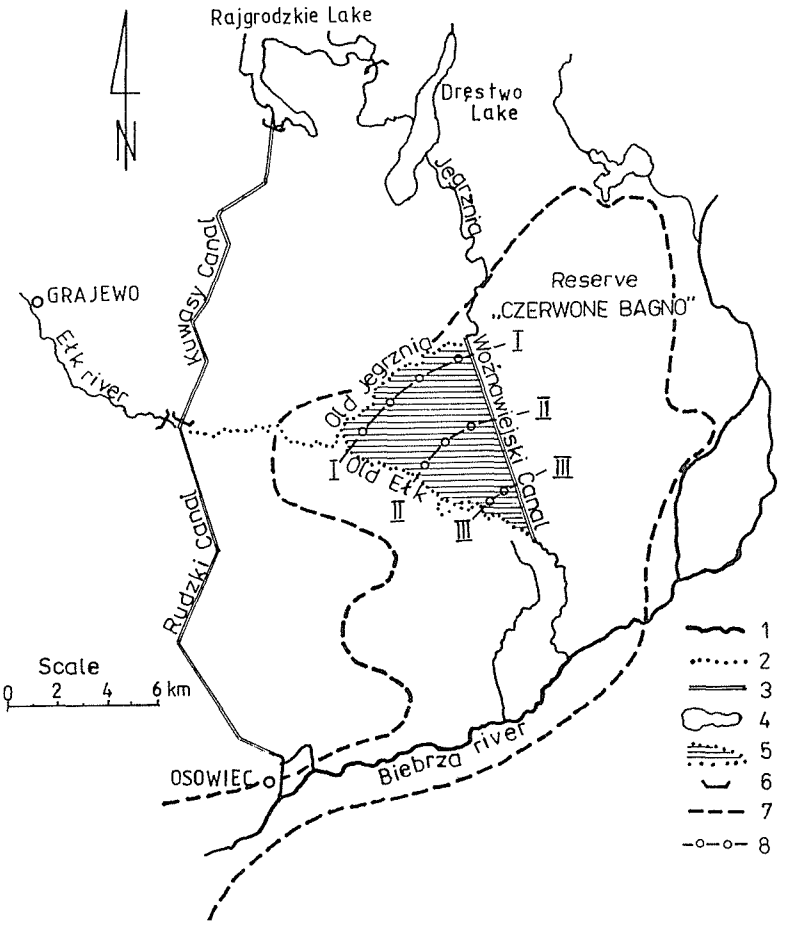

Fig. 1 Hydrographic network in the central part of the Biebrza River basin; 1—rivers, 2—old river beds, 3—canals, 4—lakes, 5—study area, 6—hydrotechnical structures, 7—boundary of the Biebrza National Park, 8—transects with piezometers.

Field investigations demonstrated that virtually the entire study area is covered by shallow peat soils with a saturated hydraulic conductivity ranging between 0.1 and 2.0 m day^{-1}. Below the peat layer, sand and silt can be found. The thickness of this layer is 15–20 m with an average hydraulic conductivity of 5.0 m day^{-1}. Impermeable clay underlies the sand in the whole area.

The "Triangle" area covers about 3000 ha and land use is predominantly low yielding meadow and pasture (45%). The remaining area is overgrown with natural marsh plants (20%) and forest or bushes (35%). The last years natural marsh plants have disappeared and the study area has overgrown with unwanted bushes.

Lysimeter research, which has been undertaken for many years in this area, has enabled the assessment of the crop coefficient to compute evapotranspiration both for marshland vegetation and cultivated grass (Szuniewicz & Chrzanowski, 1995).

In the "Triangle" area 29 piezometers were installed in three transects (Fig. 1). Groundwater levels were measured every ten days from early spring until late autumn (Fig. 2). In spring the groundwater and surface water levels are high and in some years they reach the soil surface. Drainage by the rivers and Woźnawiejski canal and increased evapotranspiration of the expanding bush resulted in a decrease of the groundwater levels to a depth of 1.0–1.5 m below the soil surface.

DESCRIPTION OF THE SIMGRO MODEL

The model SIMGRO (SIMulation of GROundwater flow and surface water levels) simulates transient regional groundwater flow in response to drainage, water supply, sprinkling, subsurface irrigation and surface water level control. To model regional groundwater flow, the system has to be schematized. Land use is schematized at the first aggregation level. The second aggregation level deals with subregions describing

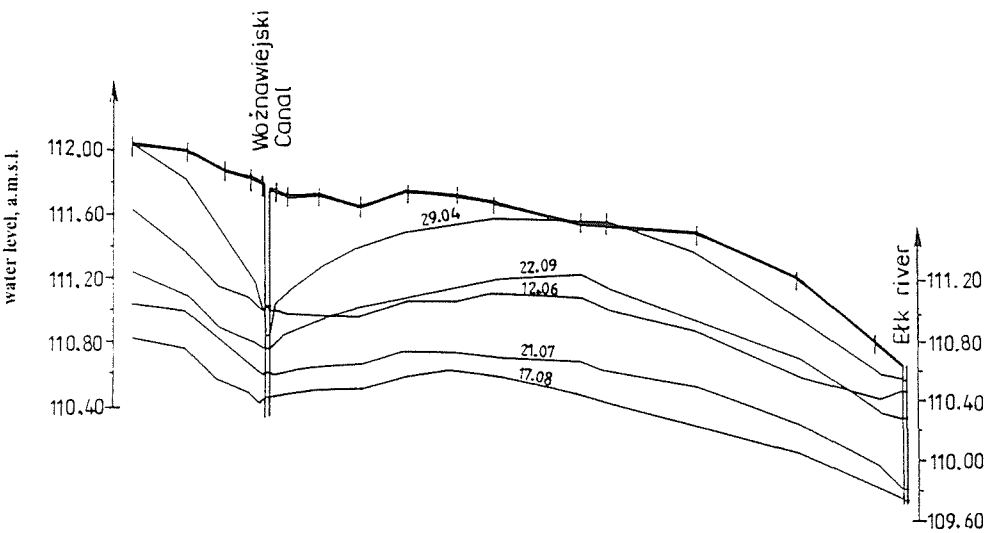

Fig. 2 Measured groundwater levels in transect II in 1992.

soils and hydrologic properties for the unsaturated zone. The third level covers various subsurface layers for saturated groundwater flow.

The unsaturated zone consists of two reservoirs, one for the root zone and one for the subsoil. If the equilibrium moisture storage for the root zone is exceeded, the excess water percolates to the saturated zone. If the moisture storage is less than the equilibrium moisture storage, then an upward flow from the saturated zone occurs. The height of the phreatic surface is calculated from the saturated flow and the water balance of the unsaturated subsoil, using a storage coefficient which is dependent on the depth of the groundwater level below soil surface. The unsaturated zone is modelled one-dimensionally per subregion and land use type (Querner, 1993). Special processes are included in the unsaturated zone model, i.e. surface runoff, perched water tables, hysteresis and preferential flow.

Actual evapotranspiration is a function of weather data, crop type and moisture content in the root zone. Measured or computed values for net precipitation and potential evapotranspiration for grassland and woodland are required as input data. The potential evapotranspiration for other crops or vegetation types is derived by the model from the values for grassland by converting with known crop coefficients. The potential evapotranspiration for forest is calculated as the sum of transpiration and interception. Potential evapotranspiration was calculated using the Penman method with the crop coefficients determined in lysimeters covered with grasses and marsh vegetation. However, there is a lack of reliable data on the potential evapotranspiration of forests and bushes. Observations and surveys made in the study area indicate that it is acceptable to assume that the potential evapotranspiration of forests is 10% larger than the potential evapotranspiration of natural marsh plants.

The saturated groundwater flow equation is solved numerically by using the finite element approach (Querner, 1988). Therefore the study area is covered with a finite element network. The groundwater subsystem reacts slowly to changes (e.g. precipitation) whereas the surface water subsystem responds quickly. Therefore both subsystems have their own time step length. The surface water module performs several time steps during one time step of the groundwater module. The interaction between groundwater and surface water is characterized by a so-called drainage resistance (Ernst, 1978).

The model area (the "Triangle" area together with the adjacent Czerwone Bagno Reserve) was divided into 611 triangular elements and 640 nodes. In each node the groundwater level was computed. The area was divided into 26 subregions (Fig. 3) with approximately uniform unsaturated conditions (i.e. similar soil type and fluctuations of groundwater levels).

Model simulations were done for climatic conditions prevailing in 1992. The model simulation starts on 1 April, the beginning of the growing season, with the groundwater levels measured on the 1 April 1992 as initial levels. The initial levels were assumed to be equal for all the scenarios.

MODEL SCENARIOS

The following scenarios were considered:

I. *Present situation*—the surface water levels in the Elk, Jegrznia and the Woźnawiejski canal were similar to the natural conditions prevailing in 1992. This scenario was used to verify the model.

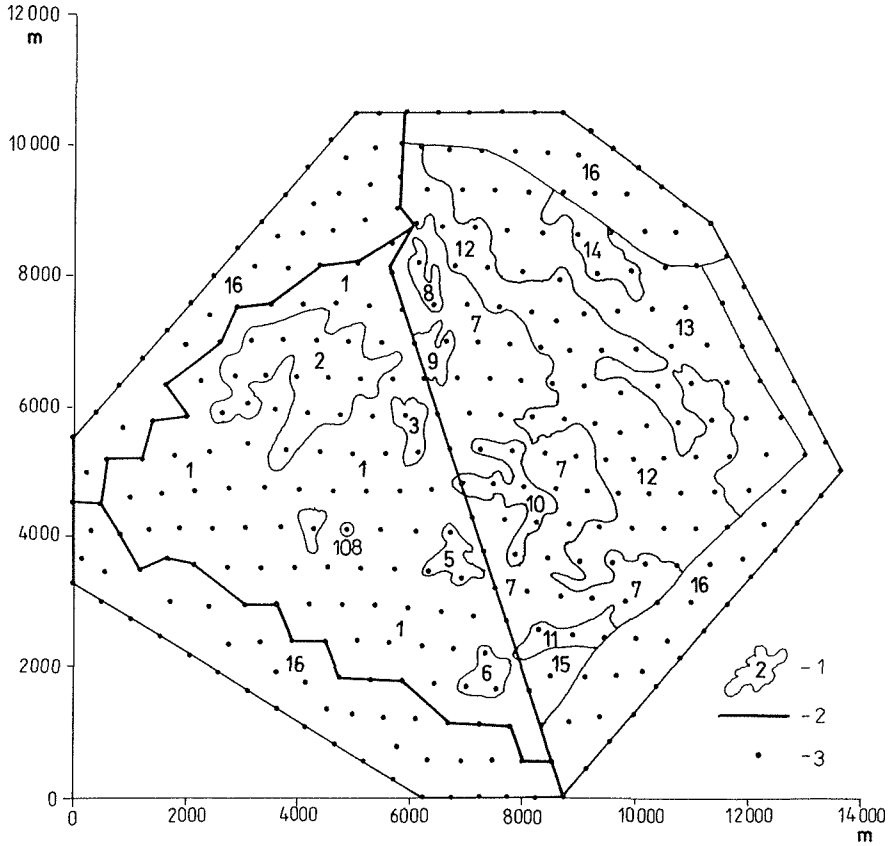

Fig. 3 Division of the model area into subregions; 1—boundaries and number of subregions, 2—canals and rivers, 3—nodal points.

II. *Triangle afforested*—this scenario represents the situation if bush expansion continues and the "Triangle" area becomes overgrown. The surface water levels were assumed to be equal to scenario I.

III. *Damming of Woźnawiejski canal*—it was assumed that hydraulic structures are built (weirs) in the Woźnawiejski canal. This would result in significantly higher water levels in the canal and in the Elk and Jegrznia rivers too. It was assumed that the surface water level of the canal and rivers remain constant throughout the whole growing season (0.5 m below the soil surface).

IV. *Woźnawiejski canal filled up*—it was assumed that the canal was eliminated. For modelling purposes the geological conditions were assumed to be the same as in the adjacent area. The water levels in the Elk and Jegrznia rivers were supposed to be identical to scenario III.

RESULTS

The model results are presented as groundwater hydrographs for the present situation and the scenarios for a nodal point in the centre of the "Triangle" area (Fig. 4). The location of the nodal point is given in Fig. 3. The simulated groundwater level for

the present situation (scenario I) is in most of the nodes in agreement with the measurements.

The negative impact of bush expansion on the groundwater levels (scenarios I and II) is significant. In scenario II groundwater levels are about 25–35 cm lower than in scenario I. Model simulation confirms the on-site observations that in woodland areas the groundwater levels are significantly lower than in the original marshland.

Raising the water levels in the rivers and canals has an insignificant impact on the groundwater levels in the central regions of the "Triangle" area (scenarios I and III). The influence of higher surface water levels on groundwater levels is limited to a narrow zone (200–400 m) directly adjacent to the rivers and canals. Fluctuation and the elevation of the groundwater levels in the central part of the "Triangle" area mainly depend on rainfall and evapotranspiration amounts.

The filling up of the Woźnawiejski canal (scenario IV) causes a pronounced increase in the groundwater level (about 0.5 m) even at a distance of 600–1000 m from the canal. This increase predominantly occurs at the beginning of the growing season. At the end of the growing season the impact of filling up of the canal is smaller. The large evapotranspiration and the drainage by the Elk River cause the decrease of the groundwater levels as in scenario III. Simulations demonstrate that

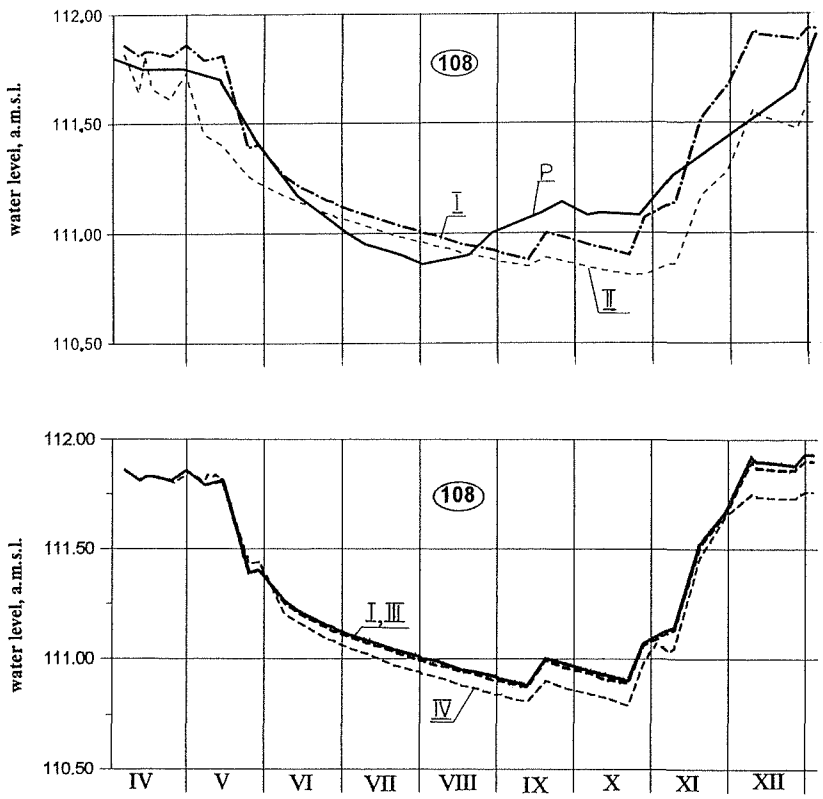

Fig. 4 Observed (P) and simulated groundwater levels for node 108 for the present situation (I) and the scenarios II, III and IV.

both the filling up of the canal and maintaining high surface water levels only improve the moisture conditions in the "Triangle" area to a certain extent.

CONCLUSIONS

Drainage by the Woźnawiejski canal causes the low observed groundwater levels in the River Jegrznia Valley. Moreover the construction of the Rudzki canal results in smaller amounts of water flowing towards the "Triangle" area through the Elk River. There has been a significant reduction of spring flooding in the valley. Before the construction of these canals the valley area was often flooded until the end of June when now already in March or April the water flows from the land via the Woźnawiejski canal to the Biebrza River.

Maintaining high water levels in rivers and canals (for example, by building weirs) does not sufficiently improve the moisture conditions in the valley. The groundwater level increases only in a narrow zone adjacent to the rivers and canals. Groundwater levels in the central part of the "Triangle" area are more controlled by precipitation and evapotranspiration than by surface water levels.

High groundwater levels and associated nature protection can only be achieved after long lasting spring flooding in the valley. Therefore the runoff of surface water via the Woźnawiejski canal should be slowed down or even more water should be directed towards this area. This would require the entire reconstruction of the hydrographic network in the region. For example, hydraulic structures should be built in the Rudzki and Woźnawiejski canals to direct part of the water to the old Elk River bed, and the Jegrznia River should be used to cause spring flooding (Fig. 1). However, these solutions would render severe problems for farmers to use the valley for agricultural purposes. Integrated water management research could try to find a balance between the protection of the natural environment and agricultural needs. This requires further detailed research, including developing a model for simulating groundwater and surface water flow in the entire middle basin of the Biebrza Valley, including all waterways and canals in the region.

REFERENCES

Ernst, L. F. (1978) Drainage of undulating sandy soils with high groundwater tables. *J. Hydrol.* **39**(3/4), 1–50.

Mioduszewski, W. (1994) Gospodarka wodna w Rajgrodzkim Weźle Wodnym (Water management in the Rajgrod water node). *Biul. Inf.* **3/4**, 15–20.

Okruszko, H. (1990) *Wetlands of the Biebrza Valley—Their Value and Future Management*. Polish Academy of Science, Warszawa.

Querner, E. P. (1988) Description of a regional groundwater flow model SIMGRO and some applications. *Agric. Wat. Manage.* **14**, 209–218.

Querner, E. P. (1993) Aquatic weed control within an integrated water management framework. Wageningen Agricultural University. Doctoral Thesis. Also as: *Report 67, DLO Winand Staring Centre, Wageningen, The Netherlands*.

Szuniewicz, J. & Chrzanowski, S. (1995) Sezonowe współczynniki roslinne do wyliczenia ewapotranspiracji lak w rejonie Polski pólnocno-wschodniej (Seasonal crop coefficient for calculating evapotranspiration in meadows in the Polish northeastern region). *Wiad. IMUZ* **14**(2), 73–81.

FRIEND'97 — Regional Hydrology: Concepts and Models for Sustainable Water Resource Management
(Proceedings of the Postojna, Slovenia, Conference, September–October 1997). IAHS Publ. no. 246, 1997.

Hydrological drought analysis in the Hupsel basin using different physically-based models

H. A. J. VAN LANEN
Department of Water Resources, Agricultural University, Nieuwe Kanaal 11, 6709 PA Wageningen, The Netherlands

L. M. TALLAKSEN
Department of Geophysics, University of Oslo, PO Box 1022, Blindern, 0315 Oslo, Norway

L. KAŠPÁREK
T.G. Masaryk Water Research Institute, Podbabská 30, 16062 Prague 6, Czech Republic

E. P. QUERNER
DLO Winand Staring Centre for Integrated Land, Soil and Water Research (SC-DLO), PO Box 125, 6700 AC Wageningen, The Netherlands

Abstract Three different physically-based models were applied to the Hupsel basin to explore their potential to simulate hydrological droughts. The models include water balance models with a simple (BILAN) or a detailed description of the evapotranspiration process (HBVMOR) and a groundwater and surface water flow model (MOGROW). Onset, duration and deficit volume of drought events were derived from observed and simulated hydrographs for the period 1980–1983. Onset of the major drought, i.e. 1982 was well predicted with HBVMOR and MOGROW, whereas BILAN has some limitations because of the monthly time step. Duration and deficit volume of the 1982 drought were underestimated by all models (10–30%). HBVMOR performs best when all droughts events were considered (differences: 15–20%). The strength of the physically-based models lies within their possibility to explore the impact of man-induced changes on droughts, but they still need some improvement if a very accurate simulation of low flows and associated droughts is required.

INTRODUCTION

Droughts seriously affect water resources and may have a detrimental impact on environment and nature reserves. This study focuses on hydrological droughts in terms of streamflow deficits. Hydrological droughts are defined as periods during which the streamflow is below a certain threshold level. Daily and monthly streamflow series were used to assess drought duration and deficit volume derived from both measured and simulated streamflow. In the framework of the FRIEND Low Flow Group two key approaches are being used, i.e. statistical modelling and physical-based modelling, which are complementary. Physically-based models were introduced: (a) to understand the underlying hydrological processes of streamflow generation in a basin more thoroughly, and (b) to simulate streamflow data for hypothetical hydrological conditions, allowing an impact assessment (e.g. change in land use or climate, or groundwater abstraction). Three different physically-based models were applied by the Low Flow Group to simulate streamflow time series and subsequently to analyse droughts. These were the BILAN, HBVMOR and MOGROW, which are using widely different concepts due to different objectives, basin characteristics and data availability. The purpose of this paper is to explore the

reliability of the models by comparing the simulated droughts with each model for the Hupsel basin in The Netherlands. Elsewhere the impact of human activities on hydrological droughts simulated with these models is presented (Querner *et al.*, 1997).

METHODS AND MATERIALS

Hupsel basin

The Hupsel experimental basin (6.5 km^2) is situated in the east of The Netherlands close to the German border (Warmerdam *et al.*, 1982). The basin is relatively flat, its altitude varies between 24 and 33 m a.m.s.l.. The average slope of the area is about 0.8%. Agricultural land use dominates in the basin, i.e. 70% grassland, 21% arable land (mainly maize) and 6% forest. Pleistocene eolian, fluviatile or glacial deposits, which usually consist of sand with some gravel, cover Tertiary, marine clays. This clay is found at a depth of 1 m in the east and dips to the west, where the top is at 8 m below soil surface. The Pleistocene sediments form a small unconfined aquifer with relatively shallow water tables. The aquifer transmissivity varies between 10 to 350 m^2 day^{-1}. The basin has a dense surface water network. The average annual precipitation is about 770 mm. Daily discharge data from 1969 to 1992 were available. The average discharge is 273 mm.

Models

BILAN ("Balance" in Czech) is a water budget model, which was developed to assess the water balance components of a basin in monthly time steps. It is a single-cell model, where the entire basin is represented as one cell (Kašpárek & Krejčová, 1994). The model aims at the evaluation of long time-series. BILAN has been developed both for mountainous and lowland groundwater basins. The hydrological processes, such as evapotranspiration, the generation of surface runoff or baseflow, are represented by a set of empirical relationships. The model uses average basin rainfall, air temperature and relative air humidity as input data, and produces monthly data of basin evapotranspiration and streamflow (total of surface runoff, interflow and baseflow). Furthermore average water storage in the snow cover, the unsaturated and saturated zone are separately simulated. The model is calibrated with an optimization technique. Therefore measured streamflow data series are a prerequisite.

HBVMOR is a single-cell water budget model too, but with a time step ranging from 1 to 24 h depending on the evapotranspiration process to be simulated (Tallaksen, 1993). It was developed for a detailed analysis of basin behaviour and associated streamflow, and it includes a comprehensive description of evapotranspiration. HBVMOR consists of a physically-based evapotranspiration sub-model and a conceptual rainfall–runoff sub-model. It combines the HBV model, which means Swedish Hydrometeorological Institute, and AutoMORecs, where AUTO stands for automatic climate stations in Norway and MORECS for the Meteorological Office (Great Britain) Rainfall and Evaporation Calculation System

(HBVMOR is not an acronym). The model includes algorithms for snow accumulation and melting, interception and transpiration, capillary rise, and runoff generation. Some principles of distributed models are included, such as separate altitude zones for the simulation of snow accumulation and melting (semi-distributed model). The model requires hourly meteorological data to compute potential evapotranspiration and interception. Parameters of the rainfall–runoff sub-model are obtained by calibration against daily time series of observed streamflow. The model output consists of daily data of interception, actual evapotranspiration, streamflow and the water content of the various reservoirs.

MOGROW (Modelling GROundwater flow and flow in surface Water systems) combines the simulation of unsaturated–saturated groundwater flow and water flow in a surface water system (Querner, 1997). It is a regional model; the region or basin is divided in triangular cells for the simulation of subsurface flow. The surface water courses, including special structures (e.g. weirs), are incorporated in a nodal network to simulate surface water flow. The distinction of cells allows the specification of a complex geometry of the basin and surface water system, and spatially varying characteristics, e.g. land use, physical properties of soils, transmissivities of the aquifers and hydraulic resistances of the aquitards. So, regional heterogeneity represented by point data can be incorporated by using different input data for each cell. A water budget rise is used for the root zone, whereas the flow equations are solved for the unsaturated subsoil, the saturated system and the surface water system. In this study a time step of 1 day was used for the specification of the time-dependent input data, such as precipitation and potential evapotranspiration. For the simulation of surface water flow a time step of half an hour was used. The output comprises daily data of actual evapotranspiration, soil moisture storage, groundwater heads in the aquifers for each cell, and streamflow for each river network section. The model is used for a detailed analysis of (sub-)basin behaviour and streamflow generation, usually for a number of years. MOGROW is developed for lowland groundwater basins, and does not account for snow or hillslope hydrology. Although the model can be run without calibrating because parameters have a physical meaning, generally a restricted calibration is carried out using observed groundwater heads and streamflow records.

The parameters of the BILAN model were optimized using data from the Hupsel experimental basin over the years 1976–1983. Average daily discharge was obtained for the BILAN model by dividing simulated monthly mean values by the number of days per month. HBVMOR was calibrated with data from 1980–1981, and validated with data from 1982–1983. Some parameters of the MOGROW model were fine-tuned with data from 1981 (e.g. parameters accounting for preferential flow in the unsaturated zone). A validation was carried out with data from 1982–1985. Then MOGROW was applied to the period 1969–1992. All three models have the years 1980–1983 in common. Measured and simulated time series of streamflow data from these 4 years were used in this study to identify droughts and to compare the models.

Drought identification

The droughts events were obtained from the measured and simulated streamflow

hydrograph by considering flow situations where the daily discharge is below a certain threshold level (low flow spells). The 70th percentile of the flow duration curve ($Q70$) of the measured streamflow was used as a threshold level, i.e. the streamflow which is exceeded in 70% of the days. Each drought event is characterized by its onset, duration (length of the low flow spell) and deficit volume (sum of daily deficits within a low flow spell). Partial duration series (PDS) of drought duration and deficit volume were preferred in this study instead of annual maximum series because of the relatively short common simulated time series available. This implies that all drought events during a year irrespective of the severity are considered. Mutually dependent droughts were pooled into single drought events for the models HBVMOR and MOGROW which use a daily time step by applying the Moving Average (MA) procedure as proposed by Tallaksen *et al.* (1997) for the PDS approach. An averaging time interval of 10 days was used (MA = 10 days). All processing of the streamflow data was done by the software code EXDEV (Řičica & Novický, 1995).

RESULTS

Observed and simulated streamflow

The observed and simulated daily streamflow data were converted to flow duration curves (FDC) to explore the nature of the basin and to evaluate model performance (Fig. 1). Because of the relatively thin aquifer, shallow water tables and dense surface water network, the streamflow of the Hupsel basin has a flashy nature resulting in a steep flow duration curve. In dry years the basin suffers from summer

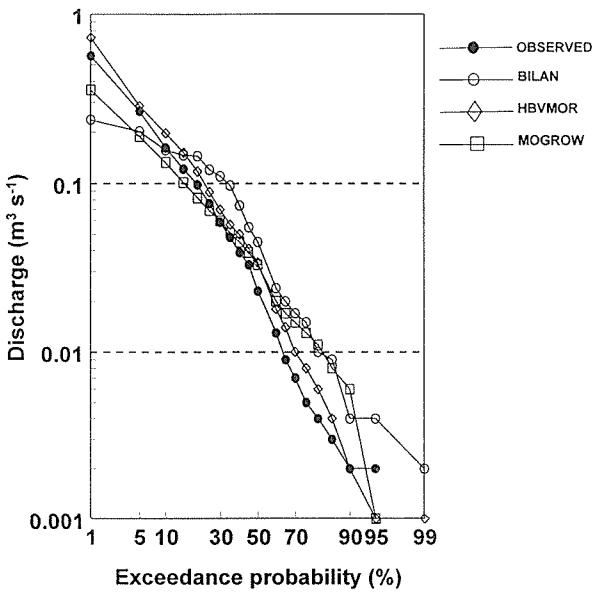

Fig. 1 Flow duration curves derived from measured and simulated data from the Hupsel basin for the period 1980–1983.

droughts, sometimes resulting in a completely drying up of the brook (<5% of the days). The $Q70$ derived from the 1980–1983 dataset equals 0.007 $m^3 s^{-1}$ (indicated as $Q70^{sh}$; sh: period 1980–1983). The flow duration curve was also computed for the observed dataset from 1969–1992, which resulted in a $Q70$ of 0.016 $m^3 s^{-1}$ ($Q70^{lo}$; lo: period 1969–1992). In the low flow range (flow with a probability exceedance of less than 30%), the 1980–1983 period was slightly dryer than the 1969–1992 period. Both $Q70$s were used in the following drought analysis.

The FDCs derived from the simulated hydrographs show that the BILAN model produced a more flat curve than the observed one, which implies an underestimation of the peak flows and an overestimation of the low flows. This is typical for a model using a monthly time step. The deviation between the FDCs from BILAN and the observed data, however, is small. The FDC derived from the HBVMOR model shows a better agreement with the observed one than the FDC based upon the MOGROW simulation. Especially, in the low flow range the MOGROW model simulates slightly higher streamflows than observed. These differences are caused by MOGROW parameters, which were not thoroughly calibrated by comparing measured and simulated streamflow as was done by the optimization procedure of BILAN and HBVMOR.

Simulation of drought characteristics

In the 1980–1983 period 10 drought events were identified based upon the observed hydrograph and the $Q70^{lo}$. The 1982 drought is the most severe one. The probability distributions derived from the 1969–1992 dataset indicate that the 1982 drought has an exceedance probability of about 5% both in terms of duration and deficit volume.

Drought onset The 1982 drought started on 11 July and 16 May for the $Q70^{sh}$ and $Q70^{lo}$ thresholds, respectively (Table 1). The estimated onset with MOGROW deviates 12 and 2 days, and with HBVMOR the difference equals 2 and 15 days. BILAN estimates the onset well for the $Q70$sh threshold (difference of 10 days). However, in case of the $Q70^{lo}$, BILAN was unable to predict the onset adequately (difference >1 month). The monthly time step as used in BILAN prevents an accurate prediction of the onset.

Drought duration The 1982 drought lasted 127 and 186 days for the $Q70^{sh}$ and $Q70^{lo}$ threshold level, respectively (Fig. 2(a) and (b)). All three models underestimate these durations. Dependent on the selected threshold level, the underestimation using

Table 1 Onset of the 1982 drought derived from measured data and simulated streamflow data for two threshold values.

Threshold $Q70$ ($m^3 s^{-1}$)	Onset: Measured	Models: BILAN	HBVMOR	MOGROW
0.007 ($Q70^{sh}$)	11 July 1982	1 July 1982	13 July 1982	29 June 1982
0.016 ($Q70^{lo}$)	16 May 1982	1 July 1982	31 May 1982	14 May 1982

BILAN equals 3 and 34%. For HBVMOR and MOGROW these deviations are 25 and 30%, and 21 and 11%.

The estimation of the duration for all drought events improves when using the $Q70^{lo}$ threshold level. The HBVMOR model shows the best agreement with the drought durations derived from the observed hydrograph. BILAN and MOGROW are unable to adequately predict the durations of the events 2, 3, 4 and 5 for the $Q70^{sh}$ (Fig. 2(a)) and the minor drought events 5 and 6 for the $Q70^{lo}$ (Fig. 2(b)). The average percentage of the absolute difference between the observed and the HBVMOR simulated drought durations for the three most severe droughts deviates 20% as the $Q70^{sh}$ threshold level is used. This percentage equals 19% for the four most severe droughts in case of using the $Q70^{lo}$ threshold. The average percentages

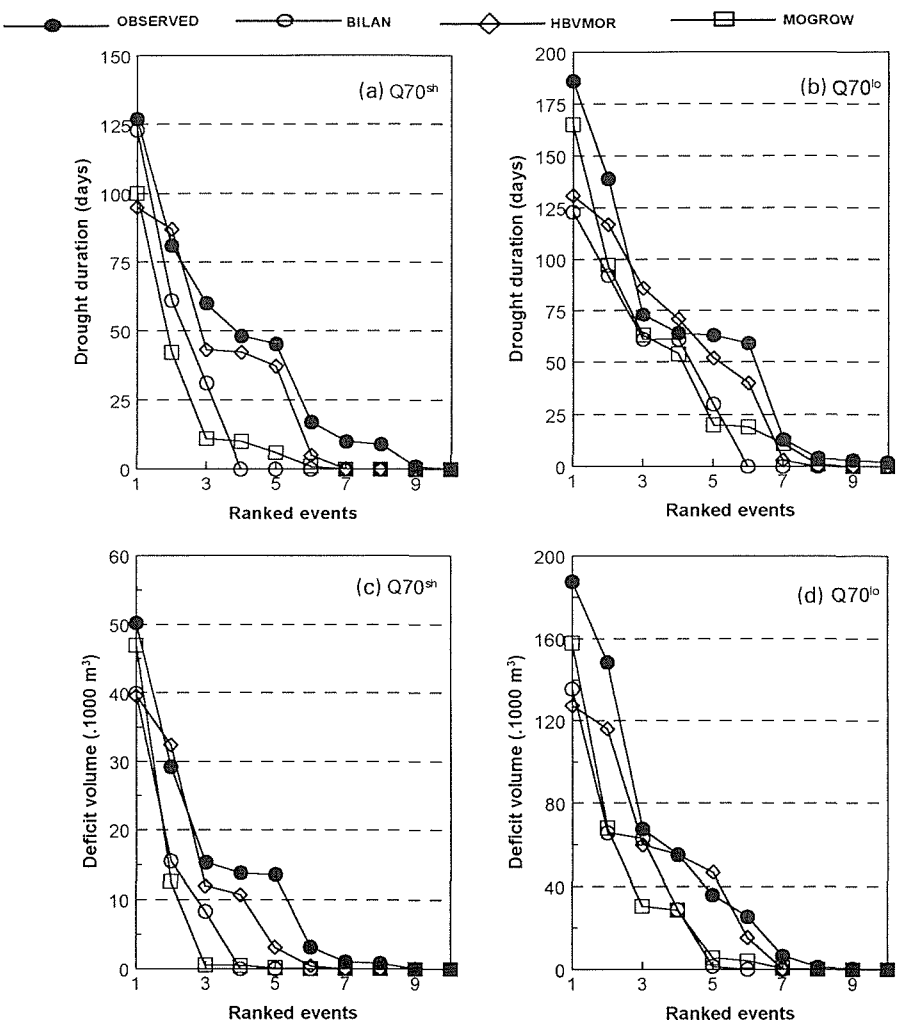

Fig. 2 Drought durations and deficit volumes for two threshold values ($Q70^{sh}$ and $Q70^{lo}$) derived from measured and simulated data from the Hupsel basin for the period 1980–1983.

for BILAN (25 and 22%) and MOGROW (50 and 18%) are higher, especially for the $Q70^{sh}$ threshold.

Deficit volumes The deficit volume of the 1982 drought was 50 241 and 187 583 m^3 for the $Q70^{sh}$ and $Q70^{lo}$ threshold levels, respectively (Fig. 2(c) and (d)). Similar to the duration, all three models underestimate these deficit volumes. BILAN underestimates the deficit volumes of the 1982 drought by 20 and 28% dependent on the threshold level. For HBVMOR and MOGROW the underestimations are 21 and 32%, and 6 and 16%.

In general HBVMOR estimates deficit volumes best. Using $Q70^{sh}$ as threshold level the average percentage of the absolute difference of the first three drought events (Fig. 2(c)) equals 18%. For the $Q70^{lo}$ this percentage of the first four drought events (Fig. 2(d)) is 16%. For BILAN and MOGROW these percentages are substantially higher, i.e. 38 and 34%, and 53 and 43%, respectively.

CONCLUSIONS

The three physically-based models included in the study can reasonably well simulate the streamflow of the Hupsel basin in the period 1980–1983. In the low flow range the HBVMOR model shows the best agreement with the observed streamflow. All three models identify the major drought in the relatively short time series, i.e. the 1982 drought. The onset of the drought is well predicted with the more comprehensive models HBVMOR and MOGROW, which use a daily time step. The prediction of the onset with the BILAN model is not very accurate in some cases because of the monthly time step. The duration and the deficit volume of the 1982 drought is underestimated by all models. Differences up to about 30% prevail between droughts derived from simulated and observed hydrographs dependent on the model and the selected threshold level. When all drought events are considered, the drought duration and deficit volume simulated with HBVMOR show the best fit with the observed series. The average difference between observed and HBVMOR simulated droughts in terms of duration and volumes equals 15–20%. For BILAN and MOGROW the average differences are between 20 and 50%. HBVMOR performs better than BILAN because of the smaller time step. Furthermore the required parameter optimization of rainfall–runoff models (BILAN and HBVMOR) usually results in a better estimation of the streamflow than a more sophisticated model which simulates groundwater flow and surface water flow without a comprehensive calibration of model parameters (MOGROW). Performance of all models is better in case of a higher threshold level, i.e. the $Q70$ of the period 1969–1992 gives better results than the $Q70$ for the period 1980–1983. The drought assessment with BILAN would improve when droughts would be derived from average monthly observed streamflow instead from daily flows as in this study.

Irrespective of the complexity of some of the models, the reliability of simulating details of all droughts is limited.

Acknowledgements The authors thank Mr J. Kole (Wageningen Agricultural

University) for providing the data from the Hupsel basin. The MSc student W. J. Werkman performed the MOGROW simulations. As members of the Low Flow Group of the FRIEND project, we appreciate the contribution of the group through the initiation of the present drought study and the valuable discussions.

REFERENCES

Kašpárek, L. & Krejčová, K. (1994) BILAN water balance model. User's guide and background information. *Report T.G. Masaryk Water Research Institute, Prague.*

Querner, E. P. (1997) Description and application of the combined surface and groundwater flow model MOGROW. *J. Hydrol.* (in press).

Querner, E. P., Tallaksen, L. M., Kašpárek, L. & Lanen, H. A. J. van (1997). Impact of land-use, climate change and groundwater abstraction on streamflow droughts, using physically-based models. In: *FRIEND'97—Regional Hydrology: Concepts and Models for Sustainable Water Resource Management* (Proc. Postojna Conference, September–October 1997) (this volume).

Řičica, J. & Novický, O. (1995) Experiments with deficit volumes (EXDEV). Description of the program. *Report Czech Hydrometeorological Institute, Prague*, April 1995.

Tallaksen, L. M. (1993) Modelling land use change effects on low flows. In: *Flow Regimes from International Experimental and Network Data FRIEND*: vol., I *Hydrological Studies* (ed. by A. Gustard), 56–58. Institute of Hydrology, Wallingford, UK.

Tallaksen, L. M., Madsen, H. & Clausen, B. (1997) On the definition and modelling of streamflow drought duration and deficit volume. *Hydrol. Sci. J.* **42**(1), 15–33.

Warmerdam, P. M. M., Stricker, J. N. M. & Kole, J. W. (1982) Current research and data collection in the experimental catchment Hupselse Beek, in The Netherlands. In: *Hydrological Research Basins and their Use in Water Resources Planning* (Proc. Bern Symp., September 1982), vol. 1, 209–216.

FRIEND'97 — Regional Hydrology: Concepts and Models for Sustainable Water Resource Management
(Proceedings of the Postojna, Slovenia, Conference, September–October 1997). IAHS Publ. no. 246, 1997.

Application of a physically-based model to identify factors causing hydrological drought in western and central European basins

LADISLAV KAŠPÁREK
T. G. Masaryk Water Research Institute, Podbabská 30, 160-62 Prague 6, Czech Republic

OLDŘICH NOVICKÝ
HYDROART, Čenětická 3126/1, 149-00 Prague 4, Czech Republic

Abstract Several approaches can be adopted for the purposes of defining and assessing hydrological drought. In the approach used in this study, the drought is a period during which the streamflow is below a certain truncation level (threshold discharge). Each drought event is characterized by its duration, severity (runoff deficit below the threshold) and onset. The causes of hydrological drought may vary under different climatic, hydrological or geological conditions. BILAN, a physically-based model simulating water balance components in a monthly step, has been applied for a number of basins in central and western Europe with the intention of identifying the main factors influencing the occurrence of severe droughts. In this paper, the results of the analysis are illustrated for five basins which have been selected to demonstrate drought causing factors in different hydrogeological and climatic conditions. The results of the analysis suggest that summer and winter drought events occurring in the studied basins are of two main types. The runoff deficit in summer occurs when potential evapotranspiration approaches or exceeds precipitation during a certain preceding period, while causal factors of the winter drought are the air temperature continuously below 0°C and temporarily low groundwater storage. The most severe drought events are caused by a combination of a dry summer and autumn with a cold winter.

INTRODUCTION

Hydrological drought is generally caused by an unfavourable combination of meteorological factors, mainly precipitation and temperature. Severity and other characteristics of drought are naturally associated with a measure used for its determination. In this study, the measure is represented by the threshold discharge (Zelenhasič & Salvai, 1987) selected as the 70 percentile monthly flow expressed in mm of runoff (R_{70}). Five basins with different hydrological and meteorological conditions illustrate the causal factors of hydrological drought. Two of the basins, the Haugland and Knappom, are situated in Norway, the Gulp and Hupselse Beek were selected from The Netherlands, and lastly, the Orlice basin is located in the Czech Republic. Basic information on individual basins and some results are summarized in Table 1.

For each basin, the parameters of the BILAN model were first calibrated and used for subsequent simulation of monthly series of water balance components. A

Table 1 Basic characteristics and results for the selected basins.

Variable	Basin name and country:				
	Haugland Norway	Knappom Norway	Gulp The Netherlands	Hupselse Beek The Netherlands	Orlice Czech Republic
Period of observation	1960–1993	1960–1991	1978–1993	1976–1983	1961–1990
Precipitation (mm year^{-1})	1820	791	764	740	1120
Runoff (mm year^{-1})	1543	442	300	255	648
Air temperature (°C)	7.4	1.9	9.7	-	5.6
Runoff R_{70} (mm month^{-1})	62.7 (48.8)	12.0 (32.5)	18.4 (73.6)	4.0 (19.0)	28.5 (52.8)
Groundwater storage (mm)	43.3 (2.8)	28.7 (6.5)	194 (64.7)	12.2 (4.8)	69.2 (10.7)
Mean runoff deficit (mm)	64.2 (4.2)	12.0 (2.7)	12.0 (4.0)	5.2 (2.0)	17.1(2.6)
Max. runoff deficit (mm)	202.2 (13.1)	39.0 (8.8)	47.4 (15.8)	22.7 (8.9)	81.7 (12.6)
Mean drought duration (months)	2.3	2.5	3.1	2.4	2.4
Maximum drought duration (months)	7	5	8	7	8

Note: Values in parentheses are in % of monthly mean runoff for R_{70} and in % of annual runoff for the other variables.

basic analysis of drought events, focused on their occurrence, duration and severity, was performed on both observed and simulated runoff series using the EXDEV computer program.

METHODS

Two main tools were used for the purposes of the study, the BILAN model simulating water balance components in a monthly step (Kašpárek & Krejčová, 1994) and EXDEV computer code (Řičica & Novický, 1995), developed for determination and analysis of low flow periods within the activities of the FRIEND Low Flow Group.

The BILAN model, which was developed in the T. G. Masaryk Water Research

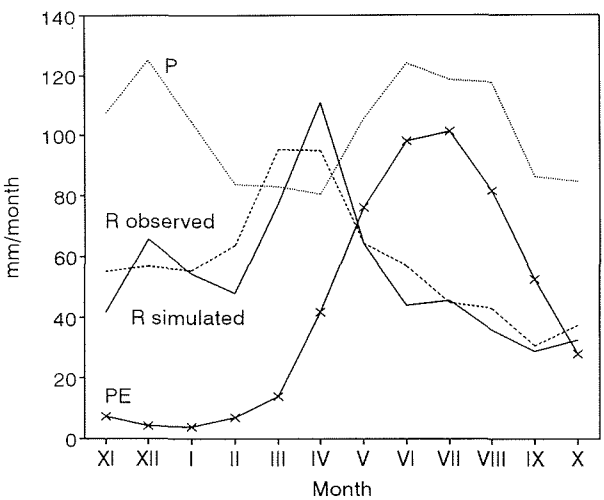

Fig. 1 Water balance components (R = runoff, P = precipitation, PE = potential evapotranspiration) of the Orlice basin.

Institute, Prague, describes the basic principles of water balance on the ground, in the zone of aeration and in the groundwater. The entry data of the model are monthly series of basin precipitation, the air temperature and relative air humidity. A runoff series at the outlet from the basin is used for model calibration. The model generates monthly series of basin potential evapotranspiration, actual evaporation, percolation to the zone of aeration, groundwater recharge and components of water storage in the snow cover, zone of aeration (soil) and groundwater aquifer. The total runoff consists of three components, namely direct runoff, interflow and baseflow.

The EXDEV program selects drought events from flow series and performs statistical analysis including the application of several probability distributions to the annual or partial series. Program options include calculation and selection of the threshold discharge, linear interpolation techniques for filling in missing data, calculation of moving average series and its subsequent analysis and graphical interpretation of results.

RESULTS

To assess the series simulated by the BILAN model, diagrams were drawn showing mean monthly precipitation, observed runoff, simulated runoff, potential evapotranspiration, basin evaporation and individual water storage components. Examples are given in Figs 1 and 2 presenting water balance components for the Orlice basin. Figure 3 shows a good fit between cumulative frequency curves of runoff deficit, derived for the Knappom basin from observed and simulated runoff series.

Knowledge of the water balance components and physical processes governing the water cycle allows us to identify the main factors causing hydrological drought in a given basin. Therefore, the drought causing factors in the selected basins were studied by an analysis of monthly series of runoff, precipitation, potential

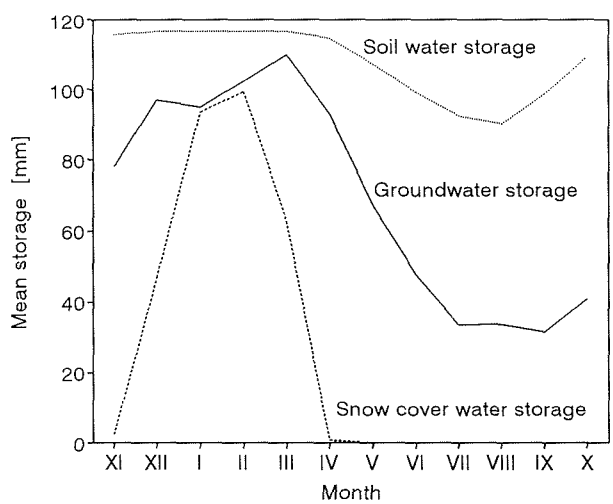

Fig. 2 Components of water storage simulated by BILAN model for the Orlice basin.

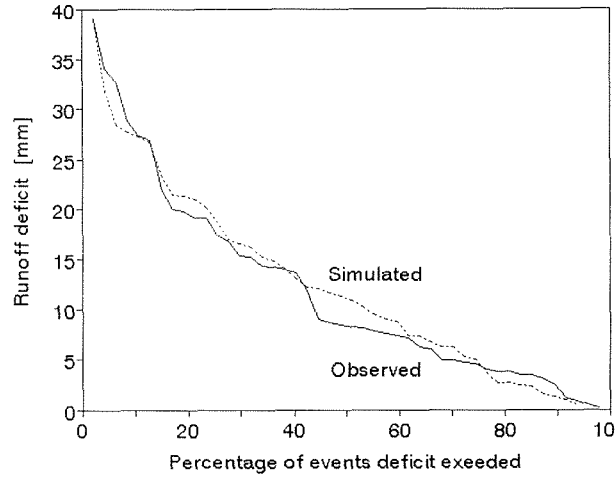

Fig. 3 Cumulative frequency curves of runoff deficit derived for the Knappom basin from observed and simulated runoff series.

evapotranspiration, groundwater storage, snow water storage and air temperature. The following are the results of the analysis for individual basins.

The *Haugland basin* (area 135 km^2) is situated on the west coast of Norway. Mean annual basin precipitation of 1820 mm is high, but the basin storage capacity, compared to the precipitation, is low. The mean groundwater storage represents only 2.8% of the total annual runoff. The snow water storage, accumulated during the winter season, is also normally low due to relatively high annual mean temperature (7.4°C) and coastal type of climate. Therefore, the runoff is closely related to precipitation in the given month and the annual runoff pattern approaches that of precipitation reduced by potential evapotranspiration (see Fig. 4). The evapotranspiration is lower than 20% compared to the precipitation and thus its inter-annual

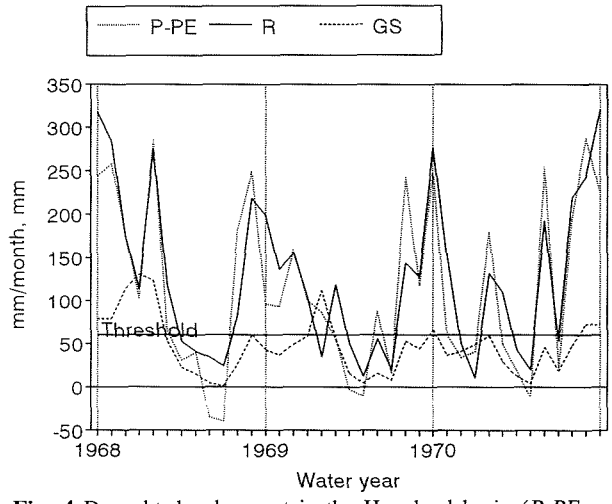

Fig. 4 Drought development in the Haugland basin (*P-PE* = precipitation reduced by potential evapotranspiration, *R* = runoff, *GS* = groundwater storage).

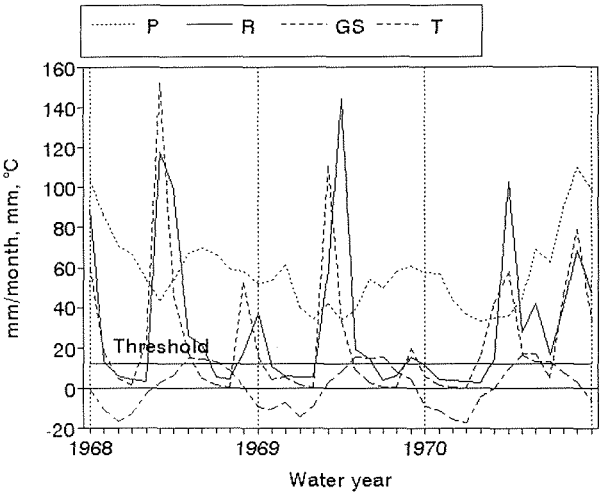

Fig. 5 Drought development in the Knappom basin (P = four-month moving average of precipitation, R = runoff, GS = groundwater storage, T = air temperature).

variability cannot significantly affect the runoff.

Under such conditions, the occurrence of drought is entirely caused by deep precipitation deficit lasting for several months. The runoff deficit begins in the same month as that of precipitation and ends in the first month when the precipitation approaches or exceeds its long-term mean.

The *Knappom basin* (area 1625 km^2), selected also from Norway, is located in the inland part of the country, and has substantially lower precipitation (790 mm) compared to the Haugland basin. Another significant difference is that, due to low annual mean temperature (2°C), the snow is normally accumulated in the basin during the period between November and March. The snow melts during March to May, feeding streamflow which rises (see Fig. 5). The spring rising limb of the hydrograph is followed by a decrease in streamflow during summer, but the low flow period is normally terminated by higher precipitation during the autumn season.

Another drought occurs in winter and the runoff deficit normally exceeds that in summer. However, the precipitation during summer and autumn plays an important role in runoff evolution in winter because, between November and April, the runoff is not fed from precipitation but is formed by outflow from groundwater storage. When precipitation during summer and autumn is low, the increase in runoff normally occurring in autumn is also low and severe drought lasting until April may occur.

Therefore, precipitation deficit occurring during summer and particularly during autumn, in combination with the air temperature below zero in the winter season, are the main factors causing hydrological drought in this type of basin.

The annual precipitation of the *Hupselse Beek basin* (area 6.5 km^2) in The Netherlands (Warmerdam *et al.*, 1982) is 740 mm and snow precipitation is rare. Potential evapotranspiration significantly affects water balance components, its annual value representing about 66% of the annual precipitation. Hydrogeological conditions of the basin allow a significant portion of water accumulated in the basin to be available for evaporation. The mean groundwater storage, estimated from the

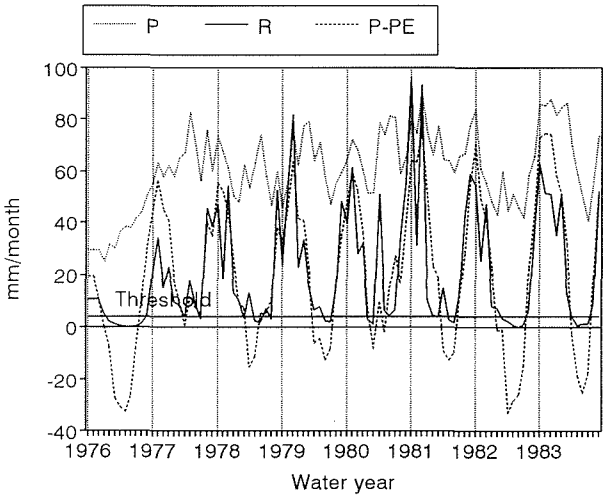

Fig. 6 Drought development in the Hupselse Beek basin (P = four-month moving average of precipitation, R = runoff, P-PE = four-month moving average of precipitation reduced by potential evapotranspiration).

simulations, is only 4% of the annual runoff. This is relevant to the fact that in a relatively short record there is a period when streamflow ceases. Under such conditions, hydrological drought can be caused by low precipitation occurring for several months during which the potential evapotranspiration is high (see Fig. 6).

The *Gulp basin* (area 46 km^2) is also situated in The Netherlands and it differs from the other basins mainly by its high groundwater storage capacity, because the basin is formed by Cretaceous aquifer with highly developed groundwater circulation. The groundwater storage reaches several hundred millimetres and its mean value is about 25% of the annual precipitation of 765 mm. This is reflected in

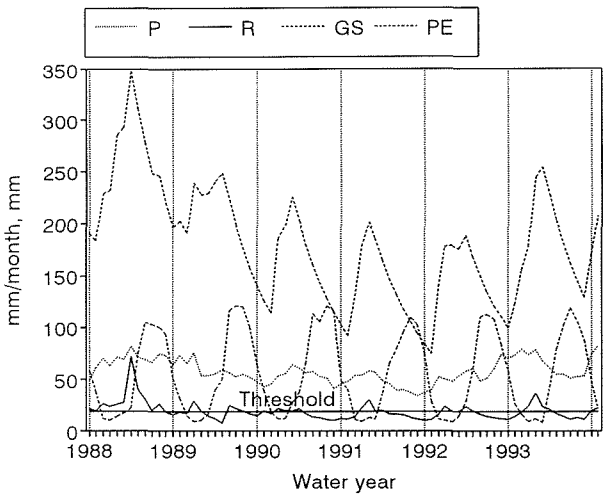

Fig. 7 Drought development in the Gulp basin (P = six-month moving average of precipitation, R = runoff, GS = groundwater storage, PE = potential evapotranspiration).

relatively low seasonal and inter-annual variability of flow.

This can be demonstrated by the 1990 drought (see Fig. 7), which occurred after a period of low precipitation lasting for the two preceding years. The drought continued in 1991 and 1992, and was not even terminated by an increase in precipitation at the end of 1992.

Therefore, in basins with high water storage capacity, a precipitation deficit lasting for several months does not cause a hydrological drought. The drought, in spite of having the attributes of a seasonal event, is a result of long-term, frequently multi-year, precipitation deficit.

The *Orlice basin*, covering an area of 155.1 km^2, is situated in the Czech Republic. The mean annual precipitation is 1220 mm and groundwater storage capacity is significant but not extremely high. The mean groundwater storage equals 10.6% of the annual precipitation and the annual potential evapotranspiration is about 42% compared to the precipitation. A drought can occur either during summer and autumn, being caused by precipitation deficit (the difference between precipitation and potential evapotranspiration is close to zero or even negative), or during the winter season when the air temperature is below zero.

Therefore, the most severe drought can occur when a dry summer and autumn are followed by a winter season with the temperature continuously below 0°C (see Fig. 8). The winter snow precipitation does not contribute to the streamflow and the drought can continue until snowmelt occurs in spring. The total duration of the drought can reach eight months. The causing factors of the drought are similar to those of the Knappom basin in Norway, however, the frequency of winter drought is lower, which is attributable to higher air temperature.

CONCLUSIONS

The results of the analysis suggest that summer and winter drought events are two

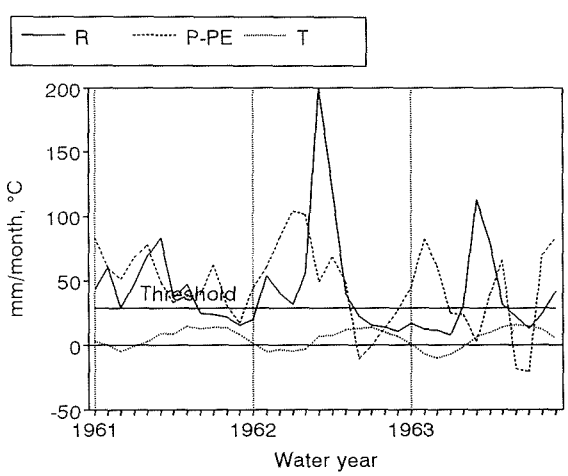

Fig. 8 Drought development in the Orlice basin (R = runoff, P-PE = two-month moving average of precipitation reduced by potential evapotranspiration, T = air temperature).

main types of drought occurring in basins in central and western Europe. Of the basins selected for the analysis, the summer drought occurs in the Haugland, Hupselse Beek and Gulp basins, while both types of drought can occur in the Knappom and Orlice basins.

The annual pattern of the air temperature is a causal factor for determining the type of drought. The effect of the temperature is reflected either in a rise in potential evapotranspiration, which contributes to the drought in summer, or in snow precipitation and unfavourable runoff conditions in winter. Winter drought, which prevails in northern Europe, does not occur in warmer regions where the air temperature is not normally below zero during the winter season. The most severe drought events are caused by a combination of dry summer and autumn with cold winter.

The causal factors of the summer and winter droughts are different. The runoff deficit in summer can occur when potential evapotranspiration approaches or exceeds precipitation during a certain preceding period whose duration, necessary to cause the drought, depends on the capacity of the basin to retain water. The causal factors of the winter drought are the air temperature continuously below 0°C and temporarily low groundwater storage.

In any case, baseflow is a substantial component of streamflow during the drought and thus the occurrence, duration and severity of drought depend on groundwater storage in the basin. The groundwater storage depends on hydrogeological conditions and on the ratio between precipitation and potential evapotranspiration. Dynamic groundwater storage is formed under conditions of favourable combination of water storage capacity of the aquifer, basin precipitation and evaporation.

Basins having sufficient water storage capacity, particularly of groundwater, are not so sensitive to short-term variability in precipitation and thus a severe drought occurs as a result of a multi-year precipitation deficit.

The results of the study demonstrate that spatial variability in the occurrence, duration and severity of drought in Europe is affected by both meteorological conditions prevailing in a given geographical area and also changing locally, e.g. with altitude, and hydrogeological conditions having high diversity also at a local scale.

REFERENCES

Kašpárek, L. & Krejčová, K. (1994) *BILAN Water Balance Model. User's Guide and Background Information*. T. G. Masaryk Water Research Institute, Prague.

Řičica, J. & Novický, O. (1995) *Experiments with Deficit Volumes (EXDEV). Description of the Program*. Czech Hydrometeorological Institute, Prague, April 1995.

Warmerdam, P. M. M., Stricker, J. N. M. & Kole, J. W. (1982) Current research and data collection in the experimental catchment Hupselse Beek, in The Netherlands. In: *Hydrological Research Basins and their Use in Water Resources Planning* (Proc. Bern Symp., September 1982), vol. 1, 209–216.

Zelenhasič, E. & Salvai, A. (1987) A method of streamflow drought analysis. *Wat. Resour. Res.* **23**(1), 156–168.

FRIEND'97 — Regional Hydrology: Concepts and Models for Sustainable Water Resource Management
(Proceedings of the Postojna, Slovenia, Conference, September–October 1997). IAHS Publ. no. 246, 1997.

Analysis of the sensitivity of water balance components to hydrogeological conditions and climatic change

H. R. NASSERY & J. BUCHTELE
Institute of Hydrogeology, Engineering Geology and Applied Geophysics, Faculty of Sciences, Charles University, Albertov 6, 128 43 Prague 2, Czech Republic

Abstract The impact of basin hydrogeological, morphological conditions and climatic changes on streamflow and water balance components was simulated in two hydrogeologically different basins using two deterministic water balance models SAC-SMA and BROOK90. The resemblance between the sub-basins of each basin is reflected in the magnitude of the calibrated parameter values. The differences between the two basins mainly concern parameters which represent the hydrogeological conditions. The BROOK90 model adequately simulates evapotranspiration components, but it cannot satisfactorily simulate streamflow in sub-basins where baseflow plays a major role in streamflow generation. The SAC-SMA model is sufficiently able to simulate streamflow under different hydrogeological conditions.

INTRODUCTION

Water balance components and streamflow generation in a basin are influenced by a multitude of factors which may be broadly classified into climatic, physiographic, geomorphologic and hydrogeologic factors. The climatic factors comprise intensity, duration, type and areal distribution of precipitation and evapotranspiration components. The physiographic, geomorphologic and hydrogeologic factors include the geometry of the basin, land use, vegetation cover, soil characteristics and physical characteristics of geological formations.

In the past many attempts have been made to assess the role of geology, geomorphology and land use on the runoff process. While some attempts found no conclusive relationships between basin characteristics or the values of model parameters and the runoff process (e.g. Braun & Renner, 1992), some other attempts stated the important role of basin characteristics and presented approaches or regional equations to evaluate the runoff process (e.g. Kobold & Brilly, 1994). The objective of this study is to explore the impact of basin characteristics, such as vegetation cover and hydrogeology, on evapotranspiration and runoff generation using two different water balance models. In this context the SAC-SMA and BROOK90 models which were applied to the Police and Spulka basins, were recently tested at different scales in central Europe (e.g. Buchtele *et al.*, 1997).

STUDY AREAS AND AVAILABLE DATA

Two river basins in the Czech Republic were chosen; one in a sedimentary region (Police River basin) located about 140 km northeast of Prague near the Polish border and one in a crystalline region (Spulka River basin) located about 120 km southwest

of Prague near the Austrian border. Basins with different geology were chosen to obtain an indication of the difference in performance of the selected hydrological models (BROOK90 and SAC-SMA) under different morphoclimatic and hydrogeologic conditions. The Spulka River basin has been subdivided into six sub-basins and the Police River basin into 14 sub-basins. The Spulka River basin covers an area of about 104 km^2 with a total length of about 13 km and an average width of 8 km. The bedrock geology of this basin is dominated by igneous and metamorphic rocks. The Czech part of Police River valley is approximately 20 km long with an average width of 8 km. The area is about 230 km^2. The outcropping rocks in the Police basin are mostly sedimentary rocks (mostly marlstones) (Table 1).

Time series of precipitation, air temperature and discharge were available to simulate the rainfall–runoff process. For the Spulka sub-basins a record of 10 years (1983–1993) was used, and for the Police sub-basins records of 5–30 years.

Table 1 Basic characteristics of some sub-basins.

Basin	Sub-basin	Area (km^2)	Forest area (%)	Annual runoff (mm year^{-1})	Geological bedrock
Police	Maršov	94	30	352	Marlstone
-	Hronov	248	30	348	-
Spulka	Zdikovsky	0.98	100	285	Migmatite
-	Albrechtec	1.61	98	333	-
-	Bohumilice	104	39	317	-

METHOD OF STUDY

The relationship between the rainfall–runoff process, basin characteristics, and the parameters of a water balance model was investigated by using the SACramento Soil Moisture Accounting (SAC-SMA) and BROOK90 models. These models have been applied to the sub-basins. Both models have been presented briefly elsewhere (Buchtele *et al.*, 1996) and detailed information can be found in Burnash *et al.* (1973) and Federer (1995).

For calibration of the SAC-SMA model, initial estimates of the following three group of parameters have been made and simultaneously analysed in an iterative procedure:

(a) storages of several soil moisture zones LZFPM, LZFSM, LZTWM, UZTWM and UZFWM, which are the main hydrogeological parameters of the model (Table 2),
(b) precipitation correction factor including snowfall and rainfall,
(c) evapotranspiration demand for individual months.

The initial estimates were optimized and the SAC-SMA model was verified by using the "differential split sample test" method. For the BROOK90 model the default parameters values recommended by Federer (1995), were first chosen to simulate streamflow for each sub-basin of the Spulka basin. Subsequently the model parameter's values were changed. The calibration was done by curve-fitting and achieving the minimum mean bias error.

The models with the parameters optimized against historical streamflow time series, were first applied with different parameter sets to find out the relationship between basin characteristics and model parameters. Subsequently the historical input data were adapted by increasing the temperature and scaling the precipitation (multiplying rainfall data by a constant factor) to define climate change scenarios. The simulations with the adapted data, using the same optimized parameter values, were then compared with the historical runoff data to obtain an estimate of the potential changes. The selected scenarios were: changes in daily precipitation by +10%, -10%, +20%, -20%, +40% and -40% and an increase in daily temperature by 1°C, 2°C and 4°C for the SAC-SMA model in the sub-basins Hronov and Zdikovsky (Table 1). The scenarios +15%, -15%, +5%, -5% and +20%, -20%, +10%, -10% (precipitation) and +3°C, -3°C, +1°C, -1°C (temperature) were selected for the BROOK90 model in the Bohumilice and Zdikovsky sub-basins.

RESULTS

The optimized values of parameters

The optimal parameter's values of SAC-SMA model for some sub-basins are summarized in Table 2. The analysis was carried out for all model parameters. The hydrogeological and geomorphological resemblance between the sub-basins of either the Police and Spulka basin is reflected in the magnitude of the obtained parameter values. The differences in values between the two basins mainly concern parameters which represent the hydrogeologic and snow characteristics. More details about the comparison of the two basins have been presented by Nassery (1997).

Table 2 The major parameters of the SAC-SMA model and statistical indexes for some sub-basins.

Acronym	Description	Sub-basin:				
		Hronov	Maršov	Zdikovsky	Albrechtec	Bohumilice
	Major snow parameters					
SCF	Snow Correction Factor	1.15	1.15	1.05	1.0	1.16
MFMAX	Maximum Melting Factor (mm/°C/6 h)	1.65	1.80	0.75	0.75	1.35
MFMIN	Minimum Melting Factor (mm/°C/6 h)	0.40	1.00	0.2	0.3	0.32
SI	Areal water equivalent (mm)	75	75	75	80	85
	Major hydrogeological parameter					
UZTWM	Upper Zone Tension Water Maximum (mm)	125	100	105	69	67
UZFWM	Upper Zone Free Water Maximum (mm)	15	15	17	12	15
LZTWM	Lower Zone Tension Water Maximum (mm)	300	275	185	185	170
LZFPM	Lower Zone Free Primary Maximum (mm)	850	480	350	350	350
LZFSM	Lower Zone Free Supplement Maximum (mm)	115	120	85	85	85
UZK	Upper Zone Coefficient	0.3	0.4	0.28	0.2	0.37
LZPK	Lower Zone Primary Coefficient	0.0011	0.0011	0.0023	0.0002	0.0018
LZSK	Lower Zone Supplement. Coefficient	0.11	0.10	0.068	0.057	0.056
ZPERC	(Max.) PERcolation rate Coefficient	75	75	100	105	65.5
REXP	EXPonent of percolation shape curve	3.96	3.5	1.65	1.4	2.15
	Major statistical index					
R	Correlation coefficient	0.8459	0.7965	0.8172	0.8160	0.8772
$\lvert\Delta\rvert$	Average absolute error of monthly flow (%)	19.43	24.02	15.80	16.73	15.21
RMS	Monthly root mean square error (%)	31.35	32.37	23.71	23.42	21.17

Generally the calibrated parameter values for sub-basins with significant groundwater storage, such as the Police sub-basins are larger than for others, e.g. Spulka sub-basins. For instance, this applies to the values of the parameters UZTWM, LZTWM, LZFSM, LZFPM and REXP. Hydrogeologic and geomorphologic conditions of both basins cause these differences (Table 2).

Analysis of runoff components

Runoff was simulated by the SAC-SMA model which has six components: PRM (primary or long term baseflow), SUP (supplementary or seasonal baseflow), INT (interflow), SUR (surface flow), DIR (direct runoff from temporarily impervious area) and IMP (runoff from permanently impervious area). Runoff was also simulated by the BROOK90 model which has four components: GWFL (groundwater flow), DSFL (downslope flow), BYFL (bypass flow) and SRFL (surface flow). Figure 1 illustrates changes in the seasonal distribution of the recorded and simulated daily flows and its runoff components as simulated by the SAC-SMA model for the Hronov and Zdikovsky sub-basins. It shows the usual annual cycle of flows for all analysed sub-basins, high discharges in spring and low flows during autumn.

The two baseflow components (PRM and SUP), which are controlled by groundwater storages, mainly determine runoff generation. The primary baseflow (PRM) is relatively constant throughout the year, whereas the supplementary baseflow (SUP) occurs mostly during periods with high streamflow. The short-term runoff components (IMP, DIR, SUR and INT) are nearly negligible compared to the baseflow. The SAC-SMA model indicates that the maximum contribution of surface and direct runoff components to the total runoff usually occurs in March and April when snowmelt causes peak runoff.

Figure 2 presents a comparison of the streamflow simulated by SAC-SMA and BROOK90 models and the observed streamflow. The SAC-SMA model simulates streamflow better than the BROOK90 model. The BROOK90 model uses a simple linear storage concept for the simulation of baseflow and therefore, it cannot adequately simulate streamflow if baseflow plays a major role, such as in the Zdikovsky sub-basin. The SAC-SMA model is adequately able to simulate streamflow under different hydrogeological conditions.

Evapotranspiration

The SAC-SMA model simulates potential and actual evapotranspiration, while the BROOK90 model is more sophisticated and can simulate five components of the total evapotranspiration, which are transpiration (TRAN), evaporation from intercepted rain (IRVP), evaporation from intercepted snow (ISVP), soil evaporation (SLVP) and snow evaporation (SNVP). The simulated evapotranspiration components by the BROOK90 model for the Spulka sub-basins are given in Table 3. The total evapotranspiration of the Bohumilice sub-basin is larger than of the Zdikovsky sub-basin because of the lower elevation of the Bohumilice sub-basin. The components TRAN, ISVP, IRVP and SNVP in the Zdikovsky sub-basin are larger than in the

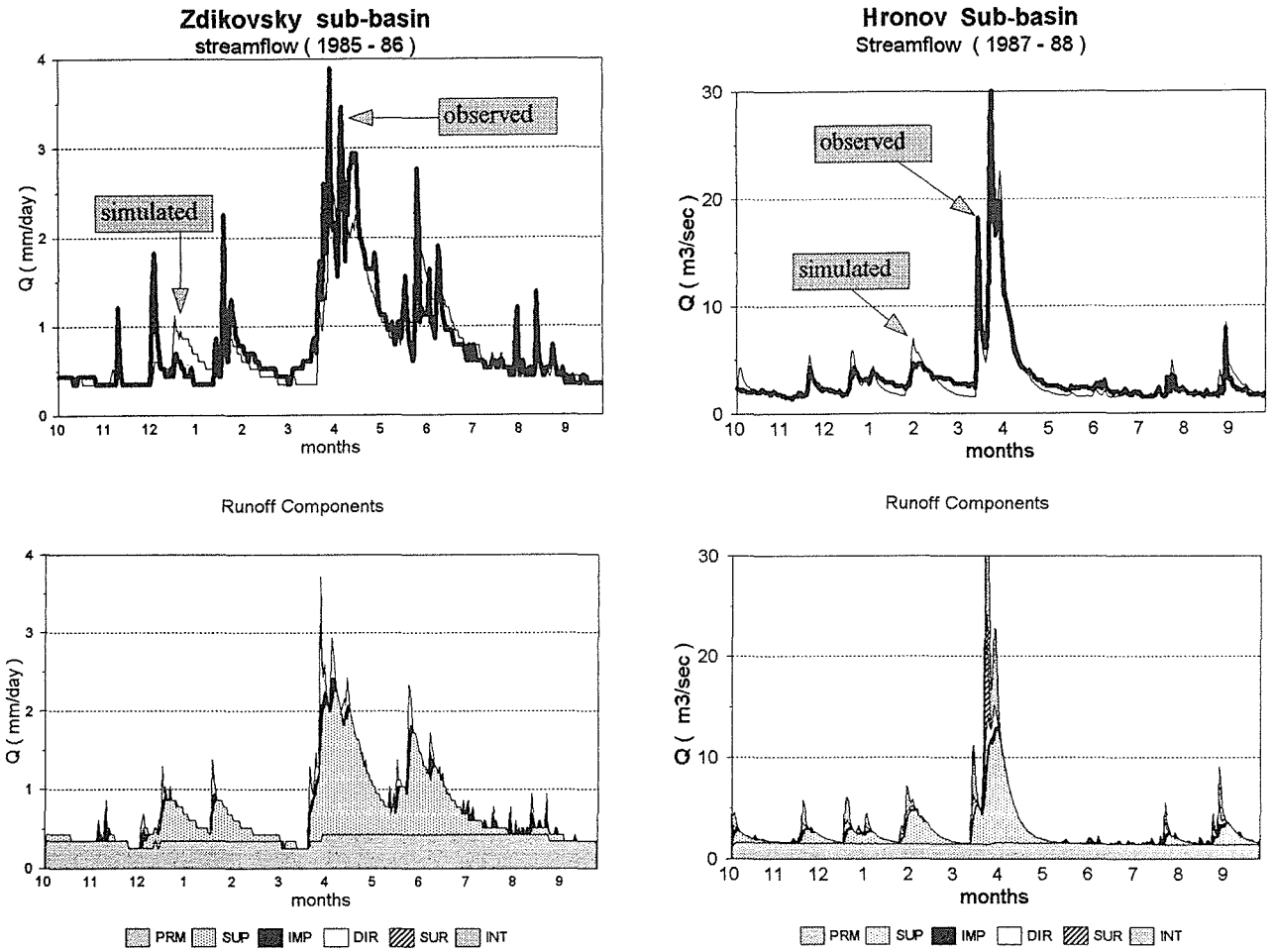

Fig. 1 Observed and simulated streamflow and its runoff components simulated by the SAC-SMA model in the Zdikovsky and Hronov sub-basins.

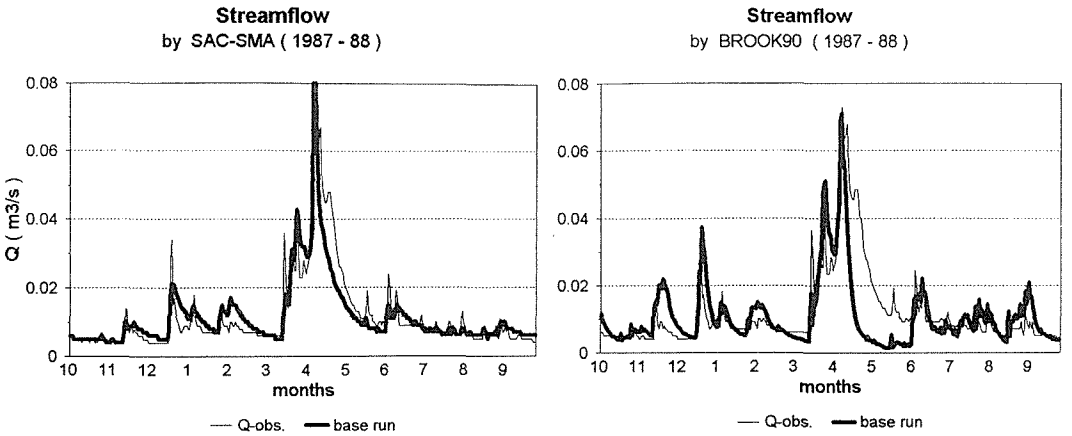

Fig. 2 Observed and simulated streamflow by the SAC-SMA and BROOK90 models in the Zdikovsky sub-basin.

Bohumilice sub-basin, which can be explained by the full forest cover in the Zdikovsky sub-basin (Table 1). The smallest total evapotranspiration occurs in the

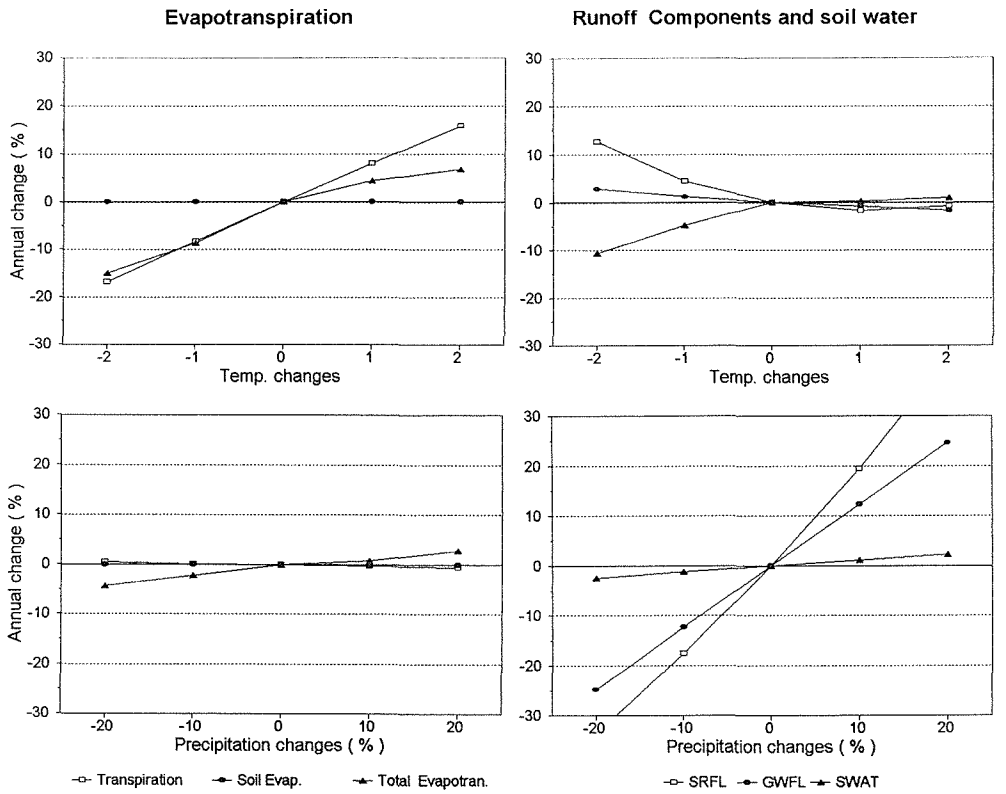

Fig. 3 Sensitivity of soil water, runoff and evapotranspiration components to precipitation and air temperature changes in the Zdikovsky sub-basin as simulated by the BROOK90 model.

Table 3 Evapotranspiration components as a percentage of total evapotranspiration in the Spulka sub-basins over the period 1984–1988 as simulated by the BROOK90 model.

Sub-basin	TRAN (%)	IRVP (%)	ISVP (%)	SLVP (%)	SNVP (%)	TOTAL (mm)
Albrechtec	79.7	7.9	1	0	11.4	184.5
Zdikovsky	67.7	10.6	1.8	0	19.9	232.4
Bohumilice	46.7	5.8	0.03	43.4	4	319.8

Albrechtec sub-basin, which is the highest area of the Spulka basin. The largest total evapotranspiration occurs in the Bohumilice sub-basin, which has the lowest mean elevation in the Spulka basin. Total evapotranspiration varies from one basin to another as affected by land use and physiographic conditions, including the altitude.

Basins hydrological responses to climatic changes

The hydrological responses of the Police and Spulka basins were simulated for several hypothetical climate change scenarios. The results were compared with the

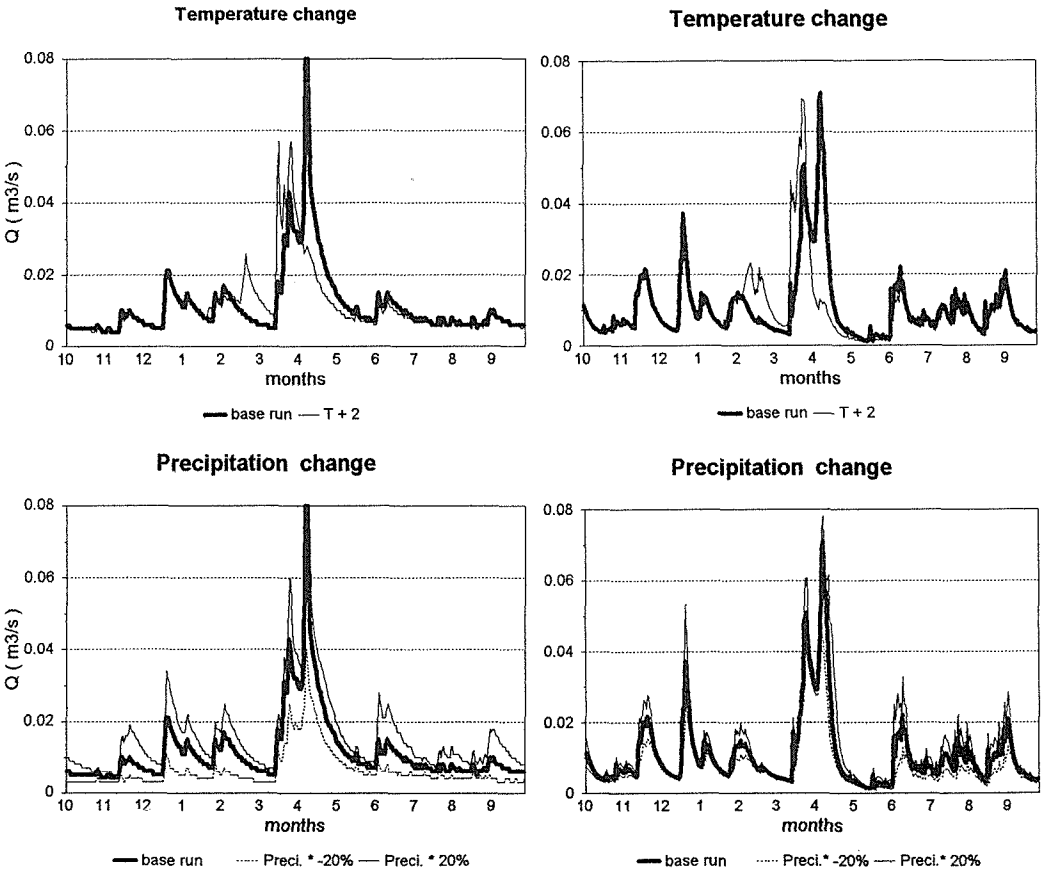

Fig. 4 Effects of temperature and precipitation changes simulated by the models SAC-SMA (left column) and BROOK90 (right column) in the Zdikovsky sub-basin over the period 1987–1988.

reference or base case (present climate conditions). Figure 3 illustrates the sensitivity of soil water, evapotranspiration, and runoff components to temperature and precipitation changes in the Zdikovsky sub-basin. The evapotranspiration components appear more sensitive to temperature changes than to precipitation changes, whereas the runoff components are more sensitive to precipitation changes. The transpiration shows a negative correlation to precipitation. This behaviour is related to rain interception. Increase of precipitation results into higher rain interception and consequently reduces transpiration.

Sensitivity of streamflow to temperature and precipitation changes as simulated by BROOK90 and SAC-SMA models is presented in Fig. 4. The SAC-SMA model shows a relatively large sensitivity to precipitation changes, while the BROOK90 model only shows a low sensitivity.

CONCLUSIONS

Two deterministic hydrological models have been applied to different basins to find out the impact of both basin conditions and climatic changes on water balance components and runoff generation. Most soil water and groundwater storage parameters of the sedimentary area (Police sub-basins) are larger than of the crystalline area (Spulka sub-basins) which correspond with the hydrogeologic and geomorphologic conditions. The total evapotranspiration varies and is affected by land use and physiographic condition, including the altitude. The evapotranspiration components are more sensitive to temperature changes than to precipitation changes, whereas the runoff components are more sensitive to precipitation changes.

REFERENCES

Braun, L. N. & Renner, C. B. (1992) Application of a conceptual runoff model in different physiographic regions of Switzerland. *Hydrol. Sci. J.* **37**(3), 217–231.

Buchtele, J., Elias, V., Tesar, M. & Herrmann, A. (1996) Runoff components simulated by rainfall–runoff models. *Hydrol. Sci. J.* **41**(1), 49–60.

Buchtele, J, Nassery, H. R., Herrmann, A. & Di Nunzio, F. (1997) Areal variability of parameters of rainfall–runoff process. In: *Int. Conf. on Regionalization in Hydrology* (10–14 March 1997, Braunschweig, Germany) (in press).

Burnash, R. J. C., Ferrel, R. L. & McGuire, R. A. (1973) *A General Streamflow Simulation System Conceptual Modelling for Digital Computers*. Report by the Joint Federal State River Forecasting Center, Sacramento, California.

Federer, C. A. (1995) *A Simulation Model for Evaporation, Soil Water, and Streamflow*, Version 3.1. USDA Forest Service, Durham, New Hampshire, USA.

Kobold, M. & Brilly, M. (1994) Low flow discharge analysis in Slovenia. In: *FRIEND: Flow Regimes from International Experimental and Network Data* (ed. by P. Seuna, A. Gustard, N. W. Arnell & G. A. Cole) (Proc. Braunschweig Symp., October 1993), 119–131. IAHS Publ. no. 221.

Nassery, H. R. (1997) Simulation of water balance components in hydrogeological distinct areas using SAC-SMA and BROOK90 models. PhD thesis submitted to Dept Hydrogeology, Faculty of Sciences, Charles University, Prague, Czech Republic.

6 Hydrological Extremes: *Rainfall Frequency*

FRIEND'97 — Regional Hydrology: Concepts and Models for Sustainable Water Resource Management
(Proceedings of the Postojna, Slovenia, Conference, September–October 1997). IAHS Publ. no. 246, 1997.

Towards a regionalization of extreme rainfall events in the Mediterranean area

MARIA-CARMEN LLASAT & ROBERTO RODRIGUEZ
Department of Astronomy and Meteorology, University of Barcelona, Avda Diagonal 647, 08028 Barcelona, Spain

Abstract The paper shows a first pluviometric characterization of the European Mediterranean area, mainly focused on the high rainfall events. First, a time series analysis of monthly data from 16 stations for the period 1940–1990 has been performed in order to compare the different trends and anomalies of rainfall. Secondly, an analysis of the distribution of events with more than 200 mm in 24 h has been made on the basis of the information gathered from 410 stations for the period 1940–1990. The results obtained for each area have been compared.

INTRODUCTION

One of the main purposes of the AMHY/FRIEND project and the FLOODAWARE project is the regionalization of different hydrological processes. This paper attempts a first regionalization of rainfall in the European Mediterranean countries, paying special attention to the extreme rainfall events.

The Mediterranean region is characterized by a great number of geographical and topographical complexities, including many separate gulfs, seas, straits and channels. The combination of the effects produced by them makes weather forecasting in the Mediterranean region exceedingly difficult. There are some general reports available related to meteorology in the Mediterranean area (Meteorological Office, 1962; Reiter, 1975; Brody & Nestor, 1980), others are devoted to the analysis of the "Mediterranean air mass" (Jansà, 1959, 1966), the cyclogenesis process (Jansà *et al.*, 1994; Radinovic, 1987), the influence of the orography on rainfall (Desurosne & Oberlin, 1991; Petrovic & Radic, 1994) or high rainfalls (Capaldo *et al.*, 1980; Ferrari *et al.*, 1990; Llasat & Puigcerver, 1992; Ramis *et al.*, 1994; Brilly *et al.*, 1995; Llasat *et al.*, 1996; Siccardi, 1996). All these publications and studies, together with the knowledge of the mesoscale processes etc., are useful for the regionalization of extreme rainfall events from a conceptual point of view, i.e. in order to understand and explain their physical and statistical features. The present contribution is far from attaining such an ambitious objective. The aim of this paper is to show the first results obtained after the application of a specific temporal and spatial analysis over different zones of the Mediterranean area.

DATA

It is not easy to obtain rainfall data for a medium or a long period of time. Sometimes a great part of the data is missing or not available. In order to do a good regionalization of rainfall it would be necessary to have data of each "homogeneous"

sub-region to be able to compare their pluviometric behaviour and the results obtained after the application of the same methodologies. Unfortunately, this information usually is not available. This paper used the database developed by the AMHY/FRIEND project and data gathered by different members of this project.

Two types of data have been used. The first consists of daily or monthly rainfall series (continuous data series). The second represents high rainfall events, and is usually discontinuous and heterogeneous information. Table 1 shows the monthly series which have been selected because they have data for more than 30 years. Data in Table 2 have been used for the analysis of high rainfalls, together with those stations of Table 1 also having daily rainfall records.

METHODOLOGY

Temporal analysis

The first part of this study deals with a temporal analysis of the monthly precipitation in the stations shown in Table 1. The common period for all the stations (1940–1990) was analysed. The purpose was to compare trends and anomalies of rainfall and the main pluviometric features at the different stations during this lapse of time. This type of analysis is most useful when considering regional features, because it allows determination of the differences and analogies in rainfall distribution from a spatial and temporal point of view.

Firstly, the 12 monthly average values and the yearly average value of the rainfall have been calculated, and the statistical properties of the series are also considered. Secondly, the data have been standardized month by month with respect

Table 1 Stations with monthly rainfall series. Asterisk denotes stations also having daily data.

Station	Period	Latitude	Longitude	Altitude (a.m.s.l.)	Country
Athens Obs*.	1871–1990	37°59′N	23°4 4′E	107 m	Greece
Thessalonica*	1930–1990	40°38′N	22°56′E	40 m	Greece
Lugoj*	1930–1993	45°41′N	21°55′E	-	Romania
Timisoara*	1922–1993	45°45′N	21°13′E	-	Romania
Caransebes*	1921–1993	45°25′N	22°13′E	-	Romania
Barcelona*	1850–1991	41°22′N	8°00′E		Spain
Murcia	1942–1993	37°57′N	1°47′W	75 m	Spain
Sevilla	1923–1993	37°21′N	6°00′W	14 m	Spain
Ciudad Real	1866–1991	38°59′N	1°13′W	629 m	Spain
Perpignan	1850–1970	42°36′N	2°54′E	-	France
Milan	1850–1983	45°30′N	9°00′E	100 m	Italy
Roma	1782–1983	41°54′N	12°29′E	-	Italy
Belvedere Sp.*	1922–1987	39°12′N	4°26′E	330 m	Italy
S. Severina*	1922–1987	39°08′N	4°28′E	326 m	Italy
Rocca di Neto*	1922–1987	39°11′N	4°33′E	183 m	Italy
Crotone*	1922–1987	39°05′N	4°41′E	6 m	Italy

to the monthly average at each station, in order to eliminate the specific characteristics of the annual position (Rodriguez *et al.*, 1994). The persistence of spells of precipitation which are either considerably above or considerably below the average, will be apparent in periods of positive and of negative anomalies that either extend through a period of successive months or prevail at the same season or part of a season but over a number of years.

It is possible to represent and identify these periods using monthly isothets on an annual-monthly graph. Anomaly is defined here as a value which falls outside the interval $x_{aver} - \sigma$, $x_{aver} + \sigma$ (standard deviation of normal distribution; the interval comprises 68% of values). The two fields of positive and negative anomalies were analysed for each station and, afterwards, the common anomalies of all stations have been obtained. In the anomalies analysis it is important to distinguish the season of the year in which they are produced. The worst case, for example, is when the negative anomaly is produced during the rainfall season (Rodriguez & Llasat, 1996).

Thirdly, the moving average analysis with a window of constant length $L = 10$ years and cadence $\tau = 1$ year has been performed. As in the previous case, standardized values were used. This technique makes it possible to analyse the different trends (long term variations) of the series.

High rainfall events

Taking into account that the information was very heterogeneous, this analysis focused on the distribution of events with daily rainfall totals exceeding 200 mm.

RESULTS

Temporal analysis

The monthly distribution shows that the spring (mainly June) is the rainiest season for the Romanian stations, while the other stations have at this time of the year the minimum. Barcelona, Murcia, Roma, Milan and Perpignan have the maximum monthly values in October; Thessalonica and the stations of Calabria, in November and Sevilla, Ciudad Real and Athens, in December.

Table 2 Regions having series of annual maximum daily rainfall with the number of stations in each region. Number of years between 1940 and 1990 in which 200 mm within 24 h have been exceeded and the most affected season.

Country	Region/basin	Num. stat.	Period	$N > 200$ mm	Season max.
Portugal	Portugal	4	1940–1992	1	Winter
France	Herault	221	1883–1991	22	Autumn
Spain	Catalonia	66	1917–1990	28	Autumn
Italy	Calabria/Basilicata	100	1920–1987	39	Autumn
Portugal	Portugal	4	1940–1992	1	Winter
Yugoslavia	Montenegro	1	1923–1984	34	Autumn
Romania	Romania	9	1934–1980	5	Summer
Moldovian Rep.	Moldovian Rep.	5	1889–1994	0	-

With the exception of the Romanian and Calabrian stations there is no significant correlation between the monthly values of the different stations (values of r between 0.1 and 0.3). In the case of the Romanian stations, the correlation between Lugoj and Timisoara has $r = 0.84$ and between Timisoara and Caransebes the value of r is 0.65. The Calabrian stations have a correlation between them of over 0.8.

The analysis of the positive anomalies or rainiest periods shows some common features. Although the correlation between the stations is low, sometimes they are affected by the same meteorological anomalies. Thessalonica and Athens have a similar distribution of anomalies. Sevilla and Ciudad Real have the same main features, with an important concentration of positive anomalies in the decade 1960–1970. Caransebes also shows this maximum, although in this station the positive anomalies last until 1981 and the monthly distribution was not the same. Lugoj and

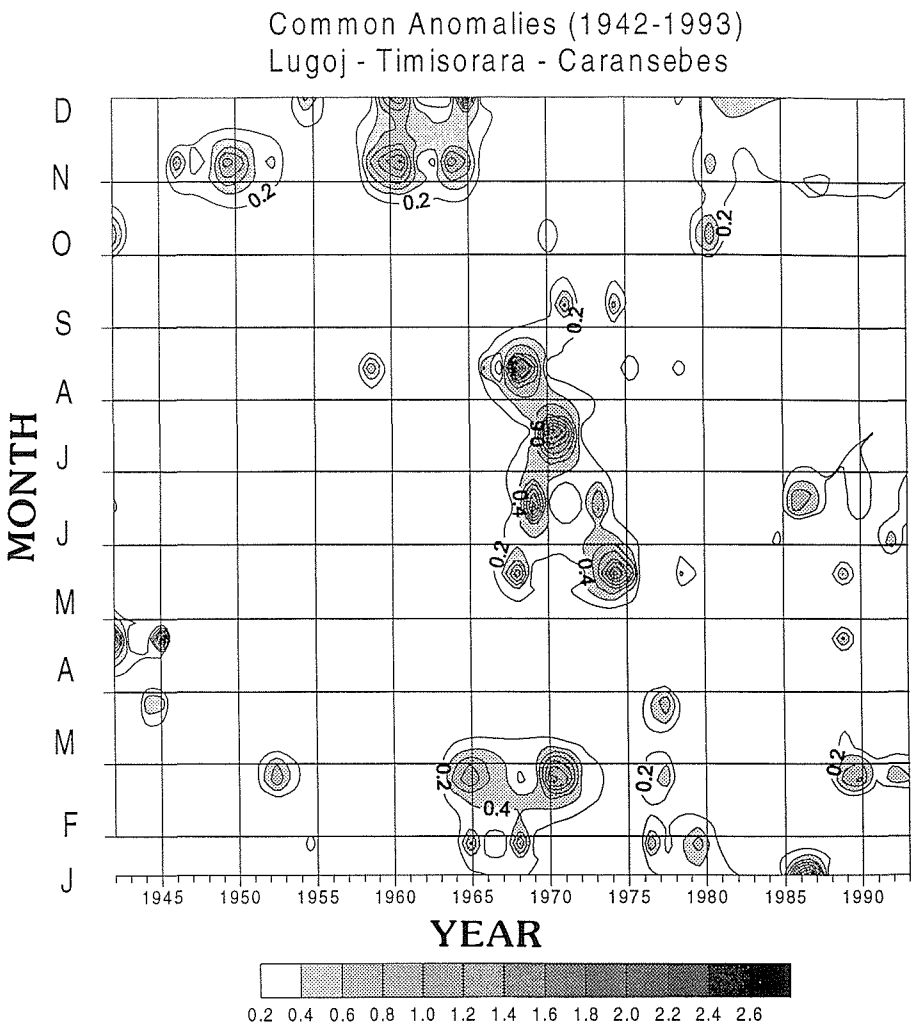

Fig. 1 Common positive pluviometric anomalies of Lugoj, Timisoara and Caransebes (Romania). Isothets are plotted in intervals of 0.2.

Timisoara have a similar behaviour, showing an important cluster of anomalies between 1965 and 1977, mainly during the first part of the year (Fig. 1). Barcelona, Perpignan and Roma have some common features although the behaviour is not so similar as between the other stations. For example, the period 1950–1960 has one concentration of positive anomalies in spring, and another common one during the second part of the year between 1975–1980. This latter anomaly is observed too in Milan. The stations of Murcia and Calabria do not show any common feature with the other stations, with the exception of the most general anomalies. This is the case of the winter months of 1940–1941 or the autumn months of 1960–1965 that can be considered the rainiest in all the European Mediterranean region.

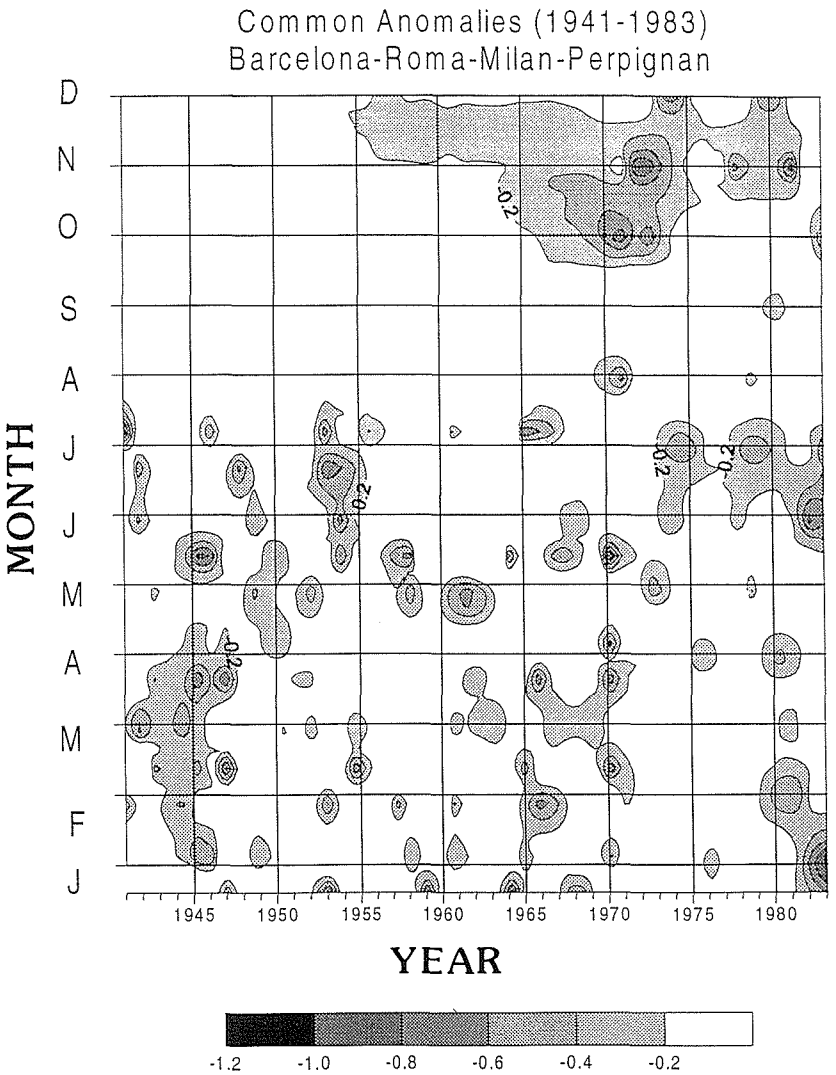

Fig. 2 Common negative pluviometric anomalies of Barcelona (Spain), Perpignan (France), Milan and Roma (Italy).

The negative anomalies or dry periods show more dispersion than in the previous case. Sevilla, Ciudad Real, Barcelona, Roma, Milan show a dry period from 1980 until the end of the series and other one during some autumn months of 1965–1975 (Fig. 2). In the other stations only the general anomalies are common. This is the case of the years between 1945 and 1950 that can be considered the driest period in the last 50 years in all the European Mediterranean countries.

The running means show an important oscillation in all the stations throughout the period analysed. It would be possible to suggest a period of between 20 and 30 years, although to confirm this we would need a spectral analysis. Figure 3 shows that Barcelona and Sevilla have a similar evolution, with a maximum between 1960 and 1962, but the other two Spanish stations have different trends. The same is observed in Thessalonica and Athens or Lugoj and Timisoara. It is interesting that Calabria, Roma, Perpignan and Ciudad Real have a similar evolution too, mainly between 1940 and 1965. Murcia reveals a different evolution from the others. However, the most important years are those with common features. This is the case of the interval 1977–1982 with a strong "trough" (minimum) at all the stations except Roma. The years 1956–1958 represent a secondary dry period. In the case of the "peaks" (maximum), the dispersion is bigger. It shows that the driest periods affect simultaneously all the European Mediterranean area, whereas the rainiest periods can depend more on the local conditions. However, it is possible to see a "peak" between 1960 and 1964 and another one between 1946 and 1954, with the exception of Sevilla.

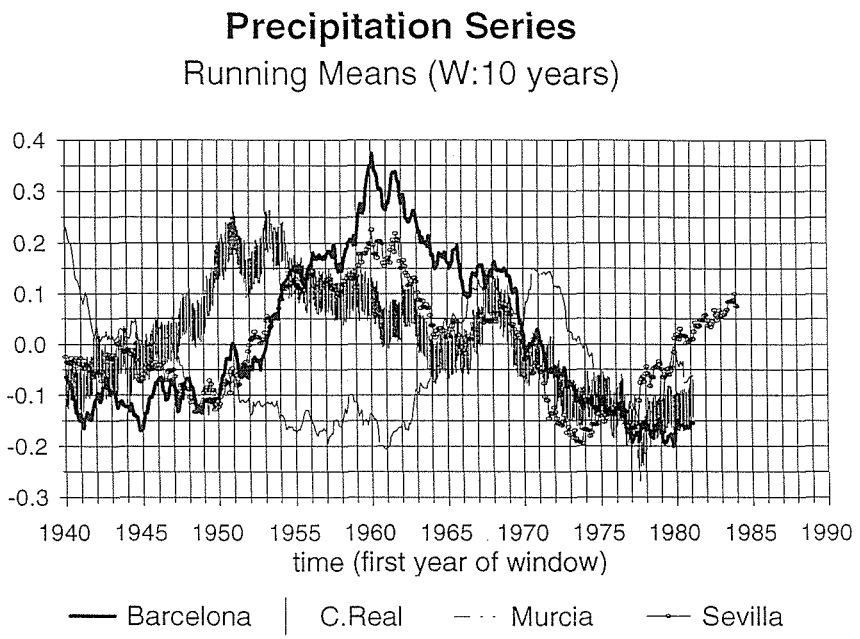

Fig. 3 Moving average of monthly rainfall for Perpignan, Milan, Roma and Rocca di Neto. Window length L = 10 years and cadence τ = 1 year. Y-axis values are standarized.

Distribution of events with total daily precipitation over 200 mm

The Montenegro region is one of the regions most affected by heavy rainfalls. In this region, 74% of the years register at least one event with daily precipitation above 200 mm. In the period 1940–1990, more than eighty days with a rainfall total over 200 mm have been recorded, occurring between September and April, the most affected months being October, November and December (50% of all the days).

In the region of the Herault, when we consider the whole series 1883–1991, the maximum daily rainfall has exceeded 200 mm only in 29 years (27% of the total number of years). However, it is possible that some old data might have been in error. If we consider only the period 1940–1990, the percentage increases to 43%. The month with the highest probability is September (31% of the events).

In Catalonia, the number of years with 200 mm or more between 1917 and 1990 has been 34, i.e. 46% of the total length of record (51% for the period 1940–1990). Forty one per cent of the events took place in October and 79% concentrated between September and November.

Calabria and Basilicato have recorded 54 years with maximum daily rainfall above 200 mm, i.e. 79% of the years (76% for the period 1940–1990). In this case, the seasonal evolution shows autumn as that most affected by extreme events.

The Moldavian Republic has recorded only one event since the beginning of its series, in August 1889. The same feature is observed in Portugal, where only the station of Faro Aeroporto recorded over 200 mm in December 1975. In Romania five events have been recorded, three of them in June.

There is a small number of common events with a maximum above 200 mm. The most important ones happened in October 1987, November 1988, October 1990 and November 1982, and affected the Herault and Catalonia regions. In September 1992 an event started in Catalonia and affected France and Italy. The meteorological conditions and the main hydrological consequences of these events have been analysed in Ramis *et al.* (1994, 1995) and Bolla *et al.* (1996), among others.

CONCLUSIONS

The paper proposes a methodology for regionalization of heavy rainfalls and presents the results of its application to different regions. The correlation between the monthly series shows that only Lugoj and Timisoara and the four stations of Calabria are well correlated. The analysis of the rainfall anomalies allows us to find common features between Sevilla and Ciudad Real, and Barcelona, Perpignan, Roma and Milan. The moving average technique points out common dry or rainy periods for all the stations. This is the case of years 1956–1958 and 1977–1982 with a minimum of rainfall, or 1946–1954 and 1960–1964, with a maximum. Sometimes the rainfall recorded at stations which are far from each other shows more similar features than rainfall records at stations nearer to each other. Finally, it is clear that events with more than 200 mm within 24 h happened only in the western and central Mediterranean regions, usually in autumn and never in spring. On the contrary, high rainfalls in the Eastern region are produced usually in spring.

Acknowledgements Our thanks to E. Ferrari (Italy), V. Vukmirovic (Yugoslavia), I. Desurosne (France), A. Gavrilita (Moldavian Republic), M. Lacerda (Portugal), L. Fugaciu (Romania) and L. Quintas (Spain) for the data provided. Our particular thanks to P. Breil for the AMHY/FRIEND data and to the Instituto Nacional de Meteorología for the Spanish data. This study has been supported by the Environment Project FLOODAWARE (ENV4-CT96-0293) and the CICYT project AMB95-0671-CO2.

REFERENCES

Bolla, R., Boni, G., La Barbera, P., Lanza, L., Marchese, M. & Zappatore, S. (1996) The tracking and prediction of high intensity rainstorms. *Remote Sensing Rev.* **14**, 151–183.

Brilly, M., Rakovec, J., Vidmar, A., Garantini, M., Cegnar, T., Divjak, M., Gorisek, M. & Mikox, M. (1995) Weather radar and storm and flood hazards. Slovenian contribution (unpublished report) CEC-PECO Project CIPDCT925090.

Brody, L. R. & Nestor, M. J. R. (1980) *Regional Forecasting Aids For the Mediterranean Basin (Handbook for Forecasters in the Mediterranean*, part 2). Tech. Report TR 80–10, Department of the Navy, Washington, DC.

Capaldo, M., Conte, M., Finizio, C. & Todisco, G. (1980) A detailed analysis of severe storms in the central Mediterranean: the case of Trapani flood. *Rivista di Meteorologia Aeronautica* **40**, 183–199.

Desurosne, I. & Oberlin, G. (1991) Intensités des pluies en zones à relief: premiers résultats sur un transect alpin de forte densité. *La Houille Blanche* **5**, 365–371.

Ferrari, E., Gabriele, S., Rossi, F., Versace, P. & Villani, P. (1990) La valutazione delle piene in calabria. Aspetti metodologici di una analisi a scala regionale. In: *XXII Convegno di Idarulica e Costruzioni Idrauliche* (Cosenza, 4–7 Octubre 1990).

Jansà, J. M. (1959) The Mediterranean air mass (in Spanish). *Rev. Geofísica* **18**, 35–50.

Jansà, J. M. (1966) Meteorology of the west Mediterranean area (in Spanish). *Tercer ciclo de Conferencias*, serie A, no. 43.

Jansà, A., Genovés, A., Picornell, M. A., Campins, J., Radinovic, D. & Alpert, P. (1994) *Mediterranean Cyclones: Subject of a WMO Project*. A: *The Life Cycle of Extratropical Cyclones*, vol. 2, Bergen, 26–31.

Llasat, M. C. & Puigcerver, M. (1992) Pluies extremes en Catalogne: influence orographique et caracteristiques synoptiques. *Hydrol. Continentale* 7, 99–115.

Llasat, M. C., Ramis, C. & Barrantes, J. (1996) The meteorology of high-intensity rainfall events over the west Mediterranean region. *Remote Sensing Rev.* **14**, 51–90.

Meteorological Office (1962) *Weather in the Mediterranean*, I. Her Majesty's Stationery Office, London.

Petrovic, J. & Radic, Z. M. (1994) Effects of topography on rainfall spatial structure in the Drina basin (in Serbian). *Vodoprivreda* **147–149**, 45–53.

Radinovic, D. (1987) *Mediterranean Cyclones and their Influence on the Weather and Climate.* WMO, PSMP Report Ser, 24.

Ramis, C., Llasat, M. C. Genovés, A. & Jansà, A. (1994) The October-87 floods in Catalonia. Synoptic and mesoscale mechanisms. *Met. Apps.* **1**, 337-350.

Ramis, C., Alonso, S. & Llasat, M. C. (1995) A comparative study between two cases of extreme rainfall events in Catalonia. *Surv. in Geophys.* **16**, 141–161.

Reiter, E. R. (1975) *Handbook for Forecasters in the Mediterranean; Weather Phenomena of the Mediterranean Basin;* Part 1: *General Description of the Meteorological Processes.* Tech. Report 5-75, Department of the Navy, Washington, DC.

Rodriguez, R., Llasat, M. C. & Rojas, E. (1994) Evaluation of climatic change through harmonic analysis. *Natural Hazards* **9**, 5–16.

Rodriguez, R. & Llasat, M. C. (1996) Features of the precipitation series of Sevilla y Murcia (in Spanish). In: *Clima y Agua: la Gestión de un Recurso Climático*, 144–153. Marzol, Dorta & Valladares.

Siccardi, F. (1996) Rainstorm hazards and related disasters in the north-west Mediterranean region. *Remote Sensing Rev.* **14**, 5–21.

FRIEND'97 — Regional Hydrology: Concepts and Models for Sustainable Water Resource Management
(Proceedings of the Postojna, Slovenia, Conference, September–October 1997). IAHS Publ. no. 246, 1997.

Regional dependence and application of DAD relationships

DIETMAR GREBNER & THOMAS ROESCH
Department of Geography, Swiss Federal Institute of Technology, Winterthurerstrasse 190, CH-8057 Zurich, Switzerland

Abstract The application of depth–area–duration (DAD) relationships as areal reduction factors (ARFs) is implying the supposition that they are unaffected by the return period and by climate, e.g. also by regional properties. These preconditions have been tested on the basis of storm centred analyses of areal precipitation for the conditions in Switzerland, being characterized by special orographic and climatic influences. The study confirms the independence of ARFs from the return period. They have proved not to be independent of climatic properties of a region. In addition the ARFs and their application depend on the method of estimation.

INTRODUCTION

The estimation of areal precipitation by suitable reduction of a point precipitation using areal reduction factors (ARFs) is a long standing concept. It has been introduced in Berlin (Frühling, 1894) about 100 years ago and has been carried on particularly in USA during the following years (Court, 1961). In Europe analyses of ARFs had not been carried out until about the 1970s (WMO, 1969; Grobe, 1974; Rodriguez-Iturbe & Mejia, 1974; NERC, 1975; Bell, 1976). Very different approaches have been developed to derive ARFs from depth–area–duration relationships (DAD). Grobe (1974) directly integrated precipitation fields in a hydrological basin and calculated depletion curves using the corresponding point maxima of each event. Rodriguez-Iturbe & Mejia (1974) have shown a derivation of ARFs by correlating a representative pair of stations. In the method of NERC (1975) the areal precipitation is parameterized by a point precipitation, the ratio to highest point precipitation then being used as ARF. Several areas of different size, from different locations in Great Britain, provide the depletion of the reduction factor with increasing area. Bell (1976) used the same data set, but calculated the reduction factors with the areal precipitation itself.

All these analyses were carried out in fixed areas or hydrological basins. The investigations of DAD-relationships in the USA since the 1950s have been carried out mostly using indirect methods and using fixed area precipitation fields (Omolayo, 1993; Grebner, 1995). Hershfield (1962) generated the reduction factors by explicitly estimated areal precipitation and its maximum amount in the field centre, i.e. his analyses are storm centred.

The resulting ARFs and their application contain several assumptions, and also restrictions concerning climate, return period, shape of the area and properties of the method. In Switzerland DAD-relationships have been investigated systematically since 1989 (Grebner, 1995).

Beside others the independence on climate and on the return period as well as the application of methods and ARFs had to be examined.

AREA AND DATA

The investigation covers the whole area of Switzerland. To detect possible differences in the characteristics of precipitation, this area has been subdivided into six main regions (Fig. 1), large enough to get representative samples from the available reference period.

Precipitation conditions in Switzerland can be differentiated by meteorological characteristics in northern, central and southern Alpine areas. The suitable central Alpine regions are the catchments of the River Rhone (canton Wallis) and of the Inn (Engadine and Münstertal). The southern Alpine region contains the areas of Tessin and Südbünden (abbreviated to Tessin), characterized by Mediterranean influence. The most extended area geographically is that part north of the Alps, but containing non-uniform precipitation conditions. The mean annual precipitation is increasing from west to east as well as from north to the Alpine crest (HADES, 1991). Some properties of extreme precipitation fields also change from west to east in this area. The fields of heavy precipitation in the western part are centred north of the Alps, whereas east of Zurich precipitation fields are dominating, which extend from south across the Alps to north (Grebner, 1993). For that reason the area north of the Alps is subdivided into three regions: West, Prealpine and East (Fig. 1).

The above regions of Switzerland are suitable to investigate the dependence of ARFs on climate conditions and on return period, due to the adjoining climatic zones, i.e. temperate humid to the north and Mediterranean to the south respectively, and due to the relatively dense standard network of precipitation gauges. In particular, the fields and centres of cyclonic precipitation events are reliably recorded.

The precipitation data originate from the gauging network of the Swiss Meteorological Institute (SMI). No data have been available from the surrounding

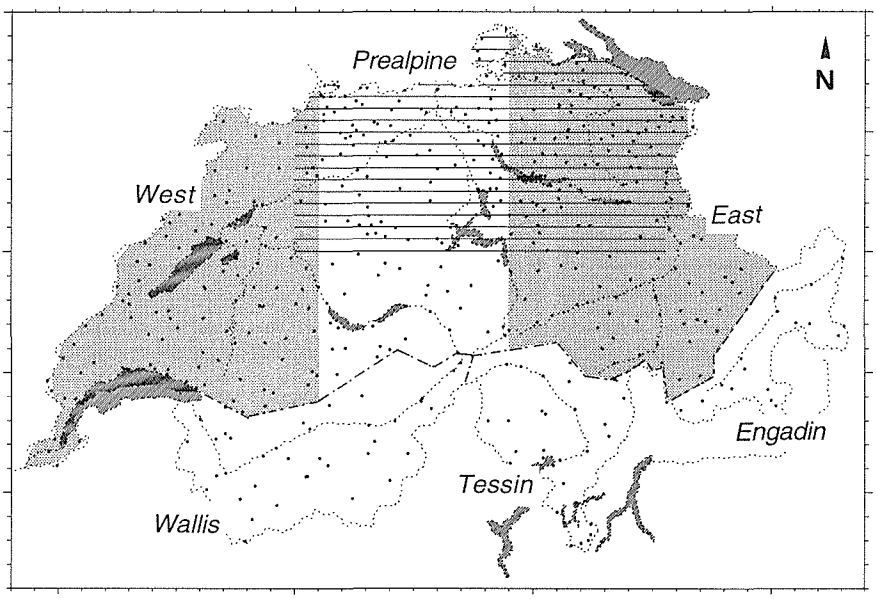

Fig. 1 Map of Switzerland showing the six main regions and the precipitation gauging network (points). Border: scale marks in steps of 10 km.

countries. The average network density is about one station per 100 km^2 (Fig. 1). However this density is not homogeneous, but decreases particularly from the pre-Alpine zone to the mountain crest, and moreover in the central Alpine area the gauging sites are usually installed in the lower parts of the valleys. About 80% of the network stations have a time step of 1 day, the other 20% are automatic stations (ANETZ) with higher resolution. The reference period is defined by the recording period of this ANETZ and includes the years from 1981 to 1993.

METHODS

The time step of the analysis is one hour. On the basis of ANETZ records the daily precipitation amounts had been resolved into hourly values. Each hourly data set of the network was interpolated on a regular 2 km grid, using the triangulation method.

Detailed studies demonstrate that the results of this simple deterministic method are not different from those of more sophisticated ones (e.g. Kriging), even if the network density is substantially reduced.

The precipitation fields have been related to that region, where the field centres have been located. The depletions of the areal precipitation have been analysed from storm centres. As a first approach the properties of precipitation fields are taken to

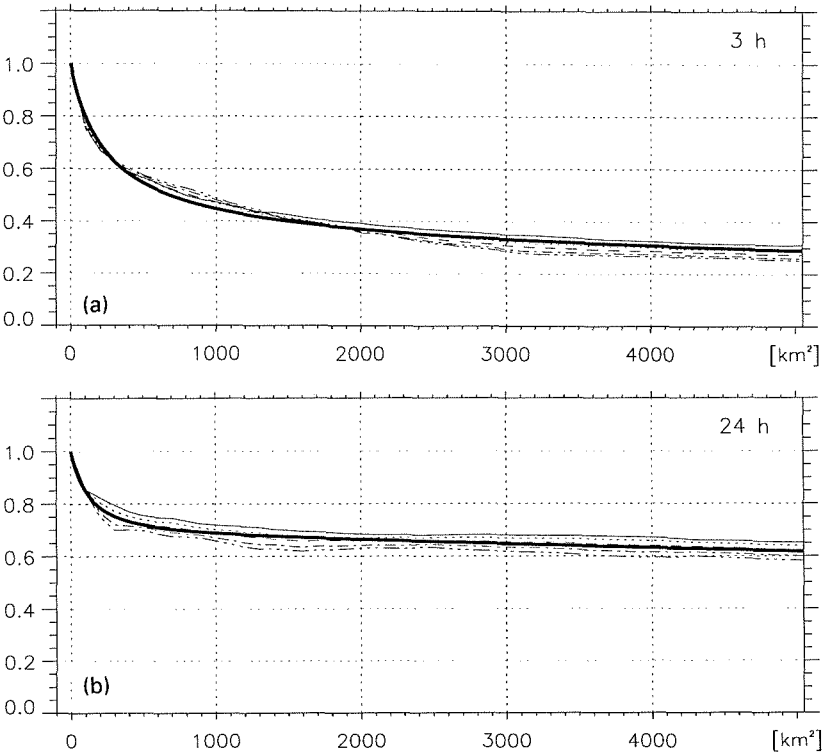

Fig. 2 Relative depletion curves of the West region for the return periods 2, 5, 10, 25 und 50 years (thin lines from the top) and fitted mean curves (ARF functions) (thick line) for duration intervals of (a) 3 and (b) 24 h.

be uniform within a region. For the field integration, region borders lying inside the country don't exist, except the mountain crest for hydrometeorological reasons. The integration has been limited by the national border.

The ARFs have been derived for the eight duration intervals 3, 6, 12, 24, 36, 48, 60 and 72 h and are shown for areas up to 5000 km^2 (Figs 2 and 3). The analyses were performed on the major events in the reference period. An event has been accepted for a duration interval only if precipitation in the central part of the field had no interruptions in the record. Secondary centres in an analysed precipitation field have been included into the estimation of areal precipitation. For generalization, envelope curves have been constructed over the individual depth–area depletion curves. These envelopes are little affected by the limiting influence of the national border.

RESULTS

The questions referred to above (see Introduction) will be discussed based on the findings for the three regions north of the Alps (Figs 2 and 3). Figure 2 shows for the West region the ARFs in relation to return periods for 3-h and 24-h duration

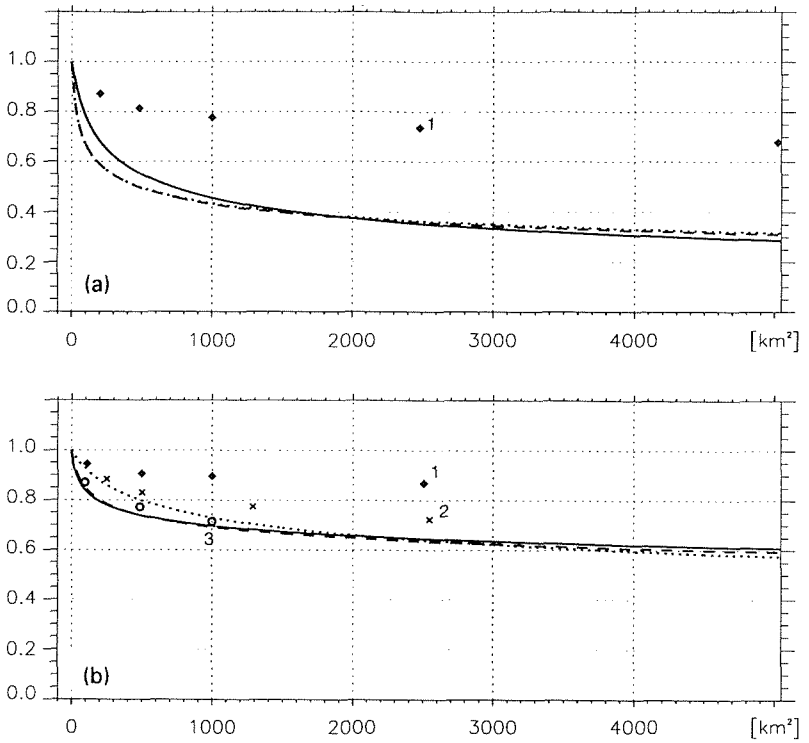

Fig. 3 Comparison of the fitted ARF functions (see Fig. 2) for the regions West (solid curve), Prealpine (dashed) and East (dotted); and in addition the results of other authors: (1) NERC, (1975), fixed area; (2) Hershfield (1960), storm centred; (3) Rodriguez-Iturbe & Mejia (1974), fixed area. Duration intervals: (a) 3 and (b) 24 h.

intervals. The curves represent the return periods 2, 5, 10, 25 and 50 years (e.g. in Fig. 2(b) from the top). The fitted mean of these curves is the thick line. In the graph for 3 h, the precipitation amounts for smaller areas (up to about 500 km^2) reflect convective conditions and for larger areas (>500 km^2) cyclonic precipitation. The curves for 24 h are completely based on cyclonic precipitation.

ARFs and return periods

Figure 2(a) illustrates the relationship between short, heavy areal precipitation (3 h) and different return periods. The analyses for the other two regions have led to similar results. To be precise, in both the Prealpine and East regions, the slopes of the curves show some variation above small areas (up to about 500 km^2) for the different return periods. But these deviations, as well as the curve variations (Fig. 2), are thought to be caused by the shortness of the reference period and the density of the gauging network regarding the detection of convection centres. No dependence of the ARFs on frequency is shown for areas larger than 500 km^2. The unreliability decreases with increasing duration interval (Fig. 2(b)) and the differences are restricted to smaller areas (less than 300 km^2).

These results confirm the independence of ARFs on the return period. They will be represented in the following by the fitted ARF functions (Fig. 2, thick lines).

ARFs and climatic influences

In Fig. 3 the fitted ARF functions of the three regions are put together. The figure presents three hourly conditions with convective events (Fig. 3(a)) and the 24 hourly functions of cyclonic precipitation (Fig. 3(b)). The curves represent: solid line = West region, dashed line = Prealpine region, dotted line = East region.

The 3-h curves of the Prealpine and East regions are congruent, West region having a deviating slope up to about 1000 km^2. That means, the centre amounts of the sampled convective precipitation fields in the West region are smaller compared with that of the two eastern regions. The congruence of the ARF functions of the Prealpine and East regions is caused by using approximately the same sampled events. They are located in the overlapping portion of both regions (Fig. 1). The remaining area of the East region covers the Alps. There, convective precipitation decreases with rising orography due to decreasing water vapour supply with altitude and a restricted advection of water vapour in the valleys. In summer the saturation mixing ratio of 2000 m a.s.l. reaches only 60 or 70% of the values at about 500 m a.s.l. Consequently, convections in this Alpine area are of low significance in the sample of major events observed in the East region.

However the difference between the two slopes for duration intervals of 3 h appears not significant. Tests show that a randomly observed high point precipitation in a convective precipitation field can cause a similar difference in the slope (Fig. 3(a)).

The 24-h heavy areal precipitation (Fig. 3(b)) results from cyclonic processes. The error caused by resolving the daily into hourly time steps is small. In contrast to

Fig. 3(a), the ARF functions of West and Prealpine are now congruent, i.e. differing from the Ost region.

These findings can be explained as follows: the important precipitation fields are generated by atmospheric systems centred north of the Alps. The main fields of the East region however arise from processes centred south of the Alps and extending across the mountains to the north (Fig. 4). Consequently the depletion of areal precipitation on the northern side is referred to a relative precipitation centre near the mountain crest. The reduction from such a point is always smaller than from a real centre. Therefore the sloping differences in Fig. 3(b) are physically significant.

Application

The principle of application of ARFs appears simple. However the practice proves essentially more difficult. For deriving and transposing of depletion relationships their properties must be considered. The previous discussion demonstrates that the ARFs are obviously not dependent on the return period, but depend on the regional boundary conditions of precipitation regimes.

Further influences on ARFs arise from the methods of analysis from network density and from generalization of individual depletion curves. Most of the direct estimations of DAD relationships, and of all conceptual approaches, observe precipitation fields in fixed areas, being defined hydrologically or otherwise (Omolayo, 1993). Therefore the samples based on these methods not only contain the variability of the intensity of the events, but in addition the variability of the position of the area within the precipitation fields. Further uncertainties are created by using areas from

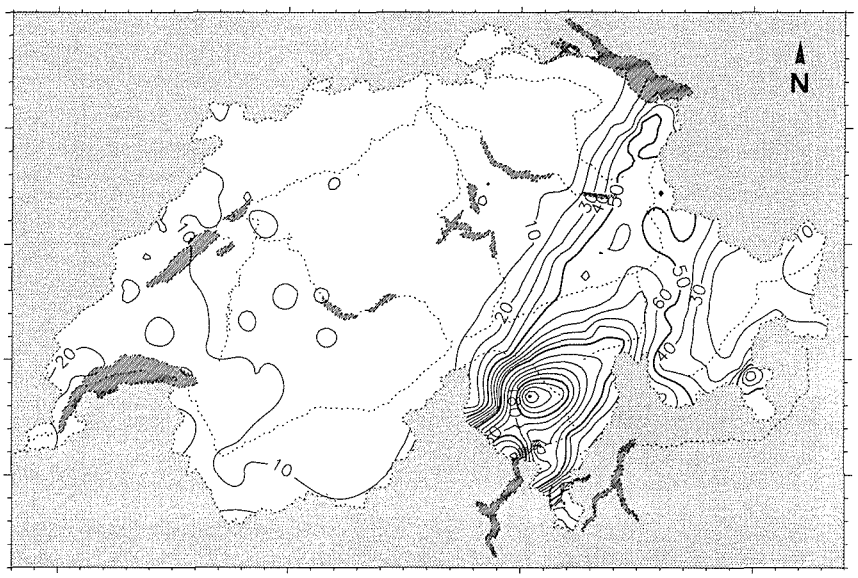

Fig. 4 Pattern of a precipitation field being centred to the south of the Alps and crossing the mountains; one day amounts (mm) of 17 July 1987. Border: scale marks in steps of 10 km.

different regions for the same sample (e.g. NERC, 1975). For such approaches long reference periods are necessary to get representative ARFs. The same requirement exists, if mean curves (e.g. from extreme series) are used as generalization.

The density of the gauging network affects both the recording of the real point maximum in a precipitation field and the calculation of the areal precipitation, in particular under convective conditions. For the frequently used Thiessen method the polygon areas have to be small compared with the investigated area.

Differences between the estimation conceptions (e.g. NERC, 1975; Rodriguez-Iturbe & Mejia, 1974) as well as the shape and the orientation of a basin can have a systematic effect on the AR factors (Figs 2 or 3 in Omolayo, 1993).

Some of these difficulties can be excluded by storm centred integration of the precipitation fields. However this approach implies the assumption that the centre of heavy precipitation fields can occur at each point of a region or zone with meteorological and orographic uniform boundary conditions for precipitation. Moreover the storm centred analysis is supplying not only (relative) ARF functions, but also (absolute) precipitation efficiency of the atmosphere. This meets the requirements as a basis for engineering design. The generalization of the depletion curves by envelopes serves the same purpose.

CONCLUSIONS

Based on the different precipitation conditions on the northern Alpine part of Switzerland, storm centred analyses of the areal reduction factors show:

- ARFs are independent of the return period in all investigated duration intervals,
- ARFs are not independent however on regional, i.e. climatic influences.

From the latter result, the transposition of methods seems to be more reliable than the transposition of ARFs. The decision between a storm centred or fixed area method depends on the objectives. Fixed area ARFs serve as a basis for engineering design tasks, but primarily for an individual basin or area, containing larger unreliabilties than storm centred analyses, for the usually short available reference periods. Storm centred absolute DAD relationships are, in addition, a tool to estimate absolute storm magnitudes.

Acknowledgements The authors gratefully thank the Swiss Meteorological Institute for the comfortable availability of the database and the Swiss National Science Foundation for kindly supporting this project.

REFERENCES

Bell, F. C. (1976) *The Areal Reduction Factor in Rainfall Frequency Estimation*. Inst. Hydrology, Wallingford, Oxfordshire, Report no. 35.

Court, A. (1961) Area-depth rainfall formulas. *J. Geophys. Res.* **66**(6), 1823–1831.

Frühling, A. (1894) Über Regen- und Abflussmengen für städtische Entwässerungskanäle. *Der Civilingenieur* (Leipzig), ser. 2, **40**, 541–558, 623–643.

Grebner, D. (1995) Synoptische Zirkulationen während Extremniederschlägen in der nordalpinen Schweiz. In: *Aktuelle Aspekte in der Hydrologie* (ed. by D. Grebner). Zürcher Geographische Schriften, Heft 53, 39–48. Verlag Geograph. Inst., ETH Zürich.

Grobe, B. (1974) *Niederschlagsgebiete in Abhängigkeit von Niederschlagshöhe und Eintrittswahrscheinlichkeit*. Wasserhaushalt und Bodennutzung; Schriftenreihe des Sonderforschungsbereichs 150 der Technischen Universität Braunschweig; Heft 3.

HADES (1992) *Hydrological Atlas of Switzerland*; 2.2 *Mean Annual Corrected Precipitation Depth 1051–1980*. Landeshydrologie und -geologie, Bern.

Hershfield, D. M. (1962) Extreme rainfall relationships. *J. Hydraul. Div.*, Proc. Am. Soc. Civil Engrs **92**, 73–92.

NERC (1975) *Flood Studies Report*, vol. 2; *Meteorological Studies*, 38–41. Natural Environment Research Council (NERC), London.

Omolayo, A. S. (1993) On the transposition of areal reduction factors for rainfall frequency estimation. *J. Hydrol.* **145**,191–205.

Rodriguez-Iturbe, I. & Mejia, J. M. (1974) On the transformation of point rainfall to areal rainfall. *Wat. Resour. Res.* **10**(4), 729–735.

WMO (1969) *Manual for Depth–Area–Duration Analysis of Storm Precipitation*. WMO No. 237, TP 129, Geneva.

FRIEND'97 — Regional Hydrology: Concepts and Models for Sustainable Water Resource Management
(Proceedings of the Postojna, Slovenia, Conference, September–October 1997). IAHS Publ. no. 246, 1997.

Regional analysis of convective storms achieved from dense hydrometeorological network data in an arid zone of the Southern Hemisphere

PEDRO C. FERNANDEZ[1], SARA RODRIGUEZ & LUIS FORNERO
National Water and Environment Institute Andean Regional Centre, PO Box 6, 5500 Mendoza, Argentina

Abstract A procedure is described for carrying out a regional analysis of convective storms over an area of 625 km^2 surrounding the metropolitan area of Mendoza City (central west Argentina). A dense hydrometeorological telemetric network of 24 stations over the area allowed detailed studies of depth–duration–frequency and time and space distribution of precipitation to be undertaken. A total of 140 network recorded storms during 12 years of operation and many other historical storms from the National Weather Service records were used to generate a composite record for a meteorologically homogeneous region. A method is described for defining homogeneous zones and finally tables for design storms are presented to use in precipitation runoff models which take into account time–space distribution and depth–duration–frequency for the convective storms of the region.

INTRODUCTION AND SCOPE

With the support of 24 telemetric stations over an of area 625 km^2 in central west Argentina (Mendoza) (Fig. 1) a detailed study of thunderstorm rainfall fields was carried out. Each telemetric station has a record of about 12 years and there are 30 years of records at two other stations from the National Weather Service.

The continuous operation of this high-density and synchronized raingauge network has provided significant new knowledge of the temporal and spatial distribution of precipitation in an arid zone of the southern hemisphere, where the lack of good quality, high resolution data becomes a major barrier for research (Fernández *et al.*, 1990, 1995).

Because the region is meteorologically homogeneous (Portman, 1991; Fernández *et al.*, 1995) it is possible to consider the assumption that the records for the same or different periods at a number of stations may be considered as a composite record for a single station (Chow, 1964) or in this case of individual storms that could be considered as a station-storm record (Farmer & Fletcher, 1972).

The aim of this study is to provide a procedure for regional analysis of convective storms using a dense telemetric network as a basic information tool and to produce practical tables (Fernández *et al.*, 1995) for design storms to be used directly as input to hydrological precipitation–runoff models.

[1] *Also with:* National Science and Technology Research Council (CONICET).

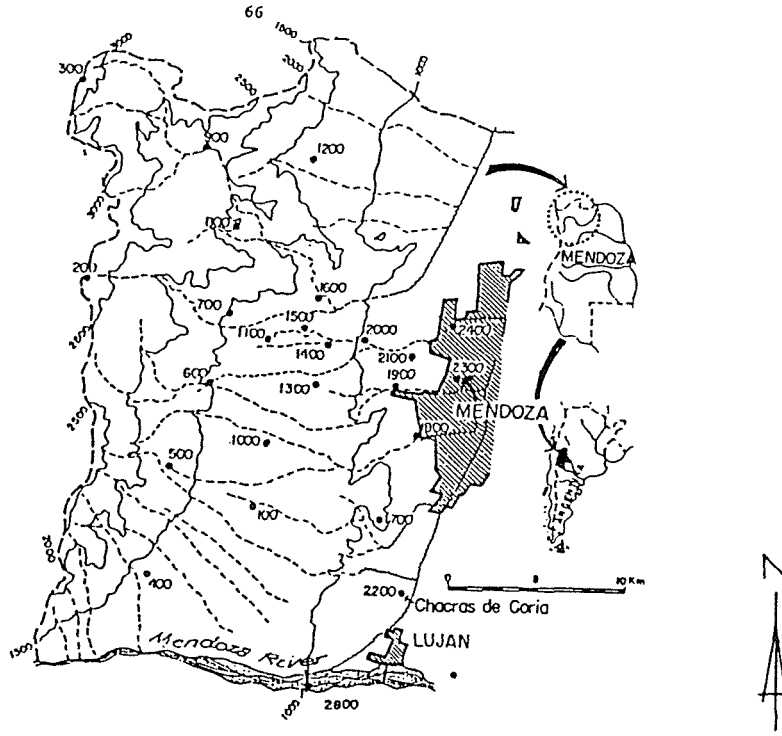

Fig. 1 Location map of the dense hydrometeorological network.

MATERIALS AND METHODS

In arid and semiarid regions where, in general, flow records are scarce, regional studies of precipitation regimes can be useful. This area has an average annual rainfall of between 200 and 300 mm and can therefore be classified as arid.

The ephemeral streams in the region are subjected to flash floods due to summer storms of high intensity and relatively limited extent, so spatial distribution of precipitation is of great importance in order to avoid over-estimation of floods. It is possible to do these studies due to the existence of a dense, synchronized telemetric network (Fernández *et al.*, 1990; 1995).

Data analysis

A database of the 24 main precipitation stations of the telemetric network for 12 years of records (1983–1994) and records since 1946 of two National Weather Service Stations at two locations within the region, were used for analysis (Portman, 1991; Fernández *et al.*, 1995).

Selection of storms

To get a homogeneous random sample, a common pattern of event selection had to be used. The criterion was hydrologic rather than meteorologic and is related to the

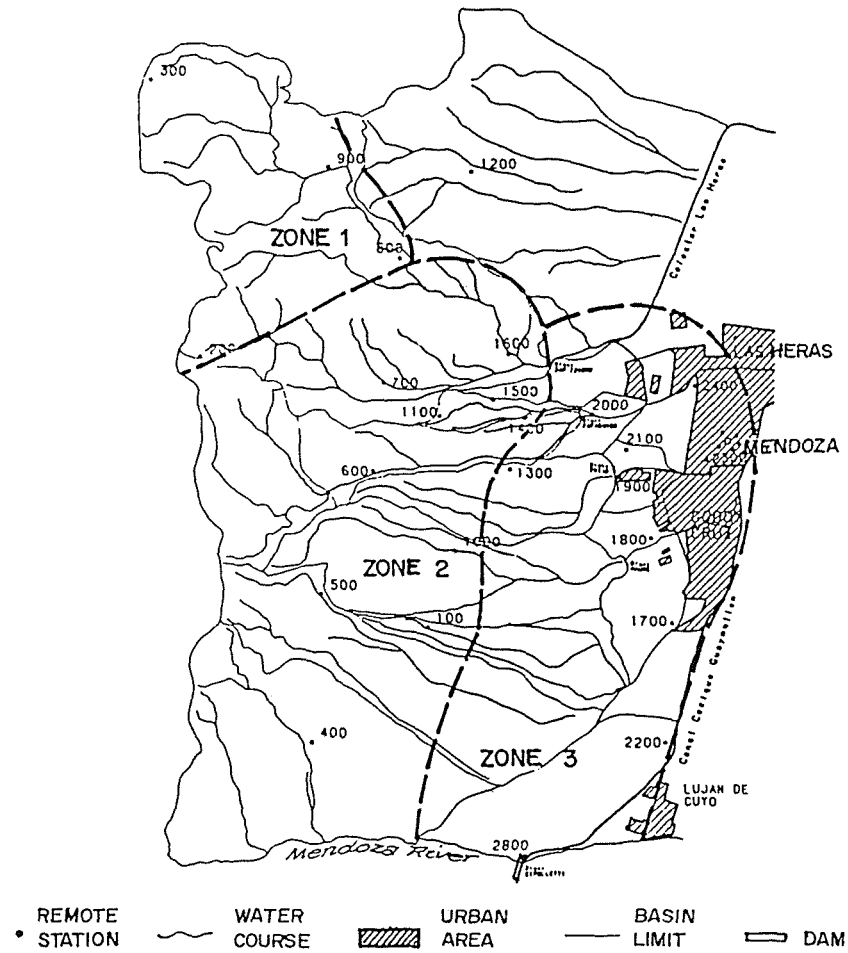

Fig. 2 Homogeneous zones.

initial abstraction and the soil infiltration capacity. Thus flash flood producing storms for the area were selected. The main focus was on precipitation greater than 20 mm in depth and intensity of 6 mm per 30 minutes.

From a total sample of 140 events 83 were finally selected. A storm was defined as a rain period separated from preceding and succeeding rainfall by one hour or more. This criterion was established because 30–45 minutes is the high-frequency duration of the storms in this region.

Regional analysis

Precipitation zones were defined according to station elevations and then a grouping of stations was made using a statistical determination of the multivariate method of Principal Component Analysis (Yevjevich, 1972; Portman, 1991; Fernández *et al.*, 1995) (Fig. 2).

The data used were the total precipitation figures for the station, as variable, of all selected precipitation events of at least four precipitation records, using only the random sample of events with more than 20 mm of total precipitation.

It is important to point out that the principal components (PC) represents an objective method of orthogonal transformation (rotation) in the multivariate analysis of random variables. For the analysis of principal components, the start point is the correlation matrix between all the variables (in this case the stations) to obtain eigenvalues and eigenvectors and with the rotation of the axis the rotated loading factor is attained (Table 1). In this case, because of the previous interpretation of altitudinal zones, it is easy to see which are the variables (for each factor) that have highest loading factor. Table 1 shows the factors for two periods of data (Portman, 1991).

The loading factor of these two periods combined showed considerable spatial linking of neighbouring stations to form groups (Fig. 2). These groups are correlated with the physical characteristic of station elevation which supports the grouping of stations (Yevjevich, 1972).

Relations between zones

From observation of the records, zones 2 and 3 present storms of the same characteristics in relation to frequency intensity, duration and spatial distribution.

On the other hand, zone 1 (the highest elevation) presents less frequency of intense precipitations and storms of lower intensity. For zones 2 and 3, tables and curves of intensity–duration–frequency were calculated.

Table 1 Rotated loading factor (patterns).

Period 1 (1984/88); n = 49					**Period 2 (1984/90); n = 72**				
	Factor 1	Factor2	Factor3	Factor4		Factor 1	Factor 2	Factor 3	Factor 4
lgp200	0.110	0.185	0.303	**0.706**	lgp200	0.107	0.132	-0.416	**0.590**
lgp300	0.107	0.087	**0.787**	0.253	lgp300	0.120	0.045	0.003	**0.719**
lgp400	**0.818**	0.078	0.367	0.208	lgp400	0.190	**0.809**	0.086	0.182
lgp500	**0.860**	0.257	0.191	0.037	lgp500	0.242	**0.791**	0.291	0.166
lgp600	**0.914**	0.135	0.163	0.084	lgp600	0.140	**0.811**	0.394	0.210
lgp700	**0.841**	0.176	0.316	0.146	lgp700	0.107	**0.659**	0.392	0.446
lgp800	0.212	-0.079	**0.856**	-0.033	lgp800	-0.041	0.102	0.296	**0.790**
lgp900	0.238	-0.026	**0.872**	0.099	lgp900	0.008	0.134	0.146	**0.876**
lgpl00	**0.706**	0.003	-0.274	0.154	lgpl00	0.283	**0.764**	-0.040	-0.141
lgpl000	**0.846**	0.317	0.105	0.163	lgpl000	0.424	**0.743**	0.274	0.088
lgpll00	**0.828**	0.300	0.261	-0.080	lgpll00	0.142	**0.609**	0.581	0.268
lgpl200	0.454	0.323	0.345	-0.269	lgpl200	0.300	0.168	0.593	0.402
lgpl300	0.579	**0.643**	0.016	-0.119	lgpl300	0.520	0.470	0.542	-0.021
lgpl400	**0.603**	0.567	-0.006	-0.235	lgpl400	0.475	0.400	**0.634**	-0.052
lgpl500	**0.755**	0.461	0.194	-0.057	lgpl500	0.277	0.543	**0.606**	0.114
lgpl600	**0.657**	0.415	0.231	-0.066	lgpl600	0.289	0.409	**0.665**	0.136
lgpl700	0.196	**0.727**	0.011	0.476	lgpl700	**0.808**	0.292	-0.022	0.134
lgpl800	0.216	**0.885**	0.028	0.247	lgpl800	**0.893**	0.259	0.112	0.082
lgpl900	0.273	**0.917**	0.013	-0.002	lgpl900	**0.877**	0.222	0.324	0.015
lgp2000	0.301	**0.841**	-0.009	-0.181	lgp2000	**0.720**	0.220	0.536	-0.060
lgp2200	0.265	**0.746**	0.043	0.467	lgp2200	**0.799**	0.385	0.002	0.068
lgp2300	0.125	**0.878**	0.065	0.172	lgp2300	**0.889**	0.160	0.177	0.114
lgp2400	0.104	**0.915**	0.006	-0.011	lgp2400	**0.801**	-0.027	0.360	0.052
(VP	7.229	6.609	2.875	1.421)	(VP	5.991	5.222	3.519	2.905)

In order to have an extending length of record using the concept of stations-storm (Chow, 1964; Farmer & Fletcher, 1972) a study was made to compare zones 2 and 3, following the general criterion of Farmer & Fletcher of obtaining a dimensionless ratio expressing the average slope of short-duration rainfall intensity curves between 5 (I5) and 10 (I10) years return period and for durations up to 30 and 60 minutes.

The ratio was computed by dividing the summation of intensities having durations of 10, 15, 20, 25, 30, 35, 40, 45, 50, 55, 60 minutes (Table 2).

RESULTS

For the general behaviour of storms and for depth–duration–frequency tables (curves) historical records of the National Weather Service from 1946 to 1976 were used in addition to records of the non-telemetric network from 1976 to 1983 and the telemetric network data from 1983 to 1994 for zones 2 and 3, except station 1200.

For rainfall temporal patterns and spatial distribution of convective storms, only the records of the telemetric network were used.

Depth–duration–frequency

A statistical analysis was done using different probability distribution functions: gamma, log-gamma, Pearson, log-Pearson, log-normal, exponential (Rodríguez, 1995). Finally the log-normal distribution was adopted (Yevjevich, 1972; Chow *et al.*, 1993).

Gamma, log-gamma and exponential show less match. Pearson and log-Pearson show best match for low durations, and none at all for durations greater than 60 minutes (Table 3).

General equations

Regression equations were calculated over the area for depth-duration–frequency (Table 4). Depth is in mm and duration in minutes. The confidence limits are vari-

Table 2 Dimensionless ratio ($I10/15$) from intensity–duration–frequency curves for zones 2 and 3.

Zone	Duration up to 30 minutes	Duration up to 60 minutes
2	1.126	1.126
3	1.140	1.141

Table 3 Depth–duration–frequency.

TR	DURATION (minutes)															
Years	5	10	15	20	25	30	35	40	45	50	55	60	65	70	75	80
5	15.7	28.0	35.2	40.3	44.3	47.5	50.3	52.7	54.8	56.6	58.3	59.9	61.3	62.6	63.8	65.0
10	18.5	33.0	41.4	47.4	52.0	55.8	59.0	61.8	64.2	66.4	68.4	70.2	71.9	73.4	74.9	76.2
25	23.7	40.8	50.8	57.9	63.4	67.9	71.7	75.0	77.9	80.5	82.8	85.0	87.0	88.8	90.5	92.1
50	27.3	46.6	57.9	66.0	72.2	77.3	81.6	85.3	88.6	91.5	94.2	96.6	98.8	100.9	102.8	104.6
100	31.6	53.3	66.1	75.1	82.1	87.8	92.7	96.9	100.6	103.9	106.9	109.6	112.1	114.5	116.6	118.6
200	36.0	60.2	74.4	84.4	92.2	98.6	104.0	108.7	112.8	116.5	119.8	122.8	125.6	128.2	130.6	132.9

able for each duration and TR, i.e. for TR = 100 years, duration = 60 minutes. The value is 109.6 mm (Table 3). The lower limit is 97 mm, the upper limit 116 mm.

Rainfall temporal patterns

The rainfall temporal patterns distribution described by Pilgrim *et al.* (1975) was adopted because of its simplicity and good results (Caamaño *et al.*, 1994). Table 5 gives the temporal patterns distribution for 30, 60 and 90 minute storms, derived from subsets of storms of these specific durations.

Spatial distribution

The high spatial variability of convective orographic precipitation makes accurate analyses of thunderstorm fields very difficult. Usually observational networks are inadequate to explain this variability. According to Huff (1970), who makes a very detailed study of this subject with a dense network, "an extremely dense raingauge network would be needed to derive real mean rates with a high degree of accuracy for a specific minute within a storm". One of the main products of this dense synchronized network is the fact that it is possible to obtain outputs from the digital data bank with as much as 1 minute intervals, to have a practically photographic sequence of the rainfall field. Using these outputs for 69 main convective storms and with a special program derived for this analysis (Fornero, 1994), isohyetal maps and depth–area curves were obtained. Figure 3 is the isohyetal map and depth/area curve for the 12 February 1990 storm. The duration is 60 minutes, the maximum point depth is 63 mm and the maximum intensity is 4 mm minute^{-1}. Table 6 shows the general relationship for the region.

Table 4 Regression equations for zones 2 and 3.

TR (years)	A	B
200	-20.255	34.948
100	-18.987	31.409
50	-17.597	27.892
25	-15.985	24.660
10	-14.962	20.808
5	-12.948	17.787
Depth = A + B ln(duration)		

Table 5 Temporal distribution patterns (%) for 30, 60 and 90 minutes.

Period minutes	5		10		15		20		25		30	
Distribution %	10.1		27.3		41.5		15.4		4.8		0.9	
Period minutes	5	10	15	20	25	30	35	40	45	50	55	60
Distribution %	4.1	2.4	8.7	15.4	20.9	28.8	11.9	5.5	1.6	0.5	0.1	0.1
Period minutes	5	10	15	20	25	30	35	40	45	50	55	
Distribution %	2.9	0.2	0.1	3.4	4.2	6.3	7.2	8.6	18.0	10.4	16.2	
Period minutes	60		65		70		75		80		85	90
Distribution %	12.9		4.7		1.8		1.8		1.0		0.2	0.1

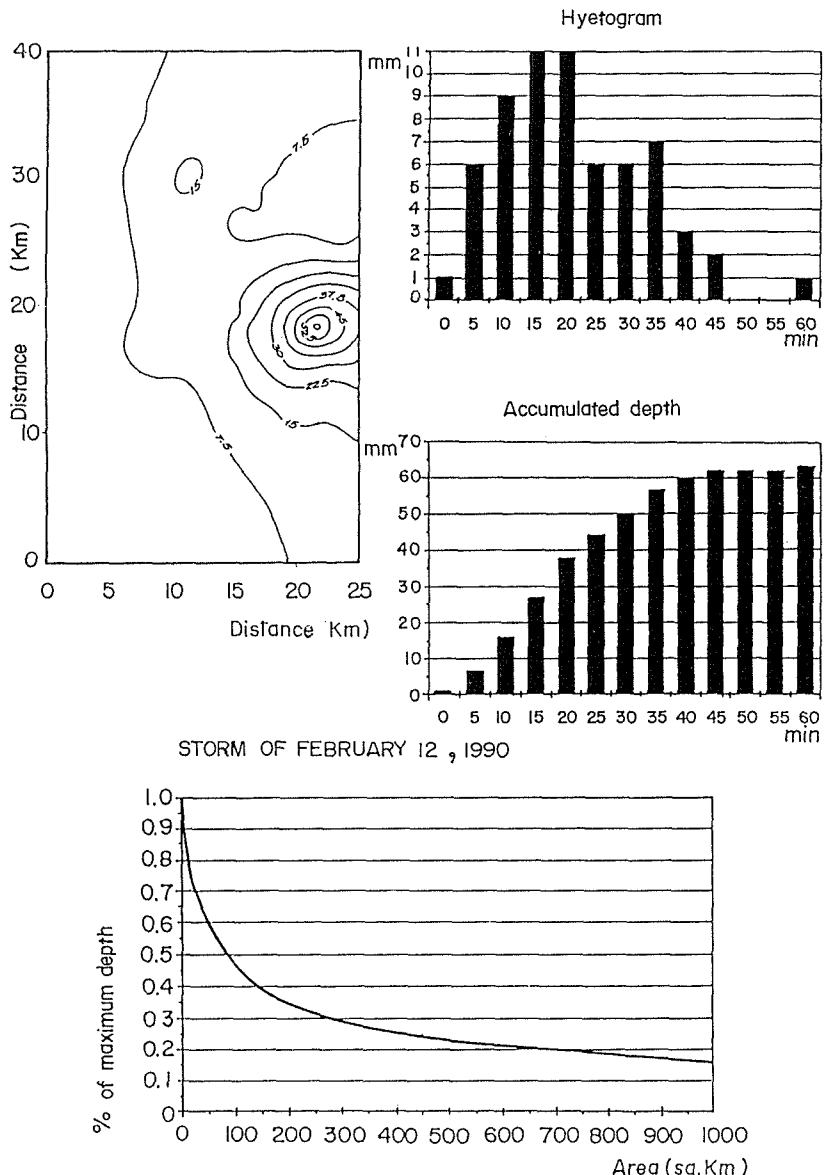

Fig. 3 Storm of 12 February 1990.

Design storms

Analyses of spatial and temporal variability of storm rainfall allows standard project storms to be constructed and provide the design criterion for engineering projects, river management and drainage works (Bell, 1969). This satisfies one of the objectives of the study; to look for a practical tool to use as input to mathematical rainfall–runoff models. The results are presented in the form of tables that bring all the factors together (Fernández *et al.*, 1995) for return periods of 5, 10, 25, 50, 100 and 200 years for 30, 60 and 90 minutes duration of the storm and areas ranging

Table 6 Depth–area relationship for convective storms (the relationship is the same for 30, 60 and 90 minute durations).

Area (km^2)	Average depth over the area as % of maximum	Standard deviation
0–0.9	1.0000	0.0000
1–4.9	0.8894	0.0570
5–9.9	0.8142	0.0710
10–14.9	0.7780	0.0876
15–19.910	0.7430	0.1032
20–24.9	0.7165	0.1113
25–44.9	0.6630	0.1240
50–74.9	0.6065	0.1574
75–99.9	0.5549	0.1498
100–199.9	0.5538	0.1948
200–299.9	0.4472	0.2056
300–499.9	0.4097	0.1689
500–599.9	0.3661	0.1661
600–699.9	0.3557	0.1359
700–1000	0.3111	0.1346

Table 7 Design storm for Mendoza (Argentina). Depths for the period (mm)—average over the area. TR = 100 years and duration = 60 minutes.

AREA	DURATION (minutes)												TOTAL
(Km^2)	5	10	15	20	25	30	35	40	45	50	55	60	DEPTH
0-0.9	4,5	2,6	9,5	16,9	22,9	31,6	13,0	6,0	1,8	0,5	0,1	0,1	109,6
1-4.9	4,0	2,3	8,5	15,0	20,4	28,1	11,6	5,4	1,6	0,5	0,1	0,1	97,5
5-9.9	3,7	2,1	7,8	13,7	18,7	25,7	10,6	4,9	1,4	0,4	0,1	0,1	89,2
10-14.9	3,5	2,0	7,4	13,1	17,8	24,6	10,1	4,7	1,4	0,4	0,1	0,1	85,3
15-19.9	3,3	2,0	7,1	12,5	17,0	23,5	9,7	4,5	1,3	0,4	0,1	0,1	81,4
20-24.9	3,2	1,9	6,8	12,1	16,4	22,6	9,3	4,3	1,3	0,4	0,1	0,1	78,5
25-44.9	3,0	1,7	6,3	11,1	15,1	20,8	8,6	4,0	1,2	0,4	0,1	0,1	72,4
50-74.9	2,7	1,6	5,8	10,2	13,9	19,1	7,9	3,7	1,1	0,3	0,1	0,1	66,5
75-99.9	2,5	1,5	5,3	9,4	12,7	17,5	7,2	3,3	1,0	0,3	0,1	0,1	60,8
100-199.9	2,5	1,5	5,3	9,3	12,7	17,5	7,2	3,3	1,0	0,3	0,1	0,1	60,7
200-299.9	2,0	1,2	4,3	7,5	10,2	14,1	5,8	2,7	0,8	0,2	0,0	0,0	49,0
300-499.9	1,8	1,1	3,9	6,9	9,4	12,9	5,3	2,5	0,7	0,2	0,0	0,0	44,9
500-599.9	1,6	1,0	3,5	6,2	8,4	11,6	4,8	2,2	0,6	0,2	0,0	0,0	40,1
600-699.9	1,6	0,9	3,4	6,0	8,1	11,2	4,6	2,1	0,6	0,2	0,0	0,0	39,0
700-1000	1.4	0.8	3.0	5,3	7,1	9.8	4,1	1,9	0,5	0,2	0,0	0,0	34,1

from 0 to 1000 km^2. Table 7 shows one example for TR = 100 years, and a 60-minute duration.

CONCLUSIONS

According to this study the zone surrounding the metropolitan area of Mendoza city (Argentina) can be divided into three climatologically homogeneous zones (Fig. 2).

For convective storms in zone 1 (elevations higher than 2500 m a.s.l.) the behaviour is different from those in zones 2 and 3. On the other hand zones 2 and 3 show a similar behaviour for intense precipitations and can be considered together. The records in these zones, for a number of stations for the same or different periods, can be considered as a composite record for the region.

The use of PCA multivariate method with the addition of some physical conditions seems to be a good approach for regionalization of meteorologically homogeneous zones.

With regard to variation of thunderstorms with elevations, the stations located at lower elevations show more intense precipitation and higher frequency.

Due to the significant changes in space and time of the convective storms a dense synchronized network is necessary for detailed studies of thunderstorm fields.

A design storm presented for the area, in the form of tables, is a practical approach for using the results of these studies as input of mathematical precipitation–runoff models.

Acknowledgement The authors thank Mr Hugo Yañez for the final revision of the English-language version of the paper as well as the final drafting of the figures.

REFERENCES

Bell, F. (1969) Generalized rainfall-duration-frequency relationships. *J. Hydraul. Div. ASCE* **95**(1), 311–327.

Caamaño, N., Benedetto, H. & Zamanillo, E. (1994) Hietogramas típicos de tormentas intensas en la estación la Suela, Pcia. de Córdoba. *XV Congreso Nacional del Agua* (La Plata, Argentina).

Chow, Ven Te (ed.) (1964) *Handbook of Applied Hydrology*. McGraw-Hill.

Chow, Ven Te, Maidment, D. & Mays, L. (1993) *Hydrología Aplicada*. McGraw-Hill.

Farmer, E. E. & Fletcher, J. E. (1972) Rainfall intensity-duration-frequency relations for the Wasatch Mountains of northern Utah. *Wat. Resour. Res.* **8**(1), 266–271.

Fernández, P., Maza, J., Roby, O. & Fornero, L. (1990) A hydrometeorological telemetric network for hydrologic research studies in Mendoza (Argentina). *Proc. International Symp. on Remote Sensing and Water Resources* (The Netherlands).

Fernández, P., Fornero, L., Rodríguez, S., Tarántola, D. & Trípodi, D. (1995) Standard project storm for Mendoza (Argentina) determined by a dense hydrometeorologic telemetric network. *International R&D Conference on Water & Energy 2001*. Central Board of Irrigation and Power, New Delhi, India.

Fornero, L. (1994) Programa para mapas de Isoyetas. INCyTH-CRA, Mendoza, Argentina. Inédito.

Huff, F. A. (1970) Spatial distribution of rainfall rates. *Wat. Resour. Res.* **6**(1), 254–260.

Pilgrim, D. H. & Cordery, I. (1975) Rainfall temporal patterns for design floods. *J. Hydraul. Div. ASCE* **101**(Hy1), 81–95.

Portman, F. (1991) Provisional Report on the temporary stay of Mr Félix Portman at INCyTH-CRA, Mendoza, Argentina. Inédito.

Rodriguez, S. (1995) Estudio hidrològico e hidràulico del barrio La Favorita Informe de beca del CONICET. Inèdito.

Yevjevich, V. (1972) *Probability and Statistics in Hydrology*. Water Resources Publications, Fort Collins, Colorado, USA.

FRIEND'97 — Regional Hydrology: Concepts and Models for Sustainable Water Resource Management
(Proceedings of the Postojna, Slovenia, Conference, September–October 1997). IAHS Publ. no. 246, 1997.

Modification des régimes d'écoulement en Afrique de l'ouest et centrale non sahélienne et conséquences sur les ressources en eau

ERIC SERVAT, JEAN-EMMANUEL PATUREL, BROU KOUAMÉ, MICHEL TRAVAGLIO
ORSTOM, Programme FRIEND AOC, 06 BP 1203, Cidex 1, Abidjan 06, Côte d'Ivoire

HÉLÈNE LUBÈS, BERTRAND MARIEU, JEAN-MARIE FRITSCH
ORSTOM, Programme FRIEND AOC, BP 5045, F-34032 Montpellier Cedex, France

JEAN-MARIE MASSON
Laboratoire Géofluides-Bassins-Eau, URA-CNRS 1767, Université Montpellier II, Place Eugène Bataillon, F-34095 Montpellier Cedex 5, France

Résumé Des études menées dans le cadre du programme ICCARE (Identification et Conséquences d'une variabilité Climatique en AfRique de l'ouest non sahElienne) au sein du projet FRIEND AOC ont montré que les régions non sahéliennes d'Afrique de l'ouest et centrale avaient subi depuis vingt cinq ans environ une importante fluctuation climatique. Celle-ci se traduit, comme dans les régions sahéliennes, par une baisse notable de la pluviométrie annuelle depuis la fin des années 1960 et le début des années 1970. Cette baisse de la pluviométrie a, bien entendu, de sérieuses conséquences sur les régimes d'écoulement des cours d'eau de cette région. Cette étude a permis de caractériser ces modifications et d'apporter une dimension régionale à leur interprétation tout en soulignant la diminution importante des volumes écoulés, et donc des ressources en eau disponibles, ce qui n'est pas sans conséquences tant au niveau économique qu'environnemental.

INTRODUCTION

Une série d'études menées dans le cadre du programme ICCARE (Identification et Conséquences d'une variabilité Climatique en AfRique de l'ouest non sahElienne) au sein du projet FRIEND AOC a montré que les régions non sahéliennes d'Afrique de l'ouest et centrale avaient subi depuis vingt cinq ans environ une importante fluctuation climatique (Servat *et al.*, 1996; Paturel *et al.*, 1997). Celle-ci se traduit, comme dans les régions sahéliennes situées plus au nord, par une baisse notable de la pluviométrie annuelle. Cette diminution des précipitations correspond à des ruptures dans les séries chronologiques de hauteurs annuelles précipitées. Un ensemble de méthodes statistiques a permis de les localiser à la fin des années 1960 et au début des années 1970. Depuis cette date, et sur l'ensemble des régions dites "humides" d'Afrique de l'ouest et centrale, on constate des déficits pluviométriques annuels pouvant atteindre 20–25%. Bon nombre de zones de savane sont également passées d'un régime climatique "guinéen" à un régime "soudanien" plus sec.

Cette baisse de la pluviométrie a, bien entendu, de sérieuses conséquences sur les régimes d'écoulement des cours d'eaux de la zone non sahélienne d'Afrique de l'ouest et centrale. Les résultats présentés ici sont les premiers obtenus dans le cadre du volet "Ecoulements" du programme ICCARE. Ils seront complétés à très court terme par un ensemble de résultats concernant le bassin du Niger. Mais il est d'ores et déjà possible de tirer certains enseignements à valeur régionale de ces premières études de la variabilité des régimes hydrologiques.

DONNEES ET METHODES

Données

Sur l'ensemble de la région étudiée, qui couvre seize pays d'Afrique de l'ouest et centrale (Sénégal, Gambie, Guinée-Bissau, Guinée, Sierra Leone, Liberia, Mali, Burkina Faso, Côte d'Ivoire, Ghana, Togo, Bénin, Nigeria, Cameroun, Tchad et Centrafrique), 88 bassins versants ont été sélectionnés. Aucun d'eux ne concerne le bassin du Niger qui est encore en cours de traitement à l'heure actuelle. Ces bassins versants ont été retenus pour la qualité et la continuité de leurs données dont les plus anciennes remontent généralement au début des années 1950. Les séries chronologiques disponibles ont été traitées sur la base de regroupements effectués non par pays mais par grands bassins hydrographiques. Ils constituent, de fait, trois grands ensembles:

(a) un premier groupe de bassins versants centré sur le bassin du Sénégal à l'ouest de la zone étudiée,
(b) un second groupe comprenant les Volta, les bassins versants des fleuves ivoiriens, togolais et béninois donc plus proches des côtes du Golfe de Guinée, et
(c) un dernier groupe situé en Afrique centrale et comprenant les bassins du Chari–Logone, de l'Oubangui et de plusieurs cours d'eau camerounais.

Différents types de variables ont été calculés à partir des données de débits journaliers. Elles permettent d'étudier de manière assez complète les manifestations de la variabilité hydrologique et concernent les débits moyens annuels ainsi que certaines variables caractéristiques des hautes eaux et des basses eaux.

Méthodes

Les séries chronologiques des différentes variables étudiées ont été analysées à l'aide de deux méthodes statistiques: (a) le test de corrélation sur le rang et (b) le test de Pettitt (Pettitt, 1979).

L'utilisation du test de corrélation sur le rang avait pour objectif de mettre en évidence l'existence d'une tendance et donc d'un caractère non aléatoire au sein des séries chronologiques. Celles-ci ont ensuite été analysées à l'aide du test de Pettitt qui a pour objet de détecter une éventuelle rupture en moyenne dans les séries chronologiques. Ce test est non-paramétrique et dérive du test de Mann-Whitney (Lubès *et al.*, 1994). L'absence d'une rupture dans la série (x_i) de taille N constitue l'hypothèse nulle.

Pettitt définit la variable $U_{t,N}$:

$$U_{t,N} = \sum_{i=1}^{t} \sum_{j=t+1}^{N} D_{ij}$$

où $D_{ij} = \sin(x_i - x_j)$ avec $\sin(Z) = 1$ si $Z > 0$, 0 si $Z = 0$ et -1 si $Z < 0$.

Il propose de tester l'Hypothèse nulle en utilisant la statistique K_N définie par le maximum en valeur absolue de $U_{t,N}$ pour t variant de 1 à $N - 1$.

A partir de la théorie des rangs, Pettitt montre que si k désigne la valeur de K_N prise sur la série étudiée, sous l'hypothèse nulle, la probabilité de dépassement de la valeur k est donnée approximativement par:

$$\text{prob}(K_N > k) \approx 2\exp\left(\frac{-6k^2}{N^3 + N^2}\right)$$

Pour un risque α de première espèce donné, si la probabilité de dépassement estimée est inférieure à α, l'hypothèse nulle est rejetée. La série comporte alors une rupture localisée au moment τ où est observé K_N.

RESULTATS

Débits moyens annuels

Les séries chronologiques de débits moyens annuels, ou modules annuels, des quatre-vingt-huit bassins versants sélectionnés ont été analysées à l'aide des méthodes présentées ci-dessus.

La Fig. 1 montre, à l'évidence, le caractère non aléatoire de l'immense majorité des séries de modules annuels (72% des bassins), traduisant en cela l'existence d'une tendance. Seuls certains bassins d'Afrique centrale, plus précisément du Cameroun et de l'ensemble Togo et Bénin, présentent un caractère aléatoire. Il convient de noter, cependant, que l'ensemble des résultats enregistrés sur les bassins du Cameroun doivent être examinés avec circonspection compte tenu des nombreux aménagements réalisés sur ces cours d'eau. Il est, en effet, difficile de faire la part exacte de ce qui est lié à la présence de ces aménagements et de ce qui relève de la variabilité naturelle.

L'utilisation du test de Pettitt a permis de montrer que 63 bassins sur les 88 étudiés présentaient une rupture dans les séries chronologiques de modules annuels (cf. Fig. 2). Ce résultat très significatif qui correspond à une diminution des débits moyens annuels souligne l'importance du phénomène dans toute la sous-région. Il est intéressant de noter la très faible dispersion des dates d'occurrence de cette rupture. Sur les 63 bassins concernés, 14% présentent une rupture qui s'est produite entre 1965 et 1968, 71% entre 1969 et 1971, 6% entre 1972 et 1975 et 6% après 1975. Un bassin présente une rupture avant 1965, mais c'est un bassin qui présenterait une augmentation du module annuel, ce qui laisse planer de sérieux doutes quant à la qualité de l'ensemble des données qui lui correspondent. D'un point de vue spatial, on constate que l'essentiel des ruptures enregistrées avant 1969 le sont sur le bassin versant du Sénégal, soit dans les régions les plus occidentales et les plus

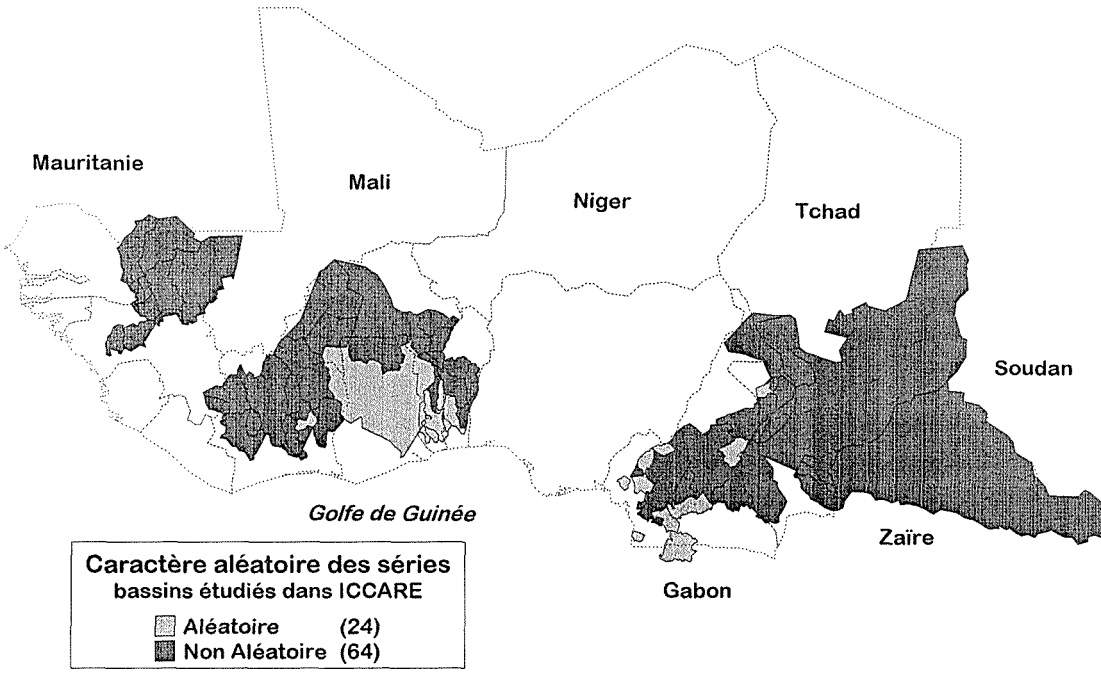

Fig. 1 Représentation cartographique du caractère aléatoire des séries de débits moyens annuels pour les bassins versants retenus dans le programme ICCARE.

septentrionales de la zone étudiée. Ceci est parfaitement conforme aux résultats de l'étude pluviométrique menée précédemment (Servat *et al.*, 1996) et qui avait révélée que les régions touchées le plus tôt par cette variabilité climatique se situait au nord-ouest de la zone étudiée. Les deux autres groupes de bassins versants, "Golfe de Guinée et Volta" d'une part "Afrique Centrale" d'autre part, ont généralement subi cette modification entre 1969 et 1971 à quelques exceptions près qui sont plus tardives.

Il est également intéressant de noter qu'en Afrique de l'ouest ce sont les régions qui présentaient la plus faible variabilité, et donc le déficit pluviométrique le plus réduit, qui ne présentent pas de ruptures dans le domaine des modules annuels. Il s'agit en particulier de certaines régions des bassins du Mono et de l'Oueme au Togo et au Bénin. Pour les mêmes raisons, certains bassins versants du Cameroun semblent ne pas avoir subi de ruptures.

S'il y a concordance avec le phénomène observé au niveau de la pluviométrie, on constate cependant que les ruptures dans les séries de débits moyens annuels sont beaucoup moins dispersées dans le temps qu'elles ne le sont pour les précipitations annuelles. Les différences qui apparaissent au niveau des cours d'eau, intégrateurs de nombreux paramètres influencés par la variabilité climatique (hauteurs précipitées, développement de la végétation, ruissellement, infiltration, recharge des nappes, évaporation, etc.), sont donc plus sensibles et détectables plus rapidement.

La Fig. 3 présente les déficits calculés pour les débits moyens annuels depuis la date de rupture estimée par le test de Pettitt. Il convient de souligner que ces déficits sont généralement extrêmement importants puisque sur les 62 bassins concernés, 52

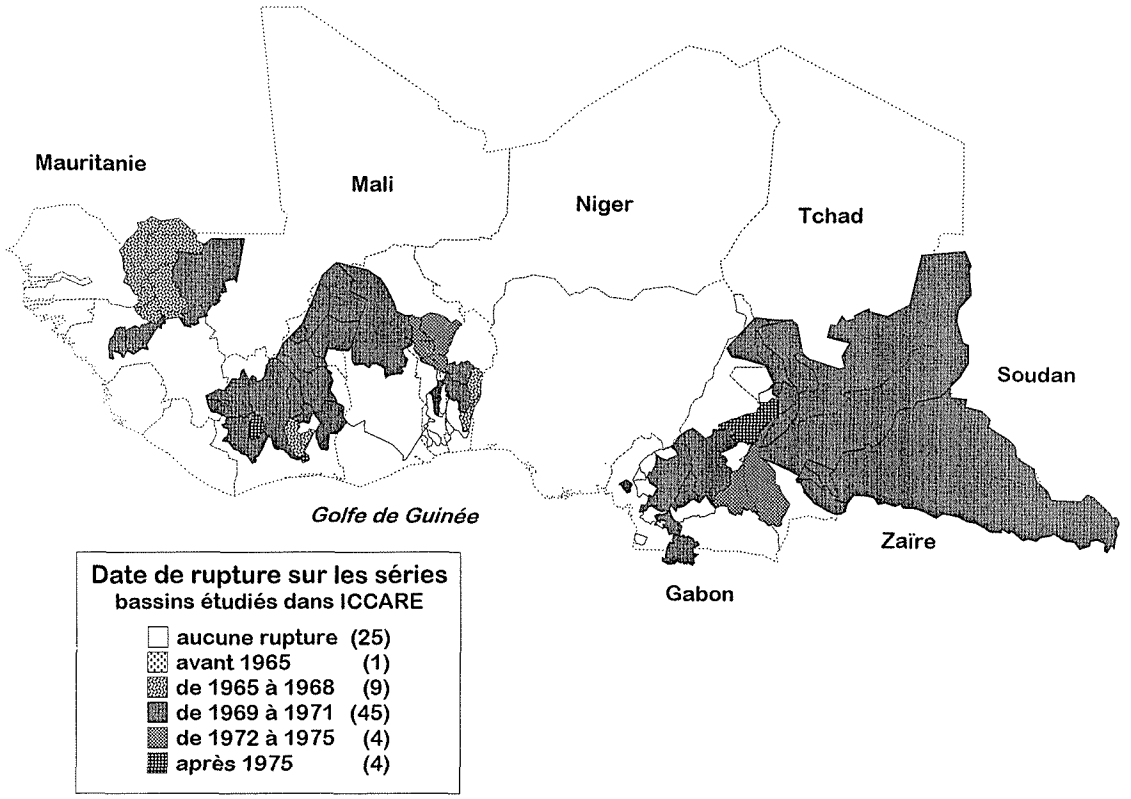

Fig. 2 Représentation cartographique de la répartition des dates de ruptures dans les séries chronologiques de débits moyens annuels.

(soit 84%) présentent un déficit supérieur ou égal à 30%, et 25 (soit 40%) un déficit supérieur ou égal à 50%. Ces chiffres montrent avec force combien les effets de la variabilité climatique mesurée sur la pluviométrie sont amplifiés au niveau des cours d'eau dont on a rappelé auparavant le rôle intégrateur. On imagine d'ores et déjà les conséquences que peuvent avoir de tels déficits sur l'exploitation des ressources en eau dans la sous-région.

Du point de vue spatial, on notera que les déficits les plus importants sont enregistrés sur le bassin du Sénégal, sur les bassins des fleuves ivoiriens et sur le bassin du Chari–Logone en Afrique centrale. L'examen de la Fig. 3 montre que, généralement, les cours d'eau prenant leur source ou dont l'alimentation se fait principalement à partir des zones de savane sont les plus touchés par ce déficit à l'inverse de ceux qui relèvent presque exclusivement des zones de forêt. On rangera dans cette dernière catégorie le bassin de l'Oubangui et la quasi totalité des bassins camerounais.

Le Tableau 1 présente quelques uns des résultats les plus significatifs en matière de débits moyens annuels. Il permet encore une fois de souligner l'importance des déficits d'écoulements enregistrés dans ces cours d'eau des régions de l'Afrique dite "humide". Ces résultats renforcent les conclusions tirées de l'étude sur la pluviométrie et confirment la réalité de la variabilité climatique subie par l'Afrique de l'ouest et centrale non sahélienne, en phase avec ce qui a été décrit auparavant au Sahel.

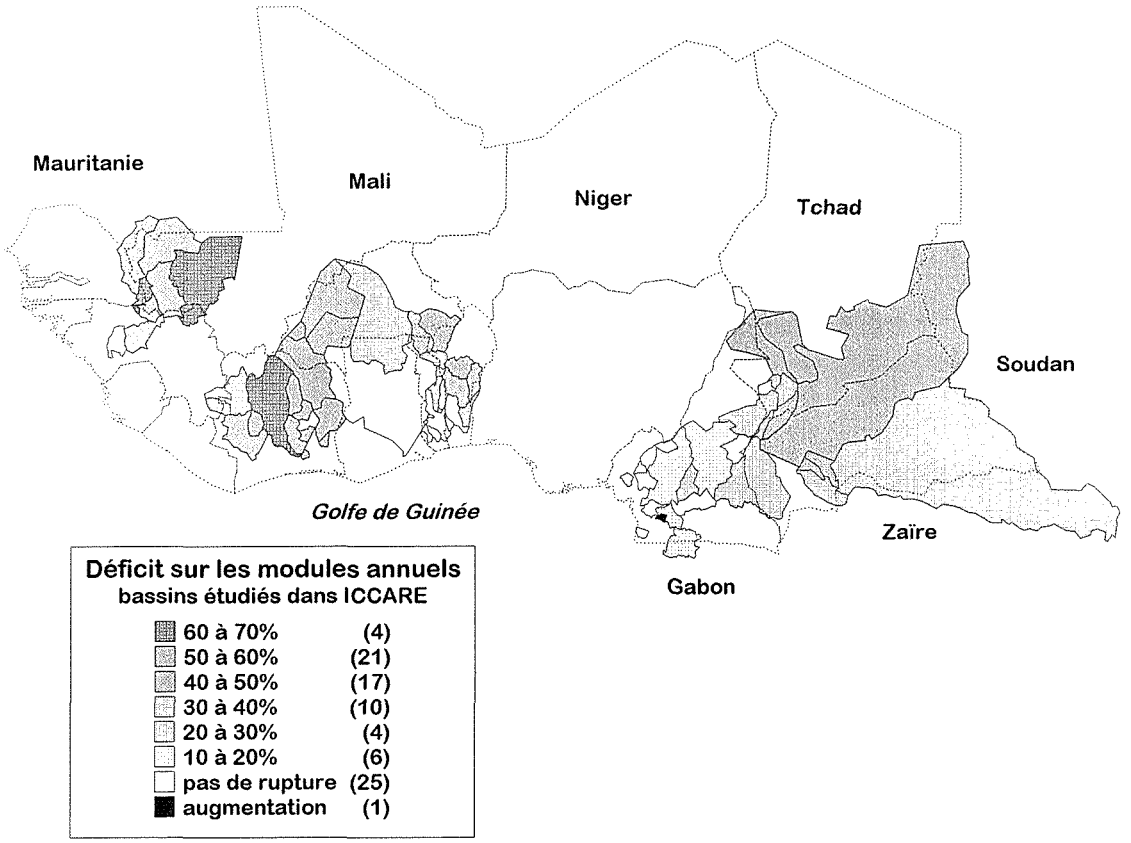

Fig. 3 Représentation cartographique des valeurs de déficits calculées de part et d'autre des dates de rupture dans les séries chronologiques de débits moyens annuels.

Autres variables caractéristiques des débits

Différents types de variables ont été définis qui concernent les débits de hautes eaux, et les débits de basses eaux:

(a) un ensemble de variables VCXn (avec n = 1, 5, 10, 20, 30, 60, 90), débits moyens maximum de n jours consécutifs,

(b) un ensemble de variables VCNn (avec n = 1, 5, 10, 20, 30, 60 voire 90 dans certains cas) débits moyens minimum de n jours consécutifs.

Le Tableau 2 regroupe certains des résultats obtenus pour les VCXn. D'une manière plus générale, pour l'ensemble des bassins étudiés, on notera que les différentes séries de VCXn présentent un caractère non aléatoire. Ce résultat suit parfaitement ceux obtenus pour les débits moyens annuels. Les dates de rupture obtenues à l'aide du test de Pettitt sont, elles aussi, très comparables à ce qui avait été obtenu pour les modules annuels et confirment que c'est durant la période 1969–1971 que cette variabilité a généralement été ressentie. L'importante corrélation qui existe d'ordinaire entre débits moyens annuels et débits maximums permet d'expliquer cette forte similarité.

L'exploitation des résultats obtenus pour les VCN*n* est plus complexe dans la mesure où, depuis la fin des années 1960 et le début des années 1970, bon nombre de cours d'eau se trouvent à sec sur des périodes relativement longues, ce qui n'était pas le cas auparavant. De même dans certaines régions (Cameroun en particulier), certains ouvrages ont été construits dans le but de soutenir les étiages, ce qui biaise les conclusions. En première analyse, on note, cependant, et dans la droite ligne de ce qui précède, que les débits de basses eaux ont également subi d'importantes modifications à la baisse décelables dans de nombreux cas durant la période 1969–1971. Une analyse plus approfondie de ces séries chronologiques de basses eaux est en cours. Elle sera complétée par une étude des tarissements et permettra, à court terme, de préciser au mieux l'ampleur de cette variabilité dans le domaine des basses eaux.

Tableau 1 Valeurs de déficits des débits moyens annuels calculés à certaines stations hydrométriques de part et d'autre de la date de rupture.

Nom station	Bassin	Rivière	A/NA	Rupture	Déficit
Mbasso	Comoe	Comoe	NA	1971	-50%
Aniassue Pont	Comoe	Comoe	NA	1971	-56%
Ndjamena	Lac Tchad	Chari	NA	1971	-51%
Bousso	Lac Tchad	Chari	NA	1971	-51%
Tchoa	Lac Tchad	Tandjile	NA	1971	-37%
Lai	Lac Tchad	Logone	NA	1970	-39%
Eseka	Nyong	Nyong	A	1971	-18%
M'Balmayo	Nyong	Nyong	A	Rien	Rien
Sagon	Oueme	Oueme	NA	1967	-42%
Logozohe-Pont	Oueme	Klou	A	Rien	Rien
Bakel	Sénégal	Sénégal	NA	1967	-50%
Fadougou	Sénégal	Falémé	NA	1967	-58%
Oualia	Sénégal	Bakoye	NA	1971	-66%
Bangui	Zaïre	Oubangui	NA	1970	-30%
Salo	Zaïre	Sangha	NA	1975	-22%
Doume	Zaïre	Doume	NA	Rien	Rien

Tableau 2 Présence et dates des ruptures détectées dans certaines des séries chronologiques de VCX.

Nom station	Bassin	Rivière	VCX1	VCX30	VCX90
Mbasso	Comoe	Comoe	1971	1971	1971
Aniassue Pont	Comoe	Comoe	1971	1971	1971
Ndjamena	Lac Tchad	Chari	1971	1971	1971
Bousso	Lac Tchad	Chari	1971	1971	1971
Tchoa	Lac Tchad	Tandjile	Rien	1970	1970
Lai	Lac Tchad	Logone	1971	1971	1970
Eseka	Nyong	Nyong	Rien	Rien	Rien
M'Balmayo	Nyong	Nyong	Rien	Rien	Rien
Sagon	Oueme	Oueme	1965	1967	Rien
Logozohe-Pont	Oueme	Klou	Rien	Rien	Rien
Bakel	Sénégal	Sénégal	1968	1972	1972
Fadougou	Sénégal	Falémé			
Oualia	Sénégal	Bakoye	1971	1971	1971
Bangui	Zaïre	Oubangui	1975	1970	1970
Salo	Zaïre	Sangha	1971	1975	1971
Doume	Zaïre	Doume	Rien	Rien	Rien

CONCLUSION

Cette étude montre que le déficit pluviométrique observé en Afrique de l'ouest et centrale depuis plus de vingt cinq ans a de sérieuses conséquences sur l'hydraulicité des cours d'eau des zones dites "humides" au sens large. Ces régions, situées au sud du 14° parallèle, et que l'on pensait épargnées par la sécheresse, présentent des déficits d'écoulement communément supérieurs à 30% et très souvent situés au delà de 50%. Les premières analyses effectuées sur le bassin du Niger sont parfaitement conformes à l'ensemble de ces résultats.

Hautes eaux et basses eaux ont subi d'importantes modifications à la baisse. Des analyses actuellement en cours viendront prochainement compléter les conclusions tirées de cette première exploitation des résultats. Elles porteront également sur des caractéristiques de forme des hydrogrammes et sur les tarissements.

Les conséquences de cette modification sur l'exploitation des ressources en eau et sur l'environnement sont évidentes. Les projets d'aménagement doivent désormais tenir compte de cette hydraulicité déficitaire. On ne citera que l'exemple du remplissage des réservoirs et du fonctionnement des installations qui leur sont liées et qui se révèlent parfois problématiques. L'impact sur la flore, comme sur la faune, de ces débits en baisse peut également se révéler important, et il convient donc d'intégrer dorénavant cette situation dans les études environnementales entreprises.

Remerciements Les auteurs souhaitent remercier Jean François Boyer pour son importante contribution à la réalisation des chaînes de traitement informatique des données.

REFERENCES

Hubert, P., Carbonnel, J. P. & Chaouche, A. (1989) Segmentation des séries hydrométriques. Application à des séries de précipitations et de débits de l'Afrique de l'Ouest. *J. Hydrol.* **110**, 349–367.

Lubès, H., Masson, J. M., Servat, E., Paturel, J. E., Kouamé, B. & Boyer, J. F. (1994) Caractérisation de fluctuations dans une série chronologique par applications de tests statistiques. *Etude Bibliographique; ORSTOM Montpellier.*

Paturel, J. E., Servat, E., Kouamé, B., Lubès, H., Ouedraogo, M. & Masson, J. M. (1996) Climatic variability in humid Africa along the Gulf of Guinea. Part two: An integrated regional approach. A paraître dans *J. Hydrol.*

Pettitt, A. N. (1979) A non-parametric approach to the change-point problem. *Appl. Statistics* **28**(2), 126–135.

Servat, E., Paturel, J. E. & Lubès, H. (1996) La secheresse gagne l'Afrique tropicale. *La Recherche*, n°290, septembre 1996.

FRIEND'97 — Regional Hydrology: Concepts and Models for Sustainable Water Resource Management
(Proceedings of the Postojna, Slovenia, Conference, September–October 1997). IAHS Publ. no. 246, 1997.

Etude de séries pluviométriques de longue durée en Afrique de l'ouest et centrale non sahélienne

J. E. PATUREL, E. SERVAT, M. O. DELATTRE
ORSTOM, Programme FRIEND AOC, 06 BP 1203 Cidex 1, Abidjan 06, Côte d'Ivoire

H. LUBES & J. M. FRITSCH
ORSTOM, Programme FRIEND AOC, BP 5045, F-34032 Montpellier Cedex, France

Résumé Dans les zones arides et semi-arides d'Afrique de l'ouest et centrale, la notion de précarité de la ressource en eau n'est pas récente. Cependant, la sécheresse qui affecte les régions tropicales africaines depuis les deux dernières décennies présente tout à la fois une sévérité, une persistance et une extension remarquables. Les séries pluviométriques annuelles enregistrées sur de longues durées sur un ensemble de stations couvrant l'Afrique de l'ouest et centrale non sahélienne (du Sénégal à la Centrafrique) ont permis d'étudier l'évolution spatio-temporelle de la pluviométrie dans cette région. Les résultats montrent l'alternance de périodes sèches et humides depuis le début du XXème siècle. La sécheresse actuelle n'a pas connu d'équivalent, ni en durée, ni en intensité, sur l'ensemble de la période étudiée. Une étude statistique, confirmée par des représentations cartographiques de ces différentes périodes, met, cependant, en évidence le caractère fortement hétérogène du phénomène dans l'espace.

INTRODUCTION

Le programme ICCARE (**I**dentification et **C**onséquences d'une variabilité du **C**limat en **AfR**ique de l'ouest non sah**E**lienne) s'inscrit dans le thème "Variabilité climatique et des ressources en eau", du projet FRIEND-AOC du PHI de l'UNESCO (Servat, 1994). Il a permis d'identifier une éventuelle fluctuation climatique en Afrique non sahélienne vers la fin des années 1960 et le début des années 1970. Cette évolution du climat se traduit par des changements notables au sein des séries chronologiques pluviométriques.

Il est cependant intéressant de chercher à situer la diminution de la pluviométrie observée depuis 25 ans dans la chronologie pluviométrique de ce siècle (Delattre, 1996).

La zone étudiée couvre 16 pays qui sont, de l'Afrique de l'ouest vers l'Afrique centrale, le Sénégal, la Gambie, la Guinée Bissau, la Guinée Conakry, la Sierra Leone, le Liberia, le Mali, le Burkina Faso, la Côte d'Ivoire, le Ghana, le Togo, le Bénin, le Nigeria, le Cameroun, le Tchad et la Centrafrique. Nous n'avons, cependant, considéré que la partie non sahélienne de cette zone, et notre étude s'est donc limitée au sud du 14ème parallèle.

L'analyse de longues séries chronologiques de pluviométries annuelles disponibles dans cette région a permis de resituer la sécheresse actuelle dans une perspective historique.

DONNEES ET METHODES

Données

Un grand nombre de postes pluviométriques ont été retenus afin de constituer une base de données annuelles pluviométriques la plus complète et la plus représentative possible de la zone d'étude du programme ICCARE. Les postes retenus, relevant de la gestion des différents services nationaux des pays concernés, obéissent à des critères de durée de l'information et de qualité des données. Le choix des postes s'est également effectué de manière à permettre une bonne couverture de la zone d'étude. Ont ainsi été retenus une centaine de postes avec des séries chronologiques qui remontent à plus de 60 ans de mesures annuelles. L'information la plus longue concerne les pays anglophones et remonte, parfois, au siècle dernier.

Méthodes

Nous avons traité la totalité de l'information contenue dans les séries chronologiques retenues. L'étude a été menée par l'application de tests statistiques de détection de "rupture" en moyenne des séries chronologiques de pluviométrie annuelle. "Rupture" doit être compris, ici, comme un changement dans la loi de probabilité de la série chronologique à un instant donné (Lubès *et al.*, 1994). Seuls les résultats du test de Pettitt (Pettitt, 1979) seront présentés dans cette étude.

Test de Pettitt Le test de Pettitt est non-paramétrique et dérive du test de Mann-Whitney. L'absence d'une rupture dans la série (x_i) de taille N constitue l'hypothèse nulle. Pettitt définit la variable $U_{t,N}$:

$$U_{t,N} = \sum_{i=1}^{t} \sum_{j=t+1}^{N} D_{ij}$$

où $D_{ij} = \mathrm{sgn}(x_i - x_j)$ avec $\mathrm{sgn}(Z) = 1$ si $Z > 0$, 0 si $Z = 0$ et -1 si $Z < 0$.

Il propose de tester l'Hypothèse nulle en utilisant la statistique K_N définie par le maximum en valeur absolue de $U_{t,N}$ pour t variant de 1 à $N - 1$.

A partir de la théorie des rangs, Pettitt montre que si k désigne la valeur de K_N prise sur la série étudiée, sous l'hypothèse nulle, la probabilité de dépassement de la valeur k est donnée approximativement par:

$$\mathrm{prob}(K_N > k) \approx 2\exp\left(\frac{-6k^2}{N^3 + N^2}\right)$$

Pour un risque α de première espèce donné, si la probabilité de dépassement estimée est inférieure à α, l'hypothèse nulle est rejetée. La série comporte alors une rupture localisée au moment τ où est observé K_N.

RESULTATS

Analyse statistique

Les résultats du test montrent qu'une rupture (équivalente à une diminution de la

pluviométrie annuelle dans le cas présent) au sein de la série chronologique s'observe majoritairement entre 1960 et 1979 avec un niveau de signification qui varie d'un poste à un autre. Le niveau de signification traduit ici l'importance réelle ou non d'un changement de la moyenne au sein de la série pluviométrique. On constate que, dans cinq cas uniquement, la rupture n'a pas été signalée durant cette période mais autour des années 1940. Il faut noter, également, que, pour six postes pluviométriques, le test révèle une augmentation de la pluviométrie annuelle. Ces six postes sont, cependant, isolés les uns des autres et leurs résultats ne traduisent donc en rien un comportement régional. Ils ne sont probablement que l'expression de sites dont les mesures sont peu fiables et qui ont été sélectionnés malgré les tests de qualité des données effectués.

Le Tableau 1 présente la probabilité associée à la statistique du test calculé pour chacun des postes. Un classement qualitatif a été effectué en tenant compte des valeurs de cette probabilité. Celles-ci ont été reportées sur une carte de la région étudiée (Fig. 1): le phénomène de déficit pluviométrique y apparaît plus marqué à l'ouest du cinquième méridien ouest et au nord des 8–10èmes parallèles nord. Ailleurs, ce phénomène est moins accentué.

Tableau 1 Probabilité associée au test de Pettitt—Rupture entre 1960 et 1979.

Probabilité associée	Classe	Dénombrement
$<1\%$	Rupture très significative	32
entre 1 et 5%	Rupture significative	10
entre 5 et 20%	Rupture peu significative	11
$>20\%$	Série homogène	32
$<5\%$	Excédent pluviométrique	6
$<1\%$	Rupture très significative en dehors de la période 1960–1979	5

Représentations graphiques et analyse cartographique

Sur la période 1925 (±5 ans)–1990, retenue comme période de référence car commune à tous les postes étudiés et présentant une forte densité d'information, nous avons, en outre, procédé à une étude cartographique. Pour chacun des postes pluviométriques, un indice pluviométrique a été calculé, défini comme une variable centrée réduite (Lamb, 1982):

$$(X_i - \overline{X}) / S$$

avec X_i: pluviométrie de l'année i; $\overline{X}$: pluviométrie moyenne interannuelle sur la période de référence; S: écart-type de la pluviométrie interannuelle sur la période de référence. Cet indice traduit un excédent ou un déficit pluviométrique pour l'année considérée par rapport à la période de référence choisie.

Les résultats ont été reportés en Fig. 2, en rangeant les stations par longitude croissante. On observe une succession de périodes déficitaires et excédentaires. Les dates indiquées ci-dessous ne sont données qu'à titre de repères chronologiques. En effet, ces fluctuations climatiques ne sont pas intervenues simultanément à une même date sur l'ensemble de la zone d'étude:

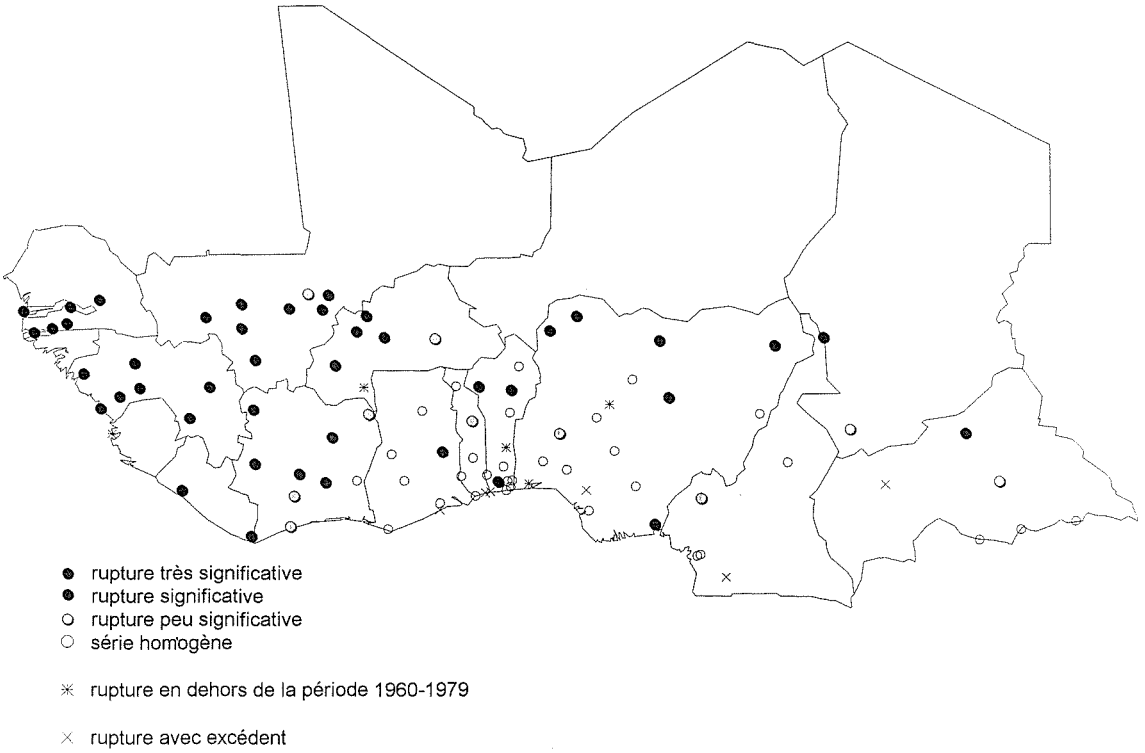

Fig. 1 Niveaux de signification des résultats du test de Pettitt.

(a) *La période 1936–1950 est déficitaire.* Ce caractère est plus marqué entre 0° et 4° de longitude est (Togo et Bénin) et il s'estompe de part et d'autre, en particulier à l'ouest;
(b) *La période 1951–1968 est excédentaire.* Ce caractère est plus marqué à l'ouest de la zone d'étude (ouest de la Côte d'Ivoire);
(c) *La période 1969-aujourd'hui est déficitaire.* Ce caractère s'observe sur l'ensemble de la zone, mais plus nettement à l'ouest (ouest de la Côte d'Ivoire).

Les résultats ont été reportés en Fig. 3 en rangeant les stations par latitude croissante. On y observe la même succession de périodes déficitaires et excédentaires que précédemment:
(a) la période 1936–1950 est déficitaire mais son caractère est peu marqué,
(b) la période 1951–1968 est excédentaire et son caractère est bien marqué,
(c) la période 1969-aujourd'hui est déficitaire et son caractère est très marqué au dessus des 8–10èmes parallèles.

La densité de l'information étant suffisamment importante, il a été possible de cartographier la moyenne par décennie des indices pluviométriques (Fig. 4). On observe alors:
(a) des zones ponctuellement déficitaires durant les décennies 1930 et 1940 (en particulier cette dernière); les valeurs des indices sont, cependant, faibles en valeur absolue,

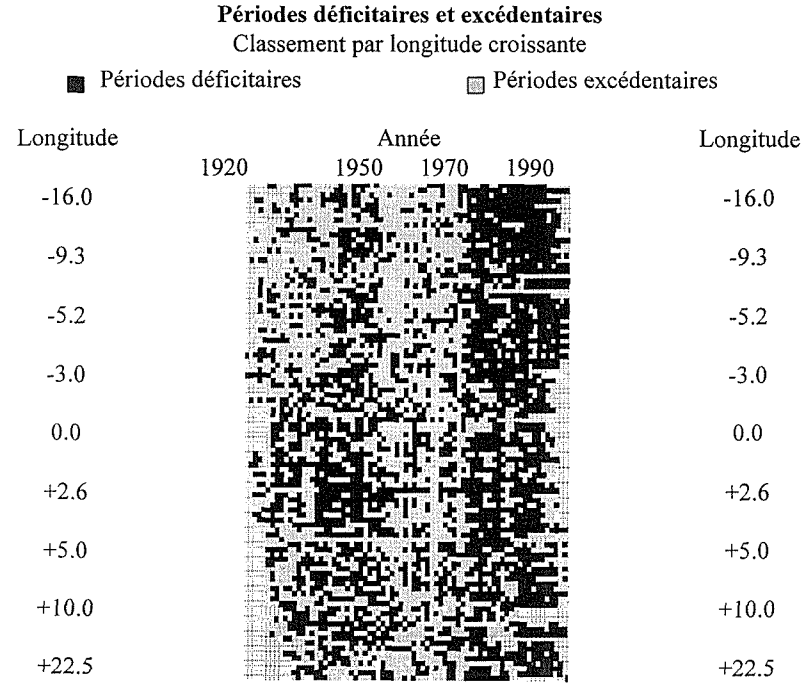

Fig. 2 Visualisation des périodes déficitaires et excédentaires en fonction de la longitude du poste de mesure.

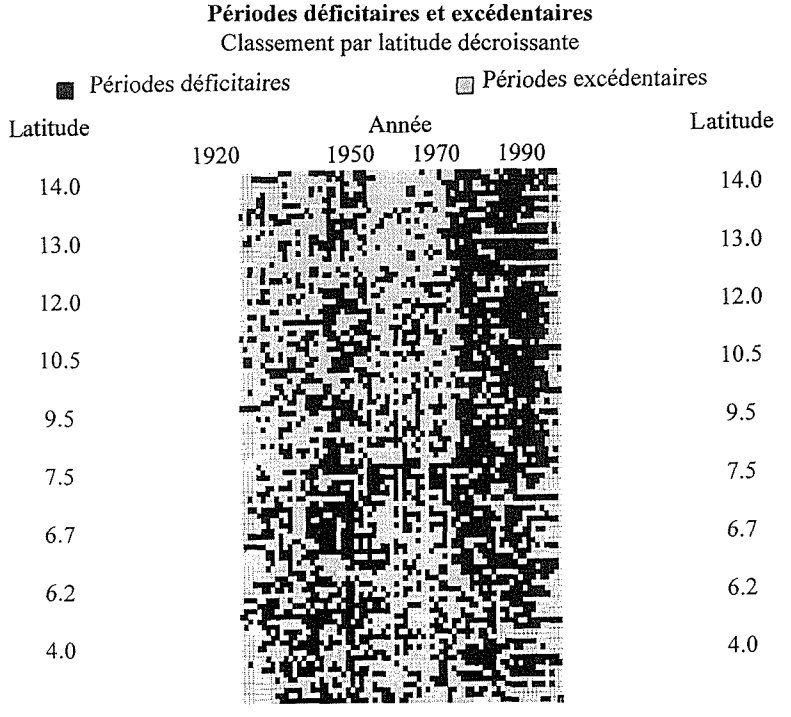

Fig. 3 Visualisation des périodes déficitaires et excédentaires en fonction de la latitude du poste de mesure.

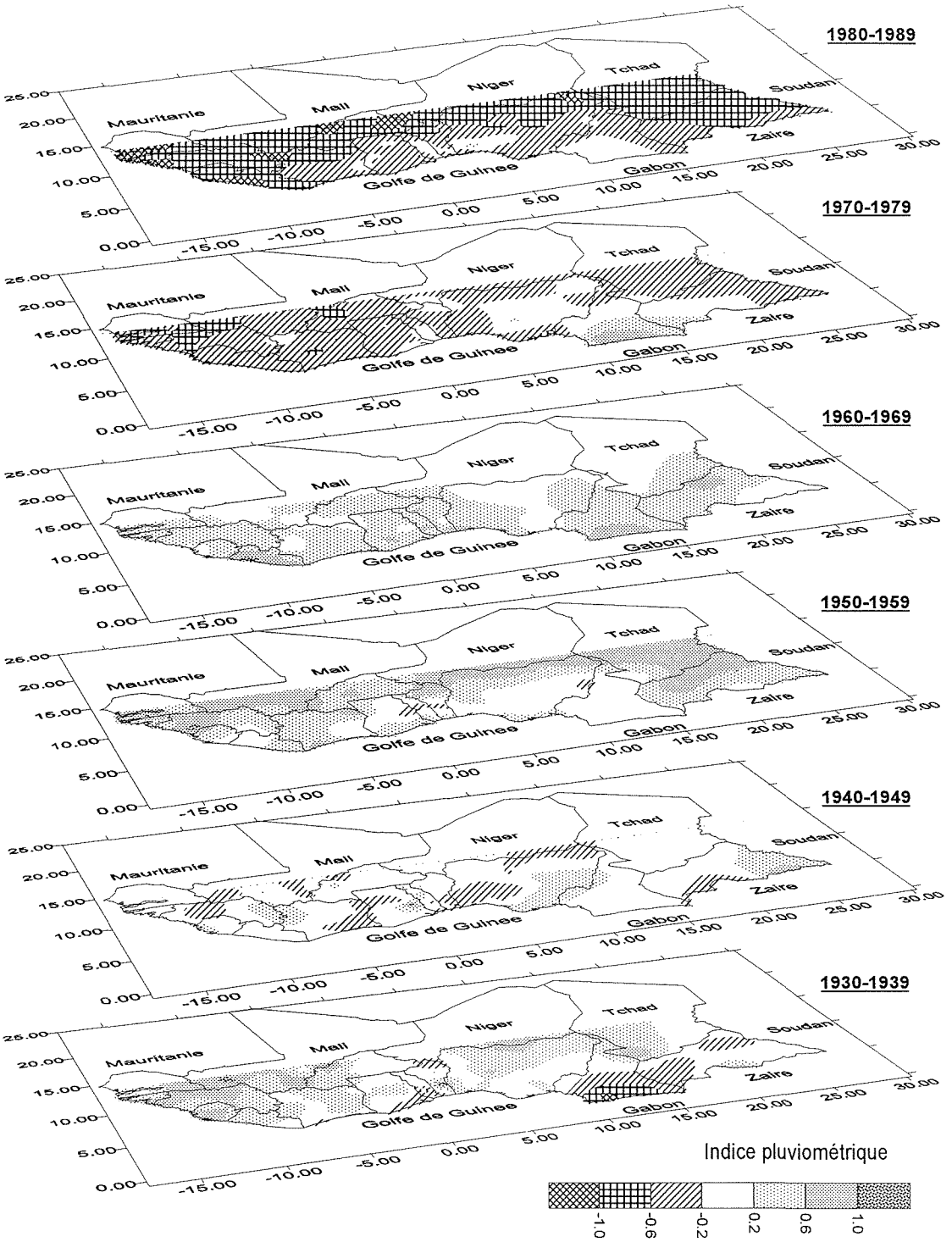

Fig. 4 Evolution des indices pluviométriques de la décennie 1930 à la décennie 1980.

(b) des zones excédentaires durant les décennies 1950 et 1960; ce caractère s'observe d'abord dans le nord puis se généralise à l'ensemble de la zone d'étude au cours de la décennie suivante,

(c) des zones déficitaires durant les décennies 1970 et 1980; ce caractère s'accentue au cours de la décennie 1980 et apparaît très marqué au nord du 10ème parallèle et à l'ouest du cinquième méridien ouest. Les valeurs des indices y sont beaucoup plus élevées qu'auparavant, en valeur absolue.

Ces différentes représentations montrent clairement l'alternance de périodes sèches et humides. L'examen des données antérieures à la période de référence choisie, et disponibles pour quelques pays seulement, révèle également une période déficitaire entre 1910 et 1922 ainsi qu'une période excédentaire entre 1922 et 1936. Cette alternance qui semble courante en Afrique de l'ouest et centrale ne constitue pas pour autant un cycle du fait de sa forte irrégularité.

Le test de Pettitt ne peu détecter qu'une seule rupture. Pour la région étudiée, il semble privilégier très nettement celle survenue autour de l'année 1970, soulignant ainsi l'importance de cette dernière variabilité au regard des séries chronologiques historiques disponibles.

CONCLUSION

Cette étude montre qu'au cours de ce siècle, l'Afrique de l'ouest et centrale a connu une succession de périodes à déficits et de périodes à excédents pluviométriques sans, toutefois, pouvoir parler de cycle. La fluctuation la plus brutale et la plus significative (au sens statistique du terme) est observée autour des années 1970, au cours desquelles on note une diminution généralement assez importante de la pluviométrie annuelle.

Cette période déficitaire se caractérise, depuis lors, par son intensité et sa durée. A l'est, ce phénomène ne semble s'inscrire que dans l'histoire des variations "normales" des séries chronologiques sans revêtir le caractère d'exception que l'on observe plus à l'ouest et au nord.

Il est probable que les activités humaines ont très certainement contribué à accroître ce phénomène de sécheresse. On peut citer l'exemple de la déforestation dans de nombreuses régions du Golfe de Guinée durant ces dernières décennies. Elle y a pris une ampleur considérable qui, même si elle ne peut être considérée comme la principale cause de cette sécheresse, ne peut pas être étrangère à la diminution de la pluviométrie annuelle.

REFERENCES

Delattre, M. O. (1996) Evolution climatique en Afrique de l'ouest et centrale non sahélienne. *Rapport de Stage de fin d'Etudes*, ISIM-Montpellier, ORSTOM, Abidjan.

Lamb, P. J. (1982) Persistence of Subsaharan drought. *Nature* **299**(September), 46–47.

Lubès, H., Masson, J. M., Servat, E., Paturel, J. E., Kouamé, B., Boyer, J. F. (1994) Caractérisation de fluctuations dans une série chronologique par application de tests statistiques—Etude bibliographique. *ORSTOM, Montpellier, Programme ICCARE, Rapport no. 3.*

Pettitt, A. N. (1979) A non-parametric approach to the change-point problem. *Appl. Statistics* **28**(2), 126–135.

Servat, E. (1994) ICCARE. Identification et Conséquences d'une variabilité du Climat en AfRique de l'ouest non sahélienne—Présentation du programme. *ORSTOM, Abidjan, Côte d'Ivoire, Programme ICCARE, Rapport no. 1.*

FRIEND'97 — Regional Hydrology: Concepts and Models for Sustainable Water Resource Management
(Proceedings of the Postojna, Slovenia, Conference, September–October 1997). IAHS Publ. no. 246, 1997.

Variations spatio-temporelles des régimes pluviométriques et hydrologiques en Afrique Centrale du début du siècle à nos jours

A. LARAQUE, J.-C. OLIVRY
Centre ORSTOM, Laboratoire d'Hydrologie, BP 5045, F-34032 Montpellier Cedex 1, France

D. ORANGE & B. MARIEU
Centre ORSTOM, LECOM, BP 84, Bamako, Mali

Résumé Une segmentation statistique sur la deuxième moitié du XXème siècle des chroniques hydropluviométriques des affluents de rive droite du Congo-Zaïre, montre que les ruptures dans les séries pluviométriques sont moins franches et moins nombreuses que celles des séries hydrologiques. Ces dernières s'accordent avec les quatre principales phases d'écoulement du Congo-Zaïre qui dispose d'une chronique hydrométrique séculaire. Ce fleuve a connu du début du siècle à 1960, une phase dite normale ou stable, une phase humide ou d'écoulement excédentaire durant la décennie 1960, puis à partir de 1971, deux phases de baisses successives de ses écoulements, la seconde de 1982 à nos jours étant plus accentuée avec une diminution de 10% de son module interannuel. C'est toute la portion septentrionale de son bassin qui a le plus souffert de l'actuelle péjoration climatique avec une baisse de régime de plus de 30% pour l'Oubangui.

INTRODUCTION

Afin d'approfondir la connaissance et la compréhension du fonctionnement hydroclimatique du bassin du Congo-Zaïre, à la suite des travaux de Nicholson *et al.* (1988), Sircoulon (1987), Hubert *et al.* (1989), Hubert & Carbonnel (1993), Olivry *et al.* (1993), Mahé (1993), Mahé & Olivry (1995), nous comparons, à partir d'une étude régionale portant sur ses sous bassins de rive droite, les variations spatio-temporelles de leurs écoulements et précipitations au cours de ce siècle.

Nous avons ainsi recherché pour chacun d'entre eux, les ruptures séparant les phases homogènes de leurs chroniques hydrométéorologiques. En nous basant sur les époques des segmentations hydrologiques du Congo-Zaïre et de l'Oubangui qui sont celles les plus couramment rencontrées dans cette zone géographique, nous avons comparé entre elles les amplitudes de ces phases homogènes, pour tous ces affluents. Cela nous a permis de définir les zones les plus sensibles à ces fluctuations.

REGION ETUDIEE, DONNEES ET METHODOLOGIE

Les bassins des affluents congolais de rive droite (Oubangui, Sangha, Likouala aux Herbes, Likouala Mossaka, Alima, Nkéni, Léfini) dont les embouchures au fleuve arrivent entre la ville zaïroise de Mbandaka et celle de Brazzaville au Congo,

couvrent près d'un million de km^2 (Fig. 1 et Tableau 1), dont 73% de la surface sont contrôlés par des stations hydrométriques.

A partir des données d'environ 250 postes pluviométriques et grâce à une chaîne de traitement automatisée (Mahé *et al.*, 1994), il a été possible de calculer pour chacun d'entre eux, les lames précipitées annuelles de 1951 jusqu'à 1993, excepté pour l'ensemble du bassin du Congo-Zaïre où les calculs se sont arrêtés en 1989 (Mahé & Olivry, 1995). Quant aux chroniques hydrologiques des cours d'eau étudiés, elles débutent aussi vers 1950, excepté pour le Congo-Zaïre à Brazzaville-Kinshasa et l'Oubangui à Bangui, son deuxième affluent, où elles remontent respectivement à 1903 et 1936 (Laraque & Maziezoula, 1995; Wesselink *et al.*, 1996).

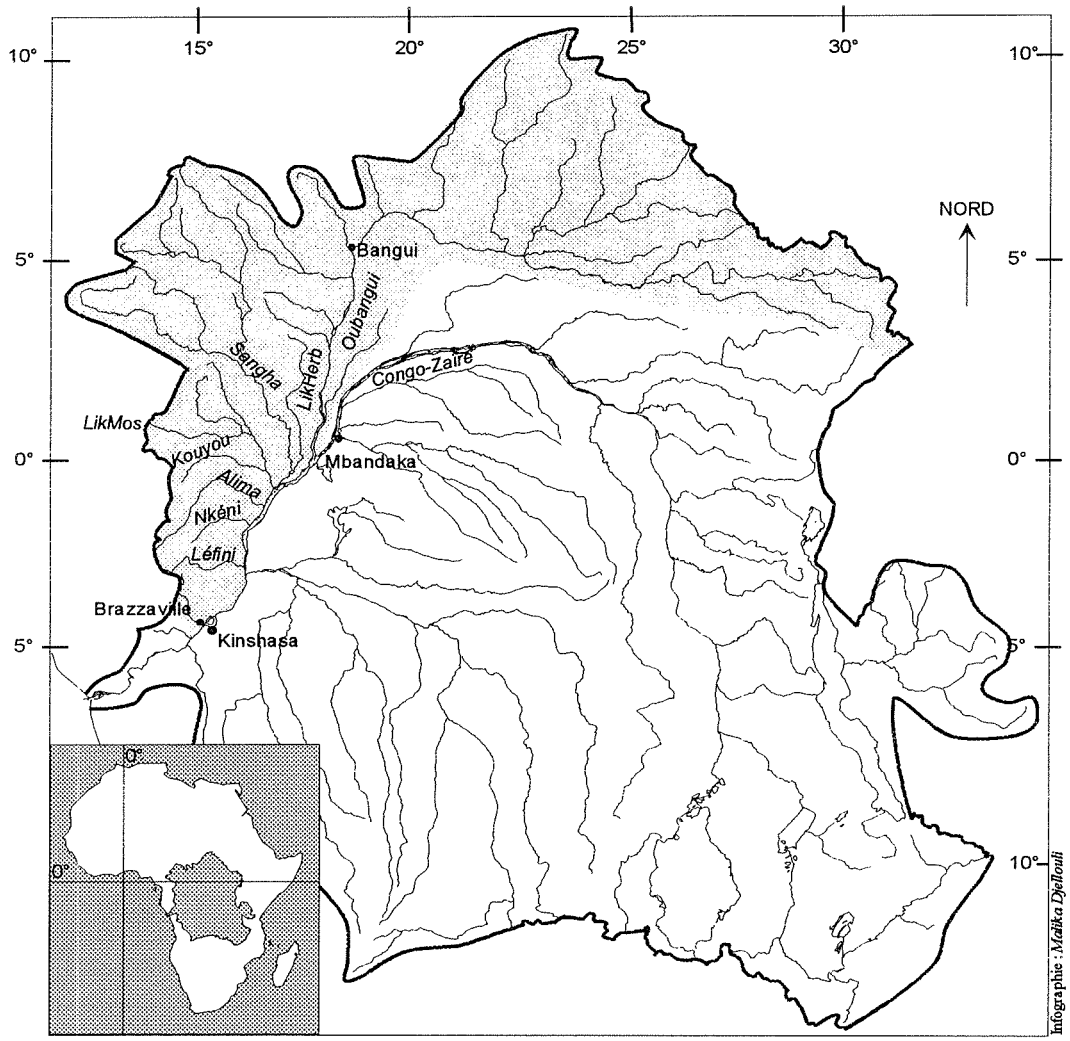

Fig. 1 Présentation des cours d'eau étudiés du bassin du Congo-Zaïre.

Sur chaque série chronologique de ces bassins, nous avons utilisé de manière systématique, quatre tests statistiques de détection de ruptures grâce aux procédures automatiques du logiciel Statisti (Lubès *et al.*, 1995). Il s'agit des tests de "Buishand", de "Pettitt", de la méthode "Bayésienne de Lee-Heghinian" et de la "segmentation de Hubert".

RESULTATS ET DISCUSSIONS

Le Tableau 1 présente les moyennes des lames précipitées et écoulées pour chaque segmentation stationnaire. On constate que les ruptures supposées des séries pluviométriques sont moins fréquentes et moins prononcées que celles des séries hydrologiques et que les dates d'apparition des premières précèdent en général d'un à trois ans, celles des secondes, aux exceptions près de la Sangha, dont la seule rupture pluviométrique de 1974 est postérieure à la rupture hydrologique de 1970, et de la Likouala aux Herbes, dont la rupture pluviométrique de 1982 se situe au milieu d'une phase d'écoulement déficitaire pourtant homogène.

La pluviométrie du bassin oubanguien est la première à diminuer de 3.2% en 1960, alors que pour tous les autres bassins, ce fléchissement se situe près de 10 ans

Tableau 1 Segmentation statistique* des séries hydropluviométriques annuelles (1951–1993) des sous bassins de rive droite du Congo-Zaïre.

Bassins versant	Stations hydro-métriques	Super-ficies (km^2)	Modules interannuels ($m^3 s^{-1}$)	Segmentation des pluies (mm)	Segmentation des écoulements (mm)
Oubangui	Bangui	488 500	3800 (1936–1993: 3900)	1951–1960: 1482 1961–1992: 1434	1936–1959: 270 1960–1970: 315 1971–1982: 230 1983–1993: 175
Sangha	Ouesso	158 300	1600	1951–1973: 1604 1974–1993: 1511	1948–1970: 360 1971–1993: 290
Likouala-aux-Herbes	Botouali	24 800	280	1951–1981: 1750 1982–1993: 1622	1949–1959: 290 1960–1970: 460 1971–1993: 335
Likouala Mossaka	Makoua	14 100	220	1951–1993: 1689	1953–1981: 503 1982–1993: 420
Kouyou	Owando	10 100	215	1951–1969: 1725 1970–1985: 1654 1986–1993: 1566	1952–1993: 575
Alima	Tchikapika	20 070	590	1951–1957: 1762 1958–1969: 1803 1970–1993: 1709	1952–1960: 860 1961–1971: 975 1972–1993: 915
Nkéni	Gamboma	6 200	200	1951–1957: 1731 1958–1969: 1802 1970–1993: 1662	1952–1993: 965
Léfini	Bwembé	13 500	420	1951–1993: 1616	1952–1993: 871
Congo–Zaïre	Brazzaville	3 500 000	40 600 (1936–1993: 40 300)	1951–1969: 1600 1970–1989: 1528	1902–1959: 355 1960–1970: 435 1971–1981: 375 1982–1993: 335

* Les ruptures indiquées sont les résultats significatifs de l'ensemble des tests du logiciel STATISTI.

plus tard avec des baisses variant de 2.5 à 8%. L'ensemble du bassin Congo-Zaïrois a vu, quant à lui, sa moyenne pluviométrique diminuer de 4.5% entre les périodes 1951–1969 et 1970–1989, en passant de 1600 à 1528 mm an^{-1}.

A l'image de la couverture pluviométrique, les débits moyens annuels des affluents rive droite, présentent également des variations spatio-temporelles, que nous commenterons à partir de celles, concomitantes, des deux principaux cours de l'Oubangui et du Congo-Zaïre. Entre 1936 et 1993, le premier présente quatre phases d'écoulements qui se superposent, cependant, avec de plus fortes amplitudes, à celles déjà signalées par Hubert & Carbonnel (1993) sur la chronique séculaire du second (Fig. 2(a) et (b)). Pour chacune de ces séries, ces phases se répartissent en deux grandes périodes, avec respectivement pour ces deux cours d'eau, des débits moyens interannuels de 4200 et 39 600 $m^3 s^{-1}$ sur la première moitié du siècle dite stable, puis pour la deuxième moitié, dite "instable", les écoulements montrent des oscillations chevauchant pratiquement les décennies calendaires. On peut distinguer une sous période "humide" entre 1960 et 1970 présentant respectivement des accroissements de 17 et 21% (soit 4900 et 48 000 $m^3 s^{-1}$). Ensuite, ce dernier connaît un retour à la "normale" entre 1971 et 1981 avec 41 400 $m^3 s^{-1}$ (soit une baisse de 14%), valeur proche de celle de la première phase et enfin à partir de 1982 une période véritablement déficitaire, avec une nouvelle baisse de 10% amenant ses écoulements interannuels à 37 500 $m^3 s^{-1}$. Par contre, pour l'Oubangui, la période

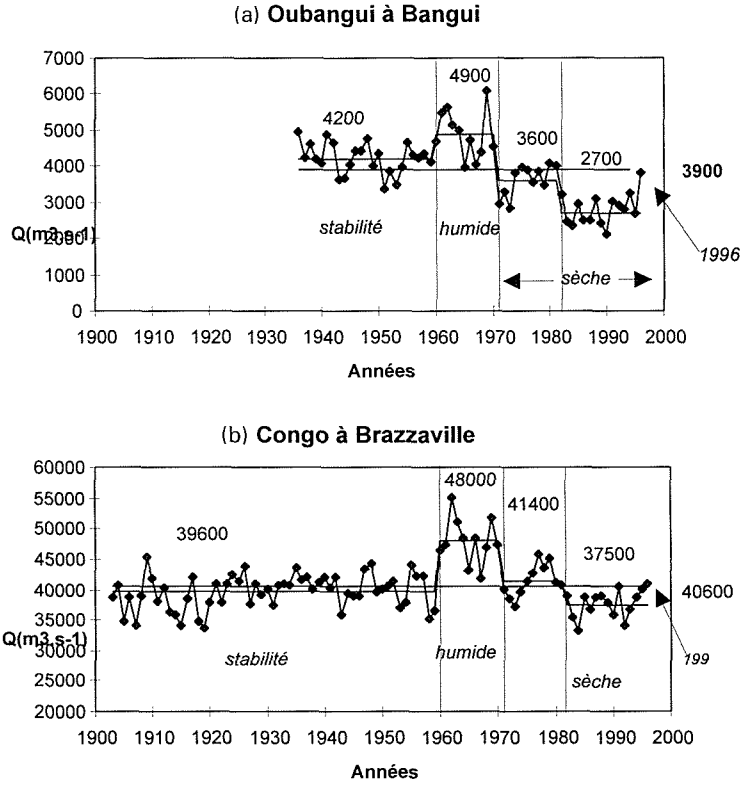

Fig. 2 Segmentation des chroniques des modules de l'Oubangui et du Congo-Zaïre.

"sèche" débute brutalement après la période humide 1960–1970, avec une chute de 26% de son module interannuel, puis s'accentue gravement à partir de 1982 avec de nouveau une baisse de 25% par rapport à la période précédente. Ainsi par rapport à leur période "stable" commune (1936–1959), la période actuelle (depuis 1982), a connu une baisse d'écoulement de près de 36% (Orange *et al.*, 1996) pour l'Oubangui contre 7.7% pour le Congo-Zaïre.

Il est à signaler pour le bassin du Congo-Zaïre, que les périodicités hydrométriques quasi décennales relativement contrastées de la deuxième moitié du siècle, qui ont succédées à une relative stabilité des écoulements durant sa première moitié, ont également été remarquées sur les fluctuations climatiques survenues ces trente dernières années sur toute sa partie zaïroise (ou versant gauche), par Kazaki & Kaoru (1996).

La Fig. 3 permet, à partir de cinq affluents de rive droite, caractéristiques des différentes régions physiographiques traversées, et par rapport aux modules interannuels de leur période d'observation commune (1951–1993), de comparer leurs variations d'hydraulicité sur les segmentations homogènes de référence régionale que sont celles de l'Oubangui et du Congo-Zaïre. C'est à partir de 1970, que pratiquement toutes les hydraulicités deviennent inférieures à l'unité. Cette décennie 1970 légèrement déficitaire, semble présenter une véritable "charnière", entre deux autres, d'hydraulicités symétriques mais opposées. En effet, la décennie 60 est excédentaire avec des valeurs variant de 1.04 à 1.3, et celle de 80, franchement déficitaire avec des variations de 0.72 à 0.99 suivant les cours d'eau. En fait, les plus faibles variations d'hydraulicité concernent les cours d'eau des plateaux Tékés avec soit aucune rupture statistiquement détectable (cas de la Nkéni et de la Léfini), soit des variations très proches de l'unité, illustrées par l'Alima avec successivement 0.93; 1.05 et 1 pour les périodes 1951–1960; 1961–1971 et 1972–1993. Pour ces dernières rivières, c'est l'immense aquifère sablo-gréseux constituant leur bassin versant qui semble à l'origine de la remarquable régulation interannuelle de leur régime (Laraque & Pandi, 1996), au point "d'effacer" les deux ruptures pluviométriques de 1957 et 1969 qui les affectent.

Enfin, pour l'Afrique Centrale, la phase hydroclimatique la plus importante par son amplitude, apparaît être la période "humide" 1960–1970, où les variations d'écoulement par rapport aux moyennes interannuelles des séries étudiées, ont toujours été supérieures à celles de la phase 1982–1993, la plus déficitaire. Ceci est confirmé par les fluctuations des modules interannuels de la période 1960–1970 du Congo-Zaïre

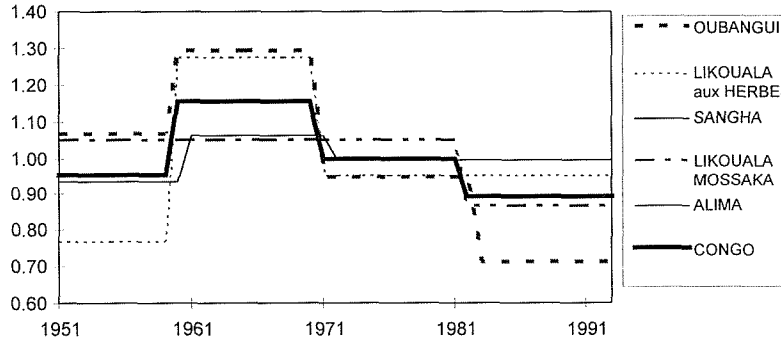

Fig. 3 Segmentation des hydraulicités de quelques cours d'eau caractéristiques.

(+20%), contre –7.6% pour 1982–1993 par rapport à celui de sa chronique séculaire.

Mais c'est bien cette persistante phase d'écoulement déficitaire enregistrée depuis 1970 et qui s'est accentuée à partir de 1982 qui est le fait marquant de ce siècle de par sa durée. A l'échelle du bassin du Congo-Zaïre, l'Oubangui en est le symbole, avec sur ses soixante années d'observations, un record d'amplitude (–31%), qui en fait son accident hydroclimatique majeur. Pour ce cours d'eau, il devance par son intensité, sa "phase humide" qui elle, n'a enregistré qu'une croissance de +25.5% de ses écoulements. Cette période sèche actuelle semblerait depuis 1993, s'achever progressivement, avec un retour à la « normale » des écoulements du Congo-Zaïre et de l'Oubangui, qui viennent juste en 1996, de retrouver leurs modules interannuels après respectivement quinze et six années d'écoulements déficitaires (Fig. 2).

Pourtant dans ce contexte apparemment favorable à la reprise des écoulements, la Sangha, deuxième affluent de rive droite, apporte une note de discordance avec une année 1996 fortement déficitaire. Son module de 1250 $m^3 s^{-1}$ dont la période de retour de 20 ans, la place pour cette seconde moitié de siècle, en deuxième position des modules les plus faibles après celui de 1983. Cela souligne bien l'hétérogénéité spatiale des phénomènes hydropluviométriques à l'échelle d'un bassin comme celui du Congo-Zaïre.

CONCLUSION

Après une grande régularité interannuelle durant la première moitié du siècle, la diminution des écoulements enregistrée sur le Congo-Zaïre depuis 1971 est cependant à nuancer. Durant la décennie 1970, on assiste en fait à leur retour à la normale après les années 60 fortement excédentaires. La baisse significative de son régime ne prend effet qu'au début des années 80 avec une diminution de 7.6% de son module interannuel, par rapport à la moyenne de toute sa chronique.

Les ruptures à la fois pluviométriques et hydrométriques les plus couramment rencontrées pour tous les bassins étudiés en Afrique Centrale sont celles de 1970 (±2 ans), qui coïncident avec l'accident hydroclimatique majeur déjà bien décrit en Afrique Occidentale (Sircoulon, 1987; Hubert *et al.*, 1989; Olivry, 1993; Aka *et al.*, 1996). L'Afrique Centrale a ainsi connue des baisses d'écoulement variant de quelques pour cent à plus de 30% suivant les bassins, sans relations spatio-temporelles apparentes avec des fluctuations pluviométriques bien plus faibles de 2 à 8%.

Cela atteste de la complexité des processus de réponse des écoulements aux précipitations, qui au sein de chaque sous bassin, doit intégrer en fonction de leur physiographie propre, des effets de mémorisation à l'échelle pluriannuelle à la fois des précipitations antérieures, comme des modifications des états de surface ou des relations rivières–aquifères. Si la situation d'Afrique Centrale est moins grave que celle d'Afrique Occidentale, elle nécessite cependant de revoir certaines options de gestion des ressources hydriques, comme notamment, le projet de relier par un canal, l'Oubangui au lac Tchad, pour combler le déficit hydrique de ce dernier.

Remerciements Nous remercions l'équipe ORSTOM du programme ICCARE pour la mise à disposition du logiciel STATISTI.

REFERENCES

Aka, A., Kouamé, B., Paturel, J. E., Servat, E., Lubès, H. & Masson, J. M. (1996) Analyse statistique de l'écoulement en Côte d'Ivoire. In: *L'hydrologie tropicale: géoscience et outil pour le développement—mélanges à la mémoire de Jean Rodier* (ed. par P. Chevallier & B. Pouyaud) (Actes de la conférence de Paris, mai 1995), 167–177. IAHS Publ. no. 238.

Hubert, P. & Carbonnel, J. P. (1993) Segmentation des séries annuelles de débits des grands fleuves africains. *Bull. de liaison du CIEH no. 92, Ouagadougou, Burkina Faso*, 3–10.

Hubert, P., Carbonnel, J. P. & Chaouch, A. (1989) Segmentation des séries hydrométéorologiques—application à des séries de précipitations et de débits de l'Afrique de l'Ouest. *J. Hydrol.* **110**, 349–367.

Kazaki, S. N. & Kaoru, F. (1996) Interannual and long term climate variability over the Zaïre River basin during the last 30 years. *J. Geophys. Res.* **101**(D16), 351–360.

Laraque, A. & Maziezoula, B. (1995) Banque de données hydrologiques des affluents congolais du fleuve Congo-Zaire et informations physiographiques. Rapport interne, Lab. Hydrol. ORSTOM, Montpellier.

Laraque, A. & Pandi, A. (1996) Rôle des données physiographiques dans la classification hydrologique des affluents congolais du fleuve Congo-Zaïre. *C. R. Acad. Sci. Paris* **323**, série IIa, 855–858.

Lubés, H., Aka, A., Masson, J. M., Servat, E., Paturel, J. E. & Kouamé, B. (1995) Essai de mise en évidence d'une variation climatique par application de test statistiques à des séries chronologiques de débit. Application aux grands fleuves de Côte d'Ivoire. In: *Statistical and Bayesian Methods in Hydrological Sciences* (Proc. International Conference in honour of J. Bernier, septembre 1995). UNESCO, Paris.

Mahé, G. (1993) Les écoulements fluviaux sur la façade atlantique de l'Afrique. Etude des éléments du bilan hydrique et variabilité interannuelle. Analyse de situations hydroclimatiques moyennes et extrêmes. Thèse de doctorat, Collection Etudes et Thèses, ORSTOM Paris.

Mahé, G., Delclaux, F. & Crespy, A. (1994) Elaboration d'une chaîne de traitement pluviométrique et application au calcul automatique de lames précipitées (bassin versant de l'Ogoué au Gabon). *Hydrol. Continent.* **9**(2), 169–180.

Mahé, G. & Olivry, J. C. (1995) Variations des précipitations et des écoulements en Afrique de l'Ouest et centrale de 1951 à 1989. *Rev. Sécher.* **6**(1), 109–117.

Nicholson, S. E., Kim, J. & Hoopingarner, J. (1988) *Atlas of African rainfall and its Interannual Variability*. Dept Meteorology, Florida State University, Tallahassee, Florida, USA.

Olivry, J. C. (1993) Evolution récente des régimes hydrologiques des grands fleuves d'Afrique de l'ouest et centrale—les écosystèmes tropicaux, fonctionnement et usages. *Journées du programme Environnement CNRS/ORSTOM, 13, 14, 15, Lyon*, janvier 1993.

Olivry, J. C., Bricquet, J. P. & Mahé, G. (1993) Vers un appauvrissement durable des ressources en eau de l'Afrique humide? In: *Hydrology of Warm Humid Regions* (ed. par J. S. Gladwell) (Proc. Yokohama Symp., juillet 1993), 67–78. IAHS Publ. no. 216.

Orange, D., Feizouré, C., Wesselink, A. J. & Callède, J. (1996) *Variabilités hydrologiques de l'Oubangui à Bangui au cours du XXième siècle* (Actes de la réunion FRIEND A.O.C., Cotonou, Bénin, décembre 1995) (sous presse). UNESCO, Paris.

Sircoulon, J. (1987) Variations des débits des cours d'eau et des niveaux des lacs en Afrique de l'Ouest depuis le 20ième siècle. In: *The Influence of Climate Change and Climatic Variability on the Hydrologic Regime and Water Resources* (ed. par S. I. Solomon, M. Beran & W. Hogg) (Proc. Vancouver Symp., août 1987), 13–25. IAHS Publ. no. 168.

Wesselink, A. J., Orange, D., Feizouré, C. & Randriamiarisoa (1996) Les régimes hydroclimatiques et hydrologiques d'un bassin versant de type tropical humide: l'Oubangui (République Centrafricaine). In: *L'hydrologie tropicale: géoscience et outil pour le développement—mélanges à la mémoire de Jean Rodier* (ed. par P. Chevallier & B. Pouyard) (Actes de la conférence de Paris, mai 1995), 179–194. IAHS Publ. no. 238.

7 Hydrological Extremes: *Flood Frequency*

FRIEND'97 — Regional Hydrology: Concepts and Models for Sustainable Water Resource Management
(Proceedings of the Postojna, Slovenia, Conference, September–October 1997). IAHS Publ. no. 246, 1997.

Non-stationary regimes: the QdF models behaviour

CHRISTEL PRUDHOMME
Institute of Hydrology, Wallingford, Oxfordshire OX10 8BB, UK

GILLES GALEA
Cemagref, 3 bis quai Chauveau, F-69336 Lyon Cedex 09, France

Abstract One of the main goals of hydrological studies is to improve our knowledge of river flood behaviour in the medium term (at least 100 years). QdF models mix regional and local information to return frequency distributions of threshold maximum discharge and mean maximum discharge for duration from instantaneous to one month and for return periods from 0.5 to 1000 years. The local hydrological descriptors used represent the production function and the transfer function of the studied catchment. To test the robustness of the QdF models in case of flood regime change, four catchments whose general flood regime in terms of the frequency distribution is non-stationary have been considered, and one of them has been chosen for a complete study. Despite the non-stationarity of the records, the use of local input parameters, representative of the regime of each given time period, enables the QdF models to produce the frequency distributions for each time period.

INTRODUCTION

Synthetic models such as Discharge–duration–Frequency models (QdF models) are based on statistical analysis of floods to estimate floods for given occurrence probabilities (Galéa & Prudhomme, 1994); they are thus series-dependent. The question is to know how they behave for non-stationary regimes. Four basins with daily discharge recorded from the beginning of the century have been studied.

(a) The stationarity of the records is studied and one catchment is selected;
(b) statistical analysis is done for different periods considered as stationary, and for the entire non-stationary period.

The frequency distributions fitted on the experimental distribution for each of the periods are compared to QdF ones. If there is a correspondence, QdF models will be considered as applicable for hydrological regimes different (in terms of frequency distribution) from the one for which they have been fitted.

PRESENTATIONS OF THE BASINS AND TEST OF STATIONARITY

Four basins situated in France in the AMHY zone have been selected. Table 1 presents the length of the records (Peak Over Threshold—POT—records or daily discharge), the administrative area and the main influence for the hydrological regime. For each basin, a POT sampling was undertaken on the instantaneous records and on daily discharge. A detailed presentation of the sampling method is

Table 1 Basin and record details.

Basin	Area (km^2)	Record periods: $Q(t)$[a]	QD[b]	Hydrological regime
Isolles at St Andre les Alpes	137	1981–1993	1904–1991	Alpes de Haute Provence—rain and snow
Ubaye at Barcelonette	549	1981–1993	1904–1993	Alpes de Haute Provence—snow
Drôme at Luc en Diois	194	1981–1991	1907–1991	Drôme—rain regime
Fier at Dingy	222	1981–1993	1906–1991	Haute Savoie—karst basin—rain and snow

[a] Instantaneous discharge.
[b] Daily discharge.

given in Lang (1995) and Galéa & Prudhomme (1997). For the Ubaye at Barcelonette, a new independence has been used for the POT selection, because of the short-term dependence of discharge data when the snow melts. Two stationarity tests have been used.

Simple accumulation

For the Ubaye at Barcelonette, the regime seems homogeneous: there is no significant difference between theoretical and experimental curves. For Drôme at Luc en Diois (Fig. 1) and Issoles at St Andre les Alpes, a main break appears (decrease of the daily discharge after the break), respectively in the early 1940s and around 1964. For Issoles, the important number of missing records between 1937 and 1959 does not seem to affect the stationarity test. The Fier basin shows a more complex behaviour, with two main breaks in 1940 and 1962.

Tolerance interval

A stationarity test has recently been proposed by Lang (1995), which allows the verification of the stationarity assumption for a POT series. It computes the tolerance interval of the number of events observed during a time interval. If the occurrence

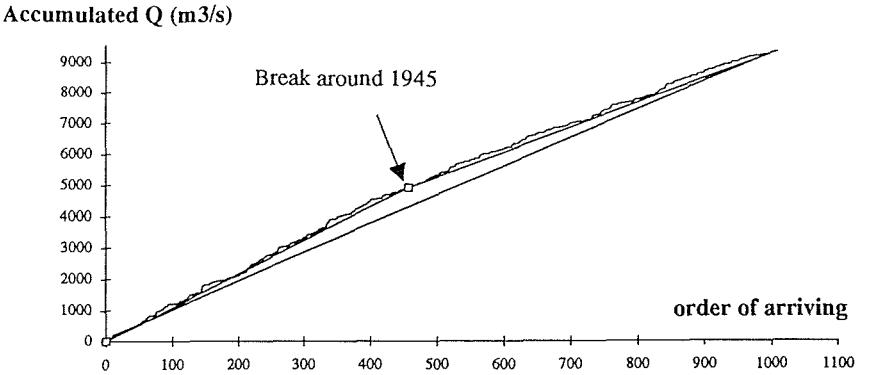

Fig. 1 Simple accumulation test- Drôme at Luc en Diois.

process is time-stationary and follows a Poisson law, one can show that the conditional probability to have k floods in the time interval $(0;t)$, if there are NC floods during $(0;t_{fin})$ is (Lang, 1995):

$$w_k^*(t) = C_{NC}^k \left(\frac{t}{t_{fin}}\right)^k \left(1 - \frac{t}{t_{fin}}\right)^{NC-k} \quad (1)$$

The 90% tolerance interval of the variable m_t (number of floods during a time interval $(0;t)$) is:

$$\text{prob}[m_t^- < m_t < m_t^+] = 0.90 \quad (2)$$

with

$$\Sigma_{k=0}^{m_t^-} w_k^*(t) = 0.05 \text{ and } \Sigma_{k=0}^{m_t^+} w_k^*(t) = 0.95$$

In practice, if NC POT values have been observed in the $(0;t_{fin})$ time interval, the following information is represented on a figure, for the dates $(t_1, t_2, \ldots, t_{NC})$:

(a) experimental curve $m_t(t)$ of the number of flood as a function of time;
(b) theoretical curve $m_t = \mu t$, for an homogeneous process of intensity $\mu = NC/t_{fin}$;
(c) curve of the 90%-tolerance interval limits of m_t, for $t = (j/NC)t_{fin}$, with j from 1 to NC.

If the experimental curve $m_t(t)$ goes out of the limits, the stationarity assumption should be rejected (with an error risk of 10%). In order to take into account missing data, the time in the abscissa corresponds to the cumulative time of observations and does not correspond exactly to the occurrence date. The advantage of this test compared to the simple accumulation one is the objective criterion of acceptance/non-acceptance of the stationarity.

The Lang-test confirms the non-stationarity for Drôme at Luc en Diois (Fig. 2) from 1907 to 1991 (complete daily records length). For the short period (1940–1991)

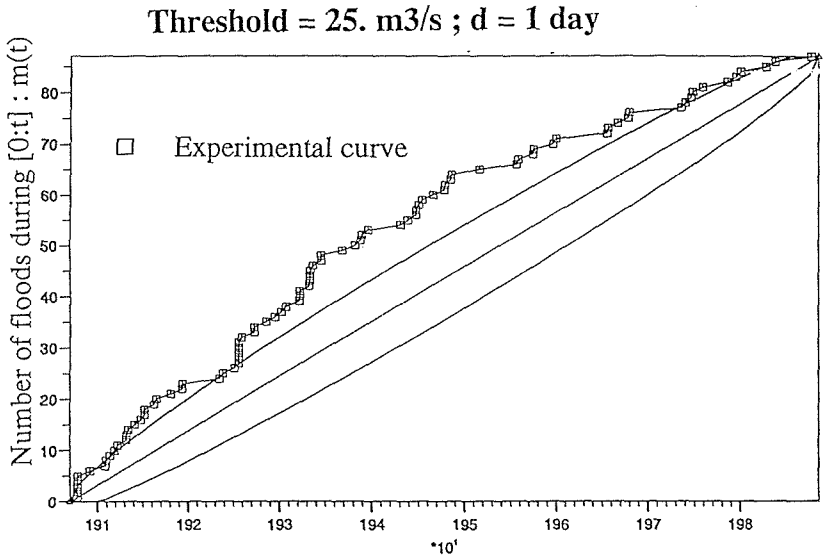

Fig. 2 Lang-test—Drôme at Luc en Diois (1907–1991).

(Fig. 3), no evidence of rejection of the stationarity is given by the Lang-test: (1940–1991) is considered as stationary. For the three other basins, the Lang-test always confirms the first assumption made by the simple accumulation test:

(a) **Fier at Dingy**: no stationarity from the beginning to the end of the records. Because of the missing years, the calculation has been done on corrected date, assuming that the series is continuous during n years ($n = n_{total} - n_{missing}$). From 1962 to 1991 (continuous record) the daily flood regime is considered as stationary.
(b) **Issoles at St Andre les Alpes**: stationarity from 1964.
(c) **Ubaye at Barcelonette**: homogeneity of the flood regime for (1904–1991).

The non-stationarity of the series in term of frequency analysis and their consequences for QdF modelling only are considered. The origin of this non-stationarity (natural in a case of climate change, or human if due to land use change for example) is not studied here.

METHODOLOGY

The complete study is presented only for one catchment, Drôme at Luc en Diois. The study is composed of two steps: (a) complete frequency analysis on the observed data; (b) QdF modelling followed by comparison of the results given by the two methods.

Frequency analysis on observed data

Definition of sampling periods The complete daily discharge chronicle (1907–1991) is divided into different sub-series to allow the study of quite homogeneous data:

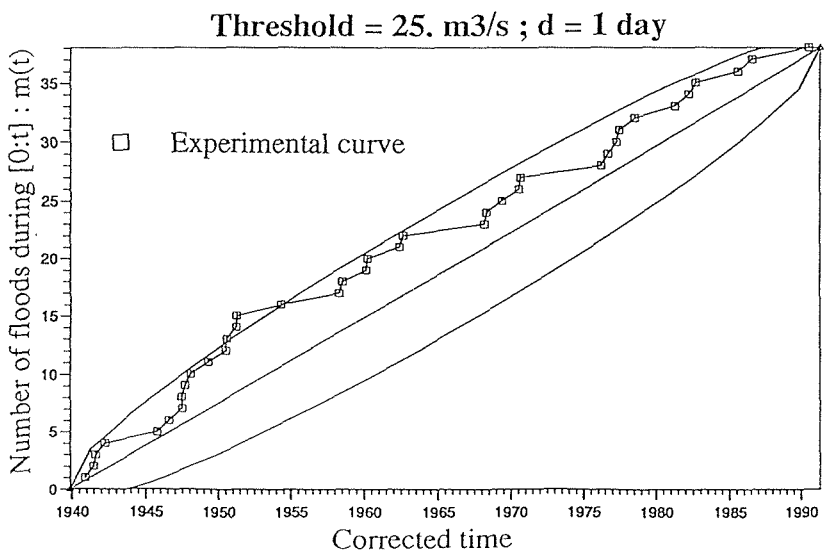

Fig. 3 Lang-test—Drôme at Luc en Diois (1940–1991).

(a) POT sampling of the maximum daily values for the whole recording duration (1907–1991). The sample will be referred to as the *long series*.
(b) POT sampling for half of the whole record period. Two samples corresponding to the periods (1907–1950) and (1951–1991) respectively referred to as *series 1* and *series 2*.
(c) POT sampling for a quarter of the whole record period. Four different samples have been considered for the periods (1907–1930), (1931–1950), (1951–1970), (1971–1991), respectively referred to as *series 1a*, *series 1b*, *series 2a*, *series 2b*.

For each period, two samplings have been used, for durations 1, 3, 6, 10 and 30 days:

(a) sampling of an average flow (**V**olume flowed during a duration ***d***) **C**haracteristic of the duration ***d***, and ma**X**imal on the sampling season (here the year), or **VCXd** (Oberlin, 1992);
(b) sampling of a **C**haracteristic threshold discharge (***Q***) exceeded during a continuous duration ***d***, ma**X**imal on the sampling season (here the year), or **QCXd** (Oberlin, 1992).

Statistical analysis For every sample, an exponential law is fitted on the experimental frequency distribution (Michel, 1989). Table 2 gives the slope parameter (or Gradex G, $m^3 s^{-1}$) and the location parameter (P, $m^3 s^{-1}$) for the series 1 and 2. The different parameters vary from one period to another, but the range of variation is not very important. Parameters of the long series are always between the ones of series 1 and 2: the evolution of the hydrological regime is taken into account and smoothed when considering the whole period of record. Table 3 presents the 10-year return period quantiles for all the different series. Let us consider the long series as

Table 2 Gradex and location parameter for long series and series 1 and 2—Drôme at Luc en Diois—VCXd—G and P in $m^3 s^{-1}$.

	1 day		3 days		6 days		10 days		30 days	
	G	*P*	*G*	*P*	*G*	*P*	*G*	*P*	*G*	*P*
long	15.2	29.3	9.01	19.8	6.54	14.7	4.89	12.0	2.73	7.72
1	17.0	31.9	9.93	21.1	7.13	16.1	5.65	13.3	3.04	8.44
2	11.7	25.0	7.28	17.8	5.02	13.5	3.47	11.0	2.23	6.96

Table 3 10-year return period discharge (in $m^3 s^{-1}$) for different durations and different periods—Drôme at Luc en Diois—VCXd.

	1 day				3 days				6 days			
long	64.3				40.5				29.8			
2 periods	71.0^{1}		51.9^{2}		44.0^{1}		34.6^{2}		32.5^{1}		25.1^{2}	
4 periods	88.3^{1a}	49.6^{1b}	45.6^{2a}	50.1^{2b}	53.2^{1a}	36.5^{1b}	31.4^{2a}	33.5^{2b}	35.1^{1a}	29.2^{1b}	22.6^{2a}	26.0^{2b}

	10 days				30 days			
long	23.3				14.0			
2 periods	26.3^{1}		19.0^{2}		15.4^{1}		12.1^{2}	
4 periods	26.2^{1a}	25.4^{1b}	16.7^{2a}	20.6^{2b}	15.9^{1a}	14.2^{1b}	11.1^{2a}	12.4^{2b}

^{1a} series 1a.
^{1b} series 1b.
^{2a} series 2a.
^{2b} series 2b.

the "reference" one, since the 10-year return period represents the general hydrological regime of Drôme at Luc en Diois (longest series). The 10-year return period quantile is not the same as the "reference" one for any of the sub-series. For short series, series 1a corresponds to the highest quantiles and series 2a to the lowest quantiles. The difference is up to 50% (daily quantile) and decreases for longer durations. Globally, the results of each of the sub-series are consistent. Series 1 has higher quantiles than series 2; series 1a and 1b have higher quantiles than series 1b and 2a. The quantiles of series 2a and 2b are quite similar, whereas the ones of series 1a and 1b are more different. These results confirm the stationarity of the period (1950–1991) (series 2).

QdF modelling

The QdF models allow us to give frequency distributions of various catchments using two local parameters (Prudhomme, 1995). The first one is the 10-years return period instantaneous peak discharge. It is referred as **QIXA10** and can be considered as the loss function of the basin. The second is the characteristic duration of the basin **D** (CTGREF *et al.*, 1980–1982), considered as the transfer function. Three different reference models have been fitted so far (Galéa & Prudhomme, 1993), corresponding to three different catchment behaviours: a fast-response regime (SOYANS model), a slow-response regime (VANDENESSE) and an intermediate regime (FLORAC). More details about the calculation of the parameters and the fitting of the models can be found in Prudhomme (1995) or in the FRIEND report 1997 (Gustard *et al.*, 1997). These two local parameters need to be known for each of the considered periods, but their definition requires peak flow data, available from 1981 for Drôme at Luc en Diois.

Definition of the characteristic duration D D is determined from the (1981–1991) peak flow records. It is assumed in the rest of the study that D is independent of the observation period (the transfer function is not changed).

10-years return period peak discharge QIXA10 The experimental frequency distribution of the peak flow QIX(T) and the maximum daily flow VCX(T,1d) are known for the period (1981–1991) period. For a given frequency, the peak rate $r(T)$ is defined by (Colin *et al.*, 1977; Margoum, 1992):

$$r(T) = \frac{\mathrm{QIX}(T)}{\mathrm{VCX}(T,1d)}$$

On the assumption that $r(T)$ is representative of the catchment behaviour, and does not depend on the sampling period, for each sampling period, one can define QIXA10 (or QIX(10)):

$$\mathrm{QIX}(10)_{\text{series a}} = r(10) \cdot \mathrm{VCX}(10,1d)_{\text{series a}}$$

For Drôme at Luc en Diois, $r(10) = 1.14$.

RESULTS OF QdF MODELLING

The modelling validation is done by graphical and numerical (Nash criterion) comparisons of theoretical (exponential law fitted on experimental frequency distribution) and QdF modelled quantiles. Depending on the length of the measurement period used for the sampling, quantiles of different return periods are considered:
(a) *long series*: quantiles of 1, 2, 5, 10, 20, 50, 80 and 100 years-return period;
(b) *series 1 and 2:* quantiles of 1, 2, 5, 10, 20, 50 and 80 years-return period;
(c) *series 1a, 1b, 2a and 2b*: quantiles of 1, 2, 5, 10 and 20 years-return period.

Model of volume-discharge VCXd

Table 4 gives the Nash criterion (Nash & Sutcliffe, 1970) calculated between theoretical quantiles and quantiles given by the QdF model of SOYANS for the different considered periods. Nashln allows us to give less weight to high values in the calculation (Prudhomme, 1995). Generally, the results are satisfactory, with Nash criterion from 87.8 (series 1b) to 97.7 (series 2b) and Nashln from 84.4 (series 1b) to 98.4 (series 2b)[1]. For series 1 and series 2 (Figs 4 and 5), the same QdF model is able to satisfactorily reproduce the frequency distributions for different durations, despite dissimilar hydrological regimes according to the parameters of the fitted frequency distributions (Table 2) and the stationarity tests (Figs 1 and 2). Actually, the use of QIXA10 as a local characteristic allows us to take into account the change of the hydrological regime. Because of its property of marking the flood regime of the catchment, it represents both runoff and climatic conditions. Thus, it is able to quantify the change of flood regime and to significantly modify the model results. Using QIXA10 equal to 80.9 $m^3 s^{-1}$ (series 1) instead of 59.2 $m^3 s^{-1}$ (series 2) moves the curves towards higher values. Because the local characteristic is representative of the flood regime for the measurement period, the same reference QdF model is able to correctly reproduce the whole range of QdF curves for periods with different flood regimes. Table 5 presents the different QIXA10 corresponding to the different series.

Model of threshold discharge QCXd

Theoretical quantiles (deduced from the observations) and QdF modelled quantiles for maximum threshold discharge (QCXd) are also compared for the durations 3, 6,

Table 4 Drôme at Luc en Diois—Validation of the QdF model (SOYANS) in VCXd for different sampling periods.

	long series	series 1	series 2	series 1a	series 1b	series 2a	series 2b
Nash	93.0	87.7	88.3	92.2	87.8	96.5	97.7
Nashln	92.5	94.5	95.1	87.6	84.4	96.9	98.4

[1] Typically, the Nash criterion lies between 0 and 100, with a value of 100 showing the perfect fit.

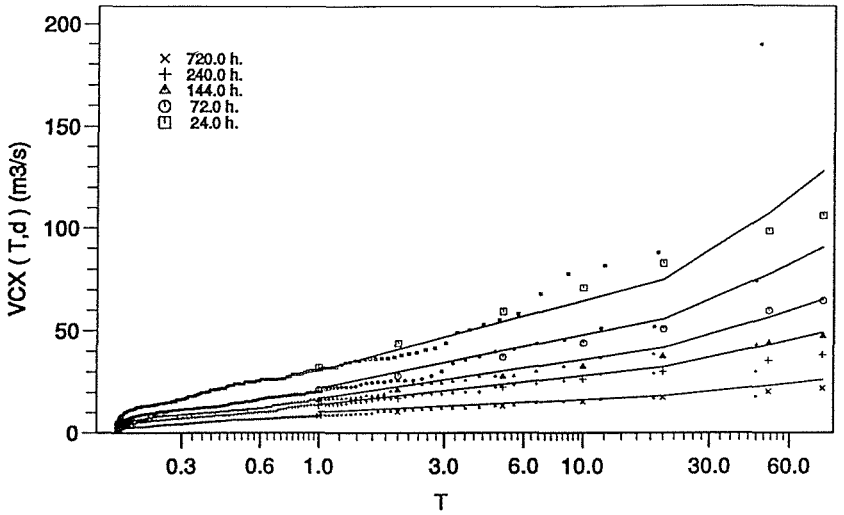

Fig. 4 Drôme at Luc en Diois—SOYANS model in VCX—series 1—D = 24 h—QIXA10 = 80.9 $m^3 s^{-1}$.

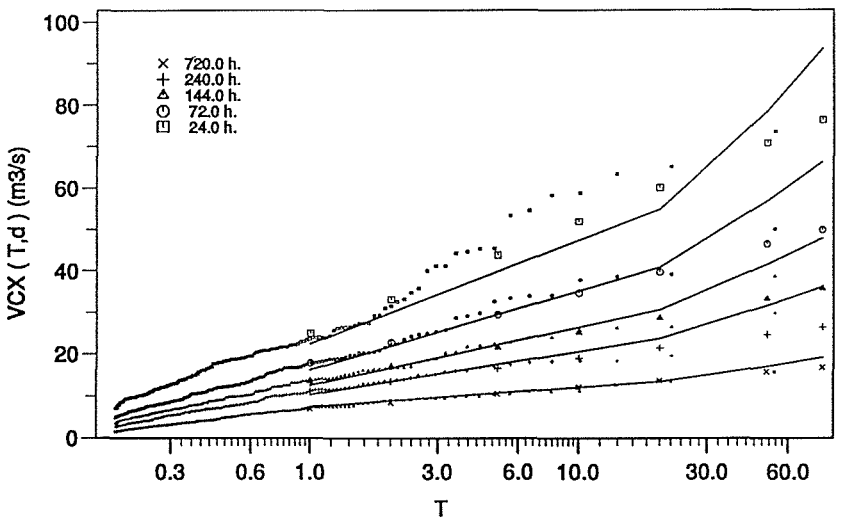

Fig. 5 Drôme at Luc en Diois—SOYANS model in VCX—series 2—D = 24 h—QIXA10 = 59.2 $m^3 s^{-1}$.

10 and 30 days (Figs 6 and 7 for series 1 and 2). Table 6 gives the Nash values calculated on the same quantiles as for VCXd. The results are consistent, but the Nash criterion is slightly smaller than for VCXd.

CONCLUSION

Changes in flood regime can be due to different causes: natural, like climate change; human, like change of the land use, modification of the river bed; or due to

Table 5 QIXA10 (m^3/s) defined by the peak rate r(10) = 1.14 for each measurement period.

long series	series 1	series 2	series 1a	series 1b	series 2a	series 2b
76.0	80.9	59.2	101.0	56.5	52.0	57.1

measurement change (change of the equipment for example). Because most hydrological studies involve medium term decisions (more than one hundred years return period), it is important to be able to take into account an eventual change in

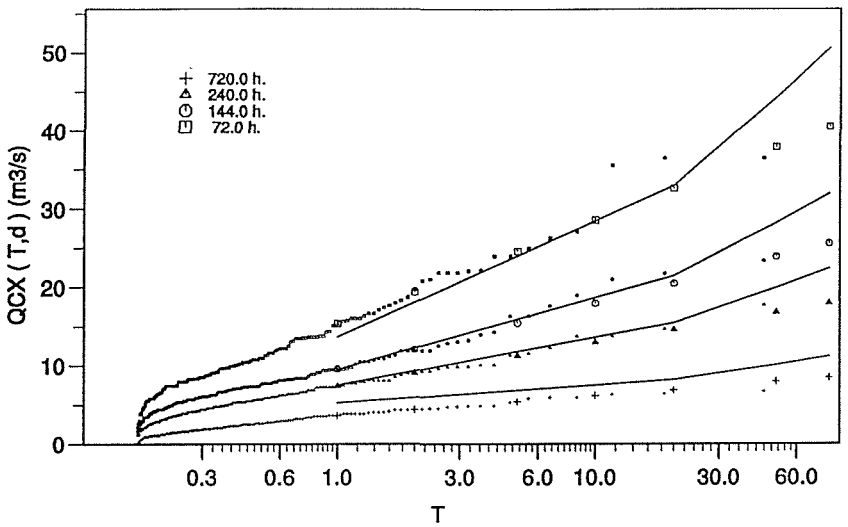

Fig. 6 Drôme at Luc en Diois—SOYANS model in QCX—series 1—D = 24 h—QIXA10 = 80.9 $m^3\ s^{-1}$.

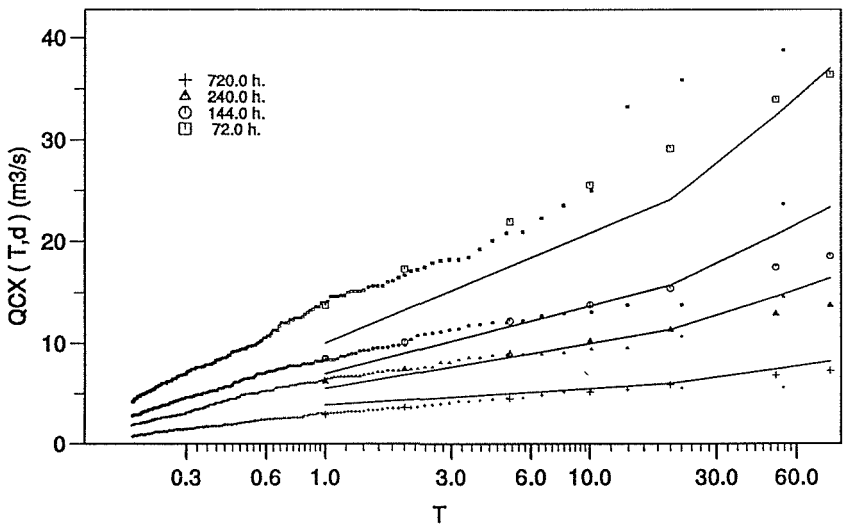

Fig. 7 Drôme at Luc en Diois—SOYANS model in QCX—series 2—D = 24 h—QIXA10 = 59.2 $m^3\ s^{-1}$.

Table 6 Drôme at Luc en Diois—Validation of the QdF model (SOYANS) in QCXd for different sampling periods.

	long series	series 1	series 2	series 1a	series 1b	series 2a	series 2b
Nash	94.5	95.2	92.2	85.9	80.8	87.6	90.4

the hydrological behaviour of a catchment. Because they use local parameters which are representative of the catchment and of the hydrological periods to be modelled, the regional QdF models, both for the volume-discharge and the threshold-discharge, are robust enough to take into account changes affecting the catchment, as soon as these changes have been taken into consideration during the definition of the local characteristics.

REFERENCES

Colin, E., Michel, C. & Oberlin, G. (1977) Application du calcul de la distribution de deux variables à l'estimation des crues. *BTGR* 120, Cemagref, Groupement Antony.

CTGREF, SRAE, DIAME, SH, (1980–1982) Synthèse nationale sur les crues des petits bassins versants. Fascicule 2: la méthode "SOCOSE"; Fascicule 3: la méthode "CRUPEDIX". *Information Technique* **38**(2).

Galéa, G. & Prudhomme, C. (1993) Characterization of large scale variations in river flow behaviour with reference to hydrological macro-regionalization. In: *FRIEND: Flow Regimes from International Experimental and Network Data* (ed. by P. Seuna, A. Gustard, N. W. Arnell & G. A. Cole) (Proc. Braunschweig Conf., October 1993), 229-239. IAHS Publ. no. 221.

Galéa, G. & Prudhomme, C. (1994) Modèles débit-durée-fréquence et conceptualisation d'un hydrogramme de crue synthétique: validation sur le BVRE de DRAIX. *Hydrol. Continent.* **9**(2), 139–151.

Galéa, G. & Prudhomme, C. (1997) Notions de base et concepts utiles à la compréhension de la modélisation synthétique des régimes de crue des bassins versants au sens des modèles QdF. *Revue des Sciences de l'Eau* (in press).

Gustard, A., Roald, L. A., Demuth, S., Lumdadjeng, H. S & Gross, R. (1997) *Flow Regimes from International Experimental and Network Data (FRIEND)*. Institute of Hydrology, Wallingford (in press).

Lang, M. (1995) Les chroniques en hydrologie: modélisation comparée par un système de gestion de bases de données relationnel et orienté-objet; traitements de base et intervalles de confiance des quantiles de crues; techniques d'échantillonnage par la méthode du renouvellement. PhD Thesis, Université Joseph Fourier—Grenoble, Cemagref—Lyon.

Margoum, M. (1992) Estimation des crues rares et extrêmes: le modèle AGREGEE. Conceptions et premières validations. PhD thesis, Ecole des Mines de Paris, Cemagref Lyon, GIS Hydrologie FRIEND-AMHY.

Michel, C. (1989) *Manuel d'Hydrologie Appliquée aux Petits Bassin Ruraux*. Cemagref—Antony, ENGREF—Paris.

Nash, J. E. & Sutcliffe, J. V. (1970) River flow forecasting through conceptual models. Part I—A discussion of principles. *J. Hydrol.* **10**, 282–290.

Oberlin, G. (1992) Normalisation des variables dans les modèles hydrologiques descriptifs. *Informations Techniques du Cemagref* **85**(4).

Prudhomme, C. (1995) Modèles synthétiques des connaissances en hydrologie—application à la régionalisation des crues en Europe Alpine et Méditerranéenne. PhD thesis, UMII, Cemagref-Lyon, UMII.

FRIEND'97 — Regional Hydrology: Concepts and Models for Sustainable Water Resource Management
(Proceedings of the Postojna, Slovenia, Conference, September–October 1997). IAHS Publ. no. 246, 1997.

Représentativité des modèles QdF—application à la régionalisation des régimes de crue du bassin versant de la Loire (France)

GILLES GALEA & JEROME SOURISSEAU
Cemagref, Groupement de Lyon, 3 bis Quai Chauveau, F-69336 Lyon Cedex 09, France

Résumé Le Cemagref a développé ces dernières années trois modèles de synthèse, dits QdF, qui permettent d'établir les courbes débit (Q)–durée (d)–Fréquence (F) relatives aux débits de crue de bassins versants observés ou non. Sur le bassin hydrographique de la Loire (S = 117 000 km^2) qui compte environ 500 bassins versants observés, les modèles ont pu être validés sur 76 bassins choisis en fonction de leur répartition géographique, de leur taille, de la qualité des chroniques de débit continu $Q(t)$, etc. Après avoir vérifié l'aptitude de ces modèles à restituer la diversité des régimes de crue qui caractérisent les 76 bassins sélectionnés, une régionalisation des deux paramètres d'entrée de ces modèles permet d'étendre leur utilisation en des sites non observés hydrométriquement. Ainsi, grâce à sa grande robustesse et à la notion de régime qu'il exprime, l'outil QdF associé à ses modalités d'application devrait contribuer à la gestion rationnelle de la ressource en eau et des écosystèmes aquatiques.

INTRODUCTION

Le Ministère de l'Environnement a confié au Cemagref la réalisation d'une étude portant sur une approche écosystémique du bassin de la Loire qui doit permettre à terme de définir des orientations de protection et de gestion des milieux aquatiques naturels du bassin. Le cadre fonctionnel des écosystèmes aquatiques étant largement dépendant de l'hydrologie des bassins versants, il a été nécessaire d'étudier la variabilité spatiale et temporelle des régimes hydrologiques en crue observés sur le bassin hydrographique de la Loire. Cette variabilité est étudiée à partir de deux variables hydrologiques (Oberlin *et al.*, 1989; Galéa & Prudhomme, 1996) traduisant deux notions de régime complémentaires (Oberlin, 1992): la notion de débit–**V**olume (moyen) **C**aractéristique sur une durée continue **d**, ma**X**imal dans la saison (noté **VCXd**) et de débit–seuil (**Q**) **C**aractéristique continûment dépassé sur la durée **d**, ma**X**imal dans la saison (noté **QCXd**). Le travail réalisé (Sourisseau & Galéa, 1996) traite essentiellement de la régionalisation des régimes de crue observés sur le bassin hydrographique de la Loire à partir de trois modèles de synthèse QdF de référence et de leur typologie. Ainsi Vandenesse (le nom du modèle est associé au site de calage) permet de représenter le régime hydrologique en crue de bassins versants dont l'écoulement est soutenu (nappe, fonte de neige par exemple) et dont les crues plutôt volumineuses sont peu rapides. Les bassins versants aux crues rapides et violentes (fort Gradex pluviométrique en général) seront représentés par les modèles de Florac et Soyans. Comparativement aux bassins représentés par Soyans, le modèle de Florac type bien en général l'écoulement de bassins rapides au comportement plus perméable et dont les crues s'inscrivent davantage dans la durée (restitution...).

L'accent a été particulièrement mis sur leur potentialité de régionalisation et donc d'usage à priori des modèles QdF en des sites non observés hydrométriquement ainsi que sur leur aptitude à couvrir un large éventail de surfaces de bassins (depuis quelques km^2 à plusieurs centaines de km^2), de durées (depuis une seconde à 30 jours) et de période moyenne de retour ($0.5 \leq T$ (an) ≤ 1000).

PRESENTATION FORMELLE DES MODELES DE SYNTHESE QdF

Le Cemagref a développé ces dernières années une méthodologie QdF, "inspirée" de la méthode d'analyse des pluies (Grissolet *et al.*, 1962) en intensité-durée-fréquence (IDF), fondée sur l'analyse probabiliste des variables VCXd et QCXd extraites des chroniques de débit continu $Q(t)$ et qui permet d'établir les courbes débit (Q)-durée (d)-Fréquence (F) relatives aux débits de crue de bassins versants observés ou non. Ces courbes synthétisent la dualité existant entre leur stabilité dans le temps et la variabilité temporelle des débits, autrement dit la notion de régime. Si l'on désigne indifféremment par Q le débit en VCXd ou en QCXd, les équations des modèles de synthèse QdF de référence sont les suivantes:

(a) pour $0.5 \leq T(an) \leq 20$, généralisation d'une loi exponentielle (1) avec d/D et $QIXA10$

$$Q(T,d) = \left(A.\ln(T) + B\right).QIXA10 \qquad (1)$$

$$A = \frac{1}{X_1.\frac{d}{D} + X_2} + X_3$$

avec

$$B = \frac{1}{X_4.\frac{d}{D} + X_5} + X_6$$

(b) pour les fréquences rares $20 < T$ (an) ≤ 1000, généralisation d'une forme d'extrapolation esthétique du Gradex (2) des pluies maximales (Michel, 1982) avec d/D et $QIXA10$.

$$Q(T,d) = Q(10,d) + \left[C.\ln\left(1 + \frac{A}{C}.\frac{T-10}{10}\right)\right].QIXA10 \qquad (2)$$

avec

$$C = \frac{1}{X_7.\frac{d}{D} + X_8} + X_9$$

où $Q(10,d)$ est obtenu par la formule (1) et où C représente le Gradex implicite des pluies maximales. Les paramètres X_i relatifs à chacun des trois modèles QdF (en VCXd ou QCXd) sont présentés au Tableau 1. Pour plus de précision sur les modèles de synthèse QdF en QCXd, notamment pour ce qui concerne les extrapolations des débits-seuils aux fréquences rares, on se reportera aux travaux de Galéa & Prudhomme (1994a,b). Les deux paramètres d'entrée des modèles QdF sont la durée caractéristique de crue du bassin versant (D) et le débit instantané maximal annuel décennal ($QIXA10$)

Tableau 1 Paramètres des modèles de synthèse QdF de référence.

Modèle QdF	Paramètres X_i								
Vandenesse	X_1	X_2	X_3	X_4	X_5	X_6	X_7	X_8	X_9
VCXd	2.635	6.19	0.016	1.045	2.385	0.172	1.083	1.750	0.000
QCXd	3.970	6.48	0.010	1.910	1.910	0.097	3.674	1.774	0.013
Florac	X_1	X_2	X_3	X_4	X_5	X_6	X_7	X_8	X_9
VCXd	1.12	3.56	0.00	0.95	3.18	0.039	1.56	1.91	0.085
QCXd	3.05	3.53	0.00	2.13	2.96	0.010	2.78	1.77	0.040
Soyans	X_1	X_2	X_3	X_4	X_5	X_6	X_7	X_8	X_9
VCXd	0.87	4.60	0.00	1.07	2.50	0.099	0.569	0.69	0.046
QCXd	2.57	4.86	0.00	2.10	2.10	0.05	1.49	0.66	0.017

qui apportent respectivement une information sur la fonction de transfert et sur la fonction de production du bassin versant. Lorsque des observations $Q(t)$ sont disponibles, D est la valeur de la médiane conditionnelle des ds pour $Qs = QIXA10$ (Fig. 1).

En l'absence de débit, D peut être estimée à partir d'une formulation sommaire (3) relative à la méthode SOCOSE (CTGREF *et al.*, 1980–1982); où S (km^2) est la superficie du bassin, PA (mm) est la pluie annuelle (moyenne interannuelle), $PJXA10$ (mm) est la pluie journalière maximale annuelle décennale du bassin, TA (°C) est la température annuelle (moyenne interannuelle) réduite au niveau de la mer.

$$\ln(D) = -0.69 + 0.32 \cdot \ln(S) + 2.2\sqrt{\frac{PA}{PJXA10 \cdot TA}} \tag{3}$$

De même que pour D, la formule sommaire CRUPEDIX (4) permet l'estimation du $QIXA10$; dans cette formule, R est un coefficient régional (CTGREF *et al.*, 1980–1982).

$$QIXA10 = S^{0.8}\left(\frac{PJXA10}{80}\right)^2 R \tag{4}$$

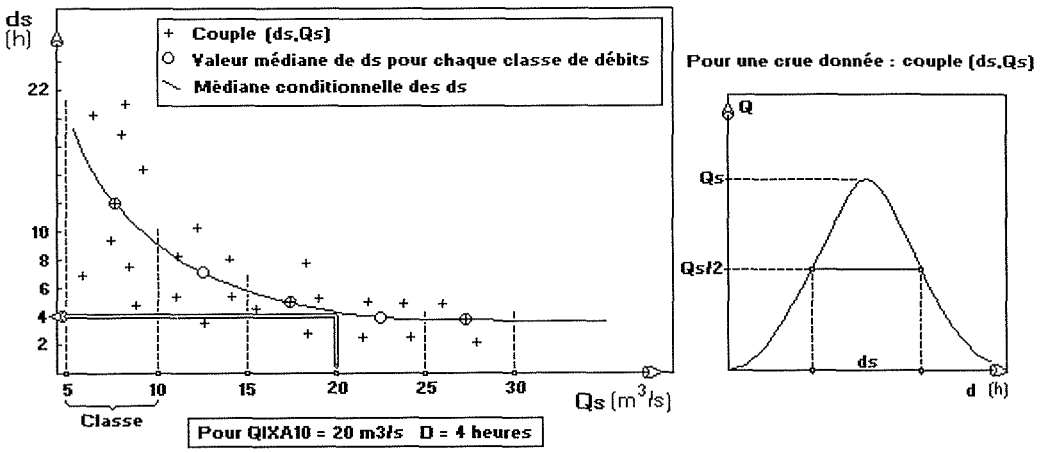

Fig. 1 Définition de la durée caractéristique de crue D (ds est la durée pendant laquelle la moitié du débit de pointe est dépassée).

REPRESENTATIVITE SPATIALE DES MODELES QdF DE REFERENCE

Dans le cadre de l'étude globale portant sur une approche écosystémique du bassin hydrographique de la Loire, l'étude hydrologique proprement dite s'est donnée trois objectifs principaux:

(a) inventorier la diversité des régimes hydrologiques en crue du bassin de la Loire,
(b) montrer que l'outil QdF permet de restituer la diversité des régimes observés,
(c) faciliter l'usage opérationnel en tout site observé ou non des modèles QdF.

Dans un premier temps, 76 bassins versants observés ($S \leq 3500$ km^2), sur les 500 environ que compte le bassin hydrographique de la Loire, ont été choisis en fonction de leur répartition géographique, de leur taille, de la qualité des chroniques, etc., afin de disposer d'un échantillon représentatif des principaux régimes observés. Les résultats, déduits de l'analyse probabiliste des chroniques observées $Q(t)$ et des modèles de synthèse, nous permettent de considérer que les deux premiers objectifs, énoncés précédemment, ont été atteints. Autrement dit, les régimes hydrologiques de l'ensemble des bassins versants sélectionnés peuvent s'identifier aux typologies d'écoulement représentées par les modèles de synthèse QdF (Fig. 2). Nous donnons (Figs 3 et 4) un exemple de validation sur le bassin du Thouet à St Generoux. Il en

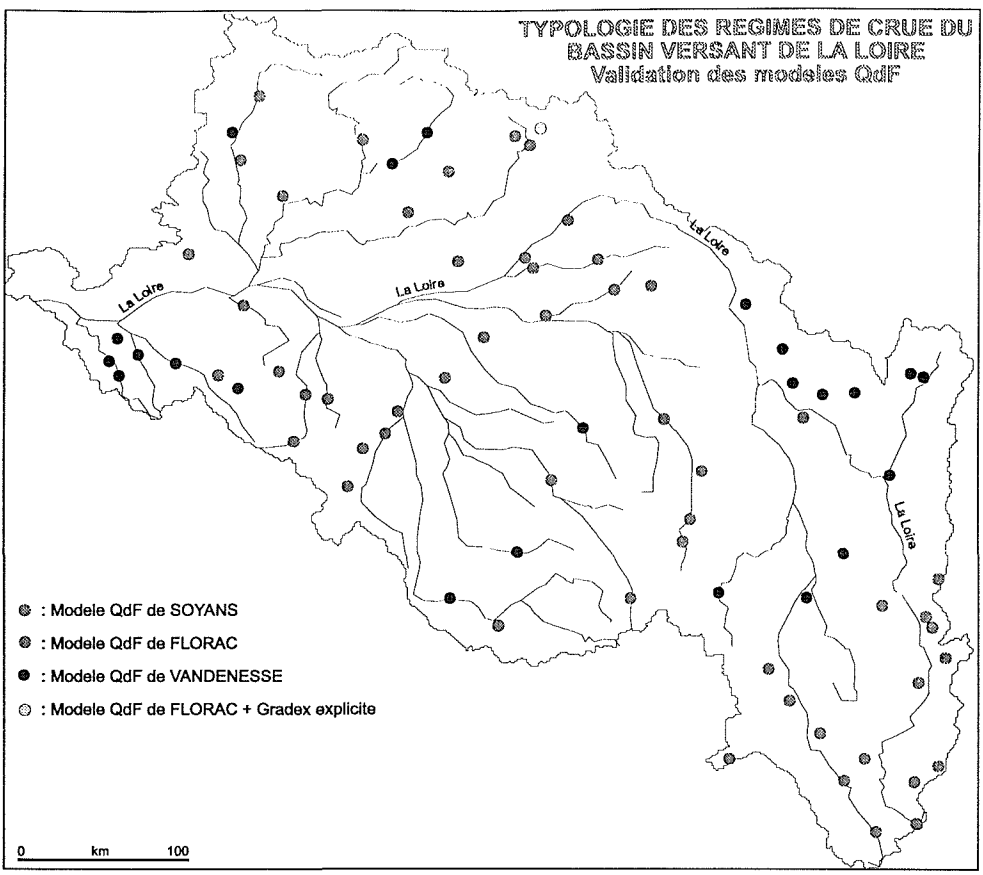

Fig. 2 Bassins versants sélectionnés, typologie des régimes de crue.

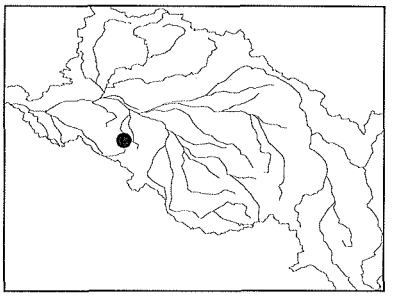

Bassin versant du Thouet à St Generoux

Code Hydrologique: L814110
Superficie: 701 km^2
Période d'observation: 1972–1992
Poste pluviométrique: 79239

Modèle QdF de FLORAC
$QIXA10$ = 302 m^3 s^{-1}
D = 15 h

Fig. 3 Situation du bassin du Thouet à St Generoux.

résulte cependant, comme pour d'autres études d'hydrologie de synthèse réalisées en France et en Europe (Prudhomme, 1995), que le choix d'un modèle de synthèse (et donc de la typologie associée) ne peut dépendre ni de la localisation géographique du bassin versant, ni de ses caractéristiques physiographiques (géologie, occupation du sol, pédologie, climat, etc.) mais plus vraisemblablement d'un critère de choix hydroclimatique, ($Lo = Gp(d)/QIXA10$) associant le Gradex des pluies maximales $Gp(d)$ et le $QIXA10$. Les valeurs de Lo obtenues pour différentes durées d ($D/2 \leq d \leq 5D$), compatibles avec la dynamique de l'écoulement, permettent à partir de la Fig. 5 d'effectuer le choix du modèle QdF de référence. Ce critère de choix n'est pas un critère absolu, il est conseillé de vérifier que la typologie d'écoulement qui lui est associée (cf. antérieurement) est bien compatible avec celle du bassin étudié (enquête auprès des riverains, etc.).

Dans un deuxième temps, pour faciliter l'usage opérationnel des modèles QdF de référence (3ème objectif), nous nous sommes intéressés à la régionalisation des descripteurs locaux de régime (D et $QIXA10$) et donc d'usage *a priori* des modèles QdF en des sites non observés hydrométriquement.

USAGE OPÉRATIONNEL DES MODÈLES QdF

Régionalisation des descripteurs locaux de régime D et $QIXA10$

En l'absence d'observation hydrométrique, les formulations sommaires (3) et (4) disponibles pour estimer respectivement les descripteurs locaux de régimes D et $QIXA10$ sont peu précises. Il a donc été nécessaire d'évaluer l'erreur commise, par référence aux valeurs de D et $QIXA10$ déduites des observations de débit, sur plus d'une centaine de bassins versants. La spatialisation du coefficient de correction des estimations effectuées à partir de (3) et (4), respectivement Fig. 6 et Fig. 7, a été obtenue par krigeage ordinaire. En règle générale, la démarche géostatistique a concerné aussi certaines variables nécessaires à l'estimation sommaire des descripteurs locaux de régime et au critère de choix du modèle QdF de référence.

Critère de choix

S'il est vrai que l'objectivité du choix du modèle (Fig. 5) et de manière générale des quantiles de crue modélisés est essentiellement liée aux paramètres d'entrée locaux (D, $QIXA10$), cela peut être cependant nuancé. En effet, les erreurs sur les descripteurs ne vont pas toujours dans le même sens, il peut donc y avoir une certaine compensation des erreurs qui globalement permet au modèle de restituer des quantiles acceptables. Par ailleurs, le critère de choix (Galéa & Prudhomme, 1994b) qui intègre ces descripteurs et donc l'erreur qui leur est associée, indique généralement le modèle donnant les résultats les plus proches du régime réel du bassin versant (Prudhomme, 1995).

Tableau 2 (de la Fig. 4).

d(h)	Période de retour T(an)								
	0.5	1	2	5	10	20	50	100	1000
0.0003	58.60	115.00	171.00	246.00	302.00	358.00	433.00	571.10	900.50
	47.95	106.75	165.55	243.28	302.08	360.88	494.32	603.45	1008.5
24	52.30	84.20	116.00	158.00	190.00	222.00	264.00	335.70	512.60
	36.92	76.03	115.15	166.85	205.96	245.08	321.14	380.71	592.16
72	31.20	54.20	77.10	107.00	130.00	153.00	183.00	-	-
	27.37	50.80	74.22	105.19	128.61	152.04	198.30	234.66	364.20
144	21.70	38.10	54.40	76.10	92.40	109.00	130.00	-	-
	21.70	36.33	50.96	70.29	84.92	99.54	131.86	158.05	254.39
240	15.50	29.20	42.80	60.90	74.50	88.20	106.00	-	-
	18.46	28.21	37.95	50.84	60.58	70.33	94.75	115.50	195.53
720	9.42	17.60	25.80	36.60	44.70	52.90	63.70	-	-
	14.32	17.97	21.62	26.45	30.10	33.75	46.02	58.41	116.67

Légende: Pour chaque d et T, quantile "observé" (ex.: 58.60), quantile modélisé (ex.: 47.95).

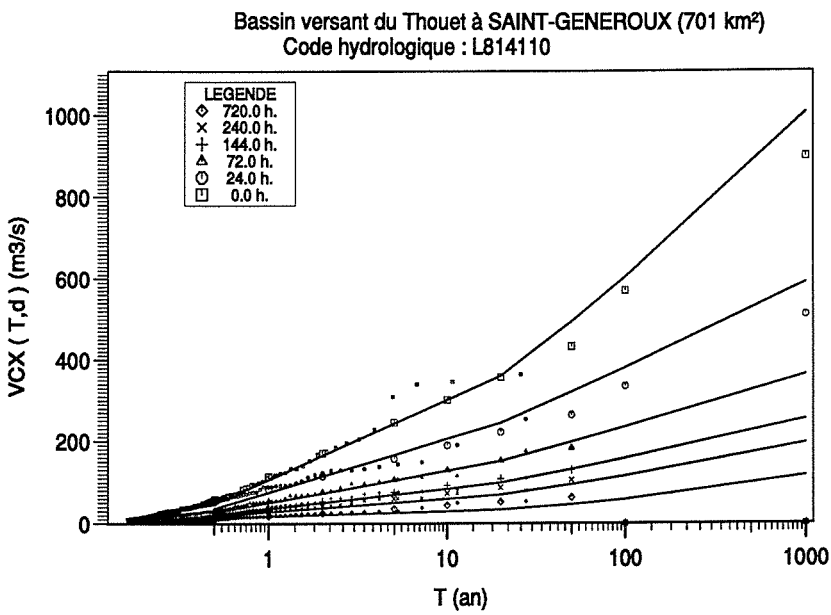

Fig. 4 Validation (*QdF FLORAC*) sur le régime des crues du Thouet à St Generoux.

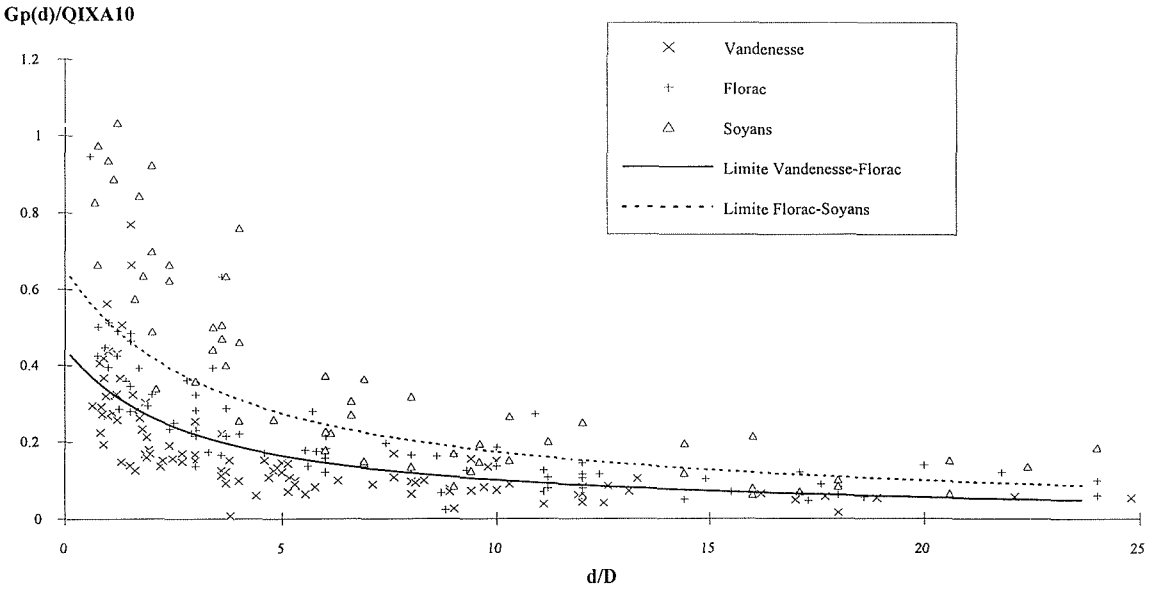

Fig. 5 Critère de choix des modèles QdF.

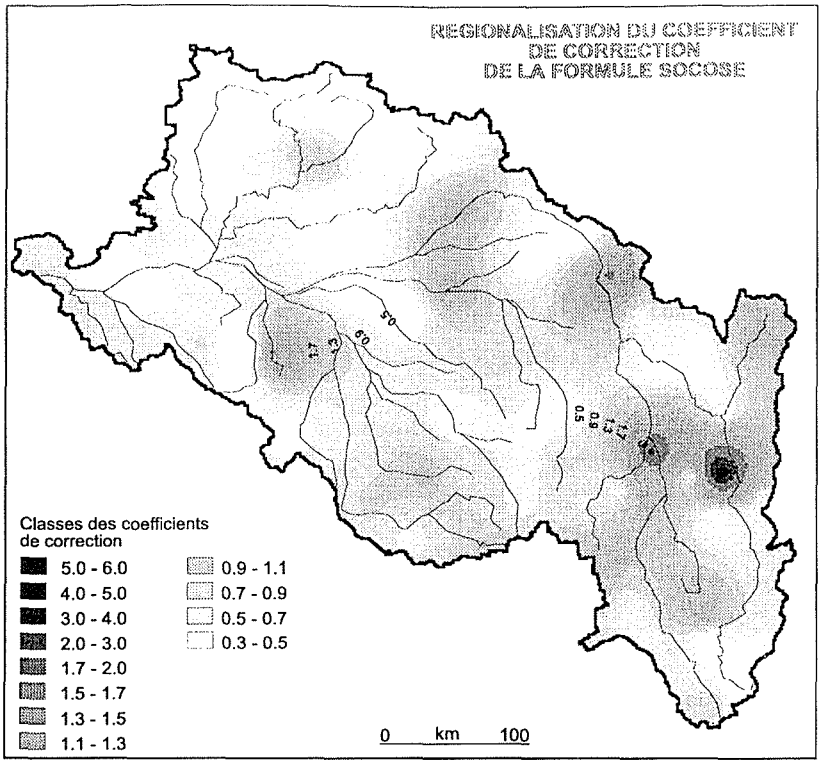

Fig. 6 Régionalisation du coefficient correcteur de D estimé selon (3).

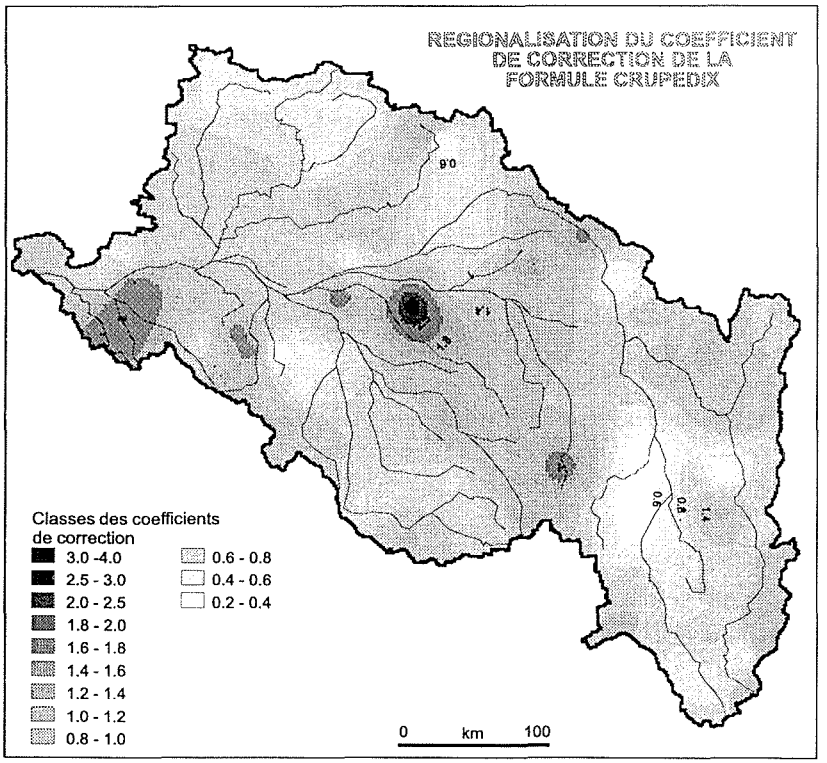

Fig. 7 Régionalisation du coefficient correcteur de *QIXA*10 estimé selon (4).

CONCLUSION

Les résultats de la régionalisation permettent de confirmer le caractère opérationnel des trois modèles QdF de référence pour typer les régimes de crue observés ou non sur le bassin hydrographique de la Loire. De mise en oeuvre facile, simples et robustes ces modèles, ne nécessitant que deux paramètres d'entrée (*D*, *QIXA*10), permettent d'obtenir des résultats finalisés, intégrant la grande variabilité spatio-temporelle des débits. Cette grande représentativité spatiale, sous leur forme mathématique adimensionnelle, est principalement due au fait que chacun d'eux est établi à partir des seules observations de débit et de pluie d'un bassin versant particulièrement choisi et représentatif d'une typologie des régimes d'écoulement en crue (Vandenesse, Soyans ou Florac). Les travaux de Prudhomme (1995) sur la régionalisation des régimes hydrologiques péri-méditerranéens ont permis aussi de confirmer cela et de constater que peu de modèles synthétiques régionaux traitant des débits–volumes (*moyens*) et des débits–seuils selon une approche multidurées et multifréquences des crues sont présents dans la littérature scientifique internationale. On peut citer les travaux de Balocki & Burges (1994) qui s'apparentent un peu à cette approche.

De manière plus exhaustive, l'aspect opérationnel des modèles QdF, c'est à dire validables et fort utiles, peut être envisagé à différents titres: caractériser le régime

de crue d'un cours d'eau, préciser une réglementation, donner des indicateurs pouvant avoir une importance écologique, ou encore pour traduire certaines demandes sociales en matière de gestion intégrée (Cemagref—Lyon, 1992) des cours d'eau et de leurs bassins versants.

Remerciements Les auteurs remercient les services de production et de gestion des débits de cours d'eau, notamment les directions régionales de l'environnement (DIREN) pour leurs conseils dans le choix des stations.

REFERENCES

Balocki, J. B. & Burges, S. J. (1994) Relationships between *n*-day flood volumes for infrequent large floods. *J. Wat. Resour. Plan. Manage.* **120**(6), 794–818.

CTGREF, SRAE, DIAME, SH (1980–1982) Synthèse nationale sur les crues des petits bassins versants. Fascicule 2: la méthode SOCOSE, Information Technique no. 38-2 (juin 1980); Fascicule 3: la méthode CRUPEDIX.

Cemagref—Lyon (1992) INONDABILITE, modélisation des connaissances hydrologiques et hydrauliques en vue d'une confrontation "Risques/Besoins de Protection" directe, Synthèse cartographique. Xème PLAN: contrat Etat-Région Rhône-Alpes, risques naturels en montagne, crues en rivières et inondations en vallées. Rapport final 1989–1992.

Galéa, G. & Prudhomme, C. (1994a) The mono frequency synthetic hydrogramme (MFSH) concept, definition, interest and construction from regional QdF models built with threshold discharges, for little mountainous basins with rapid runoff. International Conference 12–16 September 1994 Stara Lesna (Slovakia).

Galéa, G. & Prudhomme, C. (1994b) Modèles débit-durée-fréquence et conceptualisation d'un hydrogramme de crue synthétique: validation sur le BVRE de DRAIX. *Hydrol. Continentale* **9**(2).

Galéa, G. & Prudhomme, C. (1996) Notions de base et concepts utiles pour la compréhension de la modélisation synthétique des régimes de crue des bassins versants au sens des modèles QdF. Cemagref—Lyon, Division Hydrologie-Hydraulique, LHM, Université Montpellier II. Article accepté à *Sciences de l'Eau*.

Grissolet, H. Guilmet, B. & Arlery, R. (1962) *Climatologie—Méthodes et Pratiques*. Gauthiers-Villars & Cie Editeur, Paris.

Michel, C. (1982) Extrapolation par la méthode du Gradex. Note interne KG 03.05.82, Cemagref—Antony, Division Hydrologie.

Oberlin, G., Ben Mansour, H. & Ortiz, R. (1989) Generalization and standardization for 3 types of flow-duration-frequency curves in flood regime description and transfer. In: *FRIENDS in Hydrology* (Proc. First FREND Symp., Bolkesjø), *AISH Publ.* no. 187.

Oberlin, G. (1992) Normalisation des variables dans les modèles hydrologiques descriptifs. *Informations Techniques du Cemagref*, mars 1992, no. 85, note 4.

Prudhomme, C. (1995) Analyse et régionalisation des régimes hydrologiques méditerranéens. Thèse de Doctorat en Hydrologie soutenue le 8 décembre 1995. Cemagref—Lyon, Division Hydrologie-Hydraulique, LHM Montpellier II.

Sourisseau, J. & Galéa, G. (1996) Représentativité des modèles QdF, application à la régionalisation des régimes de crue du bassin versant de la Loire. Cemagref, groupement de Lyon, Division Hydrologie-Hydraulique; EPFL—IATE; Ministère de l'Environnement, Direction de l'Eau.

FRIEND'97 — Regional Hydrology: Concepts and Models for Sustainable Water Resource Management
(Proceedings of the Postojna, Slovenia, Conference, September–October 1997). IAHS Publ. no. 246, 1997.

Combining statistical and conceptual approaches for index flood estimation

ARMANDO BRATH
DISTART, University of Bologna, Viale Risorgimento 2, I-40136 Bologna, Italy

CARLO DE MICHELE & RENZO ROSSO
DIIAR, Politecnico di Milano, Piazza Leonardo da Vinci 32, I-20133 Milan, Italy

Abstract A method for index flood estimation is presented, using jointly the statistical and the derived distribution approaches, in order to combine the main features of each one. The statistical approach is used to represent the process of occurrence of peak flows, whereas the derived distribution one is adopted to relate flood frequency with climatic, geomorphologic and pedologic factors in a parsimonious representation. The proposed methodology, relating index flood to the parameters of the GEV regional growth curve and to a few parameters characterizing the relevant geomorphologic and climatic properties of the single catchment, allows the estimation of the index flood for ungauged sites. Its application to a large region of northern Italy, including Po River basin and Thyrrhenian Liguria, is presented.

INTRODUCTION

The estimation of the peak discharge with a given return period T, X_T, is often required for the design of flood control works. To this end, regionalization techniques have been largely developed in the last decades. The index flood method is the most frequently adopted technique for the purpose. It is based on the estimation of the regional growth curve of the dimensionless quantile x_T; accordingly, the T-year flood flow X_T is estimated as

$$X_T = x_T \cdot \mu_X \tag{1}$$

where μ_X (index flood) is the at-site mean annual flood. The estimation of μ_X at ungauged sites represents a critical point of this kind of approach. Normally, multiregressive techniques are used for this purpose (see e.g. NERC, 1975), even if their accuracy has been proved to be unsatisfactory in several cases. As shown by Hebson & Cunnane (1987), the estimates of the index flood obtained by regional regression are even less precise than those which can be obtained from only one year of discharge data.

The above-mentioned difficulties can be overcome by incorporating in the estimation procedure some knowledge of the physical processes involved in the rainfall–runoff transformation. This goal can be achieved by using the derived distribution approach. The approach towards obtaining derived flood frequency models, based on the analysis of the transformation of the rainfall input into runoff, was introduced by Eagleson (1972). After his pioneer paper, many researchers have devoted their attention to this problem (see e.g. Hebson & Wood, 1982; Cordova & Rodriguez-Iturbe, 1983; Diaz-Granados *et al.*, 1984; Cadavid *et al.*, 1991).

However, the results of some applications to real cases showed that the derived distributions are generally very sensitive to the parameter estimation (see e.g. Ortegon & Espezua, 1986) and that they usually could not adequately represent the entire peak discharge frequency distribution (e.g. Moughamian *et al.*, 1987).

Whereas most of the researchers attempted to derive the entire form of the peak flow distribution, Adom *et al.* (1989) proposed a different approach directed to the estimation of the moments of this distribution. The derivation of these statistics was performed by using those mathematical techniques available for the approximate evaluation of the moments of derived random variables, which are based on Taylor series expansions (Mood *et al.*, 1974). The moments of the derived distributions were found to depend both on a set of climatic parameters, which are linked with the statistics of point rainfall intensity and duration, and on three dimensionless parameters which describe the interaction of the rainfall field with the basin, i.e. its area, its absorption properties and the characteristics of its river network.

Some investigations of the approach proposed by Adom *et al.* (1989) showed its capability to reproduce in a quite satisfactory manner the central characteristics of the frequency distribution of the observed peak discharge in several cases (Brath *et al.*, 1992).

Moving from these results, we report in the present paper a methodology for index flood estimation, which uses statistical procedures jointly with this derived distribution technique, in order to combine the main features of both. The statistical approach is used to represent the process of occurrence of peak flows, whereas the derived distribution one is adopted to express the dependence of index flood on climatic, geomorphologic and pedologic factors in a synthetic representation. The methodology, relating index flood to the statistical parameters of the regional growth curve of the annual maximum peak discharge and to a few parameters characterizeng the relevant geomorphologic and climatic properties of the single catchment, allows the estimation of the index flood for ungauged sites. An application to a large area in northern Italy, including Po River basin and Thyrrhenian Liguria, is also presented.

DERIVATION OF THE MEAN OF THE PEAK DISCHARGE DISTRIBUTION

In the present paper some results of the derived distribution model developed by Adom *et al.* (1989) have been used. Therefore, in the following a brief outline of the conceptual framework adopted for the derivation is given. Point rainfall is described by means of the Poisson Rectangular Pulses model, according to Eagleson (1972). Intensity and duration are assumed to be mutually independent random variables with exponential distributions, with mean μ_i and μ_t, respectively. The effects due to the spatial reduction of precipitation over the basin area are accounted for by means of an areal reduction factor k_*. The absorption (infiltration loss) at the basin scale is described by the SCS-CN method (USDA, 1972), adopted because of its parsimonious formulation, involving only one parameter, the curve number *CN*, to be estimated. The transformation of rainfall excess into surface runoff at the basin outlet is modelled according to the linear reservoir cascade analogy. Adom *et al.* (1989) used this approach to get the mean value μ_Q of the peak discharge Q for a generic storm as

$$\mu_Q = \mu_i \eta A \left\{ \left[(1 - e^{-\chi})(1 + k_*^2) - k_*^2 \chi e^{-\chi} \left(1 + \frac{\chi}{2} \right) \right] \left[1 + 3k_*^2 (1 - \eta)^2 \right] + \left[k_*^2 (2 - \eta) e^{-\chi} (1 + \chi) - 1 \right] \right\} \tag{2}$$

In equation (2) A denotes the basin area, η and χ two dimensionless factors, i.e. $\eta = \mu_i \cdot \mu_t / (\mu_i \cdot \mu_t + S)$ and $\chi = \mu_t / t_L$, where t_L is the lag time of the basin and S the saturated infiltration capacity of the soil, which depends on the parameter CN according to the well known formula introduced by the Soil Conservation Service (USDA, 1972).

REGIONAL DISTRIBUTION OF THE ANNUAL MAXIMUM OF THE PEAK DISCHARGE

In the present study the probability distribution used to model the frequency distribution of the annual maximum of the peak discharge is the Generalized Extreme Value distribution (*GEV*), proposed by Jenkinson in 1955, which has been adopted in the UK for regional flood frequency analysis (NERC, 1975). The cumulative distribution function of the GEV is

$$F_X(x) = \exp\{-[1 - k \cdot (x - \xi)/\alpha]^{1/k}\} \tag{3}$$

with mean

$$m_X = x + (a/k) \cdot [1 - G(1 + k)] \tag{4}$$

where x, a and k are the location, scale and shape parameters of the distribution, respectively, while $G(\cdot)$ is the complete gamma function.

In the following we denote with x, a and k the parameters of the GEV local distribution of the annual maximum peak discharge X and with x', a' and k' those of the GEV regional distribution of the annual maximum of the dimensionless discharge X/μ_X. These latter ones can be estimated for each homogeneous area, descending from regional flood frequency analyses, by using the method of L-moments (Hosking, 1990). Accordingly, denoting with λ_i the ith order L-moment of the regional distribution, the following relationships allow the estimation of x', a' and k'

$$k' = 7.8590 \cdot c + 2.9554 \cdot c^2 \tag{5}$$

$$\alpha' = \frac{k' \cdot \lambda_2}{\Gamma(1 + k') \cdot (1 - 2^{-k'})} \tag{6}$$

$$\xi' = \lambda_1 + \frac{\alpha'}{k'} \cdot \left[\Gamma(1 + k') - 1 \right] \tag{7}$$

where

$$c = \frac{2\lambda_2}{\lambda_3 + 3\lambda_2} - \frac{\ln(2)}{\ln(3)} \tag{8}$$

INDEX FLOOD ESTIMATION

As previously mentioned, equation (2) gives us the mean value of the peak discharge

Q originated from a generic storm, m_Q. The mean of the annual maximum of the peak discharge, that is the index flood m_X, is a function of m_Q. However, this function depends on both the form of the cumulative distribution of Q and the rate of occurrence of the flood peaks Q.

By assuming that the annual number of occurrences of Q is a Poisson random deviate with mean 1, and that the values of peak discharges Q are independent identically distributed random variables with a cumulative distribution function $F_Q(\cdot)$, the distribution of the annual maximum of the peak discharge $F_X(\cdot)$ is related to $F_Q(\cdot)$ by (Todorovic, 1978)

$$F_X(x) = \exp\{-\lambda \cdot [1 - F_Q(x)]\} \tag{9}$$

Because the GEV distribution has been adopted as probabilistic model of the annual maximum of peak flow X, according to equation (9) the corresponding form of the probability distribution of the peak discharge of the generic flood event, Q, should be a generalized Pareto whose cumulative distribution function is

$$F_Q(x) = 1 - \left[1 - \frac{b}{a}(x - c)\right]^{1/b} \qquad x \geq c \tag{10}$$

having the mean

$$\mu_Q = c + \frac{a}{1+b} \tag{11}$$

Substituting (10) in (9) and comparing with (3), the following relationships can be easily obtained:

$$\xi = c - \frac{a}{b\lambda^b} + \frac{a}{b}, \quad \alpha = \frac{a}{b\lambda^b}, \quad k = b \tag{12}$$

which relate the parameters x, a and k of the GEV local distribution of the annual maximum peak discharge with those (a, b, c) of the underlying generalized Pareto distribution.

Assuming that the lower bound c of Q is equal to zero, from (4), (11) and (12) the dimensionless ratio m_X/m_Q can be obtained as

$$\frac{\mu_X}{\mu_Q} = \frac{(1+k)}{k}\left[1 - \frac{\Gamma(1+k)}{k\frac{\xi}{\alpha}+1}\right] \tag{13}$$

Equation (13) allows to estimate the index flood μ_X based on the knowledge of the mean of peak discharge μ_Q, which can in turn be estimated from (2). However, in order to estimate μ_X from μ_Q, in (13) the values of the parameters x, a and k of the local distribution of the annual maximum of peak discharge should be known. Accordingly, (13) can not be used for estimating the index flood for ungauged sites, because of the lack of knowledge of x, a and k for these sites.

However, it can be easily proved that the following relationships hold between the parameters x', a' and k' of the regional distribution and the corresponding parameters x, a and k of the local distribution

$$\alpha' = \frac{\alpha}{\mu_X}, \quad \xi' = \frac{\xi}{\mu_X}, \quad k' = k \tag{14}$$

Taking into account (14), (13) can be rewritten as:

$$\mu_X = \mu_Q \frac{(1+k')}{k'} \left[1 - \frac{\Gamma(1+k')}{k' \frac{\xi'}{\alpha} + 1} \right] \tag{15}$$

Equation (15) shows that the dimensionless ratio m_X/m_Q is constant within each homogeneous region, being the regional growth curve, i.e. the same for all the catchments in the region. Moreover, (15) can be used as a predictor for index flood in ungauged sites, because the parameters x', a' and k' of the GEV regional growth curve can be obtained from the regional flood frequency assessment and the value of μ_Q can be estimated for each ungauged site by means of (2), based on the knowledge of the relevant geomorphoclimatic properties of the corresponding basin.

APPLICATION

The proposed methodology for index flood estimation was applied to a large area in northern Italy. The study area includes the whole Po River basin, which is about 70 000 km^2 in area, and Thyrrhenian Liguria, with an area of about 5400 km^2 (see Fig. 1). The regional assessment of flood frequency for the study area was examined by De Michele & Rosso (1997), based on the analysis of the annual flood series available for the 74 hydrometric stations located in the area. The Generalized Extreme Value (GEV) distribution was used in order to represent the regional growth

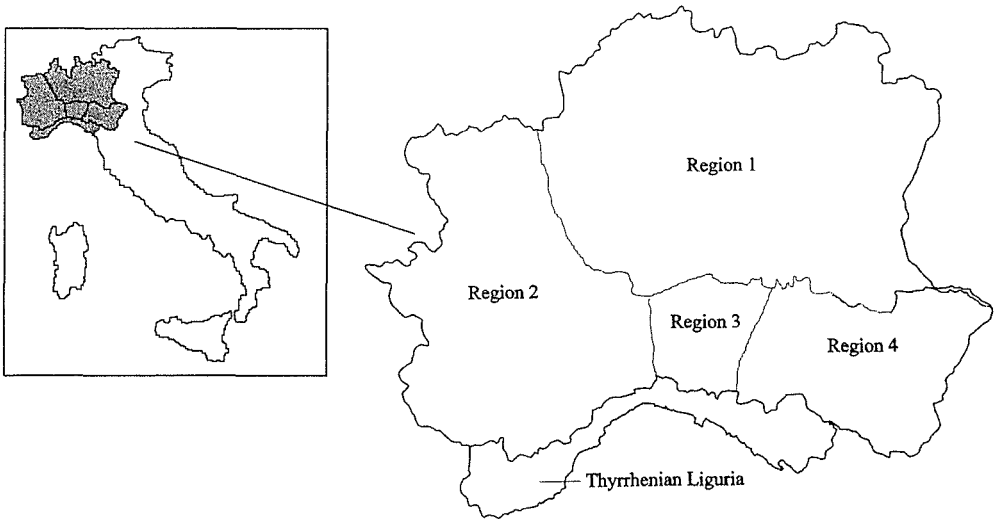

Fig. 1 Study area and boundaries of the five homogeneous regions for flood frequency analysis.

curves. Based on the analysis of the variability of the main climatic and geomorphologic characteristics, some hypotheses of regionalization were taken into consideration. Among the different hypotheses, the one leading to the most acceptable results is that depicted in Fig. 1: the Thyrrhenian Liguria was considered as an unique region, whereas in the Po River valley four geographic regions were outlined. The assumption of internal homogeneity of the five regions was found to be acceptable based on the analysis of the agreement between the growth curve of each region and frequency of the dimensionless observations available within the region. For the application presented in the following, the parameters x', a' and k' of the regional GEV growth curve for each of the five regions were taken from the above-mentioned study.

The estimation of the geomorphoclimatic parameters which control the mean of peak discharge μ_Q (see equation (2)) was performed according to the methodologies recommended by Brath *et al.* (1992). In particular, the estimation of the mean values of storm intensity m_i and duration m_l was performed on the basis of the maps of these parameters which were provided for the study area by Becciu *et al.* (1993). The areal reduction factor k_* was evaluated by the following empirical relationship derived from experimental observations collected by U.S.W.B. (Eagleson, 1972):

$$k_* = 1 - \exp(-1.1d^{1/4}) + \exp(-1.1d^{1/4} - 0.003\,861A) \tag{16}$$

in which d represents the rainfall duration in hours, while A is the basin area in km^2. According to Brath *et al.* (1992), the duration d in (16) was assumed equal to the lag time of the basin t_L.

The estimation of the parameter CN, which controls the value of the saturated infiltration capacity of the soil, S, was performed based on the criteria reported in USDA (1972) which allow to relate the value of CN to both the lithology and the land use of the basin under examination.

Finally, the estimation of the lag time of the basin, t_L, was obtained through the use of the following relationship

$$t_L = 2.3\left(\frac{R_A}{R_B}\right)^{0.3} R_L^{-0.4}\,\frac{L_\Omega}{v} \tag{17}$$

proposed by Rosso (1984). In (17), R_A, R_B, and R_L represent the Hortonian ratios of area, bifurcation and length, respectively, L_Ω is the length of the stream of highest order in the river network and v the space–time average velocity of propagation of the flood wave, which was assumed equal to 1.5 m s^{-1} for all the 74 examined catchments.

In Fig. 2 a comparison is shown between the observed values of the index flood and those calculated with the proposed methodology. As it can be observed, the results show a satisfactory predictive ability of the proposed methodology. The variance explained by the model is about 79% (R^2 = 0.786); this result is comparable to the best ones obtained by using multiregressive techniques to fit the observed index flood data for the same zones.

However, it should be noted that the proposed methodology for index flood estimation does not require any calibration procedure based on the use of the available hydrometric observations, which on the contrary is necessary in the case

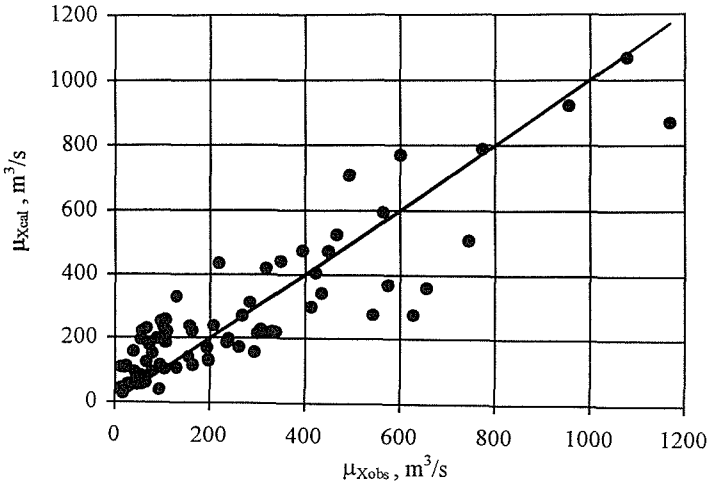

Fig. 2 Comparison between observed and predicted values of the index flood for the 74 catchments of the study area.

the multiregressive approach is adopted. Therefore, one can expect that its extrapolations, required for predicting index flood in ungauged sites, could be done with more confidence than in the case of multiregressive predictors.

In Fig. 3 we show an example of application of the proposed methodology for estimating the probability distribution of the annual maximum of the peak discharge in a given site; for the purpose, the Roya River at Airole-Piena in Thyrrhenian Liguria was considered. The estimation of the T-year peak discharge X_T was performed on the basis of the regional growth curve reported by De Michele & Rosso (1997), which gave us the dimensionless quantile x_T. The estimate of X_T was obtained according to equation (1), once by assuming μ_X equal to its observed value (solid line) and once by estimating μ_X via the proposed methodology (dashed line). One can observe that the proposed methodology for index flood estimation allows to evaluate in a quite satisfactorily manner the probability distribution of the peak flow in the examined case.

CONCLUSIONS

Index flood estimation is one of the most critical aspects of the procedures used for regional flood frequency analysis. The accuracy of the multiregressive techniques, normally used for the purpose, is often unsatisfactory. Moreover, because of their empirical nature, some doubts can arise whenever an extrapolation of the results obtained by these techniques is required in order to estimate index flood for ungauged sites. Significant improvements could be expected by incorporating in the index flood estimation procedure some knowledge of the physical processes involved in the rainfall–runoff transformation. In this framework, the paper presents a methodology for index flood estimation, which makes use of a derived distribution scheme in order to express the dependence of flood frequency on both geomorphology and climate of the basin.

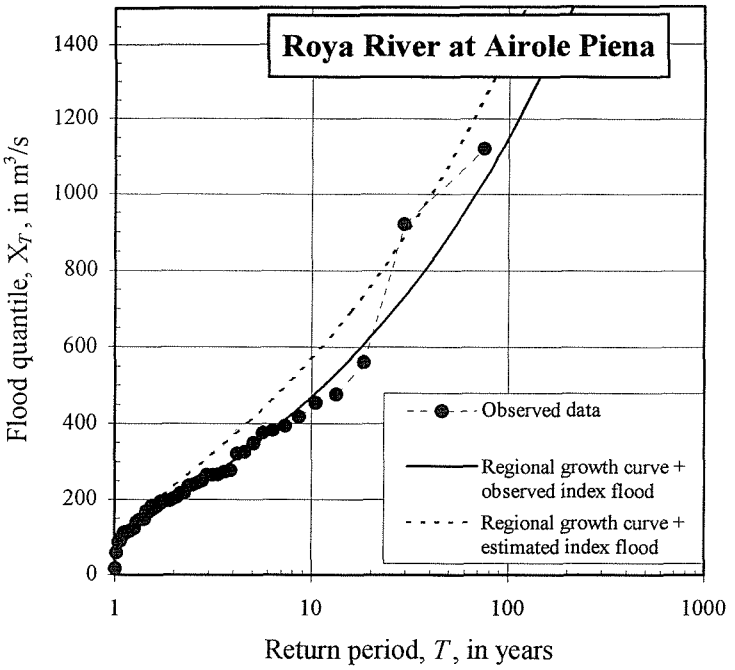

Fig. 3 Comparison between the probability distribution of the annual maximum of the peak discharge obtained by estimating the index flood via the proposed methodology, the one obtained by the observed index flood and the discharge observations for Roya River at Airole-Piena.

The methodology, relating index flood to the parameters of the GEV regional growth curve of the annual maximum of the peak discharge and to a few parameters characterizing the relevant geomorphologic and climatic properties of the single catchment, allows to estimate easily the index flood for ungauged sites. The application to a large region in northern Italy, including Po River basin and Thyrrhenian Liguria, shows its satisfactory predictive ability.

REFERENCES

Adom, D. N., Bacchi, B., Brath, A. & Rosso, R. (1989) On the geomorphoclimatic derivation of flood frequency (peak and volume) at the basin and regional scale, In: *New Directions for Surface Water Modelling* (ed. by M. L. Kavvas) (Proc. Baltimore Symp., May 1989), 165–176. IAHS Publ. no. 181.

Becciu, G., Brath, A. & Rosso, R. (1993) A physically based methodology for regional flood frequency analysis. In: *Engineering Hydrology* (ed. by C. Y. Kuo), 461–466. Am. Soc. Civ. Engrs, New York.

Brath, A., Bacchi, B. & Rosso, R. (1992) Geomorphoclimatic derivation of flood frequency (in Italian). *Idrotecnica*, no. 4, 183–200.

Cadavid, L., Obeysekera, J. T. B. & Shen, H. W. (1991) Flood-frequency derivation from kinematic wave. *J. Hydraul. Div., ASCE* **117**, 489–510.

Cordova, J. R. & Rodriguez-Iturbe, I. (1983) Geomorphoclimatic estimation of extreme flow probabilities. *J. Hydrol.* **65**, 159–173.

De Michele, C. & Rosso, R. (1997) Self-similarity as a physical basis for regionalization of flood probabilities. In: *Proc. Int. Workshop on Hydrometeorology Impacts and Management of Extreme Floods* (ed. by J. D. Salas & F. Siccardi) (Perugia, Italy, 14–17 November) (in press).

Diaz-Granados, M. A., Valdes, J. B. & Bras, R. L. (1984) A physically based flood frequency distribution. *Wat. Resour. Res.* **20**, 995–1002.

Eagleson, P. S. (1972) Dynamics of flood frequency. *Wat. Resour. Res.* **8**, 878–898.

Hebson, C. S. & Cunnane, C. (1987) Assessment of use of at-site and regional flood data for flood frequency estimation. In: *Hydrologic Frequency Modelling* (ed. by V. P. Singh), 433–448. Reidel, Dordrecht.

Hebson, C. & Wood, E. F. (1982) A derived flood frequency distribution using Horton ratios. *Wat. Resour. Res.* **18**, 1509–1518.

Hosking, J. R. M. (1990) L-moments: analysis and estimation of distributions using linear combinations of order statistics. *J. Roy. Statist. Soc.* B**52**, 105–124.

Mood, A. M., Graybill, F. A. & Boes, D. C. (1974) *Introduction to the Theory of Statistics*. McGraw-Hill Int., Singapore.

Moughamian, M. S., McLaughlin, D. B. & Bras, R. L. (1987) Estimation of flood frequency: an evaluation of two derived distribution procedures. *Wat. Resour. Res.* **23**, 1309–1319.

Ortegon, C. E. & Espezua, M. (1986) Stochastic models of rainfall and derived distribution of extreme floods (in Italian). Final Thesis VIII Advanced Course in Hydrology and Water Resources Management, Politecnico di Milano, Italy.

Natural Environment Research Council (NERC) (1975) *Flood Studies Report*. NERC, London.

Rosso, R. (1984) Nash model relation to Horton order ratio. *Wat. Resour. Res.* **20**, 914–920.

Todorovic, P. (1978) Stochastic models of floods. *Wat. Resour. Res.* **11**, 345–356.

USDA (US Department of Agriculture, Soil Conservation Service) (1972) *National Engineering Handbook. Hydrology*. Washington DC.

FRIEND'97 — Regional Hydrology: Concepts and Models for Sustainable Water Resource Management
(Proceedings of the Postojna, Slovenia, Conference, September–October 1997). IAHS Publ. no. 246, 1997.

Prediction of design storms and floods

URSZULA SOCZYÑSKA, BARBARA NOWICKA, URSZULA SOMOROWSKA
The University of Warsaw, Faculty of Geography and Regional Studies, Krakowskie Przedmieście 30, 00-927 Warsaw, Poland

ELŻBIETA KUPCZYK & ROMAN SULIGOWSKI
Pedagogical University in Kielce, Institute of Geography, Konopnickiej 15, 25-406 Kielce, Poland

Abstract In this work a method to estimate design floods based on rainfall information has been proposed and verified. A design hyetograph has been developed on the basis of 30-years of pluviographic records from 36 meteorological stations. The general formula describing rainfall intensity–duration–frequency relationship has been derived from recorded series. The spatial distribution of the derived parameters made it possible to estimate rainfall intensity quantiles at each site within the territory of Poland. The typical temporal pattern of storms have been obtained for the genetic type of rainfall and for the selected pluviographic regions. The determined synthetic storms were then transformed into outflows for the same return periods. The method has been verified by fitting probability distributions to maximum annual flows calculated from direct observations from the analysed catchments. This method, apart from giving maximum flows, gives more comprehensive information in the form of the hydrograph of stated probability (design hydrograph), as the hydrological basis for hydrotechnical design.

ESTIMATION OF THE DESIGN STORM

Frequency analysis of extreme rainfall has been based on an annual exceedance series. Frechet's model (Sevruk & Geiger, 1981) selected from the family of generalized extreme value distributions the one that proved to fit best to the empirical series and made possible the estimation of quantile values beyond the range of the observed data sets. The probability density function of Frechet's distribution is expressed as follows:

$$f(x) = \begin{cases} \frac{\beta}{\alpha}\left(\frac{x-\varepsilon}{\alpha}\right)^{-\beta-1} \exp\left[-\left(\frac{x-\varepsilon}{\alpha}\right)^{-\beta}\right] & x > \varepsilon \\ 0 & x \le \varepsilon \end{cases} \quad (1)$$

The Maximum Likelihood Method was used to estimate the two parameters (α, β). The third (ε)—displacement parameter—was derived from the rainfall data properties. The graphic form of rainfall intensity–duration–frequency relationship is illustrated in Fig. 1. The general formula developed to describe the intensity–duration–probability relationships is of the following form:

$$I_p = e^A \cdot t_r^B \quad (2)$$

where I_p is rainfall intensity (at given probability level), t_r is the rainfall duration, A and B are parameters for each range of return intervals.

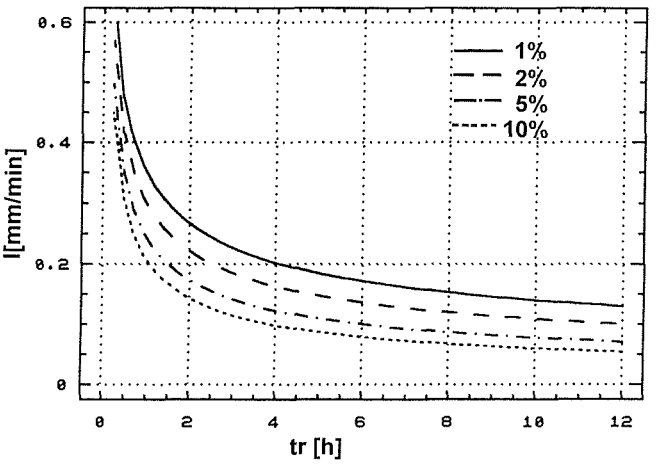

Fig. 1 Rainfall intensity–duration–probability of exceedance relationship at Gdansk.

Figures 2 and 3 illustrate spatial variations of parameters A and B respectively, for Polish areas for the return period of 100 years. The design hyetograph was developed on the basis of the detailed data covering the years 1961–1990. The maximum rainfall storms grouped into 13 classes according to their duration were extracted from independent rainfall events ranging from 10 minutes to 24 h. Rainfall series were then subdivided according to the type of events on the basis of statistical analysis of rainfall characteristics and also the main features of genetic type. The key rainfall characteristic was found to be the function of the total depth of a rainfall event to its duration. Rainfall episodes were subdivided into three sections corresponding to time of duration intervals. The variation of depth–duration relationship expressed the modification of storm characteristic and also proved the occurrence of changes within the precipitation producing mechanism. The distinction between groups of storms is due to the physical background and may be related to the original type of precipitation (Sumner, 1988). The episodes belonging to section 1 are linked with convection type processes; those in section 2 result from frontal activity, while those in section 3 result from rainfall generated by a moving depression or convergence zone on a synoptic scale. The length and slope of the selected sections obtained from the depth–duration curve at each site proved to be useful and provided objective criteria for regional analysis of rainfall. The stations were classified into the following four regions by applying the hierarchical cluster analysis method (Johnson & Wichern, 1982):

(a) sites with continental features and pre-mountainous sites,
(b) maritime sites,
(c) mountainous area sites,
(d) the group of sites strongly influenced by local circulation.

For evaluation of homogeneity of the regions, discordancy measures based on the L-moments method (Hosking & Wallis, 1993) have been estimated.

The typical temporal pattern of storms has been obtained for each type of rainfall and for selected pluviographic regions. These storm profiles can be accepted as the pattern of the design hyetograph.

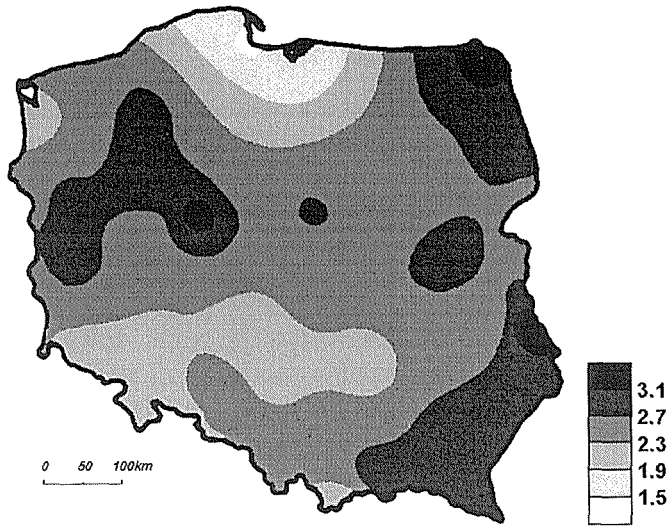

Fig. 2 Spatial distribution of parameter A at $I_p = e^{A \cdot t_r^B}$ at 1% probability of exceedance.

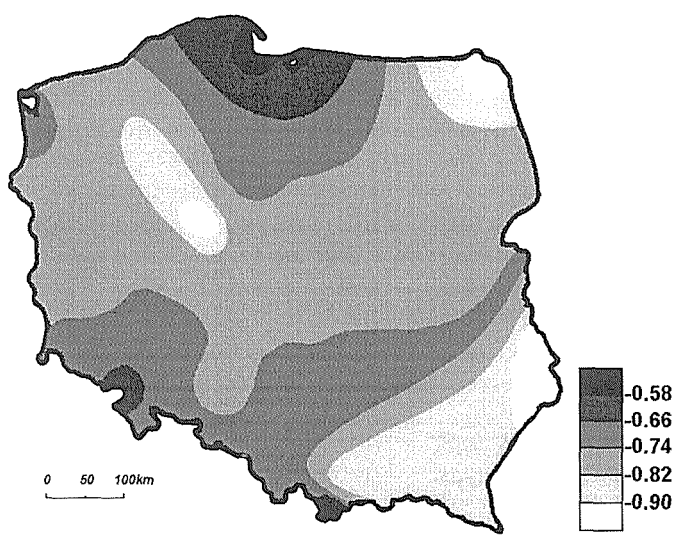

Fig. 3 Spatial distribution of parameter B at $I_p = e^{A \cdot t_r^B}$ at 1% probability of exceedance.

SELECTION AND TESTING OF MODELS

Six different conceptual models were applied for rainfall–runoff transformation. As the main objective of the study was to work out the method to estimate design storms for ungauged basins, the following criteria were applied when choosing models for the analysis:

(a) model should have small number of parameters,

(b) parameters should be easily estimated from existing topographic maps. Applied

models included:

(i) Wackermann model in original version I (Thiele & Euler, 1981) and modified one II (Ignar, 1993),

(ii) three versions of the GIUH (Rodriges-Iturbe & Valdes, 1979; Soczyñska & Nowicka, 1989; Ostrowski, 1994),

(iii) Nash model with relationship proposed by Lutz (1984).

All the above-mentioned are the lumped type of models. The models were adopted for 11 basins. Most of them are located in mountainous regions. A total of 95 different recorded flood events were used in the analysis. The SCS and runoff coefficient methods were adopted for effective rainfall determination. Thirteen different parameters were evaluated for testing of chosen models. They comprised physiographic and river bed parameters and effective rainfall characteristics. Physiographic parameters of basins were calculated from the topographical maps using the ILWIS GIS package. The type of parameters and characteristics used are summarized in Fig. 4.

A computer program in Turbo Pascal was used to simulate flood hydrographs and testing of the models. Examples of flood hydrographs simulated for Sleza River basin using different models are shown in Fig. 5.

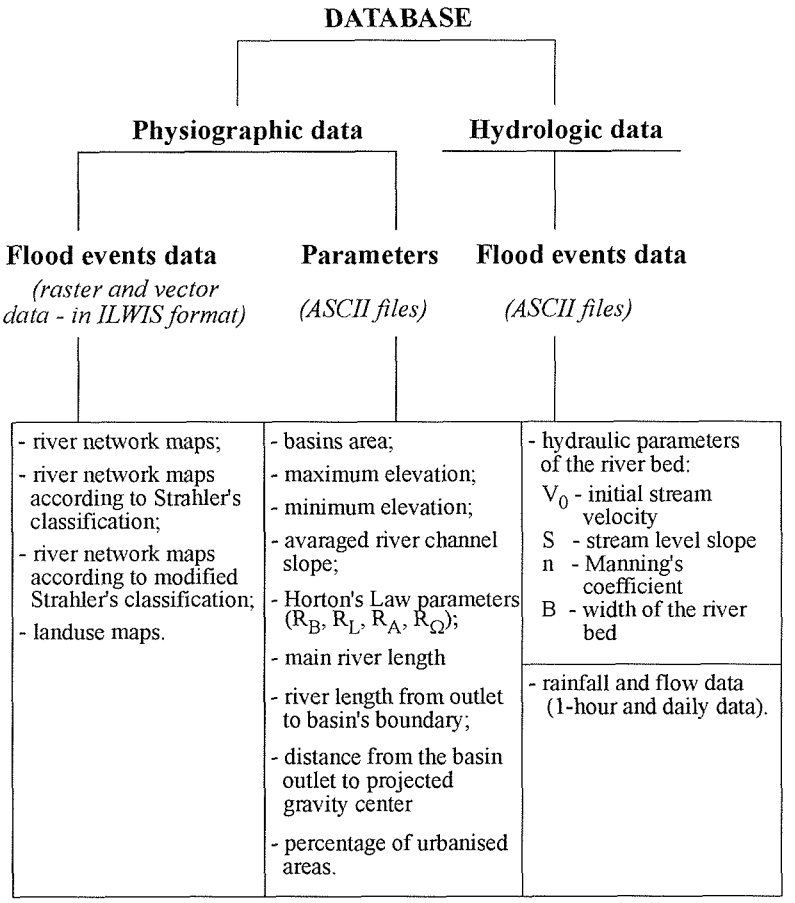

Fig. 4 Structure ot the computer database.

On the basis of the results obtained (analysis of the correlation coefficient R, special correlation coefficient RS, total square error CBK—Delleur *et al.*, 1973) four models have been selected for further research: Wackermann I and II, GIUH III and the Lutz model.

DESIGN FLOOD ESTIMATION

Design storms were transformed into the design flood hydrographs assuming the flood discharge has the same probability as the design storm. The following steps were necessary to follow in order to verify the proposed method:

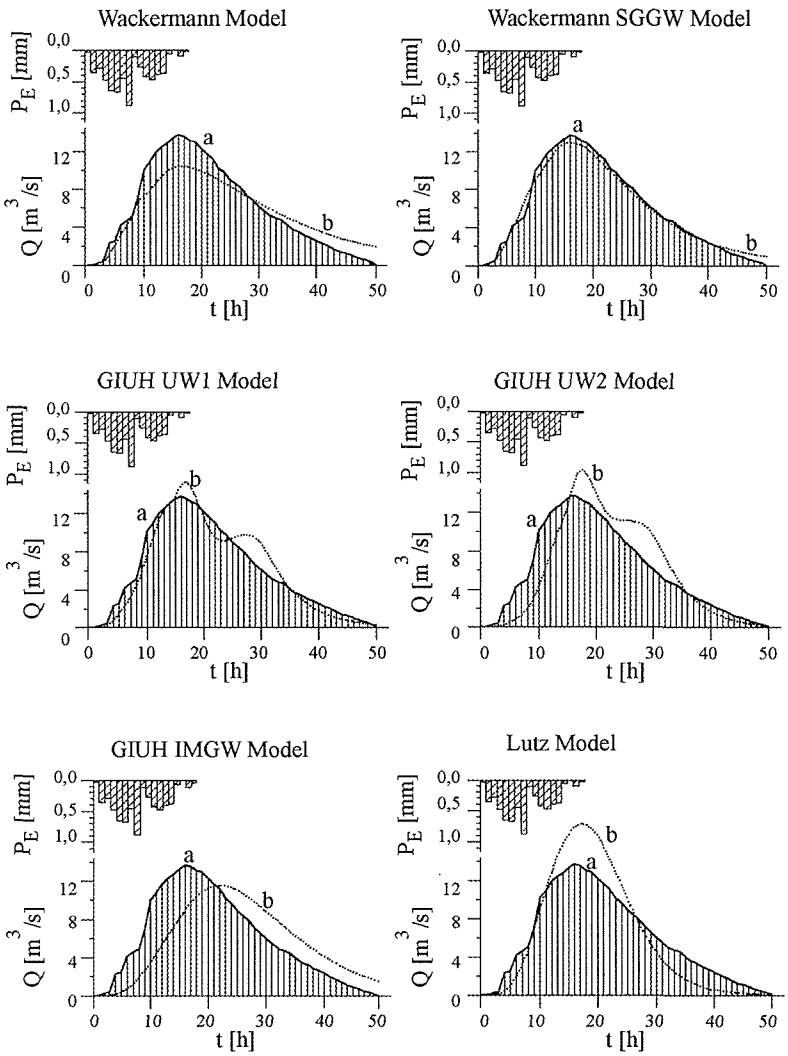

Fig. 5 Results of flood hydrograph simulation in Sleza River basin at Bialobrzezie (7 March 1980).

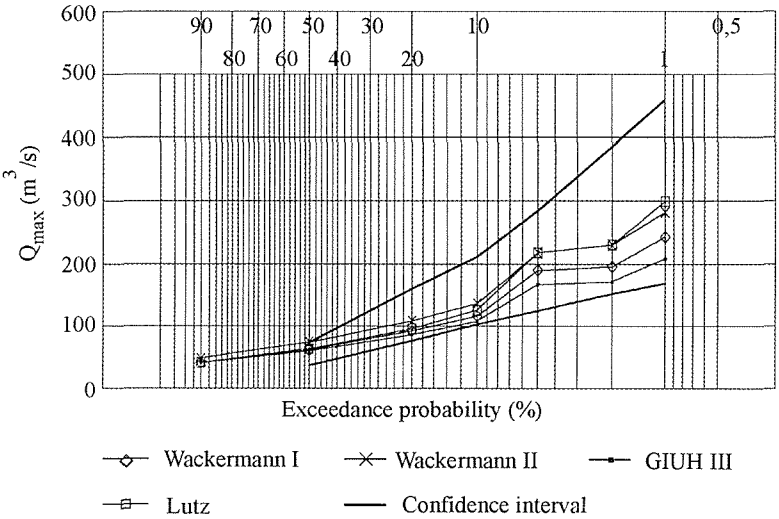

Fig. 6 Comparison of the simulated probability curves with the theoretical one calculated after Pearson III distribution model (Skawa River basin at Osielec).

(a) estimation of the maximum probable rainfall as an input to hydrological models,
(b) estimation of the maximum probable flows by statistical analysis using data series longer than 30 years,
(c) estimation of probable hydrographs using hydrological models,
(d) comparison of simulated maximum probable flows with the values of flood probability curves described by Pearson III type distribution.

Rainfall–runoff transformation was conducted with the following assumptions:

(a) CN parameter of the SCS method was equal to 100 and respectively runoff coefficient $\alpha = 1$,
(b) considered design storms were of a duration longer than 8.5 h in all rainfall–runoff transformations.

Examples of results are shown for the Skawa basin at the Osielec cross-section. Figure 6 shows a comparison of flood probabilities curves determined on the basis of applied models and the statistical distribution. Figure 7 presents example of design flood hydrographs estimated by the Lutz model for Skawa basin at the Osielec cross-section.

CONCLUSIONS

(a) Elaborated method of the design flood hydrograph estimation can be applied for the ungauged natural basins.
(b) In mountainous basins with relatively large slopes and good conditions for direct runoff creation, design storm can constitute an input to rainfall–runoff models without reduction for losses.
(c) In most cases the simulated probable flows were less than observed ones, especially for low probabilities ($p < 20\%$).
(d) Results of simulations obtained from different models were close to each other and therefore all of chosen models could be applied in practice.

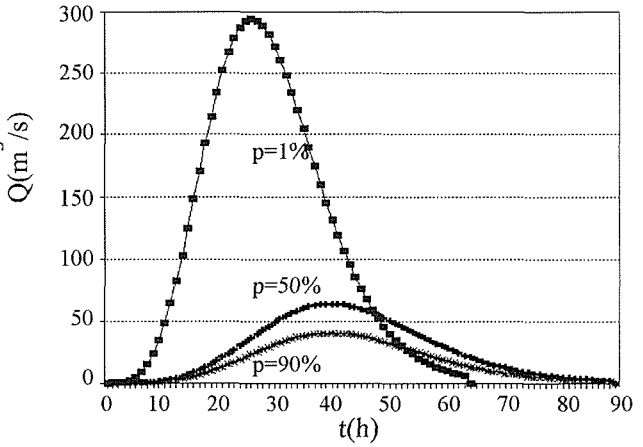

Fig. 7 Design flood hydrographs for the Skawa River basin at Osielec for probabilities p = 1%, 50%, 90%.

(e) Application of the method for lowland basins requires additional studies especially with regard to effective rainfall and concentration time determination.

Acknowledgements This project was sponsored mainly by the Committee of Scientific Research in Poland. The authors would also like to thank the Faculty of Geography and Regional Studies, Warsaw University, Institute of Geography, Pedagogical University in Kielce, the Department of Land Reclamation and Environmental Engineering, Warsaw Agricultural University and the Institute of Meteorology and Water Management for giving possibility to perform the research.

REFERENCES

Delleur, J. W., Sarma, R. B. S. & Rao, A. R. (1973) Comparison of rainfall–runoff models for urban areas. *J. Hydrol.* **18**(3–4).

Hosking, J. M. R. & Wallis, J. R. (1993) Some statistics useful in regional frequency analysis. *Wat. Resour. Res.* **29**(2), 271–281.

Ignar, S. (1993) Metodyka obliczania przeplywow wezbraniowych w zlewniach nieobserwowanych (Methodology of flood flows computations in ungauged basins). *Wydawnictwo SGGW, Warszawa.*

Johnson, A. R. & Wichern, D. W. (1982) *Applied Multivariate Statistical Analysis.* Prentice-Hall, New Jersey, USA.

Lutz, W. (1984) *Berechnung von Hochwasser Abflussen unter Anwendung von Gebietskenngrossen.* Mitteilungen IHW, H. 24, Karlsruhe.

Ostrowski, I. (1994) Model regionalny malej zlewni "MOREMAZ-1" (A small watershed regional model). *Mat. Badawcze*, seria: *Hydrologia i Oceanologia* **17**. IMGW Warszawa.

Rodrigez-Iturbe, I. & Valdas, I. B. (1979) The geomorphologic structure of hydrologic response. *Wat. Resour. Res.* **15**(6).

Sevruk, B. & Geiger, H. (1981) Selection of distribution types for extremes of precipitation. *Operational Hydrology Report no 15* (WMO no. 560). WMO Geneva.

Soczynska, U. & Nowicka, B. (1989) Application of GIUH and dimensionless hydrograph models in ungauged basins. In: *FRIENDS in Hydrology* (ed. by L. Roald, K. Nordseth & K. A. Hassel) (Proc. Bolkesjoe, Norway, Conf., April 1989), 197–203. IAHS Publ. no. 187.

Sumner, G. (1988) *Precipitation. Process and Analysis.* John Wiley & Sons.

Thiele, F. & Euler, G. (1981) *Vergleichende Untersuchung zur Ermittlung von Uebertragungsfunktionen aus Einzugsgebietsgrossen nach verschiedenen Methoden. Untersuchung fuer den DVWK-FA Niederschlag-Abflussmodelle.*

FRIEND'97 — Regional Hydrology: Concepts and Models for Sustainable Water Resource Management
(Proceedings of the Postojna, Slovenia, Conference, September–October 1997). IAHS Publ. no. 246, 1997.

Simulation de réseaux hydrographiques. Comportements géométriques et hydrologiques

ISABELLE DESUROSNE & CHRISTOPHE DUROURE
LaMP-CNRS, Université Blaise Pascal, 24 Avenue des Landais, F-63177 Clermont-Ferrand Cedex, France

Résumé Dans ce travail nous tentons d'étudier le couplage entre précipitations et topographie à l'aide de modèles volontairement simplifiés de réseaux hydrographiques. Certains comportements statistiques pourraient être conservés dans ces simplifications, en particulier ceux relatifs aux événements extrêmes. Les comparaisons sont faites entre la plus simple des topographies, et des réseaux fractals consistant en un ensemble dense de rivières décrivant chacune une marche au hasard (brownienne) sans intersections. Des modélisations introduisant certaines propriétés de "rectification" locale du chevelu sont également utilisées. Intuitivement, une complexité croissante du chevelu doit tendre à intégrer ou à "lisser" le comportement des débits observés (par exemple le débit maximal ou, plus physiquement, la densité de probabilité du débit). Nous tentons de vérifier cette hypothèse dans le cas de deux modèles extrêmes de précipitations: une précipitation uniforme ("pluie stratiforme") et l'advection aléatoire de cellules précipitantes isolées ("pluie cumuliforme").

INTRODUCTION

L'un des problèmes essentiels de l'hydrologie est de justifier physiquement le comportement asymptotique des lois de probabilité pour les valeurs extrêmes de variables telles que les pluies ou les débits extrêmes. Du fait de l'importance socio-économique de la quantification des risques associés, un grand nombre d'analyses porte depuis longtemps sur l'occurrence de ces événements catastrophiques. Des lois empiriques simples, comme la loi exponentielle pour les intensités de précipitations, ont ainsi été utilisées, mais n'ont pas encore trouvé de justification physique. La très grande complexité des processus de formation des précipitations, puis des écoulements, rend en effet illusoire toute modélisation purement déterministe. En fait, le comportement extrême des variables hydrologiques n'est probablement abordable que grâce à l'utilisation de modèles spécifiques simples ne faisant appel qu'à un minimum de lois physiques et mathématiquement maîtrisées.

L'étude présentée ci-après se place dans ce cadre et consiste à simuler des réseaux hydrographiques bidimensionnels, même si l'on sait que la troisième dimension d'altitude joue un rôle déterminant dans la transformation pluie–débit. Dans le même esprit, les simulations de pluie seront extrêmement simplifiées en épisodes purement stratiformes (précipitations uniformes sur tout le bassin) ou purement convectifs (advection d'une cellule précipitante). Ces simulations à caractère synthétique permettent de maîtriser les propriétés mathématiques des champs ainsi construits. On espère ainsi valider *in fine* les fonctionnements des modèles régionaux de régime observés (modèles QdF, par exemple Galéa &

Prudhomme, 1994), à tout le moins les quantifier mathématiquement de manière satisfaisante.

SIMULATION DE RESEAUX HYDROGRAPHIQUES REALISTES

Dans la nature, les cours d'eau s'organisent en réseaux hydrographiques hiérarchiques sur une grande gamme d'échelles spatiales. L'analyse de quelques bassins versants montre que la géométrie du tracé de leurs rivières respecte certaines lois empiriques telles que les lois de Strahler, la loi de Hack (1957) ou la dimension fractale des rivières isolées, au moins sur une plage d'échelles liée aux informations disponibles (cartes, relevés de terrain, ...). Les réseaux simulés présentés ci-après sont construits à l'aide de processus mathématiques simples et respectent, au moins approximativement, les lois empiriques précitées.

Hypothèses de construction

Des hypothèses restrictives, sévères mais incontournables, sont introduites afin de permettre une interprétation ultérieure des résultats:

(a) Isotropie et homogénéité dans l'espace, à toutes les échelles: la structure géométrique du réseau hydrographique est indépendante de la position spatiale et de l'échelle (de la macro à la micro-échelle) et la pente locale du terrain est supposée constante. Aucune modification des chenaux d'écoulement au cours des épisodes de crue (érosion, embâcles, ...) n'est envisagée même si cet aspect figé du réseau peut amener la disparition de nombreuses sources de non linéarité.

(b) Densité dans le plan: tous les pixels du plan sont considérés comme appartenant à une rivière. Dès qu'une goutte de pluie parvient au sol, elle est aussitôt introduite dans le réseau hydrographique pour ensuite s'écouler vers l'exutoire puisque tout pixel possède un et un seul pixel voisin d'écoulement. L'évaporation superficielle ainsi que l'infiltration sont donc négligées.

Méthodologie

Les résultats sont présentés dans un carré de 512×512 points, l'exutoire étant positionné au centre du réseau, ce qui diffère du modèle de Scheiddeger, où celui-ci est délocalisé au bord du réseau (Takayasu, 1990). Ce recentrage nous semble limiter les effets de bords. Excepté pour le réseau conique, la construction du chevelu hydrographique consiste à générer pixel par pixel un premier thalweg à partir de l'exutoire selon les règles les plus simples d'une marche au hasard sans intersection (Grassberger, 1985). La direction de cheminement pour le pixel suivant est choisie aléatoirement parmi les 4 directions perpendiculaires (géométrie à quatre plus proches voisins). Lorsque cette marche s'arrête, un point du réseau en construction est alors aléatoirement choisi, à partir duquel le second thalweg est construit selon le même processus. En fin de course, le chenal va rencontrer soit un bras déjà simulé, soit la frontière du domaine: dans l'un et l'autre de ces cas, la génération est

interrompue. Cette procédure récursive génère donc des chevelus strictement hiérarchiques. Le processus est itéré jusqu'au remplissage total du plan, ce qui valide la deuxième hypothèse de densité.

Réseaux générés

Les réseaux simulés sont de complexités croissantes. Le plus simple, d'un point de vue géométrique, est le réseau conique. Il est obtenu en minimisant la distance à l'exutoire de tous les points du bassin versant. Peu réaliste dans la nature, il peut éventuellement s'approcher de certains réseaux artificiels urbains.

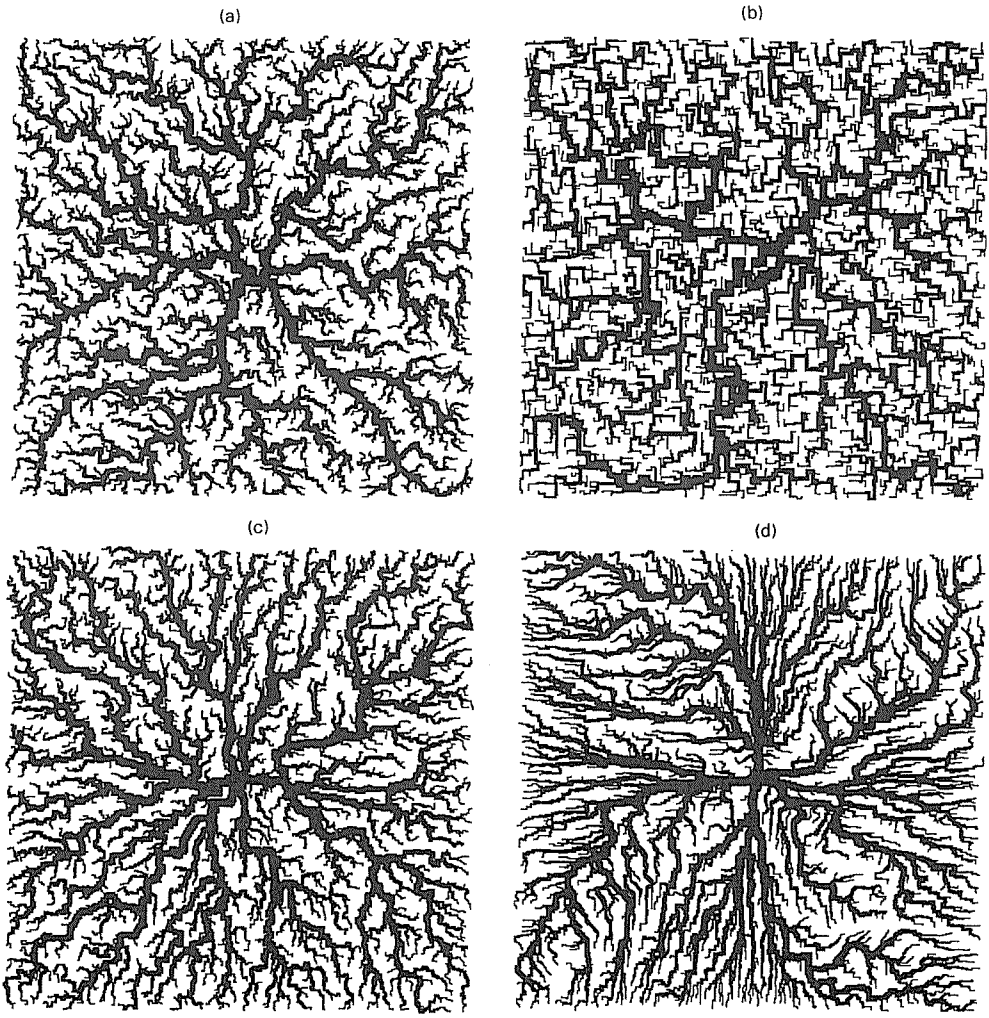

Fig. 1 Réseaux simulés browniens: pour (a), avec introduction d'une probabilité de persistance pour la direction des affluents $P_{rect} = 0.75$, (b), ainsi qu'avec une probabilité de persistance pour que l'affluent s'oriente vers l'exutoire P_{exut} de 0.25 (c) et 0.75 (d). La largeur du tracé des rivières est une fonction logarithmique de leurs débits maximaux. Seules les rivières dont le débit dépasse un certain seuil sont représentées, faute de quoi le réseau remplirait le plan (propriété de densité).

L'utilisation d'une marche au hasard sans intersection conduit à un chevelu brownien extrêmement complexe (Fig. 1(a)). Une meilleure similitude, au moins visuelle, avec un chevelu réel est obtenue par l'introduction, à chaque étape de la construction, d'une probabilité de persistance P_{rect} pour l'orientation des affluents, privilégiant leur rectification en ligne droite, indépendamment de la direction et de la position de l'exutoire (Fig. 1(b)).

Finalement, un dernier type de chevelu a été généré, en introduisant une probabilité P_{exut} pour que l'affluent s'oriente vers l'exutoire, phénomène trivialement observé dans la nature en présence d'un relief; il s'agit en pratique d'une minimisation de la distance à l'exutoire (Fig. 1(c) pour $P_{exut} = 0.25$ et Fig. 1(d) pour $P_{exut} = 0.75$) qui conduit à des réseaux moins complexes que les précédents. Si la probabilité de minimisation de la distance à l'exutoire tend vers 1, alors le réseau tend vers un chevelu conique.

Réalisme géométrique de ces simulations

La littérature hydrologique a, depuis les années 1920, proposé divers paramètres et lois expérimentales pour la description de la structure planimétrique et altimétrique des réseaux hydrographiques et des bassins versants. Citons en exemple les ordres de Strahler et les lois de Horton. Ces descripteurs, peu argumentés au plan théorique, servent en pratique de garde-fou dans la transposition des résultats d'analyse hydrologique entre bassins versants, en permettant de justifier l'éventuelle similitude des bassins en cause.

D'autre part, la géométrie fractale (Mandelbrot, 1982) permet d'analyser la complexité des chevelus de façon quantitative. Citons par exemple la mesure de la dimension fractale des rivières isolées passant de 1 pour une rivière rectifiée à 2 pour une rivière de forme suffisamment complexe pour recouvrir de façon dense le plan (courbe de Peano).

Dimension fractale de rivières isolées La dimension fractale d'un chenal d'écoulement a été observée comme étant comprise entre 1.1 et 1.3 (Mandelbrot, 1982; Takayasu, 1990; Hjelmfelt, 1988). Pour nos simulations la dimension fractale des rivières isolées est comprise entre 1.16 ($P_{exut} = 0.25$) et 1.26 ($P_{rect} = 0.75$). Ces valeurs sont incluses dans l'intervalle cité ci-dessus.

Loi de Hack Cette loi permet de relier la surface S d'un bassin versant à la longueur L de la rivière principale: $L = a.S^m$, où a et m sont deux paramètres déterminés empiriquement. La plupart des auteurs (Hack, 1957; Mandelbrot, 1982; Hjelmfelt, 1988) s'accordent à dire que m est de l'ordre de 0.6 pour les rivières naturelles, en tout cas supérieur à 0.5 (cas du chevelu conique). L'analyse, pour chaque bassin versant simulé, d'un grand nombre de sous-bassins de superficies différentes nous a conduit à $a = 1$ et $m = 0.61$, en accord avec les valeurs observées.

Lois de Horton Elles prennent appui sur la classification selon Strahler des différentes branches du réseau hydrographique à savoir que: la rencontre de deux

cours d'eau de même ordre n (les sources étant d'ordre 1) donne naissance à un cours d'eau de rang supérieur $(n + 1)$. En revanche, la confluence d'un cours d'eau principal avec une rivière d'ordre moins élevé ne modifie pas celui de la rivière principale. Pour un ordre de Strahler n donné, le rapport de confluence R_C s'exprime comme le nombre de rivières d'ordre n rapportée au nombre de rivières d'ordre $n + 1$. Expérimentalement, il a été constaté que, pour un réseau hydrographique donné, cette grandeur était à peu près constante. En d'autres termes, le nombre de cours d'eau d'ordre n suit une loi géométrique inverse. D'autre part, pour un ordre de Strahler n donné, on définit Rl comme la longueur moyenne des rivières d'ordre n rapporté à la longueur moyenne des rivières d'ordre $n + 1$. De même que précédemment, ce rapport semble être constant pour un chevelu hydrographique donné.

Ainsi, le réseau hydrographique de la Loire, digitalisé à l'échelle de 300 m puis rendu strictement hiérarchique (Pejoux, 1996), peut être analysé pour des ordres de Strahler allant jusqu'à 7 et possède un rapport de confluence de 4.25 et un rapport de longueurs moyennes de rivières de 0.46 (Alix & Roy, 1996). Il est à noter que seuls les cinq premiers ordres ont servi ces évaluations, les deux derniers étant liés à un nombre trop restreint de rivières pour être décisifs: à l'ordre le plus grand n'est lié qu'une unique rivière.

L'analyse de nos réseaux simulés avec ou sans persistance offre des résultats très proches de ces résultats expérimentaux, les deux rapports restant constants au moins pour les six premiers ordres.

Réseau	sans persistance	avec P_{rect}=0.5	avec P_{rect}=0.75	Loire
R_c	4.2	4.1	4.15	4.25
R_l	0.40	0.43	0.43	0.46

Analyse du comportement hydrologique de ces bassins

Loi de probabilité des débits à l'exutoire du bassin versant lors de l'advection de cellules précipitantes isolées Un comportement hydrologique propre à chacun des bassins simulés est mis en évidence en présence d'une situation météorologique simple: advection de cumulus illustrant, par exemple, une situation de ciel de traîne. Afin de réaliser une moyenne d'ensemble, un grand nombre de simulations est réalisé, moyennant trois hypothèses: toute quantité de pluie qui tombe ruisselle, la vitesse de propagation du courant dans le chevelu est de un pixel par unité de temps, enfin, la vitesse de propagation de la cellule pluvieuse est identique à celle de la vitesse d'écoulement.

La combinaison des deuxième et troisième hypothèses peut conduire à la formation de crues catastrophiques, dans un cas réaliste, où cellule précipitante (i.e. cumulus) et chenal d'écoulement posséderaient une trajectoire commune. On peut ainsi imaginer un nuage se déplaçant avec une vitesse de quelques km h^{-1} quand la vitesse moyenne d'écoulement serait de l'ordre de 1 m s^{-1}.

Méthodologie Le trajet d'un cumulus est simulé par le déplacement linéaire et de direction initiale aléatoire d'une cellule pluvieuse (taille de un pixel) générant une

pluie d'intensité constante dans le temps. Cette cellule est advectée sur le bassin versant avec une direction et une vitesse constantes. Lorsque le bord du bassin est atteint, la simulation de l'écoulement sur la surface du bassin versant continue jusqu'à épuisement du débit à l'exutoire; une autre cellule traverse alors le bassin versant suivant une autre direction aléatoire. Ce processus est itéré un grand nombre de fois de façon à obtenir une moyenne d'ensemble statistiquement acceptable.

A chaque étape, la réponse du bassin versant en terme de débit à l'exutoire ($Q(t)$) est donnée par la formule suivante:

$$Q(t) = \iint P[t - l(x)/V_0] \cdot dx\, dy \qquad (1)$$

où $P(t)$ représente la hauteur précipitée à l'instant t, $l(x)$ la longueur de la rivière du point x à l'exutoire et V_0 la vitesse moyenne d'écoulement des eaux sur le bassin versant, l'intégration étant effectuée sur l'ensemble du bassin.

La succession des réponses du bassin n'est pas représentative d'un épisode pluvieux réel et seules les propriétés statistiques de cette chronique de débits à l'exutoire (et non ses propriétés temporelles) ont un sens (densité de probabilité ou fonction de répartition).

Résultats Les Figs 2(a) et (b) représentent respectivement une chronique d'hydrogrammes pour les chevelus brownien et conique. L'examen comparatif de ces deux hydrogrammes conduit à remarquer que les débits maximums sont toujours largement atténués par le réseau brownien (débit instantané de pointe variant autour de 5 unités avec un maximum atteignant 25) alors que le réseau conique conduit à de

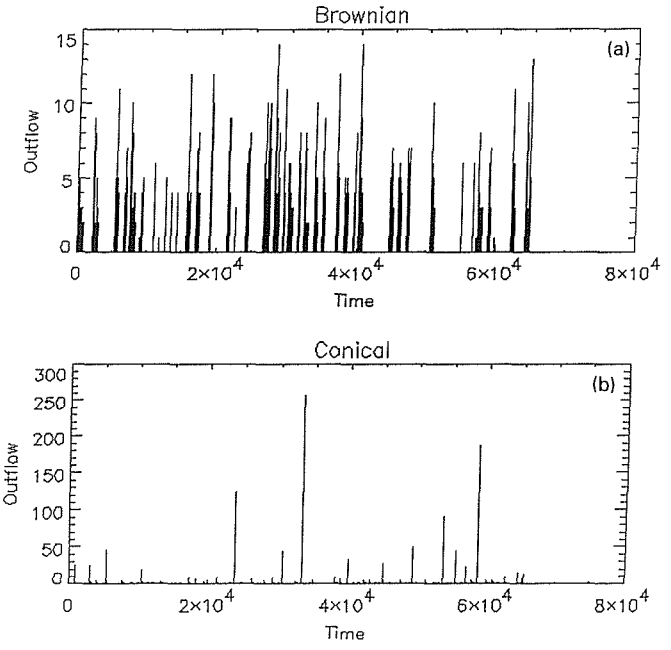

Fig. 2 Réponse d'un réseau brownien (a) et d'un réseau conique (b) au passage de cellules précipitantes d'intensité constante, dont la direction initiale de la trajectoire (rectiligne) et le point de départ sur la frontière du domaine sont aléatoires.

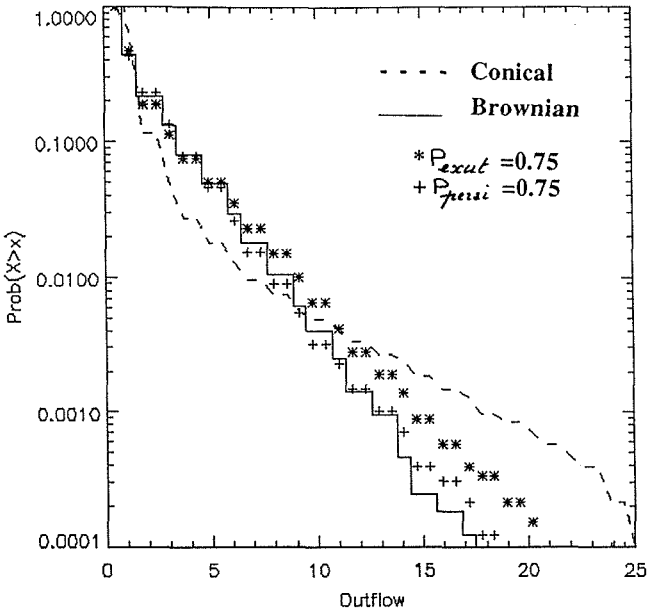

Fig. 3 Fonction de répartition des séries de débits illustrés par la Fig. 2. Elle est de forme exponentielle pour l'ensemble des réseaux (à l'exception du réseau conique).

véritables catastrophes ("flash floods") avec des pics à près de 160 unités; ces événements rares mais extrêmes sont rencontrés lorsque la cellule précipitante possède une trajectoire qui passe près de l'exutoire. Elle suit alors dans sa presque totalité un chenal d'écoulement qui va recevoir la quasi totalité de l'abat pluvieux. Cette situation peut être rencontrée en hydrologie urbaine. Une analyse plus poussée pourrait en conséquence fournir de précieux renseignements sur des erreurs à éviter en matière d'urbanisme: les terrains sont, dans les zones urbaines, imperméables et l'on cherche souvent à minimiser les temps d'écoulement et donc à évacuer les écoulements grâce à des chenaux linéaires.

Par ailleurs, il est remarquable que la loi de probabilité de ces débits (Fig. 3) soit exponentielle, excepté pour le réseau conique, cas limite non réaliste. Cette loi exponentielle semble être une caractéristique courante, les lois de probabilité des pluies, des débits (pour différents pas de temps), des hauteurs d'eau de lacs ou de rivières ... ayant en effet, dans leur grande majorité, un comportement de ce type.

Les réseaux simulés présentent des réponses hydrologiques différentes à un même événement de précipitations, de par leur structure géométrique: plus le réseau présente une structure complexe, plus le cheminement des gouttes d'eau est compliqué et plus le débit à l'exutoire est réparti de façon homogène dans le temps. En revanche, du fait de leur homogénéité spatiale, la densité de probabilité de la longueur de leurs rivières (mesurées à partir de l'exutoire) est linéaire. Cette propriété est fondamentale pour le comportement hydrologique de ce bassin car elle conditionne la forme de la partie croissante de l'hydrogramme unitaire. Elle est numériquement observée pour l'ensemble des réseaux que nous avons utilisés. La linéarité de la densité de probabilité de la longueur des rivières ne semble dépendre

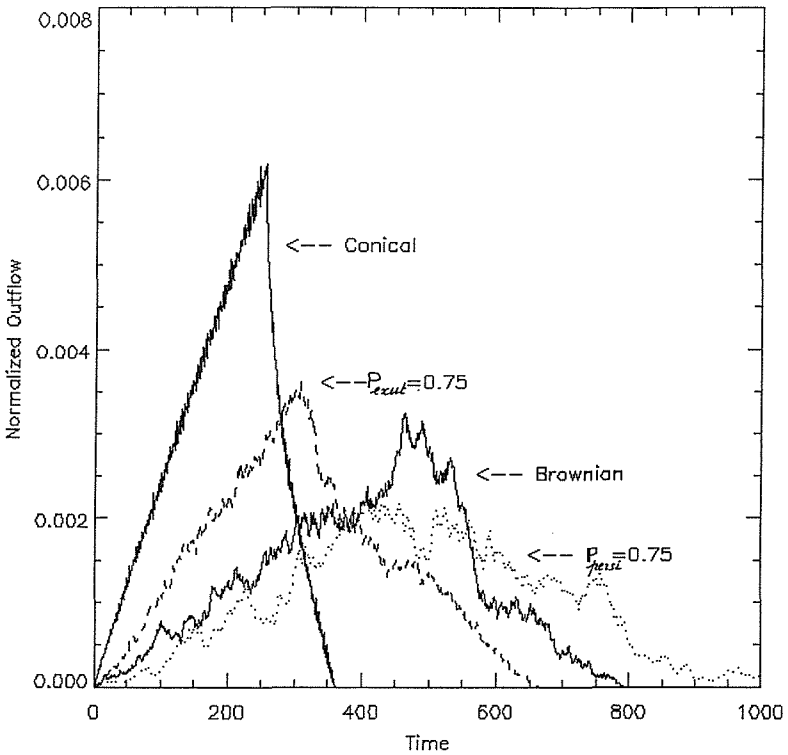

Fig. 4 Hydrogrammes unitaires pour quatre réseaux simulés, les vitesses d'écoulement étant supposées constantes. Remarquer la montée quasi linéaire pour ces quatre réseaux hydrographiques de complexité variable.

que du caractère homogène de la construction des réseaux. Cependant une démonstration générale de cette propriété n'est pas triviale.

Interprétation des hydrogrammes unitaires (HU) liés à ces réseaux artificiels

Une averse de pluie unitaire est classiquement simulée sur le bassin versant. La réponse de l'exutoire au cours du temps, c'est-à-dire l'HU, est alors donnée par la formule (1) dans laquelle $P(t)$ est remplacé par la distribution de Dirac à $t = 0$. Les Figs 4 et 5 illustrent les résultats pour quatre des bassins simulés. Il ressort de leur examen que:

(a) Quel que soit le réseau, la montée de l'HU est toujours approximativement linéaire (ceci est plus clair sur la Fig. 5 qui intègre dans le temps les HU), sa pente dépendant en revanche du type de réseau. Cette caractéristique est liée à la propriété de linéarité de la densité de probabilité des longueurs de rivières. Elle est vérifiée tant que les gouttes d'eau parvenant à l'exutoire ont été interceptées dans une zone à l'intérieur de laquelle le réseau est homogène. Au delà, les frontières du bassin sont progressivement atteintes et les gouttes interceptées vont former la décrue, dont le profil semble par conséquent largement tributaire de la forme du bassin versant et est donc difficile à modéliser.

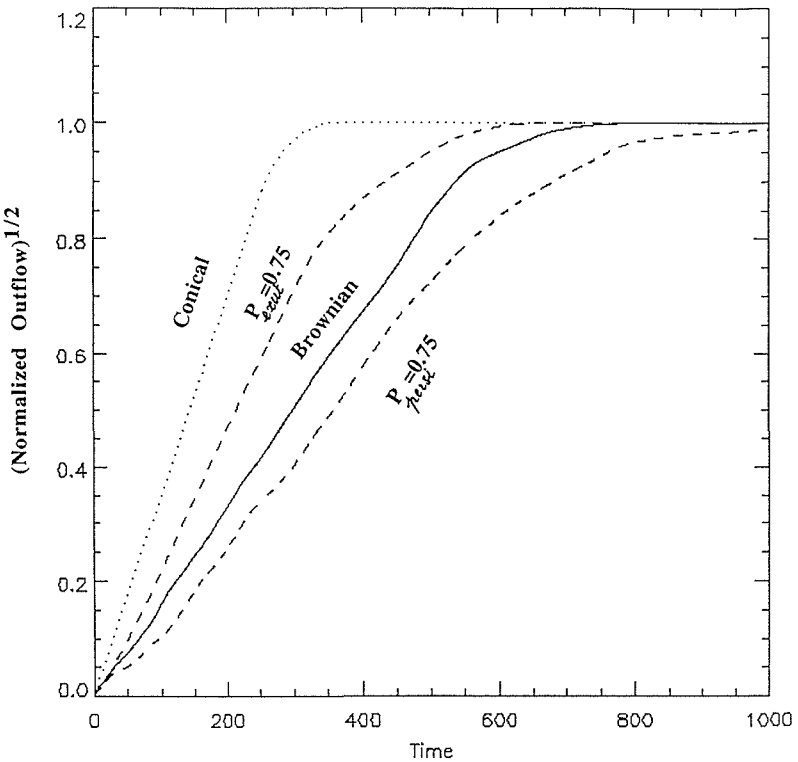

Fig. 5 Réponses des mêmes réseaux (voir Fig. 4) à un signal échelon unitaire (fonction de Heaviside) représentant une précipitation spatialement uniforme et constante dans le temps (épisode de précipitation stratiforme). En ordonnée est représentée la racine carrée du débit normalisé, de façon à mieux détecter le caractère linéaire des HU correspondants.

(b) Une complexité croissante pour la structure du réseau hydrographique tend à réduire la pente de l'HU: le temps de concentration augmente alors que le débit instantané de pointe diminue.

Si l'on avait affaire à un réseau non homogène (montagnes autour d'une plaine, par exemple), la montée de l'HU devrait probablement être décomposée en autant de parties linéaires qu'il y a de zones supposées homogènes (comme c'est en effet le cas de l'HU du réseau de la Loire). Ce travail montre par ailleurs que la montée de l'hydrogramme triangulaire, souvent utilisé comme hydrogramme de projet, semblait correcte pour modéliser la première partie de nos HU.

CONCLUSION ET PERSPECTIVES

L'exploitation de simulations de chevelus denses, homogènes et saturés, nous a permis d'interpréter l'HU utilisé lors de la transformation théorique Pluie/Débit. La partie croissante de l'HU dépend par définition du voisinage de l'exutoire: si le chevelu de ce voisinage est homogène et saturé, nos simulations indiquent que l'HU est contraint à une évolution linéaire en fonction du temps, la constante de temps

correspondante étant directement liée au "remplissage" du réseau (temps de concentration). Par voie de conséquence, les écarts expérimentaux au comportement linéaire de la partie croissante de l'HU peuvent être interprétés comme des indices de non homogénéité du chevelu, en terme de complexité géométrique ou de non saturation (infiltration ou évaporation). En revanche, la partie décroissante de l'HU ne peut être facilement modélisée, même en imposant des règles aussi restrictives que celles de posséder un chevelu homogène et saturé, la décrue étant extrêmement sensible aux limites du bassin versant. La forme du bassin est imposée par la géomorphologie, dont les constantes de temps sont arbitrairement grandes comparées aux échelles de temps utiles en hydrologie ou même en climatologie (des dizaines de millions d'années pour la formation d'un relief, des centaines ou des milliers d'années pour l'hydrologie ou la climatologie). L'interprétation de la partie décroissante de l'HU ne peut donc qu'être "géomorphologique" car elle ne dépend pas essentiellement de variables hydrologiques et météorologiques mais de constantes géographiques. Remarquons cependant que si la détermination des HU était suffisamment fiable, la forme de leurs parties décroissantes serait une "signature" unique, caractéristique de la forme et des propriétés de chaque bassin versant.

Remerciements Les auteurs remercient B. Guillemet, Y. Pointin & H. Isaka du LaMP pour leurs critiques constructives sur ce travail.

REFERENCES

Alix, P. & Roy, F. (1996) Etude hiérarchique des réseaux hydrographiques à l'aide de la classification de Horton. TER-LaMP/Université Blaise Pascal de Clermont-Ferrand.

Galéa, G. & Prudhomme, Ch. (1994) Modèles débit-durée-fréquence et conceptualisation d'un hydrogramme de crue synthétique: validation sur le BVRE de Draix. *Hydrol. Continent.* **9**(2).

Grassberger, P. (1985) Random walks without intersections. *J. Phys. A. Math. Gen.* **18**(1985) L-463.

Hack, J. T. (1957) Studies of longitudinal stream profiles in Virginia and Maryland. *US Geol. Survey Prof. Pap. 294-B*, 45–94.

Hjelmfelt, A. T. (1988) Fractals and the river length–catchment area ratio. *Wat. Resour. Bull.* 24, 455–459.

Mandelbrot, B. (1982) *The Fractal Geometry of Nature*. W. H. Freeman & Co., San Francisco.

Pejoux, R. (1996) Traitement morphologique élémentaire d'un réseau hydrographique (cas où le relief avoisinant le réseau n'est pas connu). *Note OPGC no. 135*, juin 1996.

Takayasu, H. (1990) *Fractals in the Physical Sciences. Nonlinear Science, Theory and Applications*. John Wiley & Sons.

8 Hydrological Processes

FRIEND'97 — Regional Hydrology: Concepts and Models for Sustainable Water Resource Management
(Proceedings of the Postojna, Slovenia, Conference, September–October 1997). IAHS Publ. no. 246, 1997.

In situ measurements of hillslope runoff components with different types of forest vegetation

HUBERT HOLZMANN & NORBERT SEREINIG
Institute for Water Management, Hydrology and Hydraulic Engineering, University of Agricultural Sciences (BOKU), Muthgasse 18, A-1190 Vienna, Austria

Abstract The aim of the project was to identify the components of hillslope runoff in micro catchment scale and to assess the impact of the forest vegetation types on the hydrologic response. At two experimental sites in an alpine forested catchment, measurement devices have been installed. The first is covered by coniferous trees (spruce), the second by mixed type forest (beech, spruce, fir trees) with domination of deciduous species. The subsurface runoff components have been collected and continuously autologged in trenches at three depths (20, 110 and 160 cm). Soil physical analysis and measurements of soil moisture and matric head described the soil water characteristics of the above hillslope sections. First analysis of the data showed differences of hydrologic response due to vegetation type caused by different interception and retention capacities.

INTRODUCTION

In Austria forestry plays an important role not only for economical purposes but also for the capacity of forested hillslopes for flood retention and torrent and avalanche protection. Due to increasing intensity of forestry as an economical factor the original mixed type forest in the alpine regions changed more and more to monocultural spruce forest during the last century. This may have caused changes in the hydrologic response in the catchments, but these effects are hardly to identify and not much investigated.

Therefore the aim of the project was the assessment of hillslope runoff components in different depths at specific sites considering monocultural and mixed type forests. Groups of hydrologists and forest ecologists have been involved and thus interdisciplinary approach was supported.

STUDY AREA

The study area is located in an alpine subcatchment of the River Enns in Styria, Austria. About 60–70% of the subcatchment is covered by forest. The two experimental sites, where the micro scale hillslope runoff has been measured, are at elevations of 1050–1100 m a.s.l. The first site has mixed type vegetation cover with beech, spruce and fir trees. Its slope is 35 degrees. The second site has monocultural spruce cover with a slope of 40 degrees. Slope aspect is directed from northeast to east respectively. The soil depth varies from 60 cm to 2 m. The permeable bedrock consists of fractured phyllite slate and was located in the experiment pits at a depth of 160 cm.

MEASUREMENT DEVICE AND INSTRUMENTATION

Hillslope runoff can be divided into Hortonian surface runoff—which could hardly be observed in the monitored forested slopes—and into subsurface flow. The latter consists of near-surface flow (0–20 cm), intermediate flow or interflow (20–110 cm) and of base flow near the bedrock zone. The layer boundaries are irregular and their contribution to the runoff depends on soil properties and stratifications, on actual soil moisture contents, on precipitation intensities and duration.

For the assessment of runoff components a pit has been excavated at both sites down to the bedrock layer (160 cm). Metal sheets with a width of 160 cm have been pushed about 40 cm into the front face of the pit (Fig. 1). Runoff gutters lead the flux to containers, where the accumulation of discharge is measured by pressure probes. The containers are emptied by siphon tubes. Similar hillflow measurement applications have been referred to in Atkinson (1978) and Peters *et al.* (1995).

Soil moisture characteristics of the hillslope sector above are measured by three tensiometers and 16 TDR probes. A multiplexer enables simultaneous measurements of all probes. These measurements provide data for estimating soil retention

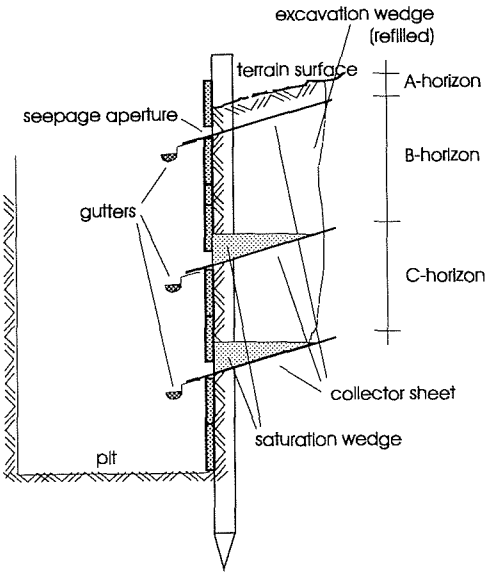

Fig. 1 Cross-section scheme of the pit for the assessment of hillslope runoff components.

Table 1 Instrumentation and measured parameters of the runoff measurement device.

Instrumentation	Measured component (dt = 15 min)
2 tipping bucket gauges	precipitation in mm
3 pressure probes (in runoff containers)	runoff depth in mm
3 tensiometers + 1 soil temperature probe	suction head in hPa
1 TDR-Trase System 1 with multiplexer and 16 TDR-probes (buriable wave guides)	Soil moisture content in vol % (dt = 60 min)
1 data logger (GEALOG S)	data storage
1 solar panel + car battery	autonomous energy supply

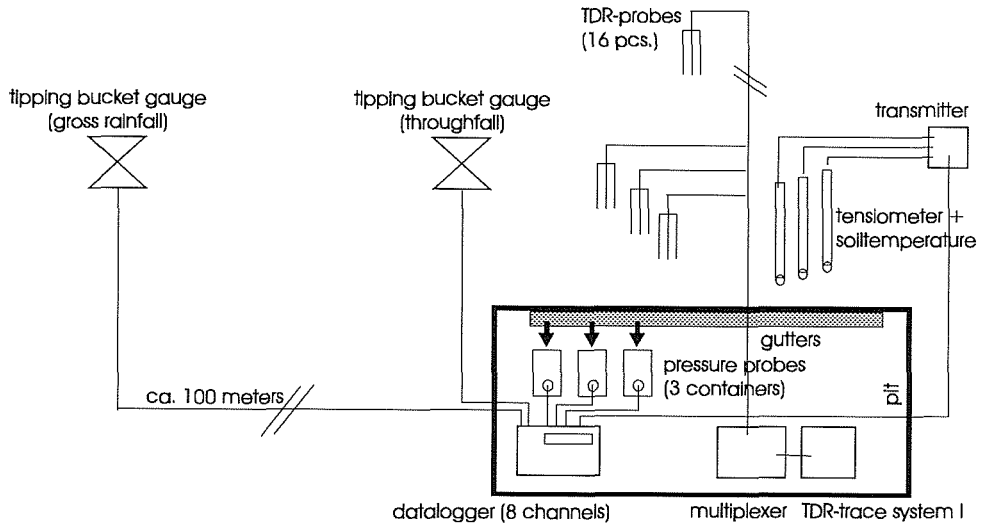

Fig. 2 Scheme of instrumentation at the experiment site.

characteristics and are reasonable to fit analytical retention curves to the *in situ* measurements (Campbell, 1985; Van Genuchten *et al.*, 1994). The latter are required for numerical modelling of the runoff process (e.g. in Simunek *et al.*, 1994). Precipitation is collected with tipping bucket gauges for non covered and forested domains (throughfall). The observations of the latter are compared and adjusted to data from the gutter collectors, which are distributed in the forest and provide more representative interception areas. Table 1 shows the installed instrumentation components. All data are stored in a data logging device at 15-minute intervals. Figure 2 shows a scheme of the instrumentation.

For the measurement of climatic parameters a portable meteorological station was installed. The instrumentation and measured parameters are summarized in Table 2. These parameters enable the computation of potential evapotranspiration (Doorenbos & Pruitt, 1975).

Table 2 Instrumentation and measured parameters at the meteorological station.

Instrumentation	Measured component (dt = 15 min)
1 wind velocimeter (Type 263)	wind velocity and direction
1 temperature sensor (Type YSI)	air temperature in °C
1 star pyranometer (Model no. 8101)	radiation
1 tipping bucket gauge(Type AP22)	precipitation in mm
1 hygrometer (Type MP)	air humidity
1 solar panel + car battery	autonomous energy supply

RESULTS OF CONTINUOUS MEASUREMENTS

In the summer period of 1995 and 1996 continuous measurements have been carried out on both experimental sites. Due to instrumentation facilities only one site could be equipped with automatic probes and data logging device. At the complementary

site only accumulated runoff components at three depths have been monitored periodically (one or two times a week). Thus comparisons and conclusions can only be made for a periodic approach, not for single events. In the summer period 1995, the automatic data-logging system has been used for the site with mixed type forest. In summer 1996 it was installed for the coniferous site. The accumulated rainfall and the runoff components are shown in Fig. 3 (1995) and Fig. 4 (1996).

The observation period 1995 started on 4 August and ended on 31 October. The total amount of precipitation for that period of 88 days is similar for both experimental sites. Single events may differ due to the distance (2 km) and regional distribution. The throughfall at the mixed type forest was 264 mm, at the coniferous forest 247 mm. The difference is caused by lower interception capacities for deciduous trees and stemflow existence, and also by different event-based rainfall intensities (Fig. 3).

At the mixed type forest, runoff was dominated by the near-surface component (0–20 cm). Its contribution to the total runoff amount is about 70%. The interflow component (20–110 cm) was about 20% and the baseflow (110–160 cm) was 10% of

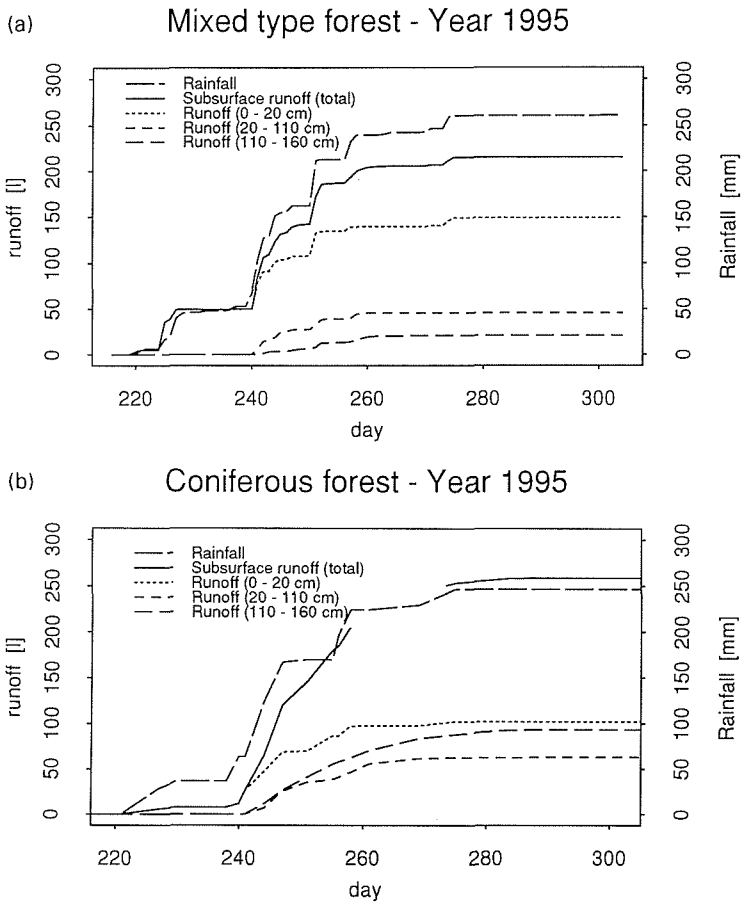

Fig. 3 Accumulated rainfall and runoff components for mixed type forest (a) and coniferous forest (b) for the vegetation period of the year 1995.

the total collected runoff. It has to be mentioned, that for both sites no impermeable bottom layer (impermeable bedrock) exists and thus the total amount of runoff could not be collected with the installed measurement device.

At the coniferous forested site the total amount of collected runoff was about 260 litres and thus higher than at mixed type forest (210 litres). The runoff contributions of the different layers were similar (Fig. 3). This may be caused by the higher conductivities in the upper layers (Table 3) but also, due to the lower root depths, the retention and transpiration capacities will be lower for coniferous vegetation and thus cause increasing hillslope runoff.

In 1996 the observation duration lasted from 8 June to 19 August. In that period of 73 days the mixed type forest site showed total surface runoff of 195 litres, 76% contributed by the near-surface flow. At the coniferous forest site the total runoff was 382 litres and thus much higher than at the mixed type site. Note the different ordinate scale for runoff in Fig. 4(b)! The rainfall amount of the coniferous forest is based on measurements of tipping bucket gauge. These values have not yet been adjusted to the rainfall gutter measurements.

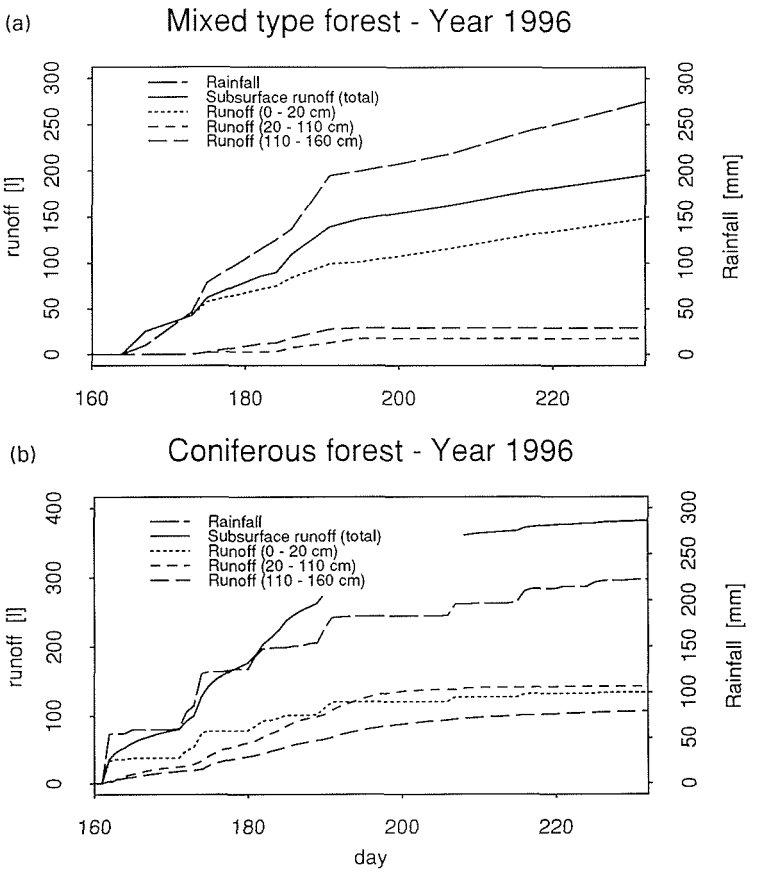

Fig. 4 Accumulated rainfall and runoff components for mixed type forest (a) and coniferous forest (b) for the vegetation period of the year 1996.

The observations for the wet summer period of 1996 showed significant higher hillslope runoff at the coniferous site. Its runoff contribution was uniformly distributed over the total depth of collection.

Table 3 Saturated hydraulic conductivities (*ks*) of the two experimental sites.

	Mixed type forest:				Coniferous forest:			
Depth (cm)	soil type	*ks*mean	*ks*min	*ks*max	soil type	*ks*mean	*ks*min	*ks*max
Hydraulic conductivity from laboratory soil sample analysis (m day^{-1})								
30	lS	23.9	8.9	34.0	siS	99.8	35.0	160.2
80	siS	50.6	1.6	177.1	S	60.3	38.4	86.7
110	siS	24.7	2.2	62.4	lS	16.5	1.6	28.8
Hydraulic conductivity from *in situ* measurements with Guelph permeameter (m day^{-1})								
30	lS	3.0	0.9	7.1	siS	8.6	2.2	21.2
70	siS	2.4	0.9	6.6	lS	2.9	1.7	4.9

lS = loamy sand
siS = silty sand
S = sand

RESULTS OF IRRIGATION EXPERIMENT

Due to the fact that the implementation of the data-logging device could only be carried out for one experimental site, there exists a deficit in the ability of direct comparison of *event-b*ased measurement values like runoff or soil moisture distribution. Thus irrigation experiments were undertaken from 19 to 23 August 1996. Under the existing circumstances the following appropriate conditions could be fulfilled at both sites:

- comparable (constant) starting conditions (dry conditions without flux);
- identical rainfall intensities and temporal distributions;
- availability of automatic measurement device as shown in Fig. 2 leads to reliable temporal resolutions of measurement parameters.

Fortunately the rainfall experiment took place under excellent weather conditions. Thus no natural rainfall effected the experiment.

The rainfall simulator covered an area of 12 m^2. The width was 2 m, the horizontal length 6 m. The required water amount has been pumped from a nearby brook and was intermediately stored in big balloons with a volume of 8 m^3. The rainfall intensities could be varied during operation by computer software. The duration of irrigation was 3 h. The rainfall depth for the first 2 h was about 60 mm h^{-1} and 100 mm h^{-1} for the third hour. This means an application of about 2700 litres for the whole area. These intensities are comparable to experiments by other authors (e.g. Markart & Kohl, 1995).

The results show very low rates of collected hillflow (Fig. 5). In the mixed type forest only 1.2% of applied rainfall discharge could be collected as subsurface runoff. At the coniferous site 8% of rainfall have been collected. The soil moisture measurements showed significant increase of moisture content. An extrapolation of the point measurement values to the representative volume of irrigated domain showed an increase of moisture storage of 1371 litres for the mixed type forest, which is 52% of the rainfall amount. In the coniferous forest 1050 litres, 39% of total rainfall, are stored in the corresponding soil domain. Figure 5 shows the time series of accumulated rainfall depth, subsurface runoff and soil moisture increase.

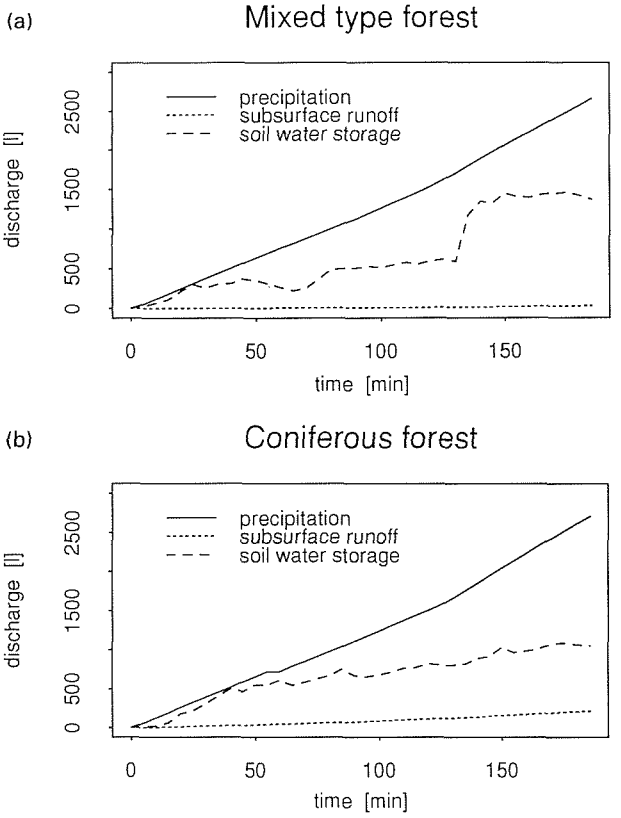

Fig. 5 Accumulated rainfall and runoff components for mixed type forest (a) and coniferous forest (b) for the rainfall experiment.

About 50% of the rainfall application could not be measured by TDR probes or runoff collectors. This amount can be interpreted as the lateral and vertical vanishing moisture flux. This shows that irrigation experiments for local domains imply three-dimensional infiltration and moisture redistribution processes, which could only partly be monitored with the installed instrumentation.

ONGOING INVESTIGATIONS

Within the research project several further investigations have been carried out, which are specified in the following section. They are described in detail in Hager & Holzmann (1995) and Hager & Holzmann (1996).

- soil physical analysis;
- measurement of plant physiological parameters like interception capacities of trees and bushes, root depths and densities, stem runoff etc.;
- modelling of subsurface slope runoff in the hydraulic laboratory;
- numerical, two-dimensional modelling of the runoff process in microscale for laboratory application and *in situ* experimental site, considering vegetation impact.

These data provide a good database for further research on hillslope runoff processes.

CONCLUSIONS

One aim of the project was the assessment of the basic hillslope runoff processes in micro catchment scale and the identification of the impact of vegetation type (forest species) on the hydrologic response. Regarding the runoff process, no surface runoff could be observed at both test sites. This is caused by the high conductivities of the existing soils and of the organic layer. Similar conclusions are found by Mosley (1979). Near surface runoff component is dominant in the mixed type forest. In the coniferous site, the quantities of near surface, intermediate and baseflow are uniformly distributed. The mixed type forest showed less runoff both in continuous observation periods and in the irrigation experiment. This may be caused by higher retention capacities of the soil due to soil physical characteristics but also due to the higher transpiration rates of deeper root zones.

Because of different soil conductivities (see Table 3) the direct impact of vegetation to the runoff process could not directly be proved. Only differences of the interception capacities between coniferous (spruce) and deciduous trees (beech) could be evaluated directly. Additional applications of numerical, physically based models, which have to be calibrated with *in situ* conditions, will give further information. These investigations are in progress and further results on that topic are expected in the near future.

Acknowledgements The authors give their special thanks to the Austrian Academy of Sciences for the financial support of the project within the Austrian Programme *Hydrology of Austria*, which is a subprogram of the IHP-IV activities.

REFERENCES

Atkinson, T. C. (1978) Techniques for measuring subsurface flow on hillslopes. In : *Hillslope Hydrology* (ed. by M. J. Kirkby), 1–42. John Wiley & Sons, Chichester, UK.

Campbell, G. S. (1985) *Soil Physics with Basic Transport Models for Soil–Plant Systems*. Elsevier , Amsterdam.

Doorenbos, J. & Pruitt, W. O. (1975) Crop water requirements. Irrigation and Drainage Paper 24, FAO, Rome.

Hager, H. & Holzmann, H. (1995) Hydrologic functions of natural forest ecosystems in an alpine catchment (in German) First annual report of research project HÖ/94 by order of the Austrian Academy of Sciences, Vienna.

Hager, H. & Holzmann, H. (1996) Hydrologic functions of natural forest ecosystems in an alpine catchment (in German). Second annual report of research project HÖ/95 by order of the Austrian Academy of Sciences, Vienna.

Markart, G. & Kohl, B. (1995) High intensity rainfall simulation and soil physical parameters as a base for estimation of runoff and infiltration characteristics of alpine soil and vegetation units (in German). *FBVA Berichte*. Ser. no. 89. Forstliche Bundesversuchsanstalt Wien.

Mosley, M. P. (1979) Streamflow generation in a forested watershed, New Zealand. *Wat. Resour. Res.* **15**(4).

Peters, D. L., Buttle, J. M., Taylor, C. H. & LaZerte, B. D. (1995) Runoff production in a forested, shallow soil, Canadian Shield basin. *Wat. Resour. Res.* **31**(5), 1291–1304.

Simunek, J., Vogel, T. & Van Genuchten, M. Th. (1994) The SWMS-2D code for simulating water flow and transport in two-dimensional variable saturated media. *Research Report no. 132, US Salinity Laboratory, US Department of Agriculture, Riverside, California.*

Van Genuchten, M. Th., Leij, F. J. & Yates, S. R. (1994) *The RETC Code for Quantifying the Hydraulic Functions of Unsaturated Soils*. US Department of Agriculture, Agricultural Research Service, Riverside.

FRIEND'97 — Regional Hydrology: Concepts and Models for Sustainable Water Resource Management
(Proceedings of the Postojna, Slovenia, Conference, September–October 1997). IAHS Publ. no. 246, 1997.

Erosion processes and their implications in sustainable management of watersheds in Nepal Himalayas

SURESH RAJ CHALISE
Mountain Natural Resources Division, International Centre for Integrated Mountain Development (ICIMOD), Jawalakhel, Kathmandu, Nepal

NARENDRA RAJ KHANAL
Central Department of Geography, Tribhuvan University, Kirtipur, Kathmandu, Nepal

Abstract The problem of soil erosion due to human and natural processes, and its consequences in terms of sedimentation and changes in hydrological regimes in downstream areas in the Himalayas in general and in Nepal in particular, has been a subject of national and global concerns. Considering the lack of long-term pertinent data the uncertainty that surrounds this debate has already been well highlighted. Recently some works at plot level, micro and meso watershed level erosion processes have been carried out in different physiographic and elevation zones in Nepal Himalaya which have been used to examine the role of land management in modifying the runoff and soil loss from the hillslopes in this area. The paper is based on secondary data and information on runoff and soil erosion processes reported from different parts of the country. Significant differences were observed in the rate of soil loss and the percentage of runoff to total precipitation with time, physiographic regions and different land cover/use and land management practices. The data so far available are limited in time and space and it is difficult to generalize these processes. However, it appears that there is a possibility of minimizing the loss of soil and enhancing productivity upstream through simple and innovative land use and land management practices which could also contribute significantly to reduce flood hazards in downstream areas of the watershed.

INTRODUCTION

Nepal Himalayas is one of the high energy environments mainly because of very active tectonic activities, high relief and seasonal concentration of precipitation. The altitude ranges from only 60 m in the south to more than 8848 m in the north within a short distance of 160 km. The recorded mean annual precipitation ranges from only 163 to 5244 mm with a weighted average of 1630 mm. More than 80% of the total precipitation occurs during the monsoon season between June and September. Daily precipitation exceeding 300 mm occurs frequently in the country and produces simultaneous disturbances of both the slopes and channel equilibrium on the regional scale (Chalise *et al.*, 1995; Khanal *et al.*, 1996; Khanal, 1995). Due to very high relief and seasonal concentration of precipitation with frequent high intensity precipitation events and frequent seismic activities, natural hazards in the form of surface erosion and landslides are common. Moreover, the high rate of growth of human and livestock population, subsistence land-based economy and scarce land resources have also caused to accelerate natural erosion processes. The total

population of the country has more than doubled from 8.3 million in 1952–1954 to 18.5 million in 1991 with an annual growth rate of more than 2% and more than 90% of the total population engaged in subsistence farming (Manandhar *et al.*, 1994). Livestock population in relation to arable land and animals per person is large by Asian standards (HMG/ADB, 1993). About 21% of the total area of the country is under agricultural use whereas only 17% of the total land with slopes less than 5° is suitable for seasonal crops. Forest lands have been brought for agricultural use in order to meet the increasing demand of food and fodder (Bajracharya, 1983). Similarly, due to the increasing demand for fuel wood which shares more than 83% of the total energy consumption in the country (HMG/ADB, 1993), the pressure on non-agricultural land has also been increasing and consequently accelerating the rate of surface erosion and environmental degradation.

Much of the discussion regarding environmental degradation in Nepal Himalayas which started in the mid 1970s have focused primarily on ecological concerns particularly on deforestation caused by fast growing human and animal population and its consequent impact on local and regional ecology and economy (Eckholm, 1975, 1976; Ives & Messerli, 1989). This paper attempts to discuss spatial and temporal variation in runoff and soil loss, its relation with land use and the implication for the sustainable management of watersheds in Nepal Himalayas.

METHODOLOGY

Present discussion on rainfall–runoff and soil loss processes is based on secondary information reported from different physiographic regions and land use types in different periods. On the basis of geology, relief and climate, Nepal is divided into five physiographic regions namely the Terai, the Churia Hills, the Middle Mountains, the High Mountains and the High Himal from south to north (Gurung & Khanal, 1987; LRMP, 1986). The Terai in the south with elevation ranging from 60 to 330 m is the extension of the Indogangetic plain. It represents about 13% of the total area of the country. The Churia (200–1500 m) including Inner Terai are similar in area and are composed of tertiary sandstone, siltstone, shale and conglomerates. The Middle Mountain with altitude between 800 and 2400 m is composed of phyllites, quartzite, limestone and isolated pocket of granites and occupies about 29% of the total area. The High Mountain between 2000 and 4000 m with relief of 3000 m is composed of gneiss, quartzite and mica schists and comprises 20% of the total area. The High Himal (>4000m) is composed of gneiss, schist, limestone and Tethys sediments and comprises about 24% of the total area of the country (LRMP, 1986). Seasonal and annual rainfall–runoff and soil loss data from erosion plots, micro, and meso watersheds have been analysed in order to understand the processes quantitatively and identify an intervention strategy for the sustainable management of land and water resources. Data on soil erosion from the High Himal used in this study are from Langtang and Khumbu (Watanabe, 1994; Byers, 1987). Rainfall–runoff and soil loss data reported from Bamti-Bhandara representing the High Mountain region (Ries, 1993) from Jhikhu khola, Chisapani, Chyandanda in Sindhupalchok district, Kulekhani and Pokhara representing the Middle Mountain and Subakuna (Surkhet district) representing the Churia hills have been analysed. In

addition, sediment discharge data from some selected watersheds have also been analysed in order to understand the process at different levels—from erosion plot to micro; and meso-watersheds in the country. The data on runoff and soil loss from plot to watershed levels referred to in this paper are not for individual events. Although these data do not represent the annual figures in all cases, all of them cover monsoon period which is critical for runoff and soil loss in Nepal.

DISCUSSION

Runoff

Data so far available on the percentage of precipitation which runs off is presented in Table 1. There is a wide variation in the percentage of runoff by time, place and land use types. The percentage of runoff from agricultural terraces ranges from only 0.5 to 33. Study on Bamti-Bhandara (the High Mountain) indicates that the runoff from agricultural terraces varies significantly by types of cultivation. Very high runoff of more than 20% was recorded from Buckma under shifting cultivation compared to only 3% from natural forest, 13% from used forest and 15% from pasture land (Ries, 1993). Studies in Dandapakhar and Bonch area showed that runoff ranges from only 5% from overgrown plots to 25% of the total rainfall from bare (weeded) plots (Schaffner, 1987). It varies from only 0.5 to 11.6% in Jhikhu khola from agricultural plots and such differences in runoff in Jhikhu khola were mainly due to the differences in soil properties and intensity of rainfall rather than slope and cropping (P. B. Shah, personal communication). At the micro-watershed level, the percentage of runoff so far reported ranges from only 12.2 to 35%. The percentage of runoff in paired catchments in Phewa (the Middle mountain) ranges from 22.4 to 29.6 whereas it is only 12.2–14.4 from Kulekhani. Study of the water budget in Likhu khola watershed (the Middle and High mountain) indicates that 35% of the total

Table 1 Percentage of runoff to total precipitation.

Places	Annual precipitation (mm)	Plot level: Agriculture	Pasture	Degraded forest/ shrubland[1]	Forest	Micro-watershed
High mountain						
Bamti-Bhandara (Ries, 1993)	1000–2200	0.2–33 (14.4)	14.8	12.6	3.2	
Dandapakhar (Schaffner, 1987)	3125		5–19			
Bonch (Schaffner, 1987)	3661		7–25			
Likhukhola (Boorman *et al.*, 1996)	4970					35
Middle mountain						
Pakribas (Sherchan & Chand, 1991)	1261	22–31 (29)				
Jhikhu khola	1393	0.5–11.6 (2.9)				
Chyandanda (Maskey & Joshi, 1991)	2104	15–24 (20.6)				
Chisapani (Maskey & Joshi, 1991)	2047	4–9 (6)				
Kulekhani (Upadhaya *et al.*, 1991 and DSC, 1995a, 1996)	1387	6–30 (16)				12.2–14.4
Phewa (DSC, 1996)						24.4–29.6

Note: Figure in parentheses indicates annual average.

[1] It also includes used forest and shrublands.

precipitation is discharged annually in the form of runoff, 34% is lost due to evaporation and the remaining 31% is lost by other processes (Boorman *et al.*, 1996).

Soil erosion

There is a wide variation with time, space and land use in the rate of soil erosion (Table 2). The annual loss of soil from agricultural plots ranges from only 0.1 to

Table 2 Annual soil erosion (t ha^{-1}).

Places	Annual precipitation (mm)	Altitude (m)	Plot level: Agriculture	Pasture	Degraded forest/ shrubland[1]	Forest	Micro-watershed
High Himal							
Khumbu (Byers, 1987)	807–1071	3300–4415		2.22–16.93		0.25–4.87 (0.6)	
Langtang (Watanabe, 1994)		3000–4900		0.43–2.95			
High mountain							
Bamti-Bhandara (Ries, 1993)	1000–2200	1995–2453	0.2–12.7 (5.8)	0.4	1.4	1.4	2.08–29.85
Dandapakhar (Schaffner, 1987)	3125	1730		0.4–18.7			
Bonch (Schaffner, 1987)	3661			3.7–66.6			
Middle mountain							
Pakribas (Sherchan & Chand, 1991)	1261		16.9–36.7 (32.9)				
Jhikhu khola (Carver & Nakarmi, 1995)	1393	1230–1260	0.1–42 (12.3)				
Chyandanda (Maskey & Joshi, 1991)	2104	1385	53.9–104.8				
Chisapani (Maskey & Joshi, 1991)	2047	1940	0.2–0.6 (0.6)				
Kathmandu (Laban, 1978)						8	
Kulekhani (Upadhaya *et al.*, 1991 and DSC, 1995a)	1387	1620–1800	0.3–3.98 (1.4)				0.2–0.3
Phewa (Mulder, 1978 and DSC, 1996)	3700			9–35		0.34	15.2–15.4
Dailekh (Carson, 1985)			2–7	20	15	5	
Churia							
Chatra (Laban, 1978)				36.8	7.8		
Lothar (Laban, 1978)				31.5–420			
Surkhet (DSC, 1995b)	923	720	1.06–2.74 (1.87)				
Nepal (Laban, 1978))							
Well managed level terraces			0–15		40–200	0–5	
Poorly managed sloping terraces			20–100				
Nepal (LRMP, 1986)							
Irrigated terraces (khet)			0				
Level terraces (pakho)			5				
Sloping terraces (pakho)			20				
Shifting cultivation			100				

Note: Figure in parentheses indicates annual average.

[1] It also includes used forest and shrublands.

104.8 t ha^{-1}. The average soil loss from different types of agricultural fields is reported to be 1.4 t ha^{-1} (10-years) in Kulekhani area, 12.27 t ha^{-1} (4-years) in Jhikhu khola and 32.9 t ha^{-1} (2-years) in Pakhribas in the Middle Mountain region. Relatively high rates of soil loss are reported from outward sloping terraces as compared to level terraces. Comparatively very high rate of soil erosion was reported from pasture and heavily utilized forest and shrubland as compared to the rate of erosion from protected and natural forest except at Bamti-Bhandara. Annual loss of soil from pasture land ranges from 9 to 35 t ha^{-1} in the Middle Mountain, 0.4–66.6 t ha^{-1} in the High Mountain and 0.43–16.93 t ha^{-1} in the High Himal region. Very high rates of soil loss from overgrazed or weeded bare ground (16.9–66.6 t ha^{-1}) were also reported from Khumbu, Danadapakhar and Bonch areas compared to the locally managed or overgrown pasture plots (Byers, 1987; Schaffner, 1987). The rate of soil loss from highly utilized degraded forest including *shrub*land ranges from 1.4 to 420 t ha^{-1} whereas it is between 0.25 and 7.8 t ha^{-1} from well managed or natural forest. Studies in micro-watersheds (less than 6 ha) show this rate to be less than 1 t ha^{-1} in Kulekhani to 15 t ha^{-1} in Phewa (the Middle Mountain) and 2–30 t ha^{-1} in Bamti-Bhandara. The estimated soil loss ranged from 0 to 15 t ha^{-1} from well managed level terraces to 20–100 t ha^{-1} from poorly managed sloping terraces, 40–200 t ha^{-1} from overgrazed degraded shrub and pasture land and

Table 3 Seasonal and annual loss of soil (t ha^{-1}).

Id	River	Station	Area (km^2)	November–February		March–June		July–October		Total
				Soil loss	%	Soil loss	%	Soil loss	%	Soil loss
Watersheds (Shankar, 1989)										
170	Surnagad	Patan	188							12
240	Karnali	Asarghat	19260	0.179	2.1	1.802	20.9	6.64	77.0	8.621
260	Seti	Banga	7460	0.43	1.5	2.537	9.1	25.051	89.4	28.018
280	*Karnali*	*Chisapani*	42890	0.372	1.9	2.699	13.4	17.034	84.7	20.105
286	Sarada	Sarada	816	0.105	2.1	0.104	2.1	4.861	95.9	5.070
290	Babai	Bargadha	3000							37
350	West Rapti	Bayasoti	3512	0.718	1.5	6.732	14.2	39.856	84.3	47.306
360	West Rapti	Jalkundi	5150	0.311	1.1	1.754	6.3	25.891	92.6	27.956
410	*Kaligandaki*	*Setibeni*	7130	0.197	0.5	4.013	9.6	37.518	89.9	41.728
430	Seti	Pokhara	582	0.632	1.2	18.793	35.6	33.434	63.3	52.859
447	Trisuli	Betrawati	4640	0.128	1.3	1.114	11.5	8.459	87.2	9.701
450	Narayani	Narayanghat	31100	0.295	0.5	4.359	7.7	52.184	91.8	56.838
470	Lothar	Lothar	169	0.1956	0.5	0.991	2.7	35.184	96.7	36.370
550	*Bagmati*	*Chobhar*	585	0.122	0.8	1.463	9.9	13.183	89.3	14.768
570	Kulekhani	Kulekhani	126	0.044	2.5	0.413	23.8	1.278	73.7	1.735
590	Bagmati	Karmaiya	2720	0.122	0.8	1.463	9.9	13.183	89.3	14.768
598	Kamala	Kamala	1550							32.3
690	Tamur	Mulghat	5640	1.217	1.2	11.954	11.7	88.881	87.1	102.052
695	*Saptakosi*	*Chatra*	59400							24.4
795	Kankaimai	Mainachuli	1148	0.263	0.5	6.071	12.6	42.021	86.9	48.355
	Average									31.1
Erosion plots										
	Dandapakhar (Schaffner, 1987)						74		26	
	Bonch (Schaffner, 1987)						71		29	
	Jhikhu khola (Carver & Nakarmi, 1995)						82		18	
	Kulekhani (Upadhaya *et al.*, 1991 and DSC, 1995a)				6		39		55	

0–5 t ha^{-1} from natural forest. The annual rate of soil loss within agricultural land ranges from 0 to 100 t ha^{-1} depending upon types of terraces.

The annual discharge of sediment from 20 watersheds is presented in Table 3 and Fig. 1. The rate of soil loss from these watersheds ranges from only 1.74 to 102.05 t ha^{-1} with an average of 31.1 t ha^{-1}. The annual loss of soil is comparatively low in the northern and middle part of the country except in Pokhara area (Setibeni and Pokhara) where the average annual precipitation is very high (more than 3700 mm) compared with other parts of the country (Fig. 2). The annual loss of soils from watersheds within the High and the Middle Mountain ranges from 1.73 t ha^{-1} in Kulekhani to 52.86 t ha^{-1} in Seti watershed (Pokhara) with an average of 19.39 t ha^{-1}, whereas it is between 14.77 t ha^{-1} in Bagmati at Karmaiya and 102.5 t ha^{-1} at Mulghat in Tamur with an average of 43.26 t ha^{-1} in the southern part of the country (the Mahabharat and Churia) and 20.11 t ha^{-1} at Chisapani in Karnali to 56.8 t ha^{-1} at Narayanghat in Narayani and 24.4 t ha^{-1} at Chatra in Saptakosi with an average of 33.8 t ha^{-1} (Fig. 1). Average annual soil loss from small watersheds with areas less than 200 km^2 is 16.7 t ha^{-1}, from watersheds with areas between 500 and 1000 km^2 is 24.23 t ha^{-1}, from watersheds with areas between 1000 and 5000 km^2 is 31.57 t ha^{-1}, from watersheds with areas between 5000 and 20 000 km^2 is 41.67 t ha^{-1} and from macro- watersheds with areas more than 20 000 km^2 is 33.78 t ha^{-1}. Average annual loss of soil in these watersheds increases with the increase in the size of watershed upto 20 000 km^2 and begins to decrease as the size becomes larger.

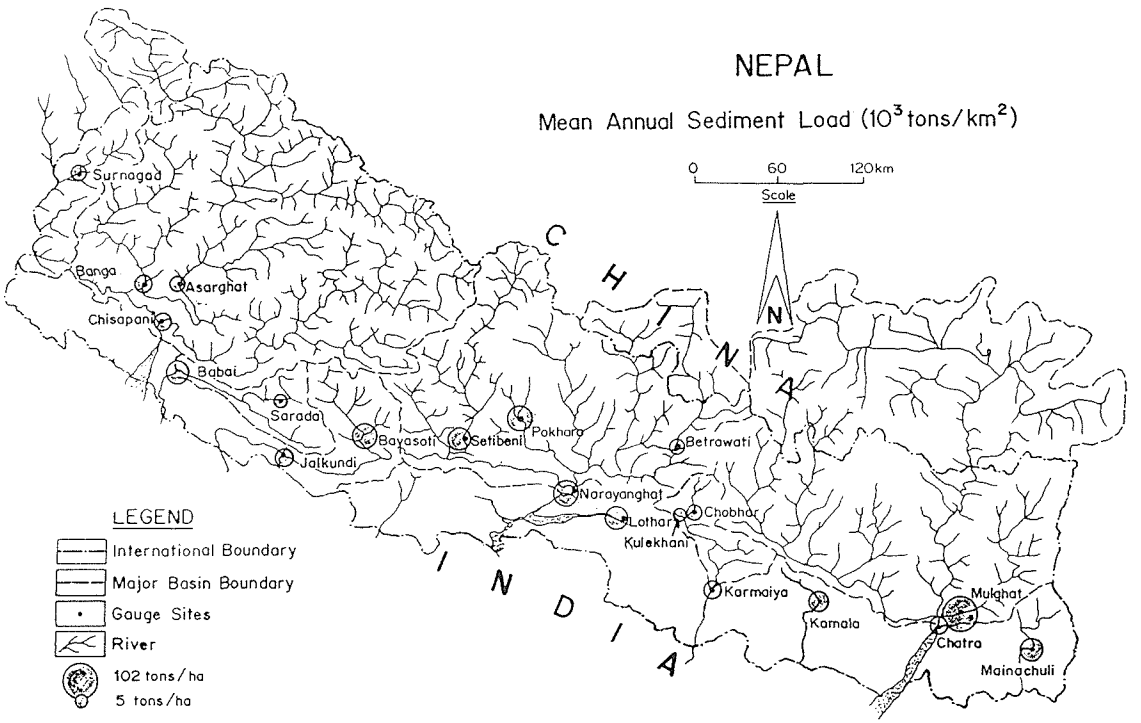

Fig. 1 Map showing drainage network and river discharge monitoring stations in Nepal and annual sediment discharge.

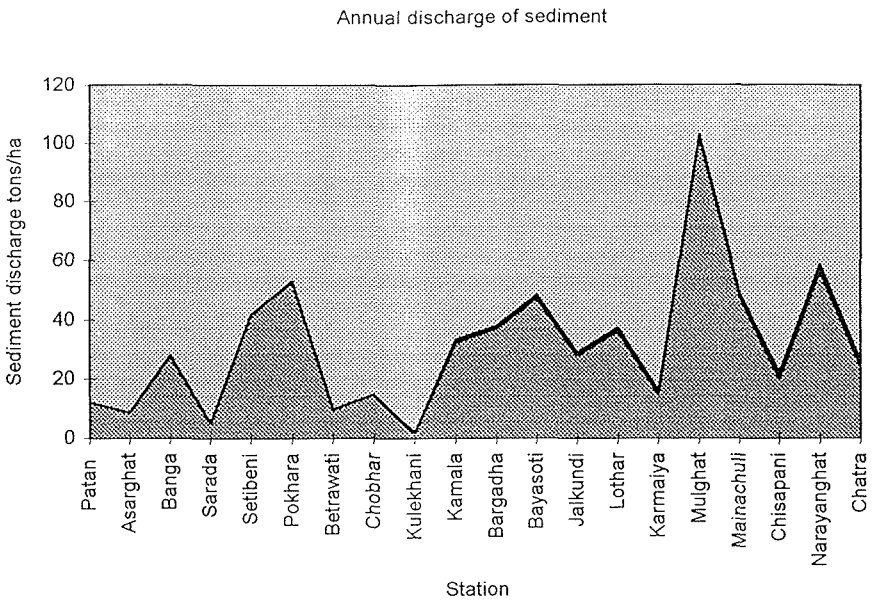

Fig. 2 Annual sediment discharge from selected watersheds in Nepal.

Annual sediment discharge from watersheds is higher than the average loss of soil from agricultural plots. Similarly, there are differences in the timing of soil loss in plots and watersheds. About 68% of the total soil loss occurs in the pre-monsoon and early monsoon period in agricultural plots whereas more than 86% of the total loads in the river is discharged during the later part of the monsoon period (Table 3). The comparatively very high loss of soil in the late monsoon period from watersheds compared to the amount of soil lost from agricultural fields indicates that the major sources of sediments in the rivers are not agricultural fields. The source of the high loss is surface erosion from degraded pasture, shrub and forest areas, and from landslides, river bank cutting and reworking of deposited materials along the gullies and river channels. The rate of soil erosion from degraded forest, shrubland and overgrazed pasture land is more than double that from agricultural fields. Several other studies also indicate that agricultural fields are well managed by the farmers and the loss of soil from these fields is less than was generally assumed in the past (Chalise, 1986; Ives & Messerli, 1989). Tree cutting alone is considered not to lead to increase in surface erosion, nor to the decrease in water resources, nor any negative consequences in the timing and distribution of water resources. However, overgrazing and the collection of litter from forest land does contribute to high runoff and soil loss (Hamilton, 1987). Since grazing of animals and collection of litters and grasses for farm manure and fodder from common lands (shrubland, forest and pasture) are commonly practised in the country, one can expect high surface runoff and sediment yield from these common lands. Studies of the soil hydraulic properties in Sindhupalchok also reveal that short term rainfall events are likely to cause more surface runoff on heavily grazed, trampled grassland than on well protected forest areas (Gilmour *et al.*, 1987).

Studies of landslides in Kakani by Caine & Mool (1982) indicate that 1% of the

total area is occupied by landslides resulting in a denudation rate of 14 mm $year^{-1}$ (approximately 250 t ha^{-1}). In Lele watershed near Kathmandu, a single precipitation event of 1981 caused many landslides (47 landslides per km^2) removing hillslope materials of more than 160 t ha^{-1} (Manandhar & Khanal, 1988). In Kulekhani watershed the estimated volume of materials removed from landslides by a single event of 1993 was more than 2000 t ha^{-1} from agricultural fields and 10 000 t ha^{-1} from degraded forest, shrubland and pasture (Khanal, 1995; Dhital *et al.*, 1993). Significantly high rates of sediment discharge from Tamur (50 $m^3 ha^{-1}$ $year^{-1}$) as compared to other watersheds such as Arun (9.7 $m^3 ha^{-1}$ $year^{-1}$), Sunkosi (28 $m^3 ha^{-1} year^{-1}$) and Saptakosi (19.5 $m^3 ha^{-1}$ $year^{-1}$) were reported to be due to a higher density of landslides in Tamur (13.8% of the total area) than in other watersheds (less than 3% of the total area covered by landslides) (HMG/JICA, 1986). Though the dominant causes of deep and large scale landslide occurrences are natural, it has been reported that large scale mass wasting (landslides) had increased by 26% as a result of human activities (Laban, 1979).

Table 4 Land use (000 ha).

Land use types	Existing area	Additional area suitable for trees
1. Total land area	14 748	
2. Total cultivated land:	3 052	
(a) Hillslope cultivation level terraces	774	
(b) Hillslope cultivation sloping terraces	511	
(c) Terai/valley cultivation	1 767	
3. Non-cultivated inclusion within cultivated land	998	789
4. Grazing land	1 745	829
5. Forest/plantation	5 518	5 518
(a) Forest with crown density 10–40%	1 417	
(b) Forest with crown density 40–70%	3 186	
(c) Forest with crown density >70%	821	
6. Shrub/degraded forest	706	706
7. Others	2 729	

Source: HMG/ADB/FINNIDA (1988) and LRMP (1986).

Land use

Earlier discussions on runoff and erosion processes have shown that the major source of sediments are other than privately owned agricultural fields. It is poorly managed common lands e.g. pasture, shrubland and used forest area which contribute to high sediment yield. Though reduction in soil and nutrient loss from the agricultural fields particularly from outward sloping terraces is essentially required to maintain the productivity, it is the common lands which should be managed from the ecohydrological view point. Table 4 shows the existing land cover/land use condition of the country. It indicates that greater attention should be paid to improving the management of about 511 000 ha of sloping terraces, 789 000 ha of non-cultivated inclusions (which include mainly grazing and shrublands), 829 000 ha of grazing land, 1 417 000 ha of thinly covered forest with crown densities between 10 and 40% and 706 000 ha of shrub and degraded land which altogether represent about 29% of the total area for the sustainable economic and ecological development of the country.

REFERENCES

Bajracharya, D. (1983) Deforestation in the food/fuel context, historical and political perspectives from Nepal. *Mountain Research and Development* **3**(3), 227–240.

Byers, A. C. (1987) A geoecological study of landscape change and man-accelerated soil loss: the case of the Sagarmatha (Mt Everest) National Park, PhD Thesis, University of Colorado, Boulder, USA.

Boorman, D., Jenkins, A. & Collins, R. (1996) Rainfall runoff data and modelling in the Likhu khola catchment, Nepal. Paper presented in International Conference on Ecohydrology of High Mountain Areas (Kathmandu, 24–28 March 1996).

Caine, N. & Mool, P. K. (1982) Landslides in the Kolpu khola drainage, middle mountains, Nepal. *Mountain Research and Development* **2**(2), 157–173.

Carson, B. (1985) Erosion and sedimentation processes in the Nepalese Himalaya, *ICIMOD Occasional Pap. no. 1, Kathmandu.*

Carver, M. & Nakarmi, G. (1995) The effect of surface conditions on soil erosion and stream suspended sediments. In: *Challenges in Mountain Resource Management in Nepal, Processes, Trends and Dynamics in Middle Mountain Watersheds* (ed. by H. Schreier, P. B. Shah & S. Brown) (Proc. Workshop, April 1995), 155–162. International Development Research Centre (IDRC), Ottawa.

Chalise, S. R. (1986) Constraints of resources and development in the mountainous regions of south Asia. In: *Nepal Himalaya, Geoecological Perspectives* (ed. by S. C. Joshi, M. J. Haigh, Y. P. S. Pangtey, D. R. Joshi & D. D. Dani), 13–26. Himalayan Research Group, Naini Tal, India.

Chalise, S. R., Shrestha, M. L. & Nayaju, R. P. (1995) Rainfall as the primary indicator of water induced disasters in Nepal (Proc. International Seminar on Water Induced Disaster (ISWID), March 1995), 191–201. Water Induced Disaster Prevention Technical Centre (DPTC). Kathmandu.

Dhital, M. R., Khanal, N. & Thapa, K. B. (1993) The role of extreme weather events, mass movements and land use changes in increasing natural hazards: A report of the preliminary field assessment and workshop on causes and recent damage incurred in south-central Nepal (July 1993). ICIMOD, Kathmandu.

DSC (Department of Soil Conservation) (1995a) Kulekhani soil loss and runoff plot. *Annual Report 1994/95—Watershed Management Project, Kathmandu.*

DSC (Department of Soil Conservation) (1995b) Soil loss and runoff study at Subbakuna Demonostration Centre, Surkhet. *Annual Report 1994/95—Watershed Management Project, Kathmandu.*

DSC (Department of Soil Conservation) (1996) Paired catchment study in Kulekhani and Pokhara. *Annual Report 1995/96—Watershed Management Project, Kathmandu.*

Eckholm, E. (1975) The deterioration of mountain environment. *Science*, 764–770.

Eckholm, E. (1976) *Losing Ground, World Watch Institute.* W. W. Norton & Co., New York.

Gilmour, D. A., Bonell, M. & Cassells, D. S. (1987) The effects of forestation on soil hydraulic properties in the middle hills of Nepal: A preliminary assessment. *Mountain Research and Development* 7(3), 239–249.

Gurung, H. B. & Khanal, N. R. (1987) Landscape processes in the Chure range, central Nepal, Nepal National Committee for Man and the Biosphere, Kathmandu.

Hamilton, L. S. (1987) What are the impacts of Himalayan deforestation on the Ganges-Brahmaputra lowlands and delta? Assumptions and facts. *Mountain Research and Development* 7(3), 256–263.

HMG/ADB (1993) *Livestock Master Plan*, vol. I: *A Strategy for Livestock Development.* Kathmandu.

HMG/ADB/FINNIDA (1988) Master plan for forestry sector, Nepal, main report. Kathmandu.

HMG/JICA (1986) Master plan study on the Kosi River water resource development. Kathmandu.

Ives, J. D. & Messerli, B. (1989) *The Himalayan Dilemma: Reconciling Development and Conservation.* The United Nations University, Routledge, London.

Khanal, N. R. (1995) The 1993 extreme event in Nepal and its consequences. Geographer's point. *J. Geogr., Centre for Nepalese Geography* **IV**(1 and 2), 18–21.

Khanal, N. R., Pokharel, A. P. & Chalise, S. R. (1996) Ecohydrology of river basins of Nepal. Paper presented at the International Conference on Ecohydrology of High Mountain Areas (Kathmandu, 24–28 March 1996).

Laban, P. (1978) Field measurements on erosion and sedimentation in Nepal. *Integrated Watershed Management Project Working Pap. no 5, Dept of Soil Conservation and Watershed Management, Kathmandu.*

Laban, P. (1979) Landslide occurrence in Nepal. *Nepal Report IWM/WP/13, HMG, Ministry of Forest, Kathmandu.*

LRMP (Land Resource Mapping Project) (1986) *Land System Report: the Soil Landscapes of Nepal.* Kenting Earth Sciences, Kathmandu.

Manadhar, I. N. & Khanal, N. R. (1988) Study on landscape processes with special reference to landslides in Lele watershed, central Nepal. Research Division, Tribhuvan University, Kirtipur, Kathmandu.

Manandhar, M., Subedi, B. P., Malla, U. M., Shrestha, C. B., Ranjitkar, N. G., Pradhan, P. K. & Khanal, N. R. (1994) *Study on Population and Environment in Nepal.* Central Department of Geography, Tribhuvan University, Kathmandu.

Maskey, R. B. & Joshi, D. (1991) Soil and nutrient losses under different soil management practices in the middle mountains of central Nepal. In: *Soil Fertility and Erosion Issues in the Middle Mountains of Nepal* (ed. by P. B. Shah, H. Schreier, S. Brown & K. W. Riley) (Proc. Workshop, Jhikhu khola Watershed, April 1991), 105–120. International Development Research Centre (IDRC), Ottawa.

Mulder, R. P. (1978) Erosion plot measurement in Phewa Tal catchment. Integrated Watershed Management Project.

Phewa Tal Tech. Report no. 6, Dept of Soil Conservation and Watershed Management, Kathmandu.

Ries, J. B. (1993) Soil erosion in the high mountain region, eastern central Himalaya. A case study in Bamti/Bhandara/Surma area, Nepal. PhD Dissertation, Geowissenschftlichen Fakultat, Albert-Ludwigs-Universität, Freiburg I Br.

Schaffner, R. (1987) Vegetation of stabilizing and eroding slopes in eastern Nepal. PhD Dissertation, Swiss Federal Institute of Technology, Zurich.

Shankar, K. (1989) Regional sediment studies of rivers of Nepal. Paper presented in Regional Workshop on Hydrology of Mountainous Areas (Kathmandu, December 1989)

Sherchan, D. P. & Chand, S. P. (1991) A review of current soils related research activities at Pakribas Regional Agricultural Centre. In: *Soil Fertility and Erosion Issues in the Middle Mountains of Nepal* (ed. by P. B. Shah, H. Schreier, S. Brown & K. W. Riley) (Proc. Workshop, Jhikhu khola Watershed, April 1991), 83–104. International Development Research Centre (IDRC), Ottawa.

Upadhaya, G. P., Sthapit, M. & Shrestha, K. N. (1991) Runoff and soil loss studies in the Kulekhani watershed: Results 1985–1990. In: Soil fertility and erosion issues in the middle mountains of Nepal. (ed. by P. B. Shah, H. Schreier, S. Brown & K. W. Riley) (Proc. Workshop, Jhikhu khola Watershed, April 1991), 25–32. International Development Research Centre (IDRC), Ottawa.

Watanabe, T. (1994) Soil erosion on Yak-grazing steps in the Langtang Himal, Nepal. *Mountain Research and Development* **14**(2), 171–179.

FRIEND'97 — Regional Hydrology: Concepts and Models for Sustainable Water Resource Management
(Proceedings of the Postojna, Slovenia, Conference, September–October 1997). IAHS Publ. no. 246, 1997.

Erosion et transport particulaire par le Niger: du bassin supérieur à l'exutoire du delta intérieur (bilan de cinq années d'observation)

J. P. BRICQUET, G. MAHE, F. BAMBA, M. DIARRA, A. MAHIEUX, T. DES TUREAUX, D. ORANGE, C. PICOUET
ORSTOM, BP 84, Bamako, Mali

J. C. OLIVRY
ORSTOM, BP 5045, F-34032 Montpellier Cedex, France

Résumé Les chroniques hydrologiques du Niger supérieur et de sa cuvette lacustre montrent un appauvrissement de la ressource en eau depuis deux décennies lié aux déficits pluviométriques et à l'amenuisement des ressources souterraines. La cuvette lacustre—delta central du Niger—constitue un hydrosystème particulier de lacs et de plaines d'inondation où les pertes annuelles, dues essentiellement à l'évaporation, sont extrêmement importantes. Les mesures de flux fluviaux de matières particulaires, entreprises depuis 1990 sur le Niger amont et son delta, ont montré une perte globale de matières en suspension à l'intérieur du delta central. Les variations saisonnières de la charge solide, en amont et en aval du delta central, permettent une première approche du fonctionnement de cet hydrosystème. La forte hydraulicité de l'année 1994/1995 a mis en évidence la complexité du phénomène de transport fluvial de matière à l'intérieur du delta.

INTRODUCTION

Le programme sur l'environnement et la qualité des apports fluviaux du Niger au Sahel (EQUANIS) a mis en place au Mali un réseau de stations d'observation des flux hydriques et de matières particulaires et dissoutes, et a développé sur le Niger les recherches biogéohydrodynamiques des grands écosystèmes relevant de la thématique du Programme sur l'Environnement de la Géosphère Intertropicale (PEGI, INSU/CNRS/ORSTOM).

Le delta central du Niger se distingue des régions avoisinantes par une relative concentration de ressources naturelles renouvelables, liée dans une très large mesure à la présence de l'eau. Par sa taille et sa grande richesse naturelle il offre, plus que d'autres régions, les conditions d'une étude exemplaire du fonctionnement actuel du milieu naturel. Les apports fluviaux de matières du Niger amont à sa cuvette lacustre constituent une ressource renouvelable importante pour l'équilibre des ressources vivantes de l'ensemble du delta. Seuls les résultats sur les flux particulaires de 1991 à 1995 seront présentés ici.

HYDROLOGIE DU NIGER ET DE SA CUVETTE LACUSTRE

Issu des monts de Guinée, le Niger, troisième fleuve d'Afrique par sa longueur (4200 km) s'écoule suivant une direction générale nord-est jusqu'aux confins du

Sahara. Il décrit une grande boucle dans sa traversée des régions sahéliennes et subdésertiques où il perd dans la cuvette lacustre une part importante de ses apports hydriques avant de retrouver la route de l'océan au fond du golfe de Guinée.

Hydrologie du Niger supérieur

Le bassin amont du Niger couvre du sud au nord les domaines climatiques guinéen, soudanien puis sahélien. La pluviométrie annuelle passe respectivement de 1500 mm an^{-1} à 600 mm an^{-1} (Fig. 1). Ensuite, le Niger entre dans sa cuvette lacustre située en domaines sahélien puis subdésertique. La pluviométrie annuelle varie alors de 600 mm an^{-1} à 250 mm an^{-1}. Pour toutes ces zones climatiques, la saison des pluies, centrée sur le mois d'août, est une saison bien marquée.

A Koulikoro, station hydrométrique installée en 1907, la superficie du bassin versant est de 120 000 km^2, dont seulement un cinquième au Mali. Le débit moyen interannuel calculé sur 83 ans est de 1420 $m^3 s^{-1}$, soit un module spécifique de 11.8 l s^{-1} km^{-2}. Avec une hauteur de précipitation interannuelle estimée à 1600 mm et une lame d'eau écoulée de 370 mm, le coefficient d'écoulement moyen pour l'ensemble du bassin amont du Niger atteint 23%. La reprise par évaporation serait de 1230 mm (Brunet-Moret *et al.*, 1986).

Les chroniques hydrologiques du Niger supérieur et de la cuvette lacustre montrent un appauvrissement de la ressource en eau depuis deux décennies lié au

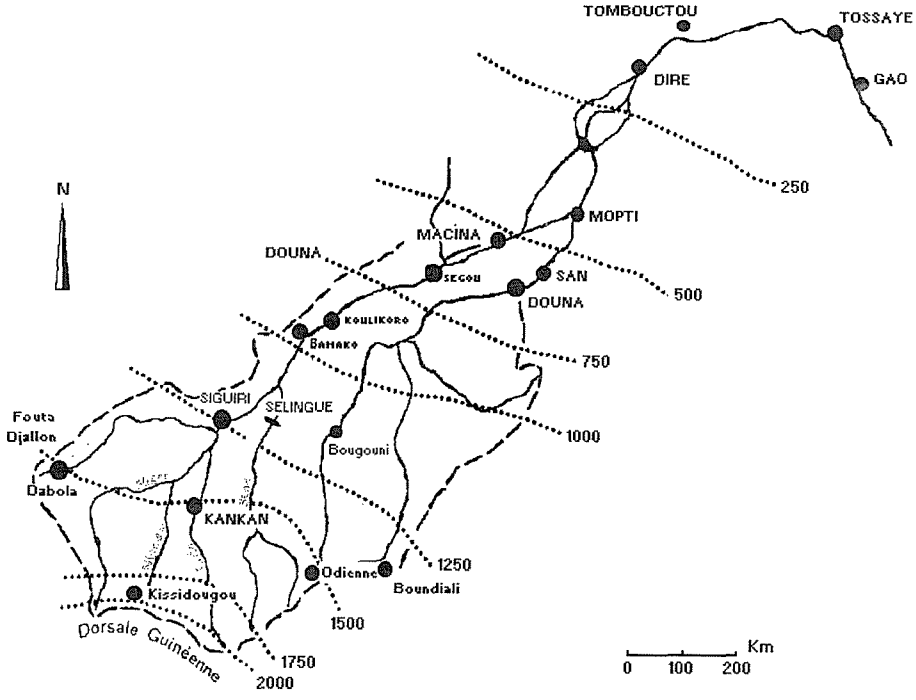

Fig. 1 Bassin supérieur du Niger et isohyètes interannuelles en mm.

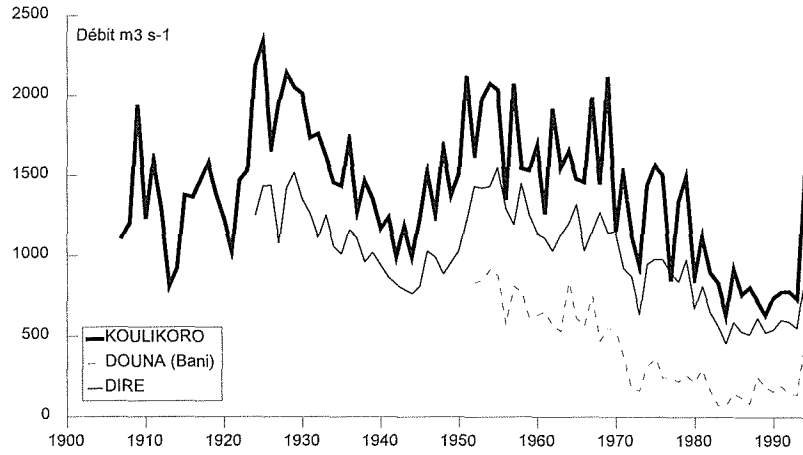

Fig. 2 Evolution des modules annuels, depuis l'origine des observations jusqu'en 1995, du Niger à Koulikoro et Diré et du Bani à Douna.

déficit pluviométrique et à l'amenuisement des ressources souterraines (Olivry, 1995a). Dans la période récente l'hydraulicité des fleuves de la région n'a cessé de se dégrader, d'abord dans les années 1972–1973, puis de manière plus importante encore dans les années 1983 et 1984 (Fig. 2).

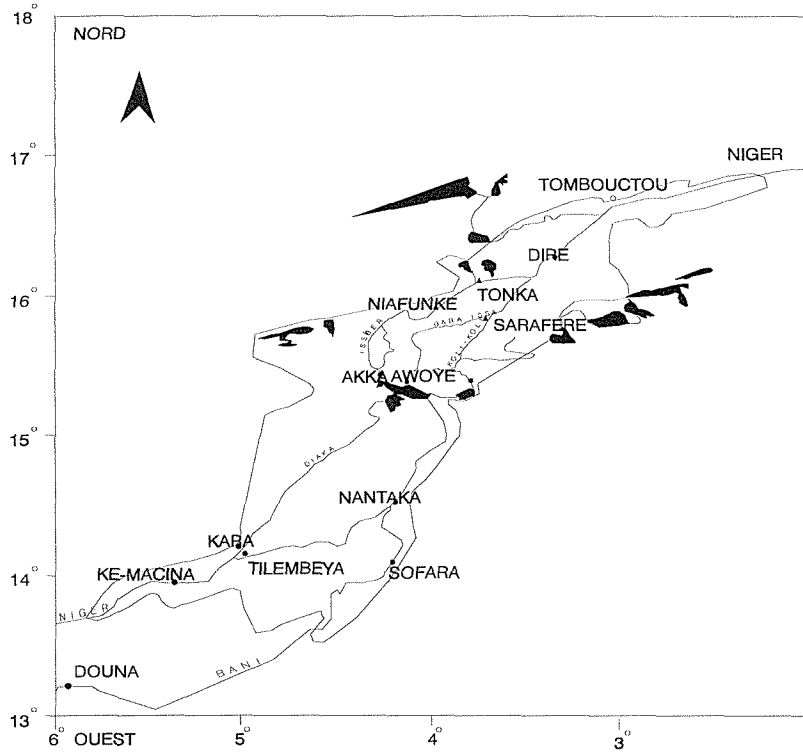

Fig. 3 Carte de situation de la Cuvette lacustre.

La cuvette lacustre

Vaste zone d'épandage des apports de matière du Niger, la cuvette lacustre constituée par un delta amont inondable et un système aval complexe de lacs, couvre une superficie de 50 000 km^2 de 450 km de long sur 125 km de large (Fig. 3).

Le fonctionnement hydrologique de la cuvette lacustre est largement dépendant:

(a) des conditions d'écoulement exogènes, l'essentiel des ressources en eau provenant des régions beaucoup plus arrosées de l'amont et donc des régimes hydroclimatiques des bassins supérieurs du Niger et du Bani;

(b) des conditions morphologiques et climatologiques propre au delta central, régissant les écoulements (défluences, inondations) et le bilan hydrologique (évaporation, infiltration).

L'examen des modules depuis l'origine des observations montre que les écoulements contrôlés à la sortie du delta à Diré perdent de 47% en année humide à 37% en année moyenne et 32% en année sèche par rapport aux entrées liquides dans le delta. En fait, les pertes sont d'autant plus importantes que les zones d'inondations

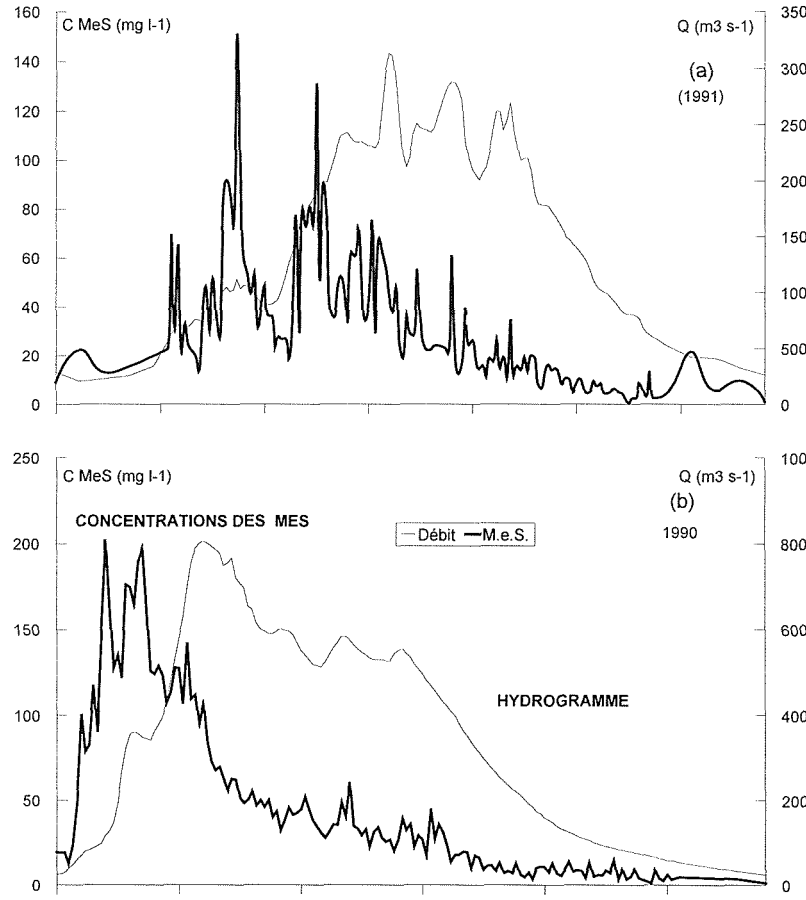

Fig. 4 Exemples d'hydrogrammes et de concentrations en MES (matières en suspension) pour le Niger à Koulikoro (a) et le Bani à Douna (b).

augmentent, mais aussi que les effluents secondaires transfèrent des volumes plus importants.

Ce sont bien évidemment ces pertes hydriques et leur ampleur qui font la caractéristique hydrologique principale de la cuvette lacustre et, de celle-ci, une formidable machine évaporatoire en Afrique de l'ouest.

REGIME DU TRANSPORT DE MATIERES EN SUSPENSION DANS LES EAUX DU BASSIN AMONT

L'étude des matières en suspension dans les eaux du bassin amont montre des variations saisonnières des concentrations caractéristiques des fleuves tropicaux (Gac, 1980; Meybeck, 1984; Orange, 1992; Olivry *et al.*, 1995b). Les concentrations les plus élevées correspondent au début de la saison des pluies. Elles dépassent rarement 100 mg l^{-1} pour le Niger et 200 à 250 mg l^{-1} pour le Bani. Elles tombent en saison de basses eaux jusqu'à 5 mg l^{-1} et, compte tenu des très faibles débits de cette période de l'année, le transport de matière devient alors pratiquement négligeable (Fig. 4).

Les pics de concentration précèdent toujours la crue hydrologique. Les concentrations ont considérablement diminué lors du maximum de la crue, suivant une décroissance assez régulière sur le Bani, plus variable sur le Niger. L'hystérésis de la relation concentrations-débits, illustrée pour le Niger en Fig. 5, correspond à un phénomène classique en zone tropicale. L'évolution mensuelle des concentrations suit toujours trois phases.

(a) Au début de la crue, il y a une érosion du bassin versant sous l'effet des précipitations et un transport par le fleuve des sédiments arrachés.

(b) Les concentrations diminuent le reste de la saison humide. La proportion des particules prêtes a être arrachées aux sols est moindre et la végétation joue son rôle protecteur. L'érosion est ralentie. Il y a dilution de la charge par le débit.

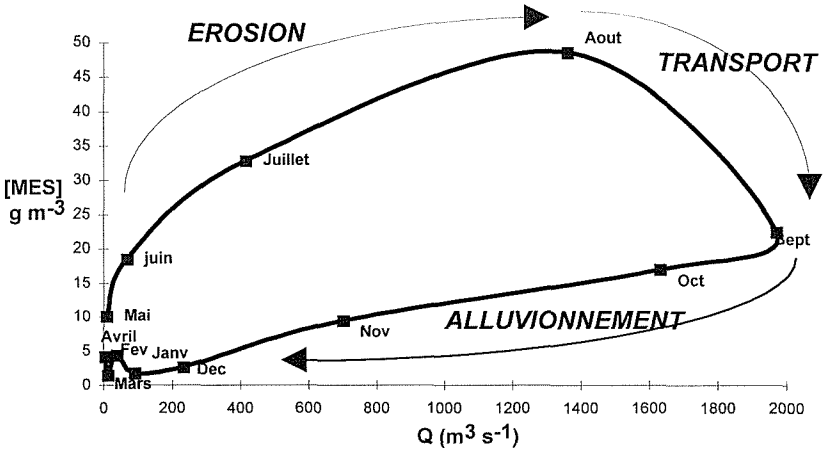

Fig. 5 Exemple de relation Concentration–Débits pour le Niger à Banankoro.

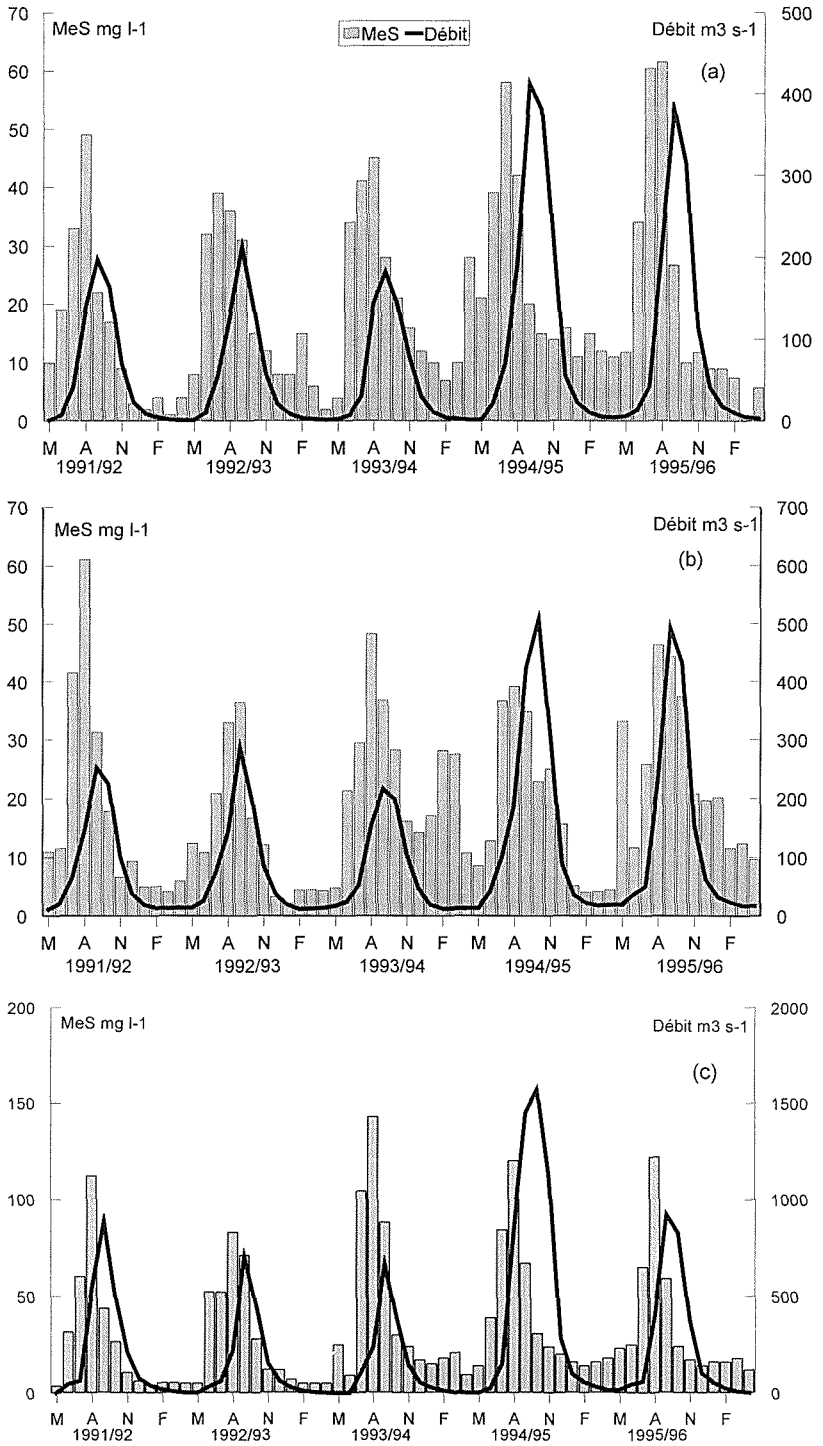

Fig. 6 Concentrations moyennes mensuelles des suspensions et débits mensuels pour le Niger à Banankoro (a), le Niger à Koulikoro (b) et le Bani à Douna (c).

(c) Le débit diminue et la rivière perd de sa compétence. Les particules sont alors déposées dans les lits majeurs ou les plaines inondées. La phase d'alluvionnement dure le reste de l'année, les concentrations en MES sont faibles, c'est la période où les eaux sont limpides.

La Fig. 6 donne pour la période d'observation les histogrammes des concentrations moyennes mensuelles des matières en suspension et la courbe de variation des débits mensuels correspondants pour les trois stations principales du bassin amont. La forte hydraulicité de l'année 1994–1995 confirme la complexité des relations concentrations en matières en suspensions et débits. En effet, on enregistre cette année-là des concentrations mensuelles plus fortes à Banankoro mais plus faibles à Douna.

Les concentrations moyennes annuelles varient de 22 à 27 mg l^{-1} sur le Niger et de 49 à 75 mg l^{-1} pour le Bani. Elles ont peu varié malgré la forte augmentation de débit de la dernière année. Enfin, ces valeurs sont très faibles en comparaison des observations effectuées dans la même zone climatique de l'Afrique. Ainsi, Gac (1980) donne dans son étude sur le bassin du lac Tchad des concentrations moyennes annuelles sur le Chari de 73 à 97 mg l^{-1}, respectivement en année humide et sèche. Sur le Sénégal (Gac & Orange, 1990), la concentration moyenne de la charge annuelle en suspension est de 230 mg l^{-1} sur neuf années de la décennie 1980.

Les bilans de matière particulaire exportée, calculés pour les années 1991/1992, 1992/1993, 1993/11994 et 1994/1995, montrent une variation importante entre l'année 1994/1995 et les années précédentes comme pour l'hydrologie, alors que les concentrations de MES sont restées dans le même ordre de grandeur (Tableau 1).

Tableau 1 Flux annuels de matières en suspension (MES) et érosions spécifiques sur le Niger et le Bani supérieurs.

Année hydrologique	Banankoro: MES (t an^{-1})	Erosion (t km^2 an^{-1})	Koulikoro: MES (t an^{-1})	Erosion (t km^2 an^{-1})	Douna: MES (t an^{-1})	Erosion (t km^2 an^{-1})
1991/1992	425 000	5.9	655 000	5.5	339 000	3.3
1992/1993	440 000	6.1	540 000	4.5	229 000	2.3
1993/1994	471 000	6.6	681 000	5.7	317 000	3.1
1994/1995	828 000	**11.5**	1 245 000	**10.4**	738 000	**7.3**

Etant donné les faibles variations de concentration moyenne annuelle, le facteur déterminant dans l'importance du flux annuel de matière particulaire transportée est le débit annuel du fleuve. De même à l'échelle mensuelle, la variation des flux de matière suit celle de l'hydrogramme de crue: les maximums d'exportation de matière coïncident avec la période des très hautes eaux.

En terme d'érosion spécifique, les valeurs de la dégradation moyenne annuelle varient de 8.1 à 6.6 t km^{-2} an^{-1} pour le Niger à Banankoro et le Niger à Koulikoro, et de 3.2 à 2.5 t km^{-2} an^{-1} seulement pour le Bani à Douna.

BILAN ET VARIATION DES FLUX DE MATIERE DANS LA CUVETTE LACUSTRE

On peut distinguer, dans le delta central, deux parties ayant leur fonctionnement propre:

(a) une *partie amont*, constituée de vastes zones d'épandage encore largement inondées par la crue annuelle malgré le déficit hydropluviométrique, qui se termine au lac Débo, anévrisme majeur et permanent du réseau hydrologique de la région;
(b) une *partie aval* où une géomorphologie très différente, caractérisée par une surimposition aux formes deltaïques antérieures d'un erg holocène orienté est-ouest, conduit à observer un réseau hydrologique très diffus, souvent commandé par des sillons interdunaires, avec des zones d'inondation plus réduites.

L'étude des transports de matière s'appuie sur les observations effectuées aux entrées amont du delta (stations de Ké-Macina et Douna), aux sorties du Lac Débo et à la sortie du delta aval à la station de Diré.

Evolution des concentrations au cours du cycle hydrologique

Au cours de l'année hydrologique, les stations du delta central du Niger montrent le même type d'évolution saisonnière des concentrations en matières en suspension (Fig. 7) pouvant être décrit en trois étapes.

(a) Les concentrations maximum de matières particulaires à Diré sont environ de 160 mg l^{-1}, elles se situent plus de 2 mois avant le maximum de crue, et seulement 23 à 45 jours après le début de la montée des eaux. Bien que la montée des eaux soit plus lente qu'à l'amont, le pic de matières en suspension se produit à la sortie du delta avant celui enregistré à l'entrée du delta. Il semble donc que les dépôts de fond de lit et des berges sont plus facilement mobilisables à l'intérieur du delta dès le début de la crue.
(b) Lors de l'étale de la crue, on observe les concentrations minimales, correspondant à la dilution de la charge par le débit et au phénomène d'alluvionnement. Aussi, le minimum de concentration correspond-il toujours au

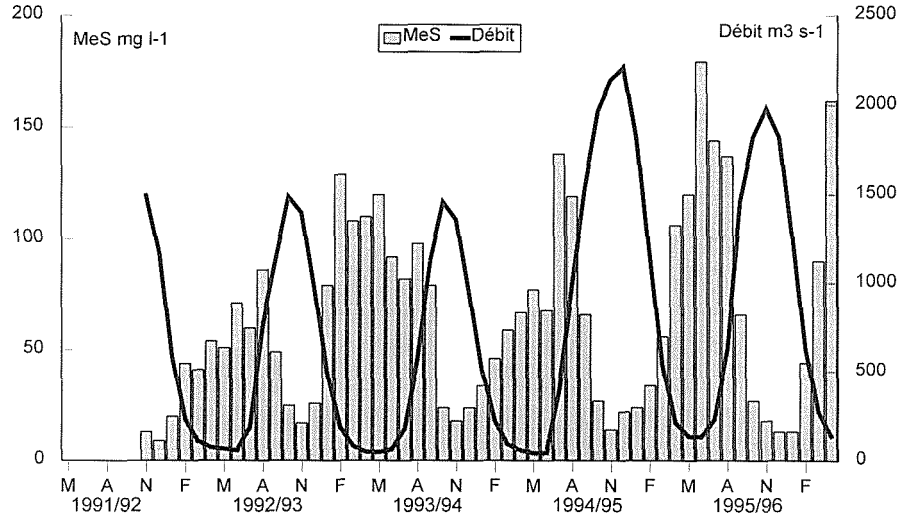

Fig. 7 Hydrogrammes et concentrations en matières en suspensions de 1992 à 1995 à la sortie du delta central du Niger (Diré).

maximum de crue, qui se situe 1 mois après celui de l'amont (alors que pour le Niger amont, le minimum de concentration est enregistré pendant l'étiage).

(c) Pendant la phase de vidange des plaines d'inondation (de décembre à février), il y a une augmentation brusque des concentrations, qu'une diminution des débits n'explique qu'en partie. Par ailleurs, pendant cette période, l'eau du fleuve drainant la région du lac Débo est également de plus en plus concentrée en matières dissoutes. On suppose qu'il y a des apports extérieurs ou des phénomène locaux de remise en suspension: apports de poussières atmosphériques par l'harmattan, action du vent créant des vaguelettes qui attaquent les berges, production algale importante dans le lac Débo.

Bilan annuel des flux de matières

Le Niger et le Bani ont apporté au delta un flux annuel de matières en suspension de 1 à 2.3 millions de tonnes par an entre 1991 et 1994. A Diré, le flux annuel de matières en suspension sortant du delta varie entre 0.8 et 1.4 millions de tonnes par an. Le bilan global entrées–sorties de ces flux de matières en suspension montre que le delta central a retenu entre 200 et 900 milliers de tonnes par an durant la période observée.

Le Tableau 2 donne le détail des flux annuels de matières mesurés en 1992/1993 et 1994/1995. Les mesures intermédiaires effectuées aux sorties du lac Débo montrent un comportement très différent des parties amont et aval du delta. En effet, le bilan annuel met en évidence un piégeage de 331 000 t et 1 283 000 t de suspensions avant le lac Débo et au contraire un gain de 87 000 t et 382 000 t entre le lac Débo et Diré, respectivement en 1992/1993 et 1994/1995 (Fig. 8).

Tableau 2 Bilan des flux de matières particulaires dans le delta central du Niger en milliers de tonnes.

	1992/1993	1994/1995
Entrées delta	1034	2311
Sortie lac Débo	703	1028
Perte Amont	331	1283
Sortie Diré	790	1411
Perte aval	87 (gain)	382 (gain)
Perte totale	244	901

Il y a décantation dans les plaines d'inondation de la zone amont de près d'un tiers de la charge solide alors que les phénomènes de reprise dans la zone aval excédent largement la décantation. Le calcul des concentrations moyennes annuelles de matières en suspension suggère deux fonctionnements:

(a) *Partie amont du delta*: la baisse de concentration des MES (–8.4 mg l^{-1}) pourrait indiquer qu'au piégeage de matière lié aux pertes en eau dans les plaines d'inondation s'ajoute une décantation des suspensions des eaux faisant retour au réseau en décrue.

(b) *Partie aval du delta*: la concentration augmente par rapport aux sorties du lac Débo; les apports complémentaires, dus probablement aux reprises de berges par effet du vent ou dépôts de poussières atmosphériques mais aussi à des possibles

transferts du dissous au particulaire d'origine biologique (diatomées), s'associent à l'évaporation au fil des écoulements pour reconcentrer les suspensions à Diré.

Le suivi des variations mensuelles des flux de matières apporte des informations complémentaires sur le fonctionnement hydrodynamique du Niger à travers le delta.

Variations saisonnières des flux de matière

Le bilan mensuel des flux de matière en suspension a été établi entre les entrées amont et les sorties du lac Débo et entre le lac Débo et la sortie aval à Diré sur les années hydrologiques 1992/1993, 1993/1994 et 1994/1995.

Les flux de sortie du delta amont sont supérieurs aux entrées en mai, juin et juillet; la fin de la saison des basses eaux se manifeste par une reprise des berges dans le lit mineur du fleuve. En août, septembre, octobre et novembre, avec l'inondation de la crue annuelle, des pertes importantes sont observées; elles sont

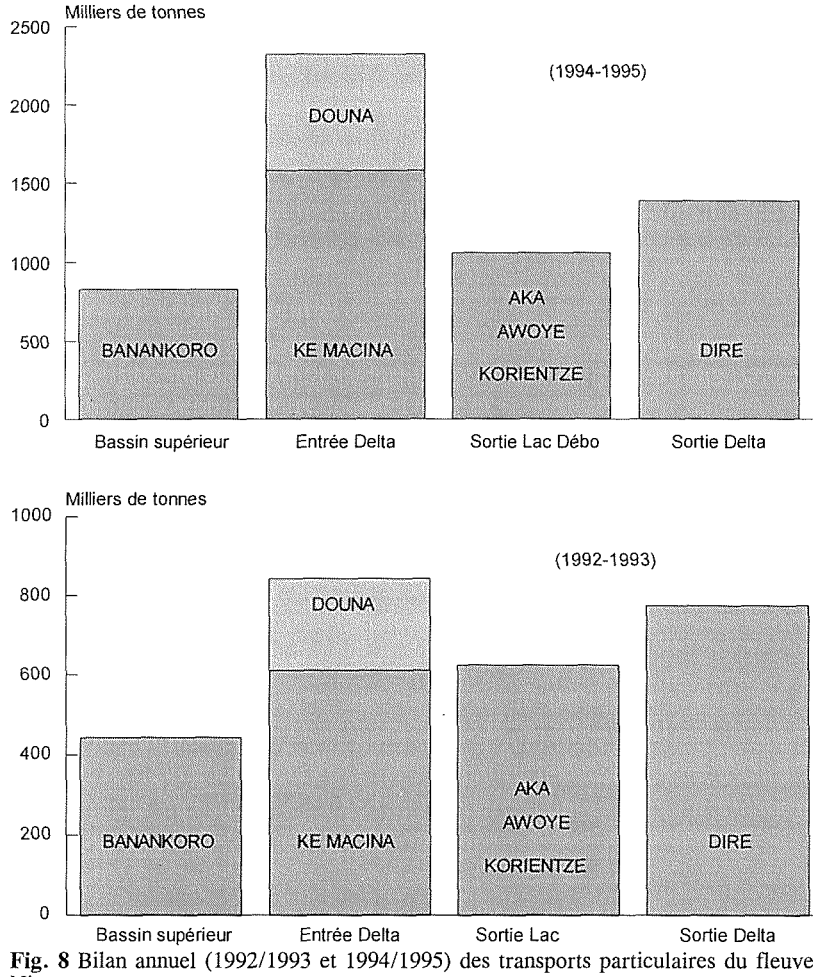

Fig. 8 Bilan annuel (1992/1993 et 1994/1995) des transports particulaires du fleuve Niger.

maximales en septembre. A partir de décembre, il y a restitution d'une petite partie du stock piégé.

Sur le delta aval, le comportement du système est tout à fait différent. Seul les mois de juillet, août et septembre montrent une perte en sédiments, avec un maximum en août. A partir de novembre, et en décembre puis janvier, les exportations de matières observées à Diré excédent les flux mesurés à la sortie du lac Débo.

Un léger excédent des sorties subsiste de février à juin. Ce gain de matière en suspension a déjà été évoqué dans le bilan annuel; limité à la période novembre–juin,

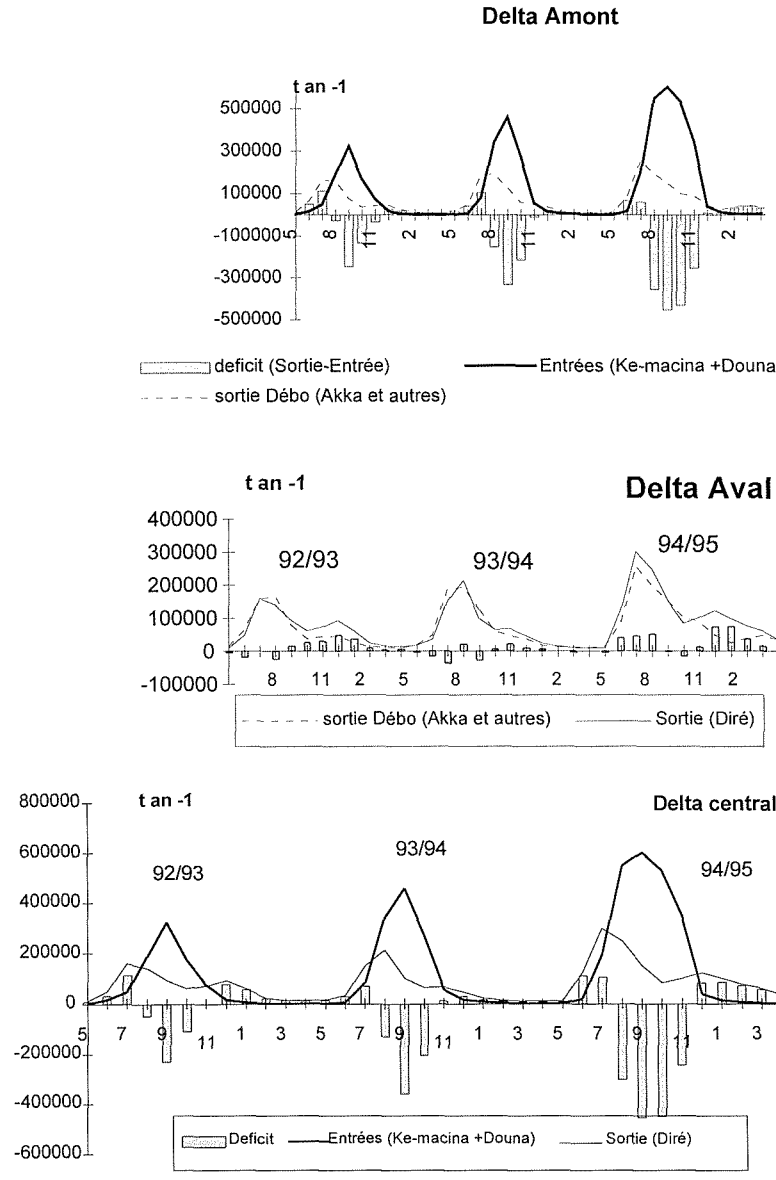

Fig. 9 Variations mensuelles du bilan sorties–entrées des transports particulaires dans le delta central du Niger de 1992 à 1994.

il correspond, en saison sèche, à l'observation de vents forts (harmattan), orientés dans la direction principale du fleuve à l'aval du lac Débo, qui favorisent une érosion des berges et une reprise des dépôts de fond dans les biefs les moins profonds. C'est la période d'apports éoliens (sables dunaires) des brumes sèches et de poussières atmosphériques; c'est aussi une période de transformations planctoniques (par exemple la transformation de silice dissoute en silice du test des diatomées). La position septentrionale du delta aval plus proche du Sahara explique ce fonctionnement différent de celui du delta amont. La Fig. 9 illustre ces variations de flux des suspensions pour les deux parties du delta et pour l'ensemble de la cuvette lacustre.

CONCLUSION

Au stade actuel des mesures disponibles, il est difficile d'aller plus loin dans l'interprétation du fonctionnement de l'hydrosystème, et en particulier de celui du delta aval. Il est clair que la traversée du delta central du Niger avec ses écoulements très lents et ses plaines d'inondation conduit à de notables modifications de la charge en suspension du fleuve.

Des mesures complémentaires sur plusieurs années permettront de vérifier la répétition des phénomènes observés. Afin de pouvoir approcher un modèle de fonctionnement du transport particulaire à l'intérieur du delta central, l'observation sur les stations principales doit être maintenue avec une fréquence régulière surtout durant la crue. Par ailleurs, un suivi des apports de poussières atmosphériques semble nécessaire, leur intervention dans le bilan global sorties-entrées de matière étant sans doute non négligeables à cause des forts vents de poussière régnant dans ce type d'environnement.

Le delta central du Niger ne correspond pas à un bassin sédimentaire ancien, comme celui du lac Tchad où l'épaisseur des dépôts correspond à une longue histoire géologique. Aussi, faute d'observer l'existence d'un bassin sédimentaire ancien, l'importance relative des dépôts de matière dans la cuvette lacustre aurait pu caractériser les phases de faible hydraulicité du Niger; or l'année 1994/1995 de bonne hydraulicité a rejeté cette hypothèse. Une augmentation de l'hydraulicité a entraîné une augmentation des flux transportés et des dépôts dans la cuvette lacustre.

REFERENCES

Brunet-Moret, Y., Chaperon, P., Lamagat, J. P. & Molinier, M. (1986) *Monographie Hydrologique du Fleuve Niger*, tome I: *Niger Supérieur*; tome II: *Cuvette Lacustre et Niger Moyen*. Collection. Monogr. Hydrol., no. 8, ORSTOM, Paris.

Gac, J. Y. (1980) *Géochimie du Bassin du Lac Tchad. Bilan de l'altération, de l'érosion et de la sédimentation*. Travaux et documents ORSTOM, no 123.

Gac, J. Y. & Orange, D. (1990) Cadre naturel du haut bassin-versant du fleuve Sénégal. *Rapport ORSTOM Dakar. Projet CEE/EQUESEN no. TS-2-0-198-F-EDB*.

Meybeck, M. (1984) Les fleuves et le cycle géochimique des éléments. Thèse Doct. Etat. Sciences, Univ. P. et M. Curie, Paris XI.

Olivry, J. C., Bricquet, J. P., Bamba, F. & Diarra, M. (1995a) Le régime hydrologique du Niger supérieur et le déficit des deux dernières décennies. In: *Grands Bassins Fluviaux* (ed. par J. C. Olivry & J. Boulègue) (Actes du Colloque PEGI, 22–24 novembre 1993), 251–266. Collection Colloques et Séminaires ORSTOM.

Olivry, J. C., Gourcy, L. & Touré, M. (1995b) Premiers résultats sur la mesure des flux de matières dissoutes et particulaires dans les apports du Niger au Sahel. In: *Grands Bassins Fluviaux* (ed. par J. C. Olivry & J. Boulègue) (Actes du Colloque PEGI, 22–24 novembre 1993), 281–292. Collection Colloques et Séminaires ORSTOM.

Orange, D. (1992) Hydroclimatologie du Fouta Djalon et dynamique actuelle d'un vieux paysage latéritique. *Sciences Géologiques, Mémoire no. 93, Strasbourg*.

FRIEND'97 — Regional Hydrology: Concepts and Models for Sustainable Water Resource Management
(Proceedings of the Postojna, Slovenia, Conference, September–October 1997). IAHS Publ. no. 246, 1997.

Regression analyses of heavy metal concentrations in urban flash floods of an arid zone

M. NOUH
Department of Civil Engineering, Sultan Qaboos University, PO Box 33, Al-Khod 123, Oman

Abstract Real data from five residential urban arid catchments of varying size, slope, and perviousness ratio were used to develop regression equations for predicting mean concentrations of selected heavy metals in the urban runoff from duststorm and flow properties. The duststorms vary in their total particulate matter concentrations, whereas the flow resulted from rainstorms of different intensity, depth and duration, spatial and temporal distribution over the catchment, and dry period between two successive rainstorms. The selected metals are copper, lead, nickel, zinc and iron. About 80% of the collected data were randomly selected and used to develop these equations, while the remaining 20% of the data were used for the verification of the equations. The R^2 of these equations varied from 0.76 to 0.88, and the significance of the regression parameters was supported by the results of the statistical inference analyses. The equations were used to identify the relative importance of the flash floods and duststorms on the concentrations of heavy metals. Based on the results, recommendations concerning water quality control in the investigated arid zone are made.

INTRODUCTION

Proper design of urban water quality management and control schemes requires identification of runoff heavy metal loads and their spaciotemporal variability. Basically, metal loads are introduced into urban runoff from three sources; namely, the land surface, catch basins, and the sewers in combined sewer systems. It has been realized that the contributions of heavy metals to urban runoff from land surfaces and catch basins are much more significant than that from combined sewers. Heavy metals from land surfaces are caused mainly by streets and sidewalk sweepings, pollutants deposited on or washed into streets from yards and other indigenous open areas, wastes and dirt from building and demolition, dirt–oil–tyre and exhaust residue contributed by automobiles, and fallout of air pollution particles. The latter cause has recently been found to play an important role in urban stormwater quality in arid areas (Nouh, 1996a). Catch basins as well as pervious areas directly connected to sewer systems are important sources of metals dissolved from sediments and carried by flash floods to downstream sites.

Previous investigations have indicated that the climate characteristics in arid areas significantly affect the processes of heavy metals generation and transportation. In Saudi Arabia, as a typical arid area, the high variability of temperature and precipitation accompanied with low levels of atmospheric and soil humidity result in soil destruction and erosion, which furnish the windstorms and flash floods with large amounts of suspended sediment to carry (Nouh & Jamjoom, 1981). It has been found that the amounts of heavy metals in the stormwater runoff increase as

suspended sediment flow rates increase (Nouh, 1992, 1995a, 1995b, 1997) and are affected to a considerable extent by properties of duststorms (Nouh, 1996a, 1996b, 1996c) as well as by rainstorms (Nouh, 1991a; Nazarov, 1996) and catchment characteristics (Nouh, 1991b, 1991c; Sansalone *et al.*, 1996). Such association of heavy metals and sediments is recently supported by others (Ershova *et al.*, 1996; Selim & Ma, 1996). The present investigation is an extension to the previous ones. The purpose is to develop a statistical methodology for the estimation of heavy metal concentrations in the flash floods of urban arid areas. Regression analyses were performed on data collected for this purpose. A description of the data used and method of analysis are given below.

DATA AND METHOD OF ANALYSIS

Five residential catchments of a typical arid climate, located in the southwest region of Saudi Arabia between latitudes 16°30′00″ and 22°00′00″ N and longitudes 39°30′00″ and 46°00′00″ E, were selected for the study. The region's temperature ranges from 2 to 53°C, with a yearly mean of 27°C. The annual relative humidity has an average value of 62%, with maximum and minimum values of about 96% and 17%, respectively. Rainfall is characterized by short duration and high intensity, with the mean number of yearly rainstorms about 7 (Nouh, 1990). Its annual average depth is about 850 mm, with maximum and minimum values of about 1450 mm and 300 mm, respectively. Details of the rainfall characteristics in this region are given elsewhere (Nouh, 1987a). The annual runoff coefficients fluctuate between 0.133 and 0.885 resulting in an overall average of 0.158 on pervious areas and 0.512 on impervious areas (Nouh, 1988a). Runoff is characterized by spates which generally last on average 12 h from start to finish. Storm runoff hydrographs have a steep rise and rapid recession. The period of the greatest total rise varies from 25 to 65 minutes. More information on the runoff generation and properties are given elsewhere (Nouh & El-Laithy, 1988b). The average total suspended sediment transport rate is about 78 gpl, with a maximum of 127 gpl and a minimum of 46 gpl. The suspended sediment consist of clay and silt of about 74% and 22%, respectively (Nouh, 1987b). The investigated catchments are characterized by intensive duststorms of an average total suspended particulate matter concentration of 2100 $\mu g\ m^{-3}$ (Nouh, 1989). The characteristics of the catchments used and their data are summarized in Table 1.

Stormwater runoff and its suspended sediments, as well as total suspended particulate matter concentrations, were sampled under different rainstorm and duststorm characteristics. The runoff and its suspended sediments were sampled every 15 minutes at the outlet of the main trunk pipe of each catchment, whereas the total suspended particulate matter concentrations were evaluated at about 17 different locations in each of the catchments using calibrated high volume air samplers operated for a period of about 36 h during the storms. Details of the runoff and suspended sediment measurements are reported by Nouh & Jamjoom (1981), and those of the total suspended particulate matter concentrations are given elsewhere (Rowe *et al.*, 1985; Nouh *et al.*, 1986).

Because properties of pollutants may vary with the grain size diameter of transported sediments (Hellmann, 1987; Nouh, 1992), the sampled suspended

sediments were separated into five divisions according to their grain size diameter d; namely, $d > 0.20$ mm, $0.20 \geq d > 0.06$ mm, $0.06 \geq d > 0.02$ mm, $0.02 \geq d > 0.002$ mm, and 0.002 mm $\geq d$. The suspended sediment samples within each division were further split by random selection into two groups of samples. The first group contains about 80% of the samples (called the regression group), and was used to develop the regression equations, while the remaining 20% of the samples (called the verification group) was used to verify the developed equations. The suspended sediment samples in both groups of each division were then analysed for selected heavy metals; namely, copper (Cu), lead (Pb), nickel (Ni), zinc (Zn) and iron (Fe). The regression group of data of each division diameter of suspended sediments and its mean concentration of heavy metals were used together with the corresponding stormwater flows in developing the following regression equations.

RESULTS AND DISCUSSIONS

Based on the previous finding that the concentrations of suspended sediments in stormwater runoff are considerably influenced by both flash floods and duststorm characteristics (Nouh, 1996b), the mean concentration of suspended sediments in the stormwater is assumed to follow the following model:

$$C_d = \lambda_d + \alpha_{1d} q^{\beta_{1d}} + \alpha_{2d} S^{\beta_{2d}} \quad (1)$$

where C is the mean concentration of suspended sediments (gpl); q is the stormwater runoff depth over catchment (mm); S is the total suspended particulate matter concentration averaged over the catchment ($\mu g\ m^{-3}$); λ, α, and β are regression parameters to be determined. The subscript d refers to the division range of suspended sediment diameters.

Table 1 Summary of catchments and data used for the study.

Data	Name of catchment:				
	Rabia	Dalia	Zubair	Hmadi	Zanbaka
Catchment size (10^4 m^2)	110	127	297	617	770
Perviousness ratio (%)	9.18	56.18	55.37	15.5	47.5
Initial infiltration (mm h^{-1})	78	69	71	83	75
Infiltration decay rate (min^{-1})	varied from 0.05 to 0.13				
Constant infiltration rate (mm h^{-1}.)	varied from 6.80 to 17.30				
Depression storage on pervious area (mm)	9.8	12.3	15.0	10.56	10.45
Depression storage on impervious area (mm)	2.7	3.17	4.33	4.05	3.18
Manning n	varied from 0.017 to 0.37				
Number of rainstorms	64	55	55	54	55
Mean rainstorm depth (mm)	54.9	92.2	88.4	74.3	59.7
Mean duration (min)	30.1	35.5	20.2	31.5	39.8
Mean period between two successive storms (days)	32.7	45.6	37.4	62.5	37.4
Coefficient of variation of rainstorm	1.12	1.19	1.23	1.15	1.32
Coefficient of kurtosis of rainstorm	0.98	1.05	1.23	1.19	1.23
Number of stormwater samples	112	98	103	89	92

Multiple regression analysis were performed on the above model using the regression group of data. The parameters of the model were estimated by using a forward stepwise algorithm, and are given in Table 2. The analysis of variance showed that not all the parameters equal zero at 95% confidence. The aptness of the model was examined. Error variance was found not to vary either with the level of the dependent variable or with the levels of the independent variables. As Table 2 indicates, the independent variables are not highly correlated (the largest value of the inter-correlation coefficient $Ir = 0.103$). The 95% confidence intervals of the majority of the regression parameters for all the division diameter ranges do not cover zero, meaning that these parameters are not zero with a risk of less than 5% of being wrong. The values of the regression parameters increase as grain size of suspended sediment decreases, meaning that the contribution of flash flood and duststorm to concentration of suspended sediments is larger in the small grain size fractions than in the large grain size fractions. It can be seen that the values of α_1 are negative but those of α_2 are positive, meaning that the concentration of suspended sediments increases as runoff depth decreases but as duststorm concentration increases. It is also seen that $\beta_1 > \beta_2$, meaning that the effect on suspended sediment concentrations of flash floods is greater than that of duststorms. However, the effect of duststorm becomes significant in the case of small grain size of sediments. From the values of R^2 (see Table 2), it is apparent that the degree of correlation between the dependent variable C and the independent variables q and S is stronger for small grain size fractions than that for large grain size fractions. Nevertheless, the values of R^2 refer to reasonable correlation between the dependent variable and the independent variables for all the grain size diameter ranges.

Since the concentrations of pollutants increase as the concentrations of suspended sediments in stormwater increase (Nouh, 1992, 1997), the mean concentration of a constituent P (mg l^{-1}) is related to the mean concentration of suspended sediment C (gpl) by the following mg l^{-1} regression model:

$$P_d = a_d C_d^{b_d} \tag{2}$$

where a and b are regression parameters, and the subscript d refers to the grain size diameter range of suspended sediment.

The regression group of data were further used to determine the regression parameters of equation (2). These parameters together with the correlation coefficients r between P and C for all the grain size diameter ranges and for all the investigated pollutants are shown in Table 3. It can be seen that the correlation coefficient between P and C, in addition to the parameters a and b, are larger in the small grain size diameter sediments than those in the large grain size diameter sediments. This means that the transport rates of the investigated pollutants with the small grain size diameter sediments are more significant than those with the large grain size diameter sediments. In addition, the degree of correlation with C of Cu and Fe, followed by Zn and Pb, is stronger than that of Ni. The strong relation between Cu and C may be explained by the organometallic complexes in the investigated catchments, which results in having Cu and Fe contents directly proportional to the amount of organic material being intensely washed out from soils during flash floods.

Table 2 Regression parameters for mean concentration of suspended sediments.

d (mm)	λ (lower, upper)	α_1 (lower, upper)	β_1 (lower, upper)	α_2 (lower, upper)	β_2 (lower, upper)	R^2	Ir
$d > 0.20$	23.3(19.6, 27.4)	-1.43(-1.49, -1.38)	0.53(0.49, 0.58)	3.62 (3.11, 3.94)	0.033(-0.008, 0.041)	0.76	0.103
$0.20 \geq d > 0.06$	37.6(31.4, 43.8)	-1.41(-1.43, -1.32)	0.67(0.61, 0.72)	4.26 (3.91, 4.72)	0.043 (0.037, 0.050)	0.81	0.101
$0.06 \geq d > 0.02$	51.3(48.6, 55.2)	-1.53(-1.62, -1.39)	0.73(0.61, 0.82)	4.93 (4.28, 5.61)	0.053 (0.042, 0.061)	0.83	0.092
$0.02 \geq d > 0.002$	67.4(63.7, 74.8)	-1.71(-1.89, -1.59)	0.92(0.88, 1.03)	5.27 (4.87, 5.63)	0.078 (0.071, 0.087)	0.88	0.087
$0.002 \geq d$	73.6(69.1, 77.3)	-1.74(-1.91, -1.62)	0.93(0.81, 0.98)	6.47 (6.11, 6.93)	0.082 (0.069, 0.093)	0.87	0.083

Table 3 Regression parameters for heavy metals concentrations.

d (mm)	Copper			Lead			Nickel			Zinc			Iron		
	a	*b*	*r*	*a*	*b*	*r*	*a*	*b*	*r*	*a*	*b*	*r*	*a*	*b*	*r*
$d > 0.20$	0.032	0.046	0.89	0.007	0.051	0.62	0.056	0.009	0.39	0.033	0.106	0.71	0.089	0.117	0.78
$0.20 \geq d > 0.06$	0.042	0.057	0.88	0.009	0.063	0.63	0.062	0.031	0.57	0.029	0.098	0.73	0.097	0.103	0.81
$0.06 \geq d > 0.02$	0.776	0.093	0.89	0.005	0.096	0.69	0.091	0.053	0.59	0.045	0.102	0.78	0.107	0.125	0.81
$0.02 \geq d > 0.002$	0.916	0.153	0.96	0.006	0.162	0.86	0.072	0.096	0.64	0.061	0.120	0.86	0.126	0.216	0.87
$0.002 \geq d$	0.103	0.196	0.93	0.011	0.123	0.77	0.083	0.104	0.69	0.097	0.155	0.85	0.133	0.238	0.91

Table 4 Accuracy of performance of the regression equations.

d (mm)	C			Copper			Lead			Nickel			Zinc			Iron		
	Rat	*Dev*	*Abs*	*Rat*	*Dev*	*Abs*	*Rat*	*Dev*	*Abs*	*Rat*	*Dev*	*Abs*	*Rat*	*Dev*	*Abs*	*Rat*	*Dev*	*Abs*
$d > 0.20$	1.08	0.24	18	1.12	0.19	11	1.26	0.33	26	1.26	0.66	59	1.18	0.29	23	1.14	0.24	19
$0.20 \geq d > 0.06$	1.06	0.22	16	1.13	0.13	15	1.17	0.29	30	1.36	0.51	53	1.12	0.22	22	1.08	0.23	17
$0.06 \geq d > 0.02$	0.92	0.20	11	1.08	0.12	12	1.12	0.23	34	1.28	0.47	47	0.92	0.23	19	1.04	0.21	15
$0.02 \geq d > 0.002$	0.96	0.16	9	0.96	0.10	9	0.87	0.22	19	1.94	0.45	42	0.96	0.21	18	0.96	0.19	15
$0.002 \geq d$	0.98	0.11	6	0.97	0.15	7	0.88	0.27	25	1.96	0.46	38	0.94	0.19	20	0.98	0.16	13

To test the performance accuracy of the developed regression equations, the verification group of data were used. Three numerical measures were used to asses such performance. These measures are:

(a) The ratio *Rat* between the estimated and observed values of the variable. This is expressed as the mean of all the storms on the catchments to indicate the average performance of a regression model in the catchments.
(b) The standard deviation *Dev* of the individual values about the overall mean, to describe the scatter in the *Rat* ratio.
(c) The absolute error *Abs* between the estimated and observed values, expressed as a percentage of the observed value. As in *Rat*, the *Abs* is expressed as the mean of all the storms on the investigated catchments.

The numerical performance accuracy measures for all the grain size diameter ranges are given in Table 4. The table shows consistent variation of the performance measures with grain size diameter of suspended sediments; the performance for small grain sizes is better than that for large grain sizes. The best performance is the regression equation for suspended sediment concentrations (equation (1)). For the heavy metals, described by equation (2), the performance of the regression for Cu, followed by that for Fe and Zn, is better than that for Pb and Ni.

CONCLUSIONS

Data from five residential arid catchments were used to develop regression equations for the estimation of heavy metal concentrations in the stormwater runoff. From the obtained results, the following conclusions are made:

- Suspended sediment concentrations in the stormwater runoff of arid residential catchments are significantly affected by the characteristics of both flash floods and duststorms over the catchments. Thus, both floods and duststorms are recommended to be considered for proper estimation of the sediments in the stormwater runoff.
- The effect on the suspended sediment concentrations of flash flood is much more significant than that of duststorms. Thus, duststorms may be neglected for rough estimation of suspended sediments in the stormwater runoff.
- The effect of the flash floods and duststorms on the suspended sediment increases as the grain size of the sediment decreases. Thus, it is recommended to control intensive duststorms and small grain size sediments from pervious areas for efficient control of drainage facilities.
- The regression equations relating the concentrations of Cu, Fe, Zn, and Pb with those of suspended sediments are of reasonable accuracy. Thus, these equations may be used for design purposes.
- The performance of the regression equations is better in the case of small grain size fractions of sediments than in the case of the large grain size fractions of sediments. Thus, these equations should be used for the estimation of metal concentrations in the stormwater runoff.
- The regression equation relating the concentration of Ni with that of the suspended sediments provides poor results. Thus, this equation may not be used in the investigated catchments.

Acknowledgement This study was supported in part by the Saudi Arabian National Water Research Funds; Grant nos AR-2-17 and AR-5-62.

REFERENCES

Ershova, E., Venitsianov, E., Kocharyan, A. & Vul'fsan, E. (1996) Heavy metals in bed-load deposits of the Kuibyshev reservoir. *Wat. Res.* **23**(1), 52–58.

Hellmann, H. (1987) *Analysis of Surface Waters.* Halsted Press–John Wiley & Sons, New York.

Nazarov, N. (1996) Assessments of erosion loss of soils and removal of biogenic substances with surface runoff of melt and rainwater in a river basin. *Wat. Res.* **23**(6), 597–604.

Nouh, M. (1987a) Analysis of rainfall in the southwest region of Saudi Arabia. *Proc. Instn Civ. Engrs* Part 2, **83**, 339–349.

Nouh, M. (1987b) Effect of very large sediment concentrations on highway sewer flows. In: *Proc. 4th Int. Conf. on Urban Storm Drainage* (IAHR/IAWPRC, Switzerland), 343–348.

Nouh, M. (1988a) On the prediction of flood frequency in Saudi Arabia. *Proc. Instn Civ. Engrs* Part 2, **85**, 121–144.

Nouh, M. (1989) A stochastic model for CO, TSP, and IP concentrations rate of protection. *Env. Software J.* **4**(3), 112–116.

Nouh, M. (1990) Design hyetographs for arabian gulf states. In: *Proc. 7th Congress of APD-IAHR* (Beijing), 161–166.

Nouh, M. (1991a) Effect of rainwater on quality and physical characteristics of flash floods in rural arid catchments. In: *Proc. XXIV Congress of IAHR* (Madrid, Spain), **A**, 169–178.

Nouh, M. (1991b) Urban stormwater quality in arid catchments. Invited Lecture, In: *Proc. Int. Conf. on Urban Drainage and New Technologies* (IAHR, Yugoslavia), 355–364.

Nouh, M. (1991c) Urban drainage in arid climates. Invited Paper, In: *Proc. Int. Conf. on Urban Drainage and New Technologies* (Dubrovnik, Yugoslavia, UNESCO/IAHR), 86–93.

Nouh, M. (1992) Sediment quality downstream of dams in extremely arid areas. In: *Proc. 5th Int. Symp. on River Sedimentation* (Karlsruhe, Germany, IAHR/IRTCES), 611–620.

Nouh, M. (1995a) Effect of urbanization on runoff quality in arid catchments. In: *Proc. 2nd Int. Conf. on Innovative Tech. in Urban Storm Drainage* (Lyon, France), 623–626.

Nouh, M. (1995b) Sediment quality in ephemeral compound channels. In: *Proc. XXVIth IAHR Congress* (London, UK), vol. 4, 54–59.

Nouh, M. (1996a) Influence of duststorms on stormwater runoff quality. In: *Proc. 3rd Int. Conf. on Environ. Pollut.* (Budapest, UNESCO), vol. 1, 350–357.

Nouh, M. (1996b) Effect of duststorms on sediment concentrations in sewer flows in an arid catchment. In: *Proc. 7th Int. Conf. on Urban Storm Drainage* (Hannover, IAHR/IAWPRC).

Nouh, M. (1996c) Simulation of water quality in sewer flows by neural networks. In: *Hydroinformatics'96* (Zurich, Switzerland, IAHR/IAWQ/UNESCO).

Nouh, M. (1997) Influence of a sheet erosion control system on sediment quality in an arid catchment. In: *Proc. XXVII IAHR Congress* (San Francisco, USA).

Nouh, M. & El-Laithy, A. (1988b) *Construction Damages Due to Floods in Wadi Addilah.* Tech. Report no. AR-5-62, KACST, Riyadh, Saudi Arabia.

Nouh, M. & Jamjoom, T. (1981) *Sediment Transport in Wadis in Saudi Arabia; A: Deposition Behind Wadi Jizan Dam.* Tech. Report no. AR-2-17, KACST, Riyadh, Saudi Arabia.

Nouh, M., Rowe, D., Al-Dowalia, K. & Mansour, M. (1986) Indoor-outdoor suspended particulate matter concentrations at four sites in Riyadh, Saudi Arabia. *Int. J. Environ. Studies* **28**,163–168.

Rowe, D., Nouh, M., Al-Dowalia, K. & Mansour, M. (1985) Indoor-outdoor relationship of suspended particulate matter in Riyadh, Saudi Arabia. *J. Air Pollut. Control Ass.* **5**(1), 24–26.

Sansalone, J., Buchberger, S. & Al-Abed, S. (1996) Fractionation of heavy metals in pavement runoff. *The Science of the Total Environment* **189/190**, 371–378.

Selim, H. & Ma, L. (1996) Solute transport of soils under conditions of variable flow velocities. *Wat. Resour. Res.* **32**(11), 3277–3283.

FRIEND'97 — Regional Hydrology: Concepts and Models for Sustainable Water Resource Management
(Proceedings of the Postojna, Slovenia, Conference, September–October 1997). IAHS Publ. no. 246, 1997.

Gestion des ressources en eau et développement durable. Un exemple dans la Province de l'extrême-nord du Cameroun

DANIEL SIGHOMNOU
Centre de Recherches Hydrologiques, Institut de Recherches Géologiques et Minières, BP 4110, Yaoundé, Cameroun

EMMANUEL NAAH
Hydrologue Régional de l'UNESCO, BP 30592, Naïrobi, Kenya

Résumé La plaine d'inondation du Logone dans la Province de l'extrême-nord du Cameroun, comme la plupart des zones humides tropicales, joue un rôle important dans le système écologique régional et même international. A la suite des travaux d'aménagement entrepris dans le cadre d'un projet hydro-agricole, les inondations annuelles de cette plaine ont considérablement diminué, ce qui a profondément perturbé ses fonctions naturelles. Cette situation est aggravée par la baisse généralisée de la pluviométrie enregistrée dans la région du Sahel au cours des deux dernières décennies. Des études ont été entreprises sur le terrain depuis 1994 en vue de la réhabilitation des inondations et de la biodiversité dans la plaine. Les premiers résultats enregistrés ont mis en évidence certaines insuffisances du Projet hydro-agricole dont la prise en considération dès le départ auraient permis d'éviter certaines conséquences négatives sur l'environnement.

DONNEES DU PROBLEME

Historique de l'inondation de la plaine

Les données hydrologiques utilisées pour l'étude des inondations avant et après la réalisation en 1979 du Projet hydro-agricole connu sous le nom: Société d'Expansion et de Modernisation de la Riziculture de Yagoua (SEMRY), sont issues de la banque de données du Centre de Recherches Hydrologiques du Cameroun (CRH) et de celle de la Commission du Bassin du Lac Tchad (CBLT). D'autre part, le mécanisme de l'inondation de la plaine du Logone est bien connu grâce aux travaux de plusieurs auteurs: Bouchardeau (1968), Benech *et al.* (1982), Olivry (1986) et Naah (1990). Connue sous le nom local de "Yaéré", la plaine d'inondation du fleuve Logone, côté camerounais, reçoit ses eaux essentiellement des crues du Logone, mais également des cours d'eau torrentiels issus des monts Mandara ainsi que des précipitations locales.

Le volume des eaux déversées dans la plaine est déterminé en utilisant les hydrogrammes des crues enregistrés au niveau de certaines stations caractéristiques des principaux cours d'eau responsables de la submersion: Logone (Bongor, Pouss et Katoa), Mayo Tsanaga (Maroua et Bogo), Mayo Boula (Dargala). Avant les aménagements de la SEMRY, les volumes d'eau reçus du Logone étaient évalués entre 3 et 4 milliards de m^3 an^{-1}, alors que les cours d'eau des monts Mandara fournissaient entre 0.5 et 1 milliard de m^3. La vidange de la plaine est assurée

essentiellement par l'El Béid dont les écoulements sont connus à Tildé, et dans une moindre mesure par le Logomatia dont le régime est connu à partir des données de la station de Zina (Fig. 1).

L'imagerie satellitaire et la photographie aérienne ont également été utilisées dans la détermination des limites des inondations suivant les années.

Les données pluviométriques utilisées sont pour partie tirées du "Document de recherche III" publié par le Centre National d'Appui à la Recherche (CNAR) tchadien sous le titre: *Travaux et Documentations Scientifiques du Tchad* (Beauvilain, 1994); complétées par d'autres données reçues de la Direction de la Météorologie Nationale du Cameroun.

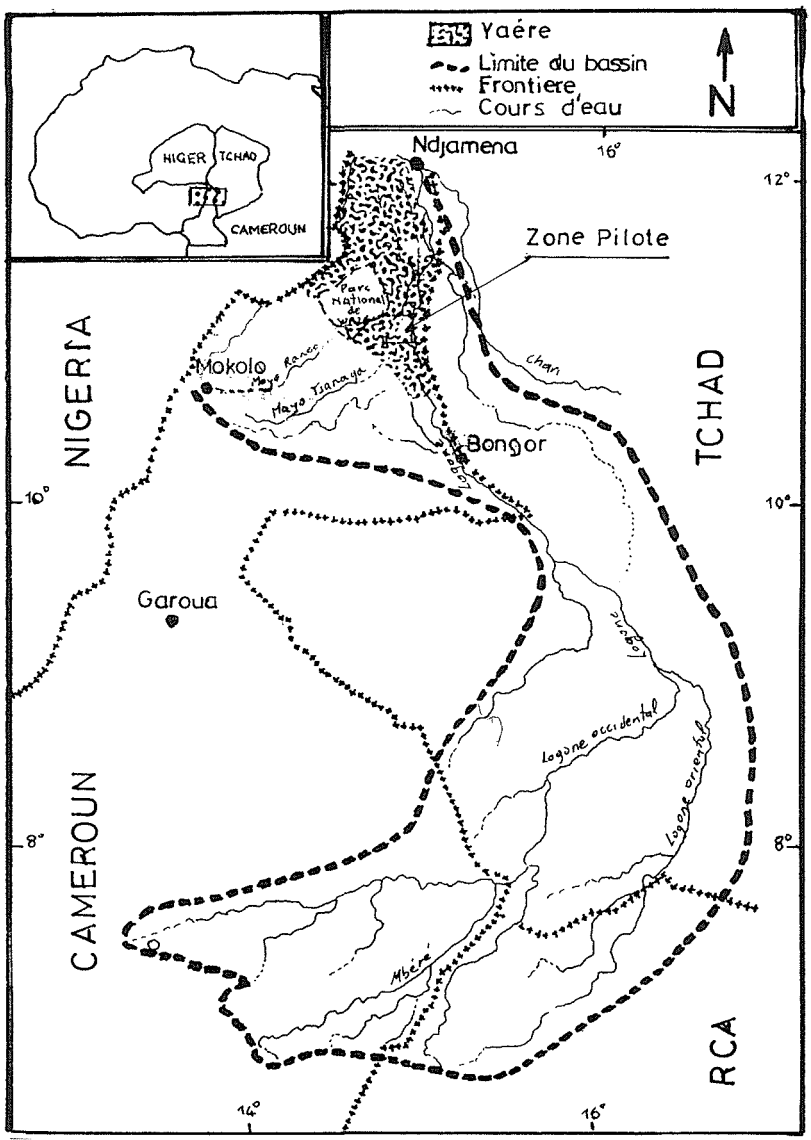

Fig. 1 Le bassin du Logone et le Yaéré.

La pluie moyenne sur le bassin du Logone est estimée par la méthode de Thiessen. Son évolution dans le temps montre une baisse prononcée depuis les années 1970 et particulièrement pendant les années 1980 (Fig. 2). Pour la plaine du Yaéré proprement dite la pluie moyenne est estimée entre 600 et 700 mm (Naah, 1990) alors que l'évapotranspiration annuelle est de l'ordre de 2000 mm (Riou, 1975).

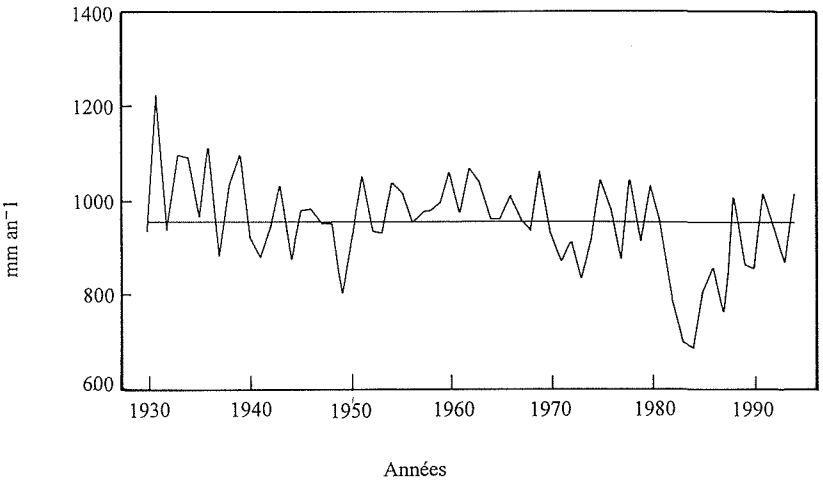

Fig. 2 Fluctuation de la pluie moyenne sur le bassin du Logone, de 1930 à 1994.

Données écologiques et socio-économiques

Les données écologiques et socio-économiques de la période ante et post Projet SEMRY sont tirées des travaux de Drijver & Van Wetten (1992) et des travaux préliminaires du Projet Waza Logone (PWL) en vue de la restauration des inondations dans la plaine. Ces études montrent, en particulier, que la population humaine et animale de la plaine a considérablement baissé au cours des deux dernières décennies, en raison de la dégradation de leur condition de vie.

La richesse de la biodiversité de la plaine avant la baisse des inondations peut être illustrée par la variété des animaux sauvages qui y vivaient, en particulier dans le parc national de Waza où la population des éléphants était supérieure au millier, celle des girafes évaluée à environ 2000 individus en plus de plusieurs autres espèces comme le lion, les antilopes, les gazelles, l'autruche, etc. D'autre part, le Yaéré joue un rôle important pour la survie des oiseaux d'eau d'Europe qui viennent y séjourner en période hivernale, et devraient y accumuler les ressources indispensables pour le voyage retour à travers le Sahara. Sur le plan de l'élevage et de la pêche, les zones inondées sont très riches en poisson (on évalue à 2000 $ USA le revenu moyen d'une famille de pécheurs pendant les 4 mois que dure la pêche) et constituent de bons pâturages de saison sèche où viennent (des pays de la sous-région) séjourner 200 à 300 000 bovins et 20 à 50 000 caprins chaque année. Sur le plan touristique, avec le parc de Waza, la région attirait un nombre important de visiteurs dont le total pouvait atteindre 6000 par an.

Les aménagements hydro-agricoles et leurs conséquences sur l'inondation de la plaine

Les données sur les aménagements réalisés sont tirées essentiellement des archives de la SEMRY à Yagoua et à Maga, et des "Audits Techniques" réalisés par la SOGREAH en 1992 sur le Projet.

En vue de la protection des populations riveraines et des périmètres cultivés le long du Logone, des travaux d'endiguement avaient été entrepris depuis les années 1950 sur les deux rives du fleuve en aval de la localité de Bongor. Ces travaux se sont poursuivis jusqu'en 1979 où ils ont été parachevés, coté Camerounais, par la construction du barrage de retenue d'eau de Maga et des 20 derniers kilomètres de digue entre les localités de Pouss et Tékélé pour protéger le périmètre rizicole de la SEMRY contre les inondations (Fig. 3) .

La capacité du barrage de Maga est évaluée à 600 millions de m^3 à sa cote de remplissage (312.19 m), pour une superficie inondée évaluée à 39 000 ha. Il est alimenté par les eaux du fleuve Logone, par celles des deux principaux cours d'eau des Monts Mandara (Mayo Tsanaga et Mayo Boula) et par les précipitations directes au-dessus de la retenue. L'ouvrage comporte un évacuateur de crue constitué d'un déversoir à paroi épaisse long de 750 m, qui permet d'évacuer le trop plein du lac vers le fleuve au niveau de la localité de Pouss. Dans le cas où le niveau d'eau est plus élevé dans le Logone, le même déversoir sert alternativement de voie d'entrée d'eau dans le lac.

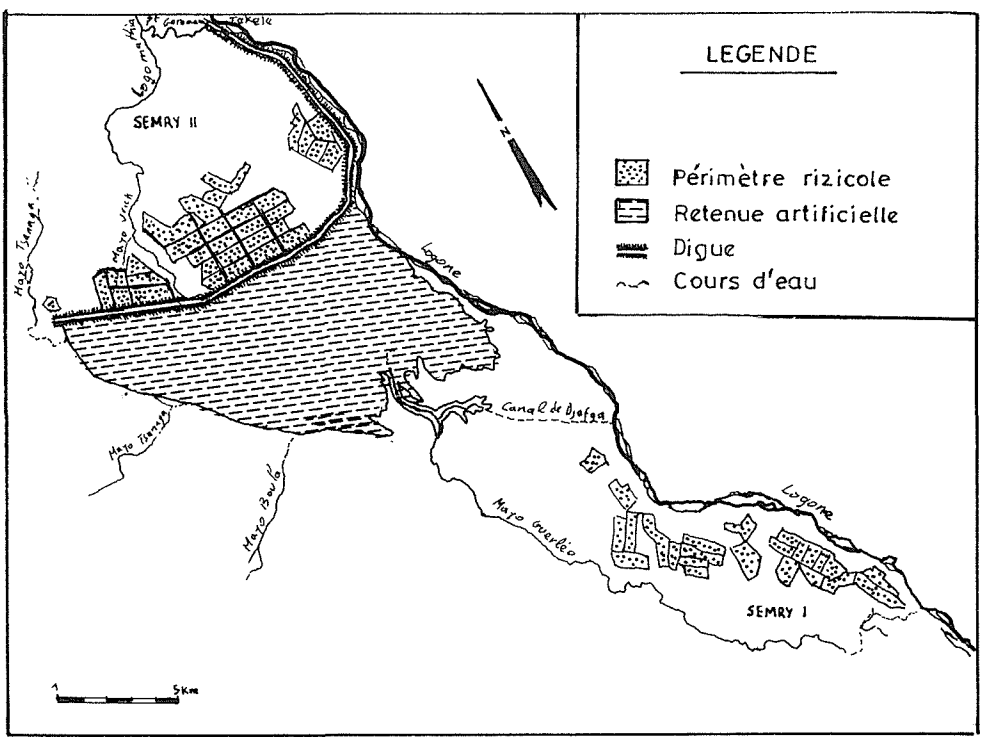

Fig. 3 Carte des aménagements de la SEMRY le long du Logone.

Du relevé journalier du niveau du plan d'eau dans la retenue ont été tirées les données du Tableau 1 qui présente les volumes d'eau excédentaires enregistrés dans le lac depuis sa construction jusqu'en 1995. Il ressort de ce tableau que la quantité d'eau excédentaire enregistrée dans le lac chaque année est importante (580 millions de m^3 en moyenne). Si cet excédent était évacué vers la plaine, il assurerait une submersion au moins partielle du secteur privé d'eau du fait de la présence du barrage.

Tableau 1 Estimation des volumes d'eau excédentaires (millions de m^3) du lac de Maga depuis 1979.

1979	**1980**	**1981**	**1982**	**1983**	**1984**	**1985**	**1986**	**1987**	**1988**	**1989**
néant	380	870	990	620	néant	110	80	néant	1065	110
1990	**1991**	**1992**	**1993**	**1994**	**1995**					
220	1910	1230	10	2010	240					

A la suite des derniers aménagements de la SEMRY en 1979, les inondations périodiques de la plaine ont considérablement baissé. D'après, Drijver & Van Wetten (1992), la superficie totale inondée jadis a diminué de 60% . Les principales conséquences sont les suivantes: diminution de la fertilité de la plaine, dégradation de la biodiversité, réduction des pâturages, recolonisation des sols par de nouvelles espèces végétales moins intéressantes pour la faune, surexploitation des pâturages résiduaires, baisse d'environ 90% de la productivité en poisson, baisse du niveau de la nappe souterraine (Detay, 1992), migration des populations, ce qui a conduit à l'abandon des systèmes traditionnels de gestion de l'environnement garants d'une exploitation durable.

ESSAI DE REINONDATION DU YAERE

En vue de la réhabilitation de la biodiversité dans le Yaéré, des études visant une restauration au moins partielle des inondations ont été entreprises en 1989 dans le cadre d'un projet dénommé "Projet Waza Logone" (PWL). Des études topographiques et une analyse détaillée du mécanisme de submersion de la plaine ont montré que la création des conditions favorables à cette opération, sur des secteurs de la plaine privés d'eau depuis 1979, était possible sans perturber les installations hydro-agricoles en place (Naah, 1993). Un "**Essai Pilote**" de réinondation a été alors envisagé et entrepris sur le terrain en mai 1994, en vue de rassembler un maximum d'informations qui permettraient d'assurer une réinondation efficace et optimale de la zone sinistrée. Les études sont prévues pour 3 ans.

L'essai pilote de réinondation consiste à la réouverture de certaines voies d'eau fermées dans le cadre des aménagements de la SEMRY, de sorte à provoquer une inondation dans un secteur de la plaine assez limité pour être facilement contrôlable. L'évaluation de l'impact de cette inondation à petite échelle permettrait alors de comprendre et maîtriser l'option finale qui vise la réinondation complète.

Au mois de mai 1994, une ouverture d'environ 15 m de large a été aménagée dans la digue en terre qui fermait l'entrée du lit du défluent Petit Goroma dans la localité de Tékélé, afin de permettre aux eaux du Logone d'entrer dans la plaine en période de crue. Le lit du Petit Goroma a été en outre faucardé et aménagé, afin de

faciliter l'écoulement des eaux. Pour le contrôle des apports et des sorties des eaux dans la zone d'impact de l'Essai Pilote, 34 stations hydropluviométriques ont été installées à des postes de mesure adéquats. Pour le suivi des inondations un quadrillage topographique représentant un réseau maillé de piquets (274 au total), placés sur des points d'altitude connue de la zone qui recevra les eaux transitant par le Petit Goroma, a été mis en place. Le suivi des variations du plan d'eau au niveau de ces piquets est assuré par une équipe de 25 observateurs (Sighomnou *et al.*, 1995, 1996).

RESULTATS

Sur le plan des inondations

Les principaux résultats enregistrés pendant les campagnes de mesures 1994 et 1995 sont regroupés dans le Tableau 2. Ils montrent que les deux campagnes de mesures se sont déroulées dans des conditions d'hydraulicité proches de la moyenne. Avec un volume d'eau total écoulé de l'ordre de 120 millions de m^3 pour un débit maximum de 20 m^3 s^{-1} obtenus à la faveur de l'ouverture du Petit Goroma, on aboutit à des inondations qui sont allées au delà de la zone d'impact escomptée. La reprise des précipitations amorcée en 1994 dans la région après près de 30 années de sécheresse peut être considérée comme le seul facteur de cette reprise des inondations observée au cours des deux années de suivi. Cependant, si les 120 millions de m^3 qui ont transité par le Petit Goroma en 1994 et 1995 représentent un très faible volume par rapport au volume total des eaux d'inondation, l'ouverture de cet ancien défluent a conduit, en particulier, B une restauration partielle de la dynamique de submersion de la plaine. L'utilisation de l'imagerie satellitaire complétée par les enquêtes sur le terrain, a permis de déterminer les contours exacts de la zone inondée durant de ces deux années. Les résultats montrent qu'en dehors de l'année 1988 où les conditions d'hydraulicité étaient exceptionnelles, les inondations enregistrées en 1994 et 1995 ont couvert une superficie supérieure, en moyenne, de 300 km^2 à toutes celles enregistrées dans la plaine depuis la fin des travaux d'aménagement de la SEMRY en 1979, même pour des conditions d'hydraulicité voisines (Rapport interne PWL; 1996). On montre sur la Fig. 4 les limites des inondations enregistrées en 1993, 1994 et 1995 ainsi que les prévisions pour l'option finale en 1998. On rappelle que la pluie moyenne dans le Yaéré en 1993 est estimée à 500 mm pour un volume écoulé de 6100 millions de m^3 enregistrés sur le Logone à la station de Pouss pour les mois d'août à octobre, contre 650 mm pour 7900 millions de m^3 en 1994 et 581 mm pour 7700 millions de m^3 en 1995.

Tableau 2 Les résultats de l'Essai Pilote en 1994 et 1995.

Année	Pluie moyen Yaéré (mm)	Volume écoulé Logone à Pouss (millions m^3)	Q_{max} Goroma à Tékélé (m^3)	Vol. écoul. Pt Goroma à Tékélé (millions m^3)	Profondeur moyenne des inondations (cm)	Durée des inondations (jours)	Etendue des inondations
1994	649.7	7895	20	123	35 à 45	50 à 60	au delà de la zone pilote
1995	580.9	7701	20	118	30 à 50	40 à 50	au delà de la zone pilote

NB: Le volume écoulé du Logone est calculé pour les trois mois les plus pluvieux (août–octobre).

Ces résultats montrent que la fermeture du Mayo Petit Goroma en 1979 n'était pas justifiée, dans la mesure où les eaux qui y transitent n'ont aucune influence sur le périmètre rizicole. Elle montre, en outre, que l'absence des inondations dans le Yaéré depuis 1979 résulte surtout de la perturbation intervenue dans la dynamique du processus d'inondation de la plaine par les crues du Logone, et pas seulement de la baisse générale de la pluviométrie enregistrée ces dernières années (Sighomnou *et al.*, 1995, 1996).

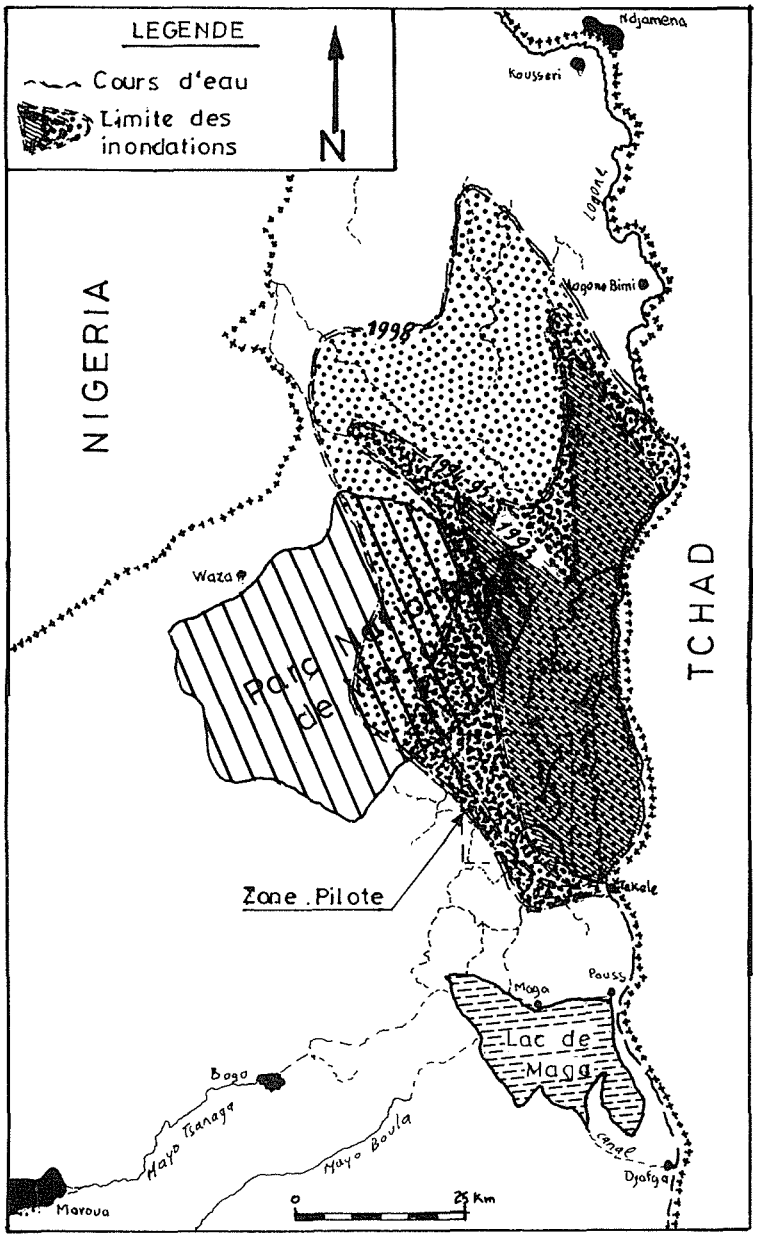

Fig. 4 Limites de la surface inondée du Yaéré en 1993, 1994, 1995 et prévisions pour 1998.

Concernant le système écologique et les activités socio-économiques de la plaine

Les inondations enregistrées en 1994 et 1995 ont conduit à une amorce de la restauration des activités socio-économiques et des systèmes écologiques de la plaine. Sur le plan social, on a enregistré le retour de certaines familles dans la région, attirées par la reprise des activités économiques et la restauration des formes traditionnelles d'utilisation des sols telles que la pêche, l'agriculture de décrue et les pâturages. Sur le plan de la végétation, les deux années de l'essai pilote ont conduit à une diminution des herbacées annuelles au profit des espèces pérennes. En particulier, on a relevé une nette diminution des surfaces occupées depuis la baisse des inondations par une espèce végétale appelée ici communément "**mil sauvage**" (*Sorghum arundinaceum*) non appréciée par les animaux, suivi d'une recolonisation par des espèces riches en protéines (*Vetiveria nigrita*, *Echinochloa pyramidalis*, etc.), plus appréciées (Rapport interne PWL, 1996).

La faune quant à elle souffre de moins en moins des problèmes de manque d'eau en même temps qu'elle bénéficie de l'amélioration des pâturages, d'où la reprise de l'accroissement des populations animales dans le Parc National de Waza, en même temps qu'une augmentation des troupeaux nomades dans la plaine. La production de la pêche s'est également considérablement améliorée. Evaluée à environ 879 t en 1994 dans l'ensemble des villages de la zone pilote, elle a été de 910 t en 1995 (Kouokam, 1996).

Toutefois, cette légère reprise des inondations a également conduit à une recrudescence de certaines maladies liées à l'eau, de même que renaissent les conflits sociaux entre les différents groupes de populations (agriculteurs, éleveurs, pécheurs, commerçants etc.) aux intérêts parfois contradictoires. Même si le niveau des inondations antérieures ne sera jamais atteint dans les conditions actuelles (Sighomnou, 1996), ces premiers résultats laissent penser que dans l'ultime étape du projet qui vise une réinondation complète, ces quelques difficultés seront plus accentuées. Un nouvel équilibre devrait cependant naître afin de favoriser la reprise des activités naturelles de la plaine pour une gestion plus durable.

L'environnement change dans le temps sous l'influence des processus d'origine naturelle ou anthropique. Comprendre ce qu'il est aujourd'hui et imaginer ce qu'il sera demain sont pour l'homme les gages de la maîtrise d'un développement acceptable socialement, biologiquement et écologiquement pour les générations futures. Pour atteindre cet objectif, des études d'impact préalables des projets d'aménagement sur l'environnement devraient permettre d'ajuster leur conception de sorte à éviter les conséquences négatives inutiles. Dans le cas du Projet SEMRY, de telles études auraient permis d'assurer une protection au moins partielle des fonctions naturelles du Yaéré. En particulier, si le trop-plein du lac de Maga avait été dirigé vers la plaine, il aurait permis d'assurer l'inondation de certains secteurs de la plaine privés d'eau, alors que la fermeture de certains défluents comme le Petit Goroma n'était pas justifiée.

Remerciements Les auteurs remercient le Gouvernement Néerlandais ainsi que les responsables des organismes suivants, sans qui cette étude n'aurait jamais été possible: Centre de Recherches Hydrologiques du Cameroun, Projet Waza Logone, Union Mondiale pour la Nature, Commission du Bassin du Lac Tchad.

REFERENCES

Beauvilain, A. (1994) Tableau de la pluviométrie dans les bassins du Tchad et de la Bénoué. De la création des stations a décembre 1994. *Travaux et Documentations Scientifiques du Tchad; Document pour la Recherche III.*

Benech, V., Quensière, J., Vidy, G. (1982) Hydrologie et physico-chimie des eaux d'inondation de la plaine d'inondation du nord-Cameroun. *Cah. ORSTOM,* sér. Hydrol. **XIX**(1).

Bouchardeau, A. (1968) *Monographie Hydrologique du Logone.* ORSTOM, Sect. Hydrologie., Paris; 8 vols.

Detay, M. (1992) Carte hydrogéologique d'aide à l'implantation d'ouvrages d'hydraulique villageoise. Notice Explicative.

Drijver, C. A. & Van Wetten, J. C. J. (1992) Les zones humides sahéliennes à l'horizon 2020. Modifier les politiques du développement ou perdre les meilleures ressources du Sahel. Un projet de Birdlife International, CML, Pays-Bas.

Kouokam, R. (1996) Synthèse analyse des résultats des études comparatives des situations socio-économiques des villages de la zone pilote du Projet Waza-Logone. Campagnes 1994/1995 et 1995/1996.

Naah, E. (1990) Hydrologie du grand Yaéré du nord Cameroun; Thèse de Doctorat es Sciences; Université de Yaoundé.

Naah, E. (1993) Restauration hydro-technique de la plaine du Yaéré de l'extrême-nord du Cameroun. Campagne Hydrologique 1993.

Olivry, J. C. (1986) *Fleuves et Rivières du Cameroun.* Collection Monographies Hydrologiques ORSTOM no. 9, ORSTOM, Paris.

Projet Waza Logone (1996) *Rapport Global du Workshop, 1996* (Maroua, avril 1996).

Riou, C. (1975) La détermination pratique de l'évapotranspiration. Application à l'Afrique centrale. *Mém. ORSTOM no. 80.* ORSTOM Paris.

Sighomnou, D., Bedimo, B. J. P., Ayissi, G., Issa, N. J., Awoua G. & Kouamou, P. (1995) Restauration hydro-technique de la plaine du Logone dans l'extrême-nord du Cameroun. Essai pilote de réinondation, première campagne de mesures.

Sighomnou, D., Djoko, A., Ayissi, G., Issa, N. J., Nkoa, F. & Kouamou, P. (1996) Restauration hydro-technique de la plaine du Logone dans l'extrême-nord du Cameroun. Essai pilote de réinondation, deuxième campagne de mesures.

Sighomnou, D. (1996) Restauration hydro-technique de plaine du Logone dans l'extrême-nord du Cameroun; prévision des inondations. Avril 1996.

SOGREAH (1992) Audits techniques; aménagements des réseaux hydrauliques, des pistes et des digues—station de pompage et gestion de l'eau. *Rapport Final, Société d'Expansion et de Modernisation de la Riziculture de Yagoua (SEMRY).*

INTERNATIONAL ASSOCIATION OF HYDROLOGICAL SCIENCES